Thèse de Doctorat

Université de BOURGOGNE FRANCHE-COMTE

Ecole Doctorale n° 554 "Environnement-Santé"

Modifications peroxysomales associées à l'oxyapoptophagie induite par le 7-cétocholestérol et identification de lipides cytoprotecteurs

Confidentiel

Thomas NURY

Thèse présentée et soutenue à Dijon le 3 Décembre 2020

Composition du Jury

Marc POIROT (Directeur de Recherche, INSERM, Toulouse)	Rapporteur / Président du Jury
Isabelle DELTON (Professeur des Universités, INSA, Lyon)	Rapporteur
Delphine MEFFRE (HDR / Maitre de Conférences, Paris)	Examinateur
David MASSON (Professeur des Universités/Praticien Hospitalier, Dijon)	Examinateur
Anne VEJUX (Maitre de Conférences, Dijon)	Co-Directrice de Thèse
Gérard LIZARD (Chargé de Recherche, INSERM, Dijon)	Directeur de Thèse
Valerio LEONI Membre extérieur invité (Professeur associé, Milan)	Examinateur

Remerciements

Ce travail a été réalisé au sein du Laboratoire Bio-PeroxIL « Biochimie du Peroxysome, Inflammation et Métabolisme Lipidique » EA7270 ; Université de Bourgogne-Franche-Comté ; Dijon ; France (https://bioperoxil.u-bourgogne.fr/).

Qu'il me soit permis de remercier, les membres du jury : les **Docteur Marc Poirot** et **Isabelle Delton,** pour avoir accepté de relire et de critiquer ce travail, ainsi que le **Docteur Delphine Meffre** et le **Professeur David Masson**, d'avoir accepté d'examiner ce travail.

Merci à mes deux encadrants **: Monsieur le Directeur du Laboratoire Bio-PeroxIL**, **Gérard Lizard**, pour m'avoir encadré et dirigé depuis maintenant dix ans et **Madame Anne Vejux**, pour m'avoir co-encadré durant ces trois ans et pour ses bons conseils. Je n'aurais sans doute jamais fait de thèse sans vos conseils et vos encouragements.

Je remercie également **Monsieur le Directeur du Centre des Sciences du goût et de l'Alimentation, Lionel Bretillon**, et **Monsieur le Professeur Jean-Marc Lobaccaro**, d'avoir accepté de suivre ce travail au cours des comités de suivi de thèse.

Je voudrais aussi remercier le **Docteur Valerio Leoni** pour ses analyses lipidiques et les collaborations toujours fructueuses que nous avons réalisées, ainsi que la plateforme lipidomique (**Jean-Paul Pais De Barros** et son équipe).

Je souhaiterais également remercier l'ensemble du personnel du Laboratoire Bio-PeroxIL, mes collègues et amis, pour leur gentillesse et la bonne ambiance que chacun contribue à maintenir. **Catherine Gondcaille** (pour me supporter dans le bureau), **Nathalie Bancod, Mustapha Cherkaoui-Malki, Stéphane Savary, Pierre Andreoletti, Doriane Trompier et Norbert Latruffe**.
Je remercie également la **Société de Défense des Animaux (SNDA)**, prix Renard (Gérard Lizrad, 2018) qui nous a permis d'aborder les effets du SSO sur des oligodendrocytes dans le cadre des maladies démyélinisantes (X-ALD, sclérose en plaques).

Je remercie ma famille et mes parents, je ne serais jamais arrivé jusqu'ici sans votre aide.
Merci à Meriem, pour ton indéfectible soutien et tes précieux encouragements.

Sommaire

Liste des travaux scientifiques

Publications associées à la thèse

2020

- **Nury T**, Zarrouk A, Yammine A, Mackrill JJ, Vejux A, Lizard G. Oxiapoptophagy: A type of cell death induced by some oxysterols. ***Br J Pharmacol***. 2020, doi:10.1111/bph.15173.

- **Nury T**, Lizard G, Vejux A. Lipids Nutrients in Parkinson and Alzheimer's Diseases: Cell Death and Cytoprotection. ***Int J Mol Sci***. 2020, 21(7), 2501.

- **Nury T**, Yammine A, Caccia C, Leoni V, Hichami A, Pande A, Majeed M, Atanasov A, Vejux A, Lizard G. Prevention of 7-ketocholesterol-induced cytotoxicity by fatty acids, Lorenzo's oil and sulfo-N-succinimdyl oleate (SSO) on 158N cells: benefits of SSO and mechanisms of cytoprotection. *(en préparation*).

- **Nury T**, Yammine A, Menetrier F, Zarrouk A, Vejux A, Lizard G. 7-hydroxycholesterols-induced peroxisomal disorders in glial and microglial cells: potential role in neurodegeneration. ***Advances in Experimental Medicine and Biology***; Lizard G (Ed.). 2021. Peroxisome Biology: Experimental Models, Peroxisomal Disorders and Neurological Diseases. Chapter 7. doi: 10.1007/978-3-030-60204-8.

2018

- **Nury T**, Sghaier R, Zarrouk A, Ménétrier F, Uzun T, Leoni V, Caccia C, Meddeb W, Namsi A, Sassi K, Mihoubi W, Riedinger JM, Cherkaoui-Malki M, Moreau T, Vejux A, Lizard G. Induction of peroxisomal changes in oligodendrocytes treated with 7-ketocholesterol: Attenuation by α-tocopherol***. Biochimie***. 2018, 153:181-202.

Ensemble des Publications : travaux de recherche

* Les publications et communications en premier et second auteur (Thomas NURY) sont surlignées (jaune 1er auteur, gris 2ème auteur)

2020

Yammine A, Zarrouk A, **Nury T**, Vejux A, Latruffe N, Vervandier-Fasseur D, Samadi M, Mackrill JJ, Greige-Gerges H, Auezova L, Lizard G. Prevention by Dietary Polyphenols (Resveratrol, Quercetin, Apigenin) Against 7-Ketocholesterol-Induced Oxiapoptophagy in Neuronal N2a Cells: Potential Interest for the Treatment of Neurodegenerative and Age-Related Diseases. *Cells*. 2020, 23;9(11):E2346.

Sruthi S, **Nury T**, Millot N, Lizard G. Evidence of a non-apoptotic mode of cell death in microglial BV-2 cells exposed to different concentrations of zinc oxide nanoparticles. *Environ Sci Pollut Res Int*. 2020, doi: 10.1007/s11356-020-11100-8.

Yammine A, **Nury T**, Vejux A, Latruffe N, Vervandier-Fasseur D, Samadi M, Greige-Gerges H, Auezova L, Lizard G. Prevention of 7-Ketocholesterol-Induced Overproduction of Reactive Oxygen Species, Mitochondrial Dysfunction and Cell Death with Major Nutrients (Polyphenols, ω3 and ω9 Unsaturated Fatty Acids) of the Mediterranean Diet on N2a Neuronal Cells. ***Molecules***. 2020, 25(10), 2296.

Nury T, Doria M, Lizard G, Vejux A. Docosahexaenoic Acid Attenuates Mitochondrial Alterations and Oxidative Stress Leading to Cell Death Induced by Very Long-Chain Fatty Acids in a Mouse Oligodendrocyte Model. ***Int J Mol Sci.*** 2020, 21(2), 641.

2019

Vejux A, Abed-Vieillard D, Hajji K, Zarrouk A, Mackrill JJ, Ghosh S, **Nury T**, Yammine A, Zaibi M, Mihoubi W, Bouchab H, Nasser B, Grosjean Y, Lizard G. 7-Ketocholesterol and 7β-hydroxycholesterol: In vitro and animal models used to characterize their activities and to identify molecules preventing their toxicity. ***Biochem Pharmacol***. 2020, 173, 113648. doi: 10.1016/j.bcp.2019.113648.

Namsi A, **Nury T**, Khan AS, Leprince J, Vaudry D, Caccia C, Leoni V, Atanasov AG, Tonon MC, Masmoudi-Kouki O, Lizard G. Octadecaneuropeptide (ODN) Induces N2a Cells Differentiation through a PKA/PLC/PKC/MEK/ERK-Dependent Pathway: Incidence on Peroxisome, Mitochondria, and Lipid Profiles. ***Molecules***. 2019, 24(18), 3310.

Sghaier R, **Nury T**, Leoni V, Caccia C, Pais De Barros JP, Cherif A, Vejux A, Moreau T, Limem K, Samadi M, Mackrill JJ, Masmoudi AS, Lizard G, Zarrouk A. Dimethyl fumarate and monomethyl fumarate attenuate oxidative stress and mitochondrial alterations leading to oxiapoptophagy in 158N murine oligodendrocytes treated with 7β-hydroxycholesterol. ***J Steroid Biochem Mol Biol***. 2019, 194, 105432.

Zarrouk A, Martine L, Grégoire S, **Nury T**, Meddeb W, Camus E, Badreddine A, Durand P, Namsi A, Yammine A, Nasser B, Mejri M, Bretillon L, Mackrill JJ, Cherkaoui-Malki M, Hammami M, Lizard G. Profile of Fatty Acids, Tocopherols, Phytosterols and Polyphenols in Mediterranean Oils (Argan Oils, Olive Oils, Milk Thistle Seed Oils and Nigella Seed Oil) and Evaluation of their Antioxidant and Cytoprotective Activities. ***Curr Pharm Des***. 2019, 25(15), 1791-1805.

Sghaier R, Zarrouk A, **Nury T**, Badreddine I, O'Brien N, Mackrill JJ, Vejux A, Samadi M, Nasser B, Caccia C, Leoni V, Moreau T, Cherkaoui-Malki M, Salhedine Masmoudi A, Lizard G. Biotin attenuation of oxidative stress, mitochondrial dysfunction, lipid metabolism alteration and 7β-hydroxycholesterol-induced cell death in 158N murine oligodendrocytes. ***Free Radic Res.*** 2019, 53(5), 535-561.

Sassi K, **Nury T**, Zarrouk A, Sghaier R, Khalafi-Nezhad A, Vejux A, Samadi M, Aissa-Fennira FB, Lizard G. Induction of a non-apoptotic mode of cell death associated with autophagic characteristics with steroidal maleic anhydrides and 7β-hydroxycholesterol on glioma cells. ***J Steroid Biochem Mol Biol***. 2019, 191:105371.

Doria M, **Nury T**, Delmas D, Moreau T, Lizard G, Vejux A. Protective function of autophagy during VLCFA-induced cytotoxicity in a neurodegenerative cell model**.** ***Free Radic Biol Med***. 2019, 137:46-58.

Sallem F, Haji R, Vervandier-Fasseur D, **Nury T**, Maurizi L, Boudon J, Lizard G, Millot N. Elaboration of Trans-Resveratrol Derivative-Loaded Superparamagnetic Iron Oxide Nanoparticles for Glioma Treatment. ***Nanomaterials (Basel)***. 2019, 18;9(2).

Singh N, Sallem F, Mirjolet C, **Nury T**, Sahoo SK, Millot N, Kumar R. Polydopamine Modified Superparamagnetic Iron Oxide Nanoparticles as Multifunctional Nanocarrier for Targeted Prostate Cancer Treatment. ***Nanomaterials (Basel)***. 2019, 22;9(2).

2018

Brahmi F, **Nury T**, Debbabi M, Hadj-Ahmed S, Zarrouk A, Prost M, Madani K1, Boulekbache-Makhlouf L, Lizard G. Evaluation of Antioxidant, Anti-Inflammatory and Cytoprotective Properties of Ethanolic Mint Extracts from Algeria on 7-Ketocholesterol-Treated Murine RAW 264.7 Macrophages. ***Antioxidants (Basel)***. 2018, 6;7(12).

Namsi A, **Nury T**, Hamdouni H, Yammine A, Vejux A, Vervandier-Fasseur D, Latruffe N, Masmoudi-Kouki O, Lizard G. Induction of Neuronal Differentiation of Murine N2a Cells by Two Polyphenols Present in the Mediterranean Diet Mimicking Neurotrophins Activities: Resveratrol and Apigenin. ***Diseases***. 2018, 22;6(3).

Meddeb W, Rezig L, Zarrouk A, **Nury T**, Vejux A, Prost M, Bretillon L, Mejri M, Lizard G. Cytoprotective Activities of Milk Thistle Seed Oil Used in Traditional Tunisian Medicine on 7-Ketocholesterol and 24S-Hydroxycholesterol-Induced Toxicity on 158N Murine Oligodendrocytes. ***Antioxidants (Basel)***. 2018, 19;7(7).

Brahmi F, Vejux A, Sghaier R, Zarrouk A, **Nury T**, Meddeb W, Rezig L, Namsi A, Sassi K, Yammine A, Badreddine I, Vervandier-Fasseur D, Madani K, Boulekbache-Makhlouf L, Nasser B, Lizard G. Prevention of 7-ketocholesterol-induced side effects by natural compounds. ***Crit Rev Food Sci Nutr***. 2018, 11:1-48.

Sruthi S, Maurizi L, **Nury T**, Sallem F, Boudon J, Riedinger JM, Millot N, Bouyer F, Lizard G. Cellular interactions of functionalized superparamagnetic iron oxide nanoparticles on oligodendrocytes without detrimental side effects: Cell death induction, oxidative stress and inflammation. ***Colloids Surf B Biointerfaces***. 2018, 1;170:454-462.

2017

Zarrouk A, **Nury T**, Karym EM, Vejux A, Sghaier R, Gondcaille C, Andreoletti P, Trompier D, Savary S, Cherkaoui-Malki M, Debbabi M, Fromont A, Riedinger JM, Moreau T, Lizard G. Attenuation of 7-ketocholesterol-induced overproduction of reactive oxygen species, apoptosis, and autophagy by dimethyl fumarate on 158N murine oligodendrocytes. ***J Steroid Biochem Mol Biol***. 2017, 169:29-38.

Debbabi M, Zarrouk A, Bezine M, Meddeb W, **Nury T**, Badreddine A, Karym EM, Sghaier R, Bretillon L, Guyot S, Samadi M, Cherkaoui-Malki M, Nasser B, Mejri M, Ben-Hammou S, Hammami M, Lizard G. Comparison of the effects of major fatty acids present in the Mediterranean diet (oleic acid, docosahexaenoic acid) and in hydrogenated oils (elaidic acid) on 7-ketocholesterol-induced oxiapoptophagy in microglial BV-2 cells. ***Chem Phys Lipids***. 2017, 207(Pt B), 151-170

Brahmi F, Hadj-Ahmed S, Zarrouk A, Bezine M, **Nury T**, Madani K, Chibane M, Vejux A, Andreoletti P, Boulekbache-Makhlouf L, Lizard G. Evidence of biological activity of Mentha species extracts on apoptotic and autophagic targets on murine RAW264.7 and human U937 monocytic cells. **Pharm Biol**. 2017, 55(1), 286-293.

Bezine M, Debbabi M, **Nury T**, Ben-Khalifa R, Samadi M, Cherkaoui-Malki M, Vejux A, Raas Q, de Sèze J, Moreau T, El-Ayeb M, Lizard G. Evidence of K+ homeostasis disruption in cellular dysfunction triggered by 7-ketocholesterol, 24S-hydroxycholesterol, and tetracosanoic acid (C24:0) in 158N murine oligodendrocytes. ***Chem Phys Lipids.*** 2017, 207(Pt B), 135-150.

Debbabi M, **Nury T**, Helali I, Karym EM, Geillon F, Gondcaille C, Trompier D, Najid A, Terreau S, Bezine M, Zarrouk A, Vejux A, Andreoletti P, Cherkaoui-Malki M, Savary S, Lizard G. Flow Cytometric Analysis of the Expression Pattern of Peroxisomal Proteins, Abcd1, Abcd2, and Abcd3 in BV-2 Murine Microglial Cells. ***Methods Mol Biol***. 2017, 1595:257-265.

Kharroubi W, **Nury T**, Ahmed SH, Andreoletti P, Sakly R, Hammami M, Lizard G. Induction by arsenate of cell-type-specific cytotoxic effects in nerve and hepatoma cells. ***Hum Exp Toxicol***. 2017, 36(12), 1256-1269.

Kharroubi W, Haj Ahmed S, **Nury T**, Andreoletti P, Sakly R, Hammami M, Lizard G. Mitochondrial dysfunction, oxidative stress and apoptotic induction in microglial BV-2 cells treated with sodium arsenate. ***J Environ Sci (China)***. 2017, 51:44-51.

Samadi M, **Nury T**, Khalafi-Nezhad A, Lizard G. Protecting group-free radical decarboxylation of bile acids: Synthesis of novel steroidal substituted maleic anhydrides and maleimides and evaluation of their cytotoxicity on C6 rat glioma cells. ***Steroids***. 2017, 125:124-130.

Haj Ahmed S, Kharroubi W, Zarrouk A, Brahmi F, **Nury T**, Lizard G, Hammami M. Protective effects of bezafibrate against elaidic acid-induced accumulation of lipid droplets in monocytic cells. ***Curr Res Transl Med***. 2017, 65(1), 20-30.

2016

Debbabi M, **Nury T**, Zarrouk A, Mekahli N, Bezine M, Sghaier R, Grégoire S, Martine L, Durand P, Camus E, Vejux A, Jabrane A, Bretillon L, Prost M, Moreau T, Ammou SB, Hammami M, Lizard G. Protective Effects of α-Tocopherol, γ-Tocopherol and Oleic Acid, Three Compounds of Olive Oils, and No Effect of Trolox, on 7-Ketocholesterol-Induced Mitochondrial and Peroxisomal Dysfunction in Microglial BV-2 Cells. ***Int J Mol Sci***. 2016, 25;17(12).

Kharroubi, W.; Ahmed, S. H.; **Nury, T**.; Andreoletti, P.; Haouas, Z.; Zarrouk, A.; Sakly, R.; Hammami, M.; Lizard, G. Evidence of hormesis on human neuronal SK-N-BE cells treated with sodium arsenate: impact at the mitochondrial level. ***Environ Sci Pollut Res Int***. 2016, 23(9), 8441-8452

Leoni, V.; **Nury, T**.; Vejux, A.; Zarrouk, A.; Caccia, C.; Debbabi, M.; Fromont, A.; Sghaier, R.; Moreau, T.; Lizard, G. Mitochondrial dysfunctions in 7-ketocholesterol-treated 158N oligodendrocytes without or with alpha-tocopherol: Impacts on the cellular profil of tricarboxylic cycle-associated organic acids, long chain saturated and unsaturated fatty acids, oxysterols, cholesterol and cholesterol precursors. ***J Steroid Biochem Mol Biol***. 2017, 169:96-110.

Nury, T.; Zarrouk, A.; Ragot, K.; Debbabi, M.; Riedinger, J. M.; Vejux, A.; Aubourg, P.; Lizard, G. 7-Ketocholesterol is increased in the plasma of X-ALD patients and induces peroxisomal modifications in microglial cells: Potential roles of 7-ketocholesterol in the pathophysiology of X-ALD. ***J Steroid Biochem Mol Biol***. 2017, 169:123-136.

Rihane, N.; **Nury, T**.; M'Rad, I.; El Mir, L.; Sakly, M.; Amara, S.; Lizard, G. Microglial cells (BV-2) internalize titanium dioxide (TiO) nanoparticles: toxicity and cellular responses. ***Environ Sci Pollut Res Int***. 2016, 23(10), 9690-9699.

Zarrouk, A.; **Nury, T**.; Karym, E. M.; Vejux, A.; Sghaier, R.; Gondcaille, C.; Andreoletti, P.; Trompier, D.; Savary, S.; Cherkaoui-Malki, M.; Debbabi, M.; Fromont, A.; Riedinger, J. M.; Moreau, T.; Lizard, G. Attenuation of 7-ketocholesterol-induced overproduction of reactive oxygen species, apoptosis, and autophagy by dimethyl fumarate on 158N murine oligodendrocytes. ***J Steroid Biochem Mol Biol***. 2017, 169:29-38.

2015

Zarrouk, A., **Nury, T**., Dauphin, A., Frère, P., Riedinger, J.M., Bachelet, C.M., Frouin, F., Moreau, T., Hammami, M., Kahn, E., Lizard, G. Impact of C24:0 on actin-microtubule interaction in human neuronal SK-N-BE cells: evaluation by FRET confocal spectral imaging microscopy after dual staining with rhodamine-phalloidin and tubulin tracker green. ***Funct Neurol***. 2015, 30(1):33-46.

Nury, T., Zarrouk, A., Mackrill, J.J., Samadi, M., Durand, P., Riedinger, J.M., Doria, M., Vejux, A., Limagne, E., Delmas, D., Prost, M., Moreau, T., Hammami, M., Delage-Mourroux, R., O'Brien, N.M., Lizard, G. Induction of oxiapoptophagy on 158N murine oligodendrocytes treated by 7-ketocholesterol-, 7β-hydroxycholesterol-, or 24(S)-hydroxycholesterol: Protective effects of α-tocopherol and docosahexaenoic acid (DHA; C22:6 n-3). ***Steroids***. 2015, 99(Pt B), 194-203.

Badreddine, A., El Mostafa, K., Zarrouk, A., **Nury, T**., El Kharrassi, Y., Nasser, B., Malki, M.C., Lizard, G., and Samadi, M. An expeditious synthesis of spinasterol and schottenol, two phytosterols present in argan oil and in cactus pear seed oil, and evaluation of their biological activities on cells of the central nervous system. ***Steroids.*** 201, 99(Pt B), 119-124.

Zarrouk, A., **Nury, T**., Riedinger, J.M., Rouaud, O., Hammami, M., and Lizard, G. Dual Effect of Docosahexaenoic Acid (Attenuation or Amplification) on C22:0-, C24:0-, and C26:0-Induced Mitochondrial Dysfunctions and Oxidative Stress on Human Neuronal SK-N-BE Cells. ***J Nutr Health Aging.*** 2015, 19(2): 198-205.

Zarrouk, A., **Nury, T**., Samadi, M., O'Callaghan, Y., Hammami, M., O'Brien, N.M., Lizard, G., and Mackrill, J.J. Effects of cholesterol oxides on cell death induction and calcium increase in human neuronal cells (SK-N-BE) and evaluation of the protective effects of docosahexaenoic acid (DHA; C22:6 n-3). ***Steroids***. 2015, 99(Pt B), 238-247.

2014

El Kharrassi Y, Samadi M, Lopez T, **Nury T**, El Kebbaj R, Andreoletti P, El Hajj HI, Vamecq J, Moustaid K, Latruffe N, El Kebbaj MS, Masson D, Lizard G, Nasser B, Cherkaoui-Malki M. Biological activities of Schottenol and Spinasterol, two natural phytosterols present in argan oil and in cactus pear seed oil, on murine miroglial BV2 cells. ***Biochem Biophys Res Commun***. 2014, 446:798-804.

Gondcaille C, Genin EC, Lopez TE, Dias AM, Geillon F, Andreoletti P, Cherkaoui-Malki M, **Nury T**, Lizard G, Weinhofer I, Berger J, Kase ET, Trompier D, Savary S. LXR antagonists induce ABCD2 expression. ***Biochim Biophys Acta***. 2014, 1841(2), 259-266.

Khelifi M, Zarrouk A, **Nury T**, Hamed H, Saguem S, Salah RB, Riedinger JM, Lizard G. Cytokine and eicosanoid profiles of phosphate mine workers. ***J Toxicol Sci***. 2014, 39:465-74.

Nury T, Zarrouk A, Vejux A, Doria M, Riedinger JM, Delage-Mourroux R, Lizard G. Induction of oxiapoptophagy, a mixed mode of cell death associated with oxidative stress, apoptosis and autophagy, on 7-ketocholesterol-treated 158N murine oligodendrocytes: Impairment by α-tocopherol**.** ***Biochem Biophys Res Commun***. 2014, 446:714-9.

Boumhras M, Ouafik S, **Nury T**, Gresti J, Athias A, Ragot K, Nasser B, Cherkaoui-Malki M, Lizard G. Determination of heavy metal content and lipid profiles in mussel extracts from two sites on the moroccan atlantic coast and evaluation of their biological activities on MIN6 pancreatic cells. ***Environ Toxicol***. 2014, 29(11), 1245-1261.

Gondcaille C, Genin EC, Lopez TE, Dias AM, Geillon F, Andreoletti P, Cherkaoui-Malki M, **Nury T**, Lizard G, Weinhofer I, Berger J, Kase ET, Trompier D, Savary S. LXR antagonists induce ABCD2 expression. ***Biochim Biophys Acta***. 2014, 1841(2), 259-266

Trompier D, Vejux A, Zarrouk A, Gondcaille C, Geillon F, **Nury T**, Savary S, Lizard G. Brain peroxisomes. ***Biochimie***. 2014; 98:102-110.

2013

Nury T, Samadi M, Zarrouk A, Riedinger JM, Lizard G. Improved synthesis and in vitro evaluation of the cytotoxic profile of oxysterols oxidized at C4 (4α- and 4β-hydroxycholesterol) and C7 (7-ketocholesterol, 7α- and 7β-hydroxycholesterol) on cells of the central nervous system. ***Eur J Med Chem***. 2013, 70:558-567.

Nury T, Samadi M, Varin A, Lopez T, Zarrouk A, Boumhras M, Riedinger JM, Masson D, Vejux A, Lizard G. Biological activities of the LXRα and β agonist, 4β-hydroxycholesterol, and of its isomer, 4α-hydroxycholesterol, on oligodendrocytes: effects on cell growth and viability, oxidative and inflammatory status. ***Biochimie.*** 2013, 95:518-530.

Ragot K, Mackrill JJ, Zarrouk A, **Nury T**, Aires V, Jacquin A, Athias A, Pais de Barros JP, Véjux A, Riedinger JM, Delmas D, Lizard G. Absence of correlation between oxysterol accumulation in lipid raft microdomains, calcium increase, and apoptosis induction on 158N murine oligodendrocytes. ***Biochem Pharmacol***. 2013, 86:67-79.

2012

Baarine M, Andréoletti P, Athias A, **Nury T**, Zarrouk A, Ragot K, Vejux A, Riedinger JM, Kattan Z, Bessede G, Trompier D, Savary S, Cherkaoui-Malki M, Lizard G. Evidence of oxidative stress in very long chain fatty acid - Treated oligodendrocytes and potentialization of ROS production using RNA interference-directed knockdown of ABCD1 and ACOX1 peroxisomal proteins. ***Neuroscience***. 2012, 28;213:1-18.

Baarine M, Ragot K, Athias A, **Nury T**, Kattan Z, Genin EC, Andreoletti P, Ménétrier F, Riedinger JM, Bardou M, Lizard G. Incidence of Abcd1 level on the induction of cell death and organelle dysfunctions triggered by very long chain fatty acids and TNF-α on oligodendrocytes and astrocytes. ***Neurotoxicology***. 2012, 33:212-228.

Zarrouk A, Vejux A, **Nury T**, El Hajj HI, Haddad M, Cherkaoui-Malki M, Riedinger JM, Hammami M, Lizard G. Induction of mitochondrial changes associated with oxidative stress on very long chain fatty acids (C22:0, C24:0, or C26:0)-treated human neuronal cells (SK-NB-E). ***Oxid Med Cell Longev***. 2012, 2012:623257.

2011

Ragot K, Delmas D, Athias A, **Nury T**, Baarine M, Lizard G. αlpha-Tocopherol impairs 7-ketocholesterol-induced caspase-3-dependent apoptosis involving GSK-3 activation and Mcl-1 degradation on 158N murine oligodendrocytes. ***Chem Phys Lipids***. 2011, 64:469-78.

Revues/Chapitres d'ouvrage

2020

Nury T, Lizard G, Vejux A. Cholesterol and oxidized cholesterol derivatives: potential biomarkers of Parkinson's disease? Neurological Disorders and Imaging Physics, Volume 5, Applications in dyslexia, epilepsy, and Parkinson's. Chapitre 4, pages 143-170. Editors: Ayman El-Baz & Jasjit S Suri (IOP Publishing, Bristol, UK). DOI 10.1088/978-0-7503-2723-7

Badreddine A, Zarrouk A, Meddeb W, **Nury T**, Rezig L, Debbabi M, Bessam FZ, Brahmi F, Vejux A, Mejri M, Nasser B, Lizard G. Antioxidant and neuroprotective properties of Mediterranean oils: Argan oil, olive oil, and milk thistle seed oil. ***Oxidative Stress and Dietary Antioxidants in Neurological Diseases.*** 1st Edition. (2020) Chapitre 10, pages 143-154 (Editors**:** Colin R. Martin Victor Preedy. DOI: 10.1016/B978-0-12-817780-8.00010-4

2019

Vejux A, Abed-Vieillard D, Hajji K, Zarrouk A, Mackrill JJ, Ghosh S, **Nury T**, Yammine A, Zaibi M, Mihoubi W, Bouchab H, Nasser B, Grosjean Y, Lizard G. 7-Ketocholesterol and 7β-hydroxycholesterol: In vitro and animal models used to characterize their activities and to identify molecules preventing their toxicity. ***Biochem Pharmacol***. 2019, 3:113648.

Brahmi F, Vejux A, Sghaier R, Zarrouk A, **Nury T**, Meddeb W, Rezig L, Namsi A, Sassi K, Yammine A, Badreddine A, Vervandier-Fasseur D, Madani K, Boulekbache-Makhlouf L, Nasser B, Lizard G. Prevention of 7-ketocholesterol-induced side effects by natural compounds. ***Critical reviews in food science and nutrition***, 2019, 59(19), 3179–3198.

2018

Bezine M, Namsi A, Sghaier R, Ben Khalifa R, Hamdouni H, Brahmi F, Badreddine I, Mihoubi W, **Nury T**, Vejux A, Zarrouk A, de Sèze J, Moreau T, Nasser B, Lizard G. The effect of oxysterols on nerve impulses. ***Biochimie***. 2018, 153:46-51.

Vejux A, Namsi A, **Nury T**, Moreau T, Lizard G. Biomarkers of Amyotrophic Lateral Sclerosis: Current Status and Interest of Oxysterols and Phytosterols. ***Front Mol Neurosci***. 2018, 31;11:12.

2014

Trompier D, Vejux A, Zarrouk A, Gondcaille C, Geillon F, **Nury T**, Savary S, Lizard G. Brain peroxisomes. ***Biochimie***. 2014, 98: 102-10.

Communications orales et sur panneaux

Communications orales

*Le présentateur est souligné

2019

Nury T, Zarrouk A, Vejux A, Lizard G**.** Impact of oxysterols on the peroxisome: physiopathological consequences. ***10th International Congress of the Turkish Society of Toxicology***, 16-19 october 2019, Antalaya.

2017

Nury T, Sghaier R, Zarrouk A, Uzun T, Ménétrier F, Lherminier J, Leoni V, Caccia C, Masmoudi A, Vejux A, Moreau T, Lizard G. Evidence of marked peroxisomal alterationassociated with minor and major mitochondrial dysfunctions in early and late phases of 7-ketocholesterol-induced cell death. ***6th ENOR Symposium***, 21-22 September 2017, Bruxelles.

2016

Debbabi M, Zarrouk A, **Nury T**, Bezine M, Meddeb W, Grégoire S, Martine L, Badreddine A, Guyot S, Lionel Bretillon, Cherkaoui Malki M, Moreau T, Nasser B, Hammami M, Lizard G; Evaluation of the effects of major compounds present in the Mediterranean diet (oleic acid, docosahexahenoic acid, α-tocopherol) and hydrogenated oils (elaidic acid) on 7KC-induced oxidative stress and cell death on microglial BV-2 cells. ***6th ENOR Symposium***, 29-30 septembre 2016, Paris.

Karym E-L, Badreddine A, **Nury T**, El Kebbaj MS, Latruffe N, Andreoletti P, Cherkaoui-Malki M, Lizard G & Nasser B; Protective role of opuntia Ficus indica on iron-induced Cytoxicity in murine microglial Bv2 cells. ***Colloque International : Substances Naturelles : Stress et métabolisme cellulaires (SNSMC 2016) FST***, 15-16 Décembre 2016, Settat.

Sudhakaran S, Rihane N, **Nury T**, Millot N, Lizard G. (Andrézieux-Bouthéon - France) 17ème Journées stéphanoises Cytométrie et Imagerie Cellulaire et Tissulaire - ***CYTIMA2016***, 31 mai-1er juin 2016.

2015

Bezine M, Zarrouk A, **Nury T**, El Ayeb M, Lizard G. (Dijon – France). Evaluation in vitro des effets de différent lipides impliqués dans la neurodégénérescence sur l'activité mitochondriale, l'intégrité de la membrane cytoplasmique et l'expression du canal potassium Kv3.1 sur des oligodendrocytes murins 158N. ***Forum des Jeunes Chercheurs***, Université de Bourgogne (18-19 juin 2015).

Nury T, Zarrouk A, Savary S, Cherkaoui-Malki M, Moreau T, Lizard G. Analysis by RT-qPCR of the modulation of peroxisomal mRNA levels on murine oligodendrocytes (158N) and murine microglial cells (BV-2) treated by 7-ketocholesterol: evidence of downregulation on BV-2 cells. ***5th ENOR Symposium***, 24-25 September 2015, Bonn.

Leoni V, Zarrouk A, **Nury T**, Caccia C, Moreau T, Lizard G. Mitochondrial dysfunctions and lipid anabolism modifications on 158N murine oligodendrocytes exposed to 7-ketocholesterol. ***5th ENOR Symposium*** 24-25 September 2015, Bonn.

2014

Doria M, **Nury T**, Lizard G, Vejux A. Induction d'une mort cellulaire présentant des caractéristiques d'autophagie par les acides gras à très longue chaîne sur des oligodendrocytes murins 158N. ***AEP Bio***, 13 juin 2014, Dijon.

Hadj Ahmed S, **Nury T**, Hammami M, Lizard G. Induction de l'accumulation de gouttelettes lipidiques et activation de la mort cellulaire par le DHA sur des cellules monocytaires (U937) et des macrophages murins (Raw264.7). ***AEP Bio***, 13 juin 2014, Dijon.

Nury T, Zarrouk A, Mackrill J, Vejux A, Lizard G. Effet protecteur du DHA (C22:6 n-3) sur la mort cellulaire induite par le 7-cétocholestérol sur des oligodendrocytes murins 158N : modèle d'étude des relations potentielles entre stress oxydant, métabolisme du cholestérol et métabolisme peroxysomal. ***AEP Bio***, 13 juin 2014, Dijon.

Terreau S, **Nury T**, Vejux A, Lizard G. Incidence de l'accumulation d'acides gras à très longues chaîne (C24 :0, C26 :0) sur l'inflammation et la mort cellulaire dans des macrophages murins RAW264.7 et des cellules microgliales murines BV-2 inactivées ou non en Abcd1. ***AEP Bio***, 13 juin 2014, Dijon.

2013

Nury T, Doria M, Zarrouk A, Begue H, Vejux A, Samadi M, Delage-Mourroux R, Lizard G. Induction of a dual mode of cell death (autophagy and apoptosis) on 7-ketocholesterol-treated 158N murine oligodendrocytes, ***3d ENOR Symposyium***, 19-20 septembre 2013, Swansea.

Zarrouk A, **Nury T**, Khelefi M, Boumhras M, Lizard G Introduction à la cytomique : applications en toxicologie, pharmacologie et biosurveillance ; ***Vèmes Journées Nationales de Cytométrie en Flux***, 7-9 mars 2013, Monastir.

2011

Nury T, Samadi M, Lizard G. Biological activities of 4alpha and 4beta-hydroxycholesterol on glial cells. 1rst ENOR symposium, 22-24 septembre 2011, Rome.

Communications sur panneaux

2019

Nury T, Hichami A, Vejux A, Lizard G. Attenuation with lipid compounds and Lorenzo's oil of 7-ketocholesterol-induced oxiapoptophagy on 158N murine oligodendrocytes. ***9th ENOR Symposium***, 19-20 September 2019, Edinburgh.

Nury T, Vejux A, Lizard G. Evaluation of the cytoprotective activity of lipid nutrients on 7 ketocholesterol induced cytotoxicity. ***Forum des jeunes chercheurs,*** 13-14 juin 2019, Dijon. **Deuxième prix posters.**

2018

Nury T, Uzun T, Pais de Barros J.P, Moreau T, Vejux A, Lizard G. : Effects of 7-ketocholesterol on biogenesis and mitochondrial function on 158N murine oligodendrocytes. ***8th ENOR Symposium*** 2018, 20-21 septembre 2018, Bologne.

Sassi K, **Nury T**, Samadi M, Fennira F, Lizard G. Characterization of the cytotoxic profile and evaluation of the expression of liver X Receptor (LXR) on rat C6 glioma cells treated with natural and synthetic sterols. ***8th ENOR Symposium*** 2018, 20-21 septembre 2018, Bologne.

Sghaier R, **Nury T**, Vejux A, Cherkaoui-Malki M, Moreau T, Masmoudi A, Zarrouk A, Lizard G. Prevention of 7β-hydroxycholesterol-induced mitochondrial dysfunction and cell death by dimethylfumarate and monomethylfumarate on 158N murine oligodendrocytes. ***NutRedOx Meeting*** 19-21st september 2018, Gdansk.

Raas Q, Gondcaille C, Trompier D, Hamon Y, Zahi F-E, Leoni V, **Nury T**, Vejux A, Andreoletti P, Nasser B, Lizard G, Cherkaoui-Malki M, Savary S. ABCD1 and ABCD2 deficiency in microglia: Towards a better understanding of the physiopathogenesis of X-ALD. ***FEBS Special Meeting*** -ATP-Binding Cassette (ABC) Proteins: From Multidrug Resistance to Genetic Disease, 6-12 mars 2018, Innsbruck.

Raas Q, Gondcaille C, Trompier D, Hamon Y, Saih F, Leoni V, Caccia C, **Nury T**, Vejux A, Andreoletti P, Nasser B, Lizard G, Cherkaoui-Malki M, Savary S. ABCD1 and ABCD2 deficiency in microglia: Towards a better understanding of the physiopathogenesis of X-ALD. ***6th Open European Peroxisome Meeting***, 25-26 octobre 2018, Groningen.

Nury T, Ménétrier F, Vejux A, Lizard G. Incidence du 7-cétocholestérol sur la morphologie et l'activité des mitochondries et des peroxysomes d'oligodendrocytes murins 158N. ***Forum des jeunes chercheurs,*** 14-15 juin 2018, Besançon.

2017

M Bezine, **T. Nury**, Ben-Khalifa R, Debbabi M3, Vejux A, De Seze J, El-Ayeb M, Moreau T, Lizard G. Involvement of P2X7 receptor and K+ channels in 7-ketocholesterol-induced cell death in 158N murine oligodendrocytes. ***7th ENOR Symposium***, 21-22 septembre 2017, Bruxelles.

Karym E.M, **Nury T**, Badreddine A, Vejux A, Cherkaoui-Malki M, Nasser B, Lizard. Iron potentiation of 7-ketocholesterol-induced cell death on murine N2a and human neuronal SK-N-BE cells. ***7th ENOR Symposium***, 21-22 septembre 2017, Bruxelles.

Karym El-M., Badreddine A, **Nury T**, Cherkaoui-Malki M, Nasser B, Lizard G & Vejux A. Contribution of Iron Overload and Cholesterol Oxidation in the Pathogenesis of Alzheimer's Disease. ***NutRedOx COST***, 27 – 29 September 2017, Strasbourg.

2016

Badreddine A, Karym El M, **Nury T**, Zarrouk A, Meddeb W, Martine L, Grégoire S, Vejux A, Bretillon L, Cherkaoui Malki M, Nasser B, Lizard G. Cytoprotective effects of alimentary and cosmetic argan oils on 7-ketocholesterol - treated 158N murine oligodendrocytes; ***ENOR 6th symposium***, 29-30 septembre 2016, Paris.

Bezine M, Debbabi M, **Nury T**, Ben Khalifa R, Samadi M, El Ayeb M, Lizard G; Evidence of K+ homeostasis disruption and potential involvement of Kv channels in cellular dysfunctions triggered by 7-ketocholesterol, 24S-hydroxycholesterol, and tetracosanoic acid on 158N oligodendrocytes; ***ENOR 6th Symposium,*** 29-30 septembre 2016, Paris.

Bezine M, Zarrouk A, Maatoug S, **Nury T**, Benkhalifa R, El Ayeb M, Lizard G. Voltage gated k+ channels are associated with 7-ketocholesterol and 24(s) hydroxycholesterol - induced mitochondrial dysfunction and cell death. 13ème réunion francophone sur la maladie d'Alzheimer et les syndromes apparentés. ***Domaine Rockfeller***, 8-10 juin 2016, Lyon.

Debbabi M, **Nury T**, Gregoire S, Bretillon L, Hammami M, Lizard G. Effect of oleic acid and its trans isomer (elaidic acid) on oxidative stress, lipid content and lipid profile in microglial BV-2 cells. 13ème réunion francophone sur la maladie d'Alzheimer et les syndromes apparentés**.** ***Domaine Rockfeller***, 8-10 juin 2016, Lyon.

Badreddine A, Karym EM, **Nury T**, Cherkaoui-Malki M, Nasser B, Lizard B. Atténuation par l'huile D'argan de la mort cellulaire Et du stress oxydant induit Par 7-cétocholésterol sur les Oligodendrocytes murins 158N. ***Colloque International : Substances Naturelles : Stress et métabolisme cellulaires (SNSMC 2016) FST***, 15-16 Décembre 2016, Settat.

Mekahli N, Karym El M, Sghaier R, **Nury T**, Zarrouk A, Vejux A, Moreau T, Lizard G. Evidence of cytoprotective effects of dimethyl fumarate and monomethyl fumarate on 158N murine oligodendrocytes treated with 7-ketocholesterol or H202. ***Fondation ARSEP - French MS Research Society***, 27 mai 2016, Paris.

Najid A, Terreau S, Seguin A, **Nury T**, Andreoletti P, Gondcaille C, Trompier D, Savary S, Cherkaoui Malki M, Vejux A, Lizard G. Effect of tetracosanoic acid (C24:0) combined (or not) with ABCD1 oe ACOX1 silencing on cell viability and inflammatory status of murine macrophages RAW264.7 ***3rd ELA Scientific Congress "Advances in molecular pathogenesis, diagnosis and management of the leukodystrophies***", 24-26 juin 2015, Paris.

Nury T, Debbabi M, Zarrouk A, Ménétrier F, Sghaier R, Badreddine A, Karym EM, Bezine M, Vejux A, Savary S, Cherkaoui Malki M, Moreau T, Aubourg P, Lizard G. Incidence of 7-ketocholesterol, a cholesterol auto-oxidation product found at enhanced level in the plasma of X-ALD patients, on oligodendrocytes and microglial cells dysfunctions. ***5th Open European Peroxisome Meeting***, 14-15 septembre 2016, Vienne.

Raas Q, Gondcaille C, Saih FE, Trompier D, Andreoletti P, Vejux A, **Nury T**, Lizard G, Cherkaoui Malki M, Savary S. Understanding the physiopathogenesis of peroxisomal leukodystrophies by generating novel microglial cell models with CRISPR/Cas9-mediated genome editing. ***2nd International Conference « Peroxisome Formation, Function and Metabolism »***, 20-22 juin 2016, Hambourg.

2015

Gondcaille C, Genin EC, Lopez TE, Dias AMM, Geillon F, Andreoletti P, Cherkaoui-Malki M, **Nury T**, Lizard G, Weinhofer I, Berger J, Kase ET, Trompier D, Savary S. Advances in molecular pathogenesis, diagnosis and management of the leukodystrophies. ***3rd ELA Scientific Congress***, 24-26 juin 2015, Paris.

Najid A, Terreau S, Seguin A, **Nury T**, Andreoletti P, Gondcaille C, Trompier D, Savary S, Cherkaoui-Malki M, Vejux A, Lizard G. (Paris - France) Effect of tetracosanoic acid (C24:0) combined (or not) with ABCD1 or ACOX1 silencing on cell viability and inflammatory status of murine macrophages RAW264.7. ***3rd ELA Scientific Congress***, 24-26 juin 2015, Paris.

Zarrouk A, **Nury T**, Vejux A, Andreoletti P, Trompier D, Savary S, Cherkaoui-Malki M, Moreau T, Lizard G. (Bonn – Germany) Attenuation of 7-ketocholesterol-induced apoptosis by dimethylfumarate on 158N murine oligodendrocytes.***5th ENOR Symposium*** 24-25 September 2015, Bonn.

2014

Badreddine A, Karym E, El Kharrasi Y, Zarrouk A, **Nury T**, Doria M, Vejux A, Nasser B, Cherkaoui-Malki M, Lizard G, Samadi M. An expeditious synthesis of spinasterol and schotenol, two phytosterols present in argan oil and in cactus pear seed oil, and evaluation of their biological activities on cells of the central nervous system. ***3rd International NutriOx workshop***, 1-3 octobre ,2014, Metz.

2013

Doria M, **Nury T**, Zarrouk A, Begue H, Delage-Mourroux R, Lizard G, Vejux A. Very long chain fatty acid- and 7-ketocholesterol-induced lipotoxicity and autophagy on 158N murine oligodendrocytes. ***NutriOx Network***, 4-6 septembre 2013, Dijon.

Gondcaille C, Genin EC, Lopez T, Dias AMM, Geillon F, Andreoletti P, Cherkaoui-Malki M, **Nury T**, Lizard G, Trompier D, Savary S. Evaluation of the therapeutic potential of LXR antagonists for X-linked adrenoleukodystrophy. ***NutriOx Network***, 4-6 septembre 2013, Dijon.

Gondcaille C, Genin EC, Lopez T, Dias AMM, Geillon F, Andreoletti P, Cherkaoui-Malki M, **Nury T**, Lizard G, Trompier D, Savary S. (Swansea, UK) Evaluation of the therapeutic potential of LXR antagonists for X-linked adrenoleukodystrophy. ***3rd ENOR Symposium***. 19-20 septembre 2013, Swansea.

Zarrouk A, **Nury T**, Athias A, Hammami M, Lizard G. Attenuation of C22:0-, and very long chain fatty acids (C24:0 and C26:0) – induced side effects (mitochondrial dysfunctions, oxidative stress) by

docosahexahenoic acid (DHA ; C22:6 n-3) on human neuronal cells SK-N-BE***. 1ère Journée Inter-régionale Recherche & Neurosciences***. 29 octobre 2013, Dijon.

2012

Zarrouk A, **Nury T**, Athias A, Vejux A, El Hajj H, Haddad M, Andreoletti P, Cherkaoui-Malki M, Lizard G. Saturated very long chain fatty acid-induced mitochondrial dysfunctions and enhancement of reactive oxygen species production in human neuronal cells (SK-NB-E). ***11ème réunion francophone sur la Maladie d'Alzheimer et les syndromes apparentés, Maladie d'Alzheimer et déclin cognitif. Recherche et Pratique Clinique,*** 22-24 mai 2012, Toulouse.

Zarrouk A, **Nury T**, Vejux A, Lizard G. Saturated very long chain fatty acid-induced neuronal dysfunctions playing essential roles in Alzheimer's disease: impairment of mitochondrial activity, induction of oxidative stress and cytoskeleton disorganization. ***16th Congress of the European Federation of Neurological Societies - EFNS 2012***, 9-10 septembre 2012, Stockholm.

Liste des Figures

Liste de Tableaux

Abréviations

AADHAP-R	Acyl/alkyl- dihydroxyacétone phosphate réductase
ABC	ATP binding cassette
ACAT	Acyl CoA cholesterol Acyl-Transférase
ACOX	Acyl-CoA oxydase
ADHAP-S	Alkyl-dihydroxyacétone phosphate synthase
ADN	Acide désoxyribonucléique
AGPI	Acide gras polyinsaturé
AGT	Alanine:glyoxylate aminotransférase
AGTLC	Acide gras à très longue chaine
ALA	Acide α-linolénique
ARN	Acide ribonucléique
ATM kinase	Ataxia-telangiectasia mutated kinase
ATP	Adénosine triphosphate
BHE	Barrière hématoencéphalique
BMP	Bis(monoacylglycéro) phosphate
CAT	Carnitine acétyltransférase
CHEH	Cholestérol époxyde hydrolase
CHOP	C/EBP-Homolgous Protein
CH25H	Cholestérol 25-hydroxylase
COT	Carnitine octanoyltransférase
CYP	Cytochrome P
D8D7I	3β-hydroxysteroid-Δ8Δ7-isomérase
DDA	Dendrogénine A
DHA	Acide docosahéxaénoïque
DHAP	Dihydroxyacétone phosphate
DHAPAT	Dihydroxyacétone phosphate acyltransférase
DHCA	Acide dihydroxycholestanoïque
DMF	Diméthylfumarate
DMLA	Dégénérescence maculaire liée à l'âge
DRP1	Dynamin-related protein 1
DUOX	Dual oxydase

EPA	Acide éïcosapentahénoïque
ERA	Espèces réactives de l'azote
ERO	Espèces réactives de l'oxygène
FIS1	Mitochondrial fission 1 protein
GSH	Glutathion réduit
GST	Glutathion-S-transférase
GTP	Guanosine triphosphate
HDL	High-density lipoprotein
HODE	Acide hydroxyoctadécanoïque
HSD	Hydroxystéroïde déshydrogénase
ICAM-1	Inter-Cellular Adhesion Molecule-1
IDH2	Isocitrate déshydrogénase 2
IFN	Interféron
INSIG	Insulin induced gene
LCAT	Lécithin-Cholestérol Acyltransférase
LDH	Lactate déshydrogénase
LDL	Low density lipoprotein
MCP-1	Monocyte chemotactic protein-1
MFF	Mitochondrial fission factor
MICI	Maladies inflammatoires chroniques de l'intestin
MIP-1β	Macrophage inflammatory protein-1β
MMF	Monométhylfumarate
MMP	Métalloprotéinase matricielle
NAC	N-Acétyl-cystéine
NADPH	Nicotinamide adénine dinucléotide phosphate
NLRP3	NOD-, LRR- and pyrin domain-containing protein 3
NOS	Nitric oxide synthase
NOX	NADPH oxydase
OxLDL	LDL oxydée
PARP	Poly(ADP-ribose) polymérase
PEX	Peroxine
PLA2	Phospholipase A2
PLTP	Plasma phospholipid transfer protein
PGE2	Prostaglandine E2

PMP	Protéine membranaire peroxysomale
PPAR	Peroxisome proliferaor-activated receptor
PPRE	Peroxisome proliferator response element
Prx5	Peroxiredoxine V
PTS	Peroxisomal Targeting Signal
PTT	Protéine de transfert du tocophérol
RE	Réticulum endoplasmique
Redox	Oxydoréducteur
RXR	Retinod-X-receptor
SLA	Sclérose latérale amyotrophique
SOD	Superoxyde dismutase
SREBP	Sterol regulatory element-binding protein
SSO	Sulfo-N-succinimidyl Oleate
SYT7	Synaptotagmine VII
SULT	Sulfotransférase
THA	Acide tétracosahexaénoïque
THCA	Acide trihydroxycholestanoïque
TLR	Toll like receptor
TNF	Tumor necrosis factor
TPP	Triphénylphosphonium
UPR	Unfold protein response
VCAM-1	Vascular cell adhesion protein-1
VLDL	Very low-density lipoprotein
VEGF	Vascular endothelial growth factor
X-ALD	Adrénoleucodystrophie liée au chromosome X
7KC	7-cétocholestérol
7α-OHC	7α-hydroxycholestérol
7β-OHC	7β-hydroxycholestérol
15-LOX	15-lipoxygénase
19-OHC	19-hydroxycholestérol
25-OHC	25-hydroxycholestérol
24S-OHC	24S-hydroxycholestérol
27-OHC	27-hydroxycholestérol

Introduction

1. Contexte : Implication des oxystérols dans des maladies liées à l'âge, certaines maladies rares et inflammatoires chroniques ainsi que dans le vieillissement

Le vieillissement et certaines maladies liées à l'âge représentent un coût très élevé pour la société. Un objectif majeur dans les prochaines décennies réside dans le développement de traitements visant à en atténuer les effets ou à les supprimer.

Au cours du vieillissement, il est connu qu'une élévation progressive du stress oxydant survient (Barja, 2019; Warraich *et al.*, 2020). Il est également bien établi qu'une augmentation de ce dernier est observée dans les maladies liées à l'âge, les maladies cardiovasculaires, les maladies oculaires (dégénérescence maculaire liée à l'âge (DMLA) et cataracte), dans les maladies inflammatoires chroniques (maladies inflammatoires chroniques de l'intestin (MICI)), mais aussi dans des maladies neurodégénératives (Alzheimer, sclérose en plaques) et dans certaines maladies génétiques rares (la maladie de Niemann Pick, adrénoleucodystrophie liée à l'X (X-ALD)).

L'augmentation du stress oxydant et la rupture de l'équilibre oxydo-réducteur (équilibre Redox) dans ces maladies se caractérise par une élévation des taux d'espèces réactives de l'oxygène (ERO) et d'espèces réactives de l'azote (ERA). Ces molécules très réactives peuvent alors provoquer des attaques radicalaires sur d'autres molécules de l'organisme en les oxydant, ce qui inhibera ou bloquera leurs fonctions biologiques. Parmi les molécules cibles du stress oxydant, on trouve les composants majeurs de la cellule : les protéines, les lipides et les acides nucléiques (acide désoxyribonucléique (ADN) et ribonucléique (ARN)). Au sein de la grande famille des lipides, un composé a une importance particulière dans la physiopathologie des maladies présentant une élévation du stress oxydant, il s'agit du cholestérol. Le cholestérol est un des

principaux composants des membranes cellulaires dont il constitue environ 50% des lipides totaux. Lorsqu'il est oxydé, le cholestérol forme des oxystérols qui peuvent perturber les fonctions cellulaires. Il existe différents oxystérols en fonction du ou des sites d'oxydation du cholestérol. Ces dérivés oxydés du cholestérol ont été découverts dans les années 1970 mais ce n'est que depuis peu, avec le développement des techniques analytiques modernes qui ont gagné en sensibilité avec des analyses de l'ordre du nanogramme, que les oxystérols peuvent être véritablement étudiés dans les tissus, les cellules et les liquides biologiques (Griffiths *et al.*, 2019a; Sottero *et al.*, 2019).

Ainsi, une quantité de plus en plus importante de données suggèrent que les oxystérols seraient impliqués dans la physiopathologie des maladies présentant une élévation du stress oxydant ainsi que dans le vieillissement par leur capacité à moduler de nombreux processus biologiques.

Les effets biologiques des oxystérols sont très variés. Les oxystérols impliqués dans les maladies inflammatoires présentent des propriétés pro-oxydantes et pro-inflammatoires participant à l'aggravation des symptômes. Il induisent la surexpression de cytokines pro-inflammatoires (Poli *et al.*, 2013).

Dans l'athérosclérose, les oxystérols retrouvés majoritairement au niveau des plaques d'athérome sont le 7α-hydroxycholestérol (7α-OHC), le 7β-hydroxycholestérol (7β-OHC), le 7-cétocholestérol (7KC), le 5,6α-époxycholestérol, le 5,6β-époxycholestérol et le cholestane-3β,5α,6β-triol. Ils peuvent atteindre des taux jusqu'à 100 fois supérieurs aux taux plasmatiques normaux (Zmyslowski *et al.*, 2019). Dans ce contexte, une augmentation du 7β-OHC semble être un biomarqueur de risque cardiovasculaire (Zieden *et al.*, 1999). Le 27-hydroxycholestérol (27-OHC) joue aussi un rôle pro-inflammatoire (Umetani *et al.*, 2014; Zmyslowski *et al.*, 2019).

Dans la maladie d'Alzheimer, une augmentation du 24(S)-hydroxycholestérol (24(S)-OHC) est observée dans le liquide céphalorachidien tandis qu'il diminue dans le plasma. Cet oxystérol

impliqué dans la régulation du métabolisme du cholestérol au niveau cérébral est formé à 98 % dans le cerveau et son taux dépend du nombre de neurones actifs (Bjorkhem, 2006). Ainsi, lorsque des neurones meurent au cours de la maladie, son taux est d'abord augmenté puis diminué dans un stade avancé de la maladie (Zmyslowski *et al.*, 2019). Lorsque la maladie d'Alzheimer atteint un stade avancé, la barrière hématoencéphalique (BHE) est souvent altérée, ce qui permet l'entrée d'autres oxystérols comme le 27-OHC qui peut potentialiser les effets toxiques de l'amyloïde Aβ 1-42 (Poli *et al.*, 2013). Les taux de 7α-OHC, 7β-OHC, 7KC, 5,6-époxycholestérol et de 4β-hydroxycholestérol sont aussi augmentés dans le cerveau des patients Alzheimer (Testa *et al.*, 2018).

Dans la maladie de Parkinson, des taux élevés de 24(S)-OHC, 27-OHC, 7β-OHC et 7KC ont été mesurés dans le cortex visuel, tandis que dans le cas de la sclérose en plaques, le niveau de 24(S)-OHC est réduit dans le plasma alors que le taux de 7KC est augmenté (Cheng *et al.*, 2011; Zmyslowski *et al.*, 2019).

Dans les maladies inflammatoires de l'intestin, les oxystérols peuvent participer à l'altération de la barrière intestinale via l'activation des métalloprotéases matricielles (MMP) qui vont dégrader les jonctions cellulaires. Un mélange d'oxystérols composé de 7KC, 7α-OHC, 7β-OHC et de 5,6-époxycholestérol sur des cellules épithéliales coliques induit leur mort par apoptose (Biasi *et al.*, 2009; Testa *et al.*, 2018).

Enfin, dans la DMLA, une augmentation du stress oxydant au niveau de la rétine entraine la formation d'oxystérols pro-oxydants comme le 7KC qui vont contribuer au développement de la maladie (Moreira *et al.*, 2009).

Les maladies liées à l'âge ainsi que le vieillissement ont donc en commun une augmentation du stress oxydant aboutissant à la formation d'oxystérols qui présentent plusieurs effets toxiques. Parmi ces oxystérols, le plus fréquemment retrouvé est le 7KC.

Il est donc important de mieux connaitre les activités biologiques de cet oxystérol et d'identifier des molécules pouvant prévenir ses effets délétères afin de s'opposer au vieillissement et aux maladies qui lui sont associées.

Jusqu'aux début des années 1990, les activités biologiques des oxystérols étaient encore peu connues et l'identification d'un certains nombres d'oxystérols au niveau des plaques d'athérome et des lipoprotéines de faible densité oxydées (OxLDL) a conduit à s'intéresser à ces molécules et en particulier à celles formées par oxygénation du cholestérol (7KC et 7β-OHC) (Helmschrodt *et al.*, 2013). La démonstration du rôle du 7KC et du 7β-OHC dans la toxicité des OxLDL a conduit à supposer que ces oxystérols pouvaient contribuer à la physiopathologie de l'athérosclérose et plus largement des maladies cardiovasculaires (Colles *et al.*, 1996; Colles *et al.*, 2001). L'intérêt pour le 7KC s'est renforcé avec la démonstration de ses propriétés pro-oxydantes et pro-inflammatoires qui sont deux composantes essentielles des maladies cardiovasculaires (Vejux *et al.*, 2009b).

Comme le développement de la DMLA évoque par certains aspects celui de la plaque d'athérome (Malvitte *et al.*, 2006), l'analyse des dépôts lipidiques rétiniens (appelés drusens) a montré une accumulation de 7KC dans ces derniers suggérant aussi une implication de cette molécule dans le développement de la DMLA (Moreira *et al.*, 2009; Rodriguez *et al.*, 2004).

Peu à peu, dans d'autres pathologies liées à l'âge comme la maladie d'Alzheimer, des accumulations de 7KC ont aussi été montrées au niveau cérébral (Testa *et al.*, 2016; Zarrouk *et al.*, 2014). Plus récemment, plusieurs arguments sont en faveur d'une implication du 7KC dans des maladies inflammatoires de l'intestin et dans certaines maladies rares (X-ALD, Niemann-Pick et syndrome de Smith Lemmli Opitz) (Anderson *et al.*, 2020; Biasi *et al.*, 2009). Etudier les activités biologiques du 7KC dans le contexte de ces différentes maladies en précisant les voies de signalisation impliquées et son impact sur les organites (mitochondrie, peroxysome et

lysosome) a pour objectif non seulement de mieux comprendre comment est impliqué le 7KC dans la physiopathologie de ces maladies, mais aussi d'identifier de nouvelles cibles thérapeutiques pour soigner les maladies associées au 7KC. Dans ce contexte, identifier des molécules naturelles et synthétiques prévenant ou atténuant la toxicité du 7KC présente un intérêt thérapeutique essentiel d'autant plus que la majorité des maladies associées au 7KC ne disposent pas de traitements efficaces.

1.1 Maladies impliquant le 7-cétocholestérol

1.1.1 Maladies cardiovasculaires

La pathologie la plus fréquente impliquant le 7KC est l'athérosclérose qui apparait généralement au cours du vieillissement et chez les personnes ayant un mode de vie à risque (sédentarité, tabagisme, hypercholestérolémie, hypertension artérielle). Cette pathologie se caractérise par l'apparition progressive de plaques d'athérome au niveau de la paroi artérielle. Ces plaques apparaissent lorsque des lipoprotéines de faible densité (*Low density lipoproteins* : LDL) s'accumulent de façon locale dans des artères. Ces LDLs, lorsqu'elles sont oxydées (formation de 7KC), deviennent pro-inflammatoires induisant le recrutement de macrophages. Les macrophages se gorgent de ces LDL oxydées pour devenir des cellules spumeuses, ce qui entraine leur mort par apoptose. Les corps apoptotiques stagnent alors sur le site et s'accumulent pour contribuer à la formation de la plaque d'athérome. Les cellules musculaires lisses de la paroi vasculaire vont ensuite former des fibres de collagène qui se calcifient, ce qui va rendre la plaque de plus en plus fragile et cassante, pouvant mener à une rupture de l'artère (Testa *et al.*, 2018).

Chez des patients hypercholestérolémiques, le 7KC est l'oxystérol majoritaire, il représente 57% des oxystérols plasmatiques : 7KC (15 ng/mg de cholestérol libre, soit 57,0%) > 7α/β-OHC (20,7%) > 5,6β-époxycholestérol (11,7%) > cholestane-3β,5α,6β-triol (10,5%) > 5,6α-époxycholestérol (inférieur à 5 ng/mL). Au niveau des plaques le 7KC représente 55% des oxystérols : 7-KC (607 ng/mg de cholestérol libre, soit 54,8%) > Triol (13,5%) > 7-α/β-OHC (11,6%) > 5,6-β-EC (10,1%) > 5,6-α-EC (10,0%) (Helmschrodt *et al.*, 2013). Il a été démontré que le 7KC contribuait à la physiopathologie des plaques d'athérome. Il induit une augmentation de l'expression des molécules d'adhésion cellulaire (InterCellular Adhesion Molecule-1 (ICAM-1), Vascular cell adhesion protein-1 (VCAM-1) et E-selectine) due à l'élévation des ERO au niveau des cellules endothéliales vasculaires, ce qui favorise le recrutement de macrophages au niveau des plaques dans les stades précoces de la pathologie (Anderson *et al.*, 2020). Il a également été montré que le 7KC perturbait la polarisation des macrophages induisant plutôt le phénotype inflammatoire M1 au détriment du phénotype anti-inflammatoire M2 (Buttari *et al.*, 2013). Le 7KC induit également une augmentation de la sécrétion d'interleukines pro-inflammatoires telles que l'IL-6, IL-1β, *Tumor necrosis factor-α* (TNFα) ou encore *Monocyte chemotactic protein-1* (MCP-1) et *Monocyte inflammatory protein-1β* (MIP-1β) par les macrophages (Prunet *et al.*, 2006). Les effets pro-apoptotiques du 7KC sur les cellules musculaires lisses vasculaires augmentent le risque de rupture des plaques et de thrombose (Testa *et al.*, 2018). En raison de ses propriétés pro-oxydantes et pro-inflammatoires, il est maintenant bien établi que le 7KC contribue au développement de l'athérosclérose (Testa *et al.*, 2018; Vejux *et al.*, 2009b).

1.1.2 Maladies neurodégénératives

Il existe plusieurs maladies neurodégénératives, démyélinisantes ou non : la sclérose latérale amyotrophique (SLA), la maladie de Parkinson, la maladie d'Alzheimer, la maladie de Huntington, la sclérose en plaques ou encore l'X-ALD. Un des points communs à ces pathologies est l'élévation du stress oxydant au niveau local et/ou systémique. L'augmentation des taux de 7KC est aussi décrite dans toutes ces maladies (Anderson *et al.*, 2020; Nury *et al.*, 2017; Poli *et al.*, 2013; Testa *et al.*, 2018; Vejux *et al.*, 2020). Dans les cerveaux de malades Alzheimer analysés *post mortem*, les taux de 7KC (de 1,5 à 5 ng/mg de tissus), 7β-OHC, 7α-OHC, 25-OHC, 27-OHC, 5,6α-époxycholestérol, 5,6β-époxycholestérol, 4β-OHC et 4α-OHC sont augmentés tandis que le 24(S)-OHC est diminué (de 20 à 12,5 ng/mg de tissus) (Testa *et al.*, 2016). Il a été montré que le 7KC était toxique pour plusieurs types cellulaires issus du système nerveux central : les neurones, la glie (oligodendrocytes) ou encore la microglie (Bezine *et al.*, 2018a; Debbabi *et al.*, 2016; Yammine *et al.*, 2020a; Zarrouk *et al.*, 2015). Le cholestérol ne peut pas traverser la BHE mais des oxystérols le peuvent, en particulier le 24(S)-OHC et le 27-OHC, ce qui sert à réguler le métabolisme du cholestérol dans le système nerveux central (Bjorkhem *et al.*, 2009; Bjorkhem *et al.*, 2019). L'élévation du stress oxydant est aussi connue pour augmenter la perméabilité de la BHE (Kuriakose *et al.*, 2019; Lochhead *et al.*, 2010). Une hypothèse suggère que le 7KC pourrait alors intervenir dans l'altération de l'intégrité de la BHE en favorisant le stress oxydant. Dans certains cas, l'augmentation de perméabilité de la BHE serait liée à une activation de la Nicotinamide adénine dinucléotide phosphate-oxydase (NADPH-oxydase ou NOX) dont l'activité est elle-même modulée par le 7KC (Kuriakose *et al.*, 2019; Pedruzzi *et al.*, 2004). En ce qui concerne le 7KC, aucune étude n'a démontré qu'il pouvait, ou non, traverser la BHE, mais sa concentration est augmentée dans le système nerveux central des patients atteints

de maladies neurodégénératives (Anderson *et al.*, 2020; Vejux *et al.*, 2020). Comme le 7KC est fortement toxique sur les cellules nerveuses (oligodendrocytes, microglies et neurones), il pourrait favoriser le développement des maladies neurodégénératives (Debbabi *et al.*, 2016; Iriondo *et al.*, 2020; Nury *et al.*, 2015; Nury *et al.*, 2014; Testa *et al.*, 2018; Testa *et al.*, 2016; Yammine *et al.*, 2020a).

Dans le cadre de la maladie d'Alzheimer, le 7KC interviendrait en agissant sur les interactions du peptide Aβ 1-42 avec la membrane plasmique et favoriserait sa présence sous forme fibrillaire (Phan *et al.*, 2018). Ces résultats sur les relations entre 7KC et Aβ 1-42 sur des membranes lipidiques de synthèse ou des cellules en culture sont en accord avec les observations *in vivo* sur des cerveaux de patients (Iriondo *et al.*, 2020). De plus, les effets du 7KC sur la microglie, en particulier au niveau lysosomal, pourraient entrainer une diminution dans l'efficacité de la phagocytose du peptide Aβ 1-42 et favoriser l'apparition des plaques amyloïdes (Debbabi *et al.*, 2016). Le 7KC, à des concentrations non toxiques (3 jours d'incubation à 10 mg/L, soit 25 µM), peut activer la microglie et déclencher sa prolifération et sa migration via le clivage de la poly(ADP-ribose) polymérase (PARP). Ceci renforce l'hypothèse selon laquelle le 7KC pourrait contribuer à augmenter la neurodégénérescence lorsque la myéline (riche en cholestérol) est dégradée par la microglie (Diestel *et al.*, 2003).

1.1.3 Maladies oculaires (dégénérescence maculaire liée à l'âge, cataracte)

L'impact du 7KC est également de plus en plus étudié sur un autre type de pathologies affectant la vision, et plus précisément la rétine. La rétine est un tissu ayant la capacité de capter la lumière. Elle est composée d'une cinquantaine de types cellulaires différents dont la finalité est d'envoyer le signal visuel au cerveau. Dans la rétine, on trouve une structure appelée la macula,

responsable de la vision centrale et de la perception des couleurs. Les affections de la macula peuvent être d'origine génétique ou bien liée à l'âge, comme la DMLA. Au cours de la DMLA, un stress oxydant apparait au niveau de cellules épithéliales pigmentaires de la rétine conduisant à la formation de 7KC (Anderson *et al.*, 2020; Pariente *et al.*, 2019). Des travaux ont montré que le 7KC s'accumulait dans la rétine de singes entre 3 et 5 fois plus que dans les contrôles (entre 5 et 8 pmol/nmol de cholestérol libre contre 1 à 1,5 pmol/nmol dans les contrôles). Cette accumulation se fait principalement au niveau de dépôts protéiques appelés drusen (Moreira *et al.*, 2009). Il a été montré que le 7KC pouvait avoir une activité chimio-attractive envers la microglie rétinienne, ce qui déclencherait son activation et sa migration dans l'espace sous-rétinien, probablement en impliquant l'inflammasome (Indaram *et al.*, 2015). Il en résulte une inflammation locale qui amplifie le développement de la maladie. De plus, sur des cellules épithéliales pigmentaires de la rétine, le 7KC induit la sécrétion de *Vascular endothelial growth factor* (VEGF) (Javitt *et al.*, 2009).

Une autre atteinte de la vision est la cataracte. Elle se manifeste par une opacification du cristallin. Du 7KC a également été détecté dans des cristallins de patients atteints de cataracte (environ 4 nmol/mol de cholestérol libre alors qu'il est indétectable dans les contrôles) (Girao *et al.*, 1998; Vejux *et al.*, 2011). Néanmoins, le rôle exact du 7KC dans la cataracte n'est pas encore bien déterminé. L'acide rosmarinique, un polyphénol présent notamment dans le romarin et la menthe, avec des activités antioxydantes et anti-inflammatoires, a montré qu'il pouvait redonner sa transparence au cristallin atteint de cataracte, il n'est pas exclu que ce dernier puisse avoir une action contre la toxicité du 7KC dans ce contexte (Chemerovski-Glikman *et al.*, 2018).

1.1.4 Maladies inflammatoires intestinales

Il existe différentes maladies touchant le système digestif qui sont souvent caractérisées par une atteinte de la muqueuse intestinale de façon chronique. On trouve parmi les plus fréquentes, la maladie de Crohn, la colite ulcéreuse et les maladies inflammatoires chroniques de l'intestin (MICI). Ces pathologies ont en commun une augmentation du stress oxydant et de l'inflammation.

Les personnes consommant beaucoup de nourriture industrielle, riche en cholestérol et en oxystérols (dont le 7KC), sont plus susceptibles de développer ces pathologies. En effet, l'estomac est un parfait « bioréacteur » favorisant l'oxydation des molécules comme le cholestérol par son pH acide, la présence de dioxygène, d'ions fer libres et de protéines héminiques contenus dans la viande rouge (réaction de Fenton) (Kanner *et al.*, 2001). La formation de 7KC est alors facilitée et les activités pro-oxydantes et pro-inflammatoires de ce dernier vont alors affecter la muqueuse intestinale.

Dans ce contexte, une sécrétion de cytokines pro-inflammatoires (IL-8, Interferon-β (IFN-β) et TNFα) impliquant les Toll like Receptors 2 et 4 (TLR2 et TLR4) a été décrite sur des cellules épithéliales du colon (Caco-2) traitées avec un mélange d'oxystérols à 60 µM (composition : 42,96 % 7KC, 32,3 % 5,6α-époxycholestérol, 5,76 % 5,6β-époxycholestéol, 4,26 % 7α-OHC and 14,71 % 7β-OHC) (Rossin *et al.*, 2019). Les cellules Caco-2 incubées avec du 7KC ont montré une élévation des niveaux d'ERO via NOX entrainant une mort cellulaire par apoptose (Biasi *et al.*, 2009; Poli *et al.*, 2013). Il a aussi été décrit que le 7KC diminuait la perméabilité des cellules épithéliales intestinales, ce qui est souvent à l'origine des maladies intestinales (Chalubinski *et al.*, 2014). Le 7KC pourrait alors contribuer à l'évolution et l'aggravation de ces pathologies par ses effets pro-inflammatoires et pro-oxydants.

1.1.5 Maladies génétiques

Il existe plusieurs maladies génétiques dans lesquelles le 7KC pourrait être impliqué. Ces maladies pouvant aboutir à la mort sont généralement accompagnées d'une dérégulation du métabolisme du cholestérol et peuvent avoir des symptômes très différents allant de l'atteinte cardiaque à la neurodégénérescence. Parmi elles, la maladie de Niemann Pick (de type A et B) qui a pour origine une déficience en sphyngomyélinase acide dont le rôle est de métaboliser la sphyngomyéline dans les lysosomes. La maladie de Niemann Pick (A-B) se traduit par une accumulation intracellulaire lysosomale de sphingomyéline. Il existe un troisième type de maladie de Niemann Pick, la maladie de Niemann Pick de type C. Elle est caractérisée par une mutation des gènes NPC1 ou NPC2 qui se traduit par une perturbation du transport intracellulaire du cholestérol et son accumulation dans les endolysosomes / lysosomes. Il en résulte une accumulation de cholestérol et d'oxystérols dans les cellules qui affecte majoritairement le cerveau, le foie et la rate. Cette pathologie est généralement mortelle avant l'âge de 20 ans (Porter *et al.*, 2010). La maladie de Gaucher est une autre maladie génétique touchant le métabolisme lysosomal (déficience en glucocérébrosidase) provoquant également des atteintes aux organes en raison d'une accumulation de lipides (cholestérol en particulier) (Boenzi *et al.*, 2016). Les plasmas de patients atteints par ces maladies montrent un taux élevé de 7KC qui est corrélé à la sévérité des symptômes pour la maladie de Niemann Pick de type C. Des taux de 7KC pouvant aller jusqu'à 86 ng/mL de plasma contre 16 ng/mL pour les contrôles ont été mesurés (Boenzi *et al.*, 2016).

Le 7KC plasmatique est également augmenté dans le cas de la maladie de Batten (ou céroïdes-lipofuscinoses neuronales). Il s'agit également d'une maladie lysosomale provoquant des atteintes neurologiques chez l'enfant (Anderson *et al.*, 2020).

La déficience en lipase acide lysosomale (LAL) est une atteinte lysosomale présentant des sévérités variables et entraine l'accumulation d'esters de cholestérol et de triglycérides dans le lysosome ce qui provoque une hypercholestérolémie et de l'athérosclérose. Les taux de 7KC sont aussi plus élevés que la normale dans cette maladie (69 ng/mL contre 16 ng/mL chez les contrôles) (Boenzi *et al.*, 2016).

Dans le cas de la xanthomatose cérébrotendineuse, maladie causée par une mutation du gène codant pour la 27-hydroxylase et provoquant des atteintes au niveau du cerveau, le 7KC plasmatique est aussi augmenté. Cela pourrait être dû à une accumulation de 7-déhydrocholestérol qui serait convertie en 7KC par la 7α-hydroxylase ou cytochrome 7A1 (CYP7A1) (Bjorkhem *et al.*, 2014).

Dans le syndrome de Smith-Lemli-Optiz (SLOS), caractérisé par une mutation de la 7-déhydrocholestérol réductase, le cholestérol ne peut être synthétisé normalement et des précurseurs s'accumulent (7-déhydrocholestérol et lanostérol). Comme dans la xanthomatose cérébrotendineuse, du 7KC peut alors être généré par la CYP7A1 et se retrouver en taux élevé dans le plasma. Des taux médians de 7KC ont été mesuré à 129 ng/mL dans le plasma des patients contre 16 chez les contrôles) (Anderson *et al.*, 2020; Bjorkhem *et al.*, 2014).

Des taux augmentés de 7KC ont aussi été mesurés dans les globules rouges de patients atteints de drépanocytose (Yalcinkaya *et al.*, 2019).

Enfin, dans le cas de l'X-ALD, une maladie causée par une déficience partielle ou totale d'un transporteur peroxysomal (ATP binding cassette de type D1 (ABCD1)) et entrainant une accumulation d'acides gras à très longue chaine associée ou non à une démyélinisation, les taux de 7KC (de 0.1 µmol/L à environ 2 µmol/L), 7β-OHC, 7α-OHC et de 25-OHC sont aussi augmentés (Jang *et al.*, 2016; Nury *et al.*, 2017).

1.1.6 Maladies pulmonaires

Les fibroses idiopathiques pulmonaires font partie des pneumonies chroniques progressives. Ce sont des atteintes graves du poumon pour lesquelles il n'existe pas de traitement efficace. Elles se caractérisent par une accumulation de cellules fibroblastiques dans le tissu pulmonaire qui produisent de la matrice extracellulaire en excès. L'expression de NOX4 (augmentée par le 7KC) et la production d'ERO sont augmentées dans ces pathologies (Liu *et al.*, 2017), ce qui suggère une implication du 7KC.

Dans la maladie pulmonaire obstructive chronique, les niveaux d'ERO et d'oxystérols (7KC, 24(S)-OHC et 27-OHC) sont augmentés (Fischer *et al.*, 2015). Dans la fibrose cystique, les taux de 7KC sont aussi augmentés et le profil en acides gras est modifié (augmentation des acides gras saturés, mono-insaturés, poly-insaturés). Le taux de 7KC plasmatique passe ainsi de 8 à 11 ng/mL et celui du 7β-OHC de 9 à 14 ng/mL (Iuliano *et al.*, 2009). Dans l'infection au SARS-CoV-2 (COVID-19), le taux plasmatique de 27-OHC est diminué (diminution pouvant aller jusqu'à 50 % chez les patients graves) tandis que les taux de 7KC et 7β-OHC sont légèrement mais significativement augmentés (Marcello *et al.*, 2020). Le 7KC est aussi augmenté dans une affection pulmonaire grave : la silicose (Aksu *et al.*, 2020).

Ainsi, de nombreux oxystérols, incluant le 7KC, sont impliqués dans plusieurs maladies fréquemment observées et associées au vieillissement (**Figure 1**). Mieux connaitre les mécanismes cellulaires associés aux effets délétères du 7KC constitue un enjeu important dans la prévention et le traitement de ces maladies.

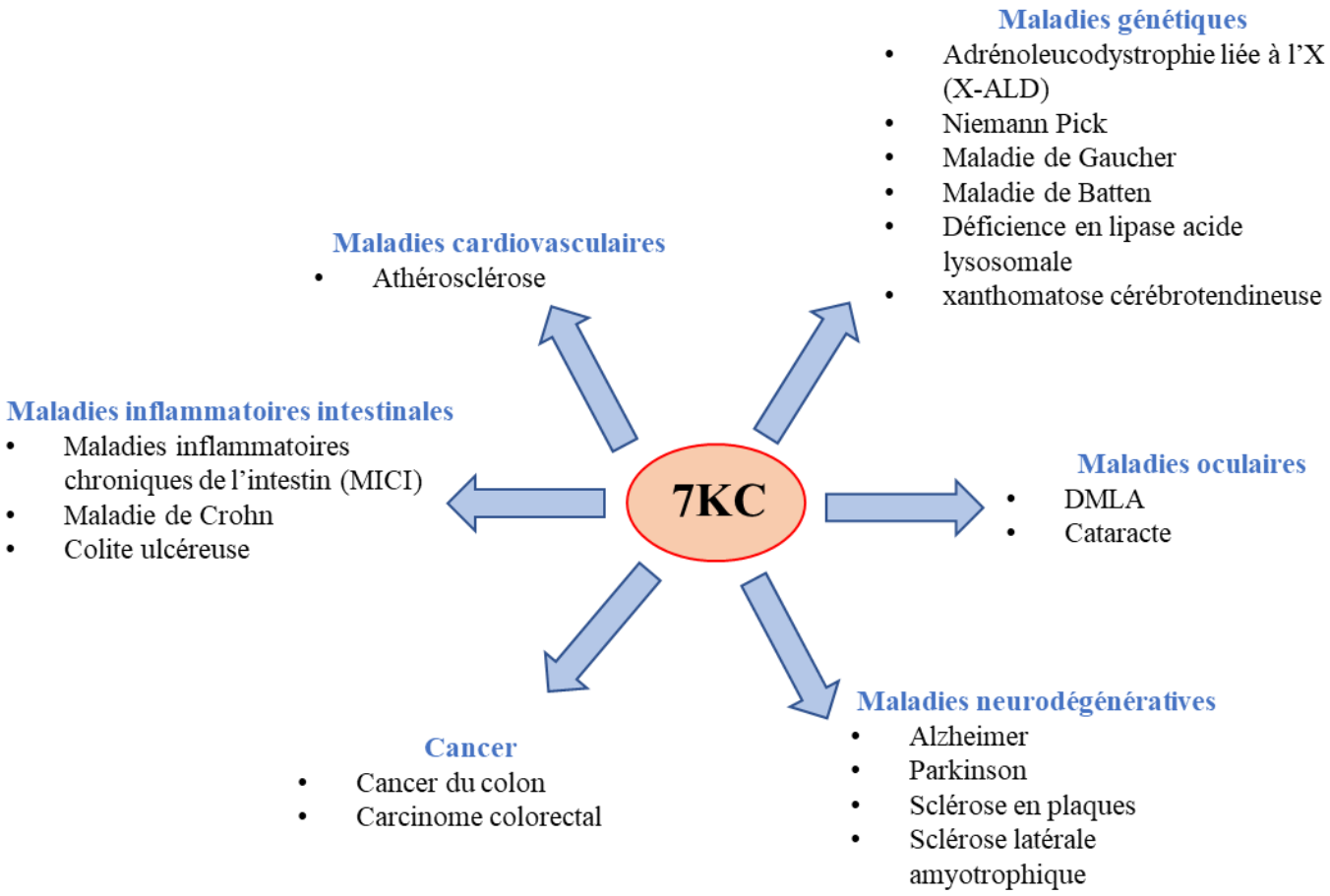

Figure 1 : Implication du 7-cétocholestérol dans les maladies liées à l'âge et les maladies inflammatoires chroniques.

Le 7KC est impliqué dans les maladies cardiovasculaires (athérosclérose), des maladies neurodégénératives (Alzheimer, Parkinson, sclérose en plaques, sclérose latérale amyotrophique), des maladies oculaires (DMLA, cataracte), des maladies inflammatoires chroniques de l'intestin et certains cancers.

2. Les oxystérols

Le cholestérol a été découvert en 1815 par le chimiste français Eugène Chevreul sous le terme de cholestérine (**Figure 2**).

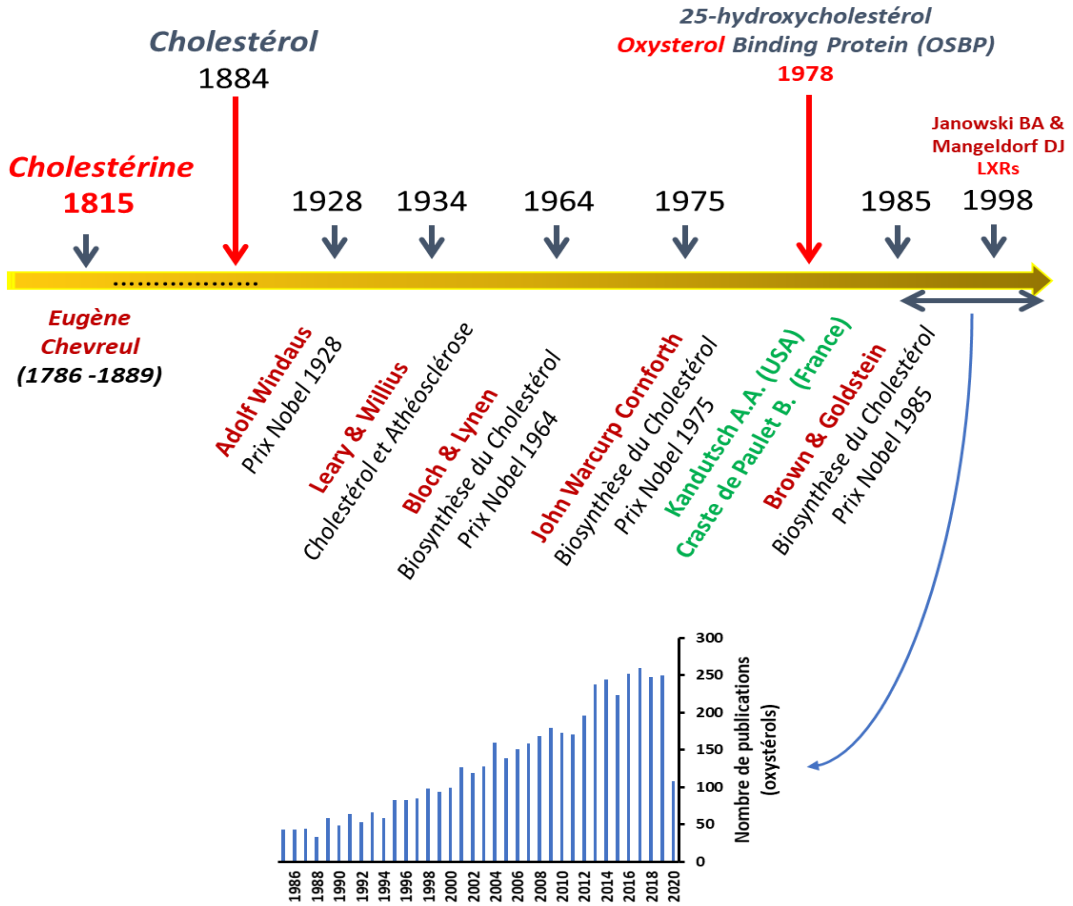

Figure 2 : Historique du cholestérol et des oxystérols.
Dans les années 1970, les travaux de Kandutsch *et al*., ainsi que ceux de Craste de Paulet *et al.*, ont fortement contribué à faire émerger la recherche sur les oxystérols qui devient de plus en plus pointue grâce aux méthodes analytiques actuellement disponibles. Le nombre de publications sur les oxystérols n'a fait qu'augmenter depuis les années 1980.

En 1884, Emile Littré l'a renommé « cholestérol », du grec « chole » (bile) et « stereos » (solide), car il avait été observé la première fois sous sa forme solide dans des calculs biliaires en 1758 par François Poulletier de la Salle. Par la suite, plusieurs prix Nobel ont récompensé des découvertes

sur les stérols, la biosynthèse du cholestérol ainsi que son implication dans des maladies. En 1928, Adolf Windaus a reçu le prix Nobel de chimie pour ses recherches sur les stérols. En 1964, Konrad Bloch et Feodor Lynen ont reçu le prix Nobel de physiologie et de médecine pour avoir découvert le métabolisme du cholestérol et des acides gras. En 1975, John Cornforth a reçu le prix Nobel de chimie pour ses études sur les enzymes lui permettant de détailler la biosynthèse du cholestérol (Cornforth *et al.*, 1947; Massaad *et al.*, 2017).

Le cholestérol est un des principaux constituants des membranes cellulaires (environ 50 % du total des lipides). Il joue un rôle majeur dans la synthèse des hormones stéroïdiennes, des acides biliaires et de la vitamine D. Les oxystérols font partie des produits d'oxygénation du cholestérol qui ont été découverts en 1913 par Lifschutz qui les avait qualifiés d'oxycholestérol (Lifschütz, 1913). Ce n'est que trente ans plus tard que Kandutsch et son équipe les ont renommés « oxystérols » (Kandutsch *et al.*, 1978).

Les produits d'oxygénation du cholestérol (communément appelés oxystérols dans le règne animal) sont des molécules d'origine biologique ou chimique de 27 atomes de carbone et comportant un noyau stéroïde ainsi qu'une chaine latérale 6-méthylheptan-2-yl. Le carbone numéro 3 du noyau stéroïde peut porter une fonction hydroxyle, comme le cholestérol, ou bien une fonction cétone. Les oxystérols (hors phytostérols) sont des dérivés du cholestérol, formés par hydroxylation ou oxydation ; ils peuvent porter une ou plusieurs fonctions hydroxyle ou cétone au niveau du noyau stéroïde et/ou de la chaine latérale (**Figure 3**).

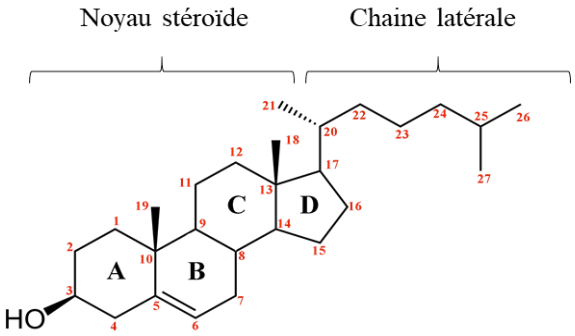

Figure 3 : Structure chimique du cholestérol.
Le cholestérol est un lipide de la famille des stérols formé d'un noyau stéroïde et d'une chaine latérale. Les quatre cycles du noyau cyclopentanoperhydrophénanthrène sont désignés par les lettres A, B, C et D. Le carbone en haut du cycle A portant le n°1, les atomes des deux cycles A et B sont numérotés à la suite en tournant dans le sens direct (1 à 10) ; on passe ensuite aux atomes du cycle C (11 à 14) puis D (15 à 17). Les radicaux méthyl liés aux carbones 13 et 10 sont désignés par les nombres 18 et 19. Enfin, ceux de la chaîne latérale sont désignés : 20 et 21 ; Au niveau du carbone 20 sont liés les carbones 22 à 25 et les deux derniers méthyl 26 et 27.

Initialement, les oxystérols étaient considérés comme de simples composés plus polaires que le cholestérol et intervenant dans son métabolisme et son élimination. Il a été découvert par la suite que les oxystérols interagissaient avec des récepteurs spécifiques et qu'ils intervenaient dans la synthèse des hormones stéroïdiennes (Luu-The, 2013). L'intérêt pour ces derniers s'est donc accru depuis les années 2000 et les preuves de leur implication dans de nombreux processus biologiques et pathologies sont de plus en plus nombreuses.

2.1 Origines et sources d'oxystérols

Il existe plusieurs sources de biogénèse des oxystérols. Ils peuvent être générés par auto-oxydation du cholestérol à la suite d'attaques radicalaires, par des enzymes spécifiques, le plus

souvent du type cytochrome ou encore être apportés par l'alimentation. Généralement, les oxystérols oxydés sur le noyau stéroïde proviennent d'une auto-oxydation tandis que ceux oxydés sur la chaine latérale proviennent plutôt d'une réaction enzymatique (Mutemberezi *et al.*, 2016).

2.1.1 Origine alimentaire des oxystérols

Le cholestérol est un composant important dans de nombreux aliments. Il peut alors être sujet à oxydation et conduire à la formation d'oxystérols qui sont alors ingérés. Les aliments riches en cholestérol tels que les œufs, la poudre d'œufs couramment utilisée dans les plats industriels, le beurre clarifié, les produits laitiers, la viande rouge, le jambon (bacon) ou encore le poisson séché ou en boites sont les plus riches en oxystérols (7KC, 7β-OHC, 7α-OHC, 5,6α-époxycholestérol, 5,6β-époxycholestérol) (Boselli *et al.*, 2001; Leonarduzzi *et al.*, 2002).

Durant le stockage et la préparation d'aliments, le cholestérol peut facilement subir une oxydation lors de l'exposition à de hautes températures (cuisson à haute température), à l'oxygène ou à l'ozone, à la lumière (exposition aux ultraviolets). Les produits déshydratés sont particulièrement sensibles à l'oxydation (Sabolova *et al.*, 2017).

Les oxystérols retrouvés en majorité dans l'alimentation sont ceux oxydés en C7 (7KC, 7β-OHC) ainsi que des époxycholestérols (5,6α/5,6β-époxycholestérol), le 25-hydroxycholestérol (25-OHC) et le 19-hydroxycholestérol (19-OHC) (Leonarduzzi *et al.*, 2002).

Dans ces produits, le taux d'oxystérols peut atteindre 10 à 100 µM (Kanner, 2007). Après l'ingestion d'un repas riche en oxystérols (salami et parmesan), des dosages ont montré après 5 heures que les concentrations plasmatiques en oxystérols (7KC, 7β-OHC et 7α-OHC) étaient augmentées principalement dans les chylomicrons. Des différences sont toutefois notables entre les différents oxystérols : le cholestane-3β,5α,6β-triol, le 7KC et les époxydes sont sous-

représentés par rapport au 7β-OHC (Linseisen *et al.*, 1998). Des résultats similaires ont été montré chez des rats après une infusion gastrique d'oxystérols (Vine *et al.*, 1997). Ceci démontre une absorption intestinale variable selon les oxystérols dont l'origine pourrait être due à leur site d'oxydation. Toujours chez des rats, il a été montré que 92 % des oxystérols alimentaires étaient absorbés (Brzeska *et al.*, 2016). Les oxystérols ingérés sont absorbés en majorité sous forme d'esters au niveau du tractus intestinal supérieur et pris en charge dans le plasma par les chylomicrons. Ensuite, les rémanents de chylomicrons sont métabolisés par le foie en lipoprotéines de très faible densité (very low density lipoprotein (VLDL)) puis en LDL et en lipoprotéines de haute densité (high density lipoprotein (HDL)). Ainsi, les oxystérols peuvent se retrouver dans tous les types de lipoprotéines mais ils sont présents en majorité dans les LDL (Addis *et al.*, 1989; Viens *et al.*, 1996). Des oxystérols non estérifiés peuvent aussi être transportés au niveau plasmatique par l'albumine. Des mesures réalisées avec du 7KC, du 20α-OHC et du 25-OHC ont montré que l'albumine transportait préférentiellement le 25-OHC (Babiker *et al.*, 1998; Brown, 2019).

2.1.2 Formation des oxystérols par voie enzymatique

Plusieurs oxystérols peuvent être produits par des oxydations enzymatiques de manière physiologique lors du métabolisme du cholestérol. Une grande proportion des oxystérols est formée de cette façon. En ce qui concerne les oxystérols majoritaires, le 4β-hydroxycholestérol (4β-OHC), le 27-hydroxycholestérol (27-OHC), le 24(S)-OHC, le 7α-hydroxycholestérol (7α-OHC) et le 25-OHC sont produits respectivement par la CYP3A4, CYP27A1, CYP46A1, CYP7A1 et la cholestérol 25-hydroxylase (CH25H) (Mutemberezi *et al.*, 2016). D'autres enzymes sont responsables de la formation d'oxystérols généralement détectés à l'état de traces

dans les liquides biologiques ou dans les tissus. Il s'agit pour la plupart d'intermédiaires dans des réactions de métabolisme du cholestérol dont certains ont probablement des durées de vie très courtes (Griffiths *et al.*, 2019b).

Les enzymes permettant l'oxydation du cholestérol sont le plus souvent des membres de la superfamille des enzymes à cytochromes P450, mais elles peuvent aussi appartenir à la famille des hydroxystéroïdes déshydrogénases (HSD). La CH25H fait figure d'exception et n'appartient pas aux deux familles précédentes. Toutes ces enzymes ne sont pas exprimées de façon ubiquitaire. Il existe des expressions spécifiques à des organes et des types cellulaires précis : **Tableau 1** et **Figure 4**.

Les principales enzymes responsables de la formation d'oxystérols sont les suivantes :

- **CYP3A4**

La CYP3A4 permet la conversion du cholestérol en 4β-OHC, l'oxystérol majoritaire retrouvé dans le plasma, mais aussi la conversion du cholestérol en 25-OHC (Nury *et al.*, 2013). Cette enzyme à cytochrome est exprimée au niveau du foie dans le RE. Elle est aussi impliquée dans le métabolisme de nombreux xénobiotiques. Il est estimé qu'elle est capable de métaboliser près de la moitié des drogues utilisées (Meaney, 2013; Mutemberezi *et al.*, 2016).

- **CYP27A1**

La CYP27A1 ou 27-hydroxylase convertit le cholestérol en 27-OHC et intervient dans la voie « acide » de formation des acides biliaires. Cette enzyme mitochondriale est exprimée dans une grande variété de tissus mais principalement dans le foie, les cellules endothéliales et les monocytes/macrophages (Meaney, 2013; Mutemberezi *et al.*, 2016).

- **CYP46A1**

La CYP46A1 ou 24-hydroxylase permet la conversion du cholestérol en 24(S)-OHC. Elle est exprimée dans le RE, essentiellement dans les neurones du système nerveux central mais également en faible quantité dans les testicules et les ovaires. Elle permet l'excrétion du cholestérol cérébral, le cholestérol ne pouvant pas traverser la BHE alors que le 24(S)-OHC le peut (Meaney, 2013; Mutemberezi *et al.*, 2016).

- **CH25H**

La CH25H ou 25-hydroxylase catalyse la transformation du cholestérol en 25-OHC. Elle est exprimée dans la plupart des tissus au niveau du RE. Elle ne fait pas partie de la famille des enzymes à cytochrome, il s'agit d'une protéine non hémique contenant du fer (Griffiths *et al.*, 2020; Meaney, 2013).

- **CYP7A1**

La CYP7A1 ou 7α-hydroxylase est la première enzyme à intervenir dans la voie « classique » de formation des acides biliaires. Elle convertit le cholestérol en 7α-OHC. Elle est fortement exprimée dans le foie et plus précisément dans les hépatocytes au niveau du RE. Son expression est régulée par les taux d'acides biliaires (Meaney, 2013). Elle peut également produire du 7KC à partir du 7-déhydrocholestérol (Mutemberezi *et al.*, 2016).

Tableau 1 : Principales enzymes impliquées dans la formation des oxystérols : localisation cellulaire et fonction
D'après (Mutemberezi *et al.*, 2016).

Enzyme	Localisation cellulaire	Substrat → Produit
Oxydoréductases		
CYP3A4	Réticulum endoplasmique	Cholestérol → 4β-OHC Cholestérol → 25-OHC
CYP3A5	Réticulum endoplasmique	Cholestérol → 4β-OHC
CYP7A1	Réticulum endoplasmique	Cholestérol → 7α-OHC 7-déhydroxholestérol → 7KC
CYP7B1	Réticulum endoplasmique	27-OHC → 7α,27-OHC 25-OHC → 7α,25-OHC
CYP11A1	Réticulum endoplasmique	Cholestérol → 22(R)-OHC 22(R)-OHC → 20(S),22(R)-diOHC
CYP27A1	Mitochondrie	Cholestérol → 27-OHC Cholestérol → 25-OHC 7KC → 27OH-7KC
CYP39A1	Réticulum endoplasmique	24(S)-OHC → 7α,24(S)-OHC
CYP46A1	Réticulum endoplasmique	Cholestérol → 24(S)-OHC Desmostérol → 24(S),25epoxychol
Déshydrogénases		
7β-HSD3	Réticulum endoplasmique	7α-OHC → 7α-OHnone
11β-HSD1	Réticulum endoplasmique	7KC → 7β-OHC
11β-HSD2	Réticulum endoplasmique	Cholestane-3β,5α,6β-triol → Oncostérone 7β-OHC → 7KC
Hydroxylase		
Cholestérol 25 hydroxyalse (CH25H)	Réticulum endoplasmique	Cholestérol → 25-OHC
Hydrolases		
Cholestérol époxyde hydrolase (CHEH)	Réticulum endoplasmique	5,6α-epoxycholestérol → Cholestane-3β,5α,6β-triol 5,6β-epoxycholestérol → Cholestane-3β,5α,6β-triol

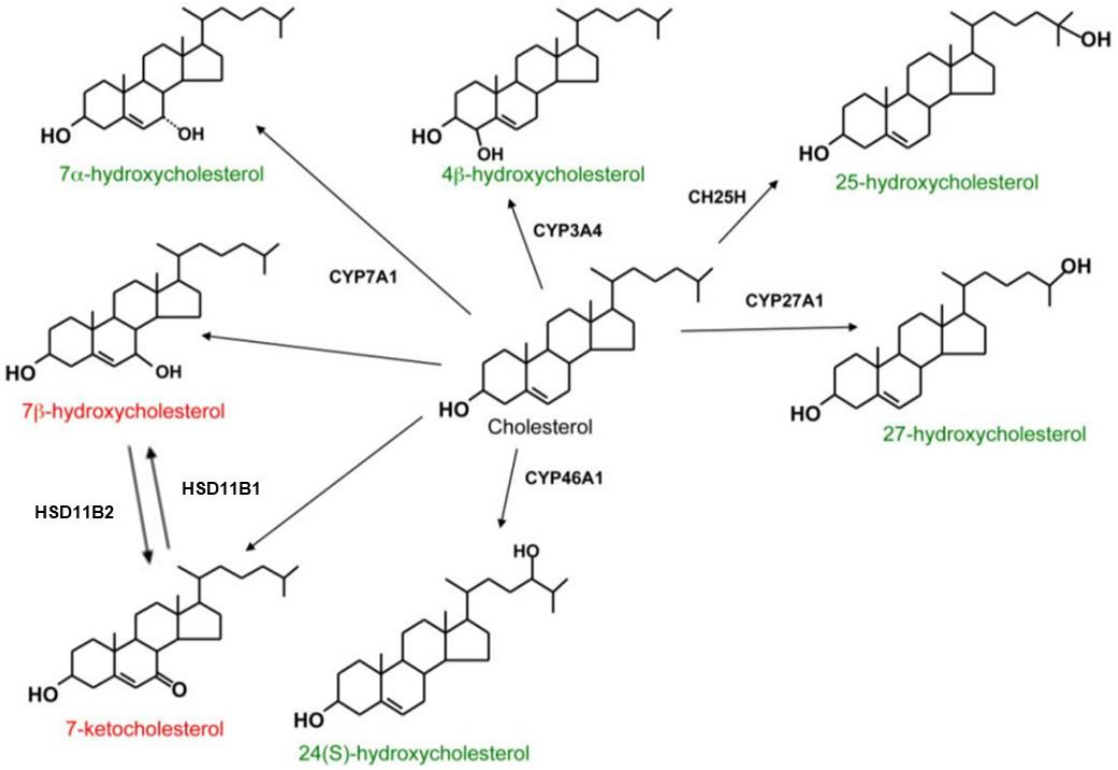

Figure 4 : Principales enzymes impliquées dans la formation des oxystérols.
Le cholestérol peut être oxydé de manière physiologique par différentes enzymes. La CYP3A4 catalyse la formation de 4β-OHC, la CYP7A1, forme le 7α-OHC, la CYP46A1 forme le 24(S)-OHC, la CYP27A1 forme le 27-OHC, la CH25H forme le 25-OHC. La 11β-HSD1 permet la conversion du 7KC en 7β-OHC et le 11β-HSD2 catalyse la réaction inverse. D'après (Olkkonen *et al.*, 2012).

2.1.3 Formation des oxystérols par auto-oxydation

L'oxydation du cholestérol peut avoir lieu dans les membranes cellulaires ou encore dans les protéines de transport du cholestérol telles que les LDL. Les LDL sont constituées d'une enveloppe de cholestérol, de protéines et de phospholipides avec un cœur d'esters de cholestérol et de triglycérides. Elles transportent les lipides du foie vers les tissus périphériques. Tous les composant de ces LDL sont susceptibles d'être oxydés pour former des LDL oxydées (OxLDL) et lorsque cette oxydation touche le cholestérol, il en résulte la formation d'oxystérols.

Les carbones des cycles A et B du noyau stéroïde sont les plus sensibles aux attaques radicalaires, en particuliers les carbones 5, 6 et 7. On distingue deux types d'auto-oxydation, celle de type I et celle de type II.

- L'auto-oxydation de type I concerne les oxydations ayant pour origine des radicaux libres (anion superoxide ($O_2^{\bullet -}$), peroxyde d'hydrogène (H_2O_2), radical hydroxyl ($HO^{\bullet}$), oxyde nitrique (NO), peroxynitrites $ONOO^-$) (**Figure 5**).

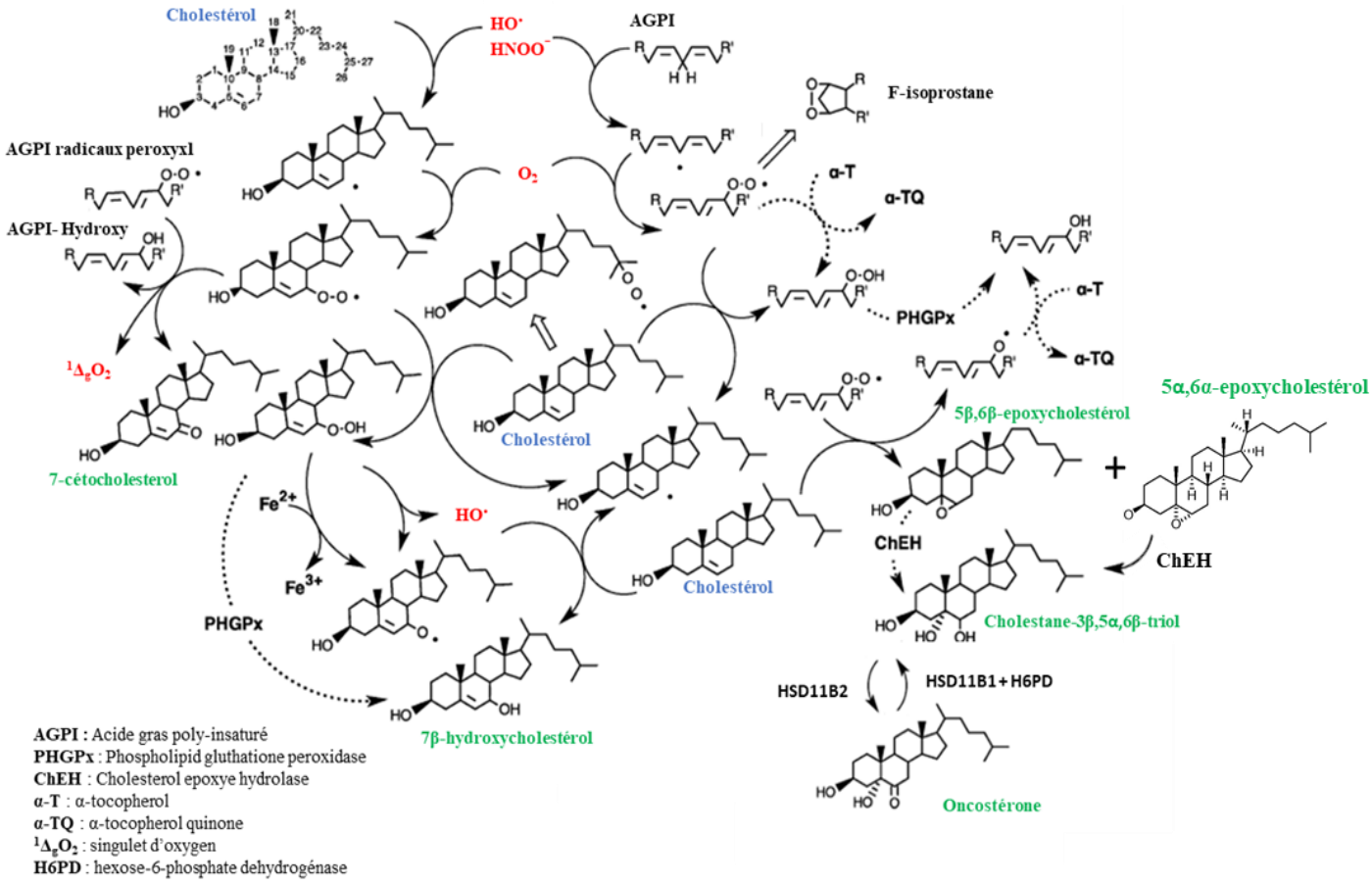

Figure 5 : Auto-oxydation radicalaire du cholestérol (oxydation de type I).
L'auto-oxydation du cholestérol de type I concerne les oxydations ayant pour origine des radicaux libres : anion superoxide ($O2^{\bullet -}$), peroxyde d'hydrogène (H_2O_2), radical hydroxyl ($HO^{\bullet}$), oxyde nitrique (NO), peroxynitrites (ONOO-). D'après (Iuliano, 2011).

Ils peuvent être générés par le métabolisme cellulaire ou bien par leur décomposition consécutive en radicaux hydroxyl par la dismutation de deux anions superoxydes en peroxyde d'hydrogène ($2O_2^{\bullet-} \rightarrow H_2O_2$) ou encore par la réaction de Fenton ($H_2O_2 + Me^{n+} \rightarrow HO^{\bullet} + Me^{(n+1)+}$) où Me est un métal de transition comme par exemple le cuivre, le fer, ou l'aluminium (Iuliano, 2011). Le plus souvent, les attaques radicalaires par les ERO ou les espèces réactives de l'azote (ERA) entrainent la perte d'un hydrogène sur le carbone 7 à cause du lien faible entre le carbone et l'hydrogène. L'énergie de dissociation de cette liaison étant de 88 kcal/mol (Zerbinati *et al.*, 2017). Cette oxydation locale en C7 étant plutôt stable, cela lui permet de réagir ensuite facilement avec de l'oxygène moléculaire pour former un radical peroxyl ($COO^{\bullet}$). Par la suite, en réagissant avec un autre hydrogène perdu par une autre molécule, le radical peroxyl va former un cholestérol hydroperoxyde (7α- ou 7β-OOHC). La fonction hydroperoxyde étant très instable, le cholestérol hydroperoxyde se décompose en 7α-OHC, 7β-OHC ou 7KC. Ces trois oxystérols oxydés en C7 sont ceux formés majoritairement par auto-oxydation (Brown *et al.*, 2009). Le 7KC est l'oxystérol majoritaire dans les OxLDL avec une proportion d'environ 30 % du total des stérols (Anderson *et al.*, 2020; Brown *et al.*, 1996).

- L'auto-oxydation de type II concerne les attaques non radicalaires par des singulets d'oxygène ($^1\Delta_gO_2$), de l'acide hypocloreux (HOCl) ou encore de l'ozone (O_3) (**Figure 6**). L'implication de l'ozone est intéressante sachant qu'il est lié à la pollution atmosphérique. Les singulets d'oxygène peuvent se former par la réaction d'un peroxyde d'hydrogène (H_2O_2) avec l'HOCl tous deux produits lors des réactions inflammatoires en présence de myéloperoxydase.

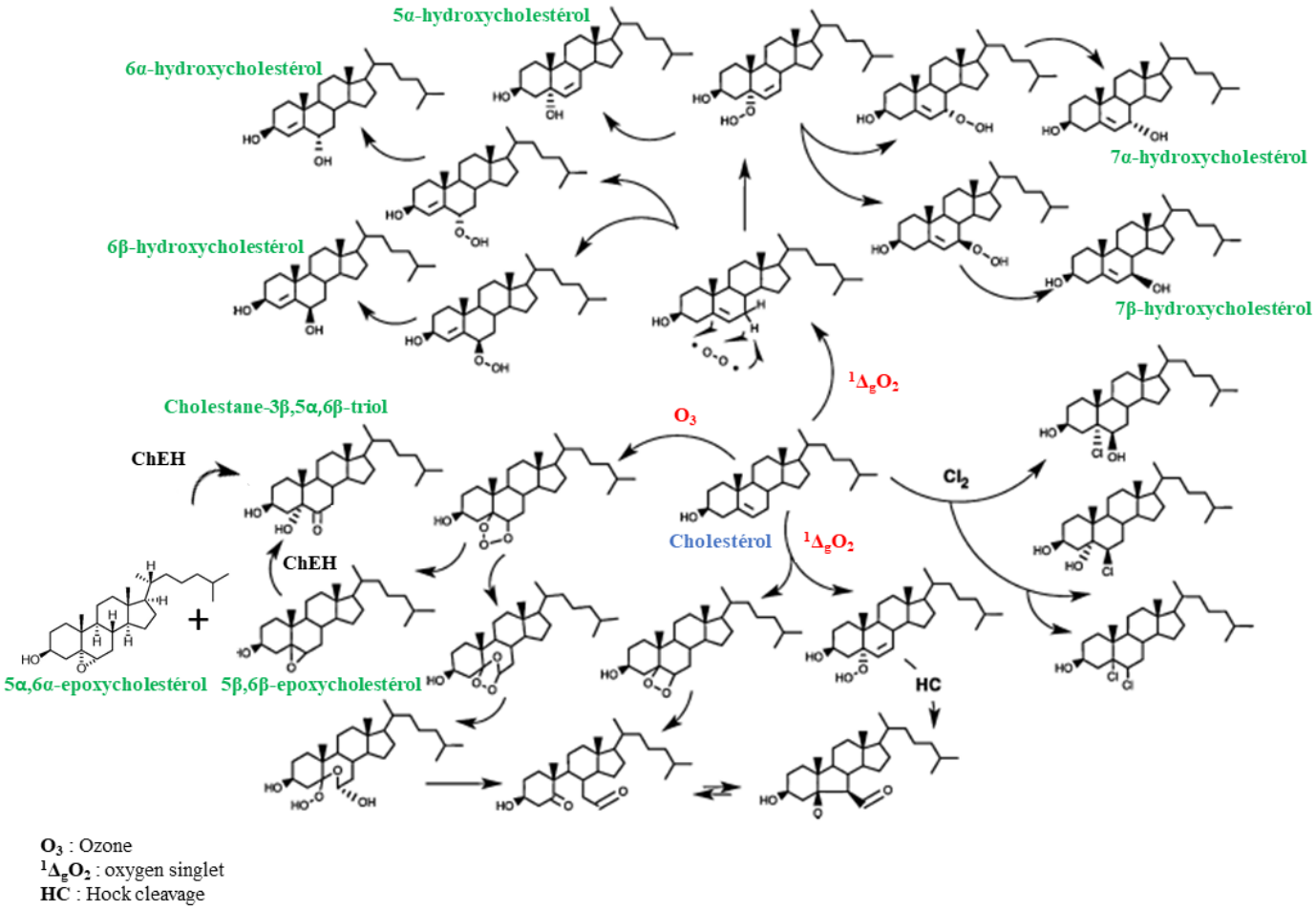

Figure 6 : Auto-oxydation non radicalaire du cholestérol (oxydation de type II).
L'auto-oxydation du cholestérol de type II concerne les attaques non radicalaires par des singulets d'oxygène ($^1\Delta_gO_2$), de l'acide hypocloreux (HOCl) ou encore de l'ozone (O_3). D'après (Iuliano, 2011).

Les hydroperoxydes en C5, C6, C7, les 5,6-epoxydes (α/β) ainsi que des secostérols sont formés comme composés primaires de ces réactions (Zerbinati *et al.*, 2017).

Les 5,6α/β-époxycholestérols peuvent être pris en charge par l'enzyme cholestérol époxyde hydrolase pour former du cholestane-3β,5α,6β-triol. Il a été montré que l'aminolyse des α-époxycholestérols pouvait donner des alkylamino-oxystérols. Parmi eux figure la dendrogénine A. La dendrogénine A peut se former lorsqu'un 5,6α-époxycholestérol réagit avec

une histamine sous l'action d'une enzyme qui reste à caractériser, la dendrogénine A synthase (de Medina *et al.*, 2020; de Medina *et al.*, 2013; Poirot *et al.*, 2018).

3. Le 7-cétocholestérol (7KC)

Parmi tous les oxystérols formés par auto-oxydation, le 7KC est certainement un des plus étudiés. Bien que son origine soit principalement due à une auto-oxydation du cholestérol, il peut aussi être formé à partir du 7β-OHC sous l'action d'une enzyme. Les enzymes 11β-HSD1 (gène HSD11B1) et 11β-HSD2 (gène HSD11B2) sont impliquées respectivement dans la conversion du 7KC en 7β-OHC et du 7β-OHC en 7KC (Raleigh *et al.*, 2018). Cependant, ces enzymes prennent aussi en charge de nombreux substrats (Griffiths *et al.*, 2019b). La conversion du 7KC en 7β-OHC par 11β-HSD1 semble survenir dans de nombreux tissus (Mitic *et al.*, 2013; Raleigh *et al.*, 2018). En revanche, la conversion du 7β-OHC en 7KC par 11β-HSD2 n'a pas été mise en évidence dans des anneaux aortiques de souris (Mitic *et al.*, 2013). Le 7KC peut aussi être formé à partir du 7-déhydrocholestérol (précurseur direct dans la synthèse du cholestérol) par la CYP7A1 (Bjorkhem *et al.*, 2014; Mutemberezi *et al.*, 2016; Vejux *et al.*, 2020) (**Figure 7**).

On trouve du 7KC partout où l'on trouve beaucoup de cholestérol dans l'organisme : c'est-à-dire dans le plasma au niveau des LDL ou fixé à l'albumine, mais aussi dans les membranes cellulaires de différents tissus (Brown *et al.*, 2009; Lin, 1995). Cette présence ubiquitaire permet au 7KC d'avoir des activités sur un très grand nombre de fonctions cellulaires et biologiques ainsi qu'une implication dans plusieurs pathologies.

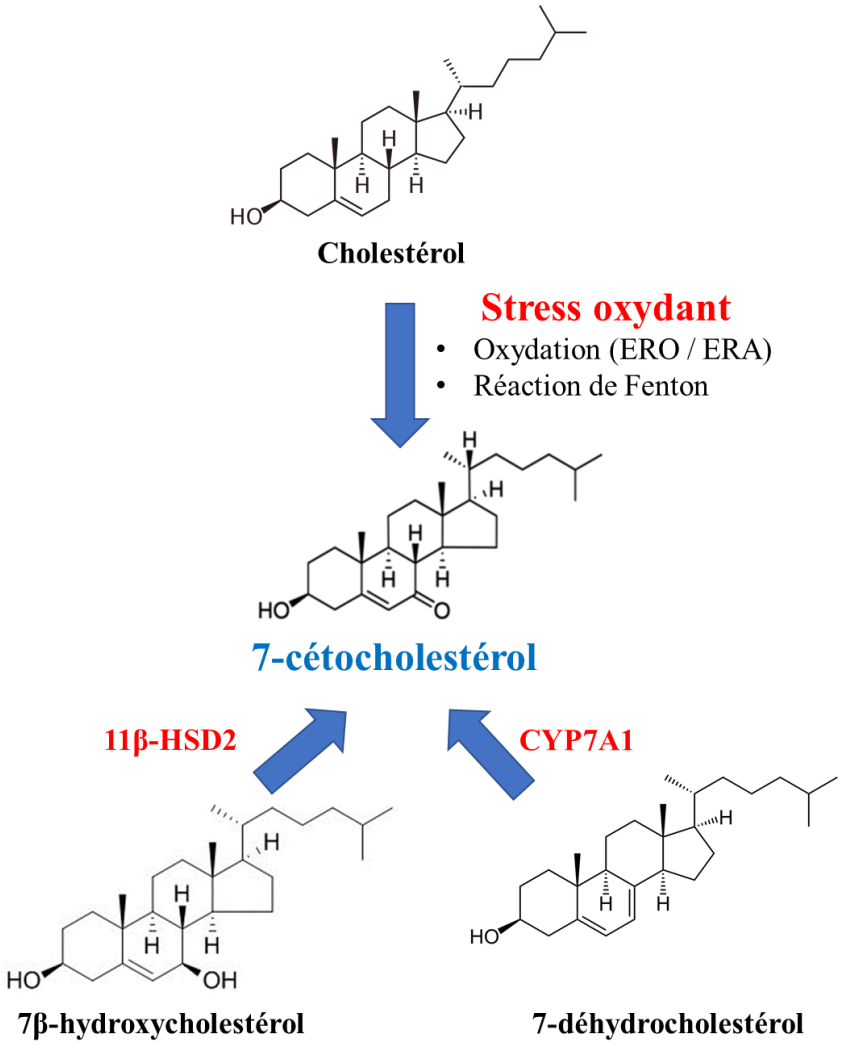

Figure 7 : Différentes voies de formation du 7-cétocholestérol.
Le 7KC peut être formé à partir du cholestérol par auto-oxydation lorsque le stress oxydant est augmenté. Il se forme également à partir du 7β-OHC par l'action de la 11β-HSD2 et à partir du 7-déhydrocholestérol par l'action de CYP7A1.

3.1 Effets du 7KC au niveau cellulaire

Le 7KC a pour cible la membrane plasmique où il se substitue au cholestérol au niveau des radeaux lipidiques. Il agit aussi sur l'activité de nombreux récepteurs membranaires et canaux ioniques. Ses effets aux niveau cellulaires se traduisent par une augmentation du stress oxydant favorisant l'induction de la mort cellulaire par une stimulation de l'inflammation (Vejux *et al.*, 2020).

3.1.1 Altération de la membrane plasmique

La membrane plasmique est sans doute la membrane biologique la plus étudiée. Elle est composée de quatre phospholipides principaux (phosphatidylcholine, phosphatidyléthanolamine, phosphatidylsérine et sphingomyéline) qui représentent plus de la moitié des lipides membranaires. Ces phospholipides sont distribués de façon asymétrique de part et d'autre de la bicouche lipidique. Le feuillet externe est composé en majorité de phosphatidylcholine et de sphingomyéline tandis que le feuillet interne se compose plutôt de phosphatidyléthanolamine et de phosphatidylsérine. Un autre phospholipide, le phosphatidylinositol, se trouve également dans le feuillet interne.

En plus des phospholipides, on trouve une grande quantité de cholestérol (près de 50% molaires) et de glycolipides sur le feuillet externe (Ayee *et al.*, 2016).

Les têtes polaires hydrophiles des phospholipides sont orientées vers l'extérieur de la membrane, tandis que les chaines d'acides gras hydrophobes sont orientées vers l'intérieur. Cette propriété rend la membrane flexible et fluide et permet aux protéines et aux lipides de circuler librement au sein de la membrane.

Du fait de sa structure, le cholestérol est inséré dans la membrane (interne et externe) avec sa tête hydroxyle dirigée du côté des têtes polaires des phospholipides. Cette caractéristique physique lui permet de diminuer la fluidité de la membrane en réduisant les mouvements des chaines d'acides gras des phospholipides.

Il existe également au sein de la membrane des régions enrichies en cholestérol et en sphingolipides (sphingomyéline et glycolipides) qui sont appelées « radeaux lipidiques ». Ces régions jouent un rôle très important dans la signalisation cellulaire par la présence de protéines

spécifiques de ces régions comme des tyrosines kinases (récepteurs des lymphocytes T et B, récepteurs à l'insuline, etc.) (Cooper, 2000; Simons *et al.*, 2000).

Tout ce cholestérol membranaire est donc une cible potentielle du stress oxydant et peut donc être une source importante d'oxystérols, en particulier de 7KC. La présence d'un ou plusieurs groupements hydroxyles supplémentaires caractérisant les oxystérols entraine une insertion différente dans la bicouche lipidique comparativement à celle du cholestérol (**Figure 8**), ce qui entraine une diminution importante de la fluidité membranaire, et donc des perturbations dans les voies de signalisation pouvant entrainer une cytotoxicité (Ayee *et al.*, 2016; Royer *et al.*, 2009).

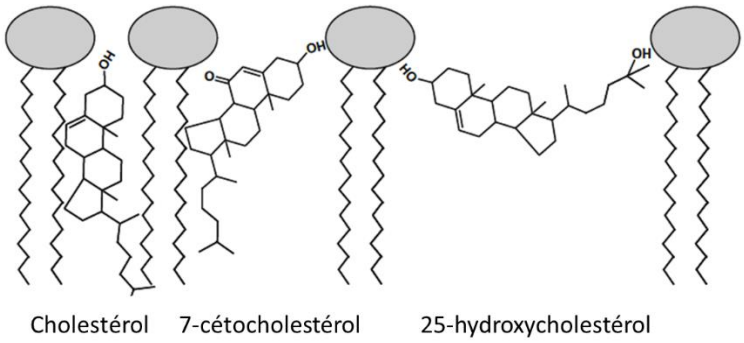

Figure 8 : Représentation schématique de l'orientation du cholestérol, du 7-cétocholestérol et du 25-hydroxycholestérol dans une bicouche lipidique.
La présence d'un ou plusieurs groupements hydroxyles supplémentaires caractérisant les oxystérols entraine une insertion différente dans la membrane plasmique par rapport à celle du cholestérol. D'après (Olkkonen *et al.*, 2012)

Des tests réalisés avec le 7KC, le 7β-OHC et le 7α-OHC, sur des membranes lipidiques de synthèse (monocouche de Langmuir) ainsi que sur des membranes d'érythrocytes humains, ont montré que le 7KC avait l'impact le plus fort sur la forme et les propriétés de la membrane caractérisé par une diminution de la fluidité (Targosz-Korecka *et al.*, 2020). Il a été montré sur les oligodendrocytes murins 158N et de cellules aortiques musculaires lisses A7R5, que le 7KC (et le

27-OHC) s'accumulait au niveau des radeaux lipidiques à l'inverse du 7β-OHC (Kahn *et al.*, 2011; Ragot *et al.*, 2013; Royer *et al.*, 2009). Cette déstabilisation des radeaux lipidiques peut engendrer des dysfonctions dans la transmission de la signalisation cellulaire. Ainsi, il a été montré que l'incorporation de 7KC dans les membranes de lymphocytes T CD4+, et plus particulièrement dans les radeaux lipidiques, impacte négativement l'expansion clonale de ces derniers (Schieffer *et al.*, 2014). Sur des cellules de phéochromocytome de rat PC12, un inhibiteur de tyrosine kinase (AG126) inhibe la mort cellulaire apoptotique induite par le 7KC (Kim *et al.*, 2010). Il a aussi été montré que le 7KC induit une activation de la tyrosine kinase PYK2 sur des cellules THP-1 qui perturbe les flux calciques et entraine l'apoptose (Berthier *et al.*, 2005).

3.1.2 Effets sur l'homéostasie ionique

Les flux ioniques tels que ceux du calcium ou encore du potassium sont des points décisifs dans l'homéostasie cellulaire ainsi que dans les signaux de survie ou de mort. L'ion calcium (Ca^{2+}) est considéré comme un second messager impliqué dans beaucoup de voies de signalisation cellulaires. Par conséquent, les effets du 7KC sur les flux ioniques ont souvent été étudiés ces dernières années sur de nombreux types cellulaires. Il a été montré que des traitements par le 7KC induisaient des variations de la concentration de Ca^{2+} intracellulaire. Sur des cellules endothéliales HUVECs, le 7KC à 150 µM pendant 2 h induit une élévation du Ca^{2+} (Millanvoye-Van Brussel *et al.*, 2004). Sur des cellules aortiques endothéliales de souris, le 7KC induit une élévation transitoire du Ca^{2+} accompagnée d'une augmentation des niveaux d'ERO et d'une mort cellulaire par apoptose (Zhou *et al.*, 2006). Sur les monocytes humains THP-1, le 7KC (100 µM) induit une augmentation du Ca^{2+} qui provoque une déphosphorylation de Bad par

la calcineurine (une phosphatase dépendante du calcium), ce qui aboutit à l'apoptose (Berthier *et al.*, 2004).

Sur des cellules musculaires lisses aortiques humaines, le 7KC (25 µM) induit des oscillations calciques ainsi qu'un stress du réticulum et une mort cellulaire par apoptose qui peut être inhibée par un bloqueur de canaux calciques, la nifédipine (Pedruzzi *et al.*, 2004; Sasaki *et al.*, 2007).

Dans des modèles cellulaires issus du système nerveux central, les oligodendrocytes murins 158N, le 7KC (50 µM) n'induit pas de changement des taux de Ca^{2+} (Ragot *et al.*, 2013). Sur des neuroblastomes humains SK-N-BE, le 7KC (100 µM) n'induit pas de modification après 10 minutes de traitement, mais entraîne une accumulation de Ca^{2+} sous forme de dépôts après 24 heures (Zarrouk *et al.*, 2015). Dans des cellules rétiniennes humaines, le 7KC (20 µM) entraine une toxicité à la suite d'une activation du récepteur P2X7 qui permet l'influx de calcium et de sodium ainsi que l'efflux de potassium (Olivier *et al.*, 2016). Ceci conduit à une élévation de l'inflammation et du stress oxydant pour aboutir par une mort cellulaire apoptotique.

En résumé, des effets calciques rapides inférieurs à la seconde, de l'ordre de la minute et même supérieurs à l'heure ou au jour ont été observés à la suite de traitements au 7KC. Les mécanismes expliquant ces différences de réaction sont encore mal connus (Mackrill, 2011).

Dans les oligodendrocytes murins 158N, le 7KC (25 µM) induit une augmentation de l'expression du canal potassique voltage dépendant Kv3.1 corrélée à une augmentation du potassium intracellulaire et à une mort par apoptose. L'augmentation de l'expression de Kv3.1 pourrait être un mécanisme de protection contre la toxicité du 7KC. De plus, le blocage de Kv3.1 par la 4-aminopyridine amplifie les effets toxiques du 7KC. Les effets du 7KC sur Kv3.1 suggèrent que cet oxystérol pourrait agir sur la qualité de l'influx nerveux (Bezine *et al.*, 2017; Bezine *et al.*, 2018b). Ces modifications au niveau des actions de canaux ioniques peuvent trouver leur origine dans des effets membranaires des oxystérols. En accord avec cette hypothèse,

le 7KC (15 µM) diminue la fluidité membranaire de cellules endothéliales humaines et inhibe l'activité de la pompe Na,K-ATPase (Duran *et al.*, 2010).

3.1.3 Activation du stress oxydant

Un des effets le plus notable du 7KC est son implication dans la génération de stress oxydant caractérisée par une augmentation de production d'ERO. En effet, le 7KC augmente la NOX. Cette enzyme catalyse la réaction d'oxydation du NADPH par l'oxygène et forme du NAPD+ ainsi qu'un proton (H^+) et un anion superoxyde ($O_2^{\cdot -}$). Il en résulte une augmentation rapide des niveaux d'ERO intracellulaires qui peuvent oxyder à leur tour des protéines, les acides nucléiques ou encore les lipides, avec parmi eux le cholestérol, ce qui amplifie la formation de 7KC dans la cellule ainsi que le stress oxydant (Leonarduzzi *et al.*, 2006; Pariente *et al.*, 2019). Il existe plusieurs NOX (NOX 1, 2, 3, 4 et 5 ainsi que deux variantes dual oxydase (DUOX 1 et 2)). Le 7KC semble agir principalement sur la NOX4 (Lee *et al.*, 2009; Pedruzzi *et al.*, 2004). La NOX 4 est principalement trouvée dans le RE, contrairement aux autres NOX qui sont plutôt membranaires (Buvelot *et al.*, 2019).

3.1.4 Inflammation cytokinique et non cytokinique

L'inflammation est une réponse biologique du système immunitaire qui peut être déclenchée par divers stimuli : pathogènes, molécules toxiques, cellules endommagées. Elle se divise en deux sous catégories. La première : l'inflammation cytokinique, se caractérise par une activation des cellules immunitaires qui vont libérer des cytokines pro-inflammatoires dans l'organisme. La seconde : l'inflammation non cytokinique, se caractérise par la sécrétion de

molécules pro-inflammatoires comme l'acide arachidonique, des prostaglandines, des leucotriènes, des thromboxanes et des prostacyclines (Chen *et al.*, 2018).

Le 7KC est connu pour être un inducteur d'inflammation dans les cellules en induisant la sécrétion de cytokines pro-inflammatoires sur plusieurs modèles cellulaires. Sur des cellules de rétine, des monocytes/macrophages, des cellules endothéliales, le 7KC induit des augmentations de niveaux de transcrits ainsi que des sécréterions d'IL-6, IL-8, IL-1β et de VEGF (Brahmi *et al.*, 2018; Pariente *et al.*, 2019; Vejux *et al.*, 2020; Yang *et al.*, 2019). Généralement, ceci passe par le récepteur TLR4 et par l'activation de la voie NFκB et une augmentation des niveaux de NOD-, LRR- and pyrin domain-containing protein 3 (NLRP3) suggérant également une activation de l'inflammasome (Huang *et al.*, 2014).

Le 7KC peut également engendrer une inflammation non cytokinique par augmentation des niveaux d'acide arachidonique et de l'activité de la phospholipase A2 (PLA2) (Freeman *et al.*, 2005; Rosenblat *et al.*, 2002). Le niveau de prostaglandine E2 (PGE2) peut également être augmenté ainsi que les activités lipoxygénases et cyclooxygénases (Tesoriere *et al.*, 2014a; Watanabe *et al.*, 2018). Enfin, les niveaux d'acide hydroxyoctadécanoïque (HODE) peuvent aussi être augmentés dans le cadre de pathologies accompagnées d'une élévation des taux de 7KC comme l'X-ALD (Nury *et al.*, 2017). Tout ceci mène généralement à une augmentation du stress oxydant qui amplifie la génération de 7KC.

3.2 Effets du 7KC sur les organites

Les différentes actions cellulaires du 7KC tant au niveau du stress oxydant, de l'intégrité membranaire, des flux ioniques et des voies de signalisation, peuvent également se répercuter directement ou indirectement sur les organites et leur fonctionnement. Ainsi, il a été montré que

le 7KC présentait une toxicité vis-à-vis du lysosome, de la mitochondrie ou encore du réticulum endoplasmique. Les travaux du laboratoire ces dernières années ont montré que le peroxysome était également une cible du 7KC et que ce dernier pouvait modifier son activité.

3.2.1 Réticulum endoplasmique

Le réticulum endoplasmique (RE) est un organite cellulaire lié à la membrane nucléaire. Il est constitué du RE lisse et du RE granuleux qui porte des ribosomes. Dans les cellules eucaryotes, le RE lisse est impliqué entre autres dans le stockage du calcium, la détoxification de drogues, la synthèse de lipides (phospholipides, stéroïdes, cholestérol) tandis que le RE granuleux participe plutôt à la synthèse des protéines et leur confère leur structure tridimensionnelle finale (Ricciardi *et al.*, 2020). Différents facteurs environnementaux tels que l'ischémie, l'hypoxie, le stress oxydant, le vieillissement et des facteurs génétiques peuvent induire un stress du réticulum. La réponse à ce stress est appelée « unfold protein response » (UPR). UPR a pour fonction d'augmenter la capacité d'élimination des protéines anormales. Lors d'un stress du RE prolongé ou trop intense, cette réponse UPR peut mener à la mort cellulaire par apoptose par l'intermédiaire de la protéine C/EBP-Homolgous Protein (CHOP). La dérégulation de la réponse UPR est impliquée dans de nombreuses pathologies comme le diabète, l'inflammation, les maladies neurodégénératives ou encore les maladies cardiovasculaires (athérosclérose) (Navas-Madronal *et al.*, 2019).

Parmi les différents inducteurs de stress du RE on trouve le 7KC, dont les effets sont plutôt bien connus. Sur des cellules ostéoblastiques MC3T3-E1, il a été montré que le 7KC induisait un stress du RE caractérisé par une augmentation de la transcription des marqueurs CHOP et GRP78. CHOP est un facteur de transcription impliqué dans la régulation de gènes pro- et anti-

apoptotiques. GRP78 est une protéine chaperonne de la lumière du RE qui joue un rôle dans le repliement des protéines. La surexpression de GRP78 protège généralement de la mort cellulaire induite par un stress du RE (Sato *et al.*, 2017). Sur des cellules rétiniennes ARPE-19, les niveaux de marqueurs du stress du RE sont également augmentés (CHOP, GRP78) (Huang *et al.*, 2014) et la voie NFκB semble être impliquée. Sur des cellules vasculaires musculaires lisses, le 7KC induit une augmentation des marqueurs protéiques de stress du RE : ATF4, ATF6, CHOP, HSPA5, IRE1, SEL1L et CREDL2 (Navas-Madronal *et al.*, 2019).

Sur des cellules monocytaires U937, le 7KC induit la formation de structures multi-lamellaires visibles au microscope électronique et appelées figures myéliniques. Il est maintenant considéré que ces figures myéliniques sont un indice de réticulophagie (autophagie du RE) (Vejux *et al.*, 2007).

3.3.2 Lysosome

Les lysosomes sont de petits organites intracytoplasmiques d'environ 0,1 à 1,2 µm de diamètre, délimités par une membrane lipidique simple (Hamer *et al.*, 2012). Leur nombre dans la cellule est variable. Leur membrane comporte des canaux ioniques qui permettent de faire entrer activement des protons à l'intérieur et de maintenir ainsi un gradient de pH (le pH des lysosomes est compris entre 3,5 et 5). Le lysosome contient un stock d'enzymes protéolytiques et hydrolytiques (lipases, glucosidases, protéases, nucléases) actives à pH acide, ce qui lui permet de jouer un rôle dans la dégradation et le recyclage des composants cellulaires ou extra-cellulaires. Il est notamment impliqué dans le processus d'autophagie au cours duquel il peut fusionner avec des autophagosomes ou des endosomes pour former des autophagolysosomes

capables de recycler des protéines mal repliées ou des organites dysfonctionnels (mitochondrie, réticulum, peroxysome).

Il est bien établi que le 7KC induit une toxicité à l'encontre du lysosome par le biais de différentes voies (Anderson *et al.*, 2020). Il peut directement induire une augmentation de la perméabilité membranaire du lysosome en raison d'une augmentation du cholestérol non estérifié dans celui-ci et induire une diminution de son pH (Li *et al.*, 2011; Sudo *et al.*, 2015). Ces modifications membranaires peuvent alors empêcher sa fusion avec les vésicules d'autophagie ou les endosomes. La toxicité du 7KC intervient aussi au niveau des enzymes lysosomales. Dans des cellules musculaires lisses vasculaires, le 7KC réduit l'expression et l'activité protéolytique des cathepsines B et D (Sudo *et al.*, 2015). Ainsi, même si les lysosomes parviennent à fusionner avec les vésicules (endosomes, autophagosomes), l'activité de dégradation s'en retrouve diminuée. Ceci a pour conséquence que des protéines ou des organites dysfonctionnels vont perdurer dans le cytoplasme et perturber le métabolisme normal de la cellule. Par exemple, des mitochondries altérées peuvent contribuer à augmenter la production de ERO alors qu'elles seraient éliminées en conditions normales (Butler *et al.*, 2006; Li *et al.*, 2012; Luchetti *et al.*, 2015).

Les lysosomes sont impliqués dans le processus normal de renouvellement des organites cellulaires via l'autophagie et sont également impliqués dans le vieillissement (Barja, 2019; Warraich *et al.*, 2020). Le 7KC induisant des dommages lysosomaux, pourrait participer de cette manière au processus de vieillissement en permettant l'accumulation de protéines et d'organites dysfonctionnels dans les cellules.

3.2.3 Mitochondrie

Les mitochondries sont des organites centraux dans le métabolisme cellulaire. Elles sont le siège de la production de l'adénosine triphosphate (ATP) et de cofacteurs (NADH, NADPH) via la phosphorylation oxydative, le cycle de Krebs et de la β-oxydation des acides gras. Elles interviennent dans diverses voies de signalisation et dans la mort cellulaire. Elles représentent la principale source d'ERO intracellulaires basale produits au cours de la phosphorylation oxydative. L'origine du 7KC étant principalement dû à la présence d'ERO, il n'est pas exclu que les mitochondries jouent un rôle important dans sa formation, en particulier lorsque leur métabolisme est perturbé et qu'il y a une surproduction d'ERO.

Il a été montré que le 7KC impactait directement les mitochondries et leur métabolisme (**Figure 9**). Dans les oligodendrocytes 158N, ces altérations sont caractérisées en premier lieu par une diminution de l'activité mitochondriale qui se traduit par une baisse du potentiel transmembranaire ($\Delta\psi m$) accompagnée par une réduction du NAD et de l'ATP. De plus, le taux de lactate est augmenté tandis que les taux de pyruvate, citrate, fumarate et succinate (intermédiaires du cycle de Krebs) sont diminués (Leoni *et al.*, 2017).

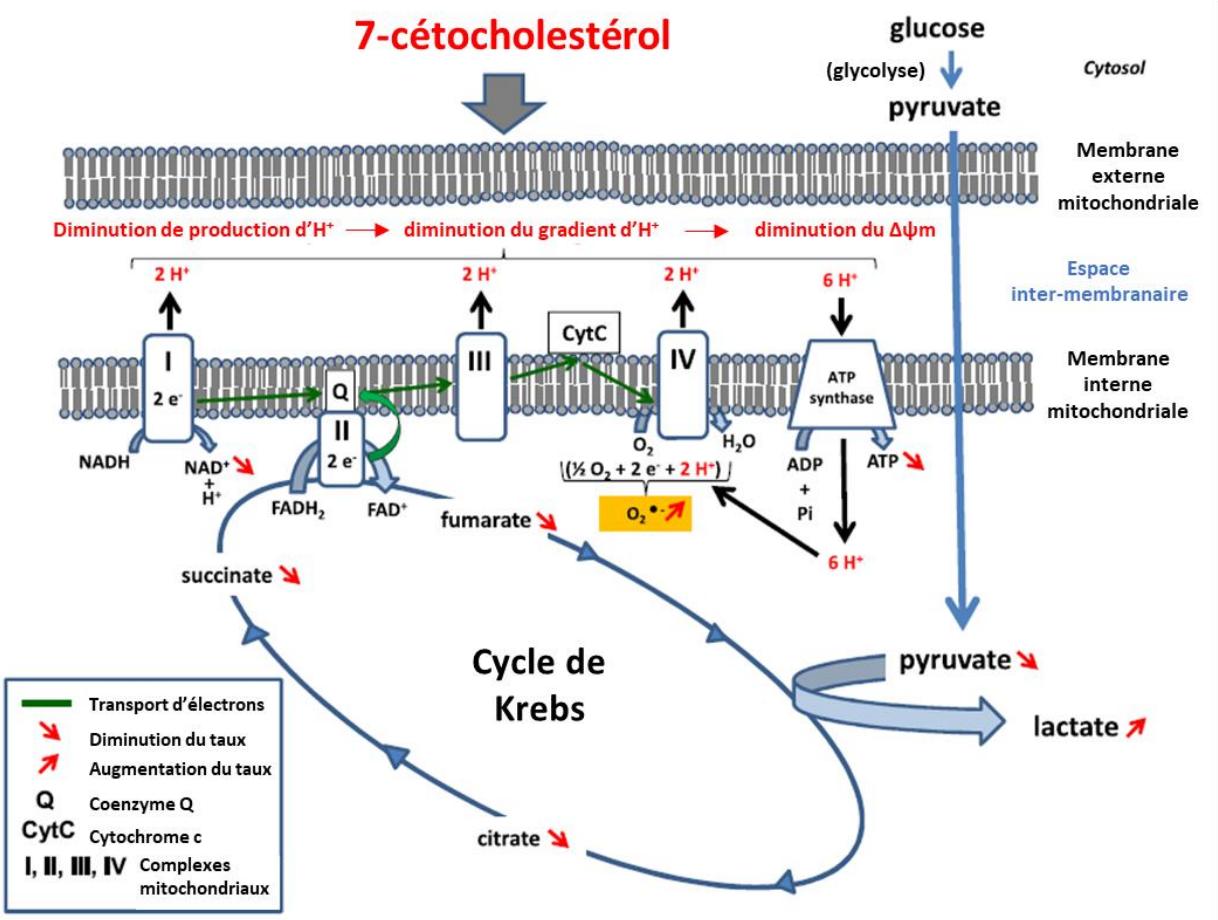

Figure 9 : Modifications de l'activité mitochondriale par le 7-cétocholestérol.
Lorsque les oligodendrocytes murins sont exposés à du 7KC, des modifications mitochondriales majeures sont observées. La chute du potentiel transmembranaire mitochondrial (Δψm) peut être considérée comme une conséquence de dysfonctionnements du cycle de Krebs conduisant par la suite à des perturbations de la phosphorylation oxydative. Cela favorise la surproduction d'anions superoxyde ($O2^{\cdot-}$) au niveau mitochondrial et contribuent à l'induction de la mort cellulaire induite par le 7KC. Adapté de (Leoni *et al.*, 2017).

Cette altération de l'activité mitochondriale, si elle est trop importante ou prolongée, conduit à la mort cellulaire par apoptose via un relargage du cytochrome c, une activation des caspases, une diminution de Bcl-2 et un clivage de PARP ainsi qu'une fragmentation internucléosomale de

l'ADN (Han *et al.*, 2007; Vejux *et al.*, 2020). D'après Fu *et al.*, le 7KC augmente la présence de miR144 qui diminue l'expression de l'isocitrate déshydrogénase 2 (IDH2) sur des cellules endothéliales aortiques et sur un modèle murin C57BL/6 (Fu *et al.*, 2014). De plus, les interactions métaboliques étroites entre les mitochondries et les autres organites (réticulum endoplasmique, peroxysomes) pourraient être perturbées en présence de 7KC, ce qui amplifierait les effets toxiques de ce dernier (Keenan *et al.*, 2020; Vejux *et al.*, 2020).

3.2.4 Peroxysome

Les effets du 7KC sur le réticulum, le lysosome et la mitochondrie sont assez bien connus et caractérisés. En revanche, les effets sur le peroxysome sont peu étudiés. Cet organite dont le métabolisme est impliqué dans de nombreuses voies et régulations métaboliques pourrait être une nouvelle cible du 7KC. Notre laboratoire a étudié la toxicité induite par le 7KC au niveau peroxysomal afin de caractériser les dysfonctions qu'il pourrait induire sur sa biogénèse et son métabolisme. Le 7KC, en perturbant le fonctionnement normal du peroxysome pourrait contribuer à l'aggravation de certaines pathologies.

Le peroxysome est présent dans le cytoplasme de toutes les cellules eucaryotes à l'exception des réticulocytes. Délimité par une membrane lipidique simple, il se présente généralement sous la forme d'une sphère de 0,1 à 1,5 µm de diamètre, il ne contient pas d'ADN (Trompier *et al.*, 2014). Il a été découvert pour la première fois par Rhodin en 1954 qui l'a d'abord qualifié de « microbody » lorsqu'il l'a observé dans le cytoplasme des cellules de rein de souris (De Duve *et al.*, 1966). Ce n'est qu'en 1956 que la désignation de « peroxysome » a été attribuée de façon définitive à cet organite à la suite de la découverte de sa première fonction par Christian de Duve, la dégradation du peroxyde d'hydrogène (H_2O_2) par la catalase en 2 molécules

d'H_2O et une molécule d'O_2. Par la suite, de nombreuses fonctions biologiques du peroxysome ont été identifiées. Le nombre et la taille des peroxysomes présents dans les cellules est très variable, il dépend notamment du type cellulaire ainsi que du statut métabolique. Afin de s'adapter aux conditions physiologiques (besoins énergétiques, statut redox, inflammation), le nombre, la morphologie et le contenu des peroxysomes sont des paramètres que les cellules doivent être en mesure de réguler rapidement et avec précision. Il existe différentes voies permettant de réguler la biogénèse et l'élimination des peroxysomes.

3.2.4.1 Biogénèse du peroxysome

A l'heure actuelle, il est admis que les peroxysomes sont formés à partir d'autres organites préexistants tels que le réticulum endoplasmique ou encore la mitochondrie (Fujiki, 2016; Kim, 2017; Sugiura *et al.*, 2017) mais aussi à partir de peroxysomes déjà matures par croissance, bourgeonnement puis fission. Ainsi, des pré-peroxysomes sont formés par bourgeonnement de membrane puis les protéines nécessaires à leur fonctionnement sont importées par différentes voies afin de former des peroxysomes matures. Depuis les années 1990, de nombreux gènes impliqués dans la biogénèse du peroxysome ont été identifiés codant pour des protéines appelées « peroxines » ou PEX. Pour l'instant, 36 peroxines ont été caractérisées (Fujiki *et al.*, 2020; Imanaka, 2019).

La formation de nouveaux peroxysomes nécessite l'action de différentes peroxines impliquées dans trois mécanismes principaux : le modelage de la membrane, l'import et l'assemblage des protéines membranaires peroxysomales (PMP) et l'import des protéines de la matrice.

Depuis leur découverte, plusieurs théories sur la biogenèse des peroxysomes se sont succédées. La première affirmait qu'il s'agissait d'organites autonomes qui se multipliaient uniquement par

fission de peroxysomes préexistants (Lazarow *et al.*, 1985), tandis que la seconde supposait que les peroxysomes pouvaient être formés à partir de bourgeonnements du RE (Geuze *et al.*, 2003). A l'heure actuelle, c'est la seconde hypothèse qui semble être la plus probable. En effet, il a été montré que la peroxine PEX16, impliquée dans la formation de la membrane du peroxysome, se trouve également dans la membrane du RE (Kim *et al.*, 2006). Depuis quelques années, il semble aussi que la mitochondrie joue également un rôle dans la biogenèse des peroxysomes. En effet, certaines protéines membranaires mitochondriales comme PEX3 ou la protéine *Mitochondrial fission factor* (MFF) et la protéine *Mitochondrial fission 1* (FIS1), qui sont impliquées dans la fission des mitochondries, se retrouvent également dans la membrane peroxysomale où elles interviennent dans la fission du peroxysome (**Figure 10**) (Hua *et al.*, 2016; Kim, 2017).

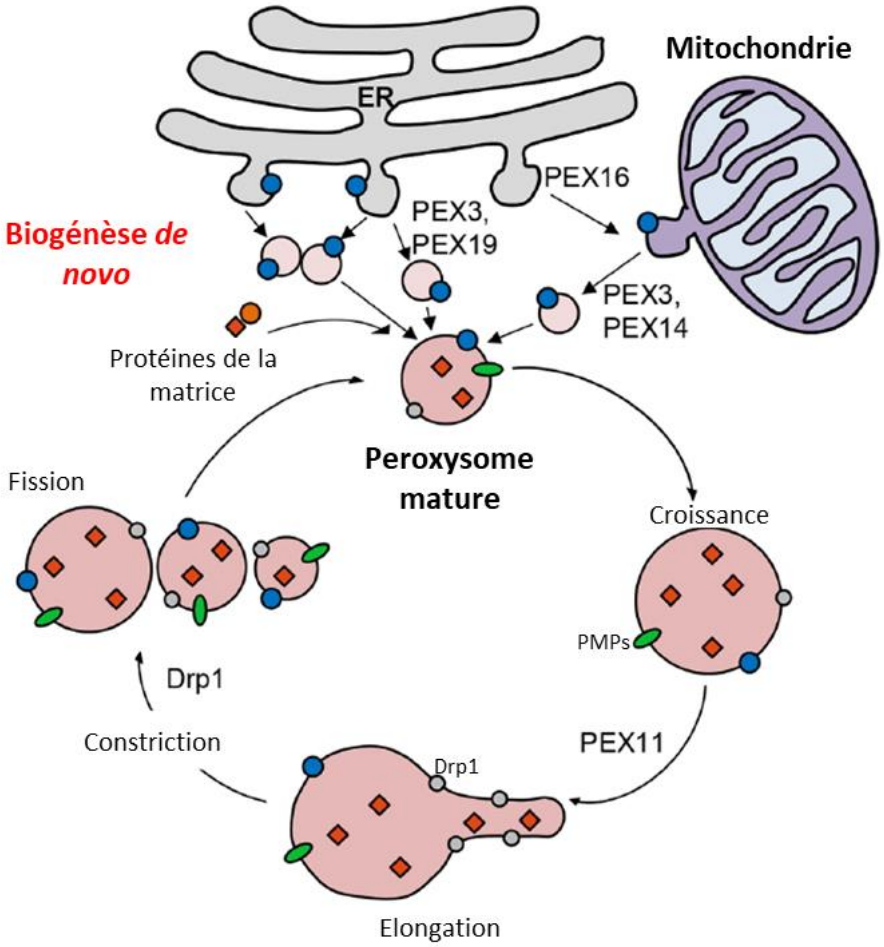

Figure 10 : Biogénèse du peroxysome chez les Mammifères
Il existe deux voies de biogénèse peroxysomale : La première est la synthèse *de novo*. Les peroxysomes peuvent être formés à partir de vésicules issues du RE et/ou de la mitochondrie (pré-peroxysome) qui portent des peroxines telles que PEX3 et PEX16 dont le rôle est de permettre la maturation des pré-peroxysomes via l'import des protéines (PMPs et protéines de la matrice). La seconde voie est la division de peroxysome existant. PEX11 et DRP1 jouent un rôle dans l'élongation et la fission des peroxysomes. Adapté de (Cho *et al.*, 2018).

3.2.4.2 Formation de la membrane peroxysomale

Chez les mammifères, trois peroxines sont impliquées dans la formation de la membrane et dans l'import des protéines membranaires peroxysomales (PMP) : PEX19, PEX3 et PEX16 (**Figure 11**) (Fujiki, 2016; Imanaka, 2019).

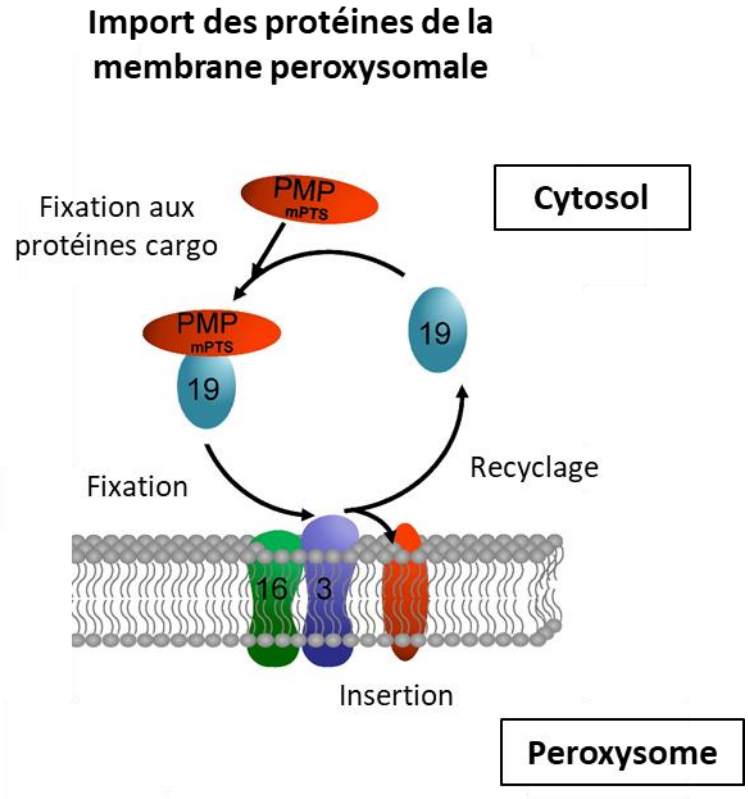

Figure 11 : Import des protéines peroxysomales membranaires
L'import des protéines de la membrane peroxysomale (PMPs) se fait via l'action de PEX19 qui reconnait le signal mPTS porté par les PMPs. PEX19 se fixe ensuite sur PEX3 tandis que PEX16 agit comme stabilisateur. La PMP est alors insérée dans la membrane du peroxysome et PEX19 est relarguée dans le cytosol pour renouveler l'opération. Adapté de (Waterham *et al.*, 2016).

PEX19 est une protéine chaperonne, principalement cytosolique, qui reconnait le « membrane Peroxisomal Targeting Signal » (mPTS) porté par les PMPs. Lorsque PEX19 est liée à une PMP, elle peut ensuite interagir avec PEX3 qui est localisée dans la membrane peroxysomale. Cela permet l'intégration de la PMP à la membrane lorsqu'elle est libérée par PEX19 qui retourne ensuite dans le cytoplasme pour renouveler l'opération. PEX16 agit comme un stabilisateur dans la fixation de PEX19 sur PEX3. PEX3 et PEX16 font aussi partie de la membrane du RE, ce qui justifie l'implication de ce dernier dans la biogénèse des peroxysomes. Des dysfonctions ou mutations de ces trois protéines entraînent des maladies peroxysomales caractérisées par une

absence de peroxysomes (ou peroxysomes fantômes) connues sous l'appellation de syndrome de Zellweger (Fujiki *et al.*, 2020).

3.2.4.3 Fission du peroxysome

Les peroxysomes sont capables de se diviser de manière autonome au même titre que la mitochondrie. Ainsi, leur nombre peut être ajusté en fonction des besoins métaboliques des cellules. La multiplication des peroxysomes par fission implique plusieurs protéines dont PEX11 ainsi que MFF, FIS1 et la *Dynamin-related protein 1* (DRP1) qui font également partie des protéines de fission mitochondriales (Schrader *et al.*, 2012). Au cours de ce processus, la membrane peroxysomale va s'allonger puis subir une constriction puis enfin une fission/division. Dans un premier temps, PEX11 (protéine transmembranaire) va s'activer au niveau de la membrane pour initier une élongation tubulaire d'un côté du peroxysome. Par la suite, cette extension commence à acquérir de nouvelles PMPs ainsi que des protéines de la matrice. PEX11 et le complexe MFF/DRP1 se concentrent aux sites de constriction en un large complexe en anneau qui hydrolyse le guanosine triphosphate (GTP) en se resserrant jusqu'à la fission en plusieurs peroxysomes. FIS1 semble jouer un rôle régulateur. Les nouveaux peroxysomes obtenus continuent à importer des protéines jusqu'à devenir matures à leur tour.

3.2.4.4 Importation des protéines matricielles peroxysomales : implication du « peroxisomal targeting signal » (PTS)

Le peroxysome étant dépourvu d'ADN, il est nécessaire que les protéines indispensables à son activité métabolique soient importées depuis le cytoplasme. Une dizaine de peroxines sont impliquées dans l'import de protéines vers le peroxysome : PEX1, PEX2, PEX5, PEX6, PEX7, PEX10, PEX12, PEX13, PEX14 et PEX26 (Fujiki, 2016).

Afin qu'une protéine puisse être dirigée vers le peroxysome, elle doit être porteuse d'un signal d'adressage appelé PTS (peroxisomal targeting signal). Il existe deux signaux différents : PTS1 et PTS2. PTS1 est un tripeptide (S/A/C)-(K/R/H)-(L/M) situé à l'extrémité COOH-terminale de la majorité des protéines de la matrice peroxysomale, tandis que PTS2 est un nonapeptide constitué d'une séquence consensus répétée (L/I/K)-X5-(Q/H)-(L/I/V) située à l'extrémité NH_2-terminale des protéines.

Les protéines synthétisées *de novo* et porteuses du signal PTS1 sont reconnues par PEX5 et celles porteuses du signal PTS2 sont reconnues par PEX7. PEX7 a ensuite besoin de reconnaitre PEX5 pour pouvoir atteindre le peroxysome.

PEX5 se fixe à la membrane peroxysomale au niveau d'un complexe oligomérique formé par PEX13 et PEX14. Ce premier complexe interagit avec un second constitué de PEX2, PEX10 et PEX12 (complexe Really Interesting New Gene : RING). Après fixation de PEX5 aux complexes, la protéine d'intérêt est transloquée à l'intérieur du peroxysome via l'action de PEX8, puis PEX5 et PEX7 sont relarguées dans le cytoplasme pour effectuer un nouvel import ou pour être dégradées par le protéasome (Waterham *et al.*, 2016). Cette étape nécessite l'activité ubiquitine ligase du complexe RING (PEX2, PEX10, PEX12), qui va mono- ou poly-ubiquitinyler PEX5. Une mono-ubiquitinylation de PEX5 va permettre son recyclage dans le cytoplasme tandis qu'une poly-ubiquitinylation la dirigera vers le protéasome pour sa dégradation. PEX1, PEX6, PEX26p forment un complexe également impliqué dans l'ubiquitinylation de PEX5 (**Figure 12**).

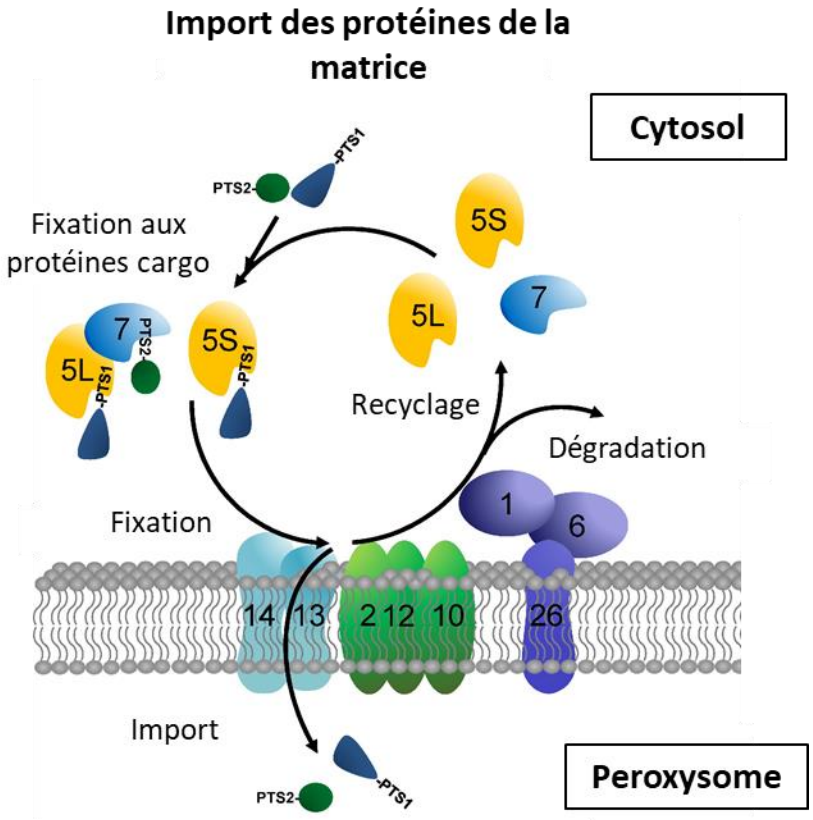

Figure 12 : Import des protéines matricielles peroxysomales
Schématisation des voies d'imports des protéines de la matrice. Les signaux PTS1 et PTS2 portés par les protéines de la matrice sont reconnus respectivement par PEX5 et PEX7. PEX5 se fixe au niveau de la membrane peroxysomale sur le complexe PEX13/PEX14 qui interagit avec le complexe RING (PEX2/PEX10/PEX12). La protéine matricielle est relarguée dans le peroxysome. Le complexe PEX1/PEX6/PEX26 est impliqué dans l'ubiquitinylation de PEX5 pour permettre son recyclage ou sa dégradation vers le protéasome. Adapté de (Waterham *et al.*, 2016).

3.2.4.5 Prolifération peroxysomale : implication du récepteur PPAR (Peroxisome Proliferator-Activated Receptor)

Les peroxysomes sont des organites dynamiques dont le nombre peut être ajusté en fonction des besoins métaboliques des cellules en réponse à des stimuli environnementaux. Leur nombre peut croitre par prolifération ou diminuer par dégradation. La prolifération peroxysomale est hautement régulée par des cascades de signalisation se terminant au niveau du noyau grâce à

des facteurs de transcription qui peuvent agir sur l'expression des gènes peroxysomaux. Généralement, les signaux d'activation de la prolifération peroxysomale sont des signaux externes tels que des acides gras ou encore des fibrates (Manickam *et al.*, 2017). Chez les mammifères, la voie principale de régulation est la voie impliquant le « peroxisome proliferator-activated receptor α » (PPARα).

Il existe trois membres de la famille PPAR : PPARα, PPARβ/δ et PPARγ. Ces derniers ne sont pas exprimés de façon équivalente en fonction des tissus et des types cellulaires. PPARα est fortement exprimé dans les tissus ayant une activité d'oxydation des acides gras élevée, comme le tissu adipeux brun, le foie, le rein, le cœur et le muscle squelettique. PPARβ est exprimé de façon ubiquitaire mais en majorité dans l'intestin, le rein et le cœur. Il est généralement plus exprimé que PPARα et PPARγ. Enfin, PPARγ est exprimé principalement dans le tissu adipeux et dans une moindre mesure dans l'intestin et les cellules du système immunitaire (Manickam *et al.*, 2017).

Lorsqu'un ligand agoniste de PPAR se fixe sur ce dernier, un changement de conformation s'opère au niveau du domaine de fixation de PPAR. Le complexe PPAR/ligand se transloque ensuite dans le noyau et s'hétérodimérise avec un autre facteur de transcription, le retinoid-X-receptor (RXR). Ce nouveau complexe PPAR/RXR est ensuite capable de reconnaitre et de se fixer sur l'ADN au niveau d'une séquence : peroxisome proliferator response element (PPRE), située dans la région promotrice des gènes peroxysomaux (Schrader *et al.*, 2016).

3.2.4.6 Dégradation des peroxysomes

La dégradation des peroxysomes est un processus aussi important que leur biogénèse afin de maintenir un équilibre métabolique dans la cellule. Ainsi, la durée de vie d'un peroxysome est de 1,5 à 2 jours. Il existe différentes voies permettant de dégrader les peroxysomes : soit par

autolyse de la membrane (20 à 30 % de la dégradation), soit par autophagie (70 à 80 % de la dégradation (Germain *et al.*, 2020) (**Figure 13**).

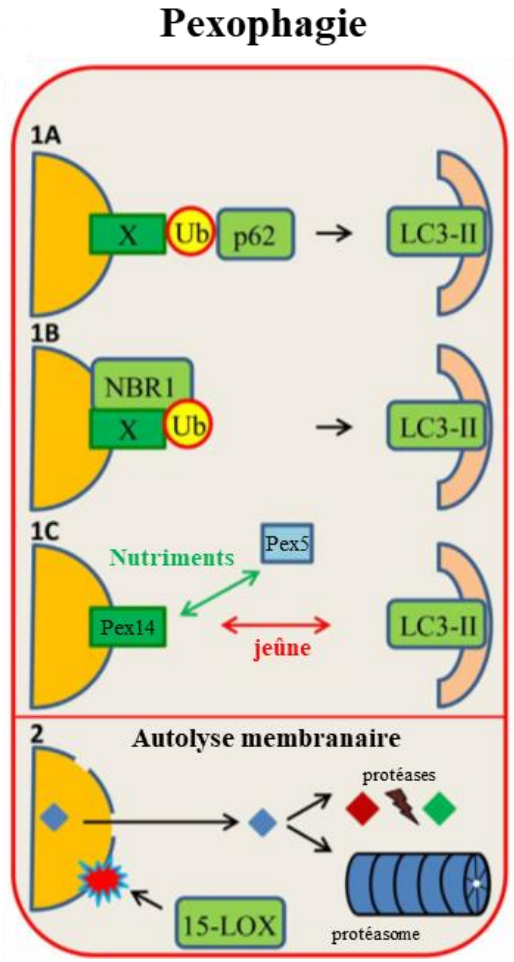

Figure 13 : Schéma des différentes voies de dégradation du peroxysome
1A) Les PMPs ubiquitinylées à la surface des peroxysomes sont reconnues par la protéine p62 qui se lie à son tour à l'autophagosome en formation via LC3-II. **1B)** La protéine NBR1 reconnait les PMPs ubiquitinylées. NBR1 peut ensuite se fixer sur LC3-II de la même manière que p62. **1C)** Dans des conditions nutritives normales, PEX14 est située dans la membrane peroxysomale et interagit avec PEX5. A l'inverse, en conditions de restrictions nutritives, l'affinité de PEX14 pour PEX5 diminue au profit de LC3-II. **2)** La voie de l'autolyse implique la 15-lipoxygénase (15-LOX). Cette dernière catalyse la conversion d'acides gras poly-insaturés en conjugués hydroperoxides, ce qui entraine une rupture de la membrane peroxysomale et sa lyse. Adapté de (Nordgren *et al.*, 2013).

La voie majoritaire de dégradation des peroxysomes consiste en une dégradation spécifique des peroxysomes par autophagie : la pexophagie. Ce processus cellulaire de recyclage consiste à ce

que les peroxysomes qui doivent être dégradés soient pris en charge par les autophagosomes pour être détruits. Il semble que ces trois processus menant à la pexophagie puissent avoir lieu :

- Le premier implique la reconnaissance de PMPs qui ont été ubiquitinylées par les E3 ubiquitine ligases à la surface des peroxysomes. Ces dernières sont reconnues par la protéine p62 qui se lie à son tour à l'autophagosome en formation via LC3-II (**Figure 13, A**).
- Le second processus implique la protéine NBR1 qui est capable de reconnaitre les PMPs ubiquitinylées ou de se fixer directement à la membrane peroxysomale. NBR1 peut ensuite se fixer sur LC3-II de la même manière que p62 (**Figure 13, B**).
- Le dernier processus se produit en cas de restriction en nutriments. Dans des conditions normales, PEX14 est située dans la membrane peroxysomale et interagit avec PEX5. En conditions de restrictions, l'affinité de PEX14 pour PEX5 diminue au profit de LC3-II, ce qui dirige le peroxysome vers l'autophagosome (**Figure 13, C**).

La voie de l'autolyse implique la 15-lipoxygénase (15-LOX). Cette dernière catalyse la conversion d'acides gras poly-insaturés en conjugués hydroperoxides (Nordgren *et al.*, 2013; Yokota *et al.,* 2001), ce qui entraine une rupture de la membrane peroxysomale et sa lyse.

3.2.4.7 Rôles du peroxysome

Le peroxysome prend part à de nombreuses voies métaboliques au sein de la cellule et peut par conséquent être impliqué dans diverses maladies. Il participe au catabolisme des ERO et ERA, à la synthèse des plasmalogènes, à la β-oxydation des acides gras, au métabolisme du glyoxylate et au catabolisme des acides aminés.

3.2.4.7.1 Métabolisme des espèces réactives de l'oxygène et de l'azote

La première fonction biologique du peroxysome qui a été découverte par Christian De Duve en 1966 est sa capacité à métaboliser le peroxyde d'hydrogène (H_2O_2) (De Duve *et al.*, 1966) : soit de façon catalytique : 2 H_2O_2 en O_2 + 2 H_2O, soit de façon peroxydique : 2 H_2O_2 +AH_2 en A + 2 H_2O où AH_2 est un donneur d'hydrogène tel que l'éthanol, le méthanol, le formaldéhyde, le formate ou encore le nitrite (Tomanek, 2015; Wanders *et al.*, 2006).

La catalase catalyse la réaction : 2 H_2O_2 en O_2 + 2 H_2O, mais d'autres enzymes peroxysomales sont aussi capables de cataboliser l'H_2O_2 : la glutathion peroxydase et la peroxyredoxine V. Des anions superoxides ($O_2^{\cdot -}$) peuvent être générés au niveau peroxysomal par la xanthine oxydase. La dégradation de l'anion superoxyde est prise en charge par les superoxyde dismutases telle que la Cu/Zn-SOD et la Mn-SOD au niveau peroxysomal (Ganguli *et al.*, 2019; Ghosh *et al.*, 1996; Schrader *et al.*, 2006).

Les peroxysomes contiennent aussi une activité nitric oxide synthase (NOS) (Del Rio, 2011). En réagissant avec les anions superoxydes, le $NO^{\cdot}$ forme des peroxynitrites ($ONOO^-$) qui sont dégradés par la peroxyredoxine V. Une activité époxyde hydrolase soluble (époxyde hydrolase 2) a également été identifiée dans les peroxysomes (Harris *et al.*, 2013; Waechter *et al.*, 1983). Enfin, le peroxysome contient une activité glutathion-S-transférase (GST), il s'agit de la GSTK1, et de la microsomal GST1 (MGST1), qui est aussi mitochondriale (Fransen *et al.*, 2012; Higgins *et al.*, 2011) (**Figure 14**).

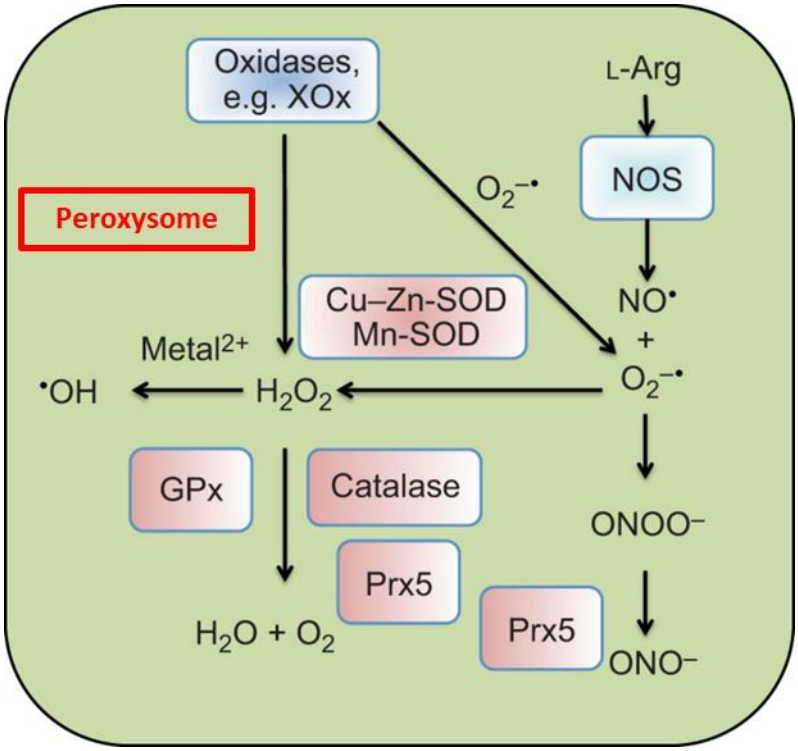

Figure 14 : Métabolisme des espèces réactives de l'oxygène et de l'azote dans le peroxysome
La production d'anions superoxydes ($O_2^{\cdot-}$) par la xanthine oxydase et de $NO^{\cdot}$ par la NOS mène à la formation de peroxynitrites ($ONOO^-$). La catalase et la glutathion peroxydase dégradent l'H_2O_2 tandis que les SOD dégradent l'$O_2^{\cdot-}$. La peroxiredoxine V (Prx5) prend en charge les peroxynitites.

3.2.4.7.2 Biosynthèse des plasmalogènes

Les éthers de phospholipides, font partie des phospholipides et sont caractérisés par la présence d'une liaison éther en position *sn-1* du glycérol (**Figure 15**). Dans la famille des éthers de phospholipides, on distingue deux groupes : ceux avec une liaison éther et ceux avec une liaison vinyl-éther qui forment les plasmalogènes. Le groupement lié en *sn-1* des plasmalogènes est un acide gras qui peut être un C16:0 (acide palmitique), un C18:0 (acide stéarique) ou C18:1 n-9 (acide oléique (AO)). La position *sn-2* est occupée par un acide gras poly-insaturé (AGPI)

tandis que le troisième groupement, lié par l'intermédiaire d'un phosphate est une éthanolamine ou une choline (Brites *et al.*, 2004).

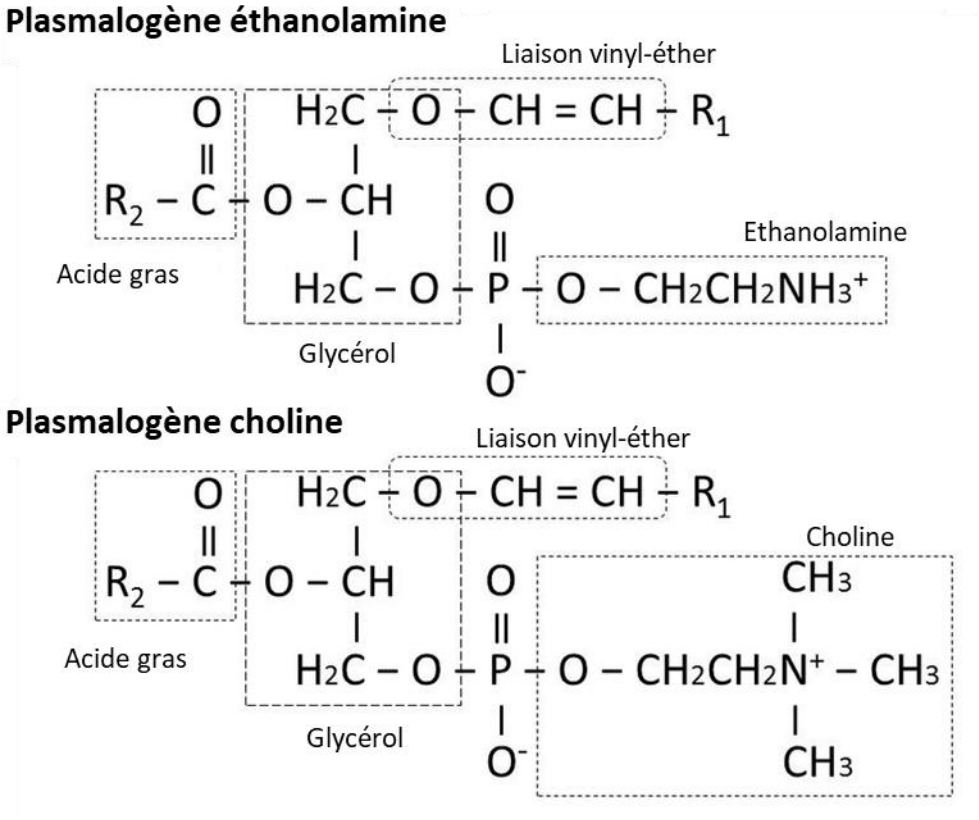

Figure 15 : Structure des plasmalogène éthanolamine et des plasmalogènes choline.
La famille des éthers de phospholipides est constituée de deux groupes : ceux avec une liaison éther et ceux avec une liaison vinyl-éther qui forment les plasmalogènes. Le groupement lié en *sn-1* des plasmalogènes est un acide gras qui peut être un C16:0 (acide palmitique), un C18:0 (acide stéarique) ou C18:1 n-9 (acide oléique (AO)). La position *sn-2* est occupée par un acide gras poly-insaturé (AGPI) tandis que le troisième groupement, lié par l'intermédiaire d'un phosphate est une éthanolamine ou une choline. Adapté de (Takeshi Arita, 2018).

Chez l'Homme, les plasmalogènes représentent 18% du total des phospholipides. La répartition des plasmalogènes peut varier en fonction des tissus et des organes. Par exemple, le cerveau et plus particulièrement la myéline, contient une majorité de plasmalogènes à éthanolamine tandis que le cœur contient plutôt des plasmalogènes à choline. Des taux de plasmalogènes plus faibles

sont retrouvés dans les reins, les muscles squelettiques, la rate, le foie et les cellules sanguines (Wanders *et al.*, 2006).

La biosynthèse des plasmalogènes à lieu en partie au niveau du peroxysome, ce qui en fait une étape limitante dans le sens où des altérations de ce dernier peuvent entrainer des problèmes de synthèse des plasmalogènes (**Figure 16**).

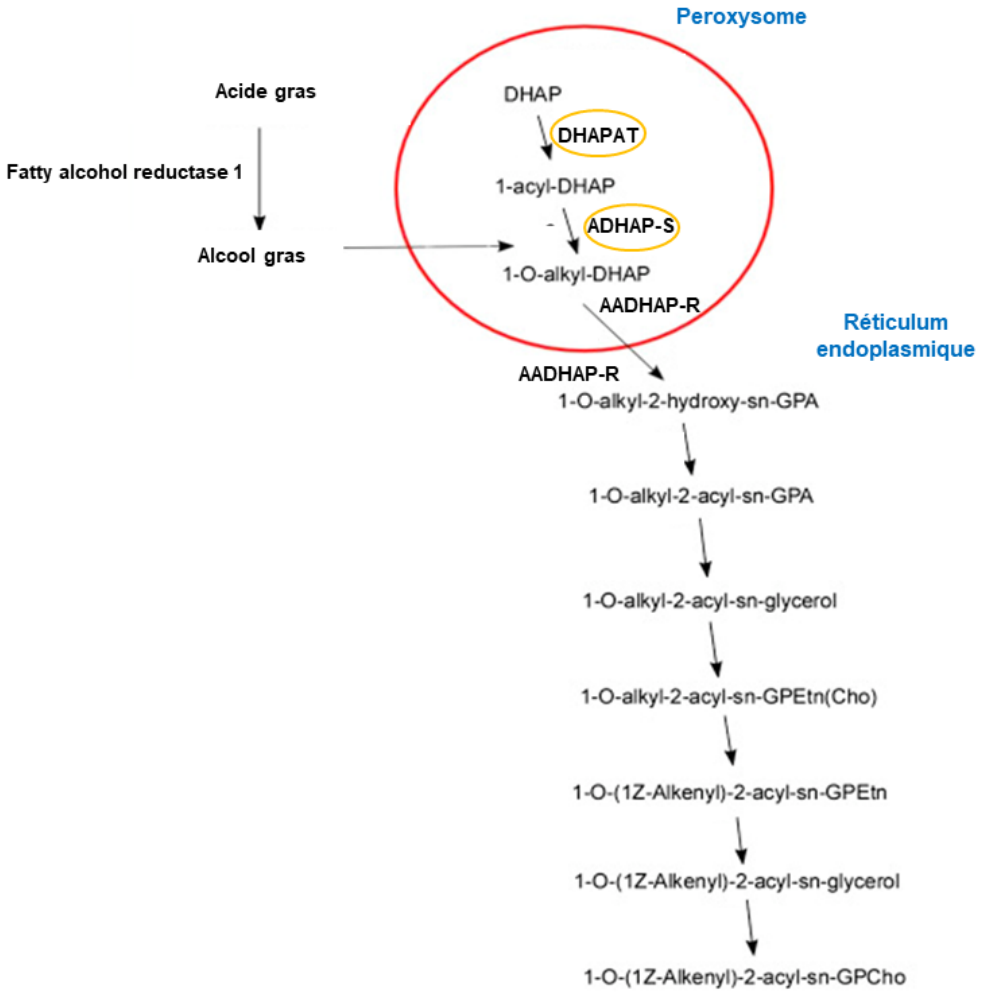

Figure 16 : Voie de synthèse des plasmalogènes
Les deux premières étapes de la synthèse des plasmalogènes ont lieu dans le peroxysome. Le dihydroxyacétone phosphate (DHAP) est converti en acyl-DHAP puis en alkyl DHAP respectivement par la dihydroxyacétone phosphate acyltransférase (DHAPAT) et l'alkyl-dihydroxyacétone phosphate synthase (ADHAP-S). La troisième étape qui transforme l'alkyl-DHAP en alkyl-G3P par action de l'acyl/alkyl- dihydroxyacétone phosphate réductase (AADHAP-R) ont lieu à la fois dans le peroxysome et dans le réticulum endoplasmique. Les autres étapes de synthèse ont lieu dans le RE. Adapté de (Braverman *et al.*, 2012).

En effet, les deux premières enzymes nécessaires à leur formation sont peroxysomales. La première étape de leur synthèse consiste en une estérification du dihydroxyacétone phosphate (DHAP) avec un acyl-CoA à longue chaine par la dihydroxyacétone phosphate acyltransférase (DHAPAT), ceci donne un 1-acyl-DHAP. La seconde étape implique l'alkyl-dihydroxyacétone phosphate synthase (ADHAP-S) qui utilise le 1-acyl-DHAP comme substrat en remplaçant en l'acide gras position *sn-1* par un alcool gras pour donner un 1-alkyl-DHAP. La DHAPAT et l'ADHAP-S forment un complexe hétérodimérique (Biermann *et al.*, 1999; Brites *et al.*, 2004). La troisième étape qui consiste à réduire la fonction cétone en position *sn-2* de l'alkyl-DHAP est effectuée par l'acyl/alkyl- dihydroxyacétone phosphate réductase (AADHAP-R), elle donne un 1-alkyl-glycérol-3-phosphate (1-alkyl-G3P). Cette réaction peut avoir lieu dans le peroxysome mais également dans le réticulum endoplasmique. Les étapes suivantes de la synthèse des plasmalogènes ont toute lieu dans le RE.

3.2.4.7.3 β-oxydation des acides gras

Une autre fonction importante du peroxysome dans le métabolisme lipidique est la β-oxydation des acides gras. Tout comme la mitochondrie, le peroxysome a la capacité de réaliser la β-oxydation de différents acides gras bien que les enzymes respectives ne soient pas codées par les mêmes gènes. En effet, les anomalies de β-oxydation chez des malades ne donnent pas les mêmes symptômes en fonction de leur origine mitochondriale ou peroxysomale (Munn *et al.*, 2003; Rinaldo *et al.*, 2002).

Une des différences entre la β-oxydation peroxysomale et mitochondriale est le substrat de départ. Les acides gras à chaine courte (C < 6) et moyenne (C6 à C12) sont β-oxydés exclusivement par la mitochondrie. Les acides gras à chaine longue (C12 à C22) sont oxydés

dans la mitochondrie et le peroxysome tandis que les acides gras à très longue chaîne (AGTLC) ($C \geq 22$) sont oxydés exclusivement dans le peroxysome avant de terminer leurs cycles de β-oxydation dans la mitochondrie.

Pour être β-oxydés, les acides gras doivent entrer dans le peroxysome. Pour cela, ils doivent être activés en acyl-CoA afin d'être pris en charge par les transporteurs membranaires peroxysomaux ABCD, dont on distingue trois transporteurs différents : ABCD1, ABCD2 et ABCD3. Ces transporteurs ont des sensibilités de substrats différents : ABCD1 et ABCD2 ont des fonctions redondantes et transportent principalement les acides gras saturés et mono-insaturés. Cependant, ABCD1 présente une spécificité plus importante pour le C24:0 et le C26:0 que ABCD2. ABCD2 présente une spécificité plus importante pour les acides gras poly-insaturés C22:6 et C24:6. ABCD3 est impliqué dans le transport des acides gras à chaine longue, des acides gras branchés, (acide pristanique et phytanique), ainsi que des acides di- et tri-hydroxycholestanoïques (DHCA et THCA) (Kawaguchi *et al.*, 2016).

A chaque cycle de β-oxydation peroxysomale plusieurs réactions enzymatiques se succèdent : α,β-déshydrogénation, hydratation (de la double liaison), déshydrogénation à nouveau et enfin clivage thiolytique. Les acides gras se retrouvent raccourcis de deux atomes de carbones et un acétyl-coenzyme A (acétyl-CoA) est formé (**Figure 17**) (Kemp *et al.*, 2011).

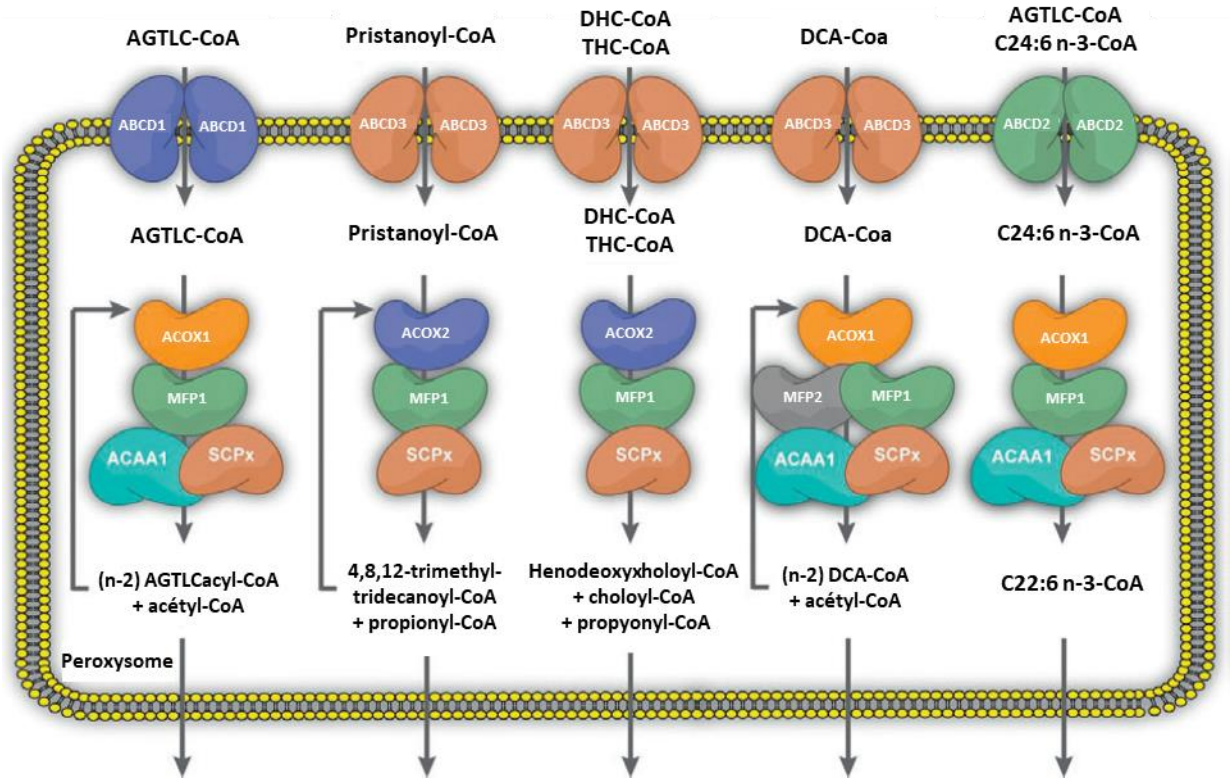

Figure 17 : Transport et β-oxydation peroxysomale des acides gras
Fonctions des transporteurs ABC peroxysomaux de mammifères dans l'importation d'AGTLC, d'acide pristanique, d'acide di- et trihydroxycholestanoïque (DHCA et THCA), d'acide dicarboxylique (DCA) et d'acide tétracosahexaénoïque (C24:6 n-3) vers le peroxysome. Les peroxysomes contiennent la machinerie enzymatique complète pour β-oxyder les acides gras. Les premières enzymes sont deux acyl-CoA oxydases (ACOX1 et ACOX2), la seconde étape implique une protéine bifonctionnelle comportant deux sous-unités (MFP1 et MFP2), la troisième étape est réalisée par deux autres enzymes, les thiolases (ACAA1 et SCPx). Pour une β-oxydation complète, les produits finaux doivent être ensuite transférés dans les mitochondries. Adapté de (Kemp *et al.*, 2011).

Parmi les enzymes nécessaires à la β-oxydation, la première à entrer en jeu est l'acyl-CoA oxydase (ACOX). Il existe trois ACOX différentes (la palmytoyl-CoA oxydase ACOX1, la cholestanoyl-CoA oxydase ACOX2 et la pristanoyl-CoA oxydase ACOX3) (Kemp *et al.*, 2011). La seconde enzyme de la β-oxydation est une enzyme bi-fonctionnelle qui comporte deux sous-unités ayant deux activités différentes : enoyl-CoA hydratase et 3-hydroxy-acyl-CoA déshydrogénase. Cette enzyme est souvent nommée MFP2 (Huyghe *et al.*, 2006). Enfin, la

dernière étape du clivage thiolytique implique une thiolase. On trouve deux thiolases chez l'Homme (ACAA1 et SCPx) et trois chez les rongeurs (thiolase A, thiolase B et SCPx).

D'autres substrats ne peuvent être dégradés que dans le peroxysome. On trouve l'acide pristanique (acide 2,4,6,10-tétraméthylpentacholestanoic) ainsi que son précurseur, l'acide phytanique (converti en acide pristanique par α-oxydation) et les précurseurs d'acides biliaires : les acides di- et tri-hydroxycholestanoïques, les acides dicarboxyliques et certains acides gras polyinsaturés comme l'acide tétracosahexaénoïque (THA ; C24:6 n-3) qui donne l'acide docosahexaénoïque (DHA ; C22:6 n-3) après un cycle de β-oxydation. On trouve également certaines prostaglandines et leucotriènes ainsi que les vitamines E et K (Wanders, 2004; Wanders *et al.*, 2006).

Les produits de la β-oxydation sont ensuite exportés vers le cytoplasme puis vers la mitochondrie pour terminer leurs cycles de β-oxydation. Pour cela, deux enzymes peroxysomales : la carnitine octanoyltransférase (COT) et la carnitine acétyltransférase (CAT) sont impliquées. Elles permettent de substituer l'acyl-CoA sur les acides gras par une acylcarnitine via une trans-estérification. Ainsi, les acides gras peuvent sortir du peroxysome pour entrer dans les mitochondries par un transporteur (carnitine-acylcarnitine translocase ACAT) (Houten *et al.*, 2020).

Le peroxysome est également capable de réaliser l'α-oxydation des acides gras. Cette réaction concerne les acides gras avec un groupement méthyl sur le carbone 3 qui bloque la β-oxydation. L'α-oxydation consiste à retirer un carbone du côté carboxyle (-COOH) de l'acide gras, de façon que le groupement méthyl se situe ensuite en position 2. De cette manière, l'acide gras résultant peut être β-oxydé classiquement dans le peroxysome. L'α-oxydation convertit l'acide phytanique en acide pristanique. Une déficience en α-oxydation induit une accumulation en acide phytanique et est connue sous le nom de maladie de Refsum (Wanders, 2004).

3.2.4.7.4 Métabolisme du glyoxylate

Chez l'Homme, le glyoxylate est formé dans les mitochondries, le cytosol ou les peroxysomes comme intermédiaire dans le cycle du glyoxylate. Ce cycle est un dérivé du cycle de Krebs qui prévient la conversion du glyoxylate en oxalate, toxique pour la cellule. On retrouve dans les peroxysomes du foie l'alanine: glyoxylate aminotransférase (AGT), qui utilise l'alanine pour convertir le glyoxylate en glycine et l'empêche de s'accumuler pour donner de l'oxalate par action de la lactate déshydrogénase (LDH) (Wanders *et al.*, 2018).

3.2.4.7.5 Catabolisme des acides aminés

Les peroxysomes contiennent une D-amino acide oxydase qui oxyde les D-isomères des acides aminés neutres et basiques, ainsi qu'une D-aspartate oxydase qui oxyde les acides aminés acides (Van Veldhoven *et al.*, 1991). De plus, les peroxysomes contiennent aussi une glutaryl-CoA oxydase (peroxysomale et mitochondriale) qui convertit la lysine, l'hydroxylysine et le tryptophane en glutaryl-CoA (Vamecq *et al.*, 1984).

3.2.4.7.6 Autres fonctions du peroxysome

Outre les fonctions métaboliques majeures décrites précédemment, le peroxysome possède d'autres activités : une implication dans la voie des pentoses phosphates (Antonenkov, 1989; Wanders *et al.*, 2006), dans l'oxydation des polyamines (Wu *et al.*, 2003), dans le métabolisme des isoprénoïdes et du cholestérol (Kovacs *et al.*, 2003). En effet, plusieurs enzymes participant à la synthèse du cholestérol sont peroxysomales : l'acétoacétyl-CoA thiolase, l'HMG-CoA synthase, l'hydroxy-méthyl-glutaryl-CoA réductase, la mévalonate kinase, la phosphomévalonate kinase, la mévalonate diphosphate décarboxylase, l'isopentényl diphosphate

isomérase et la farnésyl diphosphate synthase (Faust *et al.*, 2014; Kovacs *et al.*, 2003). Enfin, le peroxysome peut être impliqué dans la réponse immunitaire et l'inflammation (Di Cara *et al.*, 2019).

Le peroxysome contribue à de nombreuses voies métaboliques, toute modification ou perturbation de ce dernier peut avoir des conséquences importantes sur l'homéostasie cellulaire et induire des maladies graves. Des facteurs intrinsèques d'origine génétique, mais aussi extrinsèques environnementaux, pourraient participer aux dysfonctions peroxysomales. Ainsi, le 7KC formé de façon endogène ou apporté par l'alimentation pourrait prendre part à l'altération des peroxysomes.

3.2.4.7.7 Dysfonctions peroxysomales induites par le 7KC

Il a été montré que le 7KC pouvait induire des modifications peroxysomales au niveau de son métabolisme, notamment en provoquant une diminution de l'expression de transporteurs membranaires peroxysomaux tels que ABCD1, ABCD2 et ABCD3 (fréquemment utilisé en tant que marqueur de masse peroxysomale) mais également au niveau d'enzymes impliquées dans la β-oxydation des acides gras à très longue chaine (ACOX1, MFP2) sur des cellules microgliales BV-2 (Debbabi *et al.*, 2016). Sur la même lignée cellulaire, le 7KC induit également une diminution de l'expression de PEX14 (peroxine impliquée dans la biogénèse des peroxysomes) et de l'ACOX1 tandis que l'activité de la catalase est augmentée (Nury *et al.*, 2017). Dans le contexte de l'X-ALD, qui est une maladie génétique peroxysomale caractérisée par une mutation du gène ABCD1, des taux élevés de 7KC plasmatiques ainsi d'autres marqueurs de stress oxydant (9/13-HODE, 7β-OHC) ont été mesurés. Il est supposé que le 7KC amplifierait les effets

de la maladie au niveau peroxysomal mais également au niveau des autres organites (Nury *et al.*, 2017). Des effets comparables ont été montrés sur les oligodendrocytes murins 158N au niveau des transcrits ABCD1, ABCD3, ACOX1 et MFP2 (Badreddine *et al.*, 2017; Vejux *et al.*, 2020). Ces effets du 7KC sur le peroxysome et son activité se traduisent par une accumulation d'AGTLC aussi connus pour leur toxicité (Nury *et al.*, 2018).

Les mécanismes de toxicité du 7KC sur le peroxysome ne sont pas connus à l'heure actuelle. Néanmoins, il est peu probable que la toxicité du 7KC passe par une inactivation des récepteurs PPARs puisque des agonistes (fibrates) n'ont pas d'effet. L'utilisation d'agonistes et d'antagonistes de LXR ne modifie pas non plus la toxicité du 7KC. En revanche, la diminution du métabolisme du cholestérol et des altérations probables de son transport intracellulaire pourrait impacter la mitochondrie, ce qui entrainerait des problèmes de β-oxydation peroxysomale. Par ailleurs, il semble que l'inactivation de certains transporteurs du cholestérol (ORPs) diminue ou augmente la biogenèse et/ou l'activité peroxysomale.

3.3 Catabolisme du 7KC

Le 7KC est un composé que les cellules ont des difficultés à métaboliser. Il existe néanmoins des moyens pour éliminer le 7KC et diminuer ses effets toxiques. La plupart des voies du métabolisme du cholestérol peuvent s'appliquer au métabolisme des oxystérols. Les principales voies métaboliques sont l'estérification, l'oxydation, la sulfation et la réduction. Elles ont pour but de servir au transport des oxystérols et à leur élimination par exemple en formant des acides biliaires. La formation des acides biliaires intervient au niveau du foie par différentes voies : la voie de la 7α-hydroxylase, de la 27-hydroxylase, de la 24-hydroxylase et de la 25-hydroxylase (Crosignani *et al.*, 2011; Griffiths *et al.*, 2020).

Il est possible que les oxystérols, et par conséquent le 7KC, soient estérifiés au même titre que le cholestérol. L'estérification des oxystérols est aussi réalisée par l'action de l'Acyl CoA cholesterol Acyl Transferase (ACAT) dans les cellules ou de la Lecithin-Cholesterol Acyltransferase (LCAT) dans le plasma (Brown *et al.*, 2009; Szedlacsek *et al.*, 1995). De plus, la cytotoxicité des oxystérols est réduite par leur estérification en empêchant leur accumulation et en diminuant leur action pro-apoptotique (La Marca *et al.*, 2014; Monier *et al.*, 2003). Chez des patients souffrant d'une mutation de LCAT, les taux plasmatiques de 7KC libre sont augmentés tandis que le 7KC estérifié est diminué (Yamamuro *et al.*, 2020).

Le 7KC peut être sulfaté par la sulfotransférase 2B1b (SULT 2B1b), ce qui diminue sa toxicité (Fuda *et al.*, 2007). Il peut être également pris en charge par CYP27A1 pour former du 27OH-7KC (Lyons *et al.*, 2001; Pariente *et al.*, 2019).

La nature hydrophobe des oxystérols fait qu'ils sont généralement présents dans les environnements lipidiques tels que les membranes plasmiques ou les gouttelettes lipidiques. Ainsi, ils ne peuvent pas être éliminés directement des cellules mais seulement par le biais de transporteurs spécialisés. Il semble que seuls les transporteurs membranaires ATP-binding cassette, subfamilly A, member 1 (ABCA1) et ATP-binding cassette, subfamilly G, member 1 (ABCG1) soient capables d'éliminer des oxystérols en les transportant à l'extérieur des cellules. ABCA1 et ABCG1 permettent le transport des phospholipides et du cholestérol/oxystérols vers les HDL via l'ApoA1 (protéine majeure des HDL). Il a été montré sur des macrophages de souris que la protection contre la mort cellulaire induite par des OxLDL (contenant du 7KC) était spécifiquement dépendante d'ABCG1 mais pas d'ABCA1. Sur des cellules épithéliales embryonnaires de rein (HEK293), le 7α-OHC, le 7β-OHC et le 25-OHC sont aussi transportés par ABCG1. Le 25-OHC est également transporté par ABCA1 (Brown *et al.*, 2009; Terasaka *et al.*, 2007). De plus, une accumulation de 7KC est observée dans des macrophages de souris

ABCG1 -/- (Tall, 2008). Sur des macrophages murins J774, un traitement par du glycolaldhéyde et de OxLDL diminue l'expression d'ABCA1 et ABCG1, et induit une baisse de l'efflux de 7KC et son accumulation (Iborra *et al.*, 2011). Les oxystérols oxydés sur la chaine latérale (24(S)-OHC, 27-OHC et 25-OHC) font figure d'exception puisqu'ils sont capables de traverser d'eux même les membranes lipidiques (Bjorkhem, 2006).

Le 7KC peut également être pris en charge par la 11β-HSD1 (enzyme qui réduit la cortisone en cortisol) au niveau hépatique pour être réduit en 7β-OHC (Mutemberezi *et al.*, 2016; Pariente *et al.*, 2019). De plus, il existe des enzymes bactériennes (cholestérol oxydases) pouvant dégrader le 7KC (Ghosh *et al.*, 2016; Mathieu *et al.*, 2008; Mathieu *et al.*, 2010).

4. Molécules cytoprotectrices vis-à-vis du 7-cétocholestérol

Le 7KC entraine des dysfonctions des organites (mitochondrie, lysosome, peroxysome, RE) et agit sur la balance Redox, la production d'énergie, et les flux ioniques. Il contribue au développement de pathologies très variées : maladies cardiovasculaires, oculaires, pulmonaires, intestinales, neurodégénératives et maladies génétiques rares ou non. Le 7KC étant un composé qui est peu ou pas métabolisé dans les cellules, à l'exception du foie, il pourrait s'accumuler au fil du temps, ce qui favoriserait sa toxicité. Il est donc important d'identifier des molécules synthétiques ou naturelles pouvant s'opposer à ses effets toxiques. Actuellement, différents composés sont connus comme ayant des activités cytoprotectrices vis-à-vis du 7KC : des molécules naturelles (polyphénols, tocophérols, vitamines, lipides ou mélanges de lipides) et des molécules synthétiques.

4.1 Tocophérols

Le terme vitamine E caractérise un ensemble de huit isomères, quatre tocophérols avec une chaine latérale C16 saturée (α-tocophérol, β-tocophérol, γ-tocophérol et δ-tocophérol) et quatre tocotriénols avec une chaîne latérale contenant trois insaturations (α-tocotriénol, β-tocotriénol, γ-tocotriénol et δ-tocotriénol) (**Figure 18**) (Rimbach *et al.*, 2002). Ces molécules sont présentes en grande quantité dans des produits d'origine naturelle alimentaire comme les poissons gras, des huiles végétales (huile d'argan, d'olive, de pépins de raisin, de graines de chardon-Marie) ou encore dans des graines (amandes, noisettes, soja) (Badreddine *et al.*, 2017; Brahmi *et al.*, 2019; Meddeb *et al.*, 2018).

	R1	R2	R3
α	CH_3	CH_3	CH_3
β	CH_3	H	CH_3
γ	H	CH_3	CH_3
δ	H	H	CH_3

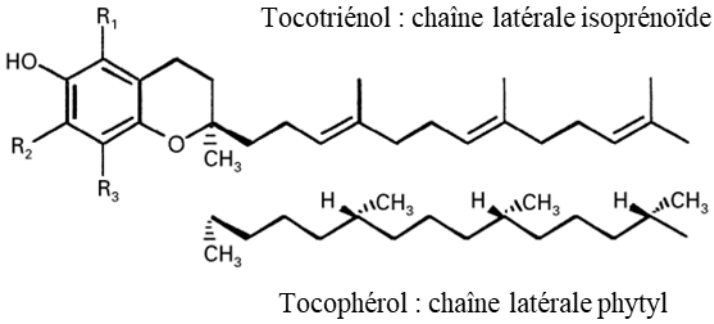

Figure 18 : Structure moléculaire des isomères de vitamine E.
La vitamine E est un ensemble de huit molécules : quatre tocophérols avec une chaine latérale C16 saturée (α-tocophérol, β-tocophérol, γ-tocophérol et δ-tocophérol) et quatre tocotriénols avec une chaîne latérale contenant trois insaturations (α-tocotriénol, β-tocotriénol, γ-tocotriénol et δ-tocotriénol). D'après (Rimbach *et al.*, 2002).

Ces molécules liposolubles ont des effets biologiques différents en fonction des isomères, mais elles ont comme point commun une activité antioxydante au sein de l'organisme en neutralisant les radicaux libres oxygénés et azotés. Leur capacité antioxydante provient du groupement phénolique hydroxyl qui peut donner un ion H^+ aux radicaux libres. La vitamine E oxydée

devient alors un radical peu réactif qui peut être régénéré par la vitamine C (Chan, 1993). L'efficacité de l'activité antioxydante de la vitamine E est modulée par deux facteurs : la mobilité de la molécule dans la membrane cellulaire déterminée par la chaine latérale et le nombre de fonctions méthyl (-CH3) portées par l'anneau chromanol (plus il est important et plus la capacité antioxydante est élevée). Ainsi, les isomères α- sont les plus actifs (Rimbach *et al.*, 2002). L'α-tocophérol est considéré comme l'isoforme la plus active biologiquement en raison de son affinité élevée pour la protéine de transfert du tocophérol (PTT) qui permet sa sécrétion dans les lipoprotéines par les hépatocytes (Thakur *et al.*, 2010). La « Plasma phospholipid transfer protein » (PLTP) transfert ensuite l'α-tocophérol plasmatique vers les tissus (Albers *et al.*, 2012). De plus, l'α-tocophérol est capable de traverser la BHE pour être actif dans le système nerveux central (Lee *et al.*, 2019).

Le rôle de l'α-tocophérol dans la protection contre les effets toxiques du 7KC est documenté sur différents types cellulaires. Sur des cellules monocytaires U937, l'α-tocophérol diminue les effets toxiques du 7KC sur le potentiel membranaire mitochondrial, le relargage de cytochrome c et l'apoptose ainsi que la formation de vésicules autophagiques (Lizard *et al.*, 2000; Miguet-Alfonsi *et al.*, 2002). L'α-tocophérol préserve l'activation de la voie PI3-K/PDK-1/Akt qui est déficiente lorsque les cellules U937 sont traitées par le 7KC (Vejux *et al.*, 2009a).

Sur des cellules musculaires lisses A7R5, l'α-tocophérol protège de la toxicité du 7KC en diminuant son incorporation dans les radeaux lipidiques ainsi qu'en activant la voie Akt/PKB. En revanche, le γ-tocophérol ne permet pas de protéger du 7KC sur ce même modèle (Royer *et al.*, 2009).

Sur des cellules de neuroblastome N2a, l'α-tocophérol inhibe le stress oxydant, la dépolarisation des mitochondries et la mort cellulaire induite par le 7KC (Yammine *et al.*, 2020a).

Sur des cellules microgliales BV-2, le 7KC induit une mort cellulaire ainsi que des dommages peroxysomaux qui peuvent être en partie inhibés par l'α-tocophérol (400 µM). Dans ce cas, le γ-tocophérol (400 µM) est également capable d'induire une cytoprotection mais le Trolox, un antioxydant synthétique dérivé de la vitamine E, n'est pas cytoprotecteur (Debbabi *et al.*, 2016; Nury *et al.*, 2017).

Sur des oligodendrocytes 158N, le 7KC induit également une mort cellulaire qui est inhibée par l'α-tocophérol. L'accumulation du 7KC dans les radeaux lipidiques est également diminuée (Leoni *et al.*, 2017; Nury *et al.*, 2018; Nury *et al.*, 2015; Nury *et al.*, 2014; Ragot *et al.*, 2011; Ragot *et al.*, 2013). Il est notable que l'α-tocotriénol, bien qu'ayant un potentiel antioxydant équivalent à celui de l'α-tocophérol, ne permet pas de protéger du 7KC (Nury *et al.*, 2018). L'origine de cette différence de protection entre les deux molécules n'est pas actuellement établie. Des résultats similaires obtenus avec du 24(S)-OHC ont été obtenus sur des neuroblastomes humains SH-SY5Y. Cette différence de cytoprotection pourrait avoir pour origine des modifications membranaires différentes puisque l'α-tocophérol diminue la fluidité membranaire alors que l'α-tocotriénol non (Nakazawa *et al.*, 2017).

4.2 Terpénoïdes

Les terpénoïdes ou isoprénoïdes, définissent un groupe de molécules dont le point commun est la présence d'un ou de plusieurs groupements isoprène (**Figure 19**). Ce sont des molécules pouvant contenir plusieurs cycles aromatiques qui sont très présentes dans le règne végétal et dont font partie les phytostérols et certains carotènes. Sur des macrophages THP-1, le lycopène (le caroténoïde majoritaire des tomates) diminue l'inflammation causée par le 7KC au niveau de la production de cytokines (IL-1β, IL-6 at IL-8) ainsi que l'augmentation d'expression

de NOX4. Le lycopène diminue également la production d'ERO et l'activation de la voie JNK, ERK1/2, p38 MAP kinase induite par le 7KC (Palozza *et al.*, 2010; Palozza *et al.*, 2011).

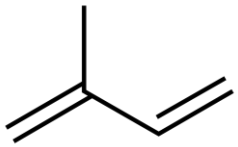

Figure 19 : Structure chimique du groupement isoprène
Les terpénoïdes (ou isoprénoïdes) forment une classe de composés organiques dérivant de l'assemblage d'unités isopréniques à cinq atomes de carbone.

4.3 Composés phénoliques

Les composés phénoliques regroupent les molécules comprenant un ou plusieurs cycles benzène portant un ou plusieurs groupements hydroxyl. On trouve parmi ces molécules les polyphénols, qui regroupent eux-mêmes différentes sous-catégories comme les acides phénoliques, des stilbènes, des lignanes ou encore des flavonoïdes (**Figure 20**) (Pandey *et al.*, 2009). Ces molécules d'origine végétale présentent de fortes capacités antioxydantes et peuvent être utilisées pour protéger contre des maladies inflammatoires chroniques, cardiovasculaires, oculaires, neurodégénératives et des cancers (Fraga *et al.*, 2019; Vauzour *et al.*, 2010). Le 7KC étant impliqué dans ces pathologies, des études ont été menées afin de définir si des polyphénols pouvaient avoir une activité cytoprotectrice à l'encontre du 7KC (Brahmi *et al.*, 2019). Des macrophages J774A.1 traitées par de l'épicatéchine (un flavonoïde) sont protégés de l'élévation des taux d'ERO et de la mort cellulaire induite par le 7KC (Leonarduzzi *et al.*, 2006). Des neuroblastomes N2a traités au 7KC sont protégés par différents polyphénols (resvératrol,

apigénine et quercétine) : inhibition de la dépolarisation des mitochondries, de l'élévation du stress oxydant et de la mort cellulaire (Yammine *et al.*, 2020a; Yammine *et al.*, 2020c).

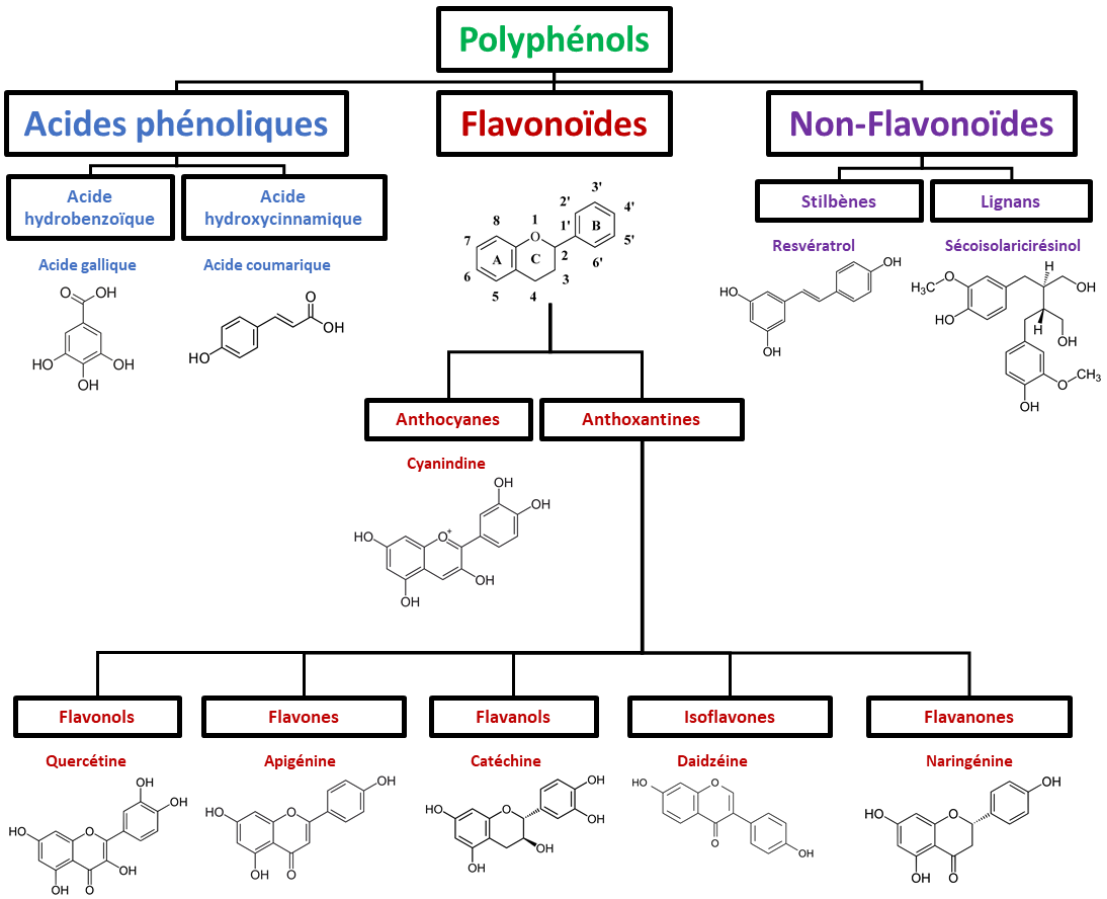

Figure 20 : Structure chimique de base des différentes classes de polyphénols.
Les polyphénols regroupent différentes sous-catégories comme les acides phénoliques, des flavonoïdes, divisés eux-mêmes en sous catégories (anthocyanes ou anthoxantines) et des non-flavonoïdes (stilbènes et lignans).

Sur des macrophages humains isolés, l'inflammation causée par le 7KC est inhibée par le resvératrol (Buttari *et al.*, 2014). Dans le cadre de la DMLA, sur des cellules ARPE-19 traitées au 7KC, la production d'ERO, de cytokines pro-inflammatoires et la mort cellulaire sont inhibées par le resvératrol (Dugas *et al.*, 2010). L'inflammation (production d'IL-6) causée par du 7KC ou du lipopolysaccharide sur les cellules ARPE-19 est inhibée par de l'acide férulique (Kohno *et al.*,

2020). En revanche, le resvératrol et un autre polyphénol, l'acide ellagique, n'ont pas d'effet sur la toxicité du 7KC sur des oligodendrocytes 158N (Ragot *et al.*, 2013). Sur des cellules entérocytaires Caco-2, l'inflammation et l'altération des jonctions serrées induite par un mélange d'oxystérols contenant du 7KC (42,96% de 7KC, 32,3% d'α-époxycholestérol, 5,76% de β-époxycholestérol, 4,26% de 7α-OHC et 14,71% de 7β-OHC) est inhibée par l'épicathéchine (Deiana *et al.*, 2017). Sur des cellules endothéliales ISO-HAS traitées au 7KC, l'adhésion de macrophages U937 est augmentée ainsi que l'expression de protéines d'adhésion : ces effets sont inhibés par l'épigallocatéchine gallate (Yamagata *et al.*, 2013). L'hydroxytyrosol et le tyrosol, deux composés phénoliques extraits de l'huile d'olive, protègent les cellules Caco-2 du stress oxydant induit par le 7KC (Atzeri *et al.*, 2016).

4.4 Acides gras

Il a aussi été montré que des acides gras pouvaient générer une cytoprotection à l'encontre du 7KC sur différents types cellulaires (Brahmi *et al.*, 2019). Sur des cellules monocytaires U937, le 7KC peut être estérifié par l'acide oléique (C18:1 n-9), ce qui serait à l'origine de la diminution de sa toxicité. L'exposition à du 7KC-oléate n'entraine aucun effet délétère sur les cellules U937 (Monier *et al.*, 2003). L'acide oléique est retrouvé en grande quantité dans des huiles naturelles alimentaires telles que l'huile d'olive, l'huile d'argan ou l'huile de graines de chardon-Marie (Meddeb *et al.*, 2017; Meddeb *et al.*, 2018; Zarrouk *et al.*, 2019). De plus, sur des oligodendrocytes murins (158N), des cellules microgliales murines (BV-2) et des neuroblastomes murins (N2a), l'acide oléique diminue les effets toxiques du 7KC sur les organites (peroxysome, mitochondrie, lysosome) ainsi que sur la production d'ERO (Badreddine *et al.*, 2017; Debbabi *et*

al., 2016; Debbabi *et al.*, 2017; Yammine *et al.*, 2020a). Il est important de noter que l'isomère trans- de l'acide oléique, l'acide élaïdique, ne protège pas contre le 7KC (Debbabi *et al.*, 2017). L'acide docosahexaénoïque (DHA ; C22:6 n-3) est aussi connu pour s'opposer aux effets du 7KC sur les cellules. Ainsi, sur les cellules 158N, BV-2 et N2a, le DHA atténue la toxicité du 7KC au niveau de la production d'ERO, et des organites (peroxysome, mitochondrie, lysosome) au même titre que l'acide oléique (Debbabi *et al.*, 2017; Nury *et al.*, 2015; Nury *et al.*, 2017; Yammine *et al.*, 2020a; Zarrouk *et al.*, 2015). Des précurseurs de synthèse du DHA, l'acide eicosapentaénoïque (EPA, C20:5 n-3) et l'acide α-linolénique (ALA ; C18:3 n-3) diminuent aussi les effets du 7KC sur les cellules N2a au niveau de la production d'ERO, du potentiel membranaire mitochondrial et de l'induction de mort cellulaire (Yammine *et al.*, 2020a). L'acide sterculique (un acide gras cyclopropène) protège les cellules rétiniennes ARPE-19 du stress du réticulum induit par le 7KC (Huang *et al.*, 2012; Huang *et al.*, 2014).

4.5 Mélanges de molécules et huiles

Des mélanges synthétiques ou naturels de molécules sont également connus pour pouvoir atténuer les effets toxiques du 7KC. Il peut s'agir d'extraits de plantes comme des huiles, ou de broyats. Sur des oligodendrocytes 158N et des cellules microgliales BV-2, l'huile de graines de chardon-Marie, l'huile d'olive et l'huile d'argan protègent de la mort cellulaire induite par le 7KC. Ces huiles sont riches en α-tocophérol, acide oléique (C18:1 n-9) et polyphénols (Badreddine *et al.*, 2017; Meddeb *et al.*, 2018; Zarrouk *et al.*, 2019). Le mélange α-tocophérol (400 µM) et DHA (50 µM) protège aussi les cellules 158N de la mort cellulaire induite par le 7KC (Nury *et al.*, 2015). De manière indirecte, la formation de 7KC induite par le stress oxydant dans une solution ou sur des cellules Caco-2, est inhibée par des traitements avec des extraits

polyphénoliques de vins rouge et blanc ainsi que par des extraits phénoliques d'huile d'olive dont les composés majoritaires sont le tyrosol, l'hydroxytyrosol et l'alcool homovanillique (Deckert *et al.*, 2002; Deiana *et al.*, 2010; Tian *et al.*, 2011). Une nourriture enrichie par un extrait de brocoli inhibe également l'oxydation du cholestérol induite par un exercice physique intense chez des rats (Cardenia *et al.*, 2017). Un extrait méthanolique de *Clinacanthus nutans* (100 µg/mL), une plante utilisée en médecine traditionnelle, inhibe la toxicité et l'inflammation induite par du 7KC (30 µM) sur des cellules microvasculaires endothéliales cérébrales humaines hCMEC/D3 (Kuo *et al.*, 2020). Enfin, l'ergothionéine, un antioxydant synthétisé par des bactéries et des champignons inhibe aussi la toxicité et l'inflammation induite par du 7KC (30 µM) sur des cellules microvasculaires endothéliales cérébrales humaines hCMEC/D3 (Koh *et al.*, 2020).

4.6 Autres molécules naturelles

Il existe d'autres molécules n'entrant pas dans les catégories précédentes qui ont montré une protection vis-à-vis du 7KC. L'indicaxanthine, un pigment jaune végétal antioxydant extrait des figues de barbarie, a montré une protection contre l'apoptose sur des monocytes/macrophages THP-1 traités par du 7KC. L'indicaxanthine empêche la suractivation de NOX4, de NF-κB et maintient l'homéostasie calcique en prévenant les dommages aux mitochondries (Tesoriere *et al.*, 2014b; Tesoriere *et al.*, 2013). De plus, à des concentrations de 1 à 5 mM, équivalentes aux niveaux plasmatiques après consommation de figues de barbarie, l'indicaxanthine empêche l'éryptose (apoptose des érythrocytes) induite par le 7KC (Tesoriere *et al.*, 2015). Des molécules antioxydantes déjà présentes dans les cellules peuvent également avoir des propriétés protectrices contre le 7KC. Le glutathion (GSH) et la N-acétyl-cystéine (NAC) protègent de l'augmentation des EROs et de l'apoptose induite par le 7KC sur des cellules U937 (Lizard *et al.*, 1998; Lizard *et*

al., 2000). Sur des cellules précurseurs d'ostéoblastes MC3T3-E1, le 7KC induit une élévation du stress oxydant, un stress du réticulum et de l'apoptose, tous ces effets sont inhibés par la NAC (Sato *et al.*, 2017).

Il a aussi été montré qu'un phospholipide présent dans les endosomes tardifs, le bis(monoacylglycéro)phosphate (BMP) pouvait réduire la formation de 7KC intracellulaire dans des macrophages RAW264.7 chargés par des OxLDL. La toxicité des OxLDL est également réduite par le BMP. Ces effets pourraient provenir de ses propriétés antioxydantes mais également d'une interaction entre BMP et ORP11 qui favoriserait l'export du cholestérol des endosomes tardifs et empêcherait ainsi son oxydation en 7KC dans ces derniers (Arnal-Levron *et al.*, 2013; Arnal-Levron *et al.*, 2019).

4.7 Molécules synthétiques

Une molécule synthétique utilisée dans le traitement de la sclérose en plaques, le diméthylfumarate (DMF) a une activité cytoprotectrice contre le 7KC. Le DMF est un activateur de Nrf2, un facteur de transcription régulant l'expression de gènes de la régulation de l'équilibre Redox. Sur des oligodendrocytes 158N, le DMF protège de l'oxyapoptophagie (référencée comme ***oxiapoptophagy*** dans les bases de données) induite par le 7KC (Zarrouk *et al.*, 2017).

4.8 Enzymes bactériennes

Une alternative pour diminuer les effets toxiques du 7KC sur les cellules serait d'augmenter son catabolisme. Il est connu que le 7KC peut être pris en charge par CYP27A1 pour former du 27OH-7KC ou bien par la 11β-HSD1 pour être converti en 7β-OHC (Heo *et al.*,

2011; Mutemberezi *et al.*, 2016). Néanmoins, ces enzymes ne sont pas exprimées de façon ubiquitaire. Depuis les années 2000, une méthode alternative appelée « bioremédiation » a été décrite. Cette méthode consiste à utiliser des enzymes (cholestérol oxydases) capables de métaboliser le 7KC pour compenser ce déficit dans la plupart des cellules humaines. En effet, des bactéries ont la capacité de métaboliser facilement le 7KC afin de l'utiliser comme source de carbone. Différentes souches ont été identifiées : *Proteobacterium*, *Sphingomonas*, *Nocardia*, *Rhodococcus* et *Pseduomonas* (Ghosh *et al.*, 2016; Mathieu *et al.*, 2008; Mathieu *et al.*, 2010). Chez *Rhodococcus jostii* RHA1, le 7KC est dégradé par la chaîne latérale en C17, puis la fonction cétone en C7 à son tour et enfin les cycles A et B du noyau stéroïde. Différents métabolites résultent de cette dégradation : parmi eux, on trouve le 3,4-dihydroxy-9,10-séconandrost-1,3,5(10)-triene-9,17-dione (3,4-DHSA) et l'acide propionique 3,4-DHSA (3,4-DHSAP) (Mathieu *et al.*, 2010).

Lorsque la cholestérol oxydase de *Chromobacterium* DS-1 (DS1-CHO) est ciblée au lysosome de fibroblastes humains, le 7KC est dégradé et la viabilité cellulaire est augmentée (Mathieu *et al.*, 2012). Dans des conditions optimales, la souche *Rhodococcus erythropolis* MTCC 3951 peut dégrader en 15 jours 93 % du 7KC d'une solution à 1 g/L (Ghosh *et al.*, 2017).

Il est possible que le microbiote intestinal ait un impact sur la formation et / ou la dégradation d'oxystérols directement dans l'intestin, ou bien en modifiant des activités d'enzymes impliquées dans le métabolisme du cholestérol (métabolisme des acides biliaires) et des oxystérols. Sur des rats sans microbiote, l'activité de CYP7A1 est augmentée ainsi que le taux de 7KC (Bhowmik *et al.*, 2012). La modification du microbiote à des visées préventives ou thérapeutiques pourrait être utilisée à l'avenir de manière à diminuer les taux d'oxystérols présents dans l'intestin avant leur passage dans l'organisme.

Problématiques et objectifs du travail de thèse

Une augmentation du stress oxydant menant à la formation de 7KC est impliquée dans de nombreuses pathologies, comme les maladies inflammatoires chroniques et liées à l'âge (maladies cardiovasculaires, maladies de l'intestin), les maladies oculaires (DMLA, cataracte) et certaines maladies neurodégénératives d'origine génétique ou non (Alzheimer, Parkinson, Sclérose en plaques, Niemann Pick et X-ALD) (Anderson *et al.*, 2020).

Dans ces maladies, la toxicité du 7KC envers les organites cellulaires comme la mitochondrie, le lysosome ou encore le RE est plutôt bien caractérisée. Cependant, jusqu'à maintenant, il n'existe pas de données concernant les effets du 7KC sur le peroxysome.

Des modifications du métabolisme peroxysomal, caractérisées par une diminution des taux de plasmalogènes (70 % des lipides de la gaine de myéline et 18 % des phospholipides totaux sont des plasmalogènes), ont été observées dans la maladie d'Alzheimer, de Parkinson et la sclérose en plaques. Le taux de plasmalogènes, dont la synthèse nécessite l'intervention de deux enzymes peroxysomales, semble être corrélé à la sévérité de la pathologie (Dragonas *et al.*, 2009; Gray *et al.*, 2014; Su *et al.*, 2019). Dans un modèle murin d'athérosclérose, une diminution des taux de plasmalogènes plasmatiques a également été mise en évidence (Rasmiena *et al.*, 2015). D'autres altérations caractérisées par un déficit de la β-oxydation peroxysomale ont également été observées dans ces maladies comme l'accumulation d'AGTLC (C22 :0, C24 :0 et C26 :0) (Jo *et al.*, 2019; Kou *et al.*, 2011).

Ces modifications du métabolisme lipidique (plasmalogènes et AGTLC) liées au peroxysome dans certaines maladies (inflammatoires chroniques et liées à l'âge, maladies rares) renforcent l'hypothèse d'une implication de cet organite dans ces pathologies et suggèrent des altérations fonctionnelles du peroxysome sous l'effet du 7KC. Cette hypothèse a été étudiée au cours des travaux de thèse qui traitent des effets du 7KC sur le peroxysome en utilisant des cellules nerveuses : oligodendrocytes murins 158N (Baarine *et al.*, 2009). Ces cellules nerveuses sont en

effet bien adaptées pour étudier le stress oxydant, la mort cellulaire (apoptose et autophagie), la contribution du peroxysome dans ces différents évènements et les relations du peroxysome avec les autres organites (Vejux *et al.*, 2020).

Le travail de thèse a abordé les points suivants :

- Caractérisation *in vitro*, sur des oligodendrocytes murins 158N, des effets du 7KC sur le stress oxydant et la mort cellulaire : notion d'oxyapoptophagie
- Caractérisation *in vitro* des effets du 7KC sur le métabolisme peroxysomal
- Identification de lipides cytoprotecteurs pour diminuer la toxicité du 7KC

Afin de répondre à ces différents objectifs, les résultats des travaux de thèse seront présentés sous la forme de plusieurs publications.

Article 1 : Nury T, Sghaier R, Zarrouk A, et al. **Induction of peroxisomal changes in oligodendrocytes treated with 7-ketocholesterol: Attenuation by α-tocopherol**. *Biochimie. 2018;153:181-202.*

Article 2 : Nury T, Yammine A, Caccia C, Leoni V, Hichami A, Pande A, Majeed M, Atanasov A, Vejux A, Lizard G. **Prevention of 7-ketocholesterol-induced cytotoxicity by fatty acids, Lorenzo's oil and sulfo-N-succinimdyl oleate (SSO) on 158N cells: benefits of SSO and mechanisms of cytoprotection.**

Article 3 : Nury T, Yammine A, Menetrier F, Zarrouk A, Vejux A, Lizard G. **7ketocholesterol and 7β-hydroxycholesterol-induced peroxisomal disorders in glial, microglial and neuronal**

cells: potential role in neurodegeneration. *Advances in Experimental Medicine and Biology*, Vol. 1299, Gérard Lizard (Eds): Peroxisome Biology: Experimental Models, Peroxisomal Disorders and Neurological Diseases. Chapter 7. 2021. doi: 10.1007/978-3-030-60204-8.

Article 4 : Nury T, Zarrouk A, Yammine A, Mackrill JJ, Vejux A, Lizard G. **Oxiapoptophagy: a type of cell death induced by some oxysterols**. *Br J Pharmacol*. 2020;10.1111/bph.15173. doi:10.1111/bph.15173.

Article 5 : Nury T, Lizard G, Vejux A. **Lipids Nutrients in Parkinson and Alzheimer's Diseases: Cell Death and Cytoprotection**. *Int J Mol Sci*. 2020;21(7):2501.

Mieux connaître les mécanismes de la cytotoxicité induite par le 7KC sur les cellules du système nerveux central, son action au niveau du peroxysome et identifier des molécules cytoprotectrices pour s'opposer aux effets délétères de cet oxystérol pourrait ouvrir de nouvelles perspectives thérapeutiques pour prévenir et/ou traiter les maladies neurodégénératives mais aussi des maladies liées à l'âge et inflammatoires chroniques qui ont en commun des taux élevés de 7KC.

Article 1

Induction of peroxisomal changes in oligodendrocytes treated with 7-ketocholesterol : Attenuation by α-tocopherol

Thomas Nury, Randa Sghaier, Amira Zarrouk, Franck Ménétrier, Tugba Uzun, Valerio Leoni, Claudio Caccia, Wiem Meddeb, Amira Namsi, Khouloud Sassi, Wafa Mihoubi, Jean-Marc Riedinger, Mustapha Cherkaoui-Malki, Thibault Moreau, Anne Vejux, Gérard Lizard

Biochimie. 2018, 153:181-202

Dans ce premier article, nous avons étudié le rôle du peroxysome dans la mort cellulaire induite par le 7KC en caractérisant les dysfonctions peroxysomales induites par ce dernier sur un modèle d'oligodendrocytes murins 158N. Nous avons aussi cherché à identifier des molécules capables d'inhiber les effets toxiques du 7KC en prévenant les dysfonctions peroxysomales, mitochondriales.

Pour cela, les cellules 158N ont été traitées pendant 24 heures par du 7KC en utilisant d'une part une concentration faiblement toxique (25 µM) n'induisant pas de mort cellulaire par apoptose, et d'autre part, une concentration toxique (50 µM) induisant de la mort cellulaire.

Dans ces conditions, les niveaux d'ERO ont été évalués : production d'anions superoxydes, de peroxyde d'hydrogène ainsi que l'activité et l'expression de la catalase. L'impact sur l'apoptose et l'autophagie a été évaluée par western blotting. Au niveau de la mitochondrie, une mesure des taux de cardiolipines, du potentiel membranaire mitochondrial ($\Delta\psi m$) et de la morphologie ont été réalisés. Enfin, l'aspect et la distribution des peroxysomes ont été étudiés par microscopie électronique à transmission en évaluant le niveau d'expression du transporteur ABCD3 en microscopie confocale. L'impact du 7KC sur le métabolisme peroxysomal a par ailleurs été étudié en mesurant les taux de plasmalogènes et d'AGTLC, ainsi que les niveaux de transcrits de transporteurs peroxysomaux (*ABCD1* et *ABCD3*) et d'enzymes peroxysomales (*ACOX1* et *MFP-2,* impliquées dans la β-oxydation, *DHAPAT* et *ADHAP-S,* impliquées dans la synthèse des plasmalogènes).

Les effets cytoprotecteurs de l'α-tocophérol et de l'α-tocotriénol, deux composants de la vitamine E, qui est bien connue pour ses propriétés protectrices contre le 7KC, ont également été mesurés en prenant en compte les effets sur les paramètres précédemment cités (Lizard *et al.,* 2000; Nury *et al.*, 2017; Ragot *et al.*, 2011; Vejux *et al.*, 2009a).

Il ressort de ce travail que le 7KC à forte concentration (50 µM), induit une augmentation du stress oxydant (augmentation de l'activité catalase et des niveaux d'ERO) et de la mort cellulaire par apoptose (Caspase-3 et PARP clivée), accompagnée de critères d'autophagie (augmentation du ratio LC3-II / LC3-I, augmentation de p62 et présence de vésicules autophagiques (incluant des peroxysomes : pexophagie) en microscopie électronique à transmission). L'ensemble de ces événements conduisant à la mort des cellules 158N a été caractérisé sous le terme d'oxyapoptophagie (**Oxy**dation + **Apopto**se + Auto**phagie**). Des modifications du métabolisme (accumulation d'AGTLC ; diminution de l'expression d'ABCD3 et des niveaux de transcrits d'*ABCD1, ABCD3, ACOX1, MFP-2* et *DHAPAT*) et de la morphologie peroxysomale ont également été observées (peroxysomes déformés et regroupés).

Lorsque le 7KC est utilisé à plus faible concentration (25 µM), il n'induit pas de mort cellulaire mais une faible augmentation des ERO. Par ailleurs, l'autophagie est activée (augmentation du ratio LC3-II / LC3-I, augmentation de p62 et présence de vésicules autophagiques) et de faibles modifications mitochondriales sont observées (baisse du $\Delta\psi m$). En revanche, les modifications peroxysomales sont équivalentes à celles induites par le 7KC à forte concentration.

Les travaux de cet article ont montré que :

- Le 7KC induit des perturbations peroxysomales fonctionnelles et morphologiques,
- Le peroxysome est plus sensible que la mitochondrie à la toxicité induite par le 7KC,
- L'autophagie (pexophagie) induite par le 7KC précède la mort cellulaire,
- L'α-tocophérol inhibe l'oxyapoptophagie ainsi que les dysfonctions peroxysomales et mitochondriales induites par le 7KC.

Biochimie 153 (2018) 181–202

Contents lists available at ScienceDirect

Biochimie

journal homepage: www.elsevier.com/locate/biochi

Research paper

Induction of peroxisomal changes in oligodendrocytes treated with 7-ketocholesterol: Attenuation by α-tocopherol

Thomas Nury [a], Randa Sghaier [a, b], Amira Zarrouk [c, d], Franck Ménétrier [e], Tugba Uzun [a], Valerio Leoni [f], Claudio Caccia [g], Wiem Meddeb [h], Amira Namsi [a, i], Khouloud Sassi [a, j], Wafa Mihoubi [k], Jean-Marc Riedinger [l], Mustapha Cherkaoui-Malki [a], Thibault Moreau [a, m], Anne Vejux [a], Gérard Lizard [a, *]

[a] Univ. Bourgogne Franche-Comté, Lab. Bio-PeroxIL, 'Biochemistry of the Peroxisome, Inflammation and Lipid Metabolism' (EA7270) / Inserm, Dijon, France
[b] Univ. Monastir, Lab. Biotechnology, Monastir, Tunisia
[c] Univ. Monastir, Lab-NAFS 'Nutrition – Functional Food & Vascular Diseases' LR12-ES-05, Monastir, Tunisia
[d] Faculty of Medicine, Sousse, Tunisia
[e] INRA – CNRS, UMR 1324 CSGA, Dijon, France
[f] Lab. Clinical Chemistry, Hospital of Varese, ASST-Settelaghi, Varese, Italy
[g] Unit of Medical Genetics and Neurogenetics, IRCCS Carlo Besta, Milano, Italy
[h] Univ. Carthage, LMMA, IPEST, Tunis, and Fac. of Science of Bizerte, Bizerte, Tunisia
[i] Univ. Tunis El Manar, Lab. Neurophysiologie Fonctionnelle et Pathologie–UR11ES/09, Tunis, Tunisia
[j] Univ. Tunis El Manar, Fac. of Medicine, Lab of Onco-Hematology, Tunis, Tunisia
[k] Centre de Biotechnologie de Sfax, Lab. Biotechnologie Moléculaire des Eucaryotes, Sfax, Tunisia
[l] Centre de Lutte Contre le Cancer GF Leclerc, Laboratoire de Biologie Médicale, Dijon, France
[m] Dept. of Neurology, Univ. Hospital of Dijon, France

ARTICLE INFO

Article history:
Received 28 March 2018
Accepted 17 July 2018
Available online 19 July 2018

Keywords:
7-Ketocholesterol
α-tocopherol
α-tocotrienol
158 N cells
Zellweger's patient fibroblasts
Mitochondria
Peroxisome
Oxiapoptophagy
Pexophagy

ABSTRACT

The involvement of organelles in cell death is well established especially for endoplasmic reticulum, lysosomes and mitochondria. However, the role of the peroxisome is not well known, though peroxisomal dysfunction favors a rupture of redox equilibrium. To study the role of peroxisomes in cell death, 158 N murine oligodendrocytes were treated with 7-ketocholesterol (7 KC: 25–50 μM, 24 h). The highest concentration is known to induce oxiapoptophagy (OXIdative stress + APOPTOsis + autoPHAGY), whereas the lowest concentration does not induce cell death. In those conditions (with 7 KC: 50 μM) morphological, topographical and functional peroxisome alterations associated with modifications of the cytoplasmic distribution of mitochondria, with mitochondrial dysfunction (loss of transmembrane mitochondrial potential, decreased level of cardiolipins) and oxidative stress were observed: presence of peroxisomes with abnormal sizes and shapes similar to those observed in Zellweger fibroblasts, lower cellular level of ABCD3, used as a marker of peroxisomal mass, measured by flow cytometry, lower mRNA and protein levels (measured by RT-qPCR and western blotting) of ABCD1 and ABCD3 (two ATP-dependent peroxisomal transporters), and of ACOX1 and MFP2 enzymes, and lower mRNA level of DHAPAT, involved in peroxisomal β-oxidation and plasmalogen synthesis, respectively, and increased levels of very long chain fatty acids (VLCFA: C24:0, C24:1, C26:0 and C26:1, quantified by gas chromatography coupled with mass spectrometry) metabolized by peroxisomal β-oxidation. In the presence of 7 KC (25 μM), slight mitochondrial dysfunction and oxidative stress were found, and no induction of apoptosis was detected; however, modifications of the cytoplasmic distribution of mitochondria and clusters of mitochondria were detected. The peroxisomal alterations observed with 7 KC (25 μM) were similar to those with 7 KC (50 μM). In addition, data obtained by transmission electron microcopy and immunofluorescence microscopy by dual staining with antibodies raised against p62, involved in autophagy, and ABCD3, support that 7 KC (25–50 μM) induces pexophagy. 7 KC (25–50 μM)-induced side effects were attenuated by α-tocopherol but not by α-tocotrienol, whereas the anti-oxidant properties of these molecules determined with the FRAP assay were in the same range. These data provide

* Corresponding author. Lab. Bio-PeroxIL, EA7270 (Biochemistry of the Peroxisome, Inflammation and Lipid Metabolism), Univ. Bourgogne Franche-Comté / Inserm, Faculté des Sciences Gabriel, 6 Bd Gabriel, 21000, Dijon, France.
E-mail address: gerard.lizard@u-bourgogne.fr (G. Lizard).

https://doi.org/10.1016/j.biochi.2018.07.009

evidences that 7 KC, at concentrations inducing or not cell death, triggers morphological, topographical and functional peroxisomal alterations associated with minor or major mitochondrial changes.

1. Introduction

Within the cell, the organelles (mitochondria, lysosomes, peroxisome, Golgi apparatus, and endoplasmic reticulum) are individual structures assuming essential functions which are required for efficient cellular activity. Besides the involvement of these organelles in cell metabolism, it is clearly established that mitochondria, lysosomes and endoplasmic reticulum contribute in different forms of cell death [1,2] whereas little is known on the part taken by the peroxisome.

The influence of mitochondria on cell death is the consequence of the key role played by this organel in apoptosis (type I cell death) [1,2]. It is well established that the two main forms of apoptosis (extrinsic pathway/cell death receptor pathway; intrinsic pathway/mitochondrial pathway) as well as the perforin/granzyme pathway (triggered by cytotoxic T cells) induce a loss of transmembrane mitochondrial potential (ΔΨm) and are associated with a cascade of caspase (**C**ysteinyl-**ASP**artate-cleaving prote**ASES**) activation [3]. In certain conditions, the loss of ΔΨm can favor the release by the mitochondria of apoptosis inducing factor (AIF) [4] and endonuclease G (EndoG) which trigger capase-independent cell death [5]. Apoptosis can lead to secondary necrosis: secondary necrotic cells are characterized by an externalization of phosphatidylserine and are progressively more permeable to propidium iodide or aminoactinomycine D (revealing alterations in the plasma membrane) whereas apoptotic cells are characterized by an externalization of phosphatidylserine but are not permeable to propidium iodide or aminoactinomycine D [6,7]. In necrosis (type III cell death/primary necrosis/accidental necrosis), no caspase activation occurs and the cells are characterized by an externalization of phosphatidylserine and by an increased permeability to propidium iodide or aminoactinomycine D [6,7]. In these conditions, mitochondrial depolarization is often associated with the mitochondrial swelling resulting from a sudden rupture of osmolarity. This rupture leads to oncosis, which precedes necrosis [8]; hence, the mitochondria plays a passive role in necrosis. In necroptosis, which, corresponds to a regulated form of necrosis [9], the RIPK3 (Receptor Interacting Protein serine/threonine Kinase 3) protein and the MLKL (Mixed Lineage Kinase Domain-like) protein are required [10]. In pyroptosis, an inflammatory form of regulated cell death, the activation of the inflammasome leads to caspase-1–dependent mitochondrial damages and dysfunctions of the organelle [11].

The concept of lysosomal cell death was mentioned by Christian de Duve, who also did pionnering work on the peroxisome [12]. Because of the hydrolytic capacity of lysosomal enzymes, de Duve defined lysosomes as 'suicide bags' that can cause cell and tissue autolysis [13]. This form of cell death is mainly carried out by lysosomal enzymes (cathepsin proteases, hydrolases) and can have necrotic or apoptotic features. This notion of lysosomal cell death/type II cell death [1] leads to the concept of autophagy [14], especially of macro-autophagy where the lysosome fuses with the autophagosome to yield the autophagolysosome [15].

Beside the role taken by mitochondria and lysosomes in cell death, it is also well established that stress on the endoplasmic reticulum can trigger cell death mechanisms. The endoplasmic reticulum is an organelle with multiple functions, notably in protein synthesis. Thus, disturbances in endoplasmic reticulum function can lead to a cell stress response, unfolded protein response (UPR), which is used to compensate cell damages but which can induce cell death if endoplasmic reticulum dysfunction is severe or prolonged [16,17].

Currently, little is known about Golgi apparatus and the cell death process. However, several proteins ensuring the structural integrity of Golgi apparatus are degradated by caspases during apoptosis [18]. Some instances of apoptosis also involve the degradation of proteins involved in anterograde vesicle transport [19]; this results in a severe secretory impairment, as well as degradation of enzymes and transporters participating in ceramide metabolism [20]. Although the cleavage of Golgi proteins often amplifies apoptotic signals, these alterations do not seem to be involved in the apical regulation of cell death [21].

At the moment, the role of the peroxisome in cell death is few investigated [22]. Peroxisomes are devoid of DNA, and have a single-limiting membrane [23]. Elongated tubular (>2 μm in length) or spherical (0.1–1 μm) peroxisomes including rod shape peroxisomes can be observed depending on the cell type [23–25]. It is hypothesized that peroxisomes (originally called microbodies) are a vestige of an ancient organelle, and thus the peroxisome is considered a 'fossil organelle', metablolizing oxygen in the ancestors of eucaryotic cells [23]. When oxygen produced by photosynthetic bacteria began to accumulate in the atmosphere, it would have been toxic to most organisms. Peroxisomes could have been used to lower the intracellular oxygen concentration but not effectively. The development of mitochondria would then have appeared with the advantage of coupling oxygen consumption to energy production in the form of ATP by means of mitochondrial oxidative phosphorylation [26]. The peroxisome contributes to several major metabolic processes: beta-oxidation of very long chain fatty acids, biosynthesis of ether phospholipids (plasmalogens) and metabolism of reactive oxygen species [23]. The name peroxisome stems from the ability of these organelles to synthetize and degrade hydrogen peroxide (H_2O_2). The evolution of peroxisomes illustrates symbiogenesis: newly born peroxisomes are hybrid organelles deriving from mitochondria and endoplasmic reticulum [27,28]. In addition, metabolic connections exist between peroxisomes and mitochondria [29,30]. In yeast, some data suggest that peroxisomes are implied in the regulation of necrosis. Thus, *S. cerevisiae PEX6* deleted cells display hallmarks of necrosis and strongly elevated formation of ROS [31]; in *H. polymorpha* methylotrophic yeast, deletion of *PMP20* leads to pronounced induction of necrosis [32]. In Pex5 knockout mice, the abscence of peroxisomes in hepatocytes causes endoplasmic reticulum and mitochondrial abnormalities [33,34]; the latter were characterized by i) reduced activity in complex I, III, and V, ii) differentially affected respiratory complexes (reduction in complexes I and III, incomplete assembly of complex V, normal activity of complexes II and IV), iii) depleted mitochondrial DNA and iv) increased permeability and fluidity in mitochondrial membranes leading to a collapse of the mitochondrial inner membrane potential [34,35]. These observations are in line with several studies which support the concept of peroxisomal interactions and cross-talk between peroxisomes and other subcellular compartments [36], and key connections between

peroxisomes and mitochondria for biogenesis and activity [29,30,37]. Furthermore, on 158 N murine oligodendrocytes, the production of reactive oxygen species (ROS) is potentiated when the peroxisomal proteins ABCD1 and ACOX1 are inactivated using RNA interference [38]. In aging and neurodegeneration, it has been proposed that peroxisomal dysfunctions could favor secondary mitochondrial alterations which could contribute to cell death [39]. Altogether, the various observations made on yeasts, cells and mice support the hypothesis that the peroxisome could play an active role in cell death. However, additional studies are required to identify the role of peroxisomes in the induction and progression of the cell death process.

In a number of old-age and chronic diseases, including Alzheimer's disease (AD) [40,41], eye diseases (cataract, age related macular degeneration (ARMD)) [42,43], colorectal inflammation [44,45] and cardiovascular diseases [46], oxidative stress, inflammation and/or organelle dysfunction (mainly mitochondrial dysfunction) are often observed. In AD and multiple sclerosis (MS), peroxisome dysfunction is also suspected [47,48]. In addition, these different diseases are frequently associated with increased levels of 7-ketocholesterol (7 KC; also named 7-oxocholesterol) in associated tissue lesions, cerebrospinal fluid and/or plasma [40,46,49,50]. 7 KC [51] is often found at increased levels in certain foods [52,53]; it results from cholesterol auto-oxidation [54,55] and can be formed endogeneously in different cell types [56]. As 7 KC is able to trigger oxidative stress, to favor cytokines secretion and to stimulate an apoptotic mode of cell death associated with autophagic criteria, named oxiapoptophagy, on numerous cell types from different species [57–60], it is strongly suspected that 7 KC could play key roles in the activation of the above mentioned diseases. In addition, as 7 KC accumulates in human cells, it is important to specify which organelles and which signaling pathways are affected by this compound,in order to identify natural and synthetic molecules [61,62] and new strategies, such as bioremediation [63–66], to impair its side effects. Currently, it is clearly established that elevated 7 KC concentrations lead to mitochondrial dysfunction contributing to the induction of apoptosis [58,67]. Lysosomal dysfunction, which could be a consequence of the accumulation of 7 KC in this organelle, has also been reported [68,69]. These lysosomal dysfunctions favor the release of proteolytic enzymes in the cytoplasm and are involved in 7 KC-induced cell death [70,71]. In addition, the observation by transmission electron microscopy (TEM) of myelin figures inside cytoplasmic vacuoles of different sizes, assimilated to phospholipidosis [58,72], evokes activation of endoplasmic reticulum autophagy (reticulophagy). With 7 KC, structures echoing mitophagy are also frequently observed. Thus, under treatment with 7 KC, data support that the lysosome contributes to different forms of autophagy [59,73,74]. Whether 7 KC-induced autophagy is protective or lethal remains to be seen. However, little is known about the impact of 7 KC on peroxisomes. It is worth noting that in the brain of patients with AD, elevated levels of 7 KC are observed [41] as well as i) enhanced numbers of peroxisomes, ii) abnormal levels of plasmalogens (the first two steps in plasmalogen biosynthesis take place in the peroxisomes via the DHAPAT (dihydroxyacetonephosphate acyltransferase) and ADHAPS (alkyldihydroxyacetonephosphate synthase) peroxisomal enzymes located on the luminal side of the peroxisomal membrane) [75–78], and iii) increased levels of very long chain fatty acid (VLCFA), which are metabolized in the peroxisome [47,79]. This leads us to suspect that 7 KC has an effect on peroxisomal biogenesis and activity. In addition, increased levels of VLCFA have been found in the plasma of patients with AD [48]. Furthermore, in 158 N and BV-2 cells treated with 7 KC, reduced mRNA and protein levels in peroxisomal transporters (ABCD1, ABCD2, ABCD3) and enzymes involved in peroxisomal β-oxidation (ACOX1, MFP2) have been described [60,80,81].

Currently, the role of mitochondria, endoplasmic reticulum and lysosome in 7 KC-induced cell death is clearly established. However, additional studies are required i) to define the role of peroxisomes in 7 KC-induced cell death and ii) to determine whether molecules which impair oxidative stress, mitochondrial and lysosomal dysfunction, caspase activation leading to apoptosis and autophagy associated with 7 KC-induced cell death also prevent peroxisomal damage.

In this context, in order to define how peroxisomes influence cell death, 158 N murine oligodendrocytes provide a relevant model i) to evaluate the relationship between oxidative stress and cell death, ii) to specify the role played by the organelles in these processes, iii) to determine the interactions between mitochondria and peroxisome, and iv) to identify natural and synthetic moleculesto prevent the cytotoxic effects of 7 KC [29,60,71,82].

In the present study, 158 N cells were cultured with 7 KC concentrations inducing minor and major cytotoxic effects, and the impact on mitochondria and peroxisomes were determined. As α-tocopherol is known to counteract 7 KC-induced cytotoxicity [59,83], its ability to prevent peroxisomal dysfunctions was also studied. Furthermore, α-tocopherol was compared with α-tocotrienol, which shares a common chromanol ring with α-tocopherol (R1 = CH3; R2 = CH3), whereas the farnesyl moiety of α-tocopherol and α-toctrienol are different: three unsaturated versus no double bonds on the farnesyl moiety of α-tocopherol and α-tocotrienol, respectively [84,85]. With 7 KC (25 μM), marked peroxisomal dysfunction associated with slight effects on mitochondria were observed, whereas with 7 KC (50 μM) both peroxysomal and mitochondrial dysfunctions were detected. Notably, the prevention of 7 KC-induced cell death was only observed with α-tocopherol which was able to impair both mitochondrial and peroxisomal dysfunction.

2. Materials and methods

2.1. Materials

7-ketocholesterol and α-tocopherol, as well as propidium iodide, dihydrorhodamine 123, Hoechst 33342, and saponin were provided by Sigma-Aldrich (St Quentin-Fallavier, France). α-tocotrienol was provided by Cayman/Interchim (# 10008377). $DiOC_6(3)$ and dihydroethidium (DHE) were from Life Technologies/Thermo Fisher Scientific (Courtaboeuf, France). Ferric chloride was obtained from Carlo-Erba (Milan, Italy), and the fluorescent mounting medium was obtained from Dako (Copenhagen, Denmark). The rabbit polyclonal antibody raised against ABCD3 (# PA1-650) was obtained from Pierce/Thermo Fisher Scientific and the goat anti-rabbit secondary antibody coupled with Alexa 488 was from Abcam (# ab150077). The caspase-3 antibody (rabbit polyclonal antibody) was from Ozyme/Cell Signaling (# 9662). The antibody raised against PARP (rabbit polyclonal antibody) was from Ozyme/Cell Signaling (# 9532S). The LC3-I/II (rabbit polyclonal antibody #L8918) and β-actin antibody (mouse monoclonal antibody #A2228) were from Sigma-Aldrich. Horseradish peroxidase-conjugated goat anti-rabbit (# 7074) was from Cell Signaling. The chemiluminescence detection kit (# 34096; Supersignal West Femto Maximum Sensitivity Substrate, Thermo-Scientific) and iScript cDNA Synthesis Kit were provided by Bio-Rad (# 1708891; Marne la Coquette, France). The RNeasy Mini Kit was obtained from Qiagen (# 74104; Courtaboeuf, France)), and the FG Power SYBR Green was from Thermo Fisher Scientific (# 10658255).

2.2. Culture and treatments of 158 N murine oligodendrocytes

Murine oligodendrocytes (158 N) [86] were seeded either in Petri dishes (30,000 cells/cm^2, 100 mm in diameter; 10 mL of culture medium), or in six-well plates (240,000 cells per well with 2 mL of culture medium). They were cultured in Dulbecco's Modified Eagle Medium (DMEM) containing 5% (v/v) heat-inactivated fetal bovine serum (Dutscher, Brumath, France) and 1% antibiotic (penicillin, streptomycin). The incubation was performed at 37 °C in a humidified atmosphere containing 5% CO_2. For subcultures, cells were trypsinized (0.05% trypsin-0.02% EDTA solution), and passaged twice a week.

7 KC (stock solution) was prepared at 2 mM as previously described [87]. After 24 h of culture, 158 N cells were incubated with 7 KC (25–50 μM) for 24 h without or with α-tocopherol or α-tocotrienol.

2.3. Ferric reducing antioxidant power (FRAP) assay

The ferric reducing antioxidant power (FRAP) assay measures the antioxidant potential of compounds or of mixtures of compounds through the reduction of ferric iron (Fe^{3+}) to ferrous iron (Fe^{2+}) [88–90]. This method, which was realized as previously described [80,81], was used to compare the antioxidant potential of α-tocopherol and α-tocotrienol, as compared with Trolox used as the positive reference. α-tocopherol, α-tocotrienol and Trolox were prepared in a range of concentrations from 0 to 5 mM in ethanol. The antioxidant potential of α-tocopherol, and α-tocotrienol evaluated with the FRAP method was estimated in Trolox equivalent (1 mol of α-tocopherol, and α-tocotrienol is equivalent to X mole of Trolox; X was determined with the calibration curve obtained with Trolox).

2.4. Fluorescein diacetate (FDA) test

Fluorescein diacetate (FDA) is a cell-permeant esterase substrate used as a viability probe [91]. The viability of 158 N murine oligodendrocytes was quantified with FDA (Sigma-Aldrich). At the end of the treatment, cells were incubated in the dark with FDA (15 μg/mL, 10 min) rinsed with PBS, and lysed with 10 mM Tris-HCl solution containing 1% sodium dodecyl sulfate (SDS). Fluorescence intensity (λ Excitation: 485 nm, λ Emission: 538 nm) was measured with a TECAN fluorescence microplate reader (Sunrise spectrophotometer, TECAN, Lyon, France). The experiments were realized in triplicate. The data were expressed as percentage of control.

2.5. Quantification of cells with depolarized mitochondria with $DiOC_6(3)$

Variations in the mitochondrial transmembrane potential (ΔΨm) were measured with 3,3′- dihexyloxacarbocyanine iodide ($DiOC_6(3)$. Cells were stained for 15 min at 37 °C with $DiOC_6(3)$ (40 nM); mitochondrial depolarization (loss of ΔΨm) is indicated by a decrease in green fluorescence collected through a 520 ± 10 nm bandpass filter on a Galaxy flow cytometer (Partec, Münster, Germany). For each sample, 10,000 cells were analyzed, and the fluorescence was measured on a logarithmic scale. Data were analyzed with Flomax (Partec) or FlowJo (Tree Star Inc., Ashland, OR, USA) software.

2.6. Measurement of reactive oxygen species with dihydroethidium and dihydrorhodamine 123

Overproduction of superoxide anion ($O_2^{\bullet -}$) and hydrogen peroxide (H_2O_2) were detected with dihydroethidium (DHE) [92] and dihydrorhodamine 123 (DHR123) [92,93], respectively. DHE (1.6 mM) was prepared in dimethyl sulfoxide (DMSO, Sigma-Aldrich), and used at 2 μM. DHR123 (2 mM) was prepared in DMSO, and used at 6 μM. After 15 min at 37 °C, the fluorescent signals of DHE and DHR123 stained cells were collected through a 590/20 nm and a 520/20 nm band pass filter, respectively, on a logarithmic scale on a Galaxy flow cytometer (Partec); 10,000 cells were acquired; data were analyzed with Flomax (Partec) or FlowJo (Tree Star Inc.) softwares.

2.7. Flow cytometric quantification of dead cells by staining with propidium iodide

Cells were stained with propidium iodide (PI: 1 μg/mL), which stains dead cells or cells with damaged cytoplasmic membranes [91]. Fluorescence was collected through a 630 longpass filter on a Galaxy flow cytometer (Partec): 10,000 cells were acquired. Data were analyzed with Flomax (Partec) or FlowJo (Tree Star Inc.) softwares.

2.8. Evaluation of mitochondrial topography by fluorescence microscopy

Cells were cultured on glass slides in six well plates. At the end of the treatment, cells were washed once with pre-warmed culture medium without FBS, and incubated with pre-warmed culture medium without FBS containing Mitotracker red (Thermo Fischer Scientific; 100 nM) for 30 min at 37 °C in a humidified atmosphere containing 5% CO_2. The cells were then washed with filtered PBS (0.2 μm) and fixed with filtered paraformaldehyde (PFA: 4%; 15 min at room temperature). After washing with filtered PBS, cells were counterstained with Hoechst 33342 (1 μg/mL). The slides were then mounted in fluorescent mounting medium (DakoCytomation, Dako, Coppenhagen, Denmark), and stored in the dark at 4 °C until examination under a fluorescent microscope coupled with an Apotome (Imager M2, Zeiss, Jena, Germany). The fluorescent signals of the samples were collected with the ZEN software (Zeiss).

2.9. Confocal microscopy evaluation of the level and topography of ABCD3 peroxisomal transporter revealed by indirect immunofluorescence

Cells were cultured on glass slides in a six well plates. After treatment, cells were washed with PBS and fixed with a 2% paraformaldehyde/PBS solution (15 min, room temperature (RT)). After washing in PBS, adherent cells were permeabilized with PBS/0.05% saponin/10% FBS, named PFS buffer (30 min, RT), and incubated with the ABCD3 antibody (1/500) diluted in PFS buffer (1 h, RT). At the end of the incubation time, cells were washed in PBS and incubated with a goat anti-rabbit antibody coupled wit 488-Alexa diluted at 1/500 in PFS buffer (30 min in the dark, RT). After washing in PBS, cells were counterstained with Hoechst 33342 (1 μg/mL). The slides were mounted in fluorescent mounting medium (Dako, Coppenhagen, Denmark), stored in the dark at 4 °C, and examined with a confocal microscope (Leica TCS SP8, Wetzlar, Germany). Hœchst fluorescence was collected as follows: excitation: 405 nm; emission 410/675 nm. 488-Alexa fluorescence was collected as follows: excitation 488 nm; emission 493/739 nm. Images were realized with the LASX software (Leica).

2.10. Flow cytometric quantification of ABCD3 peroxisomal transporter

Adherent cells were detached by trypsinization, mixed with

non-adherent cells, and fixed with paraformaldehyde (Sigma-Aldrich) diluted in PBS (2%, RT, 15 min). After two washes in PBS, the cells were incubated (RT, 30 min) in PBS/10% FBS/0.05% saponin (Sigma-Aldrich), named PFS buffer. After washing in PBS, the cells were incubated with a rabbit polyclonal antibody raised against ABCD3 (# 11523651, Pierce/Thermo Fisher Scientific). The cells were incubated (RT, 1 h) with the ABCD3 antibody diluted (1/500) in PFS buffer. After two washes in PBS, the cells were incubated (30 min) in the dark with a goat anti-rabbit secondary antibody coupled with Alexa 488 (1/500) in PFS buffer. After washing in PBS, the cells were resuspended in PBS and analyzed on a Galaxy flow cytometer (Dako/Partec). Fluorescence was collected on 10,000 cells through a 520/20 nm bandpass filter; data were analyzed with FlowJo software (Tree Star Inc.). Absolute and conjugated controls were done for the different conditions of treatments.

2.11. Visualization of LAMP1 expression pattern and evaluation of pexophagy (colocalization of p62 and ABCD3) by fluorescence microscopy

Cells were cultured on glass slides in six well plates. At the end of the treatment, cells were washed with PBS and fixed with 4% filtered PFA (0.2 μm) for 15 min at room temperature. After washing in PBS, cells were permeabilized with PBS/0.05% saponin/10% FBS (30 min, room temperature), and incubated with a rabbit polyclonal anti-ABCD3 antibody (Pierce/Thermo Fisher Scientific, diluted 1/500), a mouse monoclonal anti-p62 antibody (Abcam, Paris, France, #ab56416; diluted 1/300) or a rabbit polyclonal anti-LAMP1 antibody (Abcam #ab24170, diluted 1/300). The antibodies were diluted in PBS/0.05% saponin/10% FBS (1 h, room temperature).

At the end of the incubation time, cells were washed in PBS and incubated either with a goat anti-rabbit antibody Alexa-546 (1/500) or a goat anti-mouse Alexa 488 (1/500) diluted in PBS/0.05% saponin/10% FBS (30 min in the dark, room temperature). After washing in PBS, cells were counterstained with Hoechst 33342 (1 μg/mL). The slides were then mounted in fluorescent mounting medium (DakoCytomation), and stored in the dark at 4 °C until examination under a fluorescent microscope coupled with an Apotome (Imager M2, Zeiss). The fluorescent signals of the samples were collected with the ZEN software (Zeiss).

2.12. Transmission electron microscopy of peroxisomes and mitochondria

Transmission electron microscopy was used to simultaneously visualize and quantify peroxisomes, and to visualize mitochondria in 158 N cells cultured for 24 h in the absence or in the presence of 7 KC (25 μM) without or with α-tocopherol (400 μM); the vehicle control was ethanol (EtOH: 0.6%). Peroxisomes were quantified on 10 cells, and data were expressed as mean ± standard deviation (SD). Hepatic sections of 9- to 10-week-old C57 Black/6 males and wild type human fibroblasts were used as positive controls for peroxisomal analysis; fibroblasts from Zellweger patients were used as negative control. Normal fibroblasts and fibroblasts from Zellweger patients were a generous gift from Dr K. Heng Ng (Bicêtre Hospital, Kremlin-Bicêtre, France) [94]. For peroxisomal localization, cells and tissue sections were prepared as follows [86,95]. On cultured cells (wild type human fibroblast, fibroblasts from Zellweger patients, and untreated or treated-158 N cells), transmission electron microscopy was realized on adherent cells in culture wells. The samples were fixed for 1 h at 4 °C in 2.5% (w/v) glutaraldehyde diluted in cacodylate buffer (0.1 M, pH 7.4), washed in cacodylate buffer (0.1 M, pH 7.4), incubated in the dark for 1 h at 21 °C in Tris–HCl (0.05 M, pH 9.0) containing diaminobenzidine (2.5 mg/mL) and H_2O_2 (10 μ$props_value{literPattern}/mL of a 3% solution), washed in cacodylate buffer (0.1 M, pH 7.4) for 5 min at 21 °C, post-fixed in 1% (w/v) osmium tetroxide diluted in cacodylate sodium (0.1 M, pH 7.4) for 1 h at 21 °C in the dark, and rinsed in cacodylate buffer (0.1 M, pH 7.4). The preparations were then dehydrated in graded ethanol solutions and embedded in Epon. Ultra-thin sections (80–82 nm) were cut with an ultramicrotome, contrasted with uranyl acetate and lead citrate, and examined under an H7500 electron microscope (Hitachi, Tokyo, Japan).

2.13. Lipid extraction

For cardiolipins and plasmalogens analysis, cell pellets (around 5×10^6 cells) were spiked with 100 ng and 150 ng of 17:0/17:0 phosphatidylethanolamin and 14:0/14:0/14:0/14:0 cardiolipin used as internal standard, respectively. Total lipids were extracted with the Folch method [96]. Extracts were dissolved with 100 μL of chloroform/methanol/distilled water 60/30/4.5, and 1–8 μL were used for lipidomics analysis. Lipid standards and chemicals of the highest grade available were from Avanti Polar Lipids (Coger SAS, Paris, France) and Sigma Aldrich, respectively. LC-MS/MS quality grade solvents were from Thermo Fischer Scientific.

2.14. Characterization and quantification of cardiolipins by liquid chromatography tandem mass spectrometry (LC-MS/MS)

Cardiolipins were analyzed by LC-MS/MS (Agilent 6460 QqQ mass spectrometer, Agilent Technologies, Santa Clara, CA, USA) operating in negative selected reaction monitoring ion mode as described by Peyta et al. [97]. Lipid extracts were solubilized in 100 μL of $CHCl_3$/MeOH/H_2O (60/30/4.5); LC–MS/MS analysis of cardiolipins was conducted as previously described [98].

2.15. Characterization and quantification of plasmalogens by liquid chromatography tandem mass spectrometry (LC-MS/MS)

Phosphatidylethanolamines (PE) were analyzed by LC-MS/MS on an Agilent 6460 QqQ mass spectrometer (Agilent Technologies) using the same chromatographic conditions as previously described [98]. Acquisition was performed on an Agilent 6460 QqQ mass spectrometer operating in positive selected reaction monitoring ion mode (source temperature 325 °C, nebulizer gas flow rate 10 L/min, sheath gas flow 11 L/min, temperature 300 °C, capillary 3500 V, nozzle 1000 V). Fragmentor and collector voltages were set up at 136 V and 12 V respectively.

Transitions: $[M+H]^+ \rightarrow [M + H\text{-}141]^+$, corresponding to the neutral loss of the phosphoethanolamine moiety, were used for the quantification of phosphatidylethanolamines. Transitions: $[M+H]^+ \rightarrow 364$, $[M+H]^+ \rightarrow 392$, $[M+H]^+ \rightarrow 390$ were used for p16:0, p18:0 and p18:1 pPE species, respectively. Each PE and pPE was semi-quantified by calculating their response ratio with regard to 17:0/17:0 PE used as internal standard.

2.16. Characterization and quantification of fatty acids and sterols by gas chromatography coupled with mass spectrometry (GC/MS)

Total fatty acids, including very long chain fatty acids, were analyzed by GC/MS on a HP7890A Gas Chromatograph equipped with an HP7683 injector and a HP5975C Mass Selective Detector (Agilent Technologies) as described by Blondelle et al. [99]. Fatty acids were quantitated by calculating the relative response ratios to their closest internal standard. Calibration curves were obtained with fatty acid authentic standards (14:0, 15:0, 16:0, 17:0, 18:0, 19:0, 20:0, 21:0, 22:0, 24:0, 26:0, 16:1n-7, 18:1n-7, 18:1n-9, 18:2n-6, 18:3n-3, 18:3n-6, 20:2n-6, 20:3n-3, 20:4n-6, 20:5n-3, 22:3n-3,

22:5n-6, 22:6n-3) processed as cell pellets.

Sterol analysis (7β-hydroxycholesterol, cholestane-3β, 5α, 6β-triol) was realized by GC–MS on a Clarus 600D (Perkin Elmer, USA). The GC was equipped with an Elite column (30 m × 0.32 mm id x 0.25 mm film; Perkin Elmer, USA) and injection was performed in splitless mode using helium (1 mL/min) as carrier gas. temperature program (initial temperature of 80 °C was held for 1 min, followed by a linear ramp of 10 °C/min to 220 °C, 20 °C/min to of 280 °C and 5 °C/min up to 290 °C, which was held for 10 min. Peak integration was performed manually, and sterols were quantified from selected-ion monitoring analyses against internal standards using standard curves.

2.17. Polyacrylamide gel electrophoresis and western blotting

Adherents and floating cells were collected, washed in PBS and lysed for 30 min on ice in a RIPA buffer (10 mM Tris-HCl, pH 7.2, 150 mM NaCl, 0.5% Nonidet NP40, 0.5% Na deoxycholate, 0.1% SDS, 2 mM EDTA and 50 mM NaF) containing a complete protease inhibitor cocktail (Roche Diagnostics, Indianapolis, IN, USA) diluted 1/25. Stock solution (25X) of a complete protease inhibitor cocktail was prepared by diluting one tablet in 2 mL of distilled water. Cell lysates were cleared by centrifugation at (20 min, 20,000 g). In the supernatant, the protein concentration was measured using bicinchoninic acid assay (Thermo Fischer Scientific). Seventy micrograms of protein were diluted in a loading buffer (125 mM Tris- HCl, pH 6.8, 10% β-mercaptoethanol, 4.6% SDS, 20% glycerol, and 0.003% bromophenol blue), analyzed on a 14% SDS-PAGE gel for caspase-3 or LC-3 and β-actin, 8% for PARP, and transferred onto a nitrocellulose membrane (Thermo Fischer Scientific). After blocking nonspecific binding sites (1 h) with 5% milk powder in PBST (PBS, 0.1% Tween 20, pH 7.2), the membranes were incubated overnight (4 °C) with the primary antibody diluted in PBST. The antibodies directed against caspase-3 (detecting endogenous levels of full length casapase-3 (35 kDa) and the large fragment of caspase-3 resulting from cleavage (17 kDa) (Cell signaling/Ozymes, Trois-Rivières, Canada), and LC3-II/LC3-I (detecting LC3-I (16 kDa) and LC3-II (18 kDa)) (Sigma-Aldrich), and PARP (detecting endogenous level of full length PARP (110 kDa) and the 89 kDa cleaved fragment of PARP) (Cell signaling), ABCD3 (Thermo Fisher Scientific), ABCD1 [86,100] and MFP2 (Gentex/Euromedex, Souffelweyersheim, France; #GTX114978) were rabbit polyclonal antibodies; they were used at a final dilution of 1/1000. ACOX1 rabbit antibody [86,100] detecting two ACOX1 isoforms at 70 and 50 kDa was used at 1/250. The polyclonal goat antibody detecting catalase (R&D systems, Abingdon, UK) was used at 1/400.

An antibody directed against β-actin (mouse monoclonal antibody) was used (final concentration: 1/10,000). The membrane was then washed twice with PBST and incubated (1 h, room temperature) with horseradish peroxidase-conjugated goat anti-rabbit, rabbit anti-goat or goat anti-mouse diluted at 1/5000 in 1% milk powder in PBST (PBS, 0.1% Tween 20, pH 7.2). The membrane was washed with PBST and revealed using an enhanced chemiluminescence detection kit (Supersignal West Femto Maximum Sensitivity Substrate, Thermo-Scientific) and Chemidoc XRS$^+$ (Bio-Rad). Band intensity was determined with Image Lab software (Bio-Rad).

2.18. Quantification of gene expression asociated with peroxisomal β-oxidation (Abcd3, Acox1, and Mfp2) and plasmalogen biosynthesis (DHAPAT, ADHAPS) by RT-qPCR

Total mRNA from 158 N cells were extracted and purified using the RNeasy Mini Kit (Qiagen). Total mRNA concentration was measured with TrayCell (Hellma, Paris, France). The purity of nucleic acids was controlled by the ratio of absorbance at 260 nm and 280 nm (ratios of 1.8–2.2 were considered satisfactory). One microgram of total mRNA was used for reverse transcription with the iScript cDNA Synthesis Kit (Bio-Rad) according to the following protocol: 5 min at 25 °C, 20 min at 46 °C, 5 min at 95 °C. cDNA were amplified using the FG Power SYBR Green (Thermo Fischer Scientific). All PCR reactions were realized on an Applied Biosystem Step One plus QPCR machine (Life Science Technologies). The primer sequences were the following:

- *Abcd1: forward 5′-acatccctatcatcacacccactg -3′ and reverse 5′-gagaactcttgccacagccattg -3′*
- *Abcd2: forward 5′-gttcaaagagaaggaggatgggatg -3′ and reverse 5′-tgctcacggcactggtacattc -3′*
- *Abcd3: forward 5′-ctgggcgtgaaatgactagattg-3′ and reverse 5′-cttctcctgttgtgacaccattg-3′*
- *Acox1: forward 5′-gcccaactgtgacttccatt-3′ and reverse 5′-ggcatg-taacccgtagcact-3′*
- *Mfp2: forward 5′-aggggacttcaagggaattgg-3′ and reverse 5′-gcctgcttcaactgaatcgtaa-3′*
- *DHAPAT: forward 5′-atggacgttcctagctcctcc -3′ and reverse 5′-gcggggtgtagcacttcatt -3′*
- *ADHAPS: forward 5′-aatggatggggctacaatgattc -3′ and reverse 5′-tccagacttactccaagggtg -3′*

Thermal cycling conditions were as follows: activation of DNA polymerase at 95 °C for 10 min, followed by 40 cycles of amplification at 95 °C for 15 s, 60 °C for 30 s, and 72 °C for 30 s, followed by a melting curve analysis to test for the absence of non-specific products. Gene expression was quantified using cycle to threshold (Ct) values and normalized by the *36B4* reference gene (*forward 5′-gcgacctggaagtccaacta -3′ and reverse 5′-atctgcttggagcccacat -3′*). The quantitative expression of *Abcd1, Abcd3, Acox1, Mfp2, DHAPAT* and *ADHAPS* was determined as fold induction of the control.

2.19. Statistical analysis

The experimental data are mean ± standard deviation (SD). Statistical analyses were realized using SigmaStat 2.03 software (Systat Software) with the Mann-Whitney test. Data were considered statistically different at a *P*-value of 0.05 or less.

3. Results

3.1. Assessment of the cytoprotective effects of α-tocopherol and α-tocotrienol

Because 7-ketocholesterol (7 KC) is associated with numerous diseases and induces side effects (oxidative stress, inflammation) which lead to cell death, it is important to identify natural and synthetic compounds capable of counteracting its cytotoxic activities. Certain tocopherols have been shown to have cytoprotective activities. Trolox reportedly prevents 7 KC-induced cell death on nerve cells, PC12 and SH-SY-5Y [101,102]. On human promonocytic U937 cells, 158 N murine oligodendrocyte cells and murine microglial BV-2 cells, cytoprotective effects have been observed for α-tococopherol [80,81,87,103]. In addition, on BV-2 cells, ɤ-tocopherol was able to prevent 7 KC-induce side effects, but the same was not observed for Trolox [80]. Seeing as some tocopherols are able to impair 7 KC-induced cytotoxicity, we evaluated the ability of α-tocotrienol to prevent 7 KC (25–50 μM)-induced cell death comparatively to α-tocopherol on 158 N cells. Interestingly, with the FRAP test, similar anti-oxidant capacities were observed for α-tocopherol (1.13 ± 0.47 Trolox equivalent (mM)) and α-tocotrienol (0.98 ± 0.53 Trolox equivalent (mM)) (Fig. 1A). With α-tococopherol

A

	Trolox equivalent	SD
α-tocopherol	1.13	0.47
α-tocotrienol	0.98	0.53

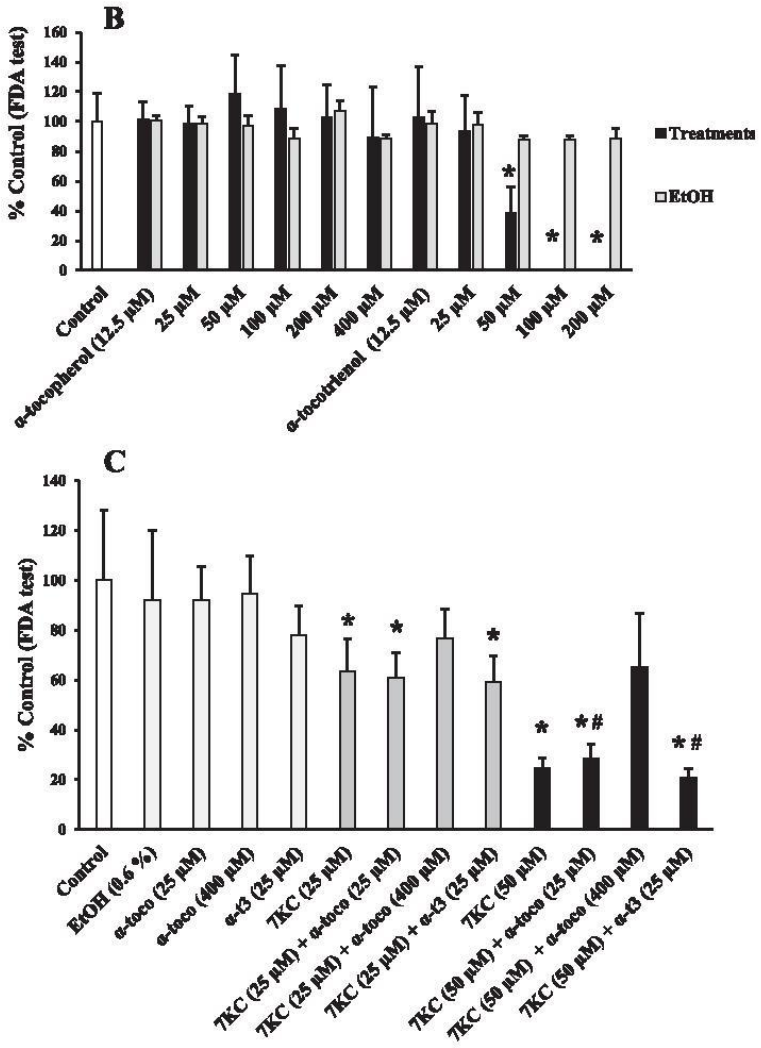

Fig. 1. Antioxidant properties of α-tocopherol (α-toco) and α-tocotrienol (α-t3), evaluation of their cytotoxicity and cytoprotective effects. The antioxidant properties of α-tocopherol (α-toco) and α-tocotrienol (α-t3) were determined with the FRAP assay as previously described [80,81] **(A)**. Their cytotoxic effects were determined by fluorimetry with the FDA test on 158 N treated for 24 h with different concentrations of α-toco (12.5, 25, 50, 100, 200 and 400 µM) and α-t3 (12.5, 25, 50, 100, and 200 µM) (**B**). Their ability to prevent 7 KC-induced cell death was evaluated on 158 N cells taken after 24 h of culture, and further cultured without and with 7 KC (25–50 µM) in the absence or in the presence of α-toco (25 and 400 µM) or α-t3 (25 µM) for an additional 24 h period of time (**C**). Significance of the differences between control (untreated cells) and 7 KC-treated cells; Mann Whitney test: *P < 0.05 or less. Significance of the differences between 7 KC-treated cells and (7 KC + α-toco (or α-t3)) - treated cells; Mann Whitney test: #P < 0.05 or less. No significant differences were found between control and vehicle-treated cells (Ethanol (EtOH0.6%).

(range of concentrations from 12.5 to 400 μM) no cytotoxic effects were found with the FDA test, whereas with α-tocotrienol (range of concentration from 12.5 to 200 μM), marked cytotoxic effects were observed at 50, 100 and 200 μM (Fig. 1B). No significant differences between control (untreated cells) and vehicle (ethanol (EtOH) 0.015%–0.85%) were observed (Fig. 1B). At the highest non-toxic concentration of α-tocotrienol (25 μM), as well as with α-tocopherol (25 μM), no cytoprotective effects were observed (Fig. 1C). However, as previously described on numerous cell types and evaluated with the FDA test, α-tococopherol (400 μM) was able to attenuate 7 KC (25–50 μM)-induced cytotoxicity (Fig. 1C). Consequently, for further experiments the ability to prevent 7 KC-induced side effects was only realized with α-tococopherol (400 μM). In addition, slight cytotoxic effects were seen with 7 KC (25 μM) and marked cytotoxic effects were observed at 7 KC (50 μM) upon FDA testing (Fig. 1C).

3.2. Concentration-dependent effect of 7-ketocholesterol on cytoplasmic membrane damage, mitochondrial dysfunction (loss of transmembrane mitochondrial potential, decreased level of cardiolipins) and mitochondrial topography

FDA test results underline that 7 KC (25 μM) induces slight cytotoxic effects whereas 7 KC (50 μM) is strongly cytotoxic. To investigate these results further, 158 N cells were cultured for 24 h with or without 7 KC (25–50 μM), and the percentage of cells with altered plasma membranes (propidium iodide (PI) positive cells considered as dead cells) [91,104] and with depolarized mitochondria ($DiOC_6(3)$ negative cells) were determined. No statistically significant differences were observed between untreated (control) and vehicle (EtOH 0.6%)-treated cells (Fig. 2A–B). In the presence of 7 KC (50 μM), in comparison with untreated (control) and vehicle (EtOH 0.6%)-treated cells, a marked and significant increase of the percentage of PI positive cells and of $DiOC_6(3)$ negative cells was found (Fig. 2A–B). In the presence of 7 KC (25 μM), in comparison with untreated (control) and vehicle (EtOH 0.6%)-treated cells, significant increases of PI positive cells and $DiOC_6(3)$ negative cells were found. This data supports the idea that 7 KC (25 μM) has onlhy slight cytotoxic effects seeing as the effects were more pronounced for 7 KC (50 μM) (Fig. 2A–B). In the presence of α-tocopherol (400 μM), the enhancement of PI positive cells was strongly attenuated, and $DiOC_6(3)$ negative cells were observed after treatment with 7 KC (25–50 μM) (Fig. 2A–B).

In 7 KC (50 μM)-treated 158 N cells, we previously have reported that the loss of transmembrane mitochondrial potential (ΔΨm) measured with DiOC6(3) was associated with a decrease of oxidative phosphorylation revealed by reduced NAD^+ and ATP levels and with lower levels of the organic acids (pyruvate, citrate, fumarate, succinate) of the tricarboxylic acid (TCA) cycle [105]. Therefore, we found it relevant to investigate whether the loss of ΔΨm was also associated with reduced levels of cardiolipins. Indeed, these specific mitochondrial phopholipids are located in the inner mitochondrial membrane and contribute to the maintenance of ΔΨm (one cardiolipin molecule interacts with two protons (H^+)) [106]. Compared to untreated (control) or vehicle (EtOH 0.6%)-treated cells, which have similar cardiolipin contents, decreased levels of total cardiolipins was observed with 7 KC (25–50 μM) treatment (Fig. 2C). Surprisingly, decreased levels of total cardiolipins were also revealed with α-tocopherol treatment in the three independent experiments, whereas no cytotoxic effects were observed with this compound (FDA, PI and $DiOC_6(3)$ tests) (Fig. 2C). In addition, the decrease of total cardiolipins observed under treatment with 7 KC was not impaired by α-tocopherol though this compound was able to attenuate 7 KC-induced loss of ΔΨm (Fig. 2C).

The mitochondrial topography was studied by fluorescence microscopy after staining with Mitotracker red (Supplementary Fig. 1). In 7 KC (25–50 μM)-treated cells, clusters of mitochondria, which could also suggest mitochondrial morphological changes, were observed. These modifications were totally counteracted when 7 KC (25 μM) was associated with alpha-tocopherol, whereas some cells with an abnormal cytoplasmic distribution of the mitochondria were still observed with 7 KC (50 μM). We did not found differences between control and vehicle-treated cells.

3.3. Concentration dependent effect of 7-ketocholesterol on superoxide anion and hydrogen peroxide overproduction, and catalase activity

Superoxide anion ($O_2^{\bullet -}$) production, hydrogen peroxide (H_2O_2) production and catalase activity were quantified on 158 N cells cultured for 24 h with or without 7 KC (25–50 μM) in the absence or in the presence of α-tocopherol (400 μM) and/or α-tocotrienol (25 μM; the highest non-cytotoxic concentration determined with the FDA test). Superoxide anions and hydrogen peroxide production were detected by flow cytometry after staining with dihydroethidium (DHE) and dihydrorhodamine 123 (DHR123). No significant differences were observed between untreated (control), vehicle (EtOH 0.6%)-treated cells, α-tocopherol (400 μM) and α-tocotrienol (25 μM) (Fig. 3A–B). A slight increase of cells overproducing superoxide anions and hydrogen peroxide were observed with 7 KC (25 μM) treatment (Fig. 3A–B). A marked and statistically significant increase of cells overproducing superoxide anions and hydrogen peroxide was observed in the presence of 7 KC (50 μM) (Fig. 3A–B). The increase in cells overproducing superoxide anions and hydrogen peroxide was impaired when 7 KC was associated with α-tocopherol (400 μM), whereas α-tocotrienol (25 μM) did not have a protective effect (Fig. 3A–B). An increase in 7 KC-induced superoxide anion production was observed in the presence of α-tocotrienol (25 μM) (Fig. 3A). The increased production of $O_2^{\bullet -}$ and H_2O_2 was associated with a lipid peroxidation process revealed by enhanced cellular levels of 7β-hydroxycholesterol and cholestane-3β,5α,6β-triol normalized in part by α-tocopherol (Supplementary Fig. 2).

In addition, as an increased proportion of cells overproducing H_2O_2 was observed with 7 KC (25–50 μM) treatment, the impact of this oxysterol on catalase, a specific peroxisomal enzyme which degrades hydrogen peroxide into water and dioxygen ($2\ H_2O_2 \rightarrow 2\ H_2O + O_2$), was defined Whereas no effect of 7 KC (25 μM) on catalase activity was observed (comparatively to untreated-, vehicle- and α-tocopherol-treated cells which demonstrated similar activity), a significant increase in catalase activity was found with 7 KC (50 μM) treatment (Fig. 3C). When α-tocopherol was associated with 7 KC, no normalization of catalase activity was detected: catalase activity in 7 KC and (7 KC + α-tocopherol)-treated cells were similar (Fig. 3C). Noteworthy, by western blotting, no increased level of catalase was found with 7 KC (25 μM); however, a significant increased level of catalase was detected under treatment with 7 KC (50 μM) supporting that the enhancement of catalase activity could be due to the higher catalase level, and that 7 KC, used at a high concentration (50 μM), favors catalase expression and/or stability (Fig. 3C). Whereas the catalase level was lower in (7 KC (50 μM) + α-tocopherol) than in 7 KC (50 μM), the catalase activity was similar in these two conditions (Fig. 3C).

3.4. Effect of 7-ketocholesterol on apoptosis and autophagy induction

Apoptosis and autophagy were biochemically evaluated on 158 N cells cultured for 24 h with or without 7 KC (25–50 μM) in the absence or in the presence of α-tocopherol. In agreement with

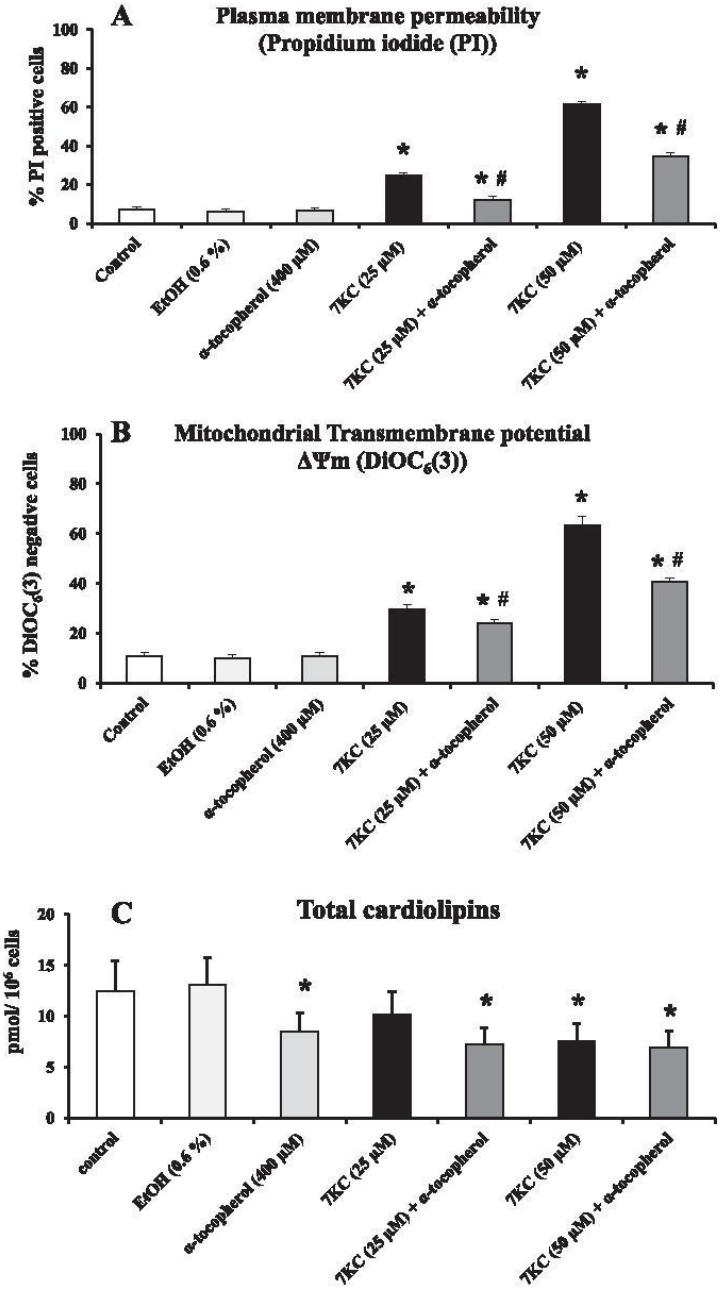

Fig. 2. Effect of 7-ketocholesterol on plasma membrane permeability, transmembrane mitochondrial potential and total cardiolipins content. 158 N murine oligodendrocytes were taken after 24 h of culture (70–80% confluency); they were further cultured without and with 7 KC (25–50 µM) associated or not with α-tocopherol (400 µM) for an additional 24 h period of time. They were analyzed by flow cytometry after staining with propidium iodide (PI) (to evaluate plasma membrane damage) (**A**) and $DiOC_6(3)$ (to evaluate transmembrane mitochondrial potential) (**B**). The percentage of PI positive cells and of cells with depolarized mitochondria were determined. In addition, total cardiolipins content was determined by LC-MS/MS (**C**). Significance of the differences between control (untreated cells) and 7 KC-treated cells; Mann Whitney test: *P < 0.05 or less. Significance of the differences between 7 KC-treated cells and (7 KC + α-tocopherol) - treated cells; Mann Whitney test: #P < 0.05 or less. No significant differences were found between control, vehicle-treated cells (Ethanol (EtOH: 0.6%) and α-tocopherol.

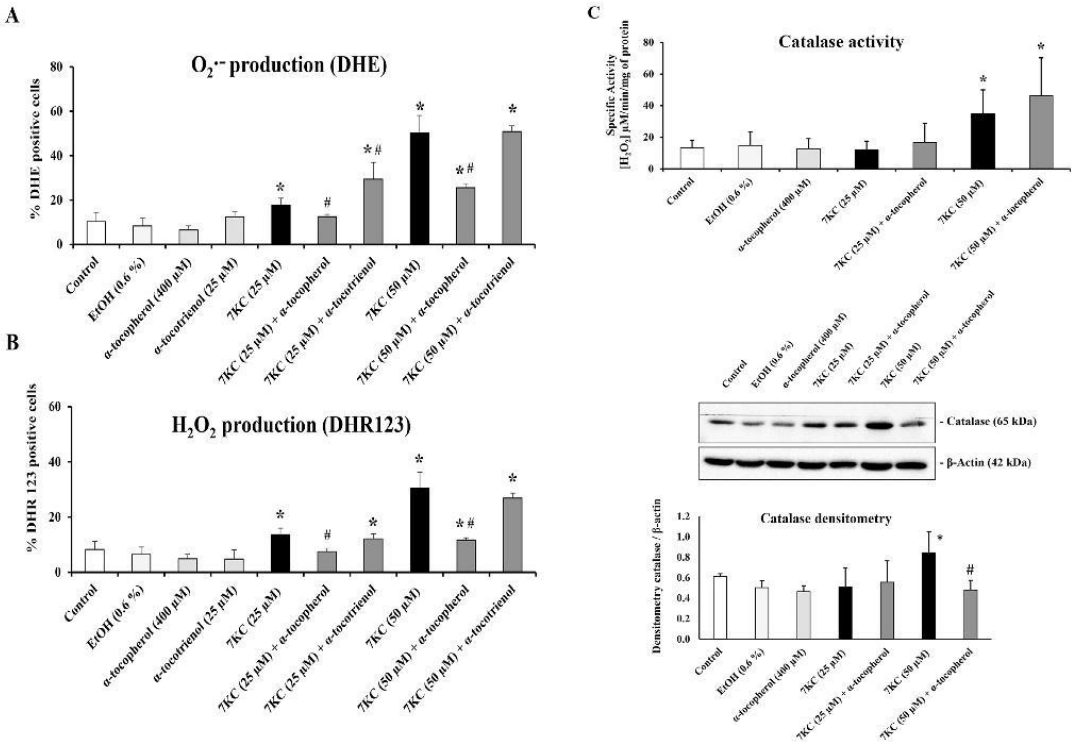

Fig. 3. Effect of 7-ketocholesterol on superoxide anion and hydrogen peroxide production, and on catalase activity and expression. 158 N murine oligodendrocytes taken after 24 h of culture, and further cultured without and with 7 KC (25–50 μM) associated or not with α-tocopherol (400 μM) or α-tocotrienol (25 μM) for an additional 24 h period of time, were analyzed by flow cytometry with dihydroethidium (DHE; evaluation of superoxide anion ($O_2^{\bullet-}$) production) (**A**) and dihydrorhodamine 123 (DHR123; evaluation of hydrogen peroxide (H_2O_2) production) (**B**); catalase activity and expression was also measured (**C**). Significance of the differences between control (untreated cells) and 7 KC-treated cells; Mann Whitney test: *P < 0.05 or less. Significance of the differences between 7 KC-treated cells and (7 KC + α-tocopherol (or α-tocotrienol)) - treated cells; Mann Whitney test: #P < 0.05 or less. No significant differences were found between control and vehicle-treated cells (Ethanol (EtOH: 0.6%).

previously reported data, western blot [59,103] revealed an induction of apoptosis and autophagy with 7 KC (50 μM): presence of cleaved caspase-3, fragmentation of poly(ADP-ribose)-polymerase (PARP), and activation of LC3-I in LC3-II (increased ratio LC3-II/LC3-I) (Fig. 4; supplementary Fig. 3). Similarly, in agreement with previous data [81], no cleaved caspase-3 and no cleaved PARP were observed under treatment with 7 KC (25 μM) (Fig. 4). At this concentration, a slight increase of the LC3-II/LC3-I ratio was observed (Fig. 4). The ability of 7 KC (25–50 μM) to induce apoptosis and autophagy was strongly attenuated by α-tocopherol: the presence of cleaved-caspase-3 was strongly reduced and at the threshold for detection, PARP cleavage was strongly attenuated but detectable, and the ratio LC3-II/LC3-I was similar to control and vehicle-treated cells (Fig. 4).

3.5. Effect of 7-ketocholesterol on the level of ABCD3, a major peroxisomal membrane component

ABCD3, the peroxisomal membrane protein (ATP binding cassette subfamily D member 3) which is a major and common constituent of peroxisomes in different tissues, is frequently used to evaluate peroxisomal mass [107,108]. In the peroxisomal membrane, ABCD3 is involved in the transport of pristanic acid, dicarboxylic acid, and of bile acid intermediates (di- and trihydroxycholestanoic acid (DHCA/THCA)) [109]. It can be detected and quantified by various complementary methods including western blotting, microscopy and flow cytometry methods [60,110]. After staining with a rabbit polyclonal antibody raised against ABCD3, stacks of confocal microscope images obtained on control, vehicle-treated cells (EtOH 0.6%), α-tocopherol (400 μM) and 7 KC (25–50 μM)-treated cells with or without α-tocopherol reveal major differences in comparison to untreated and vehicle-treated cells. A higher density of peroxisomes was observed in the cytoplasm of 7 KC (25–50 μM)-treated cells. While the peroxisomes are homogeneously distributed in the cytoplasm of the control and vehicle-treated cells, they were preferentially accumulated in a particular area of the cytoplasm in 7 KC-treated cells (Fig. 5A). It is important to underline that in our experimental conditions, confocal microscopy was used on adherent cells. Because the loss of cell adhesion occurs before the loss of ΔΨm with 7 KC treatment [111], our data suggest that the topographical peroxisomal changes might precede mitochondrial dysfunction. In addition, the effect of 7 KC on the peroxisomal mass, previously reported on 7 KC-treated BV-2 cells [60,80] was confirmed by flow cytometry. The analysis of ABCD3 levels on 158 N cells (adherent + non-adherent cells) revealed no differences between untreated- (control), vehicle- and α-tocopherol-treated cells, but a significant increase of the percentage of cells with reduced ABCD3 level under treatment with 7 KC (25–50 μM) (Fig. 5B). In addition, a significant decrease of the mean fluorescence intensity (MFI) of cells expressing ABCD3 was

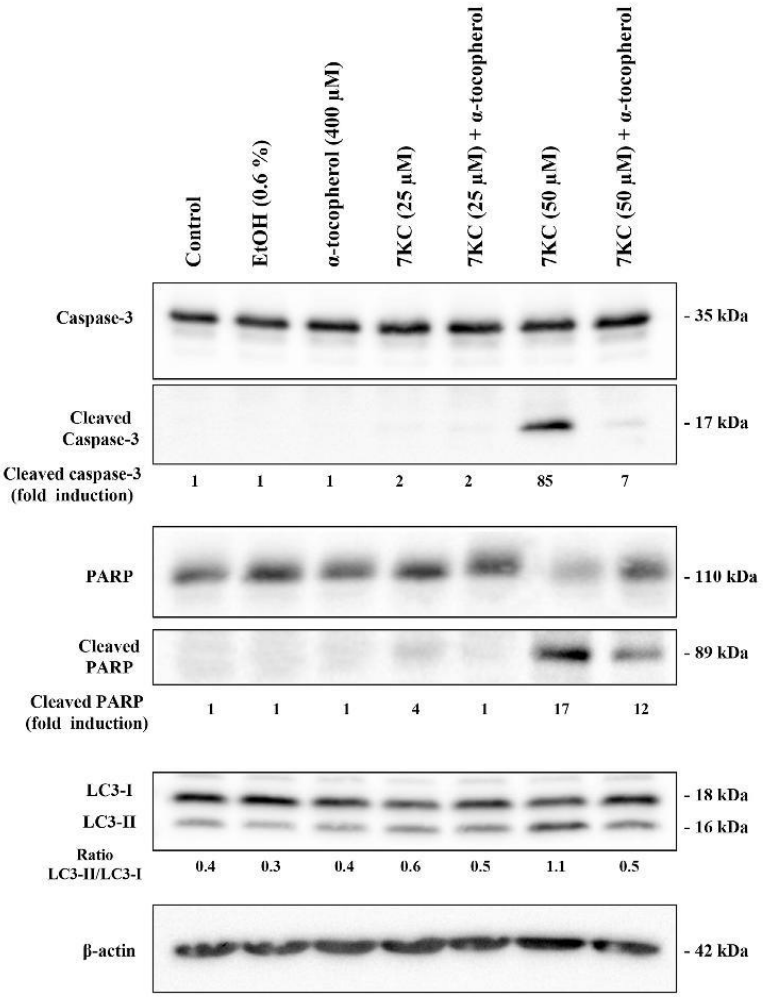

Fig. 4. Effect of 7-ketocholesterol on apoptosis and autophagy induction. 158 N murine oligodendrocytes were taken after 24 h of culture; they were further cultured without and with 7 KC (25–50 µM) associated or not with α-tocopherol (400 µM) for an additional 24 h period of time. They were analyzed by western blotting. Apoptosis was evaluated by caspase-3 activation (cleaved caspase-3), and PARP fragmentation, and autophagy by conversion of LC3-I to LC3-II [increased ratio (LC3-II/LC3-I)]. The EtOH value (0.6%) corresponds to the highest final EtOH concentration in the culture medium. No difference was observed between control and vehicle (EtOH)-treated cells. Data shown are representative of three independent experiments. The densitometric values of the ratio [LC3-II/LC3-I] are presented in Supplementary Fig. 3.

observed under treatment with 7 KC (25–50 µM) (Fig. 5B). In the presence of α-tocopherol, topographical changes in the peroxisomes were attenuated as well as the reduced expression of ABCD3 (Fig. 5B); however, the percentage of cells with reduced ABCD3 level in (7 KC + α-tocopherol)-treated cells remains higher than in vehicle treated-cells (Fig. 5B).

3.6. *Induction of morphological peroxisomal modifications under 7-ketocholesterol treatment and activation of pexophagy*

Peroxisomes are round cytoplasmic structures which can be detected by transmission electron microscopy (TEM) based on catalase activity after staining with diaminobenzidine [23,112,113]. This organelle has been previously observed by TEM in 158 N cells [39,86]. At the moment, it is well established that in patients with peroxisomal disorders, peroxisomes with abnormal shapes and sizes can be observed [112,114]. In addition, biochemical and morphological changes in peroxisomes have been described in response to infections, drugs and toxins [115]. On 158 N cells, cultured with or without 7 KC, associated with α-tocopherol or not, it was therefore of interest to study the morphological characteristics of peroxisomes. On liver tissue sections (Fig. 6A), peroxisomes and mitochondria were clearly detected. Regular peroxisomes were also observed on wild type human fibroblasts (Fig. 6B), whereas in fibroblasts from Zellweger patients, no peroxisome with round and regular shapes were detected: few DAB positive structures, which can denote morphologically abnormal peroxisomes, were observed (Fig. 6C–E).

In untreated (control) (Fig. 7A), vehicle (EtOH 0.6%)-treated (Fig. 7B), and α-tocopherol (400 µM)-treated 158 N cells (Fig. 7F),

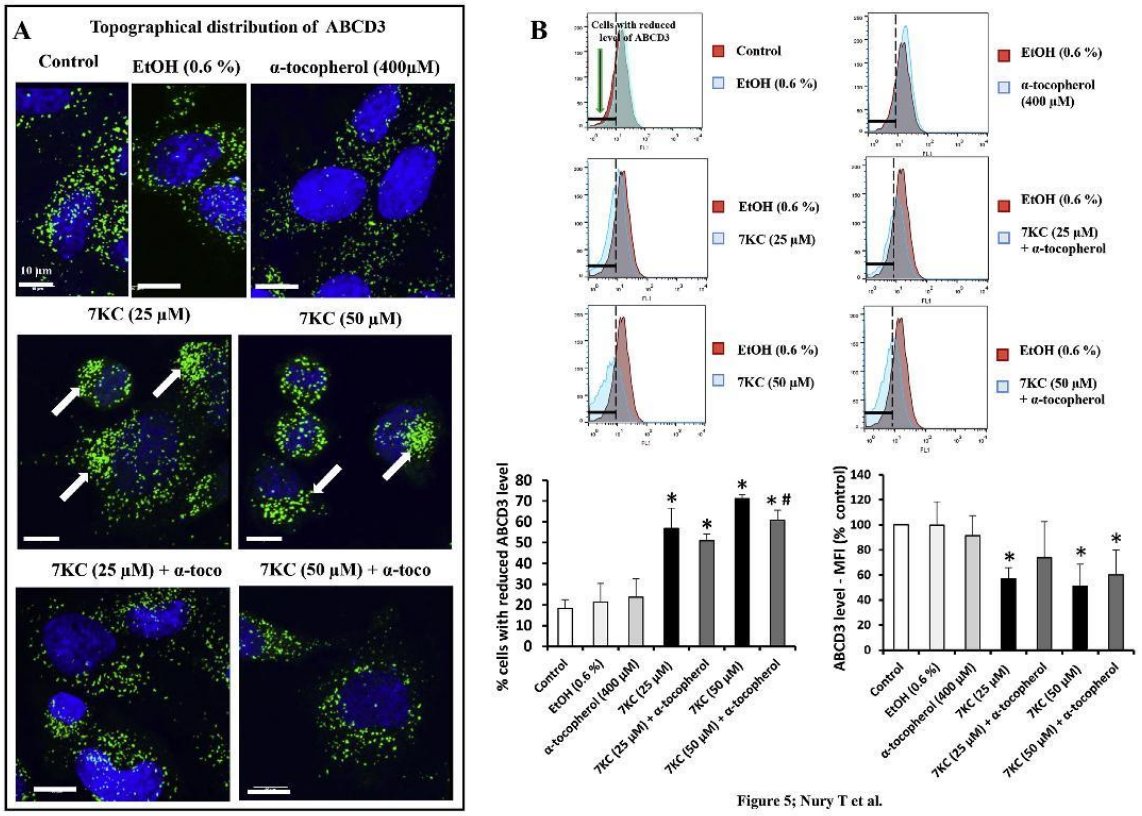

Fig. 5. Effect of 7-ketocholesterol on the topography and expression of a major peroxisomal membrane component (ABCD3). 158 N murine oligodendrocytes, taken after 24 h of culture and further cultured without and with 7 KC (25–50 μM) associated or not with of α-tocopherol (400 μM) for an additional 24 h period of time, were analyzed by confocal microscopy (**A**), and flow cytometry (**B**). ABCD3 level was revealed with a rabbit polyclonal antibody. Data shown are representative of 3 independent experiments. The white arrows point towards cells with an accumulation of peroxisomes in a particular area of the cytoplasm. Significance of the differences between control (untreated cells) and 7 KC-treated cells; Mann Whitney test: *P < 0.05 or less. Significance of the differences between 7 KC-treated cells and (7 KC + α-tocopherol) - treated cells; Mann Whitney test: #P < 0.05 or less. No significant differences were found between control and vehicle-treated cells (Ethanol (EtOH: 0.6%).

round peroxisomes and numerous mitochondria were clearly observed. The quantity of total peroxisomes was the following; control: 2.3 ± 0.8 (median: 2.5); vehicle: 2.4 ± 0.9 (median: 2.5); α-tocopherol: 2.5 ± 0.7 (median: 3.0). In 7-ketocholesterol (7 KC: 25 μM)-treated cells, peroxisomes with abnormal sizes and shapes (evoking DAB positive structures observed in Zellweger fibroblasts) were observed (Fig. 7C, D, E); DAB-positive structures were also identified in vacuoles evoking a pexophagy process (Fig. 7C). In (7 KC (25 μM) + α-tocopherol (400 μM))-treated cells, mainly round peroxisomes were observed (Fig. 7G), demonstrating the ability of α-tocopherol to impair the peroxisomal morphological changes induced by 7 KC. The quantity of total peroxisomes was the following in 7 KC– and (7 KC + α-tocopherol)-treated cells; 7 KC: 2.7 ± 1.1 (median: 2.5); (7 KC + α-tocopherol): 2.7 ± 0.8 (median: 3.0). There was no significant difference with control, vehicle and α-tocopherol. However, whereas no peroxisome with abnormal sizes and shapes were found in control, vehicle- and α-tocopherol-treated cells, there was a significant increase of peroxisomes with abnormal sizes and shapes in 7 KC-treated cells (1.7 ± 0.8; median: 1.5); this increase was significantly attenuated in the presence of α-tocopherol (7 KC + α-tocopherol: 0.7 ± 0.4 (median: 1)). It is important to underline that in our experimental conditions, TEM (specifically adapted to visualize the peroxisomes) was done on adherent cells. Thus, under treatment with 7 KC, as the loss of cell adhesion occurs before the loss of ΔΨm [111], our data suggest that the morphological peroxisomal alterations might precede mitochondrial dysfunction.

On the basis of ultrastructural features observed by electron microscopy suggesting pexophagy, complementary analyses were performed by immunofluorescence. With the use of an antibody recognizing the lysosomal-associated membrane protein 1 (LAMP1), the presence of large cytoplasmic dots, which can be considered as autolysomes [116] support the ability of 7 KC (25–50 μM) to induce autophagy; this autophagic process was strongly attenuated by α-tocopherol (Supplementary Fig. 4). To demonstrate the occurrence of pexophagy during 7 KC-induced autophagy, a dual immunofluorescence staining procedure was used. To this end, 7 KC-treated cells were simultaneously stained with a mouse monoclonal antibody raised against p62, present in the phagophore and the autophagosome [116], and with a rabbit polyclonal antibody directed against the peroxisomal transporter ABCD3, present in the peroxisomal membrane and considered as a marker of the peroxisomal mass. In those conditions, vesicles simultaneously expressing p62 and ABCD3 were considered as

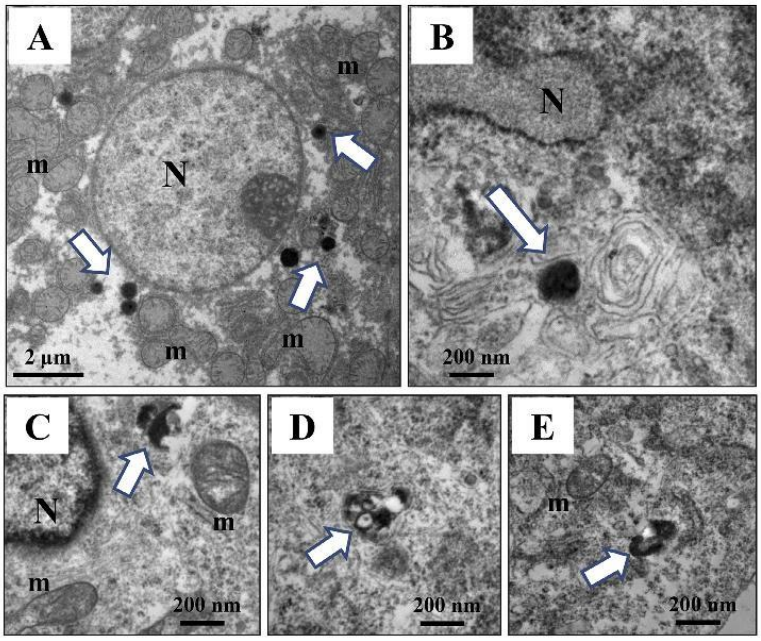

Fig. 6. Transmission electron microscopy analysis of peroxisomes and mitochondria on liver tissue sections and on wild type and Zellweger human fibroblasts. Livers of 9- to 10-week-old C57 Black/6 males (**A**) and wild type human fibroblasts (**B**) were used as positive controls for peroxisome analysis. Round **p**eroxisomes were noticeably observed in the presence of diaminobenzidine (DAB) and H_2O_2; several mitochondria (m) were also detected in the liver. In Zellweger fibroblasts (**C, D, E**), compared with murine hepatocytes and wild type fibroblasts, no round peroxisomes were observed; however, few DAB positive structures, with various shapes, which could evocate abnormal peroxisomes, were detected. Data shown are representative of three independent experiments. N: nucleus; m: mitochondria; white arrows point towards peroxisomes/DAB positive structures.

pexophagic vesicles. These vesicles correspond to yellow fluorescent spots from different sizes resulting from the colocalization of p62 (revealed with Alexa 488 which emits a green fluorescence when excited with a blue light) with ABCD3 (revealed with Alexa 546 which emits a red fluorescence when excited with a green light) (Supplementary Fig. 5A and B). This colocalization of p62 and ABCD3 supports the hypothesis that 7 KC (25–50 µM) induces pexophagy. This pexophagic process was counteracted by α-tocopherol (Supplementary Fig. 5A and B).

3.7. Effect of 7-ketocholesterol on plasmalogens and very long chain fatty acids levels

It is well establihed that the peroxisome plays key roles in lipid metabolism including etherphospholipid/plasmalogens biosynthesis and β-oxidation of very long chain fatty acids (VLCFA) [117]. In addition, it also contributes to bile acid synthesis and eicosanoid degradation [118,119]. Consequently, structural and/or functional alterations of the peroxisome can inflence plasmalogen and VLCFA levels. Therefore, the impact of 7 KC (25–50 µM) with or without α-tocopherol (400 µM) on plasmalogen and VLCFA levels was studied on 158 N cells after 24 h of treatment. Similar (C24:0, C24:1 n-9, C26:0 and C26:1 n-9) levels were found in control, vehicle- and α-tocopherol-treated cells (Ethanol (EtOH): 0.6%) (Fig. 8A–E). No modification of total plasmalogens was detected in 7 KC (25–50 µM)-treated cells with or without α-tocopherol (Fig. 8A). On the contrary, enhanced levels of C24:0 (tetracosanoic acid), C24:1 n-9 (nervonic acid), C26:0 (hexacosanoic acid) and C26:1 n-9 (ximenic acid/17-hexacosanoic acid) were increased in the presence of 7 KC (25–50 µM) (Fig. 8B–E). This increase was significantly reduced when 7 KC was associated with α-tocopherol (Fig. 8B–E). The enhanced level of VLCFA observed in the presence of 7 KC suggests peroxisomal β-oxidation deficiency. It was therefore of interest to specify the impact of 7 KC on the mRNA levels of peroxisomal transporters and enzymes.

3.8. Effect of 7-ketocholesterol on gene expression of transporters and enzymes involved in peroxisomal β-oxidation (ABCD1, ABCD2, ACOX1, MFP2), plasmalogen synthesis (DHAPAT, ADHAPS), and transport of pristanic acid, dicarboxylic acid, and bile acid intermediates (ABCD3)

The β-oxidation of VLCFA ($C \geq 22$ such as C24:0, C24:1 n-9, C26:0 and C26:1 n-9) occurs in the peroxisome and requires the peroxisomal transporter ABCD1 and enzymes of the peroxisomal β-oxidation (ACOX1, MFP2) [117]. The first two enzymes required for plasmalogen synthesis (DHAPAT, ADHAPS) are localized on the luminal side of the peroxisomal membrane [75,78]. ABCD3 protein is considered a suitable marker of peroxisomal mass [107,108], and is also a transporter of pristanic acid, dicarboxylic acid, and bile acid intermediates [109]. Therefore, the impact of 7 KC (25–50 µM), with or without α-tocopherol (400 µM), on these parameters was studied by RT-qPCR on 158 N cells after 24 h of treatment. The Ct values of the peroxisomal proteins (ABCD1, ABCD2, ACOX1, and MFP2) and ABCD3 as well as of the reference gene in untreated 158 N cells were as follows: *Abcd1*: 26.3 ± 0.3; *Abcd2* > 30: *Abcd3*: 22.0 ± 0.5; *Acox1*: 22.9 ± 0.6; *Mfp2*: 27.8 ± 0.7; *36B4*: 15.7 ± 0.1, they were in the range of those previously obtained [81]. In 158 N cells, ABCD2 mRNA, which was very weakly expressed (Ct > 30), was not further studied in different culture conditions. Similar ABCD1,

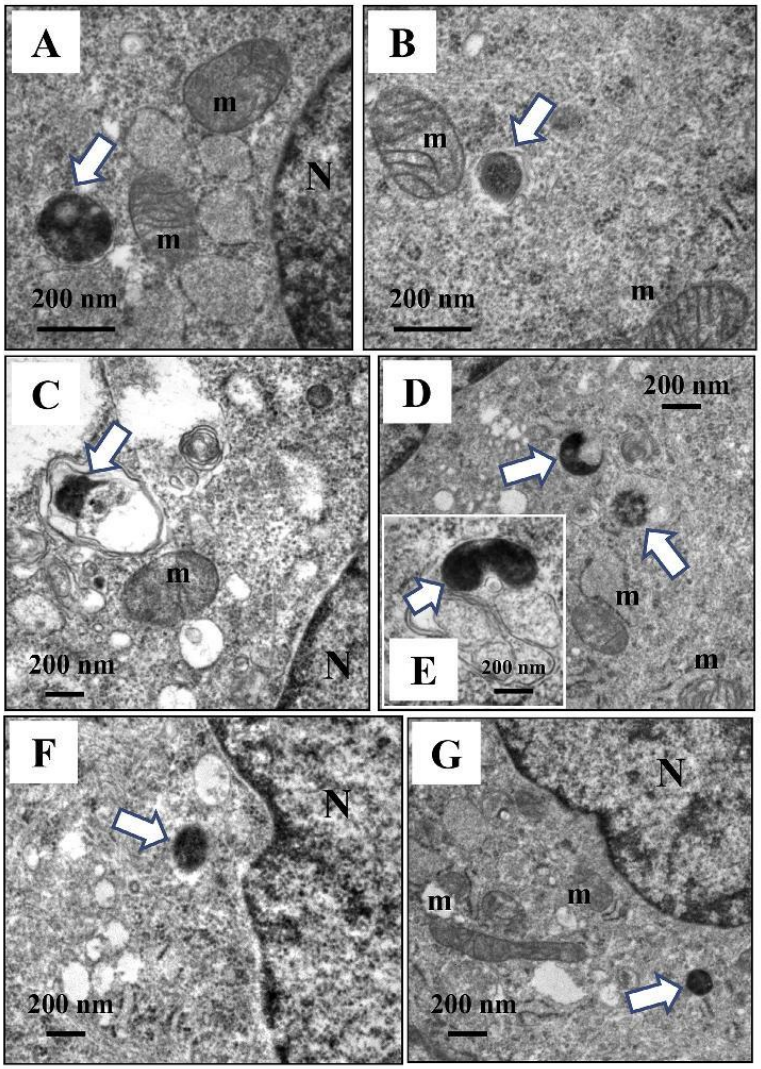

Fig. 7. Transmission electron microscopy analysis of peroxisomes and mitochondria on 158 N murine oligodendrocytes cultured with or without 7-ketocholesterol in the absence or presence of α-tocopherol. 158 N murine oligodendrocytes were taken after 24 h of culture, and further cultured without and with 7 KC (25–50 μM) associated or not with α-tocopherol (400 μM) for an additional 24 h period of time. In untreated cells (control) (**A**), vehicle (EtOH 0.6%)-treated cells (**B**), and α-tocopherol (400 μM)-treated cells (**F**), round peroxisomes were clearly detected in the presence of diaminobenzidine (DAB) and H_2O_2 as well as numerous mitochondria. In 7-ketocholesterol (25 μM)-treated cells (**C, D, E**), peroxisomes with abnormal size and shapes were observed; DAB-positive structures were also identified in vacuoles evoking a pexophagy process (**C**). In (7-ketocholesterol + α-tocopherol)-treated cells, mainly round peroxisomes were observed (**G**). Data shown are representative of three independent experiments. N: nucleus; m: mitochondria; white arrows point towards peroxisomes (DAB positive structures).

ABCD3, ACOX1 and MFP2 mRNA levels were found in control, vehicle ((Ethanol (EtOH): 0.6%) and α-tocopherol-treated cells (Fig. 9A–D). It is worth noting that the mRNA levels of ABCD1, ABCD3, ACOX1 and MFP2 were affected in 158 N cells treated with 7 KC (25 and 50 μM) (Fig. 9). The most significant decrease of mRNA levels was observed with ABCD1 (ABCD1>ABCD3>ACOX1≥MFP2) (Fig. 9A–D). Interestingly, in the presence of α-tocopherol, the decrease of ABCD1 and ACOX1 induced by 7 KC (50 μM) in mRNA levels was significantly attenuated (Fig. 9). α-tocopherol had no or slight effects on the decrease in mRNA levels of ABCD3 and MFP2 (Fig. 9A–D). The Ct values of DHAPAT and ADHAPS were 24.2 ± 0.7, and 25.9 ± 2.5, respectively. Decreased levels of DHAPAT mRNA were observed with 7 KC (25–50 μM). The decrease induced by 7 KC (25 μM) was counteracted in the presence of α-tocopherol, and no protective effect was observed for α-tocopherol with 7 KC (50 μM) (Fig. 9E). Similar levels of ADHAPS mRNA were measured in untreated cells, vehicle ((Ethanol (EtOH): 0.6%) and α-tocopherol-treated cells, as well as in 7 KC(25–50 μM) with or without α-tocopherol (Fig. 9F). As antibodies raised against ABCD1, ABCD3, ACOX1 and MFP2 were available, the corresponding protein levels

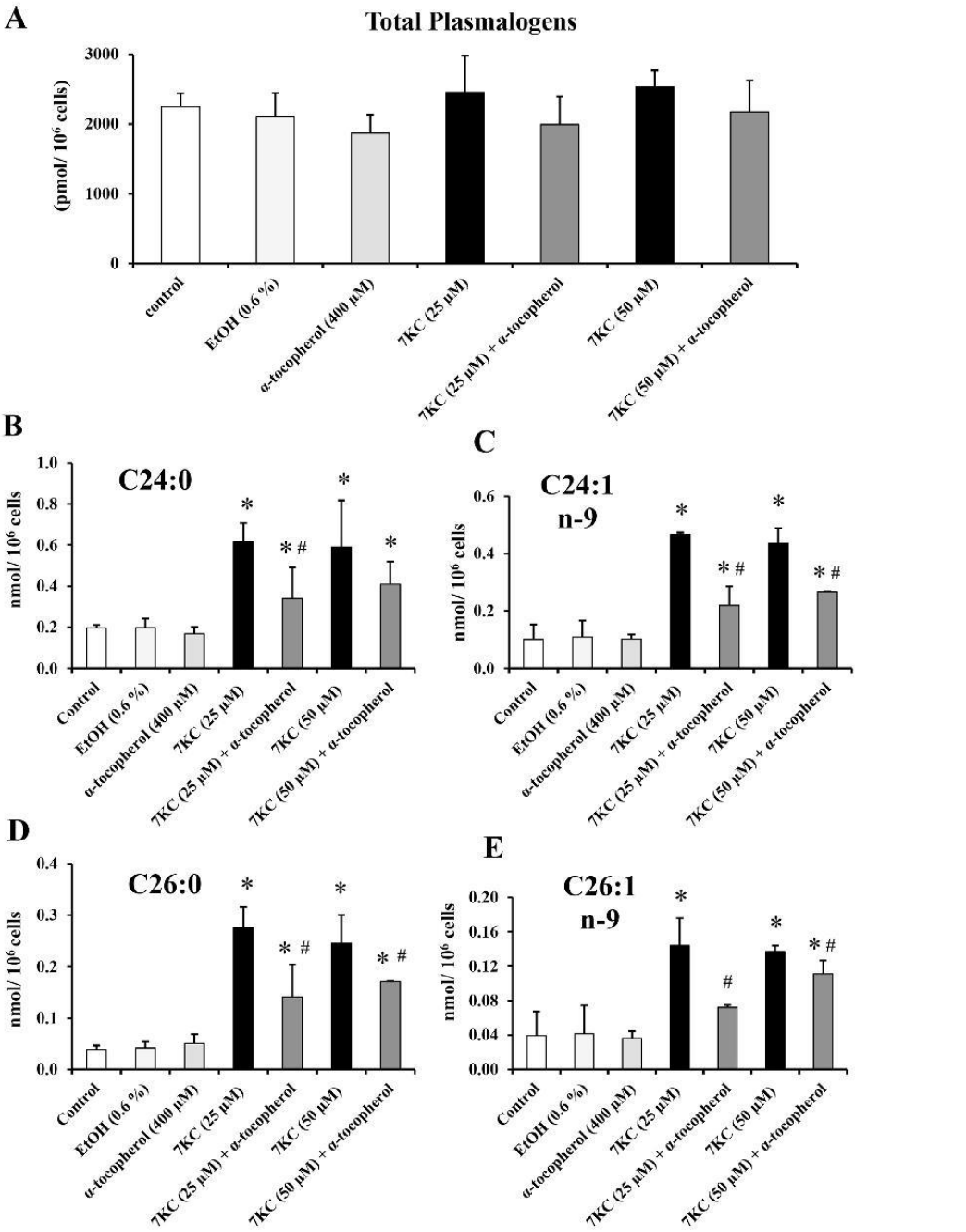

Fig. 8. Effects of 7-ketocholesterol on plasmalogens and very long chain fatty acid (VLCFA) levels. 158 N murine oligodendrocytes were taken after 24 h of culture, and were further cultured without and with 7 KC (25–50 μM) associated or not with α-tocopherol (400 μM) for an additional 24 h period of time. The level of total plasmologens was determined by liquid chromatography tandem mass spectrometry (LC-MS/MS) (**A**). The level of VLCFA (C24:0; C24:1 n-9; C26:0; C26:1 n-9) was determined by GC/MS (**B-E**). Data shown are representative of three independent experiments. Significance of the differences between control (untreated cells) and 7 KC-treated cells; Mann Whitney test: *P < 0.05 or less. Significance of the differences between 7 KC-treated cells and (7 KC + α-tocopherol (or α-tocotrienol)) - treated cells; Mann Whitney test: #P < 0.05 or less. No significant differences were found between control and vehicle-treated cells (Ethanol (EtOH: 0.6%).

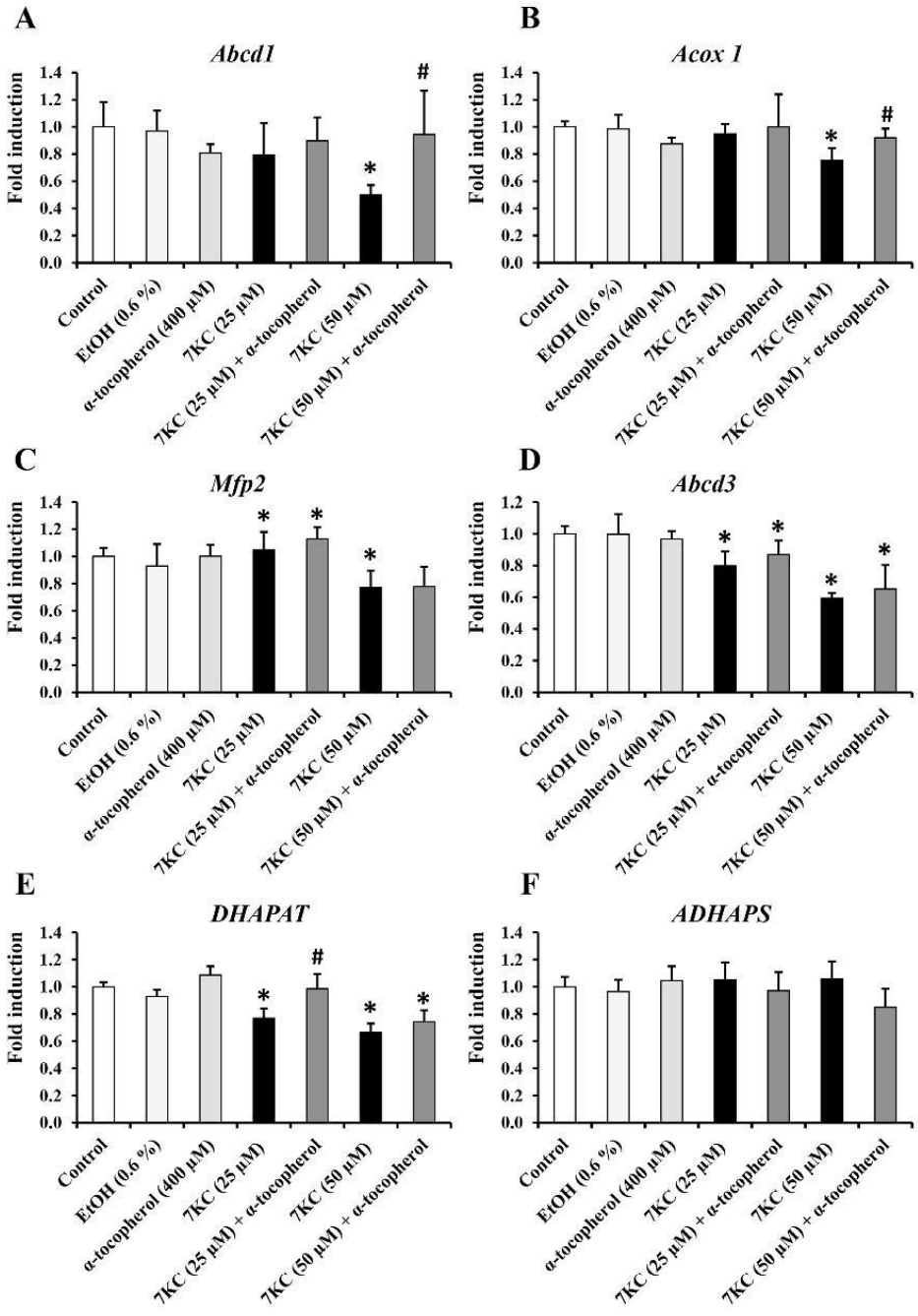

Fig. 9. Effects of 7-ketocholesterol *on peroxisomal genes expression: Abcd1, Abcd3, Acox1, Mfp2, DHAPAT and ADHAPS*. 158 N murine oligodendrocytes were taken after 24 h of culture, and were further cultured without and with 7 KC (25–50 µM) in the absence or in the presence of α-tocopherol (400 µM) for an additional 24 h period of time. The incidence of 7 KC, with or without α-tocopherol, on the mRNA expression of transporters and enzymes of the peroxisomal β-oxidation (ABCD1, ACOX1, MFP2) (**A-C**), of ABCD3 (**D**), and of the first two peroxisomal enzymes involved in plasmalogens synthesis (DHAPAT, ADHAPS) (**E-F**) was evaluated by RT-qPCR. *Abcd2* which is very slightly expressed (Ct > 30) is not represented on the figure. Data shown are representative of three independent experiments. Significance of the differences between control (untreated cells) and 7 KC-treated cells; Mann Whitney test: *P < 0.05 or less. Significance of the differences between 7 KC-treated cells and (7 KC + α-tocopherol (or α-tocotrienol)) - treated cells; Mann Whitney test: #P < 0.05 or less. No significant differences were found between control and vehicle-treated cells (Ethanol (EtOH: 0.6%).

were determined by western blotting. Data obtained are in agreement with RT-qPCR analysis mainly with the highest concentration of 7 KC (Supplementary Fig. 6A and B) supporting a peroxisomal β-oxidation deficiency rather than an activation of elongase.

4. Discussion

The enhanced levels of 7 KC in the tissues and/or fluids of patients with cardiovascular diseases, some eye diseases, neurodegenerative diseases, colorectal inflammatory diseases/Bowel diseases and some types of cancer has strongly reinforced the interest granted to this oxysterol which is essentially formed by auto-oxidation [54,55] and which accumulates during aging in different types of cells [40,46]. Due to the aging of the population, as the frequency of diseases associated with increased levels of 7 KC is expected to increase, it is important to know the molecular mechanisms associated with the toxicity of this oxysterol better, in order to identify new molecules and to develop new strategies capable of counteracting its deleterious effects. At the moment, the impact of 7 KC on the organelles, mainly mitochondria and lysosomes, is quite well recognized [51,58]. However, little is known about the effect of 7 KC on the peroxisome, which is tightly connected with mitochondria and endoplasmic reticulum [29,36,78,120], and which is important for lipid metabolism, the regulation of redox homeostasia, of non cytokinic inflammation and in the myelination process [117,119,121,122]. In addition, recent findings suggest that biochemical processes governed by the peroxisome may also play a critical role in regulating cellular aging [30,123]. In the present study realized on 158 N murine oligodendrocytes, we report the occurrence of peroxisomal alterations both with 7 KC (25 μM) and with 7 KC (50 μM) which are slightly and strongly cytotoxic, respectively. With 7 KC (25 μM), peroxisomal dysfunction associated with slight effects on mitochondria were observed, whereas with 7 KC (50 μM) both peroxysomal and mitochondrial dysfunctions, associated with an induction of oxiapoptophagy, were detected.

In agreement with previous data reported on numerous cell types, 7 KC (50 μM) is strongly cytotoxic and triggers cell death [58]. Indeed, 7 KC (50 μM) is a potent inducer of oxidative stress (including overproduction of superoxide anion and hydrogen peroxide) and induces mitochondrial dysfunction (loss of $\Delta\Psi m$) leading to a mode of cell death by apoptosis (presence of cleaved caspase-3 and cleaved PARP) associated with a marked activation of LC3-I in LC3-II, which is an autophagic criteria. This particular type of cell death, which has also been observed on 158 N cells treated with 24S-hydroxycholesterol and 7β-hydroxycholesterol as well as on murine microglial BV-2 cells treated with 7 KC, is named oxiapoptophagy (OXIdation + APOPTOsis + autoPHAGY) [57,60,103]. On 158 N cells, it is likely that 7 KC (50 μM)-induced oxiapoptophagy is associated with marked mitochondrial dysfunction, including the alteration of oxidative phosphorylation, which could result from lipid anabolism dysfunction, especially on tricarboxylic (TCA) cycle intermediates [105]. The present study brings additional information on the impact of 7 KC (50 μM) on mitochondria and on oxidative stress. Thus, 7 KC (50 μM) also decreases the quantity of cardiolipins, which are specific mitochondrial phospholipids present in the inner mitochondrial membrane and which contribute to oxidative phosphorylation [107]. In addition, the enhancement of catalase activity and of catalase level observed with 7 KC (50 μM) could occur to prevent and attenuate the increased production of H_2O_2. Altogether, these data underline that mitochondrial dysfunction and oxidative stress are major events in 7 KC (50 μM)-induced cell death, and they also reinforce the importance of developing strategies to prevent mitochondrial dysfunction and overproduction of reactive oxygen species (ROS) in order to impair 7 KC-induced side effects. Contrary to 7 KC (50 μM), slight cytotoxic effects were observed with 7 KC (25 μM): a small percentage of cells overproducing superoxide anions were detected; small percentages of cells with altered plasma membrane and depolarized mitochondria were found; no cleaved caspase-3 and cleaved PARP, which are apoptotic criteria, were revealed, and a slight increase in the (LC3-II/LC3-I) ratio was noticed. In these two situations, it was of interest to define the impact of 7 KC on the peroxisome.

Indeed, at the moment, no information is available about the role of the peroxisome in the numerous forms of cell death described [9] whereas there is lot of evidence that this organelle is tighly connected with the endoplasmic reticulum and the mitochondria [37] which play key roles in several types of cell death [124].

In 7 KC (50 μM)-induced oxiapoptophagy, the data obtained by confocal microscopy and transmission electron microscopy (TEM) for murine oligodendrocyte 158 N cells show topographical, morphological and functional dysfunction of the peroxisome. Peroxisomes of abnormal size and shapes, echoing those observed in Zellweger fibroblasts, were detected. This suggests the alteration of different partners and processes involved in peroxisome biogenesis. Decreased levels of the ABCD3 transporter (a marker of peroxisomal mass) were noticed in flow cytometry, RT-qPCR and western blotting evaluations. In addition, lower mRNA and protein levels of the ABCD1 transporter and of the enzymes ACOX1 and MFP2 associated with peroxysomal β-oxidation was found. On murine microglial BV-2 cells treated with 7 KC (50 μM, 24 h), reduced levels of ABCD3 have also been reported as well as decreased expression of *Abcd1*, *Acox1* and *Mfp2* [60,80]. The lower level of peroxisomal proteins could be due to their reduced expressions, and/or to the degradation of peroxisome in autophagic vesicles suggesting the ability of 7 KC to trigger pexophagy. This latter argument is supported by TEM, western blotting (increased ratio (LC3-II/LC3-I)) and analysis by fluorescence microscopy (LAMP1 staining pattern and colocalization of p62 with ABCD3). As 7 KC is a ligand and an inhibitor of the cholesterol-5,6-epoxide hydrolase [125] which also binds Tamoxifen and analogues [126] as well as dendrogenin A (DDA) [127,128], which are two potent inducers of autophagy, it would be important to determine whether the metabolic pathways activated by 7 KC are similar or not to those described with Tamoxifen and DDA. At the moment, 7 KC induced-autophagy is rather considered as a cellular defense mechanism and as an adaptive survival strategy that permit to recycle cellular components and to eliminate damages organelles [73]. At the opposite of 7 KC, DDA has been shown to trigger a lethal autophagic process involving the nuclear receptors Liver X Receptor-β (LXR-β)/Retinoic X Receptor (RXR) [127,128]. Therefore, it would be of interest to precise the part taken by LXR-β/RXR in 7 KC-induced autophagy, especially in 7 KC-induced pexophagy. The similar impacts of 7 KC (50 μM) on glial (oligodendrocytes) and microglial cells at the peroxisomal level [60,80,81] suggest a general phenomenom which could affect all the cells exposed to 7 KC. Consequently, peroxisomal damage could occur in numerous major diseases where increased 7 KC levels have been reported such as cardiovascular diseases, eye diseases (cataract, age related macular degeneration (ARMD)) and neurodegenerative diseases [40,129,130]. Based on data obtained on knockout mice deficient in some peroxisomal β-oxidation enzymes [131,132], the alteration of the peroxisome induced by 7 KC could have dramatic consequences on brain function. In addition, the mRNA level of the peroxisomal DHAPAT enzyme which is involved in plasmalogen biogenesis was also reduced in the presence of 7 KC (50 μM), suggesting that different enzymes located in the peroxisome could be affected. However, the mRNA level of the peroxisomal ADHAPS enzyme, also involved in plasmalogen biogenesis, was not modified, which

illustrates the selective side effects of 7 KC. Notably, the decreased mRNA and protein level of ABCD1, ACOX1 and MFP2 was associated with an intracellular accumulation of VLCFA (C24:0, C24:1, C26:0 and C26:1) suggesting alterations to the different partners of peroxisomal β-oxidation, whereas an impact of 7 KC on the activities of elongases, such as ELOVL6 (C18:0–C22:0) and ELOVL1 (C24:0–C26:0) can not be excluded [133]. However, total plasmalogens did not decrease. In the brain, the effects of 7 KC (50 μM) on the peroxisome, subsequently leading to accumulation of VLCFA which are known for their ability to favor oxidative stess and cell death on oligodendrocytes, astrocytes and neurons [38,134,135], could further amplify 7 KC-induced cytotoxicity and neurodegeneration [39]. Indeed, it is known that peroxisomal dysfunction enhances two major events associated with numerous neurodegenerative diseases: oxidative stress and mitochondrial dysfunction [29,38,39]. It is important to underline that peroxisomal dysfunction has also been described in 158 N cells treated with 7β-hydroxycholesterol and 24S-hydroxycholesterol, both of which are involved in different forms of neurodegeneration [40,129,130] and which are also potent inducers of oxiapoptophagy [59]. Therefore, cytotoxic oxysterols other than 7 KC can lead to peroxisomal dysfunction.

Interestingly, under treatment with 7 KC (25 μM, 24 h), which is slightly cytotoxic (slight increase permeability to PI, slight loss of ΔΨm, slight overproduction of superoxide anion ($O_2^{\bullet -}$) and hydrogen peroxide (H_2O_2), no induction of apoptosis (absence of cleaved-caspase-3 and cleaved PARP), slight induction of LC3-I activation which is a criteria of autophagy (higher ratio LC3-II/LC3-I)), several peroxisomal changes were observed on 158 N cells. Thus, with 7 KC (25 μM, 24 h), the cytoplasmic topography of the peroxisome as well as of mitochondria was modified, the expression of ABCD3, a peroxisomal mass marker, was reduced, and the levels of peroxisomal mRNA (*Abcd1, Abcd3,* and *DHAPAT*) were lowered. The levels of peroxisomal proteins (ABCD1, ABCD3, ACOX1 and MFP2) were also reduced. These alterations were also associated with an intracellular accumulation of VLCFA (C24:0, C24:1, C26:0 and C26:1) which was similar to those observed with 7 KC (50 μM). As observed with 7 KC (50 μM), no impact on the total plasmalogen level was detected with 7 KC (25 μM). In addition, by TEM, important morphological modifications of the peroxisomes were observed with 7 KC (25 μM). For technical reasons, as the TEM adapted to peroxisomes detection, was realized on adherent cells, and as the loss of cell adhesion occurs before the drop of ΔΨm [111], our data indicate that the morphological peroxisomal alterations probably precede mitochondrial dysfunction, especially mitochondrial activity. Indeed, mitochondrial topographical changes were observed by fluorescence microscopy after staining with Mitotracker red both on 158 N cells treated with 7 KC used at 25 and 50 μM. Altogether, our study demonstrates that a slightly cytotoxic concentration of 7 KC (25 μM) can induce morphological and functional peroxisomal alterations similar to a strongly cytotoxic concentration of 7 KC (50 μM) (Fig. 10). Altogether, these data reinforce the need to establish the role of the peroxisome in processes, such as oxidative stress and mitochondrial dysfunctions, which lead to cell death in order to precise the part taken by the peroxisome in cell death. Yeast could be an interesting complementary model to further investigate these relationships. Indeed, yeast is not only a valuable tool to study different forms of cell death, especially autophagy and apoptosis [14,136], but it is also widely used to study the peroxisome [137].

Our data also show that α-tocopherol, like oleic acid, olive oil, and argan oil (two oils rich in α-tocopherol and oleic acid), is able to attenuate both morphological and/or functional peroxisomal dysfunction induced by 7 kC at both 25 and 50 μM [80,81].

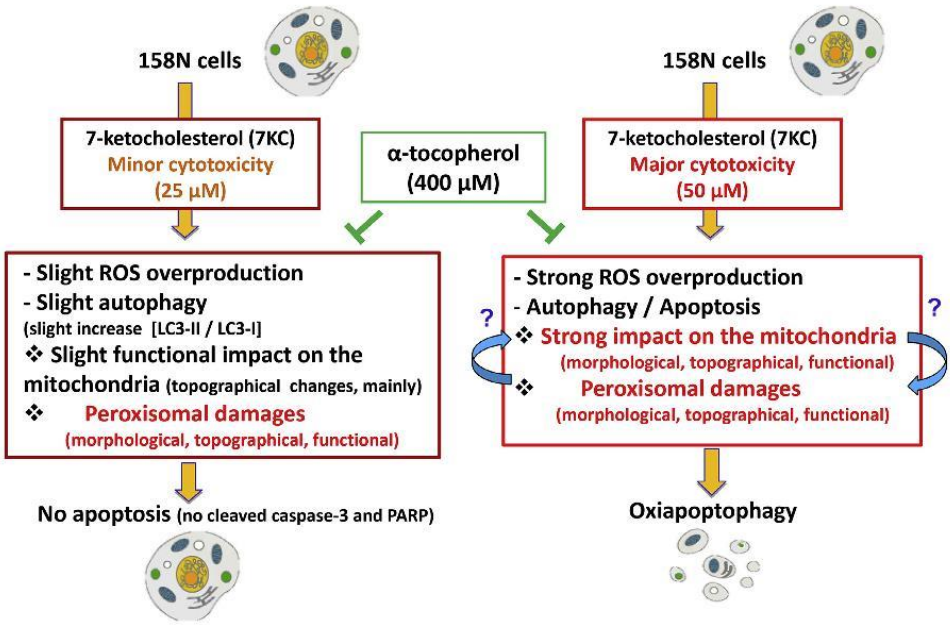

Fig. 10. Occurrence of peroxisomal damages associated with mitochondrial dysfunctions in 7-ketocholesterol-treated 158 N murine oligodendrocytes. 7 KC-induced topographical, morphological and functional peroxisomal changes are observed either with slight or strong mitochondrial dysfunctions, slight or strong ROS overproduction and with or without cell death induction (oxiapoptophagy) on 158 N cells. This cellular model (158 N cells treated with 7 KC) permits to clarify the relationships between peroxisome and mitochondria (and vis versa) during 7 KC-induced side effects leading either to slight cytotoxic effects (7 KC: 25 μM) or oxiapoptophagy (7 KC: 50 μM).

However, α-tocopherol was unable to counteract the decrease of cardiolipins observed under treatment with 7 KC. This data has similarities to the observations on BV-2 cells. Whereas α-tocopherol also attenuates 7 KC-induced loss of ΔΨm and oxiapoptophagy on these cells, it did not normalize the levels of succinic, fumaric, malic and citric acid which are tricarboxylic acid (TCA) cycle-associated organic acids [104]. This supports the idea that a full recovery of mitochondrial functions is not required to escape cell death. Therefore, as previously suggested, α-tocopherol could be used in functional foods to prevent 7 KC-associated diseases [80]. This compound is particularly interesting since it is able to cross intestinal and blood-brain barriers. As high levels of α-tocopherol are often found in oils (olive and argan oils, milk thistle seeds oil) [80,81,138], a diet rich in these products might be especially useful to prevent the bowel diseases often associated with enhanced 7 KC levels formed either endogeneously or brought on by foods [44,45]. As 7 KC (25–50 μM)-induced side effects were attenuated by α-tocopherol but not by α-tocotrienol, although the anti-oxidant properties of these molecules determined with the FRAP method were in the same range of order, these data reinforce the hypothesis that the cytoprotective properties of α-tocopherol are not only due to its antioxidant activities [80,139].

Altogether, our data underline the interest of defining the contribution of the peroxisome in oxidative stress, mitochondrial dysfunction and cell death. Our cellular model (158 N cells treated with 7 KC) is especially useful to establish the interactions between the peroxisome and the mitochondria, and to determine at which steps of cell death morphological and functional peroxisomal changes occur and their role in the process of cell death.

5. Conclusion

It is now well accepted that 7 KC, which is associated with various diseases (cardiovascular disease, eye disease, inflammatory bowel diseases and some types of cancer) induces a complex type of cell death (oxiapoptophagy) associated with various types of organelle dysfunction (mitochondria, lysosomes, endoplasmic reticulum) [71,105,140]. The results obtained demonstrate that 7 KC also induces significant topographical, morphological and functional alterations of the peroxisome. Since the proper functioning of the peroxisome is essential for the control of redox and lipid homeostasis, these results suggest that the peroxisome could also be involved in the process of cell death induced by 7 KC. In this context, it would be of interest to define the impact of other biological, physical or chemical cytotoxic agents on the peroxisome to precise the part taken by this organelle in the cell death process.

Disclosure of potential conflicts of interest

The authors have no conflicts of interest to declare.

Acknowledgements and funding

This work was presented as an oral presentation at the 7th ENOR (European Network for Oxysterol Research) Symposium 'Oxysterols and Sterol Derivatives in Health and Disease', September 21–22, 2017, Université catholique de Louvain, Brussels, Belgium (https://www.oxysterols.net/). This work was supported by grants from: Univ. Bourgogne (Dijon, France), Univ. Monastir (Tunis, Tunisia), ABASIM (Association Bourguignonne pour les Applications des Sciences de l'Information en Médecine, Dijon, France), ASSAD (Louhans, France) and the Department of Neurology (Prof. Thibault Moreau, University Hospital, Dijon, France). The authors are indebted to the following platforms: Plateforme Lipidomique: Dr J.P. Pais de Barros, Université de Bourgogne/Inserm; Plateforme DimaCell: Dr Jeannine Lherminier, Mr Benoît Gasquet, Mrs Elodie Noirot, Université de Bourgogne/Inra. We thank Mrs Suzanne Rankin for English corrections.

Appendix A. Supplementary data

Supplementary data related to this article can be found at https://doi.org/10.1016/j.biochi.2018.07.009.

References

[1] P. Boya, G. Kroemer, Lysosomal membrane permeabilization in cell death, Oncogene 27 (50) (2008) 6434–6451.
[2] G. Kroemer, L. Galluzzi, P. Vandenabeele, J. Abrams, E.S. Alnemri, E.H. Baehrecke, M.V. Blagosklonny, W.S. El-Deiry, P. Golstein, D.R. Green, M. Hengartner, R.A. Knight, S. Kumar, S.A. Lipton, W. Malorni, G. Nuñez, M.E. Peter, J. Tschopp, J. Yuan, M. Piacentini, B. Zhivotovsky, G. Melino, Nomenclature committee on cell death 2009. Classification of cell death: recommendations of the nomenclature committee on cell death 2009, Cell Death Differ. 16 (1) (2009) 3–11.
[3] G.S. Salvesen, V.M. Dixit, Caspases: intracellular signaling by proteolysis, Cell 91 (4) (1997) 443–446.
[4] N. Joza, J.A. Pospisilik, E. Hangen, T. Hanada, N. Modjtahedi, J.M. Penninger, G. Kroemer, AIF: not just an apoptosis-inducing factor, Ann. N. Y. Acad. Sci. 1171 (2009) 2–11.
[5] P. Widlak, W.T. Garrard, Discovery, regulation, and action of the major apoptotic nucleases DFF40/CAD and endonuclease G, J. Cell. Biochem. 94 (6) (2005) 1078–1087.
[6] A. Moore, C.J. Donahue, K.D. Bauer, J.P. Mather, Simultaneous measurement of cell cycle and apoptotic cell death, Meth. Cell Biol. 57 (1998) 265–278.
[7] H. Lecoeur, L.M. de Oliveira-Pinto, M.L. Gougeon, Multiparametric flow cytometric analysis of biochemical and functional events associated with apoptosis and oncosis using the 7-aminoactinomycin D assay, J. Immunol. Meth. 265 (1–2) (2002) 81–96.
[8] S.L. Fink, B.T. Cookson, Apoptosis, pyroptosis, and necrosis: mechanistic description of dead and dying eukaryotic cells, Infect. Immun. 73 (4) (2005) 1907–1916.
[9] L. Galluzzi, I. Vitale, S.A. Aaronson, J.M. Abrams, D. Adam, P. Agostinis, et al., Molecular mechanisms of cell death: recommendations of the nomenclature committee on cell death, Cell Death Differ. (2018), https://doi.org/10.1038/s41418-017-0012-4, 2018 Jan 23.
[10] S. Grootjans, T. Vanden Berghe, P. Vandenabeele, Initiation and execution mechanisms of necroptosis: an overview, Cell Death Differ. 24 (7) (2017) 1184–1195.
[11] J. Yu, H. Nagasu, T. Murakami, H. Hoang, L. Broderick, H.M. Hoffman, T. Horng, Inflammasome activation leads to Caspase-1-dependent mitochondrial damage and block of mitophagy, Proc. Natl. Acad. Sci. U. S. A. 111 (43) (2014) 15514–15519.
[12] J. Vamecq, M. Cherkaoui-Malki, P. Andreoletti, N. Latruffe, The human peroxisome in health and disease: the story of an oddity becoming a vital organelle, Biochimie 98 (2014) 4–15.
[13] S. Aits, M. Jäättelä, Lysosomal cell death at a glance, J. Cell Sci. 126 (Pt 9) (2013) 1905–1912.
[14] D.J. Klionsky, K. Abdelmohsen, A. Abe, M.J. Abedin, H. Abeliovich, A. Acevedo Arozena, et al., Guidelines for the use and interpretation of assays for monitoring autophagy (3rd edition), Autophagy 12 (1) (2016) 1–222.
[15] T. Pan, S. Kondo, W. Le, J. Jankovic, The role of autophagy-lysosome pathway in neurodegeneration associated with Parkinson's disease, Brain 131 (Pt 8) (2008) 1969–1978.
[16] C. Xu, B. Bailly-Maitre, J.C. Reed, Endoplasmic reticulum stress: cell life and death decisions, J. Clin. Invest. 115 (10) (2005) 2656–2664.
[17] I. Kim, W. Xu, J.C. Reed, Cell death and endoplasmic reticulum stress: disease relevance and therapeutic opportunities, Nat. Rev. Drug Discov. 7 (12) (2008) 1013–1030.
[18] J.D. Lane, J. Lucocq, J. Pryde, F.A. Barr, P.G. Woodman, V.J. Allan, M. Lowe, Caspase-mediated cleavage of the stacking protein GRASP65 is required for Golgi fragmentation during apoptosis, J. Cell Biol. 156 (3) (2002) 495–509.
[19] F. Brandizzi, C. Barlowe, Organization of the ER-Golgi interface for membrane traffic control, Nat. Rev. Mol. Cell Biol. 14 (6) (2013) 382–392.
[20] E. Lafont, D. Milhas, S. Carpentier, V. Garcia, Z.X. Jin, H. Umehara, T. Okazaki, K. Schulze-Osthoff, T. Levade, H. Benoist, B. Ségui, Caspase-mediated inhibition of sphingomyelin synthesis is involved in FasL-triggered cell death, Cell Death Differ. 17 (4) (2010) 642–654.
[21] L. Galluzzi, J.M. Bravo-San Pedro, G. Kroemer, Organelle-specific initiation of cell death, Nat. Cell Biol. 16 (8) (2014) 728–736.
[22] S. Manivannan, C.Q. Scheckhuber, M. Veenhuis, I.J. van der Klei, The impact of peroxisomes on cellular aging and death, Front Oncol 21 (2) (2012) 50.
[23] M. Schrader, H.D. Fahimi, The peroxisome: still a mysterious organelle, Histochem. Cell Biol. 129 (4) (2008) 421–440.
[24] M. Schrader, J.K. Burkhardt, E. Baumgart, G. Lüers, H. Spring, A. Völkl, H.D. Fahimi, Interaction of microtubules with peroxisomes. Tubular and

spherical peroxisomes in HepG2 cells and their alterations induced by microtubule-active drugs, Eur. J. Cell Biol. 69 (1) (1996) 24–35.
[25] M. Schrader, H.D. Fahimi, Growth and division of peroxisomes, Int. Rev. Cytol. 255 (2006) 237–290.
[26] B. Alberts, A. Johnson, J. Lewiset al, Peroxisomes. Molecular Biology of the Cell, fourth ed., Garland Science, 2002.
[27] D. Speijer, Evolution of peroxisomes illustrates symbiogenesis, Bioessays 39 (9) (2017).
[28] A. Sugiura, S. Mattie, J. Prudent, H.M. McBride, Newly born peroxisomes are a hybrid of mitochondrial and ER-derived pre-peroxisomes, Nature 542 (7640) (2017) 251–254.
[29] C. Lismont, M. Nordgren, P.P. Van Veldhoven, M. Fransen, Redox interplay between mitochondria and peroxisomes, Front Cell Dev Biol 3 (2015) 35.
[30] M. Fransen, M. Nordgren, B. Wang, O. Apanasets, P.P. Van Veldhoven, Aging, age-related diseases and peroxisomes, Subcell. Biochem. 69 (2013) 45–65.
[31] H. Jungwirth, J. Ring, T. Mayer, A. Schauer, S. Büttner, T. Eisenberg, D. Carmona-Gutierrez, K. Kuchler, F. Madeo, Loss of peroxisome function triggers necrosis, FEBS Lett. 582 (19) (2008) 2882–2886.
[32] E. Bener Aksam, H. Jungwirth, S.D. Sohlwein, J. Ring, F. Madeo, M. Veenhuis, I.J. van der Klei, Absence of the peroxiredoxin Pmp20 causes peroxisomal protein leakage and necrotic cell death, Free Radic. Biol. Med. 45 (8) (2008) 1115–1124.
[33] E. Baumgart, I. Vanhorebeek, M. Grabenbauer, M. Borgers, P.E. Declerc, H.D. Fahimi, M. Baes, Mitochondrial alterations caused by defective peroxisomal biogenesis in a mouse model for Zellweger syndrome (PEX5 knockout mouse), Am. J. Pathol. 159 (4) (2001) 1477–1494.
[34] R. Dirkx, I. Vanhorebeek, K. Martens, A. Schad, M. Grabenbauer, D. Fahimi, P. Declercq, P.P. Van Veldhoven, M. Baes, Absence of peroxisomes in mouse hepatocytes causes mitochondrial and ER abnormalities, Hepatology 41 (4) (2005) 868–878.
[35] A. Peeters, A.B. Shinde, R. Dirkx, J. Smet, K. De Bock, M. Espeel, I. Vanhorebeek, A. Vanlander, R. Van Coster, P. Carmeliet, M. Fransen, P.P. Van Veldhoven, M. Baes, Mitochondria in peroxisome-deficient hepatocytes exhibit impaired respiration, depleted DNA, and PGC-1α independent proliferation, Biochim. Biophys. Acta 1853 (2) (2015) 285–298.
[36] M. Schrader, S. Grille, H.D. Fahimi, M. Islinger, Peroxisome interactions and cross-talk with other subcellular compartments in animal cells, Subcell. Biochem. 69 (2013) 1–22.
[37] M. Schrader, J. Costello, L.F. Godinho, M. Islinger, Peroxisome-mitochondria interplay and disease, J. Inherit. Metab. Dis. 38 (4) (2015) 681–702.
[38] M. Baarine, P. Andréoletti, A. Athias, T. Nury, A. Zarrouk, K. Ragot, A. Vejux, J.M. Riedinger, Z. Kattan, G. Bessede, D. Trompier, S. Savary, M. Cherkaoui-Malki, G. Lizard, Evidence of oxidative stress in very long chain fatty acid—treated oligodendrocytes and potentialization of ROS production using RNA interference-directed knockdown of ABCD1 and ACOX1 peroxisomal proteins, Neuroscience 213 (2012) 1–18.
[39] D. Trompier, A. Vejux, A. Zarrouk, C. Gondcaille, F. Geillon, T. Nury, S. Savary, G. Lizard, Brain peroxisomes, Biochimie 98 (2014) 102–110.
[40] A. Zarrouk, A. Vejux, J. Mackrill, Y. O'Callaghan, M. Hammami, N. O'Brien, G. Lizard, Involvement of oxysterols in age-related diseases and ageing processes, Ageing Res. Rev. 18 (2014) 148–162.
[41] G. Testa, E. Staurenghi, C. Zerbinati, S. Gargiulo, L. Iuliano, G. Giaccone, F. Fantò, G. Poli, G. Leonarduzzi, P. Gamba, Changes in brain oxysterols at different stages of Alzheimer's disease: their involvement in neuroinflammation, Redox Biol 10 (2016) 24–33.
[42] A. Vejux, M. Samadi, G. Lizard, Contribution of cholesterol and oxysterols in the physiopathology of cataract: implication for the development of pharmacological treatments, J Ophthalmol 2011 (2011) 471947.
[43] M. Nita, A. Grzybowski, The role of the reactive oxygen species and oxidative stress in the pathomechanism of the age-related ocular diseases and other pathologies of the anterior and posterior eye segments in adults, Oxid Med Cell Longev 2016 (2016) 3164734.
[44] D. Rossin, S. Calfapietra, B. Sottero, G. Poli, F. Biasi, HNE and cholesterol oxidation products in colorectal inflammation and carcinogenesis, Free Radic. Biol. Med. 111 (2017) 186–195.
[45] B. Sottero, P. Gamba, S. Gargiulo, G. Leonarduzzi, G. Poli, Cholesterol oxidation products and disease: an emerging topic of interest in medicinal chemistry, Curr. Med. Chem. 16 (6) (2009) 685–705.
[46] G. Poli, F. Biasi, G. Leonarduzzi, Oxysterols in the pathogenesis of major chronic diseases, Redox Biol 1 (2013) 125–130.
[47] J. Kou, G.G. Kovacs, R. Höftberger, W. Kulik, A. Brodde, S. Forss-Petter, S. Hönigschnabl, A. Gleiss, B. Brügger, R. Wanders, W. Just, H. Budka, S. Jungwirth, P. Fischer, J. Berger, Peroxisomal alterations in Alzheimer's disease, Acta Neuropathol. 122 (3) (2011) 271–283.
[48] A. Zarrouk, J.M. Riedinger, S.H. Ahmed, S. Hammami, W. Chaabane, M. Debbabi, S. Ben Ammou, O. Rouaud, M. Frih, G. Lizard, M. Hammami, Fatty acid profiles in demented patients: identification of hexacosanoic acid (C26:0) as a blood lipid biomarker of dementia, J Alzheimers Dis 44 (4) (2015) 1349–1359.
[49] V.K. Senanayake, W. Jin, A. Mochizuki, B. Chitou, D.B. Goodenowe, Metabolic dysfunctions in multiple sclerosis: implications as to causation, early detection, and treatment, a case control study, BMC Neurol. 15 (2015) 154.
[50] J. Musman, S. Paradis, M. Panel, S. Pons, C. Barau, C. Caccia, V. Leoni, B. Ghaleb, D. Morin, A TSPO ligand prevents mitochondrial sterol accumulation and dysfunction during myocardial ischemia-reperfusion in hypercholesterolemic rats, Biochem. Pharmacol. 142 (2017) 87–95.
[51] M.A. Lyons, A.J. Brown, 7-Ketocholesterol, Int. J. Biochem. Cell Biol. 31 (3–4) (1999) 369–375.
[52] M.T. Rodriguez-Estrada, G. Garcia-Llatas, M.J. Lagarda, 7-Ketocholesterol as marker of cholesterol oxidation in model and food systems: when and how, Biochem. Biophys. Res. Commun. 446 (3) (2014) 792–797.
[53] B. Barriuso, D. Ansorena, I. Astiasaránl, Oxysterols formation: a review of a multifactorial process, J. Steroid Biochem. Mol. Biol. 169 (2017) 39–45.
[54] L. Iuliano, Pathways of cholesterol oxidation via non-enzymatic mechanisms, Chem. Phys. Lipids 164 (6) (2011) 457–468.
[55] C. Zerbinati, L. Iuliano, Cholesterol and related sterols autoxidation, Free Radic. Biol. Med. 111 (2017) 151–155.
[56] B. Sottero, D. Rossin, G. Poli, F. Biasi, Lipid oxidation products in the pathogenesis of inflammation-related gut diseases, Curr. Med. Chem. (2017), https://doi.org/10.2174/0929867324666170619104105.
[57] S. Monier, M. Samadi, C. Prunet, M. Denance, A. Laubriet, A. Athias, A. Berthier, E. Steinmetz, G. Jürgens, A. Nègre-Salvayre, G. Bessède, S. Lemaire-Ewing, D. Néel, P. Gambert, G. Lizard, Impairment of the cytotoxic and oxidative activities of 7 beta-hydroxycholesterol and 7-ketocholesterol by esterification with oleate, Biochem. Biophys. Res. Commun. 303 (3) (2003) 814–824.
[58] A. Vejux, G. Lizard, Cytotoxic effects of oxysterols associated with human diseases: induction of cell death (apoptosis and/or oncosis), oxidative and inflammatory activities, and phospholipidosis, Mol. Aspect. Med. 30 (3) (2009) 153–170.
[59] T. Nury, A. Zarrouk, J.J. Mackrill, M. Samadi, P. Durand, J.M. Riedinger, M. Doria, A. Vejux, E. Limagne, D. Delmas, M. Prost, T. Moreau, M. Hammami, R. Delage-Mourroux, N.M. O'Brien, G. Lizard, Induction of oxiapoptophagy on 158N murine oligodendrocytes treated by 7-ketocholesterol-, 7β-hydroxycholesterol-, or 24(S)-hydroxycholesterol: protective effects of α-tocopherol and docosahexaenoic acid (DHA; C22:6 n-3), Steroids 99 (Pt B) (2015) 194–203.
[60] T. Nury, A. Zarrouk, K. Ragot, M. Debbabi, J.M. Riedinger, A. Vejux, P. Aubourg, G. Lizard, 7-Ketocholesterol is increased in the plasma of X-ALD patients and induces peroxisomal modifications in microglial cells: potential roles of 7-ketocholesterol in the pathophysiology of X-ALD, J. Steroid Biochem. Mol. Biol. 169 (2017) 123–136.
[61] A. Cilla, A. Alegría, A. Attanzio, G. Garcia-Llatas, L. Tesoriere, M.A. Livrea, Dietary phytochemicals in the protection against oxysterol-induced damage, Chem. Phys. Lipids 207 (Pt B) (2017) 192–205.
[62] A. Zarrouk, T. Nury, E.M. Karym, A. Vejux, R. Sghaier, C. Gondcaille, P. Andreoletti, D. Trompier, S. Savary, M. Cherkaoui-Malki, M. Debbabi, A. Fromont, J.M. Riedinger, T. Moreau, G. Lizard, Attenuation of 7-ketocholesterol-induced overproduction of reactive oxygen species, apoptosis, and autophagy by dimethyl fumarate on 158N murine oligodendrocytes, J. Steroid Biochem. Mol. Biol. 169 (2017) 29–38.
[63] B.E. Rittmann, J. Schloendorn, Engineering away lysosomal junk: medical bioremediation, Rejuvenation Res. 10 (3) (2007) 359–365.
[64] J.M. Mathieu, J. Schloendorn, B.E. Rittmann, P.J. Alvarez, Medical bioremediation of age-related diseases, Microb. Cell Factories 8 (2009) 21.
[65] I. Perveen, S. Sehar, I. Naz, M.A. Raza, A.J. Khan, S. Ahmed, Biodegradation of 7-ketocholestrol (7-KC) by *Thermobifidafusca* IP1, Int. J. Biosci. 8 (4) (2016) 83–93.
[66] S. Ghosh, S.K. Khare, Biodegradation of 7-Ketocholesterol by Rhodococcus erythropolis MTCC 3951: process optimization and enzymatic insights, Chem. Phys. Lipids 207 (Pt B) (2017) 253–259.
[67] A.E. Rusinol, D. Thewke, J. Liu, N. Freeman, S.R. Panini, M.S. Sinensky, AKT/protein kinase B regulation of BCL family members during oxysterol-induced apoptosis, J. Biol. Chem. 279 (2) (2004) 1392–1399.
[68] I. Maor, H. Mandel, M. Aviram, Macrophage uptake of oxidized LDL inhibits lysosomal sphingomyelinase, thus causing the accumulation of unesterified cholesterol-sphingomyelin-rich particles in the lysosomes. A possible role for 7-Ketocholesterol, Arterioscler. Thromb. Vasc. Biol. 15 (9) (1995) 1378–1387.
[69] A.J. Brown, E.L. Mander, I.C. Gelissen, L. Kritharides, R.T. Dean, W. Jessup, Cholesterol and oxysterol metabolism and subcellular distribution in macrophage foam cells. Accumulation of oxidized esters in lysosomes, J. Lipid Res. 41 (2000) 226–237.
[70] W. Li, M. Ghosh, S. Eftekhari, X.M. Yuan, Lipid accumulation and lysosomal pathways contribute to dysfunction and apoptosis of human endothelial cells caused by 7-oxysterols, Biochem. Biophys. Res. Commun. 409 (4) (2011) 711–716.
[71] R. Sudo, F. Sato, T. Azechi, H. Wachi, 7-Ketocholesterol-induced lysosomal dysfunction exacerbates vascular smooth muscle cell calcification via oxidative stress, Gene Cell. 20 (12) (2015) 982–991.
[72] A. Vejux, S. Guyot, T. Montange, J.M. Riedinger, E. Kahn, G. Lizard, Phospholipidosis and down-regulation of the PI3-K/PDK-1/Akt signalling pathway are vitamin E inhabitable events associated with 7-ketocholesterol-induced apoptosis, J. Nutr. Biochem. 20 (1) (2009) 45–61.
[73] C. He, H. Zhu, W. Zhang, I. Okon, Q. Wang, H. Li, Y.Z. Le, Z. Xie, 7-Ketocholesterol induces autophagy in vascular smooth muscle cells through Nox4 and Atg4B, Am. J. Pathol. 183 (2) (2013) 626–637.
[74] X. Li, M. Xu, A.L. Pitzer, M. Xia, K.M. Boini, P.L. Li, Y. Zhang, Control of autophagy maturation by acid sphingomyelinase in mouse coronary arterial smooth muscle cells: protective role in atherosclerosis, J. Mol. Med. (Berl.) 92

(5) (2014) 473–485.
[75] P. Brites, H.R. Waterham, R.J. Wanders, Functions and biosynthesis of plasmalogens in health and disease, Biochim. Biophys. Acta 1636 (2–3) (2004) 219–231.
[76] R.J. Wanders, H.R. Waterham, Biochemistry of mammalian peroxisomes revisited, Annu. Rev. Biochem. 75 (2006) 295–332.
[77] N.E. Braverman, A.B. Moser, Functions of plasmalogen lipids in health and disease, Biochim. Biophys. Acta 1822 (9) (2012) 1442–1452.
[78] R.J. Wanders, H.R. Waterham, S. Ferdinandusse, Metabolic interplay between peroxisomes and other subcellular organelles including mitochondria and the endoplasmic reticulum, Front Cell Dev Biol 3 (2016) 83.
[79] G. Lizard, O. Rouaud, J. Demarquoy, M. Cherkaoui-Malki, L. Iuliano, Potential roles of peroxisomes in Alzheimer's disease and in dementia of the Alzheimer's type, J Alzheimers Dis 29 (2) (2012) 241–254.
[80] M. Debbabi, T. Nury, A. Zarrouk, N. Mekahli, M. Bezine, R. Sghaier, S. Grégoire, L. Martine, P. Durand, E. Camus, A. Vejux, A. Jabrane, L. Bretillon, M. Prost, T. Moreau, S.B. Ammou, M. Hammami, G. Lizard, Protective effects of α-tocopherol, γ-tocopherol and oleic acid, three compounds of olive oils, and No effect of Trolox, on 7-ketocholesterol-induced mitochondrial and peroxisomal dysfunction in microglial BV-2 cells, Int. J. Mol. Sci. 17 (12) (2016).
[81] A. Badreddine, A. Zarrouk, E.M. Karym, M. Debbabi, T. Nury, W. Meddeb, R. Sghaier, M. Bezine, A. Vejux, L. Martine, S. Grégoire, L. Bretillon, E. Prost-Camus, P. Durand, M. Prost, T. Moreau, M. Cherkaoui-Malki, B. Nasser, G. Lizard, Argan oil-mediated attenuation of organelle dysfunction, oxidative stress and cell death induced by 7-ketocholesterol in murine oligodendrocytes 158N, Int. J. Mol. Sci. 23 (2017) 18–49.
[82] B. Wang, P.P. Van Veldhoven, C. Brees, N. Rubio, M. Nordgren, O. Apanasets, M. Kunze, M. Baes, P. Agostinis, M. Fransen, Mitochondria are targets for peroxisome-derived oxidative stress in cultured mammalian cells, Free Radic. Biol. Med. 65 (2013) 882–894.
[83] G. Lizard, C. Miguet, G. Besséde, S. Monier, S. Gueldry, D. Neel, P. Gambert, Impairment with various antioxidants of the loss of mitochondrial transmembrane potential and of the cytosolic release of cytochrome c occurring during 7-ketocholesterol-induced apoptosis, Free Radic. Biol. Med. 28 (5) (2000) 743–753.
[84] G. Rimbach, A.M. Minihane, J. Majewicz, A. Fischer, J. Pallauf, F. Virgli, P.D. Weinberg, Regulation of cell signalling by vitamin E, Proc. Nutr. Soc. 61 (4) (2002) 415–425.
[85] W. Xia, H. Mo, Potential of tocotrienols in the prevention and therapy of Alzheimer's disease, J. Nutr. Biochem. 31 (2016) 1–9.
[86] M. Baarine, K. Ragot, E.C. Genin, H. El Hajj, D. Trompier, P. Andreoletti, M.S. Ghandour, F. Menetrier, M. Cherkaoui-Malki, S. Savary, G. Lizard, Peroxisomal and mitochondrial status of two murine oligodendrocytic cell lines (158N, 158JP): potential models for the study of peroxisomal disorders associated with dysmyelination processes, J. Neurochem. 111 (2009) 119–131.
[87] K. Ragot, J.J. Mackrill, A. Zarrouk, T. Nury, V. Aires, A. Jacquin, A. Athias, J.P. Pais de Barros, A. Véjux, J.M. Riedinger, D. Delmas, G. Lizard, Absence of correlation between oxysterol accumulation in lipid raft microdomains, calcium increase, and apoptosis induction on 158N murine oligodendrocytes, Biochem. Pharmacol. 86 (1) (2013) 67–79.
[88] M. Oyaizu, Studies on product of browning reactions: antioxidant activities of products of browning reaction prepared from glucosamine, Jpn. J. Nutr. 44 (1986) 307–316.
[89] I.F. Benzie, J.J. Strain, The ferric reducing ability of plasma (FRAP) as a measure of "antioxidant power": the FRAP assay, Anal. Biochem. 239 (1996) 70–76.
[90] K.I. Berker, K. Güçlü, I. Tor, R. Apak, Comparative evaluation of Fe(III) reducing power-based antioxidant capacity assays in the presence of phenanthroline, batho-phenanthroline, tripyridyltriazine (FRAP), and ferricyanide reagents, Talanta 72 (3) (2007) 1157–1165.
[91] G. Lizard, S. Fournel, L. Genestier, N. Dhedin, C. Chaput, M. Flacher, M. Mutin, G. Panaye, J.P. Revillard, Kinetics of plasma membrane and mitochondrial alterations in cells undergoing apoptosis, Cytometry 21 (1995) 275–283.
[92] G. Rothe, G. Valet, Flow cytometric analysis of respiratory burst activity in phagocytes with hydroethidine and 2',7'-dichlorofluorescin, J. Leukoc. Biol. 47 (1990) 440–448.
[93] G. Rothe, A. Emmendörffer, A. Oser, J. Roesler, G. Valet, Flow cytometric measurement of the respiratory burst activity of phagocytes using dihydrorhodamine 123, J. Immunol. Meth. 138 (1991) 133–135.
[94] E. Bachir Bioukar, F. Straehli, K.H. Ng, M.O. Rolland, T. Hashimoto, J.P. Carreau, J. Deschatrette, Resistance to erucic acid as a selectable marker for peroxisomal activity: isolation of revertants of an infantile Refsum disease cell line, J. Inherit. Metab. Dis. 17 (1) (1994) 41–59.
[95] M. Schrader, E. Baumgart, A. Völkl, H.D. Fahimi, Heterogeneity of peroxisomes in human hepatoblastoma cell line HepG2. Evidence of distinct subpopulations, Eur. J. Cell Biol. 64 (2) (1994) 281–294.
[96] J. Folch, M. Lees, G.H. Sloane Stanley, A simple method for the isolation and purification of total lipides from animal tissues, J. Biol. Chem. 226 (1) (1957) 497–509.
[97] L. Peyta, K. Jarnouen, M. Pinault, C. Guimaraes, J.P. Pais de Barros, S. Chevalier, J.F. Dumas, F. Maillot, G.M. Hatch, P. Loyer, S. Servais, Reduced cardiolipin content decreases respiratory chain capacities and increases ATP synthesis yield in the human HepaRG cells, Biochim. Biophys. Acta 1857 (4) (2016) 443–453.
[98] G. Vial, M.A. Chauvin, N. Bendridi, A. Durand, E. Meugnier, A.M. Madec, N. Bernoud-Hubac, J.P. Pais de Barros, E. Fontaine, C. Acquaviva, S. Hallakou-Bozec, S. Bolze, H. Vidal, J. Rieusset, Imeglimin normalizes glucose tolerance and insulin sensitivity and improves mitochondrial function in liver of a high-fat, high-sucrose diet mice model, Diabetes 64 (6) (2015) 2254–2264.
[99] J. Blondelle, J.P. Pais de Barros, F. Pilot-Storck, L. Tiret, Targeted lipidomic analysis of myoblasts by GC-MS and LC-MS/MS, Meth. Mol. Biol. 1668 (2017) 39–60. L., Galluzzi, G., Kroemer. Necroptosis: a specialized pathway of programmed necrosis. 135 (7) (2008) 1161-1163.
[100] M. Debbabi, T. Nury, I. Helali, E.M. Karym, F. Geillon, C. Gondcaille, D. Trompier, A. Najid, S. Terreau, M. Bezine, A. Zarrouk, A. Vejux, P. Andreoletti, M. Cherkaoui-Malki, S. Savary, G. Lizard, Flow cytometric analysis of the expression pattern of peroxisomal proteins, Abcd1, Abcd2, and Abcd3 in BV-2 murine microglial cells, Meth. Mol. Biol. 1595 (2017) 257–265.
[101] Y.J. Kim, J.H. Han, E.S. Han, C.S. Lee, 7-Ketocholesterol enhances 1-methyl-4-phenylpyridinium-induced mitochondrial dysfunction and cell death in PC12 cells, J. Neural. Transm. 113 (12) (2006) 1877–1885.
[102] J.H. Han, Y.J. Kim, E.S. Han, C.S. Lee, Prevention of 7-ketocholesterol-induced mitochondrial damage and cell death by calmodulin inibition, Brain Res. 1137 (1) (2007) 11–19.
[103] T. Nury, A. Zarrouk, A. Vejux, M. Doria, J.M. Riedinger, R. Delage-Mourroux, G. Lizard, Induction of oxiapoptophagy, a mixed mode of cell death associated with oxidative stress, apoptosis and autophagy, on 7-ketocholesterol-treated 158N murine oligodendrocytes: impairment by α-tocopherol, Biochem. Biophys. Res. Commun. 446 (3) (2014) 714–719.
[104] C.J. Yeh, B.L. Hsi, W.P. Faulk, Propidium iodide as a nuclear marker in immunofluorescence. II. Use with cellular identification and viability studies, J. Immunol. Meth. 43 (3) (1981) 269–275.
[105] V. Leoni, T. Nury, A. Vejux, A. Zarrouk, C. Caccia, M. Debbabi, A. Fromont, R. Sghaier, T. Moreau, G. Lizard, Mitochondrial dysfunctions in 7-ketocholesterol-treated 158N oligodendrocytes without or with α-tocopherol: impacts on the cellular profil of tricarboxylic cycle-associated organic acids, long chain saturated and unsaturated fatty acids, oxysterols, cholesterol and cholesterol precursors, J. Steroid Biochem. Mol. Biol. 169 (2017) 96–110.
[106] G. Paradies, V. Paradies, V. De Benedictis, F.M. Ruggiero, G. Petrosillo, Functional role of cardiolipin in mitochondrial bioenergetics, Biochim. Biophys. Acta 1837 (4) (2014) 408–417.
[107] N. Usuda, T. Kuwabara, R. Ichikawa, T. Hashimoto, T. Nagata, Immunoelectron microscopic evidence for organ differences in the composition of peroxisome-specific membrane polypeptides among three rat organs: liver, kidney, and small intestine, J. Histochem. Cytochem. 39 (10) (1991) 1357–1366.
[108] E. Gray, C. Rice, K. Hares, J. Redondo, K. Kemp, M. Williams, A. Brown, N. Scolding, A. Wilkins, Reductions in neuronal peroxisomes in multiple sclerosis grey matter, Mult. Scler. 20 (6) (2014) 651–659.
[109] S. Kemp, F.L. Theodoulou, R.J. Wanders, Mammalian peroxisomal ABC transporters: from endogenous substrates to pathology and clinical significance, Br. J. Pharmacol. 164 (7) (2011) 1753–1766.
[110] M. Debbabi, T. Nury, I. Helali, E.M. Karym, F. Geillon, C. Gondcaille, D. Trompier, A. Najid, S. Terreau, M. Bezine, A. Zarrouk, A. Vejux, P. Andreoletti, M. Cherkaoui-Malki, S. Savary, G. Lizard, Flow cytometric analysis of the expression pattern of peroxisomal proteins, Abcd1, Abcd2, and Abcd3 in BV-2 murine microglial cells, Meth. Mol. Biol. 1595 (2017) 257–265.
[111] J.M. Zahm, S. Baconnais, S. Monier, N. Bonnet, G. Bessède, P. Gambert, E. Puchelle, G. Lizard, Chronology of cellular alterations during 7-ketocholesterol-induced cell death on A7R5 rat smooth muscle cells: analysis by time lapse-video microscopy and conventional fluorescence microscopy, Cytometry 52 (2) (2003) 57–69.
[112] M. Depreter, M. Espeel, F. Roels, Human peroxisomal disorders, Microsc. Res. Tech. 61 (2) (2003) 203–223.
[113] M. Schrader, H.D. Fahimi, Mammalian peroxisomes and reactive oxygen species, Histochem. Cell Biol. 122 (4) (2004) 383–393.
[114] D. Ribeiro, I. Castro, H.D. Fahimi, M. Schrader, Peroxisome morphology in pathology, Histol. Histopathol. 27 (6) (2012) 661–676.
[115] S. Goldfischer, Peroxisomes in disease, J. Histochem. Cytochem. 27 (10) (1979) 1371–1373.
[116] Y. Wang, Y. Li, F. Wei, Y. Duan, Optical imaging paves the way for autophagy research, Trends Biotechnol. 35 (2) (2017) 1181–1193.
[117] R.J. Wanders, Peroxisomes, lipid metabolism, and peroxisomal disorders, Mol. Genet. Metabol. 83 (1–2) (2004) 16–27.
[118] G.P. Mannaerts, P.P. Van Veldhoven, M. Casteels, Peroxisomal lipid degradation via beta- and alpha-oxidation in mammals, Cell Biochem. Biophys. 32 (2000) 73–87. Spring.
[119] R.J. Wanders, S. Ferdinandusse, P. Brites, S. Kemp, Peroxisomes, lipid metabolism and lipotoxicity, Biochim. Biophys. Acta 1801 (3) (2010) 272–280.
[120] M. Fransen, C. Lismont, P. Walton, The peroxisome-mitochondria connection: how and why? Int. J. Mol. Sci. 18 (6) (2017).
[121] C.M. Kassmann, C. Lappe-Siefke, M. Baes, B. Brügger, A. Mildner, H.B. Werner, O. Natt, T. Michaelis, M. Prinz, J. Frahm, K.A. Nave, Axonal loss and neuroinflammation caused by peroxisome-deficient oligodendrocytes, Nat. Genet. 39 (8) (2007) 969–976.

[122] J. Berger, F. Dorninger, S. Forss-Petter, M. Kunze, Peroxisomes in brain development and function, Biochim. Biophys. Acta 1863 (5) (2016) 934–955.
[123] V.I. Titorenko, S.R. Terlecky, Peroxisome metabolism and cellular aging, Traffic 12 (3) (2011) 252–259.
[124] P.T. Daniel, Dissecting the pathways to death, Leukemia 14 (12) (2000) 2035–2044.
[125] P. de Medina, M.R. Paillasse, G. Segala, M. Poirot, S. Silvente-Poirot, Identification and pharmacological characterization of cholesterol-5,6-epoxide hydrolase as a target for tamoxifen and AEBS ligands, Proc. Natl. Acad. Sci. U. S. A. 107 (30) (2010) 13520–13525.
[126] J. Leignadier, F. Dalenc, M. Poirot, S. Silvente-Poirot, Improving the efficacy of hormone therapy in breast cancer: the role of cholesterol metabolism in SERM-mediated autophagy, cell differentiation and death, Biochem. Pharmacol. 144 (2017) 18–28.
[127] G. Segala, M. David, P. de Medina, M.C. Poirot, N. Serhan, F. Vergez, A. Mougel, E. Saland, K. Carayon, J. Leignadier, N. Caron, M. Voisin, J. Cherier, L. Ligat, F. Lopez, E. Noguer, A. Rives, B. Payré, T.A. Saati, A. Lamaziere, G. Despres, J.M. Lobaccaro, S. Baron, C. Demur, F. de Toni, C. Larrue, H. Boutzen, F. Thomas, J.E. Sarry, M. Tosolini, D. Picard, M. Record, C. Récher, M. Poirot, S. Silvente-Poirot, Dendrogenin A drives LXR to trigger lethal autophagy in cancers, Nat. Commun. 8 (1) (2017) 1903.
[128] M. Poirot, S. Silvente-Poirot, The tumor-suppressor cholesterol metabolite, dendrogenin A, is a new class of LXR modulator activating lethal autophagy in cancers, Biochem. Pharmacol. 153 (2018) 75–81.
[129] M. Doria, L. Maugest, T. Moreau, G. Lizard, A. Vejux, Contribution of cholesterol and oxysterols to the pathophysiology of Parkinson's disease, Free Radic. Biol. Med. 101 (2016) 393–400.
[130] A. Vejux, A. Namsi, T. Moreau, G. Lizard, Biomarkers of amyotrophic lateral sclerosis: current status and interest of oxysterols and phytosterols, Front. Mol. Neurosci. (2018), https://doi.org/10.3389/fnmol.2018.00012.
[131] M. Baes, P. Aubourg, Peroxisomes, myelination, and axonal integrity in the CNS, Neuroscientist 15 (4) (2009) 367–379.
[132] S. De Munter, S. Verheijden, L. Régal, M. Baes, Peroxisomal disorders: a review on cerebellar pathologies, Brain Pathol. 25 (6) (2015) 663–678.
[133] S. Kemp, J. Berger, P. Aubourg, X-linked adrenoleukodystrophy: clinical, metabolic, genetic and pathophysiological aspects, Biochim. Biophys. Acta 1822 (9) (2012) 1465–1474.
[134] S. Hein, P. Schönfeld, S. Kahlert, G. Reiser, Toxic effects of X-linked adrenoleukodystrophy-associated, very long chain fatty acids on glial cells and neurons from rat hippocampus in culture, Hum. Mol. Genet. 17 (12) (2008) 1750–1761.
[135] A. Zarrouk, A. Vejux, T. Nury, H.I. El Hajji, M. Haddad, M. Cherkaoui-Malki, J.M. Riedinger, M. Hammami, G. Lizard, Induction of mitochondrial changes associated with oxidative stress on very long chain fatty acids (C22:0, C24:0, or C26:0) treated human neuronal cells (SK-NB-E), Oxid Med Cell Longev 2012 (2012) 623257.
[136] D. Carmona-Gutierrez, M.A. Bauer, A. Zimmermann, A. Aguilera, N. Austriaco, K. Ayscough, et al., Guidelines and recommendations on yeast cell death nomenclature, Microb Cell 5 (1) (2018) 4–31.
[137] P. Dakik, V.I. Titorenko, Communications between mitochondria, the nucleus, vacuoles, peroxisomes, the endoplasmic reticulum, the plasma membrane, lipid droplets, and the cytosol during yeast chronological aging, Front. Genet. 7 (2016) 177.
[138] W. Meddeb, L. Rezig, M. Abderrabba, G. Lizard, M. Mejri, Tunisian milk thistle: an investigation of the chemical composition and the characterization of its cold-pressed seed oils, Int. J. Mol. Sci. 18 (12) (2017).
[139] T. Nakazawa, Y. Miyanoki, Y. Urano, M. Uehara, Y. Saito, N. Noguchi, Effect of vitamin E on 24(S)-hydroxycholesterol-induced necroptosis-like cell death and apoptosis, J. Steroid Biochem. Mol. Biol. 169 (2017) 69–76.
[140] E. Pedruzzi, C. Guichard, V. Ollivier, F. Driss, M. Fay, C. Prunet, J.C. Marie, C. Pouzet, M. Samadi, C. Elbim, Y. O'dowd, M. Bens, A. Vandewalle, M.A. Gougerot-Pocidalo, G. Lizard, E. Ogier-Denis, NAD(P)H oxidase Nox-4 mediates 7-ketocholesterol induced endoplasmic reticulum stress and apoptosis in human aortic smooth muscle cells, Mol. Cell Biol. 24 (24) (2004) 10703–10717.

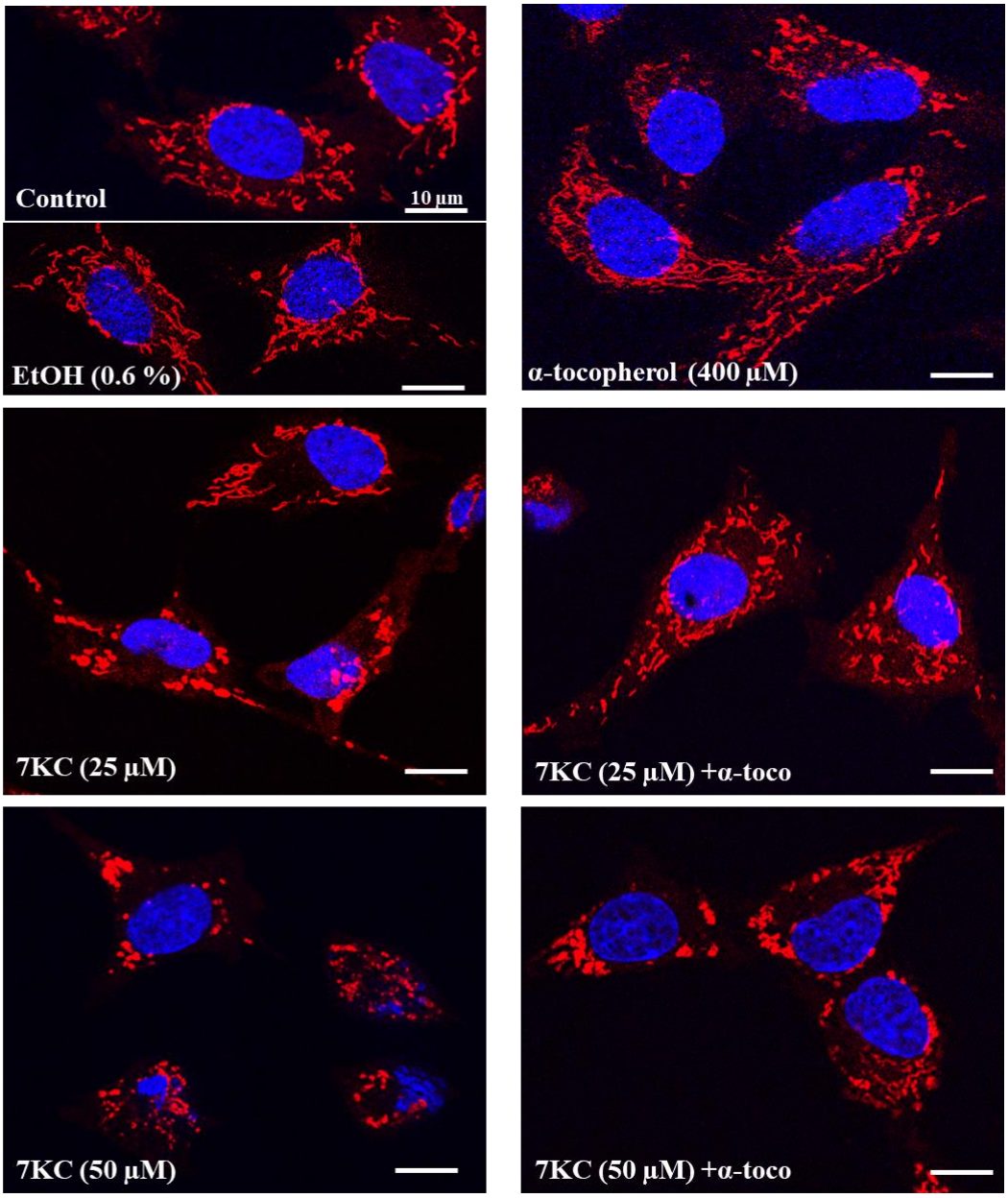

Supplementary Fig. 1: Evaluation of the effect of 7-ketocholesterol on mitochondrial topography. 158N murine oligodendrocytes were cultured on glass coverslips. They were taken after 24 h of culture and were further cultured without and with 7KC (25-50 µM) in the absence or in the presence of α-tocopherol (400 µM) for an additional 24 h period**.** The mitochondria were stained with Mitotracker red, and the nuclei were stained with Hoechst 33342. The observations were realized under a fluorescent microscope coupled with an Apotome.

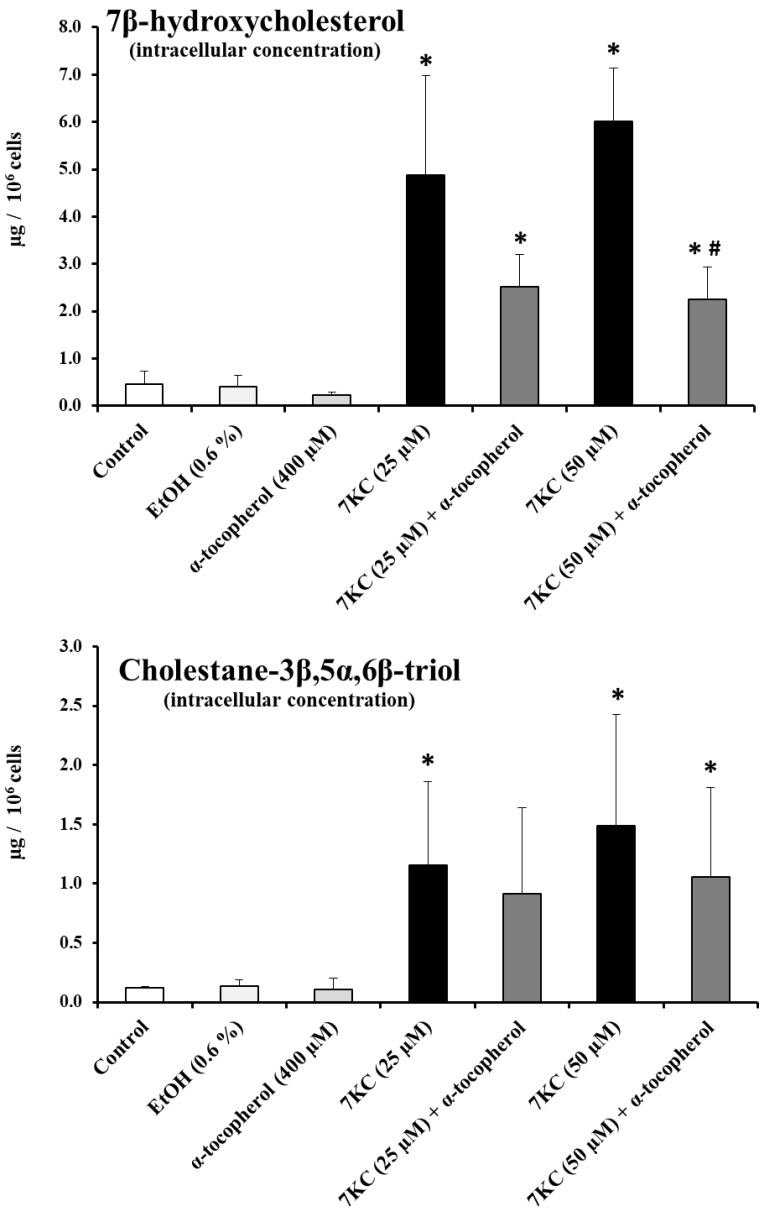

Supplementary Fig. 2: Induction of lipid peroxidation by 7-ketocholesterol. 158N murine oligodendrocytes were taken after 24 h of culture and were further cultured without and with 7KC (25-50 µM) in the absence or in the presence of α-tocopherol (400 µM) for an additional 24 h period**.** Lipid peroxidation was revealed by increased cellular levels of 7β-hydroxycholesterol and cholestane-3β,5α,6β-triol which were normalized by α-tocopherol (400 µM). Oxysterols were quantified as previously described **[104]**.

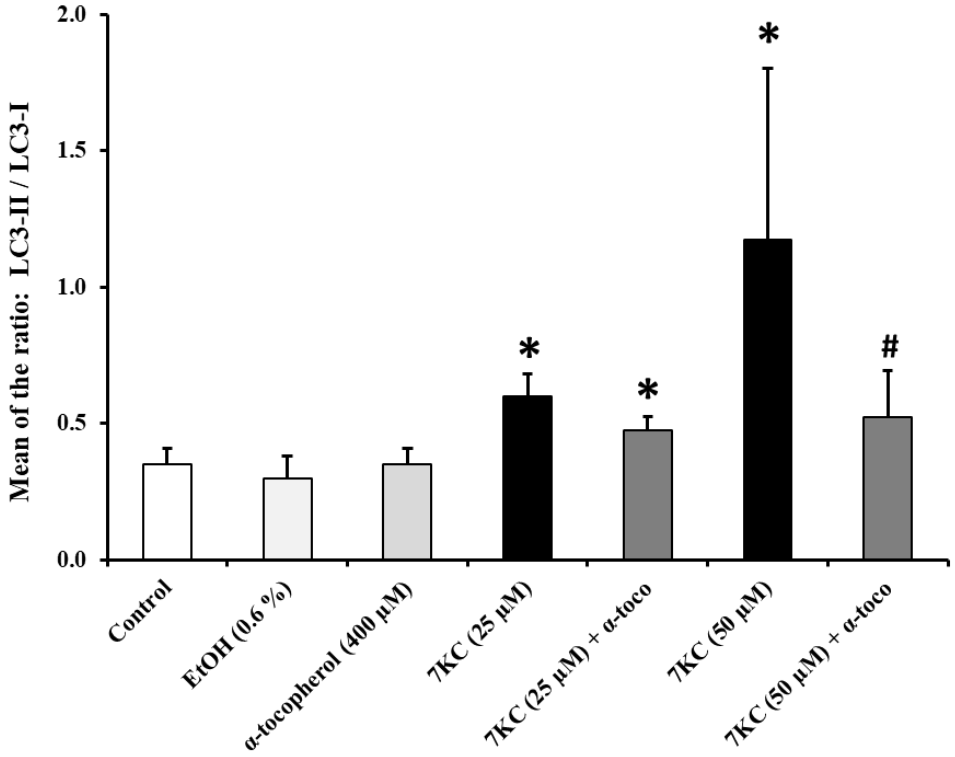

Supplementary Fig. 3: Quantitative analysis of the ratio [LC3-II / LC3-I]. The mean ± SD of the ratio [LC3-II / LC3-I] presented in **Fig. 4** have been calculated from the data obtained in 3 independent experiments. Significance of the differences between control (untreated cells) and 7KC-treated cells; Mann Whitney test: * $P<0.05$ or less. Significance of the differences between 7KC-treated cells and (7KC + α-tocopherol- treated cells; Mann Whitney test: # $P<0.05$ or less. No significant differences were found between control and vehicle-treated cells (Ethanol (EtOH: 0.6%).

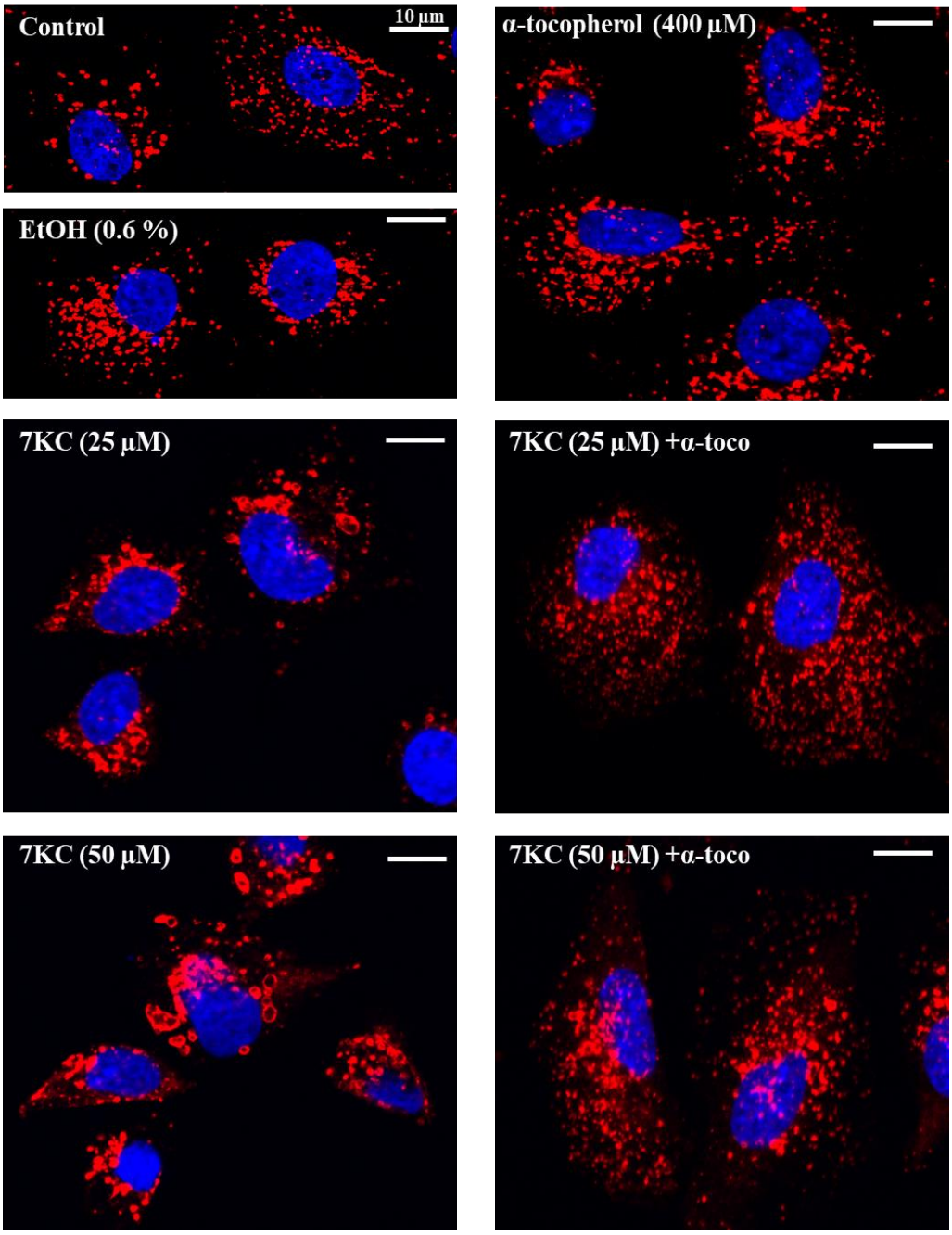

Supplementary Fig. 4: Evaluation of the effect of 7-ketocholesterol on the LAMP1 expression pattern. 158N murine oligodendrocytes were taken after 24 h of culture, and further cultured without and with 7KC (25-50 µM) in the absence or in the presence of α-tocopherol (400 µM) for an additional 24 h period of time**.** With the use of an antibody recognizing the lysosomal-associated membrane protein 1 (LAMP1), the presence of large red cytoplasmic dots, which can be considered as autolysomes support the ability of 7KC to induce autophagy which was strongly attenuated by α-tocopherol. The nuclei were stained with Hoechst 33342. The observations were realized under a fluorescent microscope coupled with an Apotome.

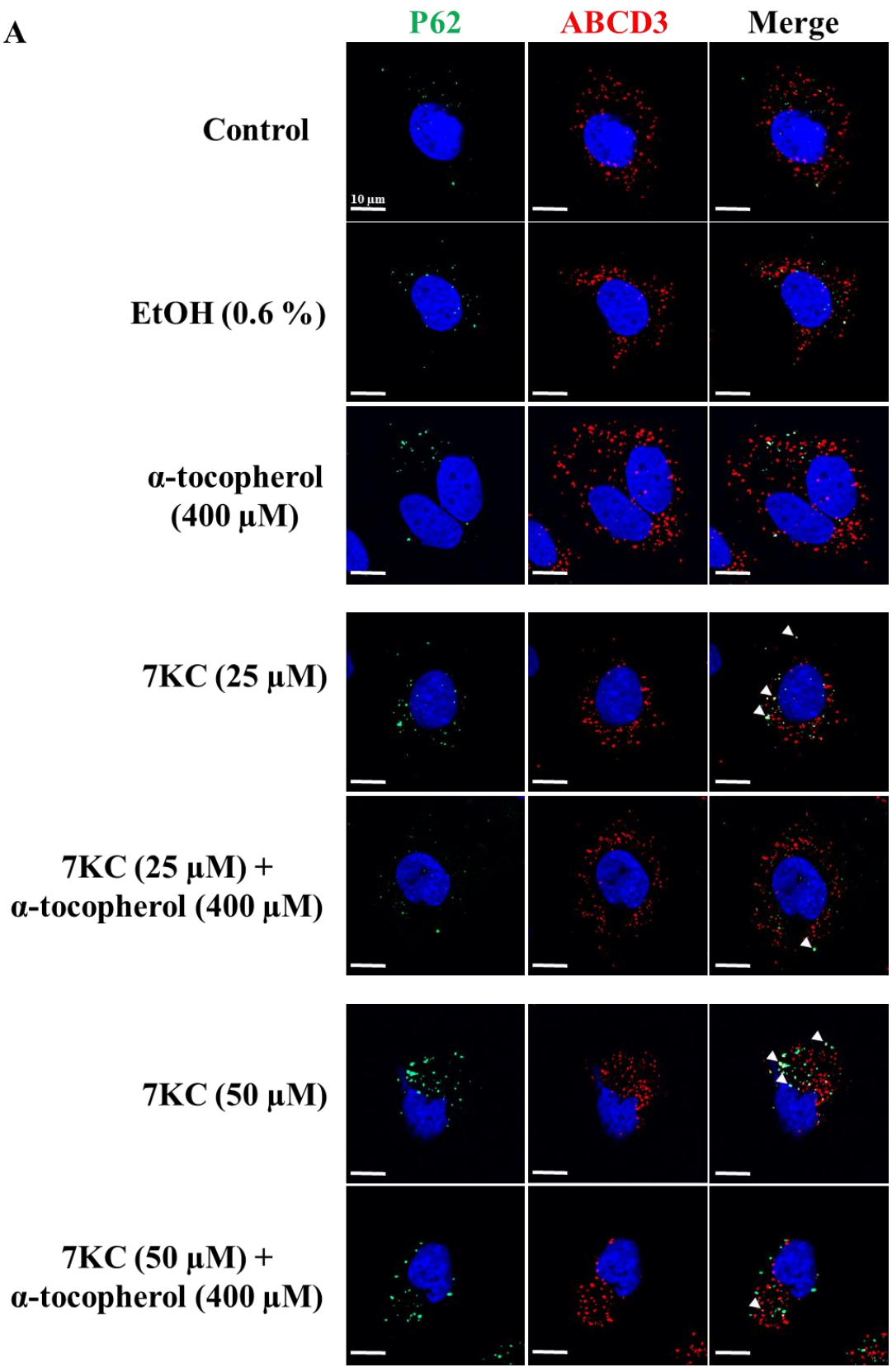
A
P62
ABCD3
Merge
Control
10 µm
EtOH (0.6 %)
α-tocopherol (400 µM)
7KC (25 µM)
7KC (25 µM) + α-tocopherol (400 µM)
7KC (50 µM)
7KC (50 µM) + α-tocopherol (400 µM)

B

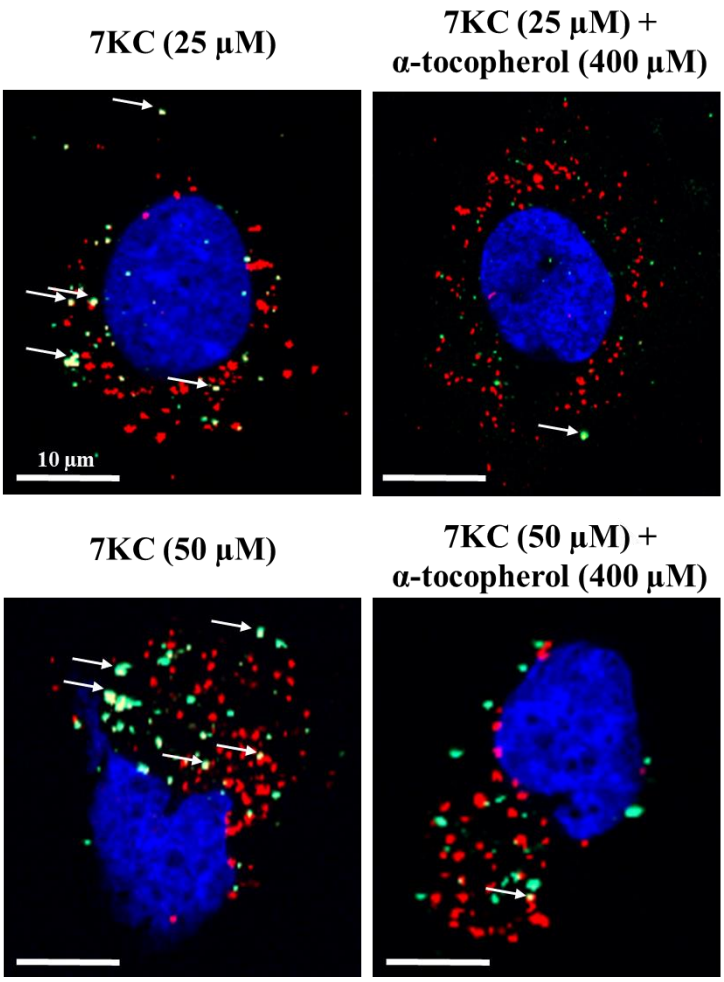

Supplementary Fig. 5: Evaluation of the effect of 7-ketocholesterol-induced pexophagy by fluorescence microscopy (colocalization of p62 and ABCD3). 158N murine oligodendrocytes were taken after 24 h of culture, and further cultured without and with 7KC (25-50 µM) in the absence or in the presence of α-tocopherol (400 µM) for an additional 24 h period of time (**A-B).** Cytoplasmic vesicles simultaneously expressing p62 and ABCD3 were considered as pexophagic vesicles. These vesicles (white arrows) correspond to yellow fluorescent spots resulting from the colocalization of p62 (revealed with Alexa 488 which emits a green fluorescence when excited with a blue light) with ABCD3 (revealed with Alexa 546 which emits a red fluorescence when excited with a green light). Pexophagic vesicles from different sizes are observed especially at high magnification (**B**). The nuclei were stained with Hoechst 33342. The observations were realized under a fluorescent microscope coupled with an Apotome.

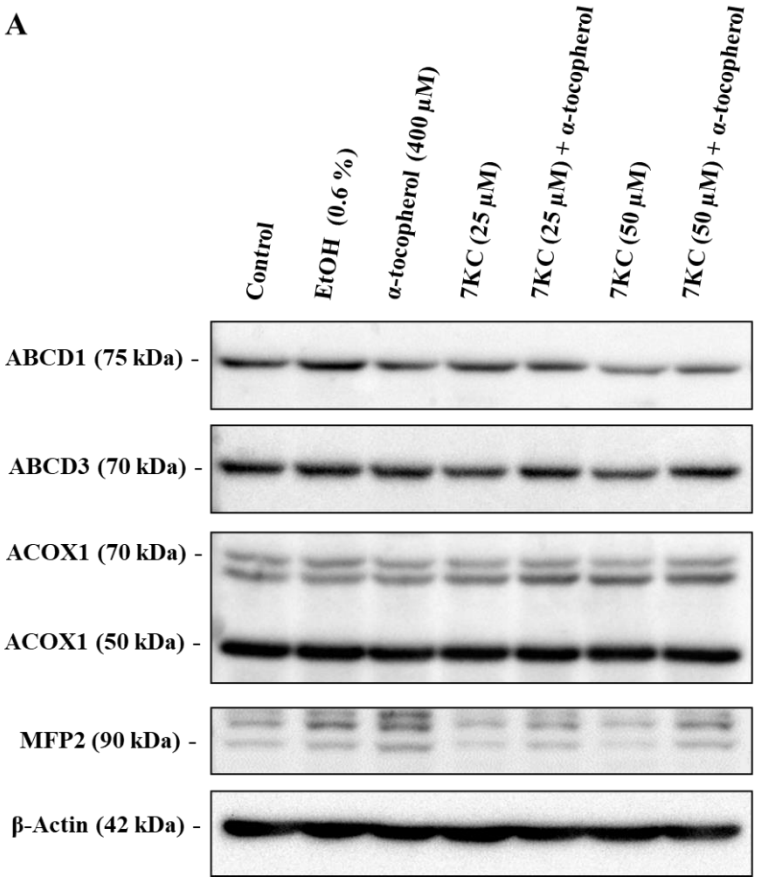
A
Control
EtOH (0.6 %)
α-tocopherol (400 μM)
7KC (25 μM)
7KC (25 μM) + α-tocopherol
7KC (50 μM)
7KC (50 μM) + α-tocopherol
ABCD1 (75 kDa) -
ABCD3 (70 kDa) -
ACOX1 (70 kDa) -
ACOX1 (50 kDa) -
MFP2 (90 kDa) -
β-Actin (42 kDa) -

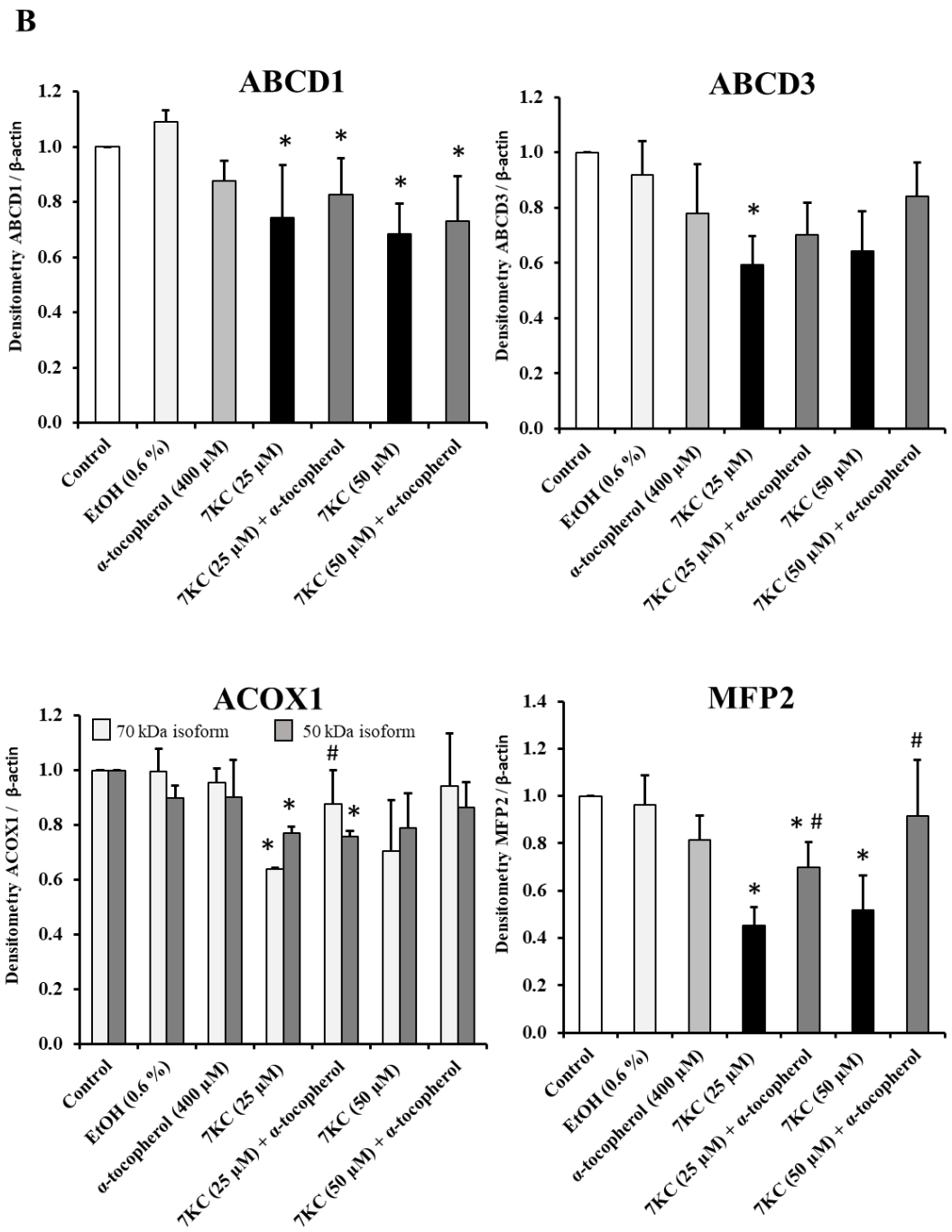

Supplementary Fig. 6: Effects of 7-ketocholesterol on peroxisomal proteins expression: ABCD1, ABCD3, ACOX1, MFP2, DHAPAT and ADHAPS. 158N murine oligodendrocytes were taken after 24 h of culture, and were further cultured without and with 7KC (25-50 µM) in the absence or in the presence of α-tocopherol (400 µM) for an additional 24 h period of time**.** The incidence of 7KC, with or without α-tocopherol, on the level of transporters and enzymes of the peroxisomal β-oxidation (ABCD1, ABCD3, ACOX1, MFP2), and on the level of the first two peroxisomal enzymes involved in plasmalogens synthesis (DHAPAT, ADHAPS) was evaluated by western blotting (**A**). Data shown are representative of

three independent experiments. Mean ± SD of the densitometric values of ABCD1, ABCD3, ACOX1, MFP2, DHAPAT, and ADHAPS obtained by western blotting from 3 independent experiments (**B**). Significance of the differences between control (untreated cells) and 7KC-treated cells; Mann Whitney test: * $P<0.05$ or less. Significance of the differences between 7KC-treated cells and (7KC + α-tocopherol) - treated cells; Mann Whitney test: # $P<0.05$ or less. No significant differences were found between control and vehicle-treated cells (Ethanol (EtOH: 0.6%).

Article 2

Prevention of 7-ketocholesterol-induced oxiapoptophagy by fatty acids and sulfo-N-succinimdyl oleate (SSO): SSO benefits and cytoprotective mechanisms

Thomas Nury, Aline Yammine, Claudio Caccia, Valerio Leoni, Aziz Hichami, Thibault Moreau, Anne Vejux, Gérard Lizard

Article en préparation

Il a été montré dans le premier article que le 7KC induit des dysfonctions mitochondriales et peroxysomales. Ces altérations sont accompagnées d'une élévation de marqueurs de l'autophagie et de l'apoptose. L'augmentation simultanée du stress oxydant, de l'apoptose et de l'autophagie sous l'effet du 7KC a été qualifiée d'oxyapoptophagie (stress **Oxy**dant + **Apopto**se + Auto**phagie**).

Le second article s'inscrit dans la continuité de ces travaux et a pour objectif d'identifier des composés lipidiques, autres que l'α-tocophérol, qui seraient capables d'inhiber l'oxyapoptophagie induite par le 7KC sur les oligodendrocytes murins 158N. Actuellement, peu de molécules possèdent ces propriétés cytoprotectrices vis-à-vis du 7KC. Les seules connues pour l'instant sont l'α-tocophérol, l'acide oléique (AO, C18:1 n-9), l'acide docosahexaénoïque (DHA, C22:6 n-3), le diméthylfumarate (DMF) ainsi que certaines huiles naturelles (huile d'argan, d'olive et de graines de chardon-Marie) (Badreddine *et al.*, 2017; Debbabi *et al.*, 2016; Meddeb *et al.*, 2018; Nury *et al.*, 2015; Nury *et al.*, 2017; Nury *et al.*, 2014; Zarrouk *et al.*, 2019; Zarrouk *et al.*, 2017).

Afin d'identifier de nouvelles molécules lipidiques protectrices, différents acides gras et dérivés ont été testés sur le modèle d'oligodendrocytes murins 158N traité par du 7KC (50 µM) pendant 24h. Le DHA et ses précurseurs : l'acide α-linolénique (ALA ; C18:3 n-9) et l'acide eicosapentaénoïque (EPA ; C20:5 n-3), l'huile de Lorenzo (mélange d'acide oléique (C18:1 n-9) et d'acide érucique (EA ; C22:1 n-9) dans un ratio 4:1) ainsi qu'un dérivé chimique de l'acide oléique, le sulfo-*N*-succinimidyl oléate (SSO). L'α-tocophérol, le DHA et l'AO ont été utilisés comme contrôles positifs de cytoprotection. La capacité de ces molécules à inhiber l'oxyapoptophagie a été évaluée en mesurant les altérations de la membrane plasmique (taux de cholestérol et marquage par la mérocyanine 540), les dysfonction mitochondriales (baisse du

Δψm) et peroxysomales (accumulation d'AGTLC), la production d'ERO (anions superoxydes, peroxyde d'hydrogène, activité catalase) l'induction d'apoptose (clivage de la caspase-3 et de PARP, expression de Bad, Mcl-1 et phospho-Mcl-1) et de l'autophagie (ratio LC3-II / LC3-I).

Ce travail a montré que l'α-tocophérol ainsi que les acides gras n-3 et n-9 (ALA (50 µM), EPA (50 µM), DHA (50 µM), OA (100 µM)), l'huile de Lorenzo (AO 100 µM + EA 25 µM), et le SSO (50 µM) atténuent l'augmentation du stress oxydant induite par le 7KC. Ils normalisent le potentiel membranaire des mitochondries (Δψm) et corrigent les dysfonction peroxysomales (normalisation de l'accumulation d'AGTLC intracellulaires). Au niveau membranaire, les perturbations lipidiques de la membrane plasmique révélées par la mérocyanine 540 et par le niveau de cholestérol ont également été en partie corrigées. Enfin, ces molécules et l'huile de Lorenzo inhibent l'autophagie (normalisation du ratio LC3-II / LC3-I) et l'apoptose (diminution du clivage de PARP et de la caspase-3, normalisation de Mcl-1 et de phospo-Mcl-1 ainsi que du ratio Bad / Mcl-1). L'acide érucique n'est pas cytoprotecteur.

L'acide oléique et l'huile de Lorenzo, bien qu'ayant montré une protection contre le 7KC, induisent la formation de gouttelettes lipidiques révélées en microscopie à fluorescence et cytométrie en flux (marquage par le BODIPY 493/503 et l'Oil Red O). La présence de gouttelettes lipidiques est également observable lorsque l'ALA, l'EPA et le DHA sont associés au 7KC. ALA, EPA, DHA et 7KC seuls, n'induisent pas la formation de gouttelettes lipidiques.

Les seules molécules permettant une inhibition de l'oxyapoptophagie induite par le 7KC sans formation de gouttelettes lipidiques sont l'α-tocophérol et le SSO. En revanche, le SSO est plus actif que l'α-tocophérol car il est cytoprotecteur à une concentration de 50 µM alors que l'α-tocophérol l'est à 400 µM.

Les travaux de cet article ont montré que :

- Les acides gras n-3 (ALA, EPA, DHA), n-9 (OA), l'huile de Lorenzo (OA + EA (4:1)), et le SSO inhibent l'oxyapoptophagie induite par le 7KC au même titre que l'α-tocophérol,
- Les dysfonctions mitochondriales et peroxysomales induites par le 7KC sont corrigées par ces molécules,
- Les acides gras n-3 (ALA, EPA, DHA associés au 7KC), l'OA et l'huile de Lorenzo induisent la formation de gouttelettes lipidiques,
- Le SSO protège du 7KC dès 50 µM sans induire la formation de gouttelettes lipidiques, ce qui lui confère un intérêt thérapeutique.

Le dépôt d'un brevet concernant le SSO et ses capacités cytoprotectrices contre le 7KC est en cours d'élaboration avec la cellule de valorisation et de transfert de technologie de l'Université de Bourgogne : SATT SAYENS.

Title: **Prevention of 7-ketocholesterol-induced oxiapoptophagy by fatty acids and sulfo-N-succinimidyl oleate (SSO): SSO benefits and cytoprotective mechanism**

Running title: **Prevention of 7KC-induced oxiapoptophagy with sulfo-N-succinimidyl oleate (SSO)**

T Nury [1], A Yammine [2], C Caccia [3], V Leoni [4], A Hichami [5], T Moreau [1,6], A Vejux [1*], G Lizard [1*]

1 - *Team Bio-PeroxIL 'Biochemistry of the Peroxysome, Inflammation and Lipid Metabolism' (EA 7270) / University Bourgogne Franche-Comté (UBFC) / Inserm, Dijon, France*

2 – *Bioactive Molecules Research Laboratory, Doctoral School of Sciences and Technologies, Faculty of Sciences, Lebanese University, Fanar, Lebanon;*

3 - *Laboratory of Medical Genetics and Neurogenetics, Fondazione IRCCS Istituto Neurologico Carlo Besta, Milan, Italy*

4 – *Laboratory of Clinical Pathology, Ospedale di Desio, ASST-Monza and Department of Medicine and Surgery, University of Milano-Bicocca*

5 – *Physiology of Nutrition & Toxicology (NUTox), Inserm U1231, University UBFC, Dijon, France*

6 - *Univ. Hospital, Department of Neurology, Dijon, France*

Correspondence (*): *Dr G Lizard,* *(PhD) and* ***Dr A Vejux****, (PhD); Laboratoire Bio-PeroxIL, Université de Bourgogne / Inserm, Faculté des Sciences Gabriel, 6 boulevard Gabriel, 21000 Dijon, France; E.mail :* gerard.lizard@u-bourgogne.fr *;* anne.vejux@u-bourgogne.fr

Word count: 3914 words (excluding abstract, Methods, references and figure legends)

Acknowledgements

This work was presented as a poster at the 9th ENOR Symposium "Metabolism and Oxysterols: Therapeutics for Lifelong Health", September 19-20, 2019, University of Edinburgh, Edinburgh, Scotland (UK) (https://www.oxysterols.net/). This work was supported by grants from: Univ. Bourgogne (Dijon, France); Lebanese University (Faculty of Sciences), Beirut, Lebanon and ABASIM (Association Bourguignonne pour les Applications des Sciences de l'Information en Médecine, Dijon, France). This work has benefited from the logistical support of the INPST network (International Natural Product Sciences Taskforce (INPST: https://inpst.net/); Prof A Atanasov, Dr A Pande, Dr G Lizard). This work has also been supported by the University of Milano Bicocca, the Italian Minister of Health and MIUR (Ministero dell'Istruzione, dell'Università e della Ricerca).

Conflict of interest

The authors state no conflict of interest.

Abstract

Background: 7-ketocholesterol is a cytotoxic oxysterol increased in many chronic inflammatory diseases and age-related diseases. Inhibiting the toxicity of 7-ketocholesterol is a major challenge in treating associated diseases.

Experimental approach: The 158N oligodendrocyte model was used to evaluate the cytoprotective effects of lipids: omega-3 and -9 fatty acids (α-linolenic acid, eicosapentaenoic acid, docosahexaenoic acid, erucic acid and oleic acid), Lorenzo's oil (a mixture of erucic acid and oleic acid, 1:4) and sulfo-N-succinimidyl oleate (SSO). The ability of these molecules to inhibit 7KC-induced oxiapoptophagy (plasma membrane alteration, loss of ΔΨm, peroxisomal dysfunction, reactive oxygen species overproduction, induction of apoptosis and autophagy) was quantified.

Key results: Unlike omega-3 and -9 fatty acids and Lorenzo's oil, SSO does not have toxic effects over a wide range of concentrations and its cytoprotective effects are not associated with the accumulation of lipid droplets.

Conclusions: These different characteristics of SSO make it possible to envisage its use for therapeutic purposes in diseases where 7KC levels are greatly increased.

Keywords: 7-ketocholesterol, α-linolenic acid, eicosapentaenoic acid, docosahexaenoic acid, oleic acid, erucic acid, Lorenzo’s oil, oxiapoptophagy, sulfo-N-succinimidyl oleate

Abbreviations: α-linolenic acid (ALA), docosahexaenoic acid (DHA), dihydroethidium (DHE); eicosapentaenoic acid (EPA), erucic acid (EA), fatty acids (FAs); fluorescein diacetate (FDA), 7-ketocholesterol (7KC), merocyanine 540 (MC540); oleic acid (OA), sulforhodamine 101 (SR101), sulfo-N-succinimidyl oleate (SSO), very long chain fatty acids (VLCFAs), X-linked adrenoleukodystrophy (X-ALD).

*** ‘What is already known’** Few natural and synthetic molecules inhibit the toxicity of 7-ketocholesterol

***‘What this study adds’** Among the fatty acids and derivatives tested, sulfo-N-succinimidyl oleate is the most promising

***'Clinical significance'** sulfo-N-succinimidyl oleate could be used to treat diseases with high 7-ketocholesterol levels

Introduction

Cholesterol provided by the diet or formed by endogenous synthesis is one of the most abundant and physiologically important lipids in the body (Bjorkhem *et al.*, 2004). Some of its oxidized derivatives (oxysterols) formed either by auto-oxidation or enzymatically, or by both processes are involved in several diseases (Mutemberezi *et al.*, 2016). Among the oxysterols formed by auto-oxidation, the most common is 7-ketocholesterol (7KC); indeed, the 7 position on cholesterol is the most reactive with oxygen and a carbonyl group the most stable form (Anderson *et al.*, 2020). 7KC is found at increased level in the biological fluids and tissue lesions of patients with aged-related diseases, some chronic inflammatory diseases and rare diseases (Brahmi *et al.*, 2019; Brown *et al.*, 1999; Testa *et al.*, 2018; Vejux *et al.*, 2020; Zarrouk *et al.*, 2014). To prevent these diseases, two strategies are possible. This consists either in promoting the degradation of 7KC, or in acting on the signaling pathways involved in the cytotoxicity of this oxysterol which induces oxidative stress and inflammation that can lead to cell death defined as oxiapoptophagy (OXIdative stress, APOPTOsis and autoPHAGY) (Klionsky *et al.*, 2016; Nury *et al.*, 2014). The alternative application of enzymes from microbial sources to degrade 7KC (medical bioremediation) is an attractive approach (Mathieu *et al.*, 2008; Schloendorn *et al.*, 2009). Pharmacological approaches consist in acting on 7KC-activated signaling pathways through strategies based on the use of natural or synthetic molecules, functionalized nanoparticles (Targeted ORganelle Nano-Therapy (TORNtherapy)) or chimeric molecules (Brahmi *et al.*, 2019). Few molecules have been shown to be effective in vitro in preventing 7KC-induced oxiapoptophagy. These are α-tocopherol, fatty acids (FAs) (oleic acid (OA; C18:1 n-9), docosahexaenoic acid (DHA; C22:6 n-3)) and dimethyl fumarate, an activator of the Nrf2

pathway, as well as its major metabolite, mono methyl fumarate (Brahmi *et al.*, 2019). Many oils (argan oil, olive oil and milk thistle seed oil) have also shown cytoprotective effects against 7KC (Zarrouk *et al.*, 2019). While the cytoprotective mechanism of α-tocopherol can be explained by its ability to prevent the accumulation of 7KC in the lipid rafts (Ragot *et al.*, 2013; Royer *et al.*, 2009), there is little information on the cytoprotection of fatty acids (FAs: OA, DHA) against 7KC (Debbabi *et al.*, 2017; Nury *et al.*, 2015). It can be assumed that they could both neutralize 7KC by esterification (Monier *et al.*, 2003) and act by reducing oxidative stress and mitochondrial dysfunction leading to cell death (Brahmi *et al.*, 2019). As OA and DHA, which are present in significant amounts in the Mediterranean diet (Schwingshackl *et al.*, 2020), are often associated with dietary supplements and can be used in functional foods, it is important to have more information on these molecules, as well as on the precursors of DHA (α-linolenic acid (ALA / C18:3 n-9) and eicosapentaenoic acid (EPA / C20:5 n-3)), by comparing their activities, assessing their deleterious effects and specifying their mechanisms of action. The effect of OA was also compared to a synthetic analogue, the membrane-impermeable sulfo-*N*-hydroxysuccinimidyl ester of oleic acid (SSO) which irreversibly binds CD36 (Coort *et al.*, 2002). On neuron-BV-2 co-culture and neuron-primary microglia co-cultures, SSO also reduced the lipopolysaccharide/interferon-γ-induced production of nitric oxide, interleukin-6 and tumor necrosis factor-α, and the protein levels of inflammatory enzymes including nitric oxide synthase 2, cyclooxygenase-2 (COX-2), and p38 mitogen-activated protein kinase in microglia, without causing cell toxicity (Dhungana *et al.*, 2017). In addition, on isolated rat liver mitochondria, an inhibition of mitochondrial membrane potential (ΔΨm) and a decrease of mitochondrial complex III activity has been reported with SSO (Drahota *et al.*, 2010). Furthermore, since X-ALD is associated with elevated plasma levels of 7KC (Nury *et al.*, 2017) and Lorenzo's oil composed of erucic acid (C22:1 n-9) and oleic acid (C18:1 n-9) in a ratio of 1:4 is sometimes administered to

patients with X-ALD in an attempt to prevent neurodegeneration by reducing levels of very long-chain fatty acids (VLCFAs) (Prieto Tenreiro *et al.*, 2013), it was considered as essential to determine the effect of this oil on 7KC-induced cytotoxicity.

In the present study, we evaluated and compared the cytoprotective effects of ALA, EPA, DHA, OA, EA and SSO as well as of Lorenzo's oil on 7KC-treated 158N cells which is a relevant model to identify natural or synthetic molecules able to prevent 7KC-induced cytotoxicity. The effects of these compounds were compared with those of α-tocopherol, the major component of Vitamin E, which was used as the reference cytoprotective molecule. Although all compounds tested, excepted EA, attenuate the toxicity of 7KC, SSO has the most interesting profile: it is not cytotoxic even at high concentrations and does not induce cytoplasmic accumulation of lipid droplets. In addition, the ability of SSO to attenuate 7KC-induced plasma membrane alteration is accompanied by a restoration of cell signaling that controls ΔΨm and prevents apoptosis.

Methods

Cell culture and treatments

Murine oligodendrocytes (158N) (Baarine *et al.*, 2009) were seeded at 30,000 cells/cm² either in 100 mm diameter Petri dishes, 12 wells plates or 96 wells plates. They were cultured in Dulbecco's Modified Eagle Medium (DMEM) containing 5% (v/v) heat-inactivated fetal bovine serum (Dutscher, Brumath, France) and 1% antibiotics (penicillin, streptomycin). The incubation was performed at 37°C in a humidified atmosphere containing 5% CO_2. For subcultures, cells were trypsinized (0.05% trypsin-0.02% EDTA solution) and passaged twice a week. 7-ketocholesterol (7KC; Sigma Aldrich, ref C2394) stock solution was prepared at 2 mM as previously described (Ragot *et al.*, 2013). After 24 h of culture, 158N cells were incubated for 24 h with 7KC, α-tocopherol (Sigma Aldrich, ref T3251), α-linolenic acid (ALA; Sigma Aldrich, ref

L2376), eicosapentaenoic acid (EPA; Enzo Life Sciences, ref BML-FA001-0100), docosahexahenoic acid (DHA; Sigma Aldrich, ref D2534), oleic acid (OA; Sigma Aldrich, ref 01008), erucic acid (EA; Interchim, ref DRE-C13203000), Lorenzo's oil (EA + OA: ratio 1:4) or sulfo-N-succinimidyl oleate **(**SSO; Interchim, ref 11211), or with 7KC associated with α-tocopherol, ALA, EPA, DHA, OA, EA, Lorenzo's oil or SSO. FAs stock solutions were prepared at 50 mM (ALA, DHA, OA, EA) or 200 mM (EPA) in absolute ethanol (Carlo-Erba, Val de Reuil, France) and stored at -20°C. SSO stock solution was prepared at 50 mM in dimethylsulfoxide (DMSO, Sigma-Aldrich). The inhibitors of autophagy (Rapamycin (Sigma-Aldrich; ref 37094); 3-methyl adenine (Sigma-Aldrich; ref M9281)) and of autophagy (z-VAD-fmk (Bachem, ref 4026865) were prepared and used as previously described (Doria *et al.*, 2019; Sassi *et al.*, 2019b; Vejux *et al.*, 2007). As we studied the effects of FAs and SSO on 158N cells, we determined the expression of PPARs and CD36 receptors on these cells. Because of the expression of PPARs and CD36 by 158N cells, we considered that these latter were suitable for studying the effects of these compounds (**Supplementary Figure 1**).

Measurement of cell viability with the fluorescein diacetate (FDA) test

The cell-permeant esterase substrate fluorescein diacetate (FDA) (Invitrogen, ref F1303) was used as a viability probe on 158N cells (Namsi *et al.*, 2018). At the end of the treatment, cells were incubated in the dark with FDA (15 µg/mL in PBS, 5 min, 37°C) and rinsed with PBS. Cell fluorescence intensity (Ex: 485 nm / Em: 538 nm) was measured with a TECAN fluorescence microplate reader (Sunrise spectrophotometer, TECAN, Lyon, France). The experiments were realized in triplicate. The data were expressed as percentage of control.

Quantification of adherent cells with the sulforhodamine 101 (SR101) test

Suforhodamine 101 (SR101; Sigma Aldrich, ref S7635) was used to evaluate the number of adherent cells by its ability to stain the total cellular protein content (Namsi *et al.*, 2019). At the end of treatments, 158N cells were fixed with ethanol 70% for 20 min at 4°C. After two washes in PBS, cells were stained with a SR101 solution (1.5 µg/mL, 30 min, 4°C). Then, the cells were washed twice with PBS and the fluorescence was measured with a fluorescent plate reader (Infinite M200, TECAN) using Ex 535nm / Em 610 nm. The experiments were realized three times in triplicate, and the data were expressed as percentage of control.

Cell condition assessment with morphological criteria by phase contrast microscopy

Cells were seeded in 12 well plates and treated with or without 7KC, FAs, Lorenzo's oil, SSO and α-tocopherol for 24 h. At the end of the treatments, cells were observed under an inverted phase contrast microscope (Primovert Zeiss microscope, Jena, Germany) at a x20 magnification. Digitalized images were obtained with a Zeiss camera (5MP HD IP).

Evaluation of CD36 expression by indirect immunofluorescence: microscopical and flow cytometric analysis

For immunofluorescence microscopy, 158N cells were seeded in 6 well plates on glass slides for 24 h before the analysis of CD36 expression. At the end of treatments, cells were washed with PBS and fixed with a 2% paraformaldehyde / PBS solution (15 min, room temperature (RT)). After washing in PBS, adherent cells were permeabilized with PBS / 0.05% saponin / 10% FBS (PFS buffer) for 30 min at RT, and incubated (1 h at RT) with the CD36 antibody (Gentex, ref GTX100642) diluted 1/200 in PFS buffer. At the end of the incubation time, cells were washed in PFS buffer and incubated (30 min in the dark, RT) with a goat anti-rabbit antibody coupled with 488-Alexa (Abcam, Paris, France; ref ab150077) diluted at 1/500 in PFS buffer. After washing in

PBS, cells were counterstained with Hoechst 33342 (Sigma-Aldrich, 1 µg/mL). The slides were mounted in fluorescent mounting medium (Dako, Coppenhagen, Denmark), stored in the dark at 4°C, and examined with a right fluorescence microspcope (Zeiss).

For flow cytometric analysis of CD36 expression, 158N cells were trypsinized and further stained in the same conditions than previously described (no counterstaining with Hoechst 33342 was realized). Cells were analyzed with a BD Accuri C6 flow cytomer (Becton-Dickinson, Franklin Lakes, NJ, USA); the green fluorescence was collected through a 520/10 nm band pass filter and analyzed on a logarithmic scale: 10,000 cells were acquired. The analysis of CD36 expression was realized using the FlowJo software (Tree Star Inc., Ashland, USA).

Flow cytometric quantification of mitochondrial membrane potential (ΔΨm) with $DiOC_6(3)$

Modifications of ΔΨm were measured with 3,3′-dihexyloxacarbocyanine iodide ($DiOC_6(3)$) (Thermo Fischer Scientific, Courtaboeuf, France). At the end of treatments, 158N cells were trypsinized and resuspended in PBS containing $DiOC_6(3)$ used at 40 nM. Cells were incubated for 15 min at 37°C in the dark. Cells were analyzed with a BD Accuri C6 flow cytomer (Becton-Dickinson); the green fluorescence was collected through a 520/10 nm band pass filter and analyzed on a logarithmic scale: 10,000 cells were acquired. The percentage of $DiOC_6(3)$ negative cells was determined using the FlowJo software (Tree Star Inc).

Flow cytometric measurement of the loss of asymmetry and altered packing of the plasma membrane with merocyanine 540

Merocyanine 540 (MC540) (Sigma Aldrich) is a negatively charged chromophore that binds to the outer leaflet of the cell membrane. The loss of asymmetry and altered packing of the membrane enhance MC540 fluorescence (Schlegel *et al.*, 1993; Vejux *et al.*, 2009a). MC540 was

prepared in absolute ethanol at 2.5 mg/mL. At the end of treatments, adherent and non-adherent cells were collected and resuspended in culture medium containing MC540 (2.5 µg/mL). Cells were incubated (10 min, RT), and analyzed with a BD Accuri C6 flow cytometer (Becton-Dickinson). The orange/red fluorescence was collected through a 590/20 nm band pass filter and analyzed on a logarithmic scale: 10,000 cells were acquired. The percentage of MC540 positive cells was determined using the FlowJo software (Tree Star Inc).

Flow cytometric quantification of reactive oxygen species after staining with dihydroethidium

The overproduction of reactive oxygen species (ROS) was detected with dihydroethidium (DHE; Life Technologies, St. Aubin, France) (Rothe *et al.*, 1990). DHE was prepared at 1.6 mM in DMSO and used at 2 µM in PBS. Cells were incubated (15 min, RT), and analyzed with a BD Accuri C6 flow cytometer (Becton-Dickinson); the orange/red fluorescence was collected through a 590/20 nm band pass filter and analyzed on a logarithmic scale: 10,000 cells were acquired. The percentage of DHE positive cells were determined using FlowJo software (Tree Star Inc).

Visualization of lipid droplets with Oil Red O (ORO): observation with brightfield microscopy

Lipid droplets are dynamic organelles and function as a storage depot for neutral lipids, including triglycerides and cholesterol esters (Walther *et al.*, 2012). The presence of neutral lipids was investigated by staining with Oil Red O (ORO; Sigma Aldrich). ORO is soluble in neutral lipids and remains dissolved in triglycerides after washing. To this end, at the end of treatments, 158N cells cultured in 6 well-plates were washed with PBS and stained with ORO solution (three parts 0.5% ORO dye in isopropanol into two parts water) for 30 min and stored in the dark at RT (Debbabi *et al.*, 2017). The stained cells were washed three times with water and three

contiguous observation fields always taken in the center of a 6-well plate were observed under an inverted phase contrast microscope (Axiovert 40 CFL, Zeiss).

Visualization by fluorescence microscopy and quantification by flow cytometry of lipid droplets stained with Bodipy 493/503

The presence of lipid droplets was also analyzed with the fluorescent neutral lipid dye 4,4-difluoro-1,3,5,7,8-pentamethyl-4-bora-3a,4a-diaza-s-indacene (Bodipy 493/503) (Sigma Aldrich, ref 790389) which permits the observation of the lipid droplets by fluorescence microscopy and their quantification per cell by flow cytometry (Qiu *et al.*, 2016). For microscopical analysis, 158N cells were seeded on glass slides in 12 well plates. After 24 h of culture, 158N cells were incubated with 7KC for 24 h without or with α-tocopherol, FAs, Lorenzo's oil or SSO. After treatments, cells were washed with PBS and stained with Bodipy 493/503 (2 µM; 15 min; 37°C). After washing, cells were fixed with 4% paraformaldehyde (10 min at RT, in the dark) and washed again with PBS. A counter staining with Hoechst 33342 (2 µg/mL in PBS, 5 min at RT, in the dark) was realized. The slides were mounted in fluorescent mounting medium (Dako), stored in the dark at 4°C, and examined under a right fluorescence microscope (Axioskop, Zeiss). For flow cytometry, 158N cells were trypsinized and stained in the same conditions (no counter-staining with Hoechst 33342 was realized). Cell suspensions were analyzed with a BD Accuri C6 flow cytometer (Becton-Dickinson); the green fluorescence was collected through a 520/10 nm band pass filter and analyzed on a logarithmic scale: 10,000 cells were acquired. The mean fluorescence intensities of Bodipy 493/503 samples were determined using FlowJo software (Tree Star Inc).

Quantification of 7-ketocholesterol and fatty acids, including very long chain fatty acids, by gas chromatography coupled with mass spectrometry

7KC and FAs were quantified on untreated and treated 158N cells as previously described (Leoni *et al.*, 2017). Cellular homogenates, prepared from pellets of about 10^7 cells suspended in water (100 µL) and sonicated for 10 min, were added to a screw capped vial sealed with a Teflon septum together with structural homologous internal standards (pentadecanoic 50 µg, heptadecanoic acid 100 µg, nonadecanoic acid 5 µg, heneicosanoic acid, 2.5 µg, tricosanoic acid 1 µg, epicoprostanol 50 µg), butylated hydroxytoluene and EDTA and flushed with argon for 10 min to remove air. Alkaline hydrolysis was allowed to proceed atroom temperature (22°C) with magnetic stirring for 60 min in the presence of ethanolic 0.5 M potassium hydroxide solution. Sterols and oxysterols were collected by liquid to liquid extraction with 5 mL of hexane. FAs were collected after correction of pH (< 3) with HCl by liquid to liquid extraction with hexane and ethylacetate. The organic solvents were evaporated under a gentle stream of argon and converted into trimethylsilyl ethers with bis(trimethylsilyl)trifluoroacetamide with 1% trimethylchlorosilane (Pierce).

Gas chromatography - mass spectrometry (GC–MS) analysis was performed on a Agilent 5973 Mass spectrometer connected to a GC 6890 Agilent equipped with an HP-5MS columns (30 m × 0.32 mm id × 0.25 mm film; Agilent, USA) and injection was performed in splitless mode using helium (1 mL/min) as carrier gas. The temperature program was as follows: initial temperature 150 °C was held for 1 min, followed by a linear ramp of 10°C/min to 250°C, 20°C/min to 300°C and held for 5 min. The mass spectrometer operates in full mass scan mode. Peak integration was performed manually, and metabolites were recognized by retention time and fragmentation patterns and quantified from total-ion count against internal standards using standard curves for

the measured FAs, cholesterol and 7KC. Recovery ranged between 94% up to 100% and precision ranged between 3 up to 7%.

Quantification of catalase gene expression by RT-qPCR

Total mRNA from 158N cells were extracted and purified using the RNeasy Mini Kit (Qiagen) and the total mRNA concentration was measured with TrayCell (Hellma, Paris, France). The purity of nucleic acids was controlled by the ratio of absorbance at 260 nm and 280 nm (ratios between 1.8 - 2.2). 1 µg of mRNA was used for reverse transcription using the iScript cDNA Synthesis Kit (Bio-Rad, Marne La Coquette, France) according to the following protocol: 5 min at 25°C, 20 min at 46°C, 5 min at 95°C. cDNA were generated using the FG Power SYBR Green (Thermo Fischer Scientific). PCR reactions were realized on an Applied Biosystem Step One plus QPCR machine (Life Science Technologies). The primer sequences were the following:

- ***Catalase****: forward 5'-agcgaccagatgaagcagtg-3' reverse 5'-tccgctctctgtcaaagtgtg-3'*
- ***36B4****: forward 5'-gcgacctggaagtccaacta -3' reverse 5'-atctgcttggagcccacat -3'*

Thermal cycling conditions were as follows: activation of DNA polymerase at 95°C for 10 min, followed by 40 cycles of amplification at 95°C for 15 s, 60°C for 30 s, and 72°C for 30 s, followed by a melting curve analysis to test for the absence of non-specific products. Gene expression was quantified using cycle to threshold (Ct) values and normalized by the 36B4 reference gene. The quantitative expression of catalase was determined as fold induction of the control.

Protein analysis by polyacrylamide gel electrophoresis and Western blotting

Protein analysis was realized as previously described by polyacrylamide gel electrophoresis and Western blotting (Nury *et al.*, 2018; Nury *et al.*, 2015; Ragot *et al.*, 2011). Cells washed in PBS were lysed in a RIPA buffer (10 mM Tris-HCl, pH 7.2, 150 mM NaCl, 0.5% Nonidet NP40, 0.5% Na deoxycholate, 0.1% SDS, 2 mM EDTA and 50 mM NaF) in the presence of 1/25 complete protease inhibitor cocktail tablets (Roche Diagnostics, Indianapolis, IN, USA) and phenylmethylsulfonyl fluoride (PMSF; 1 mM) for 30 min on ice. Cell lysates were cleared by a 20 min centrifugation at 12,000 g. The protein concentration in the supernatant was measured using the Bicinchoninic Acid Assay kit (Sigma-Aldrich). Seventy micrograms of protein were diluted in loading buffer (125 mM Tris- HCl, pH 6.8, 10% β-mercaptoethanol, 4.6% SDS, 20% glycerol, and 0.003% bromophenol blue), separated on a 14% or 8% SDS-PAGE gel depending of the molecular weight of the proteins, and transferred onto a nitrocellulose membrane (Bio-Rad, Marne La Coquette, France). After blocking nonspecific binding sites for 1 h with 5% milk powder in PBST (PBS, 0.1% Tween 20, pH 7.2), the membrane was incubated overnight at 4°C with the primary antibody diluted in PBST + 5% milk powder. The antibodies raised against caspase-3 (rabbit polyclonal antibody; Ozyme / Cell Signaling; ref: 9662; detecting endogenous levels of full length casapase-3 (35 kDa) and the large fragment of caspase-3 resulting from cleavage (17 kDa)), and LC3 (rabbit polyclonal antibody; Sigma-Aldrich, ref L8918; detecting LC3-I (18 kDa) and LC3-II (16 kDa)), Mcl-1 (monoclonal antibody; Abcam ref ab32087), Phospho-Mcl-1 (Ser159/Thr163) (rabbit polyclonal antibody; Ozyme / Cell Signalling; ref 4579), Bad (rabbit polyclonal antibody; Ozyme / Cell Signalling; ref 9292), PARP (rabbit monoclonal antibody; Ozyme / Cell Signalling; ref 9532; detecting endogenous levels of full length PARP (110 kDa) and the fragment of PARP resulting from cleavage (89 kDa)) were used at 1/1,000 final dilution. The antibody directed against β-actin (mouse monoclonal antibody; Sigma-Aldrich, ref A2228) was used at a final concentration of 1/10,000. The membrane was then

washed twice with PBST and incubated for 1 h at RT with horseradish peroxidase-conjugated goat anti-rabbit (Cell Signaling, ref 7074) or anti-mouse antibody (Santa-Cruz Biotechnology, ref sc-2005) diluted at 1/5,000. The membrane was washed with PBST and revealed using an enhanced chemiluminescence detection kit (Supersignal West Femto Maximum Sensitivity Substrate, Thermo-Scientific) and Chemidoc XRS+ (Bio-Rad). The level of bands intensity was measured with Image Lab software (Bio-Rad).

Statistical analysis

The experimental data represent the mean ± standard deviation (SD). Statistical analyses were performed using XLStat software. The Mann-Whitney U test was used to compare the different groups, and data were considered statistically different at a P value of 0.05 or less.

Results

Comparative study of the effects of α-linolenic acid (ALA), eicosapentaenoic acid (EPA), docosahexaenoic acid (DHA), oleic acid (OA), erucic acid (EA), Lorenzo's oil (EA + OA; 1:4) and sulfo-N-succinimidyl oleate (SSO) on cell growth and viability of 158N oligodendrocytes

On 158N cells, FAs (ALA, EPA, DHA, OA, EA) and SSO were used alone in a concentration range of 25 to 200 µM for a 24 h treatment. Lorenzo's oil was used for different concentrations of EA and OA (OA not exceeding 200 µM). α-tocopherol was used from 100 to 400 µM (Ragot *et al.*, 2013). With the FDA and SR101 assays, no cytotoxic effect of α-tocopherol was observed and with SSO, a slight decrease on cell growth was found at 200 µM with the SR101 assay (**Figure 1**). More or less marked cytotoxic effects were observed with FAs and Lorenzo's oil. Thus, as early as 100 µM, ALA, EPA and DHA showed cytoxicities with FDA and SR101 assays

(**Figure 1**). OA shows pronounced toxicity only at 200 µM with the FDA assay (**Figure 1**). EA only shows slight cytoxic effects at 200 µM (**Figure 1**). As for Lorenzo's oil, pronounced effects on the inhibition of cell growth measured by the SR101 assay were detected as early as the [AO (100 µM) / EA (25 µM)] concentrations (**Figure 1**). In order to subsequently determine the effects of these compounds on 7KC-induced toxicity, the highest non cytotoxic concentrations were selected: ALA (50 µM); EPA (50 µM); DHA (50 µM); OA (100 µM); EA (25 µM); SSO (50 µM); Lorenzo's oil (OA: 100 µM / EA: 25 µM).

Evaluation with the FDA and SR101 tests of the cytoprotective effects of α-linolenic acid, eicosapentaenoic acid, docosahexaenoic acid, oleic acid, erucic acid, Lorenzo's oil and sulfo-N-succinimidyl oleate (SSO) on 7-ketocholesterol-treated 158N oligodendrocytes

The effects of ALA (50 µM), EPA (50 µM), DHA (50 µM), OA (100 µM), EA (25 µM), SSO (50 µM) and Lorenzo's oil (OA: 100 µM / EA: 25 µM) as well as α-tocopherol (400 µM) associated or not with 7KC (50 µM) were evaluated with the FDA and SR101 assays after 24 h of treatment on 158N cells (**Figure 2**). The 50 µM concentration of 7KC was chosen because it decreases the number of cells by 30 to 50% using the FDA and SR101 assay, respectively; this 30-50% inhibition was confirmed by observation in phase contrast microscopy (**Figure 2, Supplementary Figure 2**). Whereas no cytoprotection was found with EA, cytoprotective effects in the same range or higher than those observed with α-tocopherol were detected with ALA, EPA, DHA, OA, SSO and Lorenzo's oil (**Figure 2; supplementary Figure 2**). The results obtained with the FDA and SR101 assays were in agreement with phase contrast microscopy observations: the cytotoxic effects of 7KC characterized by a decrease in the number of adherent cells and by an increase in the number of dead cells, which are round and float in the culture

medium, were strongly attenuated by ALA, EPA, DHA, OA, SSO, Lorenzo's oil and α-tocopherol whereas no cytoprotection was observed with EA (**Supplementary Figure 2)**.

Prevention of 7-ketocholesterol-induced oxidative stress, mitochondrial and peroxisomal dysfunction by α-linolenic acid, eicosapentaenoic acid, docosahexaenoic acid, oleic acid, Lorenzo's oil and sulfo-N-succinimidyl oleate

As it is known that 7KC (50 µM)-induced cytotoxic effects on 158N cells are associated with reactive oxygen species (ROS) overproduction, loss of ΔΨm and peroxisomal dysfunction (Nury *et al.*, 2018), the effects of ALA (50 µM), EPA (50 µM), DHA (50 µM), OA (100 µM), EA (25 µM), SSO (50 µM) and Lorenzo's oil (OA: 100 µM / EA: 25 µM) as well as α-tocopherol (400 µM) were evaluated on these parameters (**Figure 3**). An oxidative stress characterized by an increase in the percentage of cells overproducing ROS (% DHE positive cells) was detected in 7KC-treated cells (**Figure 3A**). In these latter, a drop of ΔΨm was also revealed with $DiOC_6(3)$ (**Figure 3B**) as well as peroxisomal dysfunction highlighted by an increase in VLCFAs (C24:0, C24:1, C26:0 and C26:1) since C24:0 and C26:0 are degraded in the peroxisome by β-oxidation (Wanders *et al.*, 2006) (**Figure 3C**). By RT-qPCR, an increased expression of catalase, a peroxisomal enzyme that catalyzes the dismutation of hydrogen peroxide to oxygen and water ($2\ H_2O_2 \rightarrow O_2 + H_2O$), was observed in the presence of 7KC and may be an adaptive response to ROS overproduction (**Figure 3D**). Whereas EA was inefficient to prevent 7KC-induced ROS overproduction and loss of ΔΨm, marked cytoprotective effects, in the range of those observed with α-tocopherol, were observed with ALA, EPA, DHA, OA, SSO and Lorenzo's oil (**Figure 3A-B**). When ALA, EPA, DHA, OA, SSO, Lorenzo's oil and α-tocopherol were associated with 7KC, they strongly reduced the increase in VLCFAs (**Figure 3C**); this supports that these compounds attenuate peroxisomal dysfunction and re-establish peroxisomal β-oxidation.

Moreover, decreased mRNA levels of catalase was observed when 7KC was associated with ALA, EPA, DHA, OA, SSO, Lorenzo's oil and α-tocopherol (**Figure 3D**); these data are in agreement with the ability of these compounds to decrease ROS overproduction.

Evaluation of the effects of α-linolenic acid, eicosapentaenoic acid, docosahexaenoic acid, oleic acid, erucic acid, Lorenzo's oil and sulpho-N-succinimidyl oleate on 7-ketocholesterol-induced lipid disturbances at the plasma membrane level

The effects of ALA (50 µM), EPA (50 µM), DHA (50 µM), OA (100 µM), EA (25 µM), SSO (50 µM), Lorenzo's oil (OA: 100 µM / EA: 25 µM) and SSO (50 µM) as well as α-tocopherol (400 µM) on 7KC-induced lipid disturbances at the plasma membrane level were evaluated with MC540 (Vejux *et al.*, 2009a) (**Figure 4A**) and by the quantification of total cholesterol (Cooper, 1978) (**Figure 4B**). Comparatively to untreated cells and vehicle (EtOH (0.6%))-treated cells, no effect on plasma membrane organization and cholesterol content was detected with ALA, EPA, DHA, OA, EA, SSO, Lorenzo's oil and α-tocopherol (**Figure 4A-B).** On the other hand, in the presence of 7KC, the lipid organization of the plasma membrane was strongly disturbed: the percentage of MC540 positive cells (cells strongly stained by MC540) was strongly increased (**Figure 4A**) and the total cholesterol level per cell was decreased (**Figure 4B**). Whereas EA was inefficient, the deleterious effects induced by 7KC on the lipid organization of the plasma membrane were strongly attenuated with ALA, EPA, DHA, OA, SSO and Lorenzo's oil as well as with α-tocopherol (**Figure 4A**). Similarly, with the exception of SSO, the decrease in cholesterol level induced by 7KC was attenuated by ALA, EPA, DHA, OA, Lorenzo's oil and α-tocopherol (**Figure 4B**).

Incidence of α-linolenic acid, eicosapentaenoic acid, docosahexaenoic acid, oleic acid, erucic acid, Lorenzo's oil and sulpho-N-succinimidyl oleate associated or not with 7-ketocholesterol-on lipid droplets accumulation

The use of FAs or analogues (SSO) as well as of Lorenzo's oil led us to specify the incidence of these compounds i) on the formation of lipid droplets and ii) on the accumulation of 7KC in the cells. Lipid droplet formation was evaluated with Oil Red O (ORO; brightfield microscopy) and with Bodipy 493/503 (fluorescence microscopy; flow cytometry). Quantification of 7KC and FAs was realized by GC-MS. Different effects were observed on intracellular lipid droplets accumulation with the different FAs (ALA, EPA, DHA, EA and OA), Lorenzo's oil, SSO and α-tocopherol. By staining with ORO, which colors neutral lipids, a more or less pronounced accumulation of lipid droplets was observed with ALA, EPA, DHA, OA and Lorenzo's oil and the highest quantities of lipid droplets were observed with OA and Lorenzo's oil whereas only few cells with lipid droplets were found in the presence of α-tocopherol, EA and SSO (**Supplementary Figure 3**). By brightfield microscopy, as ORO staining does not permit an accurate quantification of cells with lipid droplets and of the amount of neutral lipids per cell a staining procedure was realized with Bodipy 493/503 (**Figure 5**). By fluorescence microscopy, the visualization of lipid droplets with Bodipy 493/503 leads to similar conclusions that with ORO. Similar fluorescence staining patterns were observed with ALA, EPA, DHA, EA, SSO and α-tocopherol (weak green fluorescence) and with OA and Lorenzo's oil (strong green fluorescence) supporting a weak and a strong accumulation of lipid droplets rich in neutral lipids, respectively (**Figure 5**). With 7KC, few lipid droplets were detected with ORO (**Supplementary Figure 3**). These data are in agreement with those obtained by flow cytometry with Bodipy 493/503: a significant increase of the ratio [Mean Fluorescence Intensity (MFI) assay / MFI control] was only observed with OA and Lorenzo's oil (**Figure 5**). With 7KC, only few lipid

droplets were detected: a slight but not significant increase of the MFI ratio was found; no significant differences were identified between control, vehicle-treated cells and 7KC-treated cells (**Figure 5**). When 7KC was associated with ALA, EPA, and DHA, marked accumulation of lipid droplets characterized by a significantly higher ratio [MFI assay / MFI control] than in untreated and 7KC-treated cells was observed (the highest levels of lipid droplets per cell were observed with (7KC + OA) and (7KC + Lorenzo's oil) whereas no lipid droplets accumulation was detected when 7KC was associated with EA, SSO and α-tocopherol (**Figure 5**). Under treatment with 7KC, ALA, EPA, DHA, OA, EA and α-tocopherol, the intracellular accumulation of 7KC was also quantified as well as the intracellular levels of FAs: intracellular accumulations of 7KC and FAs were observed (**Supplementary Figure 4**). 7KC accumulation was significantly decreased with the different compounds used, at the exception of OA (**Supplementary Figure 4**).

Prevention of 7KC-induced apoptosis and autophagy with ω3 fatty acids (α-linolenic acid, eicosapentaenoic acid, docosahexaenoic acid), and sulpho-N-succinimidyl oleate

The results obtained suggest that the destabilization of plasma membrane lipid organization could lead to several cellular dysfunctions and in particular to a drop in ΔΨm. As shown on U937 cells (Vejux *et al.*, 2009a), it can be assumed that 7KC by altering the plasma membrane would lead to an inactivation of the signaling pathway which helps to control ΔΨm via the phosphorylation state of the Mcl-1 protein which allows the sequestration in the cytoplasm of the pro-apoptotic proteins Bad and Bax which promote the drop of ΔΨm when interacting with the mitochondria. In agreement with this hypothesis, 7KC induced-apoptosis was associated with a decreased level of Mcl-1 linked with an increased level of P-Mcl-1 as well as with a strong increase of the ratio Bad/Mcl-1 (**Figure 6**). As previously described on U937 cells, these two results support the

hypothesis that the increase in P-Mcl-1 leads to an inhibition of Bad sequestration in the cytoplasm thus favouring its interaction with the mitochondrial membrane to induce the drop of ΔΨm (Ragot *et al.*, 2011). In agreement with this hypothesis, supporting an activation of the mitochondrial pathway, 7KC-induced apoptosis is associated with a cleavage of caspase-3 leading to an activation of this enzyme which contributes to PARP degradation (**Figure 6**). The ability of z-VAD-fmk (a pan-caspases inhibitor) to strongly inhibit 7KC-induced cell death, demonstrates an active contribution of apoptosis in 7KC-induced cell death (**Supplementary Figure 5**). In addition, in the presence of 7KC, an activation of LC3-1 into LC3-II, which is an autophagic criteria, was observed (**Figure 6**). 7KC-induced autophagy on 158N cells can be considered as survival autophagy because cell death decreased in the presence of rapamycin (an autophagy activator) and increased in the presence of 3-methyladenine (an autophagy inhibitor) (**Supplementary Figure 5**). When 7KC was combined with FAs (ALA, EPA, DHA) or SSO, as well as α-tocopherol, the induction of apoptosis and autophagy was greatly reduced (**Figure 6**). No pro-apoptototic and pro-autophagic effects were observed when ALA, EPA, DHA, SSO and α-tocopherol were used alone (**Figure 6**). These results demonstrate the ability of ω3 FAs (ALA, EPA, DHA), SSO, and α-tocopherol to oppose mitochondrial depolarization and the induction of cell death by apoptosis as well as activation of autophagy.

Discussion and conclusions

To counter the cytotoxic effects induced by 7KC, present at increased level in several diseases (Anderson *et al.*, 2020; Zarrouk *et al.*, 2014), it is essential to identify molecules acting on its signaling pathways. In the present study, we showed on 158N cells that ω3 and ω9 FAs (ALA, EPA, DHA, OA) Lorenzo's oil, and sulfo-N-succinimidyl oleate (SSO) attenuate the toxicity of 7KC: oxidative stress, mitochondrial and peroxisomal dysfunction, oxiapoptophagy. We also

report that these cytoprotective lipid compounds enable the activation of signaling pathways that restore ΔΨm by acting on mitochondrial interaction proteins (Mcl-1 and Bad) to prevent cell death. Among these different lipids preventing 7KC toxicity, SSO presents the most attractive profile.

Currently, little is known about the mechanisms associated with the cytoprotection of FAs. However, it should be noted that among the FAs tested (ALA, EPA, DHA, OA and EA), only EA is not cytoprotective and does not prevent 7KC-induced cell death. The ability of ALA, EPA, DHA and OA to prevent 7KC-induced plasma membrane disorganization was demonstrated in our study using MC540 and cholesterol quantification. As the same FAs (ALA, EPA, DHA and OA) reduce 7KC-induced ROS overproduction revealed with DHE, it is suggested that plasma membrane alteration revealed with MC540 and observed in the presence of 7KC could be at least in part the consequence of lipid peroxidation. On U937 cells, 7KC-induced apoptosis associated with increased plasma membrane permeability was also associated with modification of free cholesterol level revealed by flow cytometry after staining with filipin (Vejux *et al.*, 2005). The lack of cytoprotection with EA could be due to the possible irreversible interactions of this fatty acid with mitochondrial cardiolipins and to changes in the phosphatidyl choline / phosphatidylethanolamine ratio at the inner membrane of the mitochondria resulting in increased mitochondrial sensitivity to toxic agents (Bozcali *et al.*, 2009). On the basis of results obtained with OA (Monier *et al.*, 2003), the hypothesis that esterification of cholesterol with FAs would reduce the toxicity of 7KC is therefore not applicable to all FAs. It can be hypothesized that ALA, EPA, DHA and OA, by modifying the plasma membrane phospholipid composition, could counter the insertion of 7KC into lipid rafts, as α-tocopherol does (Ragot *et al.*, 2013; Royer *et al.*, 2009), and restore cell signaling from the plasma membrane that helps preserve mitochondrial functionality. According to this hypothesis, based on the results obtained on U937

cells (Vejux *et al.*, 2009a), it can be thought that the functionality of the PIP3 / PDK1 / Akt signaling pathway passing through GSK3 and which is affected by 7KC (Brahmi *et al.*, 2019), could be restored by FAs thus promoting Mcl-1 / Bad interactions and the sequestration of the latter in the cytoplasm. These effects would then contribute to repressing 7KC-induced mitochondrial depolarization and inhibit apoptosis. Concerning DHA, in addition to being an important acyl chain of membrane phospholipids, it could also have cytoprotective activities thanks to biologically active derivatives such as neuroprotectin D1 (NPD1) which is an apoptosis inhibitor.(Asatryan *et al.*, 2017). This emphasizes that the ability of DHA, like other FAs (ALA, EPA and OA), to prevent mitochondrial dysfunction is a key factor in inhibiting the toxicity of 7KC. Moreover, as it has been shown that 7KC-induced autophagy on 158N cells corresponds to survival autophagy; inhibiting apoptosis by FAs (ALA, EPA, DHA an OA) should theoretically lead to a reduction in the activation of autophagy, which corresponds to what has been observed. However, this does not rule out the possibility that FAs can activate autophagy for survival. On ARPE-19 cells, it has been reported that DHA can both induce endogenous antioxidant activities and mobilizes selective autophagy of misfolded proteins (Johansson *et al.*, 2015). On DHA-treated HepG2 cells, an induction of autophagy resulting from ROS overproduction has also been described (Mei *et al.*, 2011). Although the mechanisms by which FAs induced autophagy protects against cell death are not fully understood, it is thought to involve multiple mechanisms: recycling of misfolded and aggregated proteins, removing altered organelles (mitophagy, pexophagy) and regulating fatty acid-induced lipid accumulation (lipophagy) to prevent lipotoxicity (Klionsky *et al.*, 2016; Mei *et al.*, 2011).

As a significant increase in the plasma level of 7KC was observed in X-ALD patients (Nury *et al.*, 2017), this led us to evaluate the effects of Lorenzo's oil sometimes prescribed to X-ALD patients, in order to assess its cytoprotective activity. Lorenzo's oil (EA + OA; 1:4) is used to

reduce the saturated VLCFA level (C26:0, C24:0) in X-ALD; however, its mechanism still remains elusive (Moser *et al.*, 2007). EA and OA inhibit ELOVL1 enzyme (the primary enzyme responsible for the synthesis of saturated VLCFAs), and the 1:4 mixture exhibit the most potent inhibitory activity; in addition, at the cellular level, treatment with the 1:4 mixture reduced the level of sphingomyelin with a saturated VLCFA (Sassa *et al.*, 2014). The ability of Lorenzo's oil to inhibit 7KC-induced oxiapotophagy underscores its ability to inhibit ROS overproduction and cell death induced by this oxysterol; it should be noted that the effects on these parameters are due to AO and not EA. These new elements on the cytoprotective activity of Lorenzo's oil make it possible to envisage its use in patients other than X-ALD in whom increased levels of 7KC are observed.

It is with the SSO that the most original results have been obtained. This molecule derived from AO, unlike ALA, EPA, DHA, and AO, is non-toxic over a wide range of concentrations (100 to 400 µM). SSO has been shown to interact with FAT/CD36 receptor at the Lys-164 binding site resulting in inhibition of fatty acid binding to this receptor; FAT/CD36 is a multifunctional glycoprotein that facilitates long-chain fatty acid uptake by cardiomyocytes and adipocytes and uptake of oxidized low density lipoproteins by macrophages (Kuda *et al.*, 2013). The cytoprotective effects of SSO against 7KC are potent as demonstrated by its ability to reduce 7KC-induced overproduction of ROS, apoptosis, and autophagy. Furthermore, unlike other cytoprotective FAs (ALA, EPA, DHA and OA), SSO does not induce the accumulation of triglyceride-rich lipid droplets, which is a major advantage when considering further therapeutic applications. Despite these marked differences with FAs (ALA, EPA, DHA and OA), SSO similarly prevents plasma membrane damages and restores the signaling pathway implicating Mcl-1 that prevents the loss of $\Delta\Psi m$. In agreement with previous studies, in addition to its ability to interact with CD36, our data support that SSO has other biological activities (Dhungana *et al.*, 2017; Drahota *et al.*, 2010).

Compared to the molecules already identified to inhibit the toxicity of 7KC (Brahmi *et al.*, 2019; Cilla *et al.*, 2017; Yammine *et al.*, 2020b), this study brings new elements and shows that FAs (ALA, EPA, DHA and OA), a mixture of FAs (Lorenzo's oil) and a synthetic derivative of OA (SSO) are powerful cytoprotectors: they prevent 7KC-induced plasma membrane alterations, loss of ΔΨm, apoptosis and autophagy. Among these lipids, SSO is the most promising compound: its non-toxic cytoprotective activities over a wide range of concentrations are not associated with cytoplasmic accumulation of lipid droplets. These different characteristics of SSO make it possible to envisage its use for therapeutic purposes in diseases where 7KC levels are greatly increased.

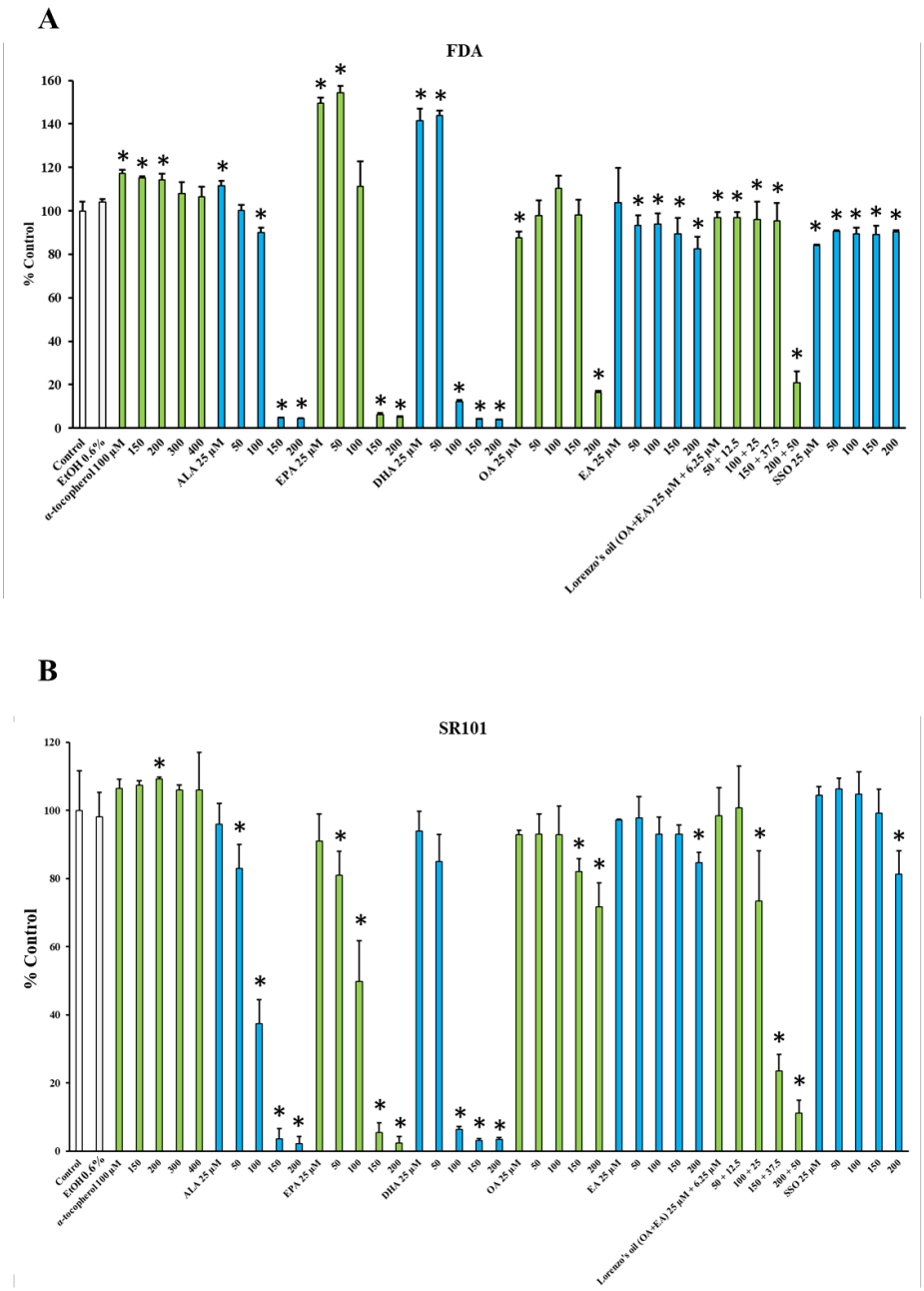

Figure 1: Evaluation of the cytotoxicity α-linolenic acid, eicosapentaenoic acid, docosahexaenoic acid, oleic acid, erucic acid, Lorenzo's oil and sulfo-N-succinimidyl oleate with the fluorescein diacetate and sulforhodamine 101 assays. 158N cells previously cultured for 24 h were further incubated with FAs (α-linolenic acid (ALA), eicosapentaenoic acid (EPA), docosahexaenoic acid (DHA), oleic acid (OA), erucic acid (EA)), sulfo-N-succinimidyl oleate (SSO), and Lorenzo's oils (EA + OA; 1:4) as well as α-tocopherol (reference cytoprotective molecule) used alone for a 24 h additional period of time. At the end of the treatment, the cytotoxicity was evaluated with the FDA and SR101 assays. Data are expressed as mean ± standard deviation (SD) of three independent experiments performed in triplicate. Significance of the differences between control (untreated cells) and ALA, EPA, DHA, OA, EA, SSO and Lorenzo's oil-treated cells; Mann Whitney test: * $P \leq 0.05$. No significant differences were observed between control (untreated cells) and vehicle control (Ethanol (EtOH) 0.6%).

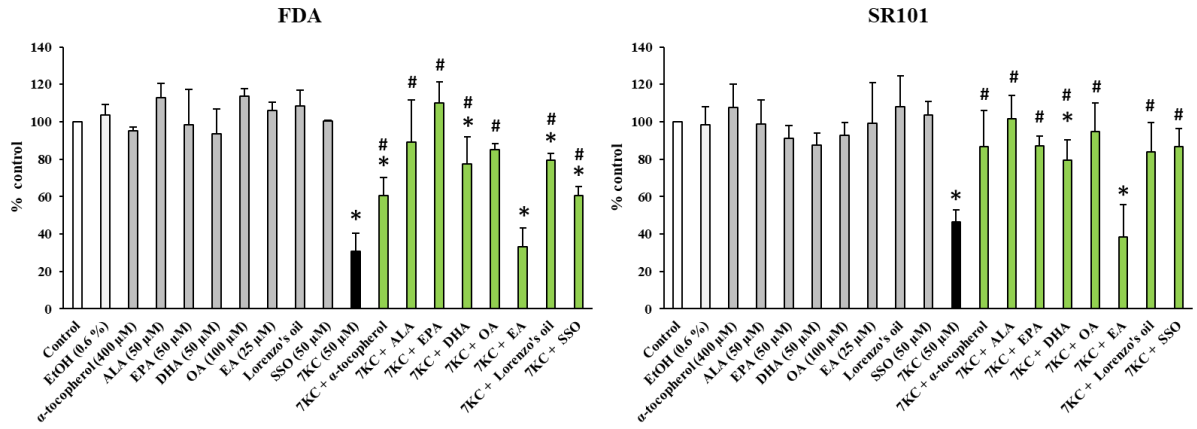

Figure 2: Evaluation with the fluorescein diacetate and sulforhodamine 101 assays on 158N cells of the cytoprotective effects of α-linolenic acid, eicosapentaenoic acid, docosahexaenoic acid, oleic acid, erucic acid, sulfo-N-succinimidyl oleate and Lorenzo's oil on 7-ketocholesterol induced-cytotoxicity. 158N cells previously cultured for 24 h were further incubated for a 24 h additional period of time with 7-ketocholesterol (7KC; 50 µM), FAs (α-linolenic acid (ALA), eicosapentaenoic acid (EPA), docosahexaenoic acid (DHA), oleic acid (OA), erucic acid (EA)), sulfo-N-succinimidyl oleate (SSO), or Lorenzo's oils (EA + OA; 1:4) as well as α-tocopherol (reference cytoprotective molecule) and with 7KC associated with ALA, EPA, DHA, OA, EA, SSO, Lorenzo's oil or α-tocopherol. At the end of the treatment, the cytotoxicity of 7KC and the cytoprotective effects of ALA, EPA, DHA, OA, EA, SSO, Lorenzo's oil and α-tocopherol were evaluated with the fluorescein diacetate (FDA) and sulforhodamine 101 (SR101) assays. Data are expressed as mean ± standard deviation (SD) of three independent experiments performed in triplicate. Significance of the differences between control (untreated cells) and ALA, EPA, DHA, OA, EA, SSO, Lorenzo's oil, and α-tocopherol-treated cells; Mann Whitney test: * $P \leq 0.05$. Significance of the differences between 7KC-treated cells and (7KC + (ALA, EPA, DHA, OA, EA, SSO, Lorenzo's oil and α-tocopherol)-treated cells; Mann Whitney test: # $P \leq 0.05$. No significant differences were observed between control (untreated cells) and vehicle control (Ethanol (EtOH) 0.6%).

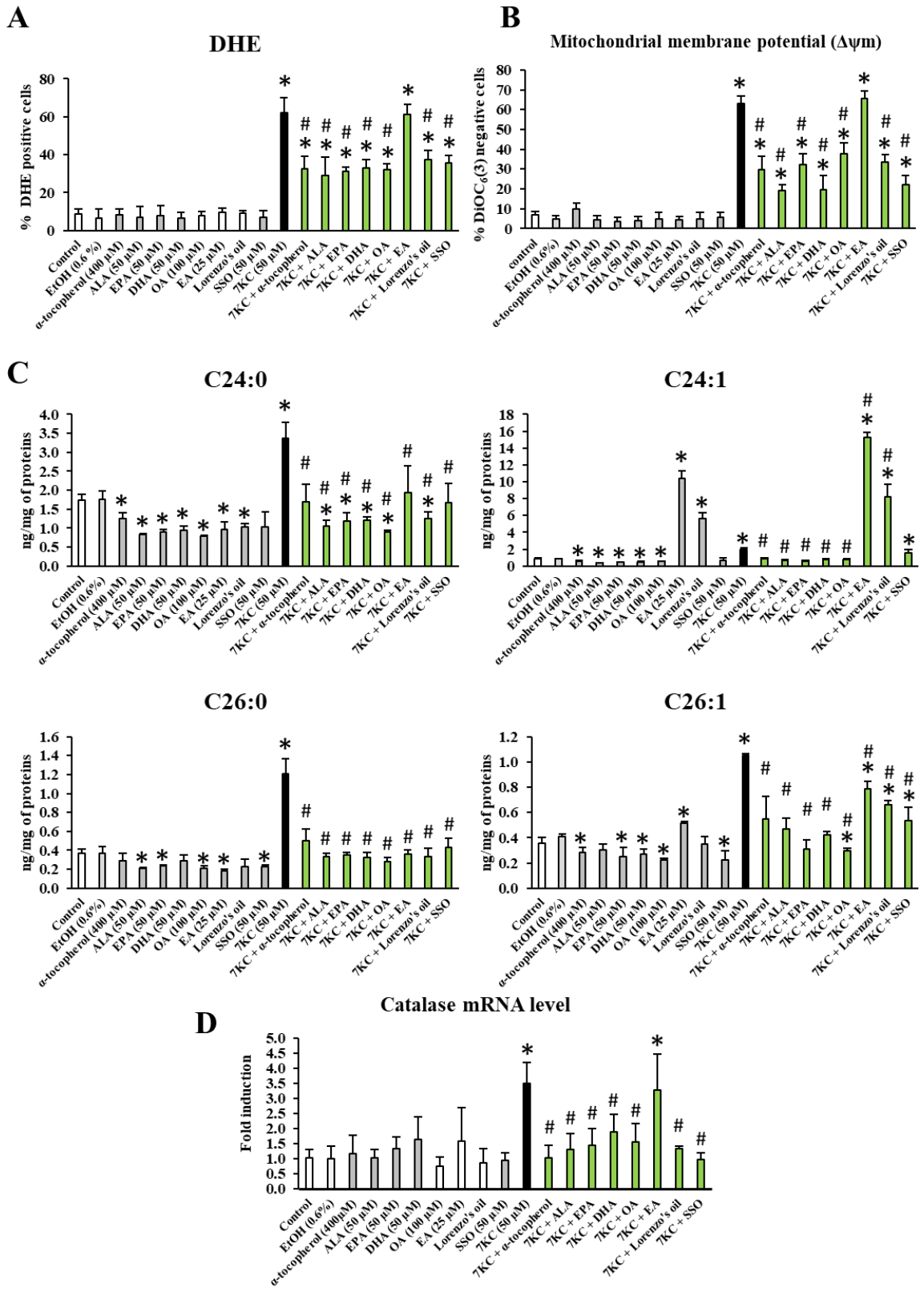

Figure 3: Effects of α-linolenic acid, eicosapentaenoic acid, docosahexaenoic acid, oleic acid, erucic acid, sulfo-N-succinimidyl oleate and Lorenzo's oil on 7-ketocholesterl-induced reactive oxygen species overproduction and on mitochondrial and peroxisomal dysfunction. 158N cells previously cultured for 24 h were further incubated for a 24 h additional period of time with 7-ketocholesterol (7KC;

50 µM), FAs (α-linolenic acid (ALA), eicosapentaenoic acid (EPA), docosahexaenoic acid (DHA), oleic acid (OA), erucic acid (EA)), sulfo-N-succinimidyl oleate (SSO), or Lorenzo's oils (EA + OA; 1:4) as well as α-tocopherol (reference cytoprotective molecule) and with 7KC associated with ALA, EPA, DHA, OA, EA, SSO, Lorenzo's oil or α-tocopherol. At the end of the treatment, the percentage of ROS overproducing cells ROS was determined by flow cytometry after staining with DHE (**A**), mitochondrial dysfunction was evaluated by the percentage of cells with altered mitochondria characterized by a loss of ΔΨm (this parameter was determined by flow cytometry after staining with $DiOC_6(3)$) (**B**), and peroxisomal dysfunction was estimated by the levels of VLCFAs (C24:0, C24:1, C26:0, C26:1) measured by GC-MS (**C**) and by the mRNA level of catalase measured by RT-qPCR (**D**). Data are expressed as mean ± standard deviation (SD) of three independent experiments performed in triplicate. Significance of the differences between control (untreated cells) and ALA, EPA, DHA, OA, EA, SSO, Lorenzo's oil, and α-tocopherol-treated cells; Mann Whitney test: * $P \leq 0.05$. Significance of the differences between 7KC-treated cells and (7KC + (ALA, EPA, DHA, OA, EA, SSO, Lorenzo's oil and α-tocopherol)-treated cells; Mann Whitney test: # $P \leq 0.05$. No significant differences were observed between control (untreated cells) and vehicle control (Ethanol (EtOH) 0.6%).

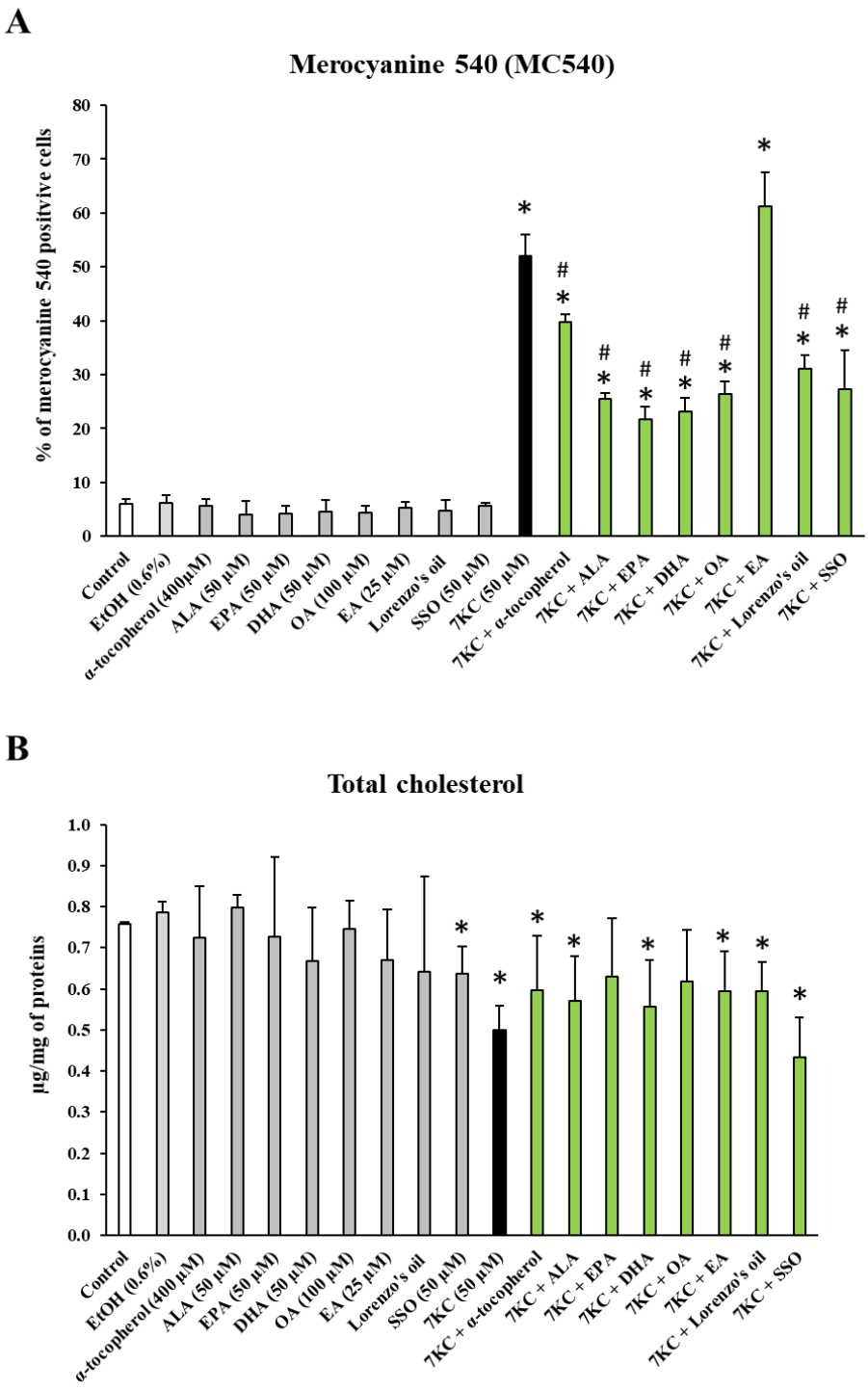

Figure 4: Effects of α-linolenic acid, eicosapentaenoic acid, docosahexaenoic acid, oleic acid, erucic acid, Lorenzo's oil and sulpho-N-succinimidyl oleate on 7-ketocholesterol-induced lipid disturbances at the plasma membrane level. 158N cells previously cultured for 24 h were further incubated for a 24 h additional period of time with 7-ketocholesterol (7KC; 50 µM), FAs (α-linolenic acid (ALA), eicosapentaenoic acid (EPA), docosahexaenoic acid (DHA), oleic acid (OA), erucic acid (EA)), sulfo-N-

succinimidyl oleate (SSO), or Lorenzo's oils (EA + OA; 1:4) as well as α-tocopherol (reference cytoprotective molecule) and with 7KC associated with ALA, EPA, DHA, OA, EA, SSO, Lorenzo's oil or α-tocopherol. At the end of the treatment, the percentage of MC540 positive cells was determined by flow cytometry (**A**), and the total cholesterol content was quantified by GC-MS (**B**). Data are expressed as mean ± standard deviation (SD) of three independent experiments performed in triplicate. Significance of the differences between control (untreated cells) and ALA, EPA, DHA, OA, EA, SSO, Lorenzo's oil, and α-tocopherol-treated cells; Mann Whitney test: * $P \leq 0.05$. Significance of the differences between 7KC-treated cells and (7KC + (ALA, EPA, DHA, OA, EA, SSO, Lorenzo's oil and α-tocopherol)-treated cells; Mann Whitney test: # $P \leq 0.05$. No significant differences were observed between control (untreated cells) and vehicle control (Ethanol (EtOH) 0.6%).

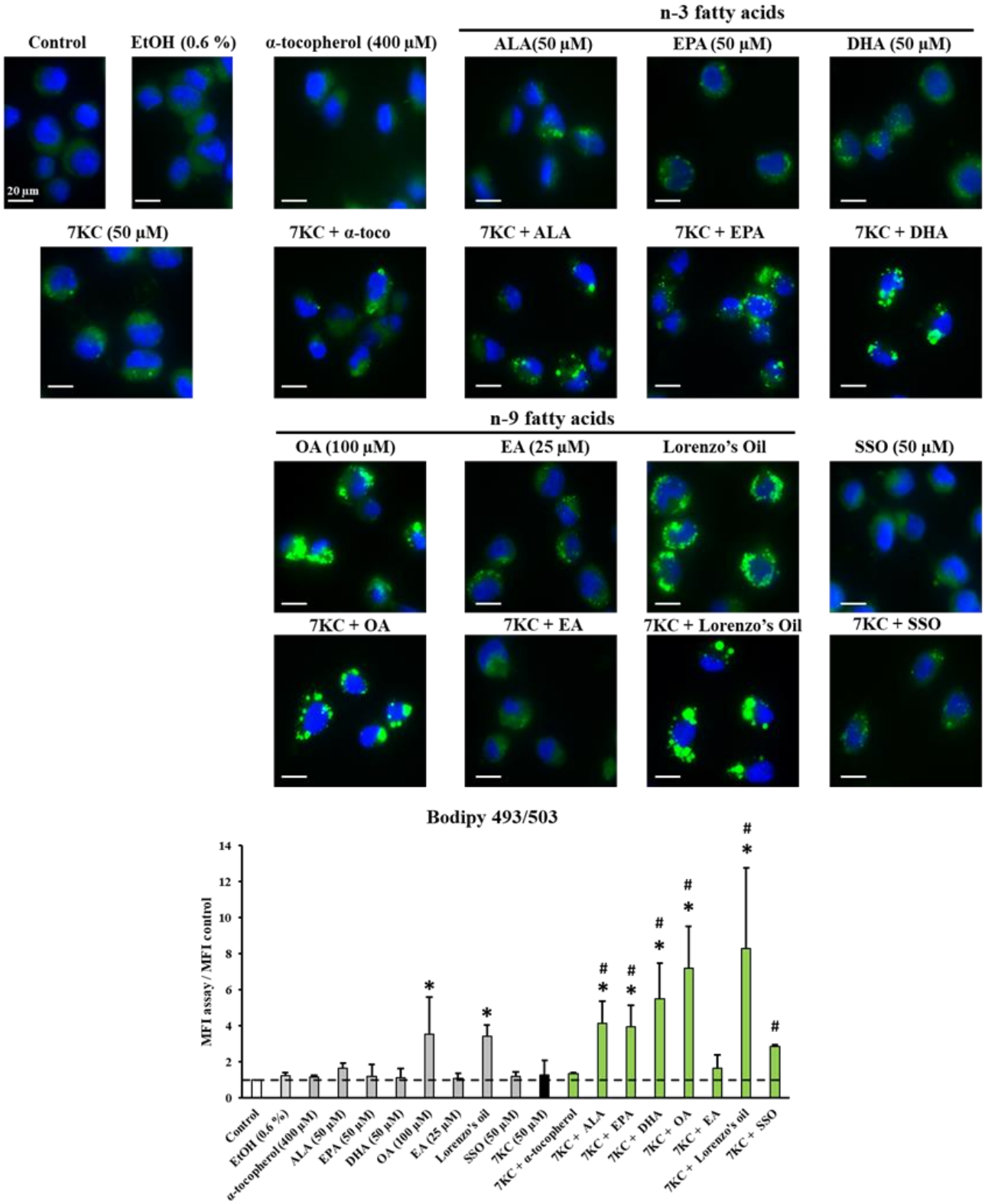

Figure 5: Evaluation of the effects of α-linolenic acid, eicosapentaenoic acid, docosahexaenoic acid, oleic acid, erucic acid, Lorenzo's oil and sulpho-N-succinimidyl oleate associated or not with 7-ketocholesterol-on lipid droplets accumulation measured with Bodipy 493/503. 158N cells previously

cultured for 24 h were further incubated for a 24 h additional period of time with 7-ketocholesterol (7KC; 50 µM), FAs (α-linolenic acid (ALA), eicosapentaenoic acid (EPA), docosahexaenoic acid (DHA), oleic acid (OA), erucic acid (EA)), sulfo-N-succinimidyl oleate (SSO), or Lorenzo's oils (EA + OA; 1:4) as well as α-tocopherol (reference cytoprotective molecule) and with 7KC associated with ALA, EPA, DHA, OA, EA, SSO, Lorenzo's oil or α-tocopherol. At the end of the treatment, the cells were stained with Bodipy 493/503. Cells were observed by fluorescence microscopy and the green fluorescence of Bodipy 493/503 was quantified by flow cytometry, data were expressed as MFI ratio [MFI assay / MFI control]. Data are expressed as mean ± standard deviation (SD) of three independent experiments performed in triplicate. Significance of the differences between control (untreated cells) and treated cells; Mann Whitney test: * $P \leq 0.05$. Significance of the differences between 7KC-treated cells and (7KC + (ALA, EPA, DHA, OA, EA, SSO, Lorenzo's oil and α-tocopherol)-treated cells; Mann Whitney test: # $P \leq 0.05$. No significant differences were observed between control (untreated cells) and vehicle control (Ethanol (EtOH) 0.6%).

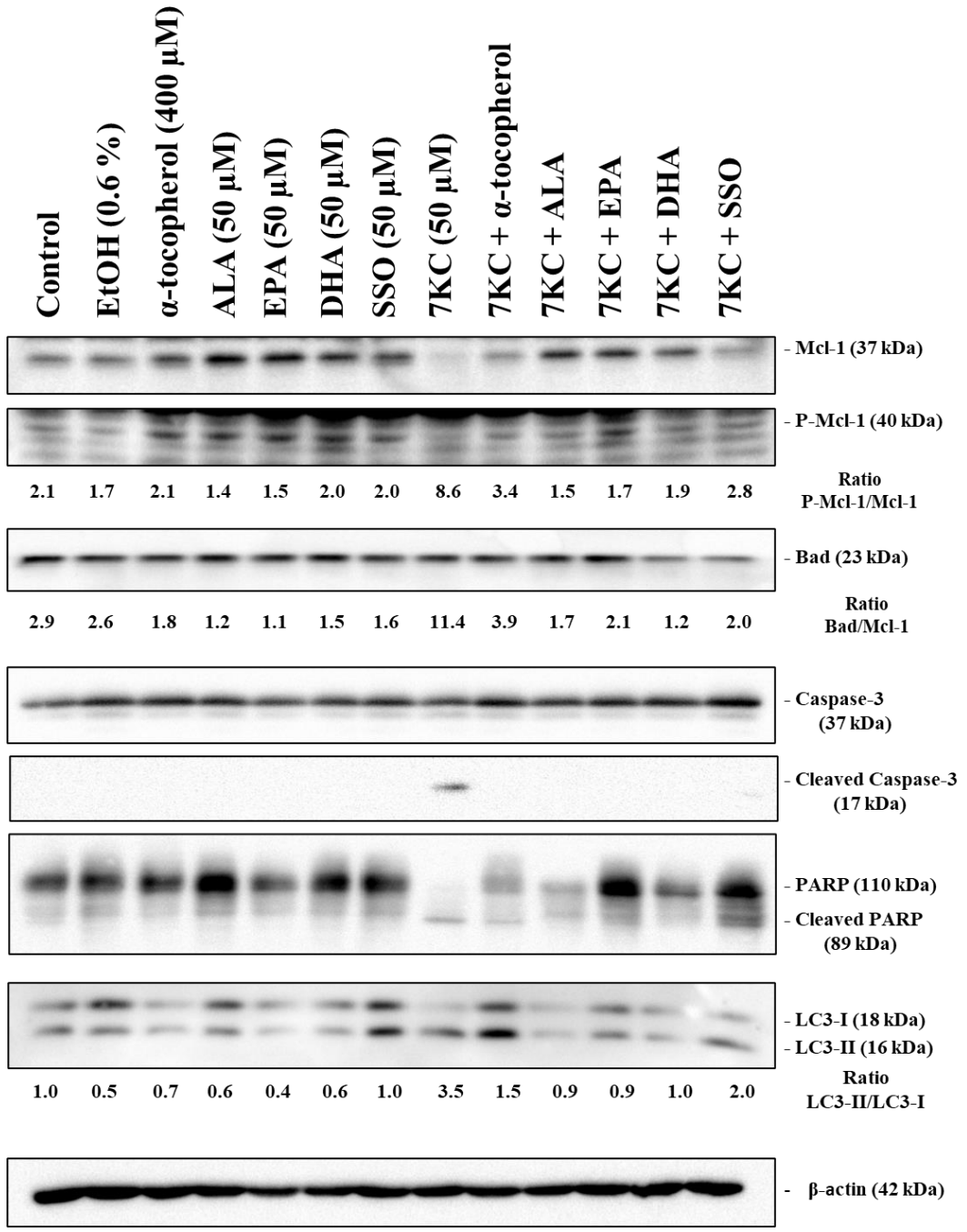

Figure 6: Evaluation of the effects of α-linolenic acid, eicosapentaenoic acid, docosahexaenoic acid, oleic acid, Lorenzo's oil and sulpho-N-succinimidyl oleate associated or not with 7-ketocholesterol-on apoptosis and autophagy. Apoptosis and autophagy were characterized by Western blotting with different antibodies. Apoptosis was evaluated by Mcl-1, P-Mcl-l and Bad levels, (Bad / Mcl-1) ratio, caspase-3 activation (cleaved caspase-3), and PARP degradation, and autophagy by conversion of LC3-I to LC3-II [ratio LC3-II/LC3-I].

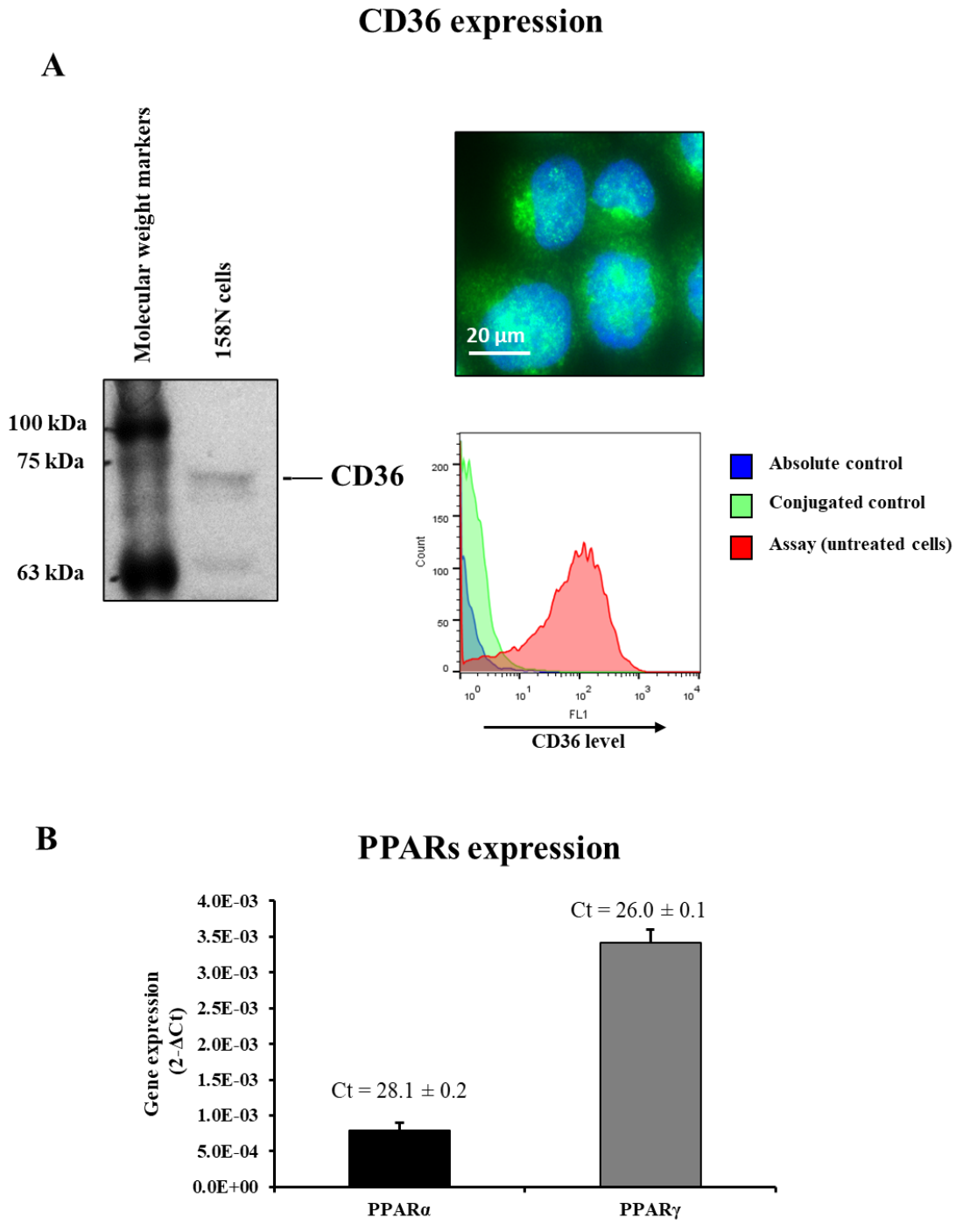

Supplementary Figure 1: Evaluation of CD36 and PPARs expression on 158N cells. A: CD36 expression was determined by immunofluorecence microscopy, flow cytometry and western blotting; these complementary methods demonstrate the expression of CD36 on 158N. **B**: Analysis of PPARs by RT-qPCR also shows expression of PPARα and PPARγ in 158N cells. Data shown are representative of three independent experiments.

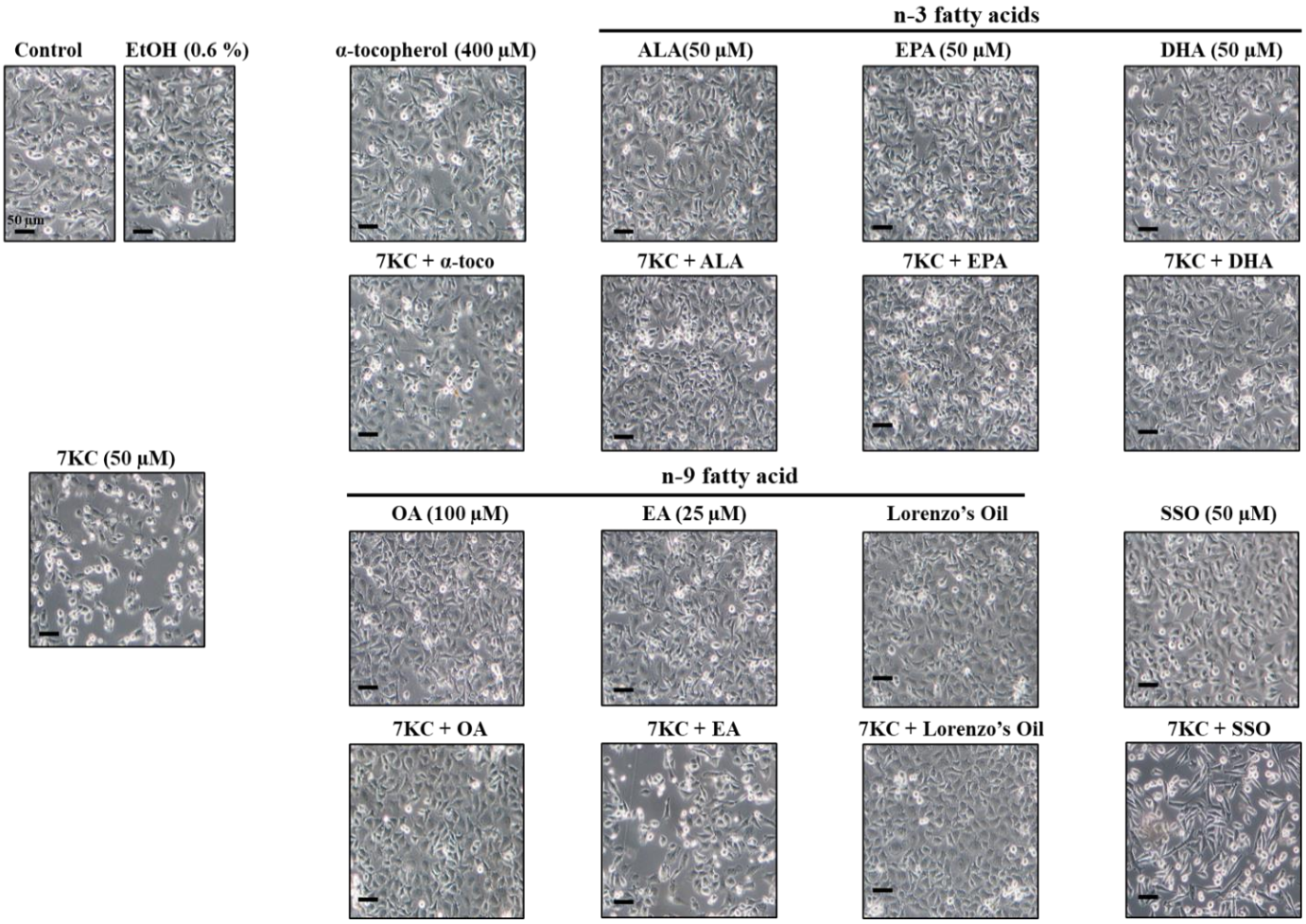

Supplementary Figure 2: Evaluation by phase contrast microscopy of the cytotoxicity of 7-ketocholesterol with or without α-linolenic acid, eicosapentaenoic acid, docosahexaenoic acid, oleic acid, erucic acid, Lorenzo's oil and sulfo-N-succinimidyl oleate on 158N cells. 158N cells previously cultured for 24 h were further incubated for a 24 h additional period of time with 7-ketocholesterol (7KC; 50 µM), FAs (α-linolenic acid (ALA), eicosapentaenoic acid (EPA), docosahexaenoic acid (DHA), oleic acid (OA), erucic acid (EA)), sulfo-N-succinimidyl oleate (SSO), Lorenzo's oils (EA + OA; 1:4) or α-tocopherol, and with 7KC associated with ALA, EPA, DHA, OA, EA, SSO, Lorenzo's oil or α-tocopherol. Cytoprotective effects were observed with all compounds excepted EA. Observations were realized under an inverted Zeiss microscope and digitalized images are shown. Data shown are representative of three independent experiments.

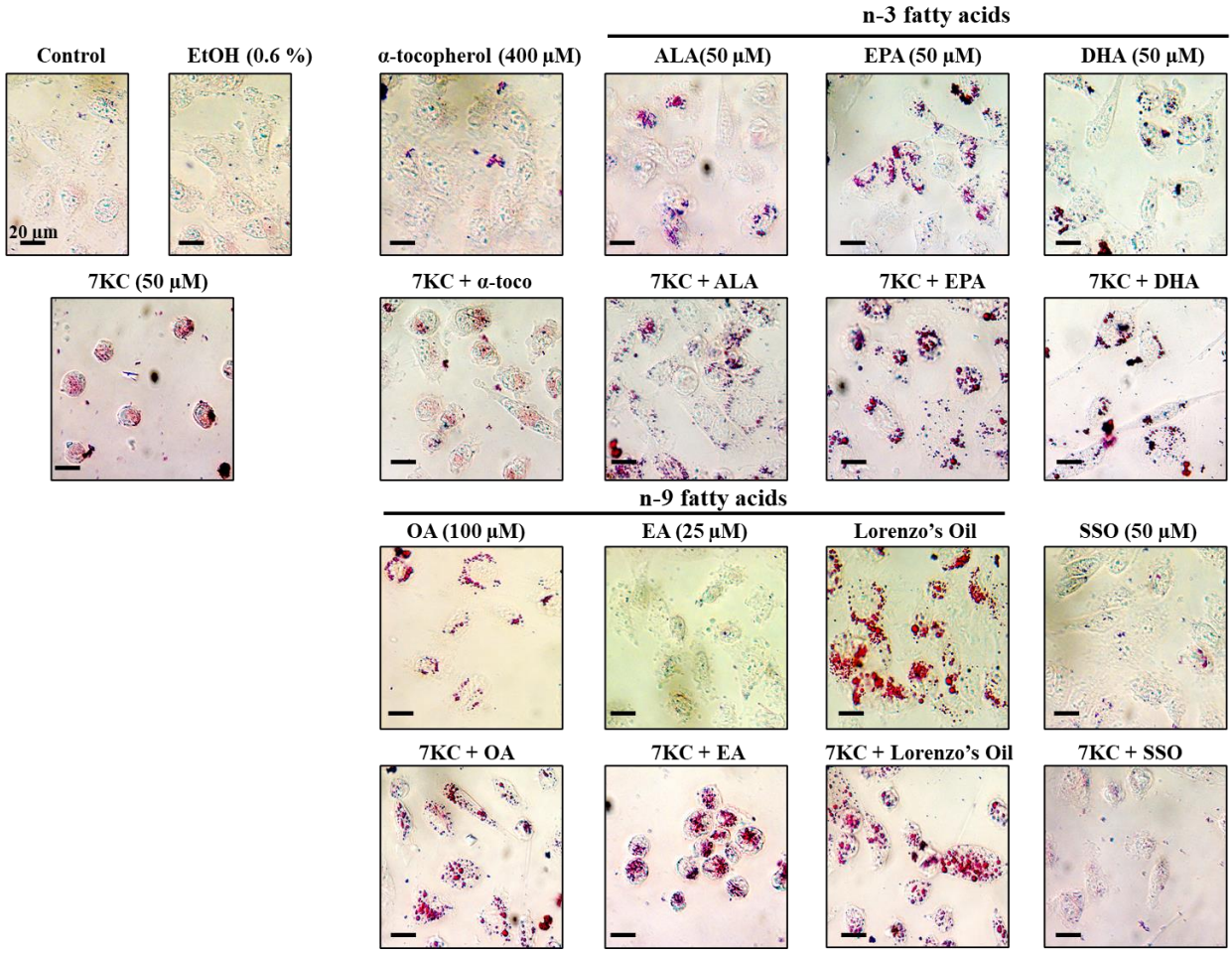

Supplementary Figure 3: Evaluation of the effects of α-linolenic acid, eicosapentaenoic acid, docosahexaenoic acid, oleic acid, erucic acid, Lorenzo's oil and sulpho-N-succinimidyl oleate associated or not with 7-ketocholesterol-on lipid droplets accumulation measured with Oil Red O. 158N cells previously cultured for 24 h were further incubated for a 24 h additional period of time with 7-ketocholesterol (7KC; 50 µM), FAs (α-linolenic acid (ALA), eicosapentaenoic acid (EPA), docosahexaenoic acid (DHA), oleic acid (OA), erucic acid (EA)), sulfo-N-succinimidyl oleate (SSO), or Lorenzo's oils (EA + OA; 1:4) as well as α-tocopherol (reference cytoprotective molecule) and with 7KC associated with ALA, EPA, DHA, OA, EA, SSO, Lorenzo's oil or α-tocopherol. At the end of the treatment, the cells were stained with Oil Red O (ORO) which stains lipid droplets which are rich in neutral lipids. Cells were observed by brightfield microscopy. Cytoplasmic red dots correspond to lipid droplets. Data shown are representative of three independent experiments.

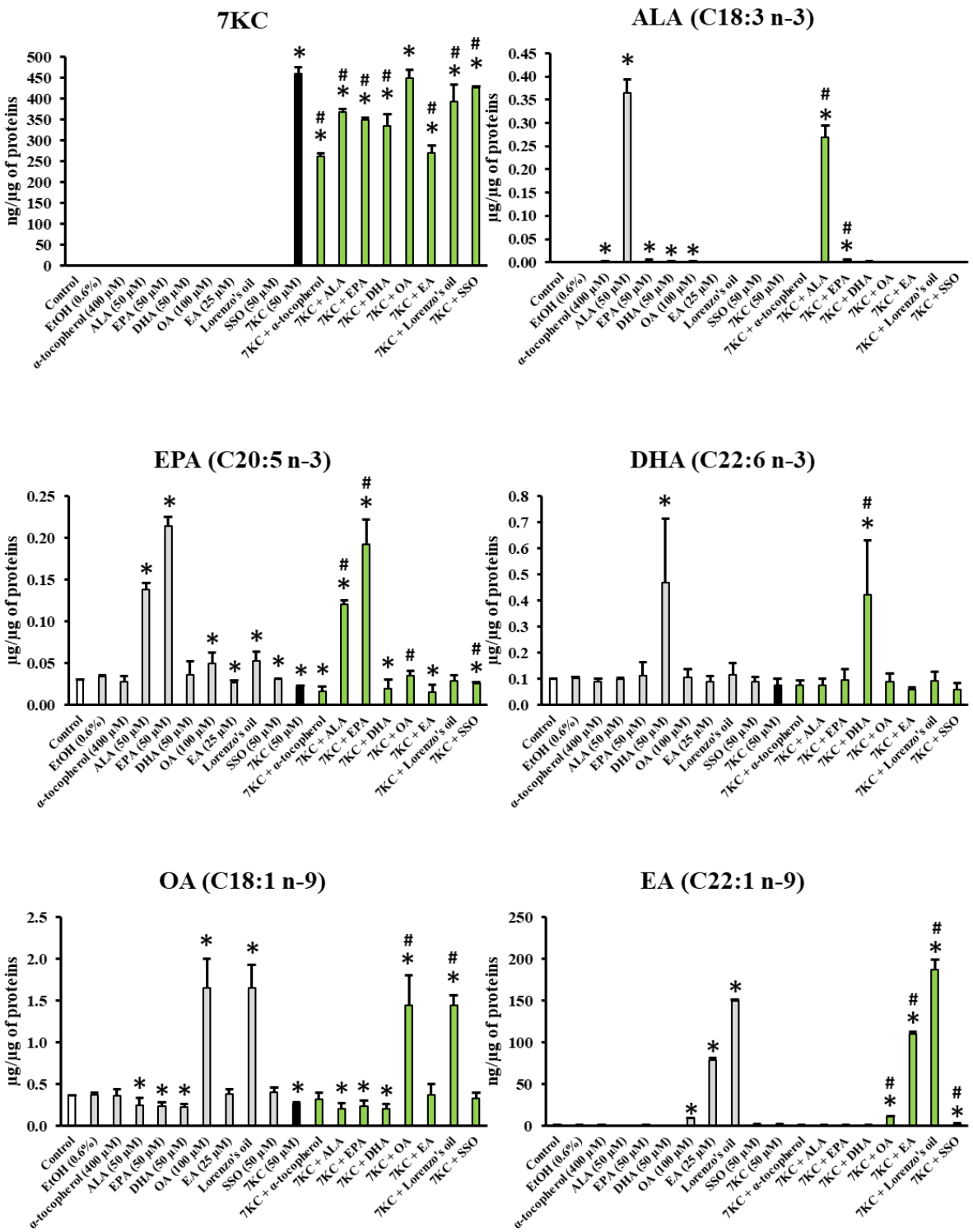

Supplementary Figure 4: Cellular quantification of 7-ketocholesterol, α-linolenic acid, eicosapentaenoic acid, docosahexaenoic acid, oleic acid and erucic acid. 158N cells previously cultured for 24 h were further incubated for a 24 h additional period of time with 7-ketocholesterol (7KC; 50 µM), FAs (α-linolenic acid (ALA), eicosapentaenoic acid (EPA), docosahexaenoic acid (DHA), oleic acid (OA), erucic acid (EA)), Lorenzo's oils (EA + OA; 1:4), sulpho-N-succinimidyl oleate (SSO) as well

as α-tocopherol (reference cytoprotective molecule) or with 7KC associated with ALA, EPA, DHA, OA, EA, SSO, Lorenzo's oil, SSO or α-tocopherol. In these different culture conditions, the quantity of 7KC, ALA, EPA, DHA, OA, and EA was quantified by GC - MS. The data are expressed in quantity of 7KC, ALA, EPA, DHA, OA, and EA (ng or µg) per µg of proteins. Data are expressed as mean ± standard deviation (SD) of three independent experiments performed in triplicate. Significance of the differences between control (untreated cells) and treated cells; Mann Whitney test: * $P \leq 0.05$. Significance of the differences between 7KC-treated cells and (7KC + (ALA, EPA, DHA, OA, EA, SSO, Lorenzo's oil and α-tocopherol)-treated cells; Mann Whitney test: # $P \leq 0.05$. No significant differences were observed between control (untreated cells) and vehicle control (Ethanol (EtOH) 0.6%).

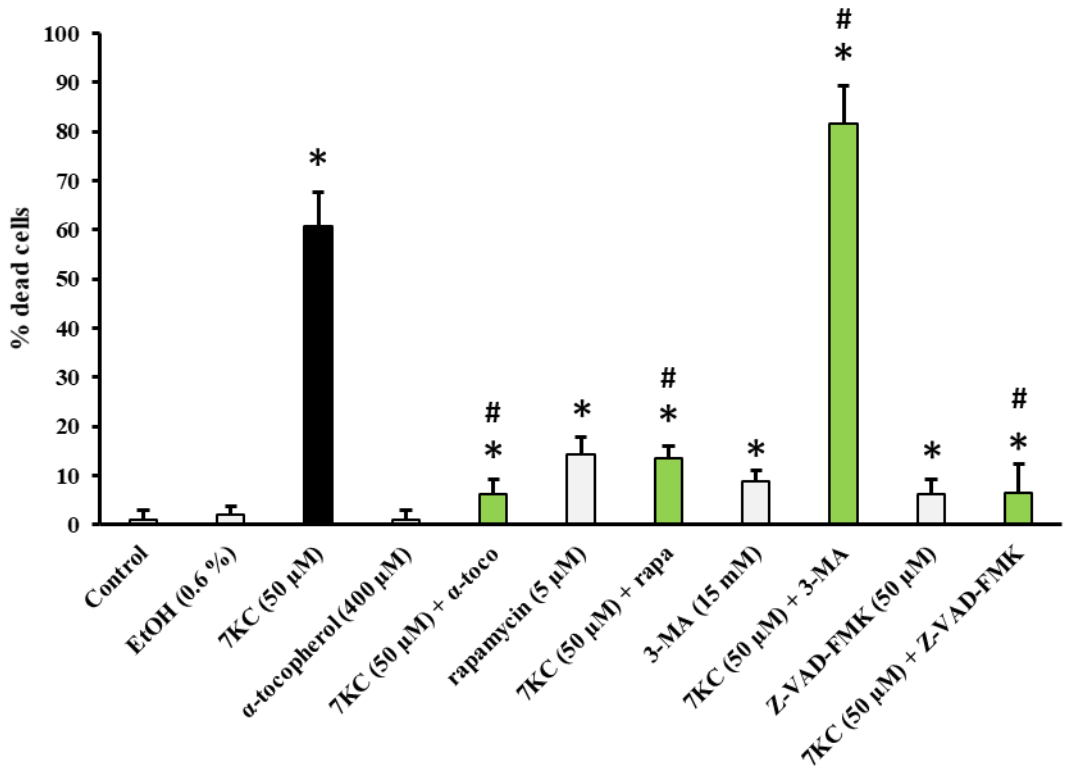

Supplementary Figure 5: Evaluation of the contribution of apoptosis and autophagy in 7-ketocholesterol-induced cell death. 158N cells previously cultured for 24 h were further incubated for a 24 h additional period of time with 7-ketocholesterol (7KC; 50 µM) associated with z-VAD-fmk (a pan-caspases inhibitor: 50 µM) or with an activator of autophagy (rapamycin (rapa): 5 µM) or an inhibitor of autophagy (3-methyl adenine (3-MA) : 15 mM). α-tocopherol (α-toco: 400 µM) was used as reference cytoprotective molecule. The incidence on cell death was morphologically quantified by phase contrast microscopy: adherent cells are considered as living cells and round cells floating in the cultured medium are considered as dead cells. A total number of 300 cells was counted. Data are expressed as mean ± standard deviation (SD) of one experiment performed in triplicate. Significance of the differences between control (untreated cells) and assays (7KC, α-toco, rapa, 3-MA or z-VAD-fmk-treated cells); Mann Whitney test: * $P \leq 0.05$. Significance of the differences between 7KC-treated cells and (7KC + (α-toco, rapa, 3-MA or z-VAD-fmk-)-treated cells; Mann Whitney test: # $P \leq 0.05$. No significant differences were observed between control (untreated cells) and vehicle control (Ethanol (EtOH) 0.6%).

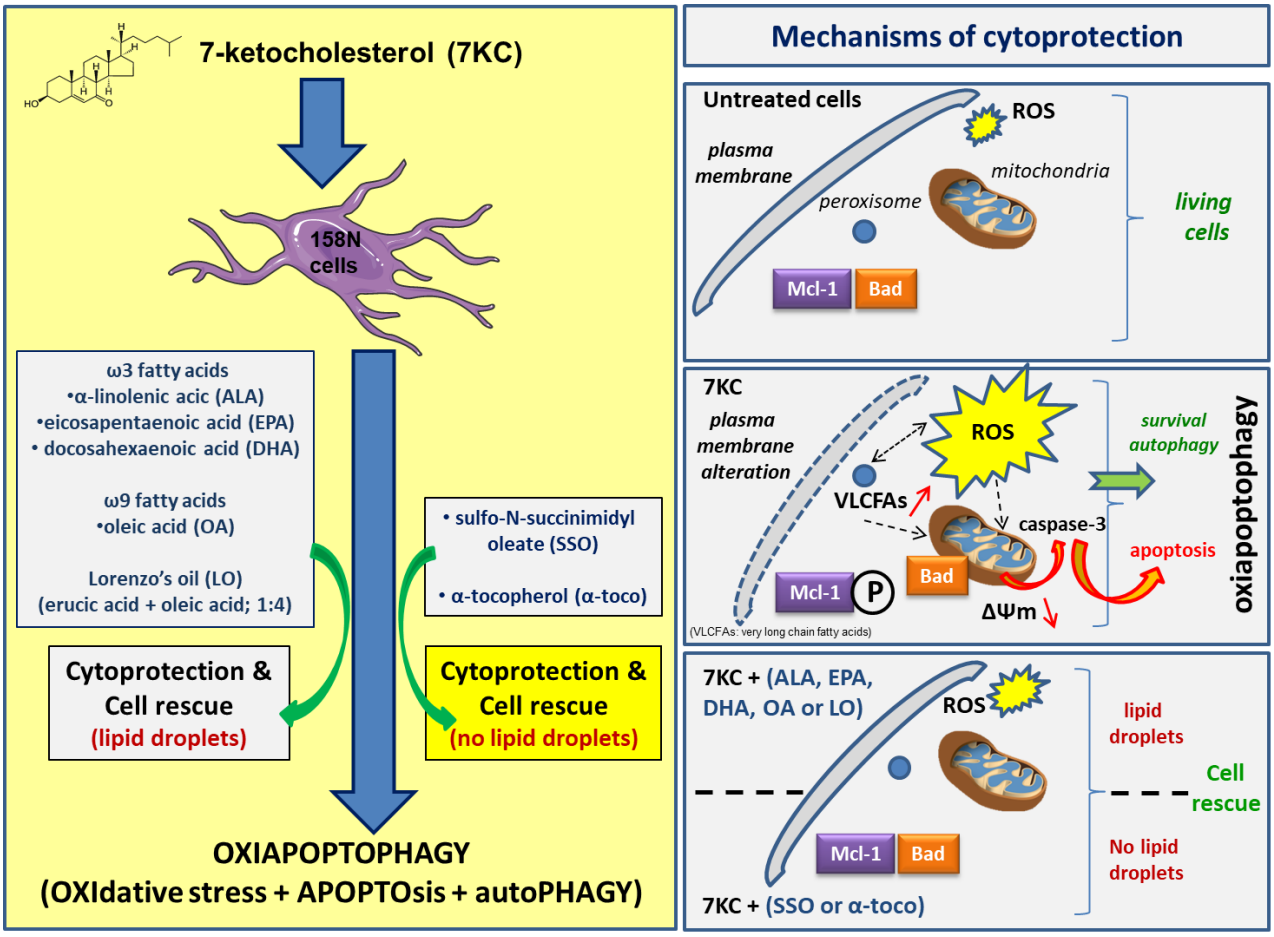

Graphical abstract: Prevention of 7-ketocholesterol-induced oxiapoptophagy by ω3 and ω9 fatty acids (α-linolenic acid, eicosapentaenoic acid, docosahexahenoic acid, oleic acid), Lorenzo's oil (erucic acid + oleic acid; 1:4) and sulfo-N-succinimidyl oleate (SSO): SSO benefits and cytoprotective mechanism

References

Anderson A, Campo A, Fulton E, Corwin A, Jerome WG, 3rd, & O'Connor MS (2020). 7-Ketocholesterol in disease and aging. Redox Biol 29**:** 101380.

Asatryan A, & Bazan NG (2017). Molecular mechanisms of signaling via the docosanoid neuroprotectin D1 for cellular homeostasis and neuroprotection. J Biol Chem 292**:** 12390-12397.

Baarine M, Ragot K, Genin EC, El Hajj H, Trompier D, Andreoletti P*, et al.* (2009). Peroxisomal and mitochondrial status of two murine oligodendrocytic cell lines (158N, 158JP): potential models for the study of peroxisomal disorders associated with dysmyelination processes. J Neurochem 111**:** 119-131.

Bjorkhem I, & Meaney S (2004). Brain cholesterol: long secret life behind a barrier. Arterioscler Thromb Vasc Biol 24**:** 806-815.

Bozcali E, Süzer O, Gürsoy HN, Atukeren P, & Gümüstas KM (2009). Effects of erucic acid supplemented feeding on chronic doxorubucin toxicity in rats. International journal of clinical and experimental medicine 2**:** 337-347.

Brahmi F, Vejux A, Sghaier R, Zarrouk A, Nury T, Meddeb W*, et al.* (2019). Prevention of 7-ketocholesterol-induced side effects by natural compounds. Crit Rev Food Sci Nutr 59**:** 3179-3198.

Brown AJ, & Jessup W (1999). Oxysterols and atherosclerosis. Atherosclerosis 142**:** 1-28.

Cilla A, Alegría A, Attanzio A, Garcia-Llatas G, Tesoriere L, & Livrea MA (2017). Dietary phytochemicals in the protection against oxysterol-induced damage. Chem Phys Lipids 207**:** 192-205.

Cooper RA (1978). Influence of increased membrane cholesterol on membrane fluidity and cell function in human red blood cells. Journal of supramolecular structure 8**:** 413-430.

Coort SL, Willems J, Coumans WA, van der Vusse GJ, Bonen A, Glatz JF*, et al.* (2002). Sulfo-N-succinimidyl esters of long chain fatty acids specifically inhibit fatty acid translocase (FAT/CD36)-mediated cellular fatty acid uptake. Molecular and cellular biochemistry 239**:** 213-219.

Debbabi M, Zarrouk A, Bezine M, Meddeb W, Nury T, Badreddine A*, et al.* (2017). Comparison of the effects of major fatty acids present in the Mediterranean diet (oleic acid, docosahexaenoic acid) and in hydrogenated oils (elaidic acid) on 7-ketocholesterol-induced oxiapoptophagy in microglial BV-2 cells. Chem Phys Lipids 207**:** 151-170.

Dhungana H, Huuskonen MT, Jaronen M, Lemarchant S, Ali H, Keksa-Goldsteine V*, et al.* (2017). Sulfosuccinimidyl oleate sodium is neuroprotective and alleviates stroke-induced neuroinflammation. Journal of neuroinflammation 14**:** 237.

Doria M, Nury T, Delmas D, Moreau T, Lizard G, & Vejux A (2019). Protective function of autophagy during VLCFA-induced cytotoxicity in a neurodegenerative cell model. Free Radic Biol Med 137**:** 46-58.

Drahota Z, Vrbacky M, Nuskova H, Kazdova L, Zidek V, Landa V*, et al.* (2010). Succinimidyl oleate, established inhibitor of CD36/FAT translocase inhibits complex III of mitochondrial respiratory chain. Biochem Biophys Res Commun 391**:** 1348-1351.

Johansson I, Monsen VT, Pettersen K, Mildenberger J, Misund K, Kaarniranta K*, et al.* (2015). The marine n-3 PUFA DHA evokes cytoprotection against oxidative stress and protein misfolding by inducing autophagy and NFE2L2 in human retinal pigment epithelial cells. Autophagy 11**:** 1636-1651.

Klionsky DJ, Abdelmohsen K, Abe A, Abedin MJ, Abeliovich H, Acevedo Arozena A*, et al.* (2016). Guidelines for the use and interpretation of assays for monitoring autophagy (3rd edition). Autophagy 12**:** 1-222.

Kuda O, Pietka TA, Demianova Z, Kudova E, Cvacka J, Kopecky J*, et al.* (2013). Sulfo-N-succinimidyl oleate (SSO) inhibits fatty acid uptake and signaling for intracellular calcium via binding CD36 lysine 164: SSO also inhibits oxidized low density lipoprotein uptake by macrophages. J Biol Chem 288**:** 15547-15555.

Leoni V, Nury T, Vejux A, Zarrouk A, Caccia C, Debbabi M*, et al.* (2017). Mitochondrial dysfunctions in 7-ketocholesterol-treated 158N oligodendrocytes without or with alpha-tocopherol: Impacts on the cellular profil of tricarboxylic cycle-associated organic acids, long chain saturated and unsaturated fatty acids, oxysterols, cholesterol and cholesterol precursors. J Steroid Biochem Mol Biol 169**:** 96-110.

Mathieu J, Schloendorn J, Rittmann BE, & Alvarez PJ (2008). Microbial degradation of 7-ketocholesterol. Biodegradation 19**:** 807-813.

Mei S, Ni HM, Manley S, Bockus A, Kassel KM, Luyendyk JP*, et al.* (2011). Differential roles of unsaturated and saturated fatty acids on autophagy and apoptosis in hepatocytes. J Pharmacol Exp Ther 339**:** 487-498.

Monier S, Samadi M, Prunet C, Denance M, Laubriet A, Athias A*, et al.* (2003). Impairment of the cytotoxic and oxidative activities of 7 beta-hydroxycholesterol and 7-ketocholesterol by esterification with oleate. Biochem Biophys Res Commun 303**:** 814-824.

Moser HW, Moser AB, Hollandsworth K, Brereton NH, & Raymond GV (2007). "Lorenzo's oil" therapy for X-linked adrenoleukodystrophy: rationale and current assessment of efficacy. Journal of molecular neuroscience : MN 33**:** 105-113.

Mutemberezi V, Guillemot-Legris O, & Muccioli GG (2016). Oxysterols: From cholesterol metabolites to key mediators. Prog Lipid Res 64**:** 152-169.

Namsi A, Nury T, Hamdouni H, Yammine A, Vejux A, Vervandier-Fasseur D*, et al.* (2018). Induction of Neuronal Differentiation of Murine N2a Cells by Two Polyphenols Present in the Mediterranean Diet Mimicking Neurotrophins Activities: Resveratrol and Apigenin. Diseases 6.

Namsi A, Nury T, Khan AS, Leprince J, Vaudry D, Caccia C*, et al.* (2019). Octadecaneuropeptide (ODN) Induces N2a Cells Differentiation through a PKA/PLC/PKC/MEK/ERK-Dependent Pathway: Incidence on Peroxisome, Mitochondria, and Lipid Profiles. Molecules 24.

Nury T, Sghaier R, Zarrouk A, Menetrier F, Uzun T, Leoni V*, et al.* (2018). Induction of peroxisomal changes in oligodendrocytes treated with 7-ketocholesterol: Attenuation by alpha-tocopherol. Biochimie 153**:** 181-202.

Nury T, Zarrouk A, Mackrill JJ, Samadi M, Durand P, Riedinger JM*, et al.* (2015). Induction of oxiapoptophagy on 158N murine oligodendrocytes treated by 7-ketocholesterol-, 7beta-hydroxycholesterol-, or 24(S)-hydroxycholesterol: Protective effects of alpha-tocopherol and docosahexaenoic acid (DHA; C22:6 n-3). Steroids 99**:** 194-203.

Nury T, Zarrouk A, Ragot K, Debbabi M, Riedinger JM, Vejux A*, et al.* (2017). 7-Ketocholesterol is increased in the plasma of X-ALD patients and induces peroxisomal modifications in microglial cells: Potential roles of 7-ketocholesterol in the pathophysiology of X-ALD. J Steroid Biochem Mol Biol 169**:** 123-136.

Nury T, Zarrouk A, Vejux A, Doria M, Riedinger JM, Delage-Mourroux R*, et al.* (2014). Induction of oxiapoptophagy, a mixed mode of cell death associated with oxidative stress, apoptosis and autophagy, on 7-ketocholesterol-treated 158N murine oligodendrocytes: impairment by alpha-tocopherol. Biochem Biophys Res Commun 446**:** 714-719.

Prieto Tenreiro A, Penacho Lazaro MA, Andres Celda R, Fernandez Fernandez M, Gonzalez Mateo C, & Diez Hernandez A (2013). Dietary treatment for X-linked adrenoleukodystrophy: is "Lorenzo's oil" useful? Endocrinologia y nutricion : organo de la Sociedad Espanola de Endocrinologia y Nutricion 60**:** 37-39.

Qiu B, & Simon MC (2016). BODIPY 493/503 Staining of Neutral Lipid Droplets for Microscopy and Quantification by Flow Cytometry. Bio-protocol 6.

Ragot K, Delmas D, Athias A, Nury T, Baarine M, & Lizard G (2011). alpha-Tocopherol impairs 7-ketocholesterol-induced caspase-3-dependent apoptosis involving GSK-3 activation and Mcl-1 degradation on 158N murine oligodendrocytes. Chem Phys Lipids 164**:** 469-478.

Ragot K, Mackrill JJ, Zarrouk A, Nury T, Aires V, Jacquin A*, et al.* (2013). Absence of correlation between oxysterol accumulation in lipid raft microdomains, calcium increase, and apoptosis induction on 158N murine oligodendrocytes. Biochem Pharmacol 86**:** 67-79.

Rothe G, & Valet G (1990). Flow cytometric analysis of respiratory burst activity in phagocytes with hydroethidine and 2',7'-dichlorofluorescin. Journal of leukocyte biology 47**:** 440-448.

Royer MC, Lemaire-Ewing S, Desrumaux C, Monier S, Pais de Barros JP, Athias A*, et al.* (2009). 7-ketocholesterol incorporation into sphingolipid/cholesterol-enriched (lipid raft) domains is impaired by vitamin E: a specific role for alpha-tocopherol with consequences on cell death. J Biol Chem 284**:** 15826-15834.

Sassa T, Wakashima T, Ohno Y, & Kihara A (2014). Lorenzo's oil inhibits ELOVL1 and lowers the level of sphingomyelin with a saturated very long-chain fatty acid. J Lipid Res 55**:** 524-530.

Sassi K, Nury T, Zarrouk A, Sghaier R, Khalafi-Nezhad A, Vejux A*, et al.* (2019). Induction of a non-apoptotic mode of cell death associated with autophagic characteristics with steroidal maleic anhydrides and 7β-hydroxycholesterol on glioma cells. J Steroid Biochem Mol Biol 191**:** 105371.

Schlegel RA, Stevens M, Lumley-Sapanski K, & Williamson P (1993). Altered lipid packing identifies apoptotic thymocytes. Immunology letters 36**:** 283-288.

Schloendorn J, Webb T, Kemmish K, Hamalainen M, Jackemeyer D, Jiang L*, et al.* (2009). Medical bioremediation: a concept moving toward reality. Rejuvenation Res 12**:** 411-419.

Schwingshackl L, Morze J, & Hoffmann G (2020). Mediterranean diet and health status: Active ingredients and pharmacological mechanisms. Br J Pharmacol 177**:** 1241-1257.

Testa G, Rossin D, Poli G, Biasi F, & Leonarduzzi G (2018). Implication of oxysterols in chronic inflammatory human diseases. Biochimie 153**:** 220-231.

Vejux A, Abed-Vieillard D, Hajji K, Zarrouk A, Mackrill JJ, Ghosh S*, et al.* (2020). 7-Ketocholesterol and 7beta-hydroxycholesterol: In vitro and animal models used to characterize their activities and to identify molecules preventing their toxicity. Biochem Pharmacol 173**:** 113648.

Vejux A, Guyot S, Montange T, Riedinger JM, Kahn E, & Lizard G (2009). Phospholipidosis and down-regulation of the PI3-K/PDK-1/Akt signalling pathway are vitamin E inhibitable events associated with 7-ketocholesterol-induced apoptosis. J Nutr Biochem 20**:** 45-61.

Vejux A, Kahn E, Dumas D, Bessède G, Ménétrier F, Athias A*, et al.* (2005). 7-Ketocholesterol favors lipid accumulation and colocalizes with Nile Red positive cytoplasmic structures formed during 7-ketocholesterol-induced apoptosis: analysis by flow cytometry, FRET biphoton spectral imaging microscopy, and subcellular fractionation. Cytometry A 64**:** 87-100.

Vejux A, Kahn E, Ménétrier F, Montange T, Lherminier J, Riedinger JM*, et al.* (2007). Cytotoxic oxysterols induce caspase-independent myelin figure formation and caspase-dependent polar lipid accumulation. Histochem Cell Biol 127**:** 609-624.

Walther TC, & Farese RV, Jr. (2012). Lipid droplets and cellular lipid metabolism. Annual review of biochemistry 81**:** 687-714.

Wanders RJ, & Waterham HR (2006). Biochemistry of mammalian peroxisomes revisited. Annual review of biochemistry 75**:** 295-332.

Yammine A, Nury T, Vejux A, Latruffe N, Vervandier-Fasseur D, Samadi M*, et al.* (2020). Prevention of 7-Ketocholesterol-Induced Overproduction of Reactive Oxygen Species, Mitochondrial Dysfunction and Cell Death with Major Nutrients (Polyphenols, ω3 and ω9 Unsaturated Fatty Acids) of the Mediterranean Diet on N2a Neuronal Cells. Molecules 25.

Zarrouk A, Martine L, Gregoire S, Nury T, Meddeb W, Camus E*, et al.* (2019). Profile of Fatty Acids, Tocopherols, Phytosterols and Polyphenols in Mediterranean Oils (Argan Oils, Olive Oils, Milk Thistle Seed Oils and Nigella Seed Oil) and Evaluation of their Antioxidant and Cytoprotective Activities. Curr Pharm Des 25**:** 1791-1805.

Zarrouk A, Vejux A, Mackrill J, O'Callaghan Y, Hammami M, O'Brien N, *et al.* (2014). Involvement of oxysterols in age-related diseases and ageing processes. Ageing Res Rev 18**:** 148-162.

Article 3

7ketocholesterol and 7β-hydroxycholesterol-induced peroxisomal disorders in glial, microglial and neuronal cells: potential role in neurodegeneration

Thomas Nury, Aline Yammine, Franck Ménétrier, Amira Zarrouk, Anne Vejux, Gérard Lizard

Advances in Experimental Medicine and Biology, Vol. 1299, Gérard Lizard (Eds): Peroxisome Biology: Experimental Models, Peroxisomal Disorders and Neurological Diseases. Chapter 7. 2021. doi: 10.1007/978-3-030-60204-8

Le 7KC induit des dysfonctions au niveaux des organites (lysosome, mitochondrie, réticulum endoplasmique) mais aussi au niveau du peroxysome sur les oligodendrocytes murins 158N. Le peroxysome serait plus sensible que la mitochondrie vis-à-vis du 7KC. En effet, les dysfonctions peroxysomales semblent apparaitre plus précocement que les dysfonctions mitochondriales et sans signe de mort cellulaire aboutissant à une démyélinisation.

Les maladies liées à des dysfonctions du peroxysome sont souvent des maladies neurodégénératives.

Les peroxysomopathies sont des maladies d'origine génétique dues à des mutations des gènes codant pour des protéines peroxysomales (peroxines, transporteurs d'acides gras, enzymes de la β-oxydation). Ces maladies rares se caractérisent généralement par des accumulations d'AGTLC (C24:0 et C26:0) et des diminutions des taux de plasmalogènes.

Le peroxysome serait aussi impliqué dans le développement des maladies neurodégénératives fréquentes comme la maladie d'Alzheimer, la maladie de Parkinson et la sclérose en plaques (Dragonas *et al.*, 2009; Gray *et al.*, 2014; Jo *et al.*, 2019; Kou *et al.*, 2011).

Dans ces maladies, le stress oxydant augmente, ce qui engendre une élévation de l'oxydation du cholestérol et la formation de 7-hydroxycholestérols toxiques (7β-OHC et 7KC). Ces derniers peuvent potentiellement prendre part à l'évolution de ces pathologies.

La revue s'inscrit dans ce contexte et présente les dysfonctions peroxysomales provoquées par les 7-hydroxycholestérols (7β-OHC et 7KC) dans des maladies neurodégénératives d'origine génétique ou non (X-ALD, maladie d'Alzheimer, maladie de Parkinson, sclérose en plaques).

Title: **7ketocholesterol and 7β-hydroxycholesterol-induced peroxisomal disorders in glial, microglial and neuronal cells: potential role in neurodegeneration**

Subtitle: **7ketocholesterol and 7β-hydroxycholesterol-induced peroxisomal disorders and neurodegeneration**

Thomas NURY[1], Aline YAMMINE[1,2], Franck MENETRIER[3], Amira ZARROUK[4], Anne VEJUX[1], Gérard LIZARD[1*]

1 - *Equipe 'Biochimie du Peroxysome, Inflammation et Métabolisme Lipidique' EA 7270 / Université de Bourgogne Franche-Comté / Inserm, Dijon, France; thomas.nury@u-bourgogne.fr; anne.vejux@u-bourgogne.fr; gerard.lizard@u-bourgogne.fr*

2 - *Laboratoire Molécules Bioactives, Faculté des Sciences-2, Ecole Doctorale des Sciences et de Technologie, Université Libanaise, Beirut, Lebanon ; alineyammine5@gmail.com*

3 - *INRA-CNRS, UMR 1324 CSGA, Dijon, France ; franck.menetrier@inra.fr*

4 - *Laboratoire 'Nutrition, Aliments Fonctionnels et Santé Vasculaire', UR12ES05 Université de Monastir, Monastir & Laboratoire de Biochimie, Faculté de Médecine, Sousse, Tunisia ; zarroukamira@gmail.com*

Correspondence: Dr Gérard LIZARD (PhD), Laboratoire Bio-PeroxIL, Université de Bourgogne / Inserm, Faculté des Sciences Gabriel, 6 Bd Gabriel, 21000 Dijon, France ; E.mail : gerard.lizard@u-bourgogne.fr; phone: 33 3 80 39 62 56 / *Fax:* 33 3 80 39 62 50

Abstract

Peroxisomopathies are qualitative or quantitative deficiencies in peroxisomes which lead to increases in the level of very long-chain fatty acids (VLCFA) and can be associated with more or less pronounced dysfunction of central nervous system cells: glial and microglial cells. Currently, in frequent neurodegenerative diseases, Alzheimer's disease (AD) and multiple sclerosis (MS), peroxisomal dysfunction is also suspected due to an increase in VLCFA, which can be associated with a decrease of plasmalogens, in these patients. Moreover, in patients suffering from

peroxisomopathies such as X-linked adrenoleukodystrophy (X-ALD), AD or MS, the increase in oxidative stress observed leads to the formation of cytotoxic oxysterols: 7-ketocholesterol (7KC), 7β-hydroxycholesterol (7β-OHC). These observations led to the demonstration that 7KC and 7β-OHC alter the biogenesis and activity of peroxisomes in glial and microglial cells. In X-ALD, AD and MS, it is suggested that 7KC and 7β-OHC affecting the peroxisome, and which also induce mitochondrial dysfunctions, oxidative stress and inflammation, could promote neurodegeneration. Consequently, the study of oxisome in peroxisomopathies, AD and MS, could help to better understand the pathophysiology of these diseases to identify therapeutic targets for effective treatments.

Keywords: oxysterol, 7-ketocholesterol, 7β-hydroxycholesterol, peroxisome, very long chain fatty acids, Alzheimer's disease, multiple sclerosis, X-linked adrenoleukodystrophy.

Abbreviations:

ABC: ATP-binding cassette; ACALD: adolescent cerebral adrenoleukodystrophy; ACOX1: Acyl-CoA oxidase 1; AD: Alzheimer’s disease; ALDP: adrenoleukodystrophy protein; AMN: adrenomyeloneuropathy; CCALD: childhood cerebral adrenoleukodystrophy; CNS: central nervous system; DHA: docosahexaenoic acid; DHAPAT: dihydroxyacetone-phosphate acyltransferase; DMF: dimethyl fumarate; DNA: deoxyribonucleic acid; LC3: protein light chain 3; LXR: Liver X receptor; MFP2: multifunctional protein 2; MMF: monomethyl fumarate; MS: multiple sclerosis; PARP: poly-ADP-ribose polymerase; PD: Parkinson’s disease; P-MS: progressive MS; PPAR: peroxisome proliferator-activated receptor; RNS: reactive nitrogen species; RR-MS: remittent recurrent-MS; ROS: reactive oxygen species; TEM: transmission electron microscopy; VLCFA: very long chain fatty acid; X-ALD: X-linked adrenoleukodystrophy; 7β-OHC: 7β-hydroxycholesterol; 7KC: 7-ketocholesterol.

1 - Neurodegeneration and peroxisomal disorders

1.1-Peroxisome and peroxisomopathies

Peroxisomes, which are devoid of DNA, are single cell membrane organelles present in nearly all eukaryotic cells [**26**]. Depending on the cell type, elongated tubular (>2 μm in length) or spherical (0.1–1 μm) peroxisomes can be observed by transmission electron microscopy (TEM) [**25**] (**Figure 1**). The identification of peroxisomes by immunofluorescence with the use of appropriated antibodies directed against specific peroxisomal antigens, such as Abcd3, gives information on the peroxisomal topography (conventional immunofluorescence, confocal microscopy) and on the peroxisomal mass per cell (flow cytomety) (**Figure 2**). Peroxisomes are essential to maintain RedOx homeostasia and have important roles in lipid metabolism: β-oxidation of very long chain fatty acids (VLCFAs) and branched fatty acids, synthesis of docosahexahenoic acid (DHA, C22:6 n-3) and of plasmalogens which are major components of the myelin sheath [**26**]. There are also several evidences that peroxisome and mitochondria are tightly connected organelles playing key roles in cellular ageing [**15**]. It is now well established that peroxisomal changes can directly or indirectly affect mitochondrial activity, and reciprocally [**15**].

Peroxisomopathies, which are rare diseases of genetic origin affecting the central and / or peripheric nervous system, include peroxisome biogenesis disorders (Zellweger syndrome), multiple peroxisomal enzyme deficiency (rhizomelic chondrodysplasia punctata) and single peroxisomal enzyme deficiency such as X-linked adrenoleukodystrophy (X-ALD, MIM 300100), Acyl-CoA oxidase deficiency, and D-Bifunctional protein deficiency [**5**]. X-ALD, which is the most frequent peroxysomal leukodystrophy of childhood, is characterized by progressive central nervous system (CNS) demyelination [**12**]. X-ALD is caused by mutations of the *ABCD1* gene

which encodes for a peroxisomal ABC half-transporter (ATP-binding cassette member 1 (ABCD1) also named adrenoleukodystrophy protein (ALDP)) involved in the import of very long chain fatty acids (VLCFAs) into the peroxisome [**2**]. These different forms of peroxysomopathies are all characterized by increased plasma levels of VLCFAs due to an impaired β-oxidation in the peroxisome and/or increased elongation [**8**]. The initial diagnosis of peroxysomopathies relies on the clinical presentation, brain imaging and biochemical analyses of VLCFAs, especially C24:0 and C26:0, which are elevated in the plasma and tissues of patients [**8**]. Newborn screening is based on the measurement of C26:0 lysophosphatidylcholine (26:0-lyso-PC) in dried blood spots [**8**]. At the moment, several studies have shown cytotoxic effects of VLCFA in vitro and in vivo [**1, 32**]. In vitro, on different types of nerve cells (neurons, glial and microglial cells), C24:0 and C26:0 often induce a non apoptotic mode of cell death associated with Ca^{2+} raise [**11**], K^{+} homeostasis disruption [**3**], reactive oxygen species (ROS) and reactive nitrogen species (RNS) overproduction [**1, 16**], and autophagic criteria [**6**]. In vivo, lysophosphatidylcholine (C24:0) injection into the parietal cortex of mice led to widespread microglial activation and apoptosis [**7**]. However, in human, there is no apparent correlation between the VLCFA level and the phenotype in X-ALD patients [**8**]. Therefore, other factors than VLCFA, including lipids and non lipid compounds, are suspected to trigger neurodegeneration in peroxisomopathies. At the moment, some signs of oxidative stress, considered as a hallmark of neurodegeneration, have been detected in the plasma and brain of X-ALD patients [**4**] and in patients with frequent neurodegenerative diseases: Alzheimer's disease (AD), Parkinson's disease (PD) and multiple sclerosis (MS) [**18**]. As VLCFA (C24:0; C26:0) are potent inducers of oxidative stress [**1, 16**], they can favor the production of protein and lipid oxidation products capable to trigger cytotoxic effects. The lipid peroxidation products generated include several aldehydes [**1**], which are

known to induce protein carbonylation, as well as some cholesterol oxidation products (oxysterols) including 7-ketocholesterol (7KC; also named 7-oxocholesterol) and 7β-hydroxycholesterol (7β-OHC) [**1**]. 7KC and 7β-OHC, which are mainly formed by cholesterol auto-oxidation, are strongly cytotoxic [**31**]. These oxysterols induce a mode of cell death by oxiapoptophagy involving oxidative stress, apoptosis and autophagy [**21**], which are hallmarks of neurodegeneration. Currently, increased levels of 7KC and 7β-OHC have been described in the plasma of patients with different forms of X-ALD [**22**]: i) cerebral demyelinating, inflammatory childhood phenotypes (CCALD: childhood cerebral ALD), which is associated with a poor prognosis and rapidly progresses to dementia and death; ii) cerebral juvenile and adult forms with demyelination in the CNS (ACALD: adolescent cerebral ALD); iii) adulthood forms without CNS demyelination (AMN: adrenomyeloneuropathy) defined as a spinal cord and peripheral nerve disease, and iiii) Addison's disease, which is characterized by adrenal insufficiency only. It is therefore hypothesized that 7KC and 7β-OHC could contribute to neurodegeneration in peroxysomopathies, especially in X-ALD, but also in other major neurodegenerative diseases [**30**].

1.2 – Potential involvement of peroxisomal changes in major neurodegenerative diseases: Alzheimer's disease and multiple sclerosis

Peroxisomal abnormalities associated with peroxysomopathies led to the clarification of the role of this organelle in neurodegeneration occurring in frequent neurodegenerative diseases such as AD and MS. Currently, potential roles of peroxisomes are suspected in AD and in dementia of the Alzheimer's type. Indeed, an accumulation of C22:0 and VLCFAs (C24:0; C26:0), all substrates for peroxisomal β-oxidation, was observed in the cortical regions of AD patients with stages V-VI of the disease compared with those modestly affected (stages I-II); conversely, the

level of plasmalogens, which need intact peroxisomes for their biosynthesis, was decreased [**13**]. In addition, in demented patients, including AD patients, the variations of fatty acid levels and the accumulation of C26:0 in the plasma and red blood cells highlight an alteration of fatty acid metabolism and point toward possible peroxisomal dysfunction **[33]**. In MS patients, a reduction in neuronal peroxisomes in MS grey matter has been reported [**10**] and alteration in the metabolism of VLCFAs, which could be a consequence of defective peroxisomes, has been described [**27**]. In the brain of patients with AD, increased levels of 7KC and 7β-OHC have also been shown [**29**]. It is important to underline that these oxysterols can be formed under the action of VLCFAs-induced oxidative stress [**1**], and under stress conditions induced by amyloid-β (Aβ) proteins, mainly Aβ42, which accumulates in brain lesions of patients with AD. High amount of 7KC have been reported in the cerebrospinal fluid of MS patients [**14**] as well as low levels [**9**]. 7KC-values might depend on the type of MS considered (Progressive-MS (P-MS) versus remittent recurrent – MS (RR-MS)) [**17**]. It is however widely accepted that oxysterols are considered as bonafide lipid mediators. To be qualified as a bonafide lipid mediator, a lipid compound should meet three conditions: i) to be endogenous; ii) to have its levels altered depending on the physiological or pathological situation, and iii) to induce a signaling response when its levels are altered. As a result, abnormal levels of 7KC (low or high) can alter cellular behavior. It is therefore hypothesized that 7KC, 7β-OHC could favor peroxisomal and mitochondrial dysfunction leading to neurodegeneration in patients with AD and MS [**30**] (**Figure 3**). This led us to specify the impact of different concentrations of 7KC and / or 7β-OHC on murine glial cells (murine oligodendrocyte 158N [**23**], murine microglial BV-2 cells [**22**], murine neuronal N2a cells, human neuroblatoma SK-N-BE cells as well as on rat C6 astrocytoma cells [**19, 24**] taking into account the effects on organelles (peroxisomes, mitochondria and

lysosomes), oxidative stress and the ability to induce cell death (apoptosis / necrosis) and to activate autophagy.

2 - In vitro evidence of 7ketocholesterol and 7β-hydroxycholesterol-induced peroxisomal damages in nerve cells

The cytotoxic effects of 7KC and 7β-OHC have been studied on several nerve cell lines: murine oligodendrocyte 158N cells; murine microglial BV-2 cells; murine neuronal N2a cells and C6 rat glioma cells. On 158N and/or BV-2 cells, 7KC and 7β-OHC induce a mode of cell death by oxiapoptophagy (OXIdative stress + APOPTOsis + autoPHAGY) characterized by ROS overproduction revealed by dihydroethidium staining, a decrease of oxidative phosphorylation associated with a loss of transmembrane mitochondrial potential ($\Delta\Psi m$) measured with $DiOC_6(3)$, reduced expression of Bcl-2, caspase-3 activation, poly-ADP-ribose polymerase (PARP) degradation, and condensation and/or fragmentation of the nuclei which are typical criteria of oxidative stress and apoptosis [**20-22, 28**]. Moreover, 7KC and 7β-OHC also enhances cytoplamic membrane permeability to propidium iodide and induces acidic vesicular organelle formation evaluated with acridine orange which evocate autophagic vesicles in agreement with observations realized by transmission electron microscopy [**20, 28**]. In addition, 7KC and 7β-OHC promotes conversion of microtubule-associated protein light chain 3 (LC3-I) to LC3-II which is characteristic of autophagy [**20, 21**], and 7KC increases the expression of p62 an autophagosome cargo protein involved in the sequestosome / aggresome formation preceding the autophagosome formation [**22, 23**]. On C6 rat glioma cells, it has been demonstrated that 7β-OHC induces survival autophagy since rapamycin, an autophagic inducer, and 3-methyladenine, an autophagic inhibitor, reduce and increase 7β-OHC-induced cell death, respectively [**24**]. On 158N cells, under treatment with 7KC used at sub-toxic (25 µM, 24 h) and toxic (50 µM, 24 h)

concentrations important peroxisomal changes were observed even in the absence of oxiapoptophagy which was only induced at 50 µM [**24**] (**Figure 4**). In the presence of 7KC (25 µM), only slight mitochondrial dysfunction and oxidative stress were found as well as modifications of the cytoplasmic distribution of mitochondria: clusters of mitochondria were detected. Thus, the peroxisomal alterations observed were similar with 7KC used at 25 and 50 µM [**23**]: presence of peroxisomes with abnormal sizes and shapes observed by transmission electron microscopy; lower cellular level of ATP-binding cassette transporter member 3 (ABCD3) used as a marker of peroxisomal mass (measured by flow cytometry); lower mRNA and protein levels (measured by RT-qPCR and western blotting) of ABCD1 and ABCD3 (two ATP-dependent peroxisomal transporters), of two peroxisomal enzymes Acyl-CoA Oxidase 1 (ACOX1) and multifunctional protein 2 (MFP2) enzymes involved in peroxisomal β-oxidation, and lower mRNA level of dihydroxyacetone-phosphate acyltransferase (DHAPAT), involved in peroxisomal β-oxidation and plasmalogen synthesis; increased levels of VLCFAs (C24:0, C24:1, C26:0 and C26:1) quantified by gas chromatography coupled with mass spectrometry metabolized by peroxisomal β-oxidation. On 158N cells, under treatment with 7β-OHC (50 µM, 24 h), morphological alterations of mitochondria and peroxisomes were simultaneously observed [**28**]. These data obtained on 158N cells support the following hypotheses: i) the peroxsisome would be more sensitive to 7KC than the mitochondria (7KC used at 25 µM induced important peroxisomal changes whereas the mitochondria was slightly affected); ii) peroxisomal changes can occur without signs of cytotoxicity (induction of oxiapoptophagy); iii) peroxisome changes could precede mitochondrial dysfunctions required to induce oxiapoptophagy. These peroxisomal dysfunctions may be associated with oligodendrocyte degeneration and may contribute to demyelination in X-ALD and MS. On BV-2 cells, 7KC also induced several peroxisomal modifications: decreased Abcd1, Abcd2, Abcd3, Acox1 and/or Mfp2 mRNA and protein levels,

increased catalase activity and decreased Acox1-activity [**22**]. In microglial cells, 7KC and 7β-OHC-induced peroxisomal alterations may favor the pro-inflammatory phenotype of these cells, thereby contributing to brain inflammation often seen in neurodegenerative diseases.

3 - Pharmacological consequences of the involvement of 7ketocholesterol and 7β-hydroxycholesterol-induced peroxisomal damages for the treatment of neurodegenerative diseases

Under the effect of 7KC and 7β-OHC, the signaling pathways involved in oxidative stress, inflammation and cell death, associated with apoptotic and autophagic criteria, have the advantage of being fairly well known [**28, 31**]. This made it possible to identify natural and synthetic molecules as well as mixtures of molecules (argan, olive and milk thistle oils) [**34**] having cytoprotective activities with respect to 7KC and 7β-OHC, and capable to prevent peroxisomal and mitochondrial dysfunctions. Several molecules are able to attenuate the cytotoxic effects of 7KC on different cell types but only few are very efficient. Currently, the only molecules identified strongly counteracting the toxicity of 7KC and 7β-OHC are α-tocopherol, docosahexaenoic acid (DHA, C22:6 n-3) and oleic acid (C18:1 n-9) [**21**]; biotin is only cytoprotective for 7β-OHC. Among the synthetic molecules, only dimethyl fumarate (DMF), marketed under the name Tecfidera for the treatment of MS, as well as its major metabolite, monomethyl fumarate (MMF), protect against oxiapoptophagy [**28**]. As more and more arguments are in favor of relationships between neurodegeneration, peroxisomal and mitochondrial dysfunction, and the involvement of oxysterols, to oppose the cytotoxic activities of these molecules could pave the way for new therapeutic approaches in both peroxisomopathies and frequent neurodegenerative diseases such as AD and MS.

4 – Conclusion

Although the auto-oxidation of cholesterol essentially leads to the formation of oxidized cholesterol derivatives in the 7-position, the formation of oxidized cholesterol derivatives at the 4-, 5- and 6-positions should be studied. An analysis of the oxisome by appropriate analytical biochemistry methods could also be informative. This approach would also take into account the metabolites of 7KC and 7β-OHC but also other enzymatically formed oxysterols (24S-hydroxycholesterol (also named cerebrosterol), 27-hydroxycholesterol, 25-hydroxycholesterol and derivatives) known to be involved in neurodegeneration. The study of the impact of oxysterols on the organelles of nerve cells (glial and microglial cells, neurons) in relation to oxidative stress, inflammation and cell death as well as the incidence of these molecules on certain nuclear receptors (peroxisome proliferator-activated receptors (PPARs), Liver X receptors (LXRs) in particular) offers many perspectives to better know and better treat neurodegenerative diseases.

References

1. Baarine M, Andréoletti P, Athias A, Nury T, Zarrouk A, Ragot K, Vejux A, Riedinger JM, Kattan Z, Bessede G, Trompier D, Savary S, Cherkaoui-Malki M, Lizard G (2012) Evidence of oxidative stress in very long chain fatty acid—treated oligodendrocytes and potentialization of ROS production using RNA interference-directed knockdown of ABCD1 and ACOX1 peroxisomal proteins. Neuroscience. 213: 1-18.

2. Berger J, Forss-Petter S, Eichler FS (2014) Pathophysiology of X-linked adrenoleukodystrophy Biochimie. 98: 135-142.

3. Bezine M, Debbabi M, Nury T, Ben-Khalifa R, Samadi M, Cherkaoui-Malki M, Vejux A, Raas Q, de Sèze J, Moreau T, El-Ayeb M, Lizard G (2017) Evidence of K(+) homeostasis disruption in cellular dysfunction triggered by 7-ketocholesterol, 24S-hydroxycholesterol, and tetracosanoic acid (C24:0) in 158N murine oligodendrocytes. Chem Phys Lipids. 207(Pt B): 135-150.

4. Deon M, Marchetti DP, Donida B, Wajner M, Vargas C (2016) Oxidative stress in patients with X-Linked Adrenoleukodystrophy. Cell Mol Neurobiol. 36(4): 497-512.

5. Depreter M, Espeel M, Roels F (2003) Human peroxisomal disorders. Microsc Res Tech. 61(2): 203-223.

6. Doria M, Nury T, Delmas D, Moreau T, Lizard G, Vejux A (2019) Protective function of autophagy during VLCFA-induced cytotoxicity in a neurodegenerative cell model. Free Radic Biol Med. 137: 46-58.

7. Eichler FS, Ren JQ, Cossoy M, Rietsch AM, Nagpal S, Moser AB, Frosch MP, Ransohoff RM (2008) Is microglial apoptosis an early pathogenic change in cerebral X-linked adrenoleukodystrophy? Ann Neurol. 63(6): 729-742.

8. Engelen M, Kemp S, de Visser M, van Geel BM, Wanders RJ, Aubourg P, Poll-The BT (2012) X-linked adrenoleukodystrophy (X-ALD): clinical presentation and guidelines for diagnosis, follow-up and management. Orphanet J Rare Dis. 7: 51.

9. Fellows Maxwell K, Bhattacharya S, Bodziak ML, Jakimovski D, Hagemeier J, Browne RW, Weinstock-Guttman B, Zivadinov R, Ramanathan M (2019) Oxysterols and apolipoproteins in multiple sclerosis: a 5 year follow-up study. J Lipid Res. 60(7): 1190-1198.

10. Gray E, Rice C, Hares K, Redondo J, Kemp K, Williams M, Brown A, Scolding N, Wilkins A (2014) Reductions in neuronal peroxisomes in multiple sclerosis grey matter. Mult Scler. 20(6): 651-659.

11. Hein S, Schönfeld P, Kahlert S, Reiser G (2008) Toxic effects of X-linked adrenoleukodystrophy-associated, very long chain fatty acids on glial cells and neurons from rat hippocampus in culture. Hum Mol Genet. 17(12): 1750-1761.

12. Kemp S, Huffnagel IC, Linthorst GE, Wanders RJ, Engelen M (2016) Adrenoleukodystrophy - neuroendocrine pathogenesis and redefinition of natural history. Nat Rev Endocrinol. 12(10): 606-615.

13. Kou J, Kovacs GG, Höftberger R, Kulik W, Brodde A, Forss-Petter S, Hönigschnabl S, Gleiss A, Brügger B, Wanders R, Just W, Budka H, Jungwirth S, Fischer P, Berger J (2011) Peroxisomal alterations in Alzheimer's disease. Acta Neuropathol. 122(3): 271-283.

14. Leoni V, Lütjohann D, Masterman T (2005) Levels of 7-oxocholesterol in cerebrospinal fluid are more than one thousand times lower than reported in multiple sclerosis. J Lipid Res. 46(2): 191-195.

15. Lismont C, Nordgren M, Van Veldhoven PP, Fransen M (2015) Redox interplay between mitochondria and peroxisomes. Front Cell Dev Biol. 3: 35.

16. López-Erauskin J, Fourcade S, Galino J, Ruiz M, Schlüter A, Naudi A, Jove M, Portero-Otin M, Pamplona R, Ferrer I, Pujol A (2011) Antioxidants halt axonal degeneration in a mouse model of X-adrenoleukodystrophy. Ann Neurol. 70(1): 84-92.

17. Mukhopadhyay S, Fellows K, Browne RW, Khare P, Krishnan Radhakrishnan S, Hagemeier J, Weinstock-Guttman B, Zivadinov R, Ramanathan M (2017) Interdependence of oxysterols with cholesterol profiles in multiple sclerosis. Mult Scler. 23(6): 792-801.

18. Niedzielska E, Smaga I, Gawlik M, Moniczewski A, Stankowicz P, Pera J, Filip M (2016) Oxidative Stress in Neurodegenerative Diseases. Mol Neurobiol. 53(6): 4094-4125.

19. Nury T, Samadi M, Zarrouk A, Riedinger JM, Lizard G (2013) Improved synthesis and in vitro evaluation of the cytotoxic profile of oxysterols oxidized at C4 (4α- and 4β-hydroxycholesterol) and C7 (7-ketocholesterol, 7α- and 7β-hydroxycholesterol) on cells of the central nervous system. Eur J Med Chem. 70: 558-567.

20. Nury T, Zarrouk A, Vejux A, Doria M, Riedinger JM, Delage-Mourroux R, Lizard G (2014) Induction of oxiapoptophagy, a mixed mode of cell death associated with oxidative stress, apoptosis and autophagy, on 7-ketocholesterol-treated 158N murine oligodendrocytes: impairment by α-tocopherol. Biochem Biophys Res Commun. 446(3): 714-719.

21. Nury T, Zarrouk A, Mackrill JJ, Samadi M, Durand P, Riedinger JM, Doria M, Vejux A, Limagne E, Delmas D, Prost M, Moreau T, Hammami M, Delage-Mourroux R, O'Brien NM, Lizard G (2015) Induction of oxiapoptophagy on 158N murine oligodendrocytes treated by 7-ketocholesterol-, 7β-hydroxycholesterol-, or 24(S)-hydroxycholesterol: Protective effects of α-tocopherol and docosahexaenoic acid (DHA; C22:6 n-3). Steroids. 99(Pt B): 194-203.

22. Nury T, Zarrouk A, Ragot K, Debbabi M, Riedinger JM, Vejux A, Aubourg P, Lizard G (2017) 7-Ketocholesterol is increased in the plasma of X-ALD patients and induces peroxisomal modifications in microglial cells: Potential roles of 7-ketocholesterol in the pathophysiology of X-ALD. J Steroid Biochem Mol Biol. 169: 123-136.

23. Nury T, Sghaier R, Zarrouk A, Ménétrier F, Uzun T, Leoni V, Caccia C, Meddeb W, Namsi A, Sassi K, Mihoubi W, Riedinger JM, Cherkaoui-Malki M, Moreau T, Vejux A, Lizard G (2018) Induction of peroxisomal changes in oligodendrocytes treated with 7-ketocholesterol: Attenuation by α-tocopherol. Biochimie. 153: 181-202.

24. Sassi K, Nury T, Zarrouk A, Sghaier R, Khalafi-Nezhad A, Vejux A, Samadi M, Aissa-Fennira FB, Lizard G (2019) Induction of a non-apoptotic mode of cell death associated with autophagic characteristics with steroidal maleic anhydrides and 7β-hydroxycholesterol on glioma cells. J Steroid Biochem Mol Biol. 191: 105371.

25. Schrader M, Fahimi HD (2006) Growth and division of peroxisomes. Int Rev Cytol. 255: 237-290.

26. Schrader M, Fahimi HD (2008) The peroxisome: still a mysterious organelle. Histochem Cell Biol. 129(4): 421-440.

27. Senanayake VK, Jin W, Mochizuki A, Chitou B, Goodenowe DB (2015) Metabolic dysfunctions in multiple sclerosis: implications as to causation, early detection, and treatment, a case control study. BMC Neurol. 15: 154.

28. Sghaier R, Nury T, Leoni V, Caccia C, Pais De Barros JP, Cherif A, Vejux A, Moreau T, Limem K, Samadi M, Mackrill JJ, Masmoudi AS, Lizard G, Zarrouk A (2019) Dimethyl fumarate and monomethyl fumarate attenuate oxidative stress and mitochondrial alterations leading to oxiapoptophagy in 158N murine oligodendrocytes treated with 7β-hydroxycholesterol. J Steroid Biochem Mol Biol. 194: 105432.

29. Testa G, Staurenghi E, Zerbinati C, Gargiulo S, Iuliano L, Giaccone G, Fantò F, Poli G, Leonarduzzi G, Gamba P (2016) Changes in brain oxysterols at different stages of Alzheimer's disease: Their involvement in neuroinflammation. Redox Biol. 10: 24-33.

30. Trompier D, Vejux A, Zarrouk A, Gondcaille C, Geillon F, Nury T, Savary S, Lizard G (2014) Brain peroxisomes. Biochimie. 98: 102-110.

31. Vejux A, Lizard G (2009)Cytotoxic effects of oxysterols associated with human diseases: Induction of cell death (apoptosis and/or oncosis), oxidative and inflammatory activities, and phospholipidosis. Mol Aspects Med. 30(3): 153-170.

32. Wanders RJ, Ferdinandusse S, Brites P, Kemp S (2010) Peroxisomes, lipid metabolism and lipotoxicity. Biochim Biophys Acta. 1801(3): 272-280.

33. Zarrouk A, Riedinger JM, Ahmed SH, Hammami S, Chaabane W, Debbabi M, Ben Ammou S, Rouaud O, Frih M, Lizard G, Hammami M (2015) Fatty acid profiles in demented patients: identification of hexacosanoic acid (C26:0) as a blood lipid biomarker of dementia. J Alzheimers Dis. 44(4): 1349-1359.

34. Zarrouk A, Martine L, Grégoire S, Nury T, Meddeb W, Camus E, Badreddine A, Durand P, Namsi A, Yammine A, Nasser B, Mejri M, Bretillon L, Mackrill JJ, Cherkaoui-Malki M,

35. Hammami M, Lizard G (2019) Profile of Fatty Acids, Tocopherols, Phytosterols and Polyphenols in Mediterranean Oils (Argan Oils, Olive Oils, Milk Thistle Seed Oils and Nigella Seed Oil) and Evaluation of their Antioxidant and Cytoprotective Activities. Curr Pharm Des. 25(15):1791-1805.

Aknowledgements

This work was supported by grants from: Univ. Bourgogne (Dijon, France); Univ. Monastir (Monastir, Tunisia); ELA fondation (grant application ELA 2010-030I4); ASSAD (Louhans, France); Applications des Sciences de l'Information en Médecine (ABASIM, Dijon, France), and Department of Neurology (University Hospital, Dijon, France).

Figures Legends

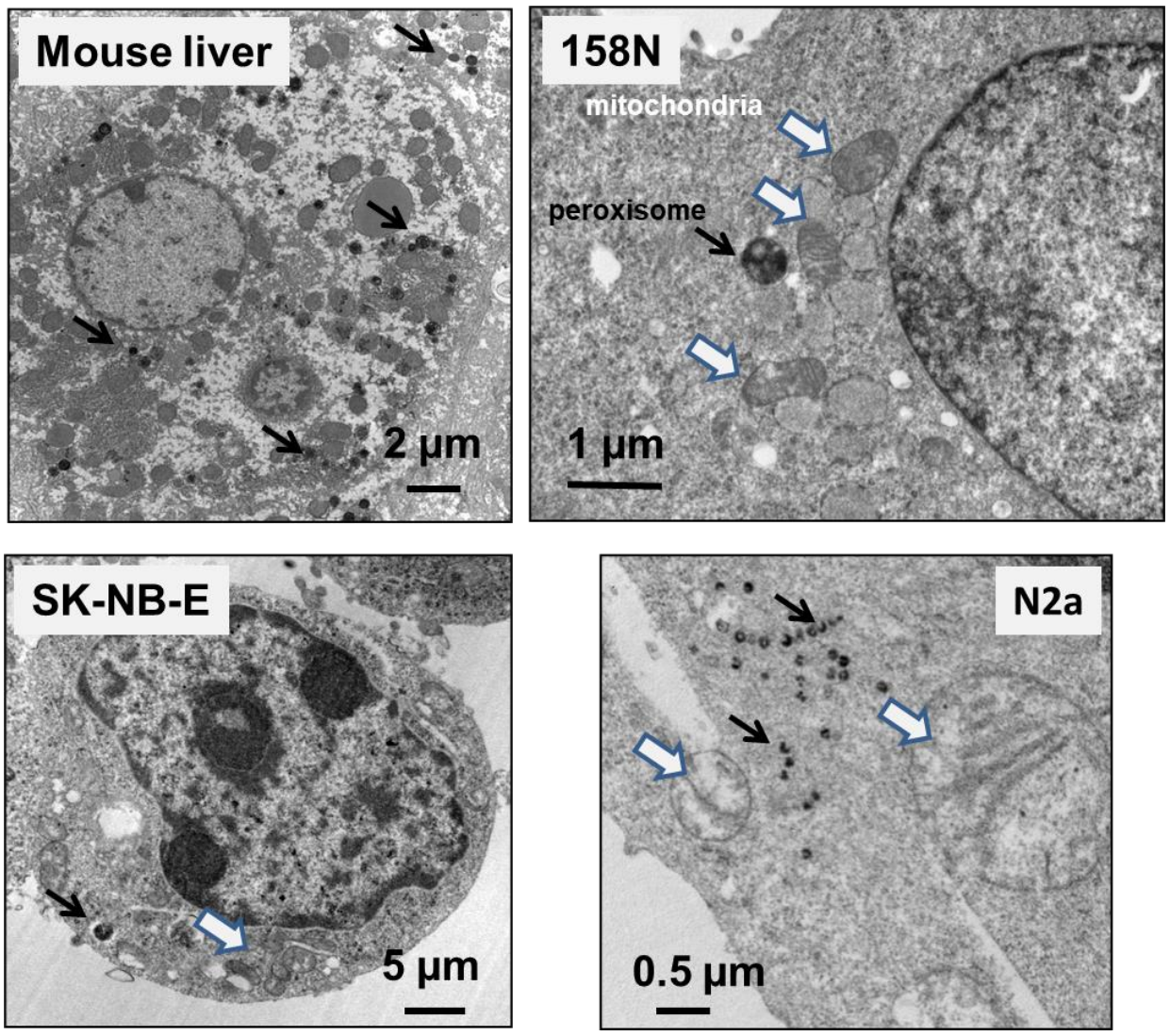

Figure 1: Identification of peroxisomes in neural cells by transmission electron microscopy. Peroxisomes can be identified by various techniques including transmission electron microscopy (TEM). Dark arrows point towards peroxisomes and white arrows towards mitochondria. Round peroxisomes were observed. The diameters were in the range of 0.5 µm in mouse liver, murine oligodendrocytes 158N and human neuronal SK-NB-E cells, and of 0.1 µm in murine neuronal N2a cells.

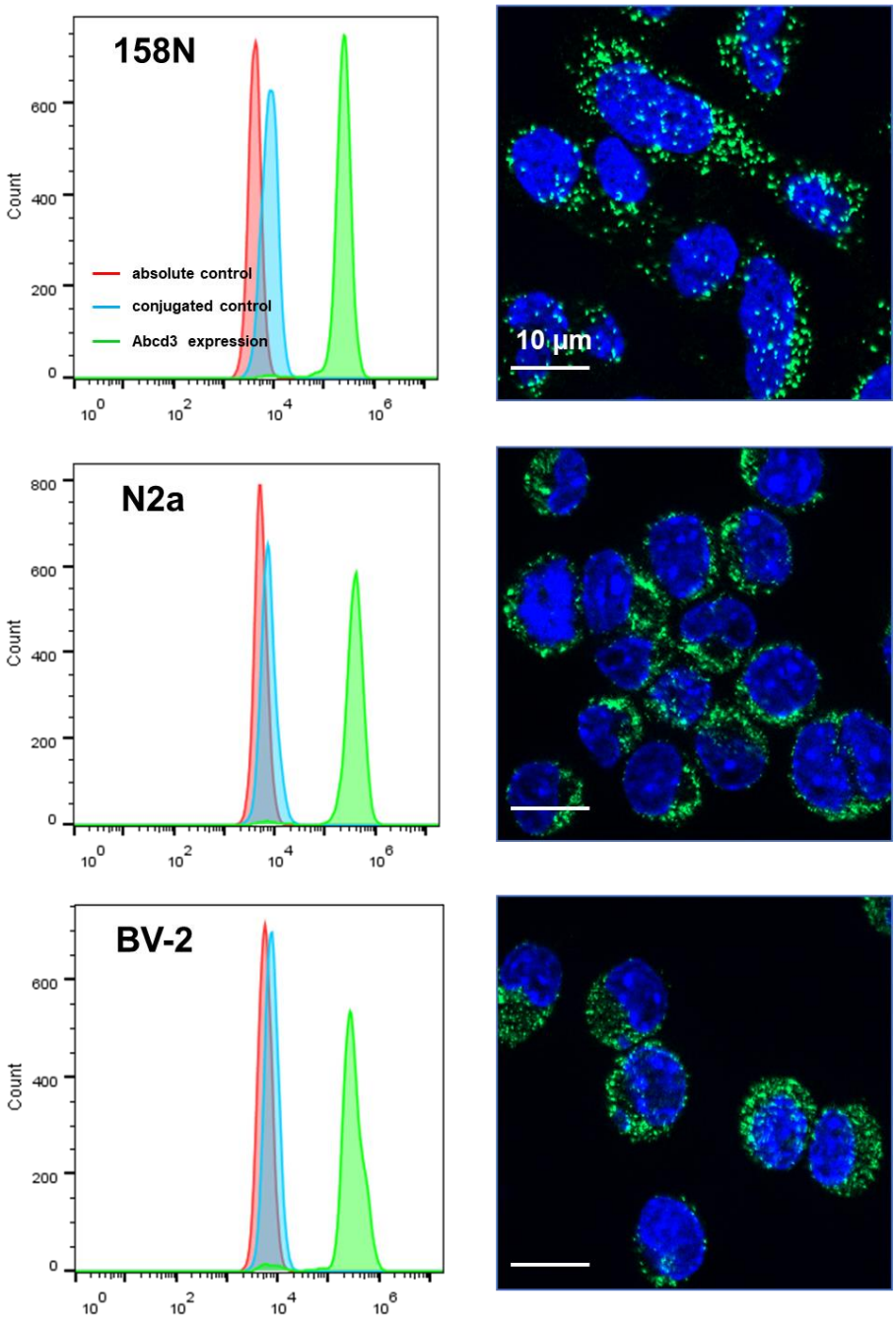

Figure 2: Analysis of peroxisomes in neural cells by flow cytometry and fluorescence microscopy. The peroxisomes were revealed by indirect immunofluorescence with a rabbit polyclonal primary antibody directed against Abcd3 (ref # 11523651, Pierce / Thermo Fisher Scientific, Montigny le Bretronneux, France), and with a secondary goat anti-rabbit antibody coupled with 488-Alexa (Thermo Fisher Scientific). The peroxisomal mass was quantified by flow cytometry. A fluorescent microscope coupled to an Apotome structured illumination system (Imager M2, Zeiss) was used to visualized the peroxisomes; the fluorescent signals of the samples were collected with the ZEN software (Zeiss). For microscopical observations, the nuclei were stained with Hoechst 33342 (2 µg/mL).

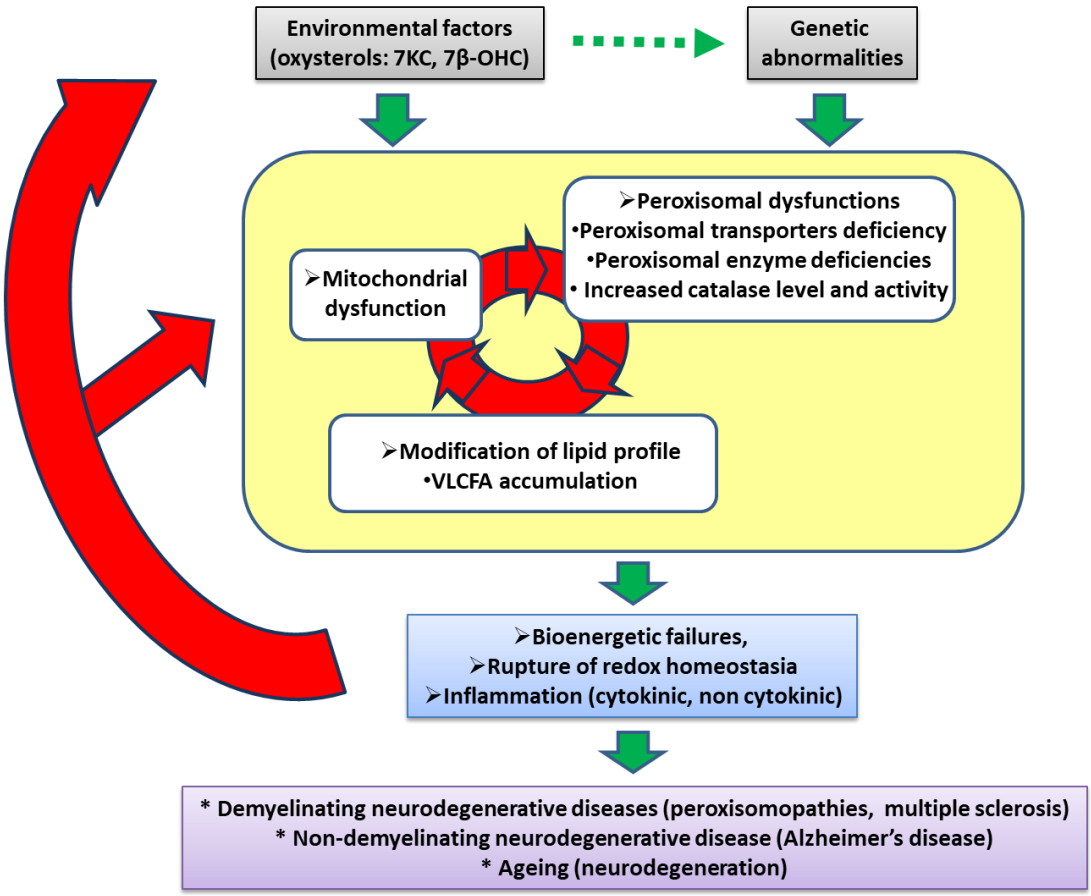

Figure 3: Incidence of peroxisomal dysfunction in neurodegeneration: hypothetic model. Environmental factors (oxysterols: 7-ketocholesterol (7KC), 7β-hydroxycholesterol (7β-OHC)) resulting from rupture or RedOx homeostasia, which is a hallmark of neurodegenerative diseases, are often enhanced in the biological fluids and in the brain of patients with neurodegenerative disease. These oxysterols could trigger peroxisomal and mitochondrial damages which could further favor bioenergetic failure, overproduction of ROS and activation of inflammatory processes. In turn, these events could contribute to amplify brain damages via secondary mitochondrial and peroxisomal dysfunctions contributing to the overproduction of oxysterols, thereby creating an amplification loop [**30**].

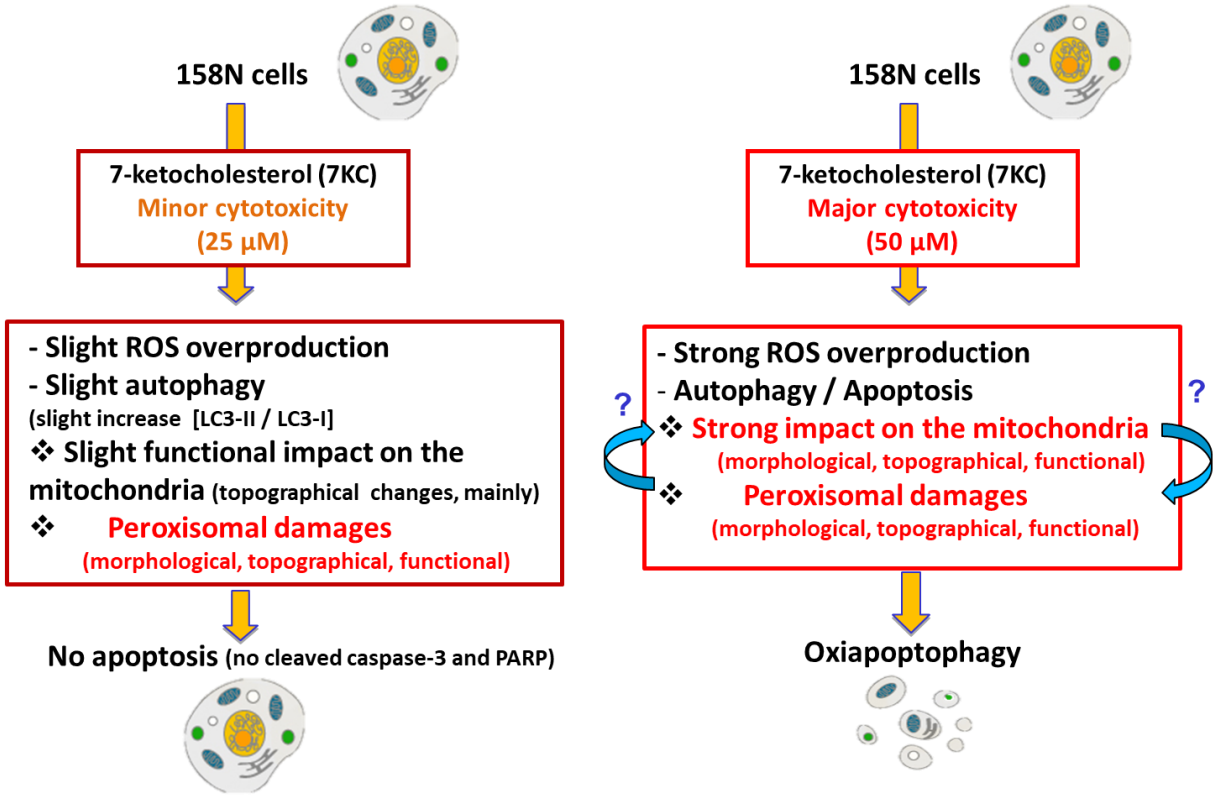

Figure 4: Association of peroxisomal damages with mitochondrial dysfunctions in 7-ketocholesterol-treated 158N murine oligodendrocytes. 7-ketocholesterol (7KC)-induced topographical, morphological and functional peroxisomal changes are observed either with slight or strong mitochondrial dysfunctions, slight or strong ROS overproduction and without or with cell death induction (oxiapoptophagy) on 158N cells. The cellular model (158N cells treated with 7KC) has been used to clarify the relationships between peroxisome and mitochondria (and vis versa) during 7KC-induced side effects leading either to slight cytotoxic effects (7KC: 25 µM) or oxiapoptophagy (7KC: 50 µM) The figure was reproduced with the written consent of Elsevier Editor (Nury T *et al.*, Induction of peroxisomal changes in oligodendrocytes treated with 7-ketocholesterol: Attenuation by α-tocopherol **[23]**).

Article 4

Oxiapoptophagy: a type of cell death induced by some oxysterols

Thomas Nury, Amira Zarrouk, Aline Yammine, John J Mackrill, Anne Vejux, Gérard Lizard

Br J Pharmacol, 2020, 10.1111/bph.15173. doi:10.1111/bph.15173

Le 7KC induit une toxicité sur les organites (mitochondrie, lysosome, peroxysome et réticulum endoplasmique) associée à la mort des cellules nerveuses (oligodendrocytes, microglie, neurones). Ce type de mort cellulaire inclus trois composantes : une élévation du stress oxydant (surproduction d'ERO), une activation de l'apoptose impliquant la mitochondrie (chute du $\Delta\psi m$, clivage de la caspas-3 et de PARP) et la présence de marqueurs autophagiques (augmentation du ratio LC3-II / LC3-I et de l'expression de p62). Cette mort cellulaire a été qualifiée d'oxyapoptophagie (stress O**xy**dant + A**popto**se + Auto**phagie**).

Cette notion d'oxyapoptophagie est apparue en 2003 lorsque des cellules monocytaires U937 traitées par du 7KC et du 7β-OHC ont présenté des caractéristiques de mort cellulaire différentes de celles induites par des agents pro-apoptotiques anti-tumoraux (Miguet-Alfonsi *et al.*, 2002; Monier *et al.*, 2003).

Mes travaux ont apporté de nouveaux éléments qui démontrent que différents oxystérols (7KC, 7β-OHC et 24(S)-OHC) sont de puissants inducteurs d'oxyapoptophagie sur des cellules nerveuses (oligodendrocytes (158N), microglie (BV-2) et neurones (N2a)). Des molécules cytoprotectrices prévenant l'oxyapoptophagie (acides gras, α-tocophérol, huiles végétales) sont également présentées.

La revue fait l'état des connaissances sur la notion d'oxyapoptophagie induite par les oxystérols et sur les molécules pouvant s'opposer à ce type de mort en soulignant l'intérêt qu'elles peuvent avoir pour traiter les maladies liées à l'âge (maladies cardiovasculaires, maladies oculaires, maladies neurodégénératives) et inflammatoires chroniques (maladies inflammatoires intestinales).

Received: 17 March 2020 | Revised: 2 June 2020 | Accepted: 10 June 2020

DOI: 10.1111/bph.15173

REVIEW ARTICLE THEMED ISSUE

Oxiapoptophagy: A type of cell death induced by some oxysterols

Thomas Nury[1] | Amira Zarrouk[2,3] | Aline Yammine[1,4] | John J. Mackrill[5] | Anne Vejux[1] | Gérard Lizard[1]

[1]Team "Biochemistry of the Peroxisome, Inflammation and Lipid Metabolism" EA 7270/ Inserm, University Bourgogne Franche-Comté, Dijon, France

[2]Faculty of Medicine, LR12ES05, Lab-NAFS "Nutrition - Functional Food & Vascular Health", University of Monastir, Monastir, Tunisia

[3]Laboratory of Biochemistry, Faculty of Medicine, University of Sousse, Sousse, Tunisia

[4]Bioactive Molecules Research Laboratory, Doctoral School of Sciences and Technologies, Faculty of Sciences, Lebanese University, Beirut, Lebanon

[5]Department of Physiology, School of Medicine, University College Cork, Cork, Ireland

Correspondence
Dr Gérard Lizard and Dr Anne Vejux, Faculté des Sciences Gabriel, Laboratoire Bio-peroxIL/EA7270, 6 Boulevard Gabriel, 21000 Dijon, France.
Email: gerard.lizard@u-bourgogne.fr; anne.vejux@u-bourgogne.fr

Funding information
ABASIM; SNDA; Association de Soins et Services à Domicile; PHC-ULYSSES; Univ. Monastir; Univ. Bourgogne

Oxysterols are oxidized forms of cholesterol generated from cholesterol by auto-oxidation, enzymatic processes, or both. Some of them (7-ketocholesterol, 7β-hydroxycholesterol and 24(S)-hydroxycholesterol), when used at cytotoxic concentrations on different cell types from different species (mesenchymal bone marrow cells, monocytic cells and nerve cells), induce a type of cell death associated with OXIdative stress and several characteristics of APOPTOsis and autoPHAGY, defined as oxiapoptophagy. Oxidative stress is associated with overproduction of ROS, increased antioxidant enzyme activities, lipid peroxidation and protein carbonylation. Apoptosis is associated with activation of the mitochondrial pathway, opening of the mitochondrial permeability pore, loss of mitochondrial membrane potential, caspase-3 activation, PARP degradation, nuclear condensation and/or fragmentation. Autophagy is characterized by autophagic vacuoles revealed by monodansylcadaverine staining and transmission electron microscopy, plus increased ratio of LC-3II/LC-3I. In addition, morphological, topographical and functional changes of the peroxisome are observed.

1 | OXYSTEROLS AND AGE-RELATED DISEASES

In vitro, some oxysterols have been shown to be cytotoxic in several human and animal cell types (Mutemberezi, Guillemot-Legris, & Muccioli, 2016; Otaegui-Arrazola, Menéndez-Carreño, Ansorena, & Astiasarán, 2010). Special attention is being paid to 7-ketocholesterol (7KC) and 7β-hydroxycholesterol (7β-OHC) in order to better understand their biological activities and the signalling pathways on which they act, as they are often found in increased amounts in the tissues and plasma of patients with various age-related diseases (Zarrouk et al., 2014). 7KC and 7β-OHC are formed by auto-oxidation but can also be the product of enzymatic reactions (Vejux et al., 2020). 7β-OHC can be formed from 7KC by the enzyme 11β-HSD1 and 7KC from 7β-OHC by the enzyme 11β-HSD2 (Vejux et al., 2020). 7KC can also be formed from 7-dehydrocholesterol, an immediate precursor of cholesterol in the Kandutsch–Russell pathway, by the enzyme CYP7A1 (Björkhem et al., 2014; Shinkyo et al., 2011). 7KC and 7β-OHC are present in high amounts in the plasma and atheromatous plaques of patients with cardiovascular

Abbreviations: 24S-OHC, 24(S)-hydroxycholesterol; 7KC, 7-ketocholesterol; 7β-OHC, 7β-hydroxycholesterol; DHA, docosahexaenoic acid; DHE, dihydroethidine/dihydroethidium; DHR123, dihydrorhodamine 123; DMF, dimethyl fumarate; MMF, monomethyl fumarate; mPTP, mitochondrial permeability transition pore; OA, oleic acid.

disease. 7KC is also present in retinal lipid deposits called drusens in patients with age-related macular degeneration and 7KC and 7β-OHC are present at elevated levels in the cortex of patients with advanced Alzheimer's disease (Anderson et al., 2020; Rodríguez & Larrayoz, 2010; Testa, Rossin, Poli, Biasi, & Leonarduzzi, 2018; Zarrouk et al., 2014). 7KC is also suspected to play an important role in inflammatory bowel disease (Sottero, Rossin, Poli, & Biasi, 2018).

In the most frequent age-related diseases, which are highly disabling and represent a high cost to society (cardiovascular, eye and neurodegenerative diseases), it is now well established that oxidative stress is increased and can lead to changes in proteins (protein carbonylation) and lipids (lipid peroxidation) (Jacob, Noren Hooten, Trzeciak, & Evans, 2013). This lipid peroxidation promotes the increase in tissue 7KC and 7β-OHC that accumulate in the lesions (Zerbinati & Iuliano, 2017). This observation has led to questions about the cytotoxic activities of 7KC and 7β-OHC in terms of the induction of oxidative stress, cell death and inflammation, which are known to contribute to the development of major age-related diseases (cardiovascular disease, age-related macular degeneration and Alzheimer's disease). The impact of 7KC and 7β-OHC on organelles (mitochondria, peroxisomes, lysosomes and endoplasmic reticulum) necessary for cellular metabolism (energy production, control of the redox balance and intracellular traffic) is also discussed, as well as the relationships between oxidative stress, organelle dysfunction and cell death. These discoveries led to the notion of oxiapoptophagy.

2 | CELL DEATH BY OXIAPOPTOPHAGY

The ability of some oxysterols (25-**hydroxycholesterol** and 7β-OHC) to induce apoptosis was first described by P. Bischoff's team in 1993 and 1995 in human monocytic U937 and HL60 cells, murine lymphoma cells and normal thymocytes (Aupeix et al., 1995; Christ, Luu, Mejia, Moosbrugger, & Bischoff, 1993). Subsequently, the pro-apoptotic potential of oxysterols (7KC, 7β-OHC, 19-hydroxycholesterol, cholesterol 5α, 6α epoxide and 25-hydroxycholesterol) was confirmed in bovine aortic endothelial cells (Lizard et al., 1996) and it was also shown by our laboratory that in human promonocytic leukaemic U937 cells, 7KC-induced apoptosis also triggers oxidative stress associated with lipid peroxidation, a decrease of reduced glutathione (GSH) levels and over production of ROS (Lizard et al., 1998). In rabbit smooth muscle cells (SMCs), it was shown by Martinet, Schrijvers, Timmermans and Bult (2008) that 7KC caused cell death, mainly via autophagic vesicle formation, with LC3 (microtubule-associated protein 1A/1B-light chain 3) processing. These observations suggested that oxysterols may induce cell death with a simultaneous combination of oxidative stress, apoptosis and autophagy. In 2003, the notion of oxiapoptophagy was introduced by demonstrating that apoptosis in U937 cells induced by 7KC and 7β-OHC presented characteristics that are clearly distinguishable from those induced by pro-apoptotic anti-tumour agents such as **vinblastine**, cytosine β-D-arabinofuranoside, **cycloheximide** and **staurosporine** (Miguet-Alfonsi et al., 2002; Monier et al., 2003). Indeed, with 7KC and 7β-OHC, but not with anti-tumour agents, we observed a type of cell death called oxiapoptophagy, simultaneously associated with oxidative stress as well as apoptotic and autophagic criteria. In oxysterol (7KC, 7β-OHC,and 24(S)-**hydroxycholesterol** [24S-OHC])-induced oxiapoptophagy, the role of mitochondria, in particular the opening of the mitochondrial permeability transition pore (mPTP) and the release of pro-apoptotic components such as cytochrome C, has been shown at an early stage on different cell types (Anderson et al., 2020; Zarrouk et al., 2014). In 2005, it was demonstrated that three pharmacologically distinct inhibitors of the mitochondrial permeability transition pore (bongkrekic acid, **cyclosporin** A and carboxyatractyloside, Briston, Selwood, Szabadkai, & Duchen, 2019) inhibited U937 oxiapoptophagy caused by 7β-OHC, but not cell death initiated by cholesterol-5β,6β-epoxide, an oxysterol which is cytotoxic via distinct mechanisms (Ryan, O'Callaghan, & O'Brien, 2005). Cell death induced by 7KC in the PC12 pheochromocytoma cell line is abolished by **trifluoperazine**, which antagonizes both the mitochondrial permeability transition pore and the Ca^{2+} effector protein, **calmodulin** (Han, Kim, Han, & Lee, 2007).

The notion of oxiapoptophagy has been gradually confirmed and it has been clearly established that certain oxysterols (7KC, 7β-OHC and 24S-OHC) are strong inducers of oxiapoptophagy (Klionsky et al., 2016; Nury et al., 2014, 2015). These data established that oxysterols oxidized either on the steroid nucleus or on the side chain, resulting either from the auto-oxidation of cholesterol (7KC and 7β-OHC) or enzymatically formed from cholesterol via the enzyme cholesterol 24-hydroxylase (CYP46A1) such as 24S-OHC (also called cerebrosterol) (Russell, 2000), can induce oxiapoptophagy. In our laboratory, oxiapoptophagic cell death was subsequently demonstrated in human U937 cells and murine nerve cells (oligodendrocyte 158N cells, microglial BV-2 cells and neuroblastoma Neuro-2a/N2a cells) (Leoni et al., 2017; Nury et al., 2015, 2017). Oxiapoptophagy has also been described on 7KC-treated bone marrow mesenchymal stem cells from patients with acute myeloid leukaemia (Paz et al., 2019).

Notably, in these different cells, oxiapoptophagy presents the same characteristics (Figure 1). In 158N, BV-2 and/or N2a cells, the oxysterols (7KC, 7β-OHC, and 24S-OHC) trigger an overproduction of ROS revealed by staining with dihydroethidine/dihydroethidium (DHE), dihydrorhodamine 123 (DHR123) and/or MitoSOX which could trigger an enhanced activity of glutathione peroxidase (GPx), superoxide dismutase (SOD) and catalase as well as lipid peroxidation and protein carbonylation, a loss of mitochondrial membrane potential ($\Delta\Psi m$) measured with $DiOC_6(3)$, **caspase-3** activation, **PARP** degradation, reduced expression of **Bcl-2**, and condensation and/or fragmentation of the nuclei, which are typical criteria of oxidative stress and apoptosis. They also favour the formation of large cytoplasmic vacuoles revealed by staining with monodansylcadaverine, considered as autophagic vacuoles and the activation of LC3-I into LC3-II considered as autophagic criteria connected with the autophagosome formation (Nury et al., 2015, 2017; Sghaier, Nury, et al., 2019; Sghaier, Zarrouk, et al., 2019). In BV-2 cells treated with 7KC, an increase in p62 levels was also reported (Nury et al., 2017). Increased

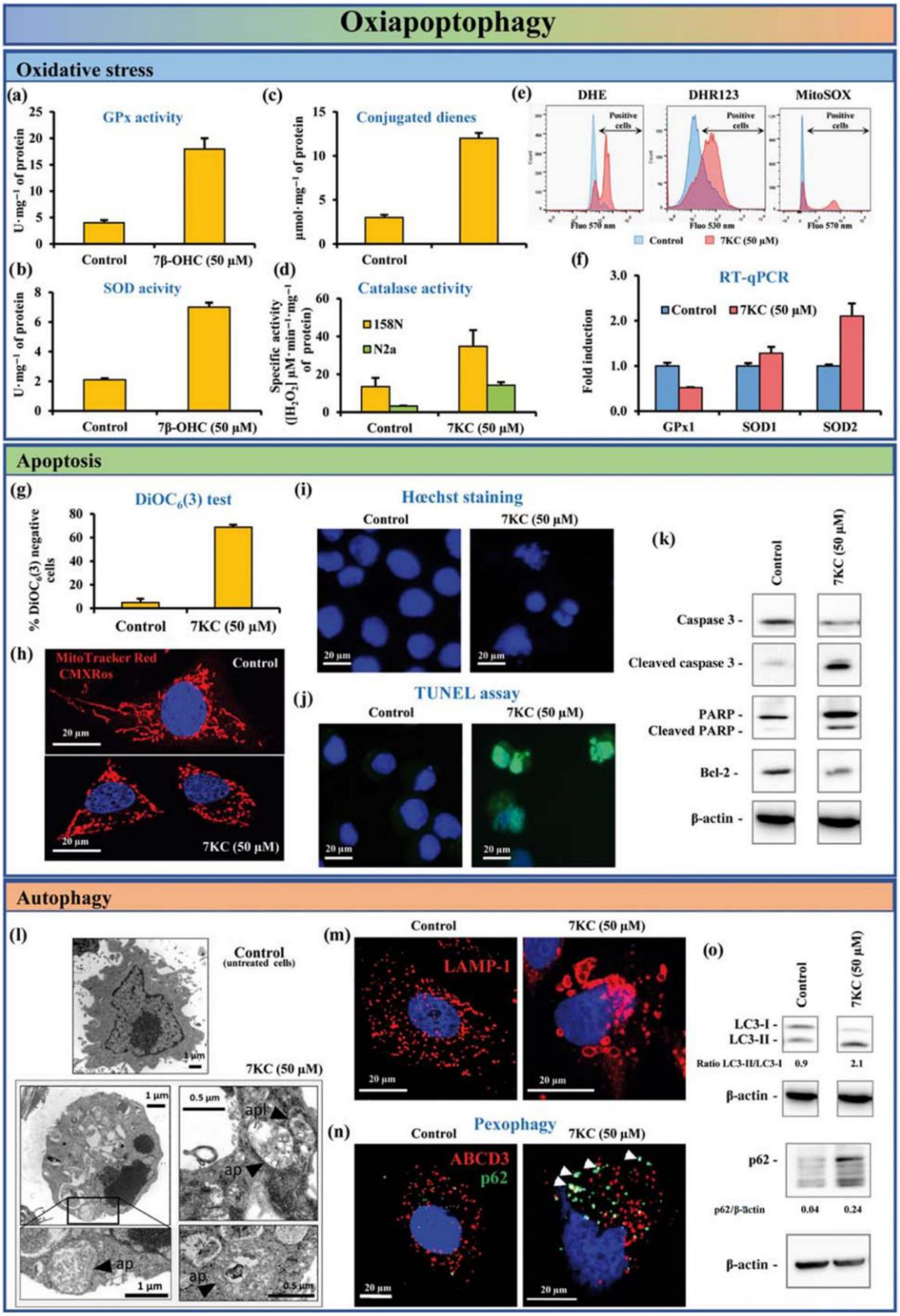
Oxiapoptophagy
Oxidative stress
(a)
GPx activity
U·mg⁻¹ of protein
Control
7β-OHC (50 µM)
(b)
SOD acivity
U·mg⁻¹ of protein
Control
7β-OHC (50 µM)
(c)
Conjugated dienes
µmol·mg⁻¹ of protein
Control
(d)
Catalase activity
Specific activity ([H2O2] µM·min⁻¹·mg⁻¹ of protein)
158N
N2a
Control
7KC (50 µM)
(e)
DHE
DHR123
MitoSOX
Positive cells
Fluo 570 nm
Fluo 530 nm
Control
7KC (50 µM)
(f)
RT-qPCR
Control
7KC (50 µM)
Fold induction
GPx1
SOD1
SOD2
Apoptosis
(g)
DiOC6(3) test
% DiOC6(3) negative cells
Control
7KC (50 µM)
(h)
MitoTracker Red CMXRos
Control
7KC (50 µM)
20 µm
(i)
Hœchst staining
Control
7KC (50 µM)
(j)
TUNEL assay
Control
7KC (50 µM)
(k)
Control
7KC (50 µM)
Caspase 3 -
Cleaved caspase 3 -
PARP -
Cleaved PARP -
Bcl-2 -
β-actin -
Autophagy
(l)
Control
(untreated cells)
7KC (50 µM)
ap
apl
1 µm
0.5 µm
(m)
Control
7KC (50 µM)
LAMP-1
20 µm
(n)
Pexophagy
Control
7KC (50 µM)
ABCD3
p62
20 µm
(o)
Control
7KC (50 µM)
LC3-I -
LC3-II -
Ratio LC3-II/LC3-I
0.9
2.1
β-actin -
p62 -
p62/β-actin
0.04
0.24
β-actin -

FIGURE 1 Morphological and biochemical characteristics of oxiapoptophagy. Oxiapoptophagy is a type of cell death induced by some oxysterols (7KC, 7β-OHC and 24S-OHC) but not by anti-tumoural drugs (vinblastine, cytosine β-D-arabinofuranoside, cycloheximide and staurosporine). It is characterized by OXIdative stress, APOPTOsis and autoPHAGY. Data obtained from murine nerve cells (oligodendrocytes 158N, microglial BV-2 cells, and neuroblastoma N2a cells) are summarized. In 158N, BV-2 and N2a cells, under treatment with 7KC, 7β-OHC and 24S-OHC, oxidative stress is characterized by an overproduction of ROS (e) revealed after staining with DHE, DHR123 and MitoSOX (detection of ROS overproduction at the mitochondrial level) (Nury et al., 2015; Nury et al., 2018; Yammine et al., 2020), which is considered to contribute to lipid peroxidation leading to enhanced levels of conjugated dienes (c); in turn, ROS overproduction could trigger an enhanced activity of GPx, SOD and catalase (a, b, d) (Sghaier, Nury, et al., 2019; Sghaier, Zarrouk, et al., 2019); in N2a cells, under treatment with 7KC, compared to untreated cells (control), lower mRNA levels of GPx1 were observed whereas higher levels of SOD1 and SOD2 were detected (f). Whatever the cell type considered (158N, BV-2, and N2a cells), a mode of cell death by apoptosis was observed under treatment with 7KC, 7β-OHC and 24S-OHC; it was characterized by a loss of ΔΨm (g: increased % of $DiOC_6(3)$ negative cells); by a modification of the subcellular distribution of the mitochondria (h: clusters of mitochondria were often observed in oxysterols-treated cells); by a condensation and/or fragmentation of the nuclei (i) which is characteristic of apoptotic cells; by an internucleosomal DNA fragmentation revealed by the TUNEL assay (Ragot et al., 2013) (j); and by caspase-3 activation, PARP degradation and lower Bcl-2 level (k); these characteristics support an activation of the mitochondrial pathway during oxysterol-induced apoptosis. As for autophagy, whatever the cell type considered (158N, BV-2 and N2a cells), it was characterized by both morphological and biochemical criteria. In 158N and BV-2 cells treated with either 7KC or 7β-OHC, autophagic vacuoles evocating autophagosome (ap) and autophagolysosome (apl) (Nury et al., 2015) were observed by transmission electron microscopy in the cytoplasm of cells with condensed and/or fragmented nuclei (apoptotic cells) (l): some of these vacuoles have double membranes and evocate autophagosome (ap), whereas some others have parts of membranes or no membranes and evocate autophagolysosome (apl) (pictures obtained by transmission electron microscopy [Nury et al., 2015] were reproduced with the agreement of Elsevier; copyright transfer agreement, licence: 4834241280326, Dr Gérard Lizard/Elsevier). Moreover, with an antibody raised against the lysosomal-associated membrane protein 1 (*LAMP-1*) also known as lysosome-associated membrane glycoprotein 1 or CD107a, large vacuoles resembling autophagic vacuoles were detected (m). In addition, by dual staining with an antibody directed against the p62 protein localized at the membrane level of the autophagosome and of the autolysosome (revealed with Alexa 488; green fluorescence) and with an antibody raised against the ABCD3 peroxisomal transporter (revealed with Alexa 546; red fluorescence), a colocalization of p62 and ABCD3 (yellow dots indicated by white arrows) was observed under a fluorescent microscope coupled with an Apotome (Zeiss) supporting the occurrence of pexophagy (n) (Nury et al., 2018). In 158N and BV-2 cells treated with 7KC, 7β-OHC or 24S-OHC, compared to untreated cells (control), an activation of LC3-I into LC3-II associated with a higher ratio (LC3-II/LC3-I) was observed (Nury et al., 2015; Nury et al., 2017; similar data were obtained on N2a cells: unpublished results) and on BV-2 cells treated with 7KC, an enhancement of p62 level was found (o) (Nury et al., 2017). It is considered that the most suitable and minimal criteria required to demonstrate the occurrence of oxiapoptophagy are ROS overproduction, condensation and/or fragmentation of the nuclei associated with caspase-3 activation and PARP degradation as well as conversion of LC3-I into LC3-II

p62 levels have also been observed with different drugs and when ROS production results in cytotoxic effects associated with an increase in potential autophagy substrates (protein aggregates and misfolded proteins plus altered mitochondria and lysosomes), endoplasmic reticulum stress may be activated (Chu, 2019; Lamark, Svenning, & Johansen, 2017; Li, Tan, Miao, Lei, & Zhang, 2015). It should be noted that whatever the cells considered, 7KC and 7β-OHC always induce ROS overproduction and that in human aortic SMCs, 7KC triggers endoplasmic reticulum stress involving NADPH oxidase-Nox-4, which leads to ROS overproduction and cell death by apoptosis (Pedruzzi et al., 2004). Few elements are currently available to define whether the observed autophagy is lethal or survival autophagy. However, activation of an autophagic process at low 7KC concentrations favours survival autophagy (Nury et al., 2018).

In 158N cells, organelle dysfunction (mitochondria and peroxisomes) induced by 7KC during oxiapoptophagy were well characterized. The loss of $\Delta\Psi_m$ is associated with a decrease of oxidative phosphorylation revealed by reduced NAD^+ and ATP, in addition the cellular lactate is higher while pyruvate, citrate, fumarate and succinate (tricarboxylic acid [TCA] cycle intermediates) are significantly reduced (Leoni et al., 2017). In 158N and BV-2 cells, 7KC-induced oxiapoptophagy, which is associated with an activation of the mitochondrial apoptotic pathway, also induces several marked peroxisomal changes (Nury et al., 2017, 2018). Morphological, topographical and functional peroxisome alterations linked with modifications of the cytoplasmic distribution of mitochondria and mitochondrial dysfunction (loss of ΔΨm and decreased level of cardiolipins) were observed. This includes the presence of peroxisomes with abnormal sizes and shapes, lower cellular levels of **ABCD3**, used as a marker of peroxisomal mass, lower mRNA and protein levels of ABCD1 and ABCD3 (two ATP-dependent peroxisomal transporters) and of acyl-CoA oxidase 1 (ACOX1) and multifunctional protein 2 (MFP2) enzymes involved in peroxisomal β-oxidation and plasmalogen synthesis, respectively, and increased levels of very long chain fatty acids (VLCFA: C24:0, C24:1, C26:0, and C26:1) metabolized by peroxisomal β-oxidation. It has also been shown that 7KC favours pexophagy (Nury et al., 2018). As the inactivation of peroxisomal biogenesis or of peroxisomal β-oxidation induces important mitochondrial modification and a rupture of redox homeostasis both *in vitro* and *in vivo*, it is suggested that oxysterol-induced peroxisomal dysfunction could amplify oxidative stress and cell death (Lismont, Nordgren, Van Veldhoven, & Fransen, 2015).

Currently, no study has been carried out on the detection of oxiapoptophagic cells *in vivo*. These are envisaged in readily available in atheromatous lesion tissues in which markers of oxidative stress, apoptosis, and autophagy have been revealed (Luo et al., 2016; Yang et al., 2017) and in which 7KC can be detected and quantified either by gas chromatography coupled with MS or by immunostaining with

specific antibodies. It is therefore technically possible and expected to demonstrate the highly probable *in vivo* existence of 7KC-induced oxiapoptophagy using histological sections of atheromatous lesions in which 7KC is present in significant amounts.

3 | INHIBITORS OF OXIAPOPTOPHAGY

Considering that cell death by oxiapoptophagy may be associated with age-related or chronic inflammatory diseases because it is induced by 7KC and 7β-OHC, it is important to identify natural or synthetic molecules as well as mixtures of molecules to inhibit or mitigate this type of death. At the moment, only few molecules (vitamins: α- and γ-tocopherol which are components of vitamin E; biotin which is also named vitamin B8, H or B7; ω-3 and ω-9 fatty acids: docosahexaenoic acid [DHA: C22:6 n-3] and oleic acid [OA: C18:1 n-9]; drugs: monomethyl fumarate [MMF] and dimethyl fumarate [DMF] and inhibitors of the mitochondrial permeability transition pore: bongkrekic **acid**, **cyclosporin A** and **carboxyatractyloside**) or mixtures of molecules (oils:- argan, olive and milk thistle seed oils) are able to counteract 7KC-, 7β-OHC- and/or 24S-OHC-induced oxiapoptophagy (Table 1). In this context, the most studied molecule is α-tocopherol, a major component of vitamin E (vit E:- a fat-soluble vitamin which covers a set of eight organic molecules, four tocopherols [α-, β-, γ-, and δ-tocopherol] and four tocotrienols [α-, β-, γ-, and δ-tocotrienol]), which prevents 7KC-, 7β-OHC- and 24S-OHC-induced oxiapoptophagy on 158N cells (Nury et al., 2015, 2018) and 7KC-induced oxiapoptophagy on BV-2 and N2a cells (Nury et al., 2017; Yammine et al., 2020). Currently, it is well described in various cell types that α-tocopherol counteracts 7KC-induced oxiapoptophagy by reducing the accumulation of 7KC in the lipid rafts preventing thus the cascade of signals leading to the loss of ΔΨm, mitochondrial and peroxisomal changes, caspase cascade activation, apoptosis and autophagy (Brahmi et al., 2019; Vejux et al., 2020). However, in 158N cells, 7KC-induced side effects were not attenuated by α-tocotrienol, whereas the antioxidant properties of α-tocotrienol and α-tocopherol determined with the ferric reducing antioxidant power (FRAP) assay were in the same range (Nury et al., 2018). In BV-2 cells, cytoprotective effects of α-tocotrienol and γ-tocopherol were observed, whereas Trolox was inefficient (Debbabi et al., 2016). In 158N cells, compared to α-tocopherol, the polyphenols (ellagic acid, **resveratrol**) as well as ferulic acid have no cytoprotective effects (Badreddine et al., 2015; Ragot et al., 2013), whereas in human retinal epithelial pigment cells (ARPE-19), resveratrol has some protective effects against 7KC- and 7β-OHC-induced cell death and vascular endothelial growth factor (**VEGF**) secretion (Dugas et al., 2010). As it is well established that α-tocopherol attenuates oxysterol-induced oxidative stress and apoptosis in a wide range of cells, it is often used as a reference molecule for the identification of new cytoprotectants (Brahmi et al., 2019). It has also been reported that biotin (also named Vitamin B8 or H) reduces 7β-OHC-induced oxiapoptophagy in 158N cells, whereas it is inefficient in preventing 7KC-induced cell death (Sghaier, Zarrouk, et al., 2019). Mediterranean and Okinawan diets are rich in ω-3 and ω-9 fatty acids such as docosahexaenoic acid (**DHA**) and oleic acid (**OA**) and are also associated with improved age-related health (Wahl et al., 2019). Consequently, the cytoprotective effects of DHA and OA were also studied. In 158N cells, DHA prevents 7KC-, 7β-OHC- and 24S-OHC-induced oxiapoptophagy (Nury et al., 2015). In addition, greater cytoprotection was observed when α-tocopherol and DHA were combined (Nury et al., 2015). In BV-2 cells, DHA and OA attenuate 7KC-induced side effects characteristic of oxiapoptophagy associated with mitochondrial and peroxisomal dysfunction (Debbabi et al., 2016; Debbabi et al., 2017).

In murine 158N oligodendrocytes, DMF and MMF attenuate the different effects of 7KC and 7β-OHC, namely, cell growth inhibition and/or loss of cell adhesion, decrease of ΔΨm, ROS overproduction, caspase-3 and PARP cleavage, nuclear condensation and fragmentation and activation of LC3-I into LC3-II (Sghaier, Nury, et al., 2019; Zarrouk et al., 2017).

In 158N and BV-2 cells, edible oils of Mediterranean origin (argan, olive and milk thistle seed oils), rich in tocopherols and/or OA, also attenuate oxysterol (7KC, 24S-OHC)-induced oxiapoptophagy and associated organelle alterations (mitochondria, peroxisome, and lysosome) (Badreddine et al., 2017; Meddeb et al., 2018; Zarrouk et al., 2019).

Mechanistically, in addition to the knowledge already acquired on the cell dysfunctions involved in the induction of oxiapoptophagy (Brahmi et al., 2019; Vejux et al., 2020), the ability of the different molecules currently identified to prevent 7KC-, 7β-OHC- and 24S-OHC-induced oxiapoptophagy allows for the development of new hypotheses on the receptors and signalling pathways that could be affected by these oxysterols. For 7KC and 7β-OHC, interactions with the antiestrogen binding site (AEBS) should be considered (de Medina, Paillasse, Segala, Poirot, & Silvente-Poirot, 2010). For 24S-OHC, which is a liver X receptor (LXR: **LXR**-α and **LXR**-β) agonist (Björkhem, 2013; Janowski et al., 1999; Lehmann et al., 1997), the role of this nuclear receptor in 24S-induced oxiapoptophagy is yet to be specified. In addition, as several oxysterol-binding protein (OSBP)-related (ORP) proteins regulate organelle lipid composition and cell signalling (Olkkonen, 2013), an involvement of ORPs in oxiapoptophagy cannot be excluded. The identification of receptors associated with oxiapoptophagy should make it possible to better control this type of death in order to activate or repress it, depending on the pathologies considered. Furthermore, the cytoprotective activities of **dimethyl fumarate** (DMF) and **monomethyl fumarate** (MMF), described to activate the nuclear factor, erythroid 2 like 2 (NFR2) transcription factor, which induces the expression of genes coding for antioxidant enzymes under stress conditions (Koss-Mikołajczyk et al., 2019), also open new perspectives to act on oxiapoptophagy via the NRF2 signalling pathway. In terms of mitochondrial drug targets for the prevention of oxiapoptophagy the structure of the mitochondrial permeability transition pore has not been defined to date, preventing docking-based routes for the design of new ligands and there have been multiple limitations to the application of known mitochondrial permeability transition pore antagonists to clinical

TABLE 1 Inhibitors of oxiapoptophagy

Inhibitors of oxiapoptophagy	Inducers of oxiapoptophagy	Cells	References
Natural molecules			
α-Tocopherol (major component of Vit E)	7KC	Oligodendrocytes—158N	Nury T et al., Biochem Biophys Res Commun. 2014; 446(3): 714–719 Nury T et al., Steroids. 2015; 99(Pt B): 194–203 Nury T et al., Biochimie. 2018; 153: 181–202
		Microglial cells—BV-2	Debbabi M et al., Int J Mol Sci. 2016; 17(12)
	7β-OHC	Oligodendrocytes—158N	Nury T et al., Steroids. 2015; 99(Pt B): 194–203 Sghaier R et al., Free Radic Res. 2019; 53(5): 535–561 Sghaier R et al., J Steroid Biochem Mol Biol. 2019; 194: 105432
	24S-OHC	Oligodendrocytes—158N	Nury T et al., Steroids. 2015; 99(Pt B): 194–203 Meddeb W et al., Antioxidants (Basel). 2018; 7(7)
γ-Tocopherol (component of Vit E)	7KC	Microglial cells—BV-2	Debbabi M et al., Int J Mol Sci. 2016; 17(12)
Biotin (Vit B8 or H)	7β-OHC	Oligodendrocytes—158N	Sghaier R et al., J Steroid Biochem Mol Biol. 2019; 194: 105432
DHA (docosahexaenoic acid; C22:6 n-3)	7KC, 7β-OHC, 24S-OHC	Oligodendrocytes—158N	Nury T et al., Steroids. 2015; 99(Pt B): 194–203
	7KC	Microglial cells—BV-2	Debbabi et al., Chem Phys Lipids. 2017; 207(Pt B): 151–170
OA (oleic acid; C18:1 n-9)	7KC	Microglial cells—BV-2	Debbabi M et al., Int J Mol Sci. 2016; 17(12) Debbabi et al., Chem Phys Lipids. 2017; 207(Pt B): 151–170
Drugs			
Dimethyl fumarate (DMF, commercialized under the name TECFIDERA)	7KC	Oligodendrocytes—158N	Zarrouk A et al., J Steroid Biochem Mol Biol. 2017; 169: 29–38
DMF and monomethyl fumarate (MMF, major metabolite of DMF)	7β-OHC	Oligodendrocytes—158N	Sghaier R et al., Free Radic Res. 2019; 53(5): 535–561
mPTP antagonists (bongkrekic acid, cyclosporin A, carboxyatractyloside)	7β-OHC	Monocyte/macrophage—U937	Ryan L et al., Br J Nutr. 2005; 94(4): 519–525
Mixture of molecules			
α-Tocopherol + DHA	7KC, 7β-OHC, 24S-OHC	Oligodendrocytes—158N	Nury T et al., Steroids. 2015; 99(Pt B): 194–203
Argan oil	7KC	Oligodendrocytes—158N	Badreddine A et al., Int J Mol Sci. 2017; 18(10)
Milk thistle seed oil	7KC, 24S-OHC	Oligodendrocytes—158N	Meddeb W et al., Antioxidants (Basel). 2018; 7(7)
Olive oil	7KC	158N and BV-2	Zarrouk A et al., Curr Pharm Des. 2019; 25(15): 1791–1805

settings (Briston et al., 2019). However, several molecules that are known to block oxysterol-induced cell death are also inhibitors of the mitochondrial permeability transition pore, including DHA in rat heart mitochondria (Khairallah et al., 2012), α-tocopherol in rat liver (Gumpricht et al., 2008), and the olive oil component hydroxytyrosol in a myocardial ischaemia–reperfusion injury model (Miao et al., 2019). Finally, there is considerable interplay between steroid biosynthesis, transport, and mitochondrial function. One key mechanism involved in these processes is the translocator protein, which is involved in cholesterol import into the mitochondria and is also a putative component of the mitochondrial permeability transition pore (Briston et al., 2019). Caprospinol is a drug based on the structure of the naturally occurring oxysterol 22R-hydroxycholesterol, which acts on the translocator protein and restores cognitive

impairment in a rat model of AD (Papadopoulos & Lecanu, 2012). These observations raise the possibility of generating oxysterol-based ligands for targeting mitochondrial dysfunction in oxiapoptophagic pathologies, such as Alzheimer's disease, cardiovascular disease and age-related macular degeneration.

4 | CONCLUSION

Since some age-related diseases involve oxidative stress, apoptosis, and autophagy, it is very likely that cell death by oxiapoptophagy will occur at the lesion level in patients affected by these pathologies. The identification of this type of death could lead to new approaches to the pathophysiology of these diseases, the identification of new therapeutic targets, and the development of new treatments. Moreover, the cellular models available to study oxiapoptophagy are relevant to define the relationships between oxidative stress, apoptosis, and autophagy but also to clarify the contribution of peroxisome in cell degeneration and to deepen understanding of the relationships between mitochondria and peroxisome during this process.

4.1 | Nomenclature of targets and ligands

Key protein targets and ligands in this article are hyperlinked to corresponding entries in http://www.guidet opharmacology.org, the common portal for data from the IUPHAR/BPS Guide to PHARMACOLOGY (Harding et al., 2018), and are permanently archived in the Concise Guide to PHARMACOLOGY 2019/20 (Alexander, Fabbro, et al., 2019; Alexander, Kelly, et al., 2019) and in the IUPHAR/BPS Guide to Pharmacology Database (McDonnell & Safi, 2019).

ACKNOWLEDGEMENTS

This work was supported by grants from Univ. Bourgogne (Dijon, France), Univ. Monastir (Tunis, Tunisia), PHC-ULYSSES (University College of Cork [UCC], Ireland/Univ. Bourgogne, France), ASSAD (Association de Soins et Services à Domicile, Louhans, France), SNDA (Société Nationale de Défense des Animaux; Prix Renard 2018), and ABASIM (Association Bourguignonne pour les Applications des Sciences de l'Information en Médecine, Dijon, France).

CONFLICT OF INTEREST

The authors declare no conflicts of interest.

REFERENCES

Alexander, S. P. H., Fabbro, D., Kelly, E., Mathie, A., Peters, J. A., Veale, E. L., … CGTP collaborators. (2019). The Concise Guide to PHARMACOLOGY 2019/20: Enzymes. *British Journal of Pharmacology*, *176*, S297–S396.

Alexander, S. P. H., Kelly, E., Mathie, A., Peters, J. A., Veale, E. L., Armstrong, J. F., … CGTP collaborators. (2019). The Concise Guide to PHARMACOLOGY 2019/20: Transporters. *British Journal of Pharmacology*, *176*, S397–S493.

Anderson, A., Campo, A., Fulton, E., Corwin, A., Jerome, W. G. 3rd, & O'Connor, M. S. (2020). 7-Ketocholesterol in disease and aging. *Redox Biology*, *29*, 101380. https://doi.org/10.1016/j.redox.2019.101380

Aupeix, K., Weltin, D., Mejia, J. E., Christ, M., Marchal, J., Freyssinet, J. M., & Bischoff, P. (1995). Oxysterol-induced apoptosis in human monocytic cell lines. *Immunobiology*, *194*(4–5), 415–428.

Badreddine, A., Zarrouk, A., Karym, E. M., Debbabi, M., Nury, T., Meddeb, W., … Lizard, G. (2017). Argan oil-mediated attenuation of organelle dysfunction, oxidative stress and cell death induced by 7-ketocholesterol in murine oligodendrocytes 158N. *International Journal of Molecular Sciences*, Oct, 23, *18*(10). https://doi.org/10.3390/ijms18102220

Badreddine, A., Zarrouk, A., Nury, T., El Kharrassi, Y., Nasser, B., Malki, M. C., … Samadi, M. (2015). An expeditious synthesis of spinasterol and schottenol, two phytosterols present in argan oil and in cactus pear seed oil, and evaluation of their biological activities on cells of the central nervous system. *Steroids*, *99*(Pt B), 119–124.

Björkhem, I. (2013). Five decades with oxysterols. *Biochimie*, *95*(3), 448–454.

Björkhem, I., Diczfalusy, U., Lövgren-Sandblom, A., Starck, L., Jonsson, M., Tallman, K., … Guengerich, F. P. (2014). On the formation of 7-ketocholesterol from 7-dehydrocholesterol in patients with CTX and SLO. *Journal of Lipid Research*, *55*(6), 1165–1172.

Brahmi, F., Vejux, A., Sghaier, R., Zarrouk, A., Nury, T., Meddeb, W., … Lizard, G. (2019). Prevention of 7-ketocholesterol-induced side effects by natural compounds. *Critical Reviews in Food Science and Nutrition*, *59*(19), 3179–3198.

Briston, T., Selwood, D. L., Szabadkai, G., & Duchen, M. R. (2019). Mitochondrial permeability transition: A molecular lesion with multiple drug targets. *Trends in Pharmacological Sciences*, *40*(1), 50–70.

Christ, M., Luu, B., Mejia, J. E., Moosbrugger, I., & Bischoff, P. (1993). Apoptosis induced by oxysterols in murine lymphoma cells and in normal thymocytes. *Immunology*, *78*(3), 455–460.

Chu, C. T. (2019). Mechanisms of selective autophagy and mitophagy: Implications for neurodegenerative diseases. *Neurobiology of Disease*, *122*, 23–34.

de Medina, P., Paillasse, M. R., Segala, G., Poirot, M., & Silvente-Poirot, S. (2010). Identification and pharmacological characterization of cholesterol-5,6-epoxide hydrolase as a target for tamoxifen and AEBS ligands. *Proceedings of the National Academy of Sciences of the United States of America*, *107*(30), 13520–13525.

Debbabi, M., Nury, T., Zarrouk, A., Mekahli, N., Bezine, M., Sghaier, R., … Lizard, G. (2016). Protective effects of α-tocopherol, γ-tocopherol and oleic acid, three compounds of olive oils, and no effect of trolox, on 7-ketocholesterol-induced mitochondrial and peroxisomal dysfunction in microglial BV-2 cells. *International Journal of Molecular Sciences*, 17(12). https://doi.org/10.3390/ijms17121973

Debbabi, M., Zarrouk, A., Bezine, M., Meddeb, W., Nury, T., Badreddine, A., … Lizard, G. (2017). Comparison of the effects of major fatty acids present in the Mediterranean diet (oleic acid, docosahexaenoic acid) and in hydrogenated oils (elaidic acid) on 7-ketocholesterol-induced oxiapoptophagy in microglial BV-2 cells. *Chemistry and Physics of Lipids*, *207*(Pt B), 151–170.

Dugas, B., Charbonnier, S., Baarine, M., Ragot, K., Delmas, D., Ménétrier, F., … Lizard, G. (2010). Effects of oxysterols on cell viability, inflammatory cytokines, VEGF, and reactive oxygen species production on human retinal cells: Cytoprotective effects and prevention of VEGF secretion by resveratrol. *European Journal of Nutrition*, *49*(7), 435–446.

Gumpricht, E., Devereaux, M. W., Dahl, R., Soden, J. S., Sparagna, G. C., Leonard, S. W., … Sokol, R. J. (2008). Resistance of young rat hepatic mitochondria to bile acid-induced permeability transition: Potential role of α-tocopherol. *Pediatric Research*, *64*(5), 498–504.

Han, J. H., Kim, Y. J., Han, E. S., & Lee, C. S. (2007). Prevention of 7-ketocholesterol-induced mitochondrial damage and cell death by calmodulin inhibition. *Brain Research*, *1137*(1), 11–19.

Harding, S. D., Sharman, J. L., Faccenda, E., Southan, C., Pawson, A. J., Ireland, S., … NC-IUPHAR. (2018). The IUPHAR/BPS Guide to PHARMACOLOGY in 2018: Updates and expansion to encompass the new guide to IMMUNOPHARMACOLOGY. *Nucleic Acids Research*, *46*(D1), D1091–D1106.

Jacob, K. D., Noren Hooten, N., Trzeciak, A. R., & Evans, M. K. (2013). Markers of oxidant stress that are clinically relevant in aging and age-related disease. *Mechanisms of Ageing and Development*, *134*(3–4), 139–157.

Janowski, B. A., Grogan, M. J., Jones, S. A., Wisely, G. B., Kliewer, S. A., Corey, E. J., & Mangelsdorf, D. J. (1999). Structural requirements of ligands for the oxysterol liver X receptors LXRα and LXRβ. *Proceedings of the National Academy of Sciences of the United States of America*, *96*, 266–271.

Khairallah, R. J., Kim, J., O'Shea, K. M., O'Connell, K. A., Brown, B. H., Galvao, T., … Stanley, W. C. (2012). Improved mitochondrial function with diet-induced increase in either docosahexaenoic acid or arachidonic acid in membrane phospholipids. *PLoS ONE*, *7*(3), e34402. https://doi.org/10.1371/journal.pone.0034402

Klionsky, D. J., Abdelmohsen, K., Abe, A., Abedin, M. J., Abeliovich, H., Acevedo Arozena, A., et al. (2016). *Autophagy*, *12*(1), 1–222.

Koss-Mikołajczyk, I., Baranowska, M., Todorovic, V., Albini, A., Sansone, C., Andreoletti, P., … Bartoszek, A. (2019). Prophylaxis of non-communicable diseases: Why fruits and vegetables may be better chemopreventive agents than dietary supplements based on isolated phytochemicals? *Current Pharmaceutical Design*, *25*(16), 1847–1860.

Lamark, T., Svenning, S., & Johansen, T. (2017). Regulation of selective autophagy: The p62/SQSTM1 paradigm. *Essays in Biochemistry*, *61*(6), 609–624.

Lehmann, J. M., Kliewer, S. A., Moore, L. B., Smith-Oliver, T. A., Oliver, B. B., Su, J. L., … Willson, T. M. (1997). Activation of the nuclear receptor LXR by oxysterols defines a new hormone response pathway. *The Journal of Biological Chemistry*, *272*, 3137–3140.

Leoni, V., Nury, T., Vejux, A., Zarrouk, A., Caccia, C., Debbabi, M., … Lizard, G. (2017). Mitochondrial dysfunctions in 7-ketocholesterol-treated 158N oligodendrocytes without or with α-tocopherol: Impacts on the cellular profil of tricarboxylic cycle-associated organic acids, long chain saturated and unsaturated fatty acids, oxysterols, cholesterol and cholesterol precursors. *The Journal of Steroid Biochemistry and Molecular Biology*, *169*, 96–110.

Li, L., Tan, J., Miao, Y., Lei, P., & Zhang, Q. (2015). ROS and autophagy: Interactions and molecular regulatory mechanisms. *Cellular and Molecular Neurobiology*, *35*(5), 615–621.

Lismont, C., Nordgren, M., Van Veldhoven, P. P., & Fransen, M. (2015). Redox interplay between mitochondria and peroxisomes. *Frontiers in Cell and Development Biology*, *3*, 35. https://doi.org/10.3389/fcell.2015.00035

Lizard, G., Deckert, V., Dubrez, L., Moisant, M., Gambert, P., & Lagrost, L. (1996). Induction of apoptosis in endothelial cells treated with cholesterol oxides. *The American Journal of Pathology*, *148*(5), 1625–1638.

Lizard, G., Gueldry, S., Sordet, O., Monier, S., Athias, A., Miguet, C., … Gambert, P. (1998). Glutathione is implied in the control of 7-ketocholesterol-induced apoptosis, which is associated with radical oxygen species production. *The FASEB Journal*, *12*(15), 1651–1663.

Luo, Y., Lu, S., Zhou, P., Ai, Q. D., Sun, G. B., & Sun, X. B. (2016). Autophagy: An exposing therapeutic target in atherosclerosis. *Journal of Cardiovascular Pharmacology*, *67*(3), 266–274.

Martinet, W., Schrijvers, D. M., Timmermans, J. P., & Bult, H. (2008). Interactions between cell death induced by statins and 7-ketocholesterol in rabbit aorta smooth muscle cells. *British Journal of Pharmacology*, *154*(6), 1236–1246.

McDonnell DP, Safi R (2019) Liver X receptor-like receptors (version 2019.4) in the IUPHAR/BPS Guide to Pharmacology Database. *IUPHAR/BPS Guide to Pharmacology CITE*. 2019(4).

Meddeb, W., Rezig, L., Zarrouk, A., Nury, T., Vejux, A., Prost, M., … Lizard, G. (2018). Cytoprotective activities of milk thistle seed oil used in traditional Tunisian medicine on 7-ketocholesterol and 24S-hydroxycholesterol-induced toxicity on 158N murine oligodendrocytes. *Antioxidants (Basel)* Jul, 19, *7*(7). https://doi.org/10.3390/antiox7070095

Miao, J., Huang, Z., Liu, S., Li, X., Jia, P., Guo, Y., … Jia, D. (2019). Hydroxytyrosol protects against myocardial ischemia reperfusion injury by inhibiting mitochondrial permeability transition pore opening. *Experimental and Therapeutic Medicine*, *17*(1), 671–678.

Miguet-Alfonsi, C., Prunet, C., Monier, S., Bessède, G., Lemaire-Ewing, S., Berthier, A., … Lizard, G. (2002). Analysis of oxidative processes and of myelin figures formation before and after the loss of mitochondrial transmembrane potential during 7β-hydroxycholesterol and 7-ketocholesterol-induced apoptosis: Comparison with various pro-apoptotic chemicals. *Biochemical Pharmacology*, *64*(3), 527–541.

Monier, S., Samadi, M., Prunet, C., Denance, M., Laubriet, A., Athias, A., … Lizard, G. (2003). Impairment of the cytotoxic and oxidative activities of 7β-hydroxycholesterol and 7-ketocholesterol by esterification with oleate. *Biochemical and Biophysical Research Communications*, *303*(3), 814–824.

Mutemberezi, V., Guillemot-Legris, O., & Muccioli, G. G. (2016). Oxysterols: From cholesterol metabolites to key mediators. *Progress in Lipid Research*, *64*, 152–169.

Nury, T., Sghaier, R., Zarrouk, A., Ménétrier, F., Uzun, T., Leoni, V., … Lizard, G. (2018). Induction of peroxisomal changes in oligodendrocytes treated with 7-ketocholesterol: Attenuation by α-tocopherol. *Biochimie*, *153*, 181–202.

Nury, T., Zarrouk, A., Mackrill, J. J., Samadi, M., Durand, P., Riedinger, J. M., … Lizard, G. (2015). Induction of oxiapoptophagy on 158N murine oligodendrocytes treated by 7-ketocholesterol-, 7β-hydroxycholesterol-, or 24(S)-hydroxycholesterol: Protective effects of α-tocopherol and docosahexaenoic acid (DHA; C22:6 n-3). *Steroids*, *99*(Pt B), 194–203.

Nury, T., Zarrouk, A., Ragot, K., Debbabi, M., Riedinger, J. M., Vejux, A., … Lizard, G. (2017). 7-Ketocholesterol is increased in the plasma of X-ALD patients and induces peroxisomal modifications in microglial cells: Potential roles of 7-ketocholesterol in the pathophysiology of X-ALD. *The Journal of Steroid Biochemistry and Molecular Biology*, *169*, 123–136.

Nury, T., Zarrouk, A., Vejux, A., Doria, M., Riedinger, J. M., Delage-Mourroux, R., & Lizard, G. (2014). Induction of oxiapoptophagy, a mixed mode of cell death associated with oxidative stress, apoptosis and autophagy, on 7-ketocholesterol-treated 158N murine oligodendrocytes: Impairment by α-tocopherol. *Biochemical and Biophysical Research Communications*, *446*(3), 714–719.

Olkkonen, V. M. (2013). OSBP-related proteins: Liganding by glycerophospholipids opens new insight into their function. *Molecules*, *18*(11), 13666–13679.

Otaegui-Arrazola, A., Menéndez-Carreño, M., Ansorena, D., & Astiasarán, I. (2010). Oxysterols: A world to explore. *Food and Chemical Toxicology*, *48*(12), 3289–3303.

Papadopoulos, V., & Lecanu, L. (2012). Caprospinol: Discovery of a steroid drug candidate to treat Alzheimer's disease based on 22R-hydroxycholesterol structure and properties. *Journal of Neuroendocrinology*, *24*(1), 93–101.

Paz, J. L., Levy, D., Oliveira, B. A., de Melo, T. C., de Freitas, F. A., Reichert, C. O., … Bydlowski, S. P. (2019). 7-Ketocholesterol promotes oxiapoptophagy in bone marrow mesenchymal stem cell from patients with acute myeloid leukemia. *Cells May*, *21*, 8(5). https://doi.org/10.3390/cells8050482

Pedruzzi, E., Guichard, C., Ollivier, V., Driss, F., Fay, M., Prunet, C., … Ogier-Denis, E. (2004). NAD(P)H oxidase Nox-4 mediates

7-ketocholesterol-induced endoplasmic reticulum stress and apoptosis in human aortic smooth muscle cells. *Molecular and Cellular Biology*, *24*(24), 10703–10717.

Ragot, K., Mackrill, J. J., Zarrouk, A., Nury, T., Aires, V., Jacquin, A., … Lizard, G. (2013). Absence of correlation between oxysterol accumulation in lipid raft microdomains, calcium increase, and apoptosis induction on 158N murine oligodendrocytes. *Biochemical Pharmacology*, *86*(1), 67–79.

Rodríguez, I. R., & Larrayoz, I. M. (2010). Cholesterol oxidation in the retina: Implications of 7KCh formation in chronic inflammation and age-related macular degeneration. *Journal of Lipid Research*, *51*(10), 2847–2862.

Russell, D. W. (2000). Oxysterol biosynthetic enzymes. *Biochimica et Biophysica Acta*, *1529*(1–3), 126–135.

Ryan, L., O'Callaghan, Y. C., & O'Brien, N. M. (2005). The role of the mitochondria in apoptosis induced by 7β-hydroxycholesterol and cholesterol-5β,6β-epoxide. *The British Journal of Nutrition*, *94*(4), 519–525.

Sghaier, R., Nury, T., Leoni, V., Caccia, C., De Barros, J. P. P., Cherif, A., … Mackrill, J. J. (2019). Dimethyl fumarate and monomethyl fumarate attenuate oxidative stress and mitochondrial alterations leading to oxiapoptophagy in 158N murine oligodendrocytes treated with 7β-hydroxycholesterol. *The Journal of Steroid Biochemistry and Molecular Biology*. Nov, *194*, 105432. https://doi.org/10.1016/j.jsbmb.2019.105432

Sghaier, R., Zarrouk, A., Nury, T., Badreddine, I., O'Brien, N., Mackrill, J. J., … Lizard, G. (2019). Biotin attenuation of oxidative stress, mitochondrial dysfunction, lipid metabolism alteration and 7β-hydroxycholesterol-induced cell death in 158N murine oligodendrocytes. *Free Radical Research*, *53*(5), 535–561.

Shinkyo, R., Xu, L., Tallman, K. A., Cheng, Q., Porter, N. A., & Guengerich, F. P. (2011). Conversion of 7-dehydrocholesterol to 7-ketocholesterol is catalyzed by human cytochrome P4507A1 and occurs by direct oxidation without an epoxide intermediate. *The Journal of Biological Chemistry*, *286*(38), 33021–33028.

Sottero, B., Rossin, D., Poli, G., & Biasi, F. (2018). Lipid oxidation products in the pathogenesis of inflammation-related gut diseases. *Current Medicinal Chemistry*, *25*(11), 1311–1326.

Testa, G., Rossin, D., Poli, G., Biasi, F., & Leonarduzzi, G. (2018). Implication of oxysterols in chronic inflammatory human diseases. *Biochimie*, *153*, 220–231.

Vejux, A., Abed-Vieillard, D., Hajji, K., Zarrouk, A., Mackrill, J. J., Ghosh, S., … Lizard, G. (2020). 7-Ketocholesterol and 7β-hydroxycholesterol: in vitro and animal models used to characterize their activities and to identify molecules preventing their toxicity. *Biochemical Pharmacology*, *173*, 113648. https://doi.org/10.1016/j.bcp.2019.113648

Wahl, D., Solon-Biet, S. M., Cogger, V. C., Fontana, L., Simpson, S. J., Le Couteur, D. G., & Ribeiro, R. V. (2019). Aging, lifestyle and dementia. *Neurobiology of Disease*, *130*, 104481. https://doi.org/10.1016/j.nbd.2019.104481

Yammine, A., Nury, T., Vejux, A., Latruffe, N., Vervandier-Fasseur, D., Samadi, M., … Lizard, G. (2020). Prevention of 7-ketocholesterol-induced overproduction of reactive oxygen species, mitochondrial dysfunction and cell death with major nutrients (polyphenols, ω3 and ω9 unsaturated fatty acids) of the Mediterranean diet on N2a neuronal cells. *Molecules*, *25*(10), E2296. https://doi.org/10.3390/molecules25102296

Yang, X., Li, Y., Li, Y., Ren, X., Zhang, X., Hu, D., … Shang, H. (2017). Oxidative stress-mediated atherosclerosis: Mechanisms and therapies. *Frontiers in Physiology*, *8*, 600. https://doi.org/10.3389/fphys.2017.00600

Zarrouk, A., Martine, L., Grégoire, S., Nury, T., Meddeb, W., Camus, E., … Lizard, G. (2019). Profile of fatty acids, tocopherols, phytosterols and polyphenols in Mediterranean oils (argan oils, olive oils, milk thistle seed oils and nigella seed oil) and evaluation of their antioxidant and cytoprotective activities. *Current Pharmaceutical Design*, *25*(15), 1791–1805.

Zarrouk, A., Nury, T., Karym, E. M., Vejux, A., Sghaier, R., Gondcaille, C., … Lizard, G. (2017). Attenuation of 7-ketocholesterol-induced overproduction of reactive oxygen species, apoptosis, and autophagy by dimethyl fumarate on 158N murine oligodendrocytes. *The Journal of Steroid Biochemistry and Molecular Biology*, *169*, 29–38.

Zarrouk, A., Vejux, A., Mackrill, J., O'Callaghan, Y., Hammami, M., O'Brien, N., & Lizard, G. (2014). Involvement of oxysterols in age-related diseases and ageing processes. *Ageing Research Reviews*, *18*, 148–162.

Zerbinati, C., & Iuliano, L. (2017). Cholesterol and related sterols autoxidation. *Free Radical Biology & Medicine*, *111*, 151–155.

How to cite this article: Nury T, Zarrouk A, Yammine A, Mackrill JJ, Vejux A, Lizard G. Oxiapoptophagy: A type of cell death induced by some oxysterols. *Br J Pharmacol*. 2020;1–9. https://doi.org/10.1111/bph.15173

Article 5

Lipids Nutrients in Parkinson and Alzheimer's Diseases: Cell Death and Cytoprotection

Thomas Nury, Gérard Lizard, Anne Vejux

Int J Mol Sci, 2020, 21(7),2501

Le 7KC induit une mort par oxyapoptophagie (stress **Oxy**dant + **Apopto**se + Auto**phagie**) sur les oligodendrocytes murins 158N. Cette mort cellulaire peut être inhibée par différents composés lipidiques : l'α-tocophérol, l'acide docosahexaénoïque (DHA) et ses précurseurs (acide eicosapentaénoïque (EPA) et acide α-linolénique (ALA)), l'acide oléique, l'huile de Lorenzo (acide oléique + acide érucique (4:1)) ainsi qu'un dérivé chimique de l'acide oléique : le sulfo-N-succinimidyl Oléate (SSO).

Ces composés lipidiques pourraient donc jouer un rôle non négligeable dans la prévention et le traitement des maladies impliquant le 7KC notamment la maladie d'Alzheimer la maladie de Parkinson.

Ces deux pathologies ont en commun des dysfonctions cellulaires telles qu'une élévation du stress oxydant, de l'inflammation, de la mort cellulaire impliquant la mitochondrie, et une accumulation de protéines dont l'élimination normale fait défaut (le peptide Aβ et la protéine tau pour la maladie d'Alzheimer et l'α-synucléine dans la maladie de Parkinson). Il existe actuellement plusieurs études *in vitro* et *in vivo* montrant que certains nutriments lipidiques, incluant des huiles végétales et animales, des huiles fonctionnalisées et des acides gras, pourraient être utilisés dans la maladie d'Alzheimer et dans la maladie de Parkinson.

La revue présentée fait état des différents nutriments lipidiques neuroprotecteurs (acides gras, huiles végétales et animales) ayant montré des propriétés *in vitro* et/ou *in vivo*.

International Journal of
Molecular Sciences

MDPI

Review

Lipids Nutrients in Parkinson and Alzheimer's Diseases: Cell Death and Cytoprotection

Thomas Nury, Gérard Lizard * and Anne Vejux *

Biochemistry of the Peroxisome, Inflammation and Lipid Metabolism' EA 7270, Team Bio-peroxIL, Université de Bourgogne Franche-Comté /Inserm, 21000 Dijon, France; thomas.nury@u-bourgogne.fr

* Correspondence: gerard.lizard@u-bourgogne.fr (G.L.); anne.vejux@u-bourgogne.fr (A.V.); Tel.: +33-3-80-39-37-01 (A.V.); Fax.: +33-3-80-39-62-50 (A.V. & G.L.)

Received: 5 March 2020; Accepted: 1 April 2020; Published: 3 April 2020

Abstract: Neurodegenerative diseases, particularly Parkinson's and Alzheimer's, have common features: protein accumulation, cell death with mitochondrial involvement and oxidative stress. Patients are treated to cure the symptoms, but the treatments do not target the causes; so, the disease is not stopped. It is interesting to look at the side of nutrition which could help prevent the first signs of the disease or slow its progression in addition to existing therapeutic strategies. Lipids, whether in the form of vegetable or animal oils or in the form of fatty acids, could be incorporated into diets with the aim of preventing neurodegenerative diseases. These different lipids can inhibit the cytotoxicity induced during the pathology, whether at the level of mitochondria, oxidative stress or apoptosis and inflammation. The conclusions of the various studies cited are oriented towards the preventive use of oils or fatty acids. The future of these lipids that can be used in therapy/prevention will undoubtedly involve a better delivery to the body and to the brain by utilizing lipid encapsulation.

Keywords: lipids nutrients; apoptosis; oxidative stress; mitochondria; synuclein; amyloid; Tau; Parkinson's disease; Alzheimer's disease

1. Introduction

Neurodegenerative diseases, a major societal issue, are pathological conditions that affect neurons, condemning them to certain death. This term covers a heterogeneous group of diseases affecting different populations of neurons of the nervous system (brain and spinal cord), i.e., around 100 pathologies. In this review, we will focus on the most frequent: Alzheimer's disease and Parkinson's disease. The mechanisms of cell death have been well-studied in vitro and in vivo, both in animal models of these pathologies and in humans. Many mechanisms are common to these different pathologies; what differentiates them is the type of neurons affected and its environment. Parkinson's disease is a chronic pathology characterized by the destruction of dopaminergic neurons at the level of the substantia nigra. These innervate the central grey nuclei and, more particularly, a structure involved in the control of motor functions, the striatum. One of the common mechanisms of neurodegeneration is the toxic aggregation of proteins. Once their synthesis is complete, proteins acquire a three-dimensional organization that allows them to perform their function. Under normal conditions, if misfolding occurs, it is either corrected or the misfolded proteins are eliminated by either the ubiquitin-proteasome pathway or by autophagy. Under pathological conditions, these misfolded proteins are not eliminated; they will aggregate and take the form of intranuclear or intracytoplasmic inclusions, or extracellular aggregates called senile plaques, which inhibit many subcellular functions [1–3]. For example, in Alzheimer's disease, there are senile plaques and tau protein aggregates. In Parkinson's disease, there are α-synuclein aggregates in the form of Lewy bodies or Lewy neurites. A loss of activity of these proteins, a gain in neurotoxic function or the induction of an inflammatory process could

explain the toxicity of these aggregates. These aggregates could also induce apoptosis of neurons associated with mitochondrial dysfunction; another process common to various neurodegenerative pathologies. Since the mitochondria are closely related to the peroxisomes, mitochondrial dysfunction can adversely affect peroxisomal activity. The third common process in neurodegeneration is the presence of oxidative stress with increased production of reactive oxygen species: the superoxide ion $O_2^{\cdot -}$, the peroxynitrite ion ONOO-, the hydroxyl radical HO and other molecular species such as hydrogen peroxide H_2O_2. Firstly, this review will present the commonalities between Parkinson's and Alzheimer's disease: protein accumulation, mitochondrial dysfunction and cell death, followed by oxidative stress. Subsequently, the lipids that can protect against cell death will be discussed in the form of vegetable, animal and functionalized oils and by individual fatty acids.

2. Mechanisms Common to Neurodegenerative Diseases

Among the mechanisms common to the two most-frequent neurodegenerative diseases in humans, Parkinson's and Alzheimer's disease, protein aggregation associated with altered protein degradation systems, mitochondrial dysfunction associated with cell death and oxidative stress were identified. These characteristics and common features will be described for these two neurodegenerative pathologies.

2.1. Protein Aggregation and Alteration of Protein Degradation Systems

In Parkinson's and Alzheimer's disease, the proteins that primarily aggregate are α-synuclein, Tau and β-amyloid proteins, respectively, although the latter are also found in Parkinson's disease. Insoluble α-synuclein fibrils make up the Lewy bodies and Lewy neurites. These are predominantly present in the pigmented neurons of the substantia nigra and in other neuronal populations at the peripheral and central levels [4–6]. Lewy bodies are present in the dopaminergic neurons of substantia nigra pars compacta and are round intraneuronal and positive round inclusions of α-synuclein and ubiquitin [6]. Lewy neurites are abnormal neurites with α-synuclein filaments and granular material that accumulate in the amygdala and striatum of Parkinsonian patients [7]. Lewy neurites can inhibit neuronal transport and, thus, compromise neuronal function and survival. In Alzheimer's disease, the alterations identified are amyloid plaques and neurofibrillary degeneration. The role of two proteins have been identified: Tau protein and Amyloid precursor protein (APP). The APP protein can be proteolyzed to generate the Aβ peptide. When this peptide aggregates, amyloid plaques are formed [8]. Neurofibrillary degeneration consists of argentophilic neurofilaments located in the pericaryon of certain cortical neurons but are also found within myelinated axons, dendrites and synapses [9]. The density of these neurofibrillary accumulations in the neocortex is directly correlated with the severity of the disease [10]. Neurofibrillary tangles consist of hyper-phosphorylated Tau proteins organized in paired helical filaments. Amyloid plaques consist of extracellular deposits of peptide Aβ. These plaques are surrounded by glial cells containing phagocytic lysosomes, as well as amyelinic neurites. These plaques are preferentially located in certain areas of the brain, particularly the cortex, striatum and cerebellum. They undergo maturation during their evolution and, thus, present a specific morphology. The less mature plaques are referred to as diffuse plaques. They are formed of amorphous, low-density aggregates of peptides Aβ. Mature plaques contain very dense aggregates of the peptide Aβ. They are associated with neurodegeneration and astroglial reactivity.

There are different systems for the removal of malformed proteins, including the two pathways involved in the degradation of α-synuclein: the ubiquitin-proteasome system (UPS) and the autophagy-lysosome pathway (ALP) [11,12]. What differs between these two pathways is the type of proteins that are recognized—for the UPS system: short-lived soluble proteins and for the ALP pathway: long-lived macromolecules, cytosolic components and dysfunctional organelles. In the case of Parkinson's disease, one of the pathways of the ALP system, chaperone-mediated autophagy (CMA), is involved. It is known that CMA activity is linked to levels of LAMP-2A (the receptor of the CMA pathway which bind to chaperones who have recognized proteins possessing the KFERQ motif), and in

the substantia nigra of patients' brains, the expression of LAMP-2A is particularly diminished [13–15]. This reduction is thought to be related to the accumulation of α-synuclein and nigral cell death [16]. In addition to the deregulation of the CMA system, an accumulation of autophagosomes and changes in enzyme content and acidification of the lysosomes were observed [17–19]. In Alzheimer's disease, it has been suggested that proteasome inhibition may explain the accumulation of Aβ inside cells in multivesicular bodies [20]. Similarly, proteasome inhibition, both in vitro and in vivo, increases peptide levels Aβ [21]. In addition, extracellular Aβ entering the cytosolic compartment can inhibit proteasome activity in cultured neurons, leading to its accumulation in the cytosol [21].

2.2. Mitochondrial Dysfunction and Cell Death

In the case of Parkinson's disease, it has been established that mitochondria are involved via a deficiency in the complex I of the respiratory chain at the level of the patient's black matter in the neurons and in the glia but, also, at the level of skeletal muscle and platelets [22–25]. This dysfunction contributes to the increase of mitochondria-dependent apoptotic processes [26]. Changes in mitochondrial dynamics, at the bioenergetic level, as well as the inhibition of complex I of the respiratory chain, have been identified on experimental models but, also, in patients [27,28]. Moreover, the genes involved in Parkinson's disease are important for mitochondrial function. For example, mutations in the LRRK2 gene are associated with alterations in the mitochondria [29]. The proteins encoded by the PARK2 and PINK1 genes are involved in the clearance of mitochondria damaged by mitophagy [29]. In patients with Parkinson's disease, degradation of the MIRO protein (outer mitochondrial membrane protein involved in the binding between the mitochondria and microtubules) is reduced, leading to loss of mitophagic function, which may result in increased oxidative stress [30]. Beyond the involvement of genetic factors and observed functional changes, α-synuclein can also interact with the mitochondria and modulate their function. α-synuclein can be located at the mitochondrial outer membrane, interact with members of the TOM complex (translocase/receptor system) and, thus, inhibit the mitochondrial import of proteins in Parkinson's disease [31]. These interactions between mitochondria and α-synuclein may also be accompanied by excessive production of oxidative stress [32]. α-synuclein can also disrupt mitochondrial dynamics, particularly the fusion process, and inhibits complex I [33,34]. Histological evidence implicates cell death as the process responsible for Parkinson's disease, as indicated by the presence of fragmented DNA and, therefore, apoptosis in patients' brains (TUNEL methods) and of active forms of caspases -1, -3, -8 and -9 at the level of the black substance [35,36]. It was also shown that the mitochondrial pathway (p53-GAPDH-Bax pathway) is involved, as is the Fas/FADD death receptor pathway, again thanks to post-mortem studies (high levels of Fas, FADD and caspase-8 in the brains of Parkinsonian patients) [37].

In Alzheimer's disease, a major feature is a loss of neurons in the cortical II layer of the entorhinal cortex [38]. Neurons in the entorhinal cortex that synthesize acetylcholine and innervate the hippocampus and neocortex can also die in Alzheimer's disease. The accumulation of amyloid plaques and neurofibrillary degeneration would be the main trigger for neuronal death of these cells. Neuronal death can be induced by exogenous Aβ and pseudo-hyperphosphorylated Tau, as shown in various cell cultures and animal models of Alzheimer's disease [39]. Indeed, neurons can internalize the extracellular Aβ peptide [40]. The Aβ peptide could thus disrupt mitochondrial membranes and alter the enzymatic activities of the respiratory chain associated with it, thereby leading to the production of a reactive oxygen species [41]. In response to induced oxidative stress, various enzymes, including calpains and caspases, are activated, leading to the cell death of neurons [42].

2.3. Oxidative Stress

Oxidative stress is a process induced by different free radicals, reactive oxygen species (ROS) and reactive oxygen and nitrogen species (RONS). Among these species are hydrogen peroxide (H_2O_2), which, in the presence of iron (in ionic form), gives two hydroxyl radicals ($^{\cdot}OH$), nitrogen monoxide ($NO^{\cdot}$) and superoxide ($O_2^{\cdot -}$). Free radicals cause damage to proteins, lipids and DNA.

This type of damage is found in the substantia nigra of Parkinson's patients. This would contribute to neuronal degeneration. At the level of patients' substantia nigra, damage to proteins, lipids and DNA related to free radicals has been identified in postmortem studies [43]. The dysfunctions of the complex I of the mitochondria mentioned earlier induce an increase in the production of free radicals, and conversely, oxidative stress leads to dysfunction of the mitochondria [43]. As in the case of mitochondria, genes may be involved in setting up oxidative stress. Mutations in the DJ-1 or PARK7 genes, coding for a protein suspected of having antioxidant activity, are concomitant with increased oxidative stress. In DJ-1-deficient mice, there is increased protein oxidation in stressed dopaminergic neurons [44]. Mitochondrial dysfunction and oxidative stress can lead to lysosome depletion and functional impairment of the autophagy/lysosome system, highlighting the interconnection between the different processes responsible for the pathology [45].

In Alzheimer's disease, in addition to the activation of certain enzymes indicated in the previous paragraph, ROS disrupts the cytoskeleton, which undergoes various disorganization phenomena, particularly at the level of dendrites [42] but, also, the plasma membrane and the membranes of the cell organelles. This activates the BACE protein and, consequently, diverts the metabolism of the APP protein towards the amyloidogenesis pathway with increased production of the peptide Aβ. As in the case of Parkinson's disease, oxidative damage has been found in proteins, nucleic acids and lipids [46,47]. The Aβ peptide can also act as a pro-oxidant directly or by impacting NMDA receptor-dependent calcium influxes, leading to mitochondrial dysfunction and, thus, ROS production [48,49].

2.4. Inflammation and Immunity

The central nervous system (CNS) has an endogenous immune system coordinated by immunocompetent cells. The main actors involved in the inflammatory process during Alzheimer's disease are microglial cells, glial cells (astrocytes) and, possibly, neurons [50,51]. Both microglial cells and astrocytes respond rapidly to the disease with changes in morphology, antigenicity and function [52]. Microglial cells are cells that support and protect neurons. They act as immunocompetent defense cells that orchestrate the endogenous immune response of the CNS. They can express major histocompatibility complex type II (MHCII) and produce proinflammatory cytokines, chemokines, ROS and complement proteins. These cells play a central role in the cellular response to pathological lesions such as Aβ and senile plaques [53]. In fact, Aβ can attract and activate microglial cells, leading to their accumulation around amyloid deposits. Exposure of microglial cells to Aβ causes their activation, leading to increased MHC II cell expression and increased secretion of proinflammatory cytokines (interleukin-1 (IL-1), interleukin-6 (IL-6) and TNF-α (tumor necrosis factor-α)), as well as chemokines (interleukin-8 (IL-8), MIP-1α (macrophage inflammatory protein-1α) and MCP1 (monocyte chemoattractant protein-1)) [54,55]. Aβ may promote passage of peripheral circulating macrophages through the blood-brain barrier following recruitment by chemokines, which could increase the extent of inflammation. Kopec & Carroll (1998) showed that Aβ can induce a phagocytic response in microglial cells in a dose- and time-dependent manner [56]. Internalization and co-localization of the lysosome and Aβ associated with damage to neighboring neurons were observed by Bolmont et al., which coincided with the arrival of microglial cells, while plaque resolution was not observed for weeks [57,58]. Reactive astrocytes also contribute to neurodegeneration by stimulating apoptotic processes [59]. In Alzheimer's disease, astrocytes are found associated with amyloid deposits, where they secrete several proinflammatory molecules such as interleukins, prostaglandins, leukotrienes, thromboxanes and complement factors. These molecules are like, and co-localized with, those secreted by microglial cells. One study detected diffuse plaques associated with astrocytes, consisting of granules of Aβ, in the brains of nondemented elderly people. This observation suggests that astrocytes may be involved in the phagocytosis of Aβ [60] and that, probably, a deficit in the elimination of Aβ by astrocytes is part of the pathology of Alzheimer's disease. In the brains of Alzheimer's disease patients [52] and transgenic models of Alzheimer's disease mice [61], reactive astrocytes occupy positions near the

plaques, encircling the deposits of Aβ, a mechanism by which the cells could act as a barrier between healthy tissue and tissue with inflammation [52]. In addition, the fibrillar form of amyloid peptide interacts with complement proteins and thereby activates the innate immune system [62]. In particular, the interaction Aβ/C1q, which involves the 11 N-terminal residues of Aβ, activates the classical complement pathway [63]. This process induces a cascade of activations that leads to the formation of lytic complexes, partly responsible for neuronal death, and inflammatory activation [64]. Neurons themselves may play a role in the inflammatory process through the production of certain cytokines such as IL-1 [65], IL-6 [66], TNF-α [67] and some pentraxins, namely CRP and Ap (amyloid P) [68]. The mRNA expression levels of proteins of the classical complement pathway are similarly increased in the brains of Alzheimer's patients compared to those of controls [69].

Numerous studies have implicated neuroinflammation and, more specifically, microglial cells in the development and progression of death of the dopaminergic neurons of the substantia nigra [70]. Positron emission tomography (PET) imaging has made it possible to visualize microglial activation in the pons, central gray nuclei, striatum and frontal and temporal cortical regions of patients with Parkinson's disease [71,72]. Post-mortem immunohistological analyses also show morphological and functional signs of microglial activation in the CNS: increased cell density, retraction of branches and hypertrophy of the cell body; expression of MHC II molecules [73–76] and increased expression of the lysosomal marker CD68 [75,77]. Phagocytosis and antigenic presentation are classically the two main functions attributed to microglial cells. In the 6-hydroxydopamine (6-OHDA) model, analysis of the lysosomal marker CD68, reflecting phagocytosis activity, and of MHC II molecules, reflecting the role of antigen presentation, shows that these two functions may evolve according to independent kinetics [78–81]. Peak phagocytic activity, as determined by the level of CD68 expression, has been reported to occur either before or after maximal neuronal death [79,82]. These contradictory results lead to conflicting hypotheses as to the role of microglial activation. It might be assumed that a process of deregulation of phagocytic functions amplifies the autonomous mechanisms of neuronal death. It could also be assumed that the main function of microglial cells is the removal of neuronal cell debris. Activated microglia also have the important property of secreting a set of cytokines that are either proinflammatory or anti-inflammatory. Potentially neurotoxic proinflammatory proteins are expressed in the brains of patients with Parkinson's disease, including COX and iNOS, TNFα, IL1β and IFNγ [83,84]. T-lymphocytes are the main cells that produce IFNγ, a cytokine known to activate macrophages (including microglia). Numerous animal studies have demonstrated a deleterious role of IFNγ in the pathophysiology of Parkinson's disease [85–88]. Since Th1 lymphocytes are the main source of IFNγ and macrophages are the main target cell for this cytokine, these results suggest that the dialogue between Th1 and microglial cells in the substantia nigra of patients with Parkinson's disease could be a key event in dopaminergic neuronal loss. In the MPTP model, the regulatory T-lymphocytes (Tregs) prevent the degeneration of dopaminergic neurons by altering the molecular behavior of microglial cells [89,90]. Thus, microglial cells are likely to exert distinct and possibly opposing effects depending on the stage of Parkinson's disease progression, the immunogenetic terrain and a set of instructional signals delivered by infiltrating T lymphocytes, among other factors.

3. Cytoprotector Effects of Vegetable Oil

In this paragraph, we will discuss the effects of oils or molecules derived from vegetable oils as a potential therapeutic or preventive avenue against cell death (mitochondria, apoptosis and oxidative stress) and inflammation. These effects are reported in Figure 1, which summarizes the different signaling pathways potentially involved in Parkinson's and Alzheimer's disease, as well as the sites of action of lipid nutrients that will be described in this section (Figure 1).

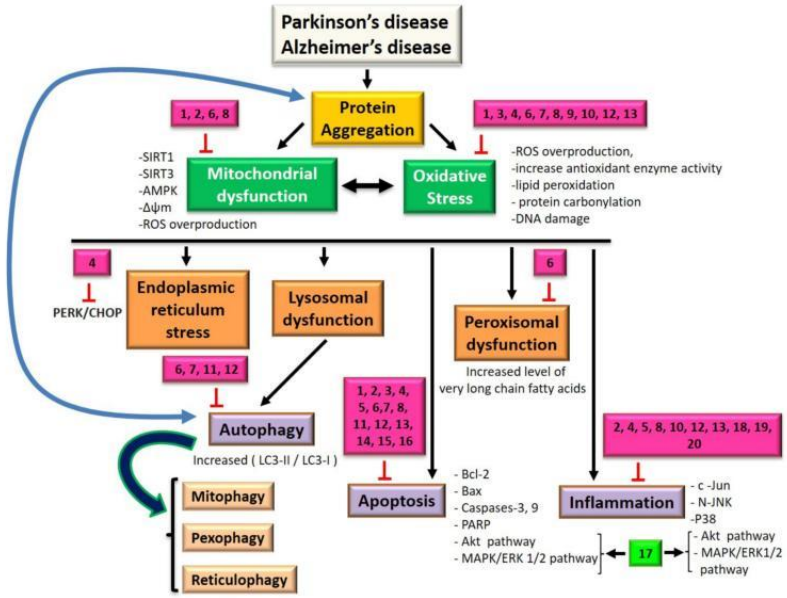

Figure 1. Signaling pathways impacted by lipid nutrients at the level of target organelles and common processes involved in Parkinson's and Alzheimer's disease: autophagy, apoptosis, oxidative stress and inflammation. (**1**) Compounds derived from sesame oil and sesame seeds, (**2**) red ginseng oil, (**3**) coriander volatile oil, (**4**) compounds of *Nigella sativa* seed oil, (**5**) olive oil, (**6**) argan oil, (**7**) milk thistle seed oil, (**8**) krill oil, (**9**) sea urchin egg oil, (**10**) compounds of Lorenzo's oil, (**11**) oleic acid, (**12**) docosahexaenoic acid, (**13**) eicosapentaenoic acid, (**14**) α-linolenic acid, (**15**) linoleic acid, (**16**) arachidonic acid, (**17**) plasmalogens, (**18**) compounds of *Cyperus rotundus* oil, (**19**) compounds of dietary tuna oil and (**20**) fish oil.

In SH-SY5Y cells, sesamin and sesamol (concentration 1 μM), two compounds derived from sesame oil and sesame seeds, are capable of reducing H_2O_2-induced cell death, as well as the production of intracellular ROS [91]. The signaling pathway involved in this neuroprotection involves activation of SIRT1-SIRT3-FOXO3a expression, inhibition of the proapoptotic protein Bax and positive regulation of the antiapoptotic protein Bcl-2 [91]. In 6-OHDA-treated rats (PD model), sesamin decreases ROS levels, increases superoxide dismutase activity and decreases caspase-3 activity [92]. In another cellular model of Parkinson's disease (use of 1-methyl-4-phenyl-pyridine (MPP(+)) ion), sesamin also protects PC12 cells from cell death by reducing oxidative stress [93].

Red ginseng oil is able to protect PC-12 cells treated with Aβ(25–35) peptides from cell death. This oil attenuates apoptosis by acting on calcium influx and loss of mitochondrial membrane potential but, also, on the proteins involved in the death pathways: Bax, Bcl-2 and caspases-3 and -9, as well as PARP [94]. It also has an anti-inflammatory effect by negatively regulating the c-Jun/N-JNK/p38 pathway [94]. Red ginseng oil extract is composed mainly of linoleic acid, β-sitosterol and stigmasterol. These three compounds inhibit the toxicity induced by Aβ(25–35) by regulating oxidative stress, apoptosis and inflammation but using different molecular mechanisms in PC12 cells [95]. For example, at the level of cell death, linoleic acid and stigmasterol regulate mitochondrial membrane potential; intracellular calcium; Bax/Bcl-2 ratio and caspases-9, -3 and -8, while β-sitosterol blocks only the intrinsic apoptotic pathway [95].

Inhaled coriander volatile oil was tested in a rat model for Alzheimer's disease and decreased markers of oxidative stress on hippocampal tissues: decreased superoxide dismutase and lactate dehydrogenase activities, increased glutathione peroxidase activity and decreased malondialdehyde

levels [96]. This inhaled oil may also decrease antiapoptotic activity [96]. Studies on *Coriandrum sativum* leaves have confirmed that this species has antioxidant, anti-inflammatory and, especially, ERK-signaling inhibitory properties that are beneficial for Alzheimer's patients [97].

Thymoquinone is the most abundant ingredient in *Nigella sativa* seed oil. This molecule protects human-induced pluripotent stem cell (hiPSC)-derived cholinergic neurons treated with Aβ(1–42) from cell death, oxidative stress and synaptic toxicity [98]. Thymoquinone reduces inflammation in a model of Alzheimer's disease by likely acting on the TLR pathway and NF-κB-signaling pathway [99,100].

Total ginsenosides and volatile oil of *Acorus tatarinowii* administered together to AD mice inhibit apoptosis, decrease malondialdehyde content in the cortex and hippocampus and increase superoxide dismutase activity [101]. *Acorus tatarinowii* Schott volatile oil, via its compound β-asarone (1,2,4-trimethoxy-5-([Z]-prop-1-enyl)benzene), is able to regulate autophagy and stress of the endoplasmic reticulum in a 6-OHDA-induced Parkinsonian rat model by inhibiting the PERK/CHOP/Bcl-2/Beclin-1-signaling pathway [102].

Olive oil, a major constituent of the Mediterranean diet, through its two components tyrosol and hydroxytyrosol, decreases the cell death of N2a cells treated with Aβ(25–35) but cannot prevent the decrease of glutathione induced by H_2O_2 or Aβ [103]. In SH-SY5Y cells treated with dopamine and 6-hydroxydopamine, hydroxythyrosol protects against death induced by these compounds [104]. Oleocanthal, one of the active components of extra-virgin olive oil, reduces interleukin-6 increase and glial fibrillary acidic protein upregulation, characteristic processes of inflammation induced by Aβ oligomers [105].

α-cyperone, one of the main ingredients of *Cyperus rotundus* oil, exerts neuroprotective effects in BV-2 microglial cells by reducing the production of inflammatory cytokines: IL-1β, TNF-α and IL-6. This action occurs by activating Akt/Nrf2/HO-1 and suppressing the NF-κB pathway [106].

The consumption of dietary tuna oil (0.55% EPA and 0.36% DHA, % of total diet weight) for eight weeks, in a mouse model of age-related pathologies such as Alzheimer's disease, prevents elevation of hippocampal TNF-α and monocytic marker CD11b protein levels, whereas GFAP and IL-1β increase despite this dietary supplementation [107].

Some oils have not been tested in a model for Parkinson's or Alzheimer's disease, but their actions have been evaluated in cell models where oxidative stress and organelle dysfunction have been induced by oxysterols (oxidized derivatives of oxysterols) in cells of the nervous system: oligodendrocytes. Indeed, when their concentration is abnormal, oxysterols are associated with demyelinating or neurodegenerative diseases such as Parkinson's or Alzheimer's disease [108,109]. 7-ketocholesterol (7KC) is capable of inducing cell death and oxidative stress in 158N oligodendrocyte cells [110].

Argan oil is capable of inhibiting processes induced by 7KC: loss of cell adhesion; cell growth inhibition; increased plasma membrane permeability; mitochondrial, peroxisomal and lysosomal dysfunction and the induction of oxiapoptophagy (OXIdation + APOPTOsis + autoPHAGY) in oligodendrocytes [111].

In the 158N oligodendrocyte cell model, OSS of cell adhesion, increased plasma membrane permeability, mitochondrial dysfunction, ROS overproduction, induction of apoptosis and autophagy induced by 7KC are attenuated by milk thistle seed oil [112].

All these oils can be potential natural resources for the functionalized food industry, as well as being used as neural protective agents.

4. Cytoprotective Effects of Animal Oils

Seafood can have neuroprotective effects. Data are available, not on models strictly mimicking Alzheimer's and Parkinson's disease, but on models adapted to resemble certain features of neurodegenerative diseases. These effects are reported in Figure 1.

Krill oil protects PC-12 cells from methamphetamine-induced cell death by increasing cell viability, decreasing cleaved caspase-3 and regulating mitochondrial membrane potential [113]. It also protects from oxidative stress by increasing superoxide dismutase and glutathione enzyme activities and

decreasing ROS and NO production [113]. The authors suggest that apoptosis and oxidative stress are key processes in the pathophysiology of many neurodegenerative diseases and that this oil could be beneficial in these pathologies [113]. Antarctic krill oil reduces oxidative stress in the brains of SAMP8 mice, but the effects are barely visible in the serum and liver [114].

Fish oil decreases the expression of neuroinflammatory genes in response to amyloid-β [115]. Short-term fish oil supplementation, used in the presymptomatic stage of Alzheimer's disease, influences the behavior of microglia/macrophages, inducing them to establish a physical barrier around the amyloid plaques [116]. In the mu-p75 saporin (SAP)-induced mouse model of Alzheimer's disease, a mixture of tart cherry extract, Nordic fish oil and refined emu oil protects from inflammation and the loss of neurons induced by SAP [117]. Sprague Dawley rats, aged eight weeks and LPS-injected, were fed for two weeks with food containing 15% fish oil (% of total diet weight). Dopaminergic lesions were decreased in this model. as well as OX42 (also known as CD11b) protein, a monocytic marker, TNF-α and IL-1β [118].

Oxysterols may be involved in the development of neurodegenerative diseases [108]. Based on this hypothesis, mouse 158N oligodendrocytes were treated with 7β-hydroxycholesterol. This induces cell death associated with oxidative stress (alterations in superoxide dismutase and glutathione peroxidase activities, increased lipid peroxidation and protein carbonylation) [119]. Sea urchin egg oil attenuates the cytotoxicity induced by 7β-hydroxycholesterol. This result led to the hypothesis that this oil could be useful in the prevention of neurodegenerative diseases and, therefore, possibly Alzheimer's and Parkinson's disease [119].

5. Cytoprotective Effects of Functionalized Oil

Functionalized oils, or compounds of these oils, may eventually become therapeutic avenues through their actions on cell death and oxidative stress. These actions are reported in Figure 1.

Erucic acid (monounsaturated ω9-fatty acid, denoted 22:1ω9) is one of the components of Lorenzo's oil, used in adrenoleukodystrophy. It is consumed in some Asian countries and by the Eskimos of Greenland as an edible oil. Erucic acid has an antioxidative activity that could counteract the oxidative stress present in neurodegenerative diseases, particularly Alzheimer's disease [120]. Indeed, it has been shown in various studies that erucic acid could reduce oxidative damage to DNA and is capable of modifying catalase activity (a peroxisomal enzyme involved in the protection of cells against ROS) but also of protecting the mitochondrion and stimulating its biogenesis (via its PPARδ ligand action) [120]. Erucic acid, present at high levels in mustard, can also inhibit inflammatory enzymes. Many oils contain erucic acid, such as corn oil, rapeseed oil, soybean oil, safflower oil, perilla oil and mustard oil, and it has been shown that these oils can have a positive effect on locomotor activity and memory [120].

6. Cytoprotective Effects of Fatty Acids

In the case of individual lipids, which are components of oils or seafood products, various studies have been carried out on cells of the nervous system, suggesting possible actions in Parkinson's and Alzheimer's disease. Their actions are reported in Figure 1.

In a mouse microglial cell model BV-2, oleic acid (OA), a major compound of olive and argan oil, and docosahexaenoic acid (DHA; C22:6 n-3) present in fatty fishes, such as sardines, are able to inhibit the major toxic effects of 7KC: caspase-3 activation and increased LC3-II/LC3-I ratio (autophagy indicator) [121].

Some n-3 polyunsaturated fatty acids (PUFAs), such as docosahexaenoic acid (DHA) and eicosapentaenoic acid (EPA; C20:5 n-3), are known to have beneficial effects in neurodegenerative diseases. In a model using differentiated SH-SY5Y cells treated with Aβ(25–35), DHA, EPA and mixtures of these two compounds at DHA/EPA ratios 1:1 and 2:1 are able to modulate the neurotoxicity of the Aβ(25–35) peptide by decreasing cell death (Bax/Bcl-2 ratio and caspase-3) and oxidative stress [122]. DHA and EPA can be provided in different forms (glycerophosphatides, triglycerides or

ethyl esters). The effects of these different modifications are considered. Chinese hamster ovary cells (CHO) stably transfected with amyloid precursor protein (APP) and presenilin 1 (PS1) and SAMP8 mice fed with high-fat diets (HFDs, known to induce metabolic stress, leading to cognitive impairment and aging) have been used to mimic Alzheimer's disease. DHA-enriched phosphatidylcholine (DHA-PC) and EPA-enriched phosphatidylcholine (EPA-PC) were tested in these models, and it was shown that these two compounds can reduce oxidative stress by inducing antioxidant systems (SOD, T-AOC, GSH and GSH-PX) and inhibiting oxidative systems (reduced MDA, NO and NOS levels). They also inhibit apoptosis [123]. In an Alzheimer's rat model (induction Aβ1–42), EPA-PC and DHA-ethyl ester are able to decrease lipid peroxidation rates and mitochondrial-dependent cell deaths [124]. In HFD-induced Alzheimer's disease mice models, DHA-PC and DHA-phosphatidylserine (DHA-PS) can inhibit oxidative stress, and DHA-PS is more effective than DHA-PC in the inhibition of mitochondrial damage [125].

One study tested the abilities of PUFAs n-3 and n-6: DHA, EPA, α-linolenic acid (α-LNA; C18:3 n-3), linoleic acid (LA; C18:2 n-6), arachidonic acid (AA; C20:4 n-3) and γ-linolenic acid (γ-LNA; C18:3n-6) to inhibit cell death. Different known inducers of cell death etoposide, okadaic acid and AraC have been used in mouse neuroblastoma cells (Neuro2a). All these PUFAs inhibit cell death when used separately but had no effect when used together. These results therefore prompted the authors to propose PUFAs as molecules that could delay the onset of diseases and/or their rates of progression [126].

The use of DHA and EPA, for six months, prevents a decrease in the levels of specialized protective mediators, involved in inflammation, produced by peripheral blood mononuclear cells (PBMC) of Alzheimer's patients [127]. This effect is accompanied by improvements in cognitive function [127]. EPA supplementation appears to improve glial overactivation and to have effects on n3/n6 imbalance and the negative regulation of BDNF, which contribute to the anti-inflammatory actions [128]. The same supplementation, given as part of the OmegAD study, induces the regulation of different genes involved in inflammation, e.g., CD63, MAN2A1, CASP4, LOC399491, NAIP and SORL1 and in ubiqutination processes, e.g., ANAPC5 and UBE2V1 [129]. Additionally, DHA and EPA supplementation decreased the release of IL-1β, IL-6 and granulocyte colony-stimulating factor from the PBMC of Alzheimer's patients [130]. DHA, in combination with (-)epigallocatechin-3-gallate and α-lipoic acid promoted anti-inflammatory (microglial activation) and neuroprotective effects in male Tg2576 transgenic mice [131]. Human CHME3 microglial cells, treated with the peptide Aβ42, also received DHA and EPA. This combination of omega-3 fatty acids stimulates microglial phagocytosis of Aβ42, decreases proinflammatory M1 markers CD40 and CD86 and increases neurotrophin production [132].

A model of Parkinson's disease can be created using rotenone, a mitochondrial I-complex inhibitor, which induces dopaminergic neuronal death. Rats are therefore treated with DHA to test its effectiveness, followed by rotenone. Pretreating these rats with DHA protects dopaminergic neurons against this mode of death [133].

In an experimental rat model of Parkinson's disease created with 1-methyl-4-phenyl-1,2,3, 6-tetrahydropyridine (MPTP), DHA induces phosphorylation of the Akt protein, thus activating the Akt-dependent survival pathway, and also acts on the Bcl-2 pathway [134]. The same team also showed that DHA would decrease lipid oxidation in the brain [135].

In a model using the herbicide paraquat that induces dopaminergic neuron loss through the excessive production of ROS, DHA inhibits neuronal cell death by increasing glutathione homeostasis via Nrf2 [136].

Plasmalogens, glycerophospholipids containing vinyl ether linkage at the sn-1 position, can attenuate the neuronal cell death in Neuro-2A cells upon the serum starvation. The plasmalogens would activate the PI3K/Akt-signaling pathway by promoting its phosphorylation and the MAPK/ERK 1/2 pathway. Plasmalogens are also able to inhibit nutrient-deprivation-induced neuronal cell death in the hippocampus via inhibition of caspase-9 and caspase-3 activity [137].

Mice treated with MPTP and fed a diet containing 0.8% ethyl EPA (% of total diet weight) showed a reduction in striatal TNF-α and IFN-γ proteins [138]. The IL-10 protein is reduced in the midbrain following treatment with ethyl EPA. On the other hand, the expression of COX-2 and calcium-dependent cytosolic PLA2, enzymes involved in inflammatory signaling, are not altered.

7. Conclusions

Parkinson's and Alzheimer's disease have common physiopathological processes, such as protein aggregation and accumulation and altered protein breakdown systems, mitochondrial malfunction associated with cell death and oxidative stress. To prevent these side effects, some nutrients could be used as nutraceuticals or a as part of functionalized foods. There are indeed several lines of evidence that oils and fatty acids used alone could be employed because of their actions on protein aggregation, dysfunctional protein degradation systems, cell death, oxidative stress and/or inflammation to prevent or slow down the development of these diseases (Figure 2). Furthermore, interactions between nutraceutical products could have inverse, negative results; it is important not to value the additive or synergistic effects of combination products in vivo without testing them in animal models and human clinical studies. In the future, micro- and nanoencapsulation of oils and fatty acids associated with targeted therapies could help to optimize the efficiency of these compounds, whose activities depend both on the degree of degradation in the gastrointestinal tract and on the passage through the blood-brain barrier. Lipid nutrients are certainly a valuable source for developing therapies, but there are also other molecules such as polyphenols, whose properties have already been demonstrated in neurodegenerative diseases and which could be used in combination with these lipids [139,140].

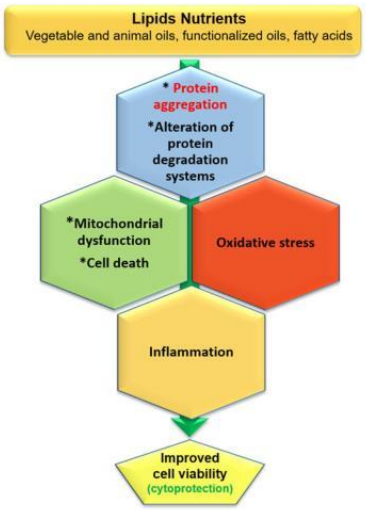

Figure 2. The potential of lipid nutrients to prevent Parkinson's and Alzheimer's disease. Several lipid nutrients, including vegetable and animal oils, functionalized oils and fatty acids, could be used to treat or attenuate Parkinson's and Alzheimer's disease. These disorders have in common protein aggregation and the alteration of protein degradation systems, which can trigger mitochondrial dysfunction and oxidative stress, leading to cell death and inflammation. There are now several in vitro and in vivo arguments that lipid nutrients can be efficient in the prevention of neurodegeneration associated with protein aggregation (β-amyloids in Alzheimer's disease and α-synuclein in Parkinson's disease). In the future, the cytoprotective activity of lipid nutrients could be enhanced by micro- or nanoencapsulation. Nanotherapy targeting the mitochondria may be considered (Targeted Organelle Nanotherapy (TORN therapy)).

Author Contributions: Writing—original draft preparation, A.V.; writing—review and editing, A.V., T.N. and G.L. and visualization, A.V., T.N. and G.L. All authors have read and agreed to the published version of the manuscript.

Funding: This research was supported by the Université de Bourgogne.

Acknowledgments: The authors thank John J Mackrill (University College of Cork, Cork, Ireland) for the English corrections.

Conflicts of Interest: The authors declare no conflicts of interest.

Abbreviations

·OH	hydroxyl radicals
6-OHDA	6-hydroxydopamine
7KC	7-ketocholesterol
AA	arachidonic acid
ALP	autophagy-lysosome pathway
APP	Amyloid precursor protein
Aβ	amyloid beta
BACE	beta-site APP cleaving enzyme
CHO	Chinese hamster ovary cells
CMA	chaperone mediated autophagy
CNS	central nervous system
DHA	docosahexaenoic acid
DHA-PC	DHA-enriched phosphatidylcholine
DHA-PS	DHA-phosphatidylserine
EPA	eicosapentaenoic acid
EPA-PC	EPA-enriched phosphatidylcholine
GSH	reduced glutathion
GSH-PX	glutathion peroxydase
H_2O_2	hydrogen peroxide
HFD	high-fat diet
hiPSC	human-induced pluripotent stem cell
IL	Interleukin
LA	linoleic acid
LRRK2	Leucine-rich repeat kinase 2
MCP1	monocyte chemoattractant protein-1
MHCII	major histocompatibility complex type II
MIP-1α	macrophage inflammatory protein-1α
MPP(+))	1-methyl-4-phenylpyridinium
MPTP	1-methyl-4-phenyl-1,2,3,6-tetrahydropyridine
NMDA	N-methyl-D-aspartate
NO.	nitrogen monoxide
$O_2^{\cdot -}$	superoxide
OA	oleic acid
PET	Positron emission tomography
PINK1	PTEN-induced putative kinase 1
PUFA	polyunsaturated fatty acids
RONS	reactive oxygen nitrogen species
ROS	reactive oxygen species
SAP	saporin
SOD	superoxide dismutase
T-AOC	total antioxidant capacity
TNF-α	tumor necrosis factor-α
TOM	translocase of the outer membrane
Tregs	regulatory T-lymphocytes
UPS	ubiquitin-proteasome system
α-LNA	α-linolenic acid
γ-LNA	γ-linolenic acid
TORN	Targeted Organelle Nanotherapy

References

1. Sweeney, P.; Park, H.; Baumann, M.; Dunlop, J.; Frydman, J.; Kopito, R.; McCampbell, A.; Leblanc, G.; Venkateswaran, A.; Nurmi, A.; et al. Protein misfolding in neurodegenerative diseases: Implications and strategies. *Transl. Neurodegener.* **2017**, *6*, 6. [CrossRef] [PubMed]
2. Colla, E.; Jensen, P.H.; Pletnikova, O.; Troncoso, J.C.; Glabe, C.; Lee, M.K. Accumulation of toxic alpha-synuclein oligomer within endoplasmic reticulum occurs in alpha-synucleinopathy in vivo. *J. Neurosci.* **2012**, *32*, 3301–3305. [CrossRef]
3. Winner, B.; Jappelli, R.; Maji, S.K.; Desplats, P.A.; Boyer, L.; Aigner, S.; Hetzer, C.; Loher, T.; Vilar, M.; Campioni, S.; et al. In vivo demonstration that alpha-synuclein oligomers are toxic. *Proc. Natl. Acad. Sci. USA* **2011**, *108*, 4194–4199. [CrossRef] [PubMed]
4. Spillantini, M.G.; Schmidt, M.L.; Lee, V.M.; Trojanowski, J.Q.; Jakes, R.; Goedert, M. Alpha-synuclein in Lewy bodies. *Nature* **1997**, *388*, 839–840. [CrossRef] [PubMed]
5. Jellinger, K. Neuropathological substrates of Alzheimer's disease and Parkinson's disease. *J. Neural Transm. Suppl.* **1987**, *24*, 109–129.
6. Takahashi, H.; Wakabayashi, K. The cellular pathology of Parkinson's disease. *Neuropathology* **2001**, *21*, 315–322. [CrossRef]
7. Duda, J.E.; Giasson, B.I.; Mabon, M.E.; Lee, V.M.; Trojanowski, J.Q. Novel antibodies to synuclein show abundant striatal pathology in Lewy body diseases. *Ann. Neurol.* **2002**, *52*, 205–210. [CrossRef]
8. Selkoe, D.J. Alzheimer's disease is a synaptic failure. *Science* **2002**, *298*, 789–791. [CrossRef]
9. Kosik, K.S.; Duffy, L.K.; Dowling, M.M.; Abraham, C.; McCluskey, A.; Selkoe, D.J. Microtubule-associated protein 2: Monoclonal antibodies demonstrate the selective incorporation of certain epitopes into Alzheimer neurofibrillary tangles. *Proc. Natl. Acad. Sci. USA* **1984**, *81*, 7941–7945. [CrossRef]
10. Delacourte, A. Biochemical and molecular characterization of neurofibrillary degeneration in frontotemporal dementias. *Dement. Geriatr. Cogn. Disord.* **1999**, *10* (Suppl. 1), 75–79. [CrossRef]
11. Goldberg, A.L. Protein degradation and protection against misfolded or damaged proteins. *Nature* **2003**, *426*, 895–899. [CrossRef] [PubMed]
12. Klionsky, D.J.; Emr, S.D. Autophagy as a regulated pathway of cellular degradation. *Science* **2000**, *290*, 1717–1721. [CrossRef] [PubMed]
13. Alvarez-Erviti, L.; Rodriguez-Oroz, M.C.; Cooper, J.M.; Caballero, C.; Ferrer, I.; Obeso, J.A.; Schapira, A.H. Chaperone-mediated autophagy markers in Parkinson disease brains. *Arch. Neurol.* **2010**, *67*, 1464–1472. [CrossRef]
14. Cuervo, A.M.; Dice, J.F. Regulation of lamp2a levels in the lysosomal membrane. *Traffic* **2000**, *1*, 570–583. [CrossRef] [PubMed]
15. Cuervo, A.M.; Gomes, A.V.; Barnes, J.A.; Dice, J.F. Selective degradation of annexins by chaperone-mediated autophagy. *J. Biol. Chem.* **2000**, *275*, 33329–33335. [CrossRef] [PubMed]
16. Xilouri, M.; Brekk, O.R.; Polissidis, A.; Chrysanthou-Piterou, M.; Kloukina, I.; Stefanis, L. Impairment of chaperone-mediated autophagy induces dopaminergic neurodegeneration in rats. *Autophagy* **2016**, *12*, 2230–2247. [CrossRef] [PubMed]
17. Cuervo, A.M.; Stefanis, L.; Fredenburg, R.; Lansbury, P.T.; Sulzer, D. Impaired degradation of mutant alpha-synuclein by chaperone-mediated autophagy. *Science* **2004**, *305*, 1292–1295. [CrossRef]
18. Yu, W.H.; Dorado, B.; Figueroa, H.Y.; Wang, L.; Planel, E.; Cookson, M.R.; Clark, L.N.; Duff, K.E. Metabolic activity determines efficacy of macroautophagic clearance of pathological oligomeric alpha-synuclein. *Am. J. Pathol.* **2009**, *175*, 736–747. [CrossRef]
19. Spencer, B.; Potkar, R.; Trejo, M.; Rockenstein, E.; Patrick, C.; Gindi, R.; Adame, A.; Wyss-Coray, T.; Masliah, E. Beclin 1 gene transfer activates autophagy and ameliorates the neurodegenerative pathology in alpha-synuclein models of Parkinson's and Lewy body diseases. *J. Neurosci.* **2009**, *29*, 13578–13588. [CrossRef] [PubMed]
20. Almeida, C.G.; Takahashi, R.H.; Gouras, G.K. Beta-amyloid accumulation impairs multivesicular body sorting by inhibiting the ubiquitin-proteasome system. *J. Neurosci.* **2006**, *26*, 4277–4288. [CrossRef] [PubMed]
21. Oh, S.; Hong, H.S.; Hwang, E.; Sim, H.J.; Lee, W.; Shin, S.J.; Mook-Jung, I. Amyloid peptide attenuates the proteasome activity in neuronal cells. *Mech. Ageing Dev.* **2005**, *126*, 1292–1299. [CrossRef] [PubMed]

22. Mizuno, Y.; Ohta, S.; Tanaka, M.; Takamiya, S.; Suzuki, K.; Sato, T.; Oya, H.; Ozawa, T.; Kagawa, Y. Deficiencies in complex I subunits of the respiratory chain in Parkinson's disease. *Biochem. Biophys. Res. Commun.* **1989**, *163*, 1450–1455. [CrossRef]
23. Schapira, A.H.; Cooper, J.M.; Dexter, D.; Jenner, P.; Clark, J.B.; Marsden, C.D. Mitochondrial complex I deficiency in Parkinson's disease. *Lancet* **1989**, *1*, 1269. [CrossRef]
24. Bindoff, L.A.; Birch-Machin, M.; Cartlidge, N.E.; Parker, W.D., Jr.; Turnbull, D.M. Mitochondrial function in Parkinson's disease. *Lancet* **1989**, *2*, 49. [CrossRef]
25. Parker, W.D., Jr.; Boyson, S.J.; Parks, J.K. Abnormalities of the electron transport chain in idiopathic Parkinson's disease. *Ann. Neurol.* **1989**, *26*, 719–723. [CrossRef] [PubMed]
26. Perier, C.; Tieu, K.; Guegan, C.; Caspersen, C.; Jackson-Lewis, V.; Carelli, V.; Martinuzzi, A.; Hirano, M.; Przedborski, S.; Vila, M. Complex I deficiency primes Bax-dependent neuronal apoptosis through mitochondrial oxidative damage. *Proc. Natl. Acad. Sci. USA* **2005**, *102*, 19126–19131. [CrossRef] [PubMed]
27. Ryan, B.J.; Hoek, S.; Fon, E.A.; Wade-Martins, R. Mitochondrial dysfunction and mitophagy in Parkinson's: From familial to sporadic disease. *Trends Biochem. Sci.* **2015**, *40*, 200–210. [CrossRef]
28. Winklhofer, K.F.; Haass, C. Mitochondrial dysfunction in Parkinson's disease. *Biochim. Biophys. Acta* **2010**, *1802*, 29–44. [CrossRef]
29. Gonzalez-Casacuberta, I.; Juarez-Flores, D.L.; Moren, C.; Garrabou, G. Bioenergetics and Autophagic Imbalance in Patients-Derived Cell Models of Parkinson Disease Supports Systemic Dysfunction in Neurodegeneration. *Front. Neurosci.* **2019**, *13*, 894. [CrossRef]
30. Hsieh, C.H.; Shaltouki, A.; Gonzalez, A.E.; Bettencourt da Cruz, A.; Burbulla, L.F.; St Lawrence, E.; Schule, B.; Krainc, D.; Palmer, T.D.; Wang, X. Functional Impairment in Miro Degradation and Mitophagy Is a Shared Feature in Familial and Sporadic Parkinson's Disease. *Cell Stem Cell* **2016**, *19*, 709–724. [CrossRef]
31. Devi, L.; Raghavendran, V.; Prabhu, B.M.; Avadhani, N.G.; Anandatheerthavarada, H.K. Mitochondrial import and accumulation of alpha-synuclein impair complex I in human dopaminergic neuronal cultures and Parkinson disease brain. *J. Biol. Chem.* **2008**, *283*, 9089–9100. [CrossRef]
32. Di Maio, R.; Barrett, P.J.; Hoffman, E.K.; Barrett, C.W.; Zharikov, A.; Borah, A.; Hu, X.; McCoy, J.; Chu, C.T.; Burton, E.A.; et al. alpha-Synuclein binds to TOM20 and inhibits mitochondrial protein import in Parkinson's disease. *Sci. Transl. Med.* **2016**, *8*, 342ra78. [CrossRef]
33. Kamp, F.; Exner, N.; Lutz, A.K.; Wender, N.; Hegermann, J.; Brunner, B.; Nuscher, B.; Bartels, T.; Giese, A.; Beyer, K.; et al. Inhibition of mitochondrial fusion by alpha-synuclein is rescued by PINK1, Parkin and DJ-1. *EMBO J.* **2010**, *29*, 3571–3589. [CrossRef]
34. Reeve, A.K.; Ludtmann, M.H.; Angelova, P.R.; Simcox, E.M.; Horrocks, M.H.; Klenerman, D.; Gandhi, S.; Turnbull, D.M.; Abramov, A.Y. Aggregated alpha-synuclein and complex I deficiency: Exploration of their relationship in differentiated neurons. *Cell Death Dis.* **2015**, *6*, e1820. [CrossRef]
35. Mochizuki, H.; Goto, K.; Mori, H.; Mizuno, Y. Histochemical detection of apoptosis in Parkinson's disease. *J. Neurol. Sci.* **1996**, *137*, 120–123. [CrossRef]
36. Andersen, J.K. Does neuronal loss in Parkinson's disease involve programmed cell death? *Bioessays* **2001**, *23*, 640–646. [CrossRef]
37. Hartmann, A.; Troadec, J.D.; Hunot, S.; Kikly, K.; Faucheux, B.A.; Mouatt-Prigent, A.; Ruberg, M.; Agid, Y.; Hirsch, E.C. Caspase-8 is an effector in apoptotic death of dopaminergic neurons in Parkinson's disease, but pathway inhibition results in neuronal necrosis. *J. Neurosci.* **2001**, *21*, 2247–2255. [CrossRef]
38. Murray, H.C.; Swanson, M.E.V.; Dieriks, B.V.; Turner, C.; Faull, R.L.M.; Curtis, M.A. Neurochemical Characterization of PSA-NCAM(+) Cells in the Human Brain and Phenotypic Quantification in Alzheimer's Disease Entorhinal Cortex. *Neuroscience* **2018**, *372*, 289–303. [CrossRef]
39. Shahani, N.; Subramaniam, S.; Wolf, T.; Tackenberg, C.; Brandt, R. Tau aggregation and progressive neuronal degeneration in the absence of changes in spine density and morphology after targeted expression of Alzheimer's disease-relevant tau constructs in organotypic hippocampal slices. *J. Neurosci.* **2006**, *26*, 6103–6114. [CrossRef]
40. Clifford, P.M.; Zarrabi, S.; Siu, G.; Kinsler, K.J.; Kosciuk, M.C.; Venkataraman, V.; D'Andrea, M.R.; Dinsmore, S.; Nagele, R.G. Abeta peptides can enter the brain through a defective blood-brain barrier and bind selectively to neurons. *Brain Res.* **2007**, *1142*, 223–236. [CrossRef]

41. Reddy, P.H. Amyloid precursor protein-mediated free radicals and oxidative damage: Implications for the development and progression of Alzheimer's disease. *J. Neurochem.* **2006**, *96*, 1–13. [CrossRef]
42. Fifre, A.; Sponne, I.; Koziel, V.; Kriem, B.; Yen Potin, F.T.; Bihain, B.E.; Olivier, J.L.; Oster, T.; Pillot, T. Microtubule-associated protein MAP1A, MAP1B, and MAP2 proteolysis during soluble amyloid beta-peptide-induced neuronal apoptosis. Synergistic involvement of calpain and caspase-3. *J. Biol. Chem.* **2006**, *281*, 229–240. [CrossRef]
43. Jenner, P. Oxidative stress in Parkinson's disease. *Ann. Neurol.* **2003**, *53* (Suppl. 3), S26–S36, discussion S36-8. [CrossRef]
44. Di Nottia, M.; Masciullo, M.; Verrigni, D.; Petrillo, S.; Modoni, A.; Rizzo, V.; Di Giuda, D.; Rizza, T.; Niceta, M.; Torraco, A.; et al. DJ-1 modulates mitochondrial response to oxidative stress: Clues from a novel diagnosis of PARK7. *Clin. Genet.* **2017**, *92*, 18–25. [CrossRef]
45. Dehay, B.; Bove, J.; Rodriguez-Muela, N.; Perier, C.; Recasens, A.; Boya, P.; Vila, M. Pathogenic lysosomal depletion in Parkinson's disease. *J. Neurosci.* **2010**, *30*, 12535–12544. [CrossRef]
46. Nunomura, A.; Honda, K.; Takeda, A.; Hirai, K.; Zhu, X.; Smith, M.A.; Perry, G. Oxidative damage to RNA in neurodegenerative diseases. *J. Biomed. Biotechnol.* **2006**, *2006*, 82323. [CrossRef]
47. Sultana, R.; Butterfield, D.A. Role of oxidative stress in the progression of Alzheimer's disease. *J. Alzheimers Dis* **2010**, *19*, 341–353. [CrossRef]
48. Butterfield, D.A.; Swomley, A.M.; Sultana, R. Amyloid beta-peptide (1-42)-induced oxidative stress in Alzheimer disease: Importance in disease pathogenesis and progression. *Antioxid. Redox Signal.* **2013**, *19*, 823–835. [CrossRef]
49. De Felice, F.G.; Velasco, P.T.; Lambert, M.P.; Viola, K.; Fernandez, S.J.; Ferreira, S.T.; Klein, W.L. Abeta oligomers induce neuronal oxidative stress through an N-methyl-D-aspartate receptor-dependent mechanism that is blocked by the Alzheimer drug memantine. *J. Biol. Chem.* **2007**, *282*, 11590–11601. [CrossRef]
50. Akiyama, H. Inflammation and Alzheimer's disease. *Neurobiol. Aging* **2000**, *21*, 383–421. [CrossRef]
51. Akiyama, H.; Arai, T.; Kondo, H.; Tanno, E.; Haga, C.; Ikeda, K. Cell Mediators of Inflammation in the Alzheimer Disease Brain. *Alzheimer Dis. Assoc. Disord.* **2000**, *14*, S47–S53. [CrossRef]
52. Sofroniew, M.V.; Vinters, H.V. Astrocytes: Biology and pathology. *Acta Neuropathol.* **2010**, *119*, 7–35. [CrossRef]
53. Kalaria, R.N. Microglia and Alzheimer's disease. *Curr. Opin. Hematol.* **1999**, *6*, 15. [CrossRef]
54. Rogers, J.; Lue, L.-F. Microglial chemotaxis, activation, and phagocytosis of amyloid β-peptide as linked phenomena in Alzheimer's disease. *Neurochem. Int.* **2001**, *39*, 333–340. [CrossRef]
55. Dionisio-Santos, D.A.; Olschowka, J.A.; O'Banion, M.K. Exploiting microglial and peripheral immune cell crosstalk to treat Alzheimer's disease. *J. Neuroinflamm.* **2019**, *16*, 74. [CrossRef]
56. Kopec, K.K.; Carroll, R.T. Alzheimer's β-Amyloid Peptide 1-42 Induces a Phagocytic Response in Murine Microglia. *J. Neurochem.* **2002**, *71*, 2123–2131. [CrossRef]
57. Bolmont, T.; Haiss, F.; Eicke, D.; Radde, R.; Mathis, C.A.; Klunk, W.E.; Kohsaka, S.; Jucker, M.; Calhoun, M.E. Dynamics of the Microglial/Amyloid Interaction Indicate a Role in Plaque Maintenance. *J. Neurosci.* **2008**, *28*, 4283–4292. [CrossRef]
58. Meyer-Luehmann, M.; Spires-Jones, T.L.; Prada, C.; Garcia-Alloza, M.; de Calignon, A.; Rozkalne, A.; Koenigsknecht-Talboo, J.; Holtzman, D.M.; Bacskai, B.J.; Hyman, B.T. Rapid appearance and local toxicity of amyloid-β plaques in a mouse model of Alzheimer's disease. *Nature* **2008**, *451*, 720–724. [CrossRef]
59. Malchiodi-Albedi, F.; Domenici, M.R.; Paradisi, S.; Bernardo, A.; Ajmone-Cat, M.A.; Minghetti, L. Astrocytes contribute to neuronal impairment in βA toxicity increasing apoptosis in rat hippocampal neurons. *Glia* **2001**, *34*, 68–72. [CrossRef]
60. Yamaguchi, H.; Sugihara, S.; Ogawa, A.; Saido, T.C.; Ihara, Y. Diffuse plaques associated with astroglial amyloid β protein, possibly showing a disappearing stage of senile plaques. *Acta Neuropathol.* **1998**, *95*, 217–222. [CrossRef]
61. Perez, J.L.; Carrero, I.; Gonzalo, P.; Arevalo-Serrano, J.; Sanz-Anquela, J.M.; Ortega, J.; Rodriguez, M.; Gonzalo-Ruiz, A. Soluble oligomeric forms of beta-amyloid (Aβ) peptide stimulate Aβ production via astrogliosis in the rat brain. *Exp. Neurol.* **2010**, *223*, 410–421. [CrossRef]
62. Emmerling, M.R.; Watson, M.D.; Raby, C.A.; Spiegel, K. The role of complement in Alzheimer's disease pathology. *Biochim. Biophys. Acta (BBA) Mol. Basis Dis.* **2000**, *1502*, 158–171. [CrossRef]

63. Carroll, M.C. The role of complement and complement receptors in induction and regulation of immunity. *Annu. Rev. Immunol.* **1998**, *16*, 545–568. [CrossRef]
64. Tenner, A. Complement in Alzheimer's disease: Opportunities for modulating protective and pathogenic events. *Neurobiol. Aging* **2001**, *22*, 849–861. [CrossRef]
65. Friedman, W.J. Cytokines Regulate Expression of the Type 1 Interleukin-1 Receptor in Rat Hippocampal Neurons and Glia. *Exp. Neurol.* **2001**, *168*, 23–31. [CrossRef]
66. Yuekui, L.; Barger, S.W.; Liu, L.; Mrak, R.E.; Griffin, W.S.T. S100β Induction of the Proinflammatory Cytokine Interleukin-6 in Neurons. *J. Neurochem.* **2001**, *74*, 143–150. [CrossRef]
67. Renauld, A.E.; Spengler, R.N. Tumor necrosis factor expressed by primary hippocampal neurons and SH-SY5Y cells is regulated by α_2-adrenergic receptor activation. *J. Neurosci. Res.* **2002**, *67*, 264–274. [CrossRef]
68. Yasojima, K.; Schwab, C.; McGeer, E.G.; McGeer, P.L. Human neurons generate C-reactive protein and amyloid P: Upregulation in Alzheimer's disease. *Brain Res.* **2000**, *887*, 80–89. [CrossRef]
69. Shen, Y.; Li, R.; McGeer, E.G.; McGeer, P.L. Neuronal expression of mRNAs for complement proteins of the classical pathway in Alzheimer brain. *Brain Res.* **1997**, *769*, 391–395. [CrossRef]
70. Tansey, M.G.; Goldberg, M.S. Neuroinflammation in Parkinson's disease: Its role in neuronal death and implications for therapeutic intervention. *Neurobiol. Dis.* **2010**, *37*, 510–518. [CrossRef]
71. Ouchi, Y.; Yoshikawa, E.; Sekine, Y.; Futatsubashi, M.; Kanno, T.; Ogusu, T.; Torizuka, T. Microglial activation and dopamine terminal loss in early Parkinson's disease. *Ann. Neurol.* **2005**, *57*, 168–175. [CrossRef]
72. Gerhard, A.; Pavese, N.; Hotton, G.; Turkheimer, F.; Es, M.; Hammers, A.; Eggert, K.; Oertel, W.; Banati, R.B.; Brooks, D.J. In vivo imaging of microglial activation with [11C](R)-PK11195 PET in idiopathic Parkinson's disease. *Neurobiol. Dis.* **2006**, *21*, 404–412. [CrossRef]
73. McGeer, P.L.; Itagaki, S.; Boyes, B.E.; McGeer, E.G. Reactive microglia are positive for HLA-DR in the substantia nigra of Parkinson's and Alzheimer's disease brains. *Neurology* **1988**, *38*, 1285. [CrossRef]
74. Imamura, K.; Hishikawa, N.; Sawada, M.; Nagatsu, T.; Yoshida, M.; Hashizume, Y. Distribution of major histocompatibility complex class II-positive microglia and cytokine profile of Parkinson's disease brains. *Acta Neuropathol.* **2003**, *106*, 518–526. [CrossRef]
75. Croisier, E.; Moran, L.B.; Dexter, D.T.; Pearce, R.K.; Graeber, M.B. Microglial inflammation in the parkinsonian substantia nigra: Relationship to alpha-synuclein deposition. *J. Neuroinflamm.* **2005**, *2*, 14. [CrossRef]
76. Orr, C.F.; Rowe, D.B.; Mizuno, Y.; Mori, H.; Halliday, G.M. A possible role for humoral immunity in the pathogenesis of Parkinson's disease. *Brain* **2005**, *128*, 2665–2674. [CrossRef]
77. Banati, R.B.; Daniel, S.E.; Blunt, S.B. Glial pathology but absence of apoptotic nigral neurons in long-standing Parkinson's disease. *Mov. Disord.* **1998**, *13*, 221–227. [CrossRef]
78. Akiyama, H.; McGeer, P.L. Microglial response to 6-hydroxydopamine-induced substantia nigra lesions. *Brain Res.* **1989**, *489*, 247–253. [CrossRef]
79. Marinova-Mutafchieva, L.; Sadeghian, M.; Broom, L.; Davis, J.B.; Medhurst, A.D.; Dexter, D.T. Relationship between microglial activation and dopaminergic neuronal loss in the substantia nigra: A time course study in a 6-hydroxydopamine model of Parkinson's disease. *J. Neurochem.* **2009**, *110*, 966–975. [CrossRef]
80. Vázquez-Claverie, M.; Garrido-Gil, P.; San Sebastián, W.; Izal-Azcárate, A.; Belzunegui, S.; Marcilla, I.; López, B.; Luquin, M.-R. Acute and Chronic 1-Methyl-4-Phenyl-1,2,3,6-Tetrahydropyridine Administrations Elicit Similar Microglial Activation in the Substantia Nigra of Monkeys. *J. Neuropathol. Exp. Neurol.* **2009**, *68*, 977–984. [CrossRef]
81. Sanchez-Guajardo, V.; Febbraro, F.; Kirik, D.; Romero-Ramos, M. Microglia Acquire Distinct Activation Profiles Depending on the Degree of α-Synuclein Neuropathology in a rAAV Based Model of Parkinson's Disease. *PLoS ONE* **2010**, *5*, e8784. [CrossRef]
82. Henry, V.; Paillé, V.; Lelan, F.; Brachet, P.; Damier, P. Kinetics of Microglial Activation and Degeneration of Dopamine-Containing Neurons in a Rat Model of Parkinson Disease Induced by 6-Hydroxydopamine. *J. Neuropathol. Exp. Neurol.* **2009**, *68*, 1092–1102. [CrossRef]
83. Hunot, S.; Boissière, F.; Faucheux, B.; Brugg, B.; Mouatt-Prigent, A.; Agid, Y.; Hirsch, E.C. Nitric oxide synthase and neuronal vulnerability in Parkinson's disease. *Neuroscience* **1996**, *72*, 355–363. [CrossRef]
84. Knott, C.; Stern, G.; Wilkin, G.P. Inflammatory Regulators in Parkinson's Disease: iNOS, Lipocortin-1, and Cyclooxygenases-1 and -2. *Mol. Cell. Neurosci.* **2000**, *16*, 724–739. [CrossRef]

85. Litteljohn, D.; Mangano, E.; Shukla, N.; Hayley, S. Interferon-γ deficiency modifies the motor and co-morbid behavioral pathology and neurochemical changes provoked by the pesticide paraquat. *Neuroscience* **2009**, *164*, 1894–1906. [CrossRef]
86. Barcia, C.; Ros, C.M.; Annese, V.; Gómez, A.; Ros-Bernal, F.; Aguado-Yera, D.; Martínez-Pagán, M.E.; de Pablos, V.; Fernandez-Villalba, E.; Herrero, M.T. IFN-γ signaling, with the synergistic contribution of TNF-α, mediates cell specific microglial and astroglial activation in experimental models of Parkinson's disease. *Cell Death Dis.* **2011**, *2*, e142. [CrossRef]
87. Chakrabarty, P.; Ceballos-Diaz, C.; Lin, W.-L.; Beccard, A.; Jansen-West, K.; McFarland, N.R.; Janus, C.; Dickson, D.; Das, P.; Golde, T.E. Interferon-γ induces progressive nigrostriatal degeneration and basal ganglia calcification. *Nat. Neurosci.* **2011**, *14*, 694–696. [CrossRef]
88. Mangano, E.N.; Litteljohn, D.; So, R.; Nelson, E.; Peters, S.; Bethune, C.; Bobyn, J.; Hayley, S. Interferon-γ plays a role in paraquat-induced neurodegeneration involving oxidative and proinflammatory pathways. *Neurobiol. Aging* **2012**, *33*, 1411–1426. [CrossRef]
89. Reynolds, A.D.; Banerjee, R.; Liu, J.; Gendelman, H.E.; Mosley, R.L. Neuroprotective activities of CD4+CD25+ regulatory T cells in an animal model of Parkinson's disease. *J. Leukoc. Biol.* **2007**, *82*, 1083–1094. [CrossRef]
90. Kosloski, L.M.; Kosmacek, E.A.; Olson, K.E.; Mosley, R.L.; Gendelman, H.E. GM-CSF induces neuroprotective and anti-inflammatory responses in 1-methyl-4-phenyl-1,2,3,6-tetrahydropyridine intoxicated mice. *J. Neuroimmunol.* **2013**, *265*, 1–10. [CrossRef]
91. Ruankham, W.; Suwanjang, W.; Wongchitrat, P.; Prachayasittikul, V.; Prachayasittikul, S.; Phopin, K. Sesamin and sesamol attenuate H2O2 -induced oxidative stress on human neuronal cells via the SIRT1-SIRT3-FOXO3a signaling pathway. *Nutr. Neurosci.* **2019**, 1–12. [CrossRef] [PubMed]
92. Baluchnejadmojarad, T.; Mansouri, M.; Ghalami, J.; Mokhtari, Z.; Roghani, M. Sesamin imparts neuroprotection against intrastriatal 6-hydroxydopamine toxicity by inhibition of astroglial activation, apoptosis, and oxidative stress. *Biomed. Pharmacother.* **2017**, *88*, 754–761. [CrossRef] [PubMed]
93. Lahaie-Collins, V.; Bournival, J.; Plouffe, M.; Carange, J.; Martinoli, M.G. Sesamin modulates tyrosine hydroxylase, superoxide dismutase, catalase, inducible NO synthase and interleukin-6 expression in dopaminergic cells under MPP+-induced oxidative stress. *Oxid. Med. Cell. Longev.* **2008**, *1*, 54–62. [CrossRef] [PubMed]
94. Lee, S.; Youn, K.; Jeong, W.S.; Ho, C.T.; Jun, M. Protective Effects of Red Ginseng Oil against Abeta25-35-Induced Neuronal Apoptosis and Inflammation in PC12 Cells. *Int. J. Mol. Sci.* **2017**, *18*, 2218. [CrossRef]
95. Lee, S.; Youn, K.; Jun, M. Major compounds of red ginseng oil attenuate Abeta25-35-induced neuronal apoptosis and inflammation by modulating MAPK/NF-kappaB pathway. *Food Funct.* **2018**, *9*, 4122–4134. [CrossRef] [PubMed]
96. Cioanca, O.; Hritcu, L.; Mihasan, M.; Hancianu, M. Cognitive-enhancing and antioxidant activities of inhaled coriander volatile oil in amyloid beta(1-42) rat model of Alzheimer's disease. *Physiol. Behav.* **2013**, *120*, 193–202. [CrossRef]
97. Liu, Q.F.; Jeong, H.; Lee, J.H.; Hong, Y.K.; Oh, Y.; Kim, Y.M.; Suh, Y.S.; Bang, S.; Yun, H.S.; Lee, K.; et al. Coriandrum sativum Suppresses Abeta42-Induced ROS Increases, Glial Cell Proliferation, and ERK Activation. *Am. J. Chin. Med.* **2016**, *44*, 1325–1347. [CrossRef]
98. Alhibshi, A.H.; Odawara, A.; Suzuki, I. Neuroprotective efficacy of thymoquinone against amyloid beta-induced neurotoxicity in human induced pluripotent stem cell-derived cholinergic neurons. *Biochem. Biophys. Rep.* **2019**, *17*, 122–126. [CrossRef]
99. Abulfadl, Y.; El-Maraghy, N.; Ahmed, A.E.; Nofal, S.; Abdel-Mottaleb, Y.; Badary, O. Thymoquinone alleviates the experimentally induced Alzheimer's disease inflammation by modulation of TLRs signaling. *Hum. Exp. Toxicol.* **2018**, *37*, 1092–1104. [CrossRef]
100. Cobourne-Duval, M.K.; Taka, E.; Mendonca, P.; Soliman, K.F.A. Thymoquinone increases the expression of neuroprotective proteins while decreasing the expression of pro-inflammatory cytokines and the gene expression NFκB pathway signaling targets in LPS/IFNγ -activated BV-2 microglia cells. *J. Neuroimmunol.* **2018**, *320*, 87–97. [CrossRef]
101. Deng, M.Z.; Huang, L.P.; Fang, Y.Q. Effects of Total Ginsenosides and Volatile Oil of Acorus tatarinowii Co-Administration on Ability of Learning and Memory and Apoptosis in Alzheimer's Disease Mice Model Induced By D-Galactose and Aluminium Chloride. *Zhong Yao Cai* **2015**, *38*, 1018–1023. [PubMed]

102. Ning, B.; Zhang, Q.; Wang, N.; Deng, M.; Fang, Y. beta-Asarone Regulates ER Stress and Autophagy Via Inhibition of the PERK/CHOP/Bcl-2/Beclin-1 Pathway in 6-OHDA-Induced Parkinsonian Rats. *Neurochem. Res.* **2019**, *44*, 1159–1166. [CrossRef] [PubMed]
103. St-Laurent-Thibault, C.; Arseneault, M.; Longpre, F.; Ramassamy, C. Tyrosol and hydroxytyrosol, two main components of olive oil, protect N2a cells against amyloid-beta-induced toxicity. Involvement of the NF-kappaB signaling. *Curr. Alzheimer Res.* **2011**, *8*, 543–551. [CrossRef] [PubMed]
104. Yu, G.; Deng, A.; Tang, W.; Ma, J.; Yuan, C.; Ma, J. Hydroxytyrosol induces phase II detoxifying enzyme expression and effectively protects dopaminergic cells against dopamine- and 6-hydroxydopamine induced cytotoxicity. *Neurochem. Int.* **2016**, *96*, 113–120. [CrossRef]
105. Batarseh, Y.S.; Mohamed, L.A.; Al Rihani, S.B.; Mousa, Y.M.; Siddique, A.B.; El Sayed, K.A.; Kaddoumi, A. Oleocanthal ameliorates amyloid-β oligomers' toxicity on astrocytes and neuronal cells: In vitro studies. *Neuroscience* **2017**, *352*, 204–215. [CrossRef]
106. Huang, B.; He, D.; Chen, G.; Ran, X.; Guo, W.; Kan, X.; Wang, W.; Liu, D.; Fu, S.; Liu, J. α-Cyperone inhibits LPS-induced inflammation in BV-2 cells through activation of Akt/Nrf2/HO-1 and suppression of the NF-κB pathway. *Food Funct.* **2018**, *9*, 2735–2743. [CrossRef]
107. Labrousse, V.F.; Nadjar, A.; Joffre, C.; Costes, L.; Aubert, A.; Grégoire, S.; Bretillon, L.; Layé, S. Short-term long chain omega3 diet protects from neuroinflammatory processes and memory impairment in aged mice. *PLoS ONE* **2012**, *7*, e36861. [CrossRef]
108. Doria, M.; Maugest, L.; Moreau, T.; Lizard, G.; Vejux, A. Contribution of cholesterol and oxysterols to the pathophysiology of Parkinson's disease. *Free Radic. Biol. Med.* **2016**, *101*, 393–400. [CrossRef]
109. Testa, G.; Staurenghi, E.; Zerbinati, C.; Gargiulo, S.; Iuliano, L.; Giaccone, G.; Fantò, F.; Poli, G.; Leonarduzzi, G.; Gamba, P. Changes in brain oxysterols at different stages of Alzheimer's disease: Their involvement in neuroinflammation. *Redox Biol.* **2016**, *10*, 24–33. [CrossRef]
110. Brahmi, F.; Vejux, A.; Sghaier, R.; Zarrouk, A.; Nury, T.; Meddeb, W.; Rezig, L.; Namsi, A.; Sassi, K.; Yammine, A.; et al. Prevention of 7-ketocholesterol-induced side effects by natural compounds. *Crit. Rev. Food Sci. Nutr.* **2019**, *59*, 3179–3198. [CrossRef]
111. Badreddine, A.; Zarrouk, A.; Karym, E.M.; Debbabi, M.; Nury, T.; Meddeb, W.; Sghaier, R.; Bezine, M.; Vejux, A.; Martine, L.; et al. Argan Oil-Mediated Attenuation of Organelle Dysfunction, Oxidative Stress and Cell Death Induced by 7-Ketocholesterol in Murine Oligodendrocytes 158N. *Int. J. Mol. Sci.* **2017**, *18*, 2220. [CrossRef] [PubMed]
112. Meddeb, W.; Rezig, L.; Zarrouk, A.; Nury, T.; Vejux, A.; Prost, M.; Bretillon, L.; Mejri, M.; Lizard, G. Cytoprotective Activities of Milk Thistle Seed Oil Used in Traditional Tunisian Medicine on 7-Ketocholesterol and 24S-Hydroxycholesterol-Induced Toxicity on 158N Murine Oligodendrocytes. *Antioxidants* **2018**, *7*, 95. [CrossRef] [PubMed]
113. Xiong, Q.; Ru, Q.; Tian, X.; Zhou, M.; Chen, L.; Li, Y.; Li, C. Krill oil protects PC12 cells against methamphetamine-induced neurotoxicity by inhibiting apoptotic response and oxidative stress. *Nutr. Res.* **2018**, *58*, 84–94. [CrossRef] [PubMed]
114. Li, Q.; Wu, F.; Wen, M.; Yanagita, T.; Xue, C.; Zhang, T.; Wang, Y. The Protective Effect of Antarctic Krill Oil on Cognitive Function by Inhibiting Oxidative Stress in the Brain of Senescence-Accelerated Prone Mouse Strain 8 (SAMP8) Mice. *J. Food Sci.* **2018**, *83*, 543–551. [CrossRef]
115. Hopperton, K.E.; Trépanier, M.-O.; James, N.C.E.; Chouinard-Watkins, R.; Bazinet, R.P. Fish oil feeding attenuates neuroinflammatory gene expression without concomitant changes in brain eicosanoids and docosanoids in a mouse model of Alzheimer's disease. *Brain Behav. Immun.* **2018**, *69*, 74–90. [CrossRef]
116. Jović, M.; Lončarević-Vasiljković, N.; Ivković, S.; Dinić, J.; Milanović, D.; Zlokovic, B.; Kanazir, S. Short-term fish oil supplementation applied in presymptomatic stage of Alzheimer's disease enhances microglial/macrophage barrier and prevents neuritic dystrophy in parietal cortex of 5xFAD mouse model. *PLoS ONE* **2019**, *14*, e0216726. [CrossRef]
117. Matchynski, J.J.; Lowrance, S.A.; Pappas, C.; Rossignol, J.; Puckett, N.; Sandstrom, M.; Dunbar, G.L. Combinatorial treatment of tart cherry extract and essential fatty acids reduces cognitive impairments and inflammation in the mu-p75 saporin-induced mouse model of Alzheimer's disease. *J. Med. Food* **2013**, *16*, 288–295. [CrossRef]

118. Ji, A.; Diao, H.; Wang, X.; Yang, R.; Zhang, J.; Luo, W.; Cao, R.; Cao, Z.; Wang, F.; Cai, T. n-3 polyunsaturated fatty acids inhibit lipopolysaccharide-induced microglial activation and dopaminergic injury in rats. *NeuroToxicology* **2012**, *33*, 780–788. [CrossRef]
119. Zarrouk, A.; Ben Salem, Y.; Hafsa, J.; Sghaier, R.; Charfeddine, B.; Limem, K.; Hammami, M.; Majdoub, H. 7beta-hydroxycholesterol-induced cell death, oxidative stress, and fatty acid metabolism dysfunctions attenuated with sea urchin egg oil. *Biochimie* **2018**, *153*, 210–219. [CrossRef]
120. Altinoz, M.A.; Ozpinar, A. PPAR-delta and erucic acid in multiple sclerosis and Alzheimer's Disease. Likely benefits in terms of immunity and metabolism. *Int. Immunopharmacol.* **2019**, *69*, 245–256. [CrossRef]
121. Debbabi, M.; Zarrouk, A.; Bezine, M.; Meddeb, W.; Nury, T.; Badreddine, A.; Karym, E.M.; Sghaier, R.; Bretillon, L.; Guyot, S.; et al. Comparison of the effects of major fatty acids present in the Mediterranean diet (oleic acid, docosahexaenoic acid) and in hydrogenated oils (elaidic acid) on 7-ketocholesterol-induced oxiapoptophagy in microglial BV-2 cells. *Chem. Phys. Lipids* **2017**, *207*, 151–170. [CrossRef] [PubMed]
122. Zhang, Y.P.; Brown, R.E.; Zhang, P.C.; Zhao, Y.T.; Ju, X.H.; Song, C. DHA, EPA and their combination at various ratios differently modulated Abeta25-35-induced neurotoxicity in SH-SY5Y cells. *Prostaglandins Leukot. Essent. Fatty Acids* **2018**, *136*, 85–94. [CrossRef] [PubMed]
123. Che, H.; Zhou, M.; Zhang, T.; Zhang, L.; Ding, L.; Yanagita, T.; Xu, J.; Xue, C.; Wang, Y. Comparative study of the effects of phosphatidylcholine rich in DHA and EPA on Alzheimer's disease and the possible mechanisms in CHO-APP/PS1 cells and SAMP8 mice. *Food Funct.* **2018**, *9*, 643–654. [CrossRef] [PubMed]
124. Wen, M.; Ding, L.; Zhang, L.; Cong, P.; Zhang, T.; Xu, J.; Chang, Y.; Wang, Y.; Xue, C. A comparative study of eicosapentaenoic acid enriched phosphatidylcholine and ethyl ester in improving cognitive deficiency in Alzheimer's disease model rats. *Food Funct.* **2018**, *9*, 2184–2192. [CrossRef]
125. Zhou, M.M.; Ding, L.; Wen, M.; Che, H.X.; Huang, J.Q.; Zhang, T.T.; Xue, C.H.; Mao, X.Z.; Wang, Y.M. Mechanisms of DHA-enriched phospholipids in improving cognitive deficits in aged SAMP8 mice with high-fat diet. *J. Nutr. Biochem.* **2018**, *59*, 64–75. [CrossRef]
126. Wu, Y.; Tada, M.; Takahata, K.; Tomizawa, K.; Matsui, H. Inhibitory effect of polyunsaturated fatty acids on apoptosis induced by etoposide, okadaic acid and AraC in Neuro2a cells. *Acta Med. Okayama* **2007**, *61*, 147–152.
127. Wang, X.; Hjorth, E.; Vedin, I.; Eriksdotter, M.; Freund-Levi, Y.; Wahlund, L.-O.; Cederholm, T.; Palmblad, J.; Schultzberg, M. Effects of n-3 FA supplementation on the release of proresolving lipid mediators by blood mononuclear cells: The OmegAD study. *J. Lipid Res.* **2015**, *56*, 674–681. [CrossRef]
128. Dong, Y.; Xu, M.; Kalueff, A.V.; Song, C. Dietary eicosapentaenoic acid normalizes hippocampal omega-3 and 6 polyunsaturated fatty acid profile, attenuates glial activation and regulates BDNF function in a rodent model of neuroinflammation induced by central interleukin-1β administration. *Eur. J. Nutr.* **2018**, *57*, 1781–1791. [CrossRef]
129. Vedin, I.; Cederholm, T.; Freund-Levi, Y.; Basun, H.; Garlind, A.; Irving, G.F.; Eriksdotter-Jönhagen, M.; Wahlund, L.-O.; Dahlman, I.; Palmblad, J. Effects of DHA-rich n-3 fatty acid supplementation on gene expression in blood mononuclear leukocytes: The OmegAD study. *PLoS ONE* **2012**, *7*, e35425. [CrossRef]
130. Vedin, I.; Cederholm, T.; Freund Levi, Y.; Basun, H.; Garlind, A.; Faxén Irving, G.; Jönhagen, M.E.; Vessby, B.; Wahlund, L.-O.; Palmblad, J. Effects of docosahexaenoic acid-rich n-3 fatty acid supplementation on cytokine release from blood mononuclear leukocytes: The OmegAD study. *Am. J. Clin. Nutr.* **2008**, *87*, 1616–1622. [CrossRef]
131. Sharman, M.J.; Gyengesi, E.; Liang, H.; Chatterjee, P.; Karl, T.; Li, Q.-X.; Wenk, M.R.; Halliwell, B.; Martins, R.N.; Münch, G. Assessment of diets containing curcumin, epigallocatechin-3-gallate, docosahexaenoic acid and α-lipoic acid on amyloid load and inflammation in a male transgenic mouse model of Alzheimer's disease: Are combinations more effective? *Neurobiol. Dis.* **2019**, *124*, 505–519. [CrossRef] [PubMed]
132. Hjorth, E.; Zhu, M.; Toro, V.C.; Vedin, I.; Palmblad, J.; Cederholm, T.; Freund-Levi, Y.; Faxen-Irving, G.; Wahlund, L.-O.; Basun, H.; et al. Omega-3 fatty acids enhance phagocytosis of Alzheimer's disease-related amyloid-β42 by human microglia and decrease inflammatory markers. *J. Alzheimers Dis.* **2013**, *35*, 697–713. [CrossRef]
133. Serrano-Garcia, N.; Fernandez-Valverde, F.; Luis-Garcia, E.R.; Granados-Rojas, L.; Juarez-Zepeda, T.E.; Orozco-Suarez, S.A.; Pedraza-Chaverri, J.; Orozco-Ibarra, M.; Jimenez-Anguiano, A. Docosahexaenoic acid protection in a rotenone induced Parkinson's model: Prevention of tubulin and synaptophysin loss, but no association with mitochondrial function. *Neurochem. Int.* **2018**, *121*, 26–37. [CrossRef]

134. Hacioglu, G.; Seval-Celik, Y.; Tanriover, G.; Ozsoy, O.; Saka-Topcuoglu, E.; Balkan, S.; Agar, A. Docosahexaenoic acid provides protective mechanism in bilaterally MPTP-lesioned rat model of Parkinson's disease. *Folia Histochem. Cytobiol.* **2012**, *50*, 228–238. [CrossRef] [PubMed]
135. Ozsoy, O.; Seval-Celik, Y.; Hacioglu, G.; Yargicoglu, P.; Demir, R.; Agar, A.; Aslan, M. The influence and the mechanism of docosahexaenoic acid on a mouse model of Parkinson's disease. *Neurochem. Int.* **2011**, *59*, 664–670. [CrossRef] [PubMed]
136. Lee, H.J.; Han, J.; Jang, Y.; Kim, S.J.; Park, J.H.; Seo, K.S.; Jeong, S.; Shin, S.; Lim, K.; Heo, J.Y.; et al. Docosahexaenoic acid prevents paraquat-induced reactive oxygen species production in dopaminergic neurons via enhancement of glutathione homeostasis. *Biochem. Biophys. Res. Commun.* **2015**, *457*, 95–100. [CrossRef] [PubMed]
137. Hossain, M.S.; Ifuku, M.; Take, S.; Kawamura, J.; Miake, K.; Katafuchi, T. Plasmalogens rescue neuronal cell death through an activation of AKT and ERK survival signaling. *PLoS ONE* **2013**, *8*, e83508. [CrossRef]
138. Luchtman, D.W.; Meng, Q.; Song, C. Ethyl-eicosapentaenoate (E-EPA) attenuates motor impairments and inflammation in the MPTP-probenecid mouse model of Parkinson's disease. *Behav. Brain Res.* **2012**, *226*, 386–396. [CrossRef]
139. Kujawska, M.; Jodynis-Liebert, J. Polyphenols in Parkinson's Disease: A Systematic Review of In Vivo Studies. *Nutrients* **2018**, *10*, 642. [CrossRef]
140. Bureau, G.; Longpré, F.; Martinoli, M.-G. Resveratrol and quercetin, two natural polyphenols, reduce apoptotic neuronal cell death induced by neuroinflammation. *J. Neurosci. Res.* **2008**, *86*, 403–410. [CrossRef]

Discussion

Les effets toxiques du 7KC sur cellules ont été établis dans le contexte de nombreuses maladies : cardiovasculaires, oculaires, neurodégénératives, inflammatoires chroniques et génétiques rares (Anderson *et al.*, 2020). Ces effets délétères se caractérisent par une élévation du stress oxydant pouvant mener à la mort cellulaire (Vejux *et al.*, 2020).

- ✓ Au niveau cellulaire, les effets du 7KC sont bien documentés mais de nombreux aspects de sa toxicité sont encore méconnus. Nos résultats obtenus sur cellules 158N confirment l'induction d'une mort par oxyapoptophagie incluant une activation du stress oxydant, une induction d'apoptose et la présence de critères d'autophagie. La complexité de ce type de mort et des voies de signalisation qui lui sont associées sont représentées sur la **Figure 21**.

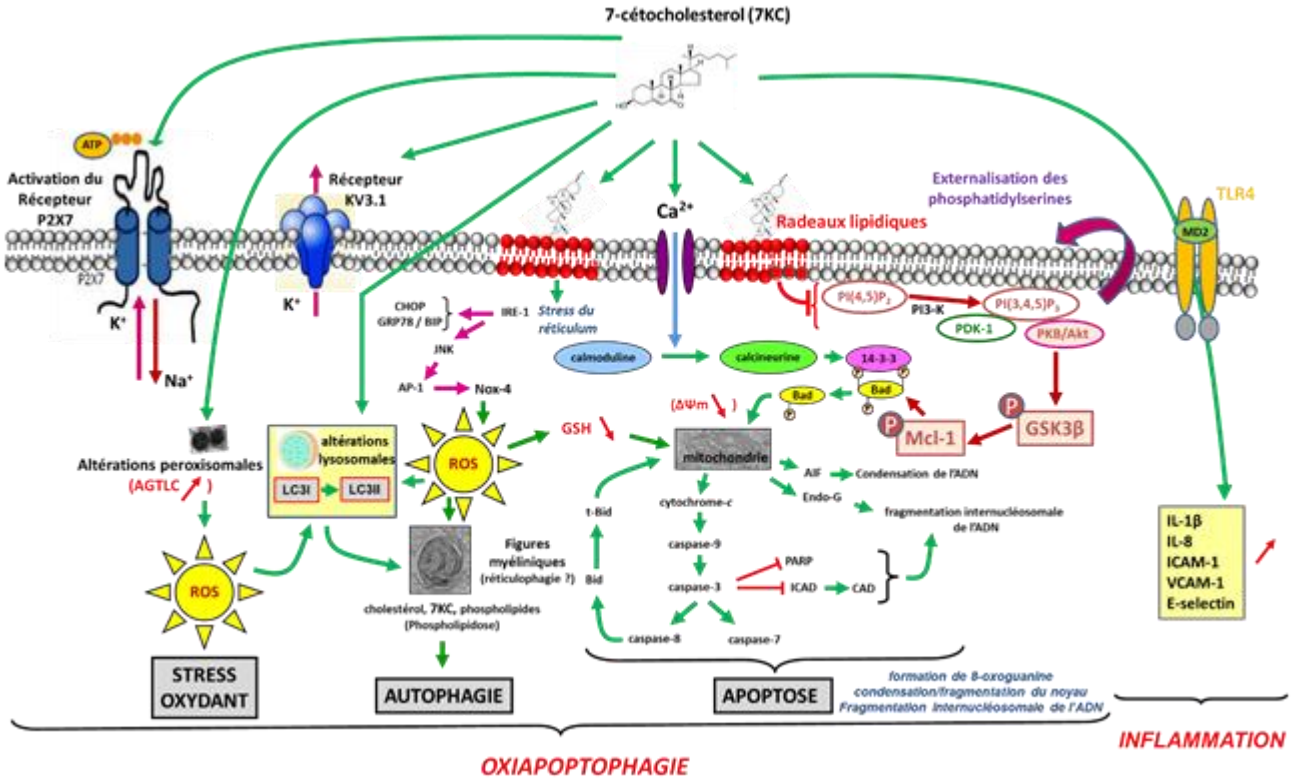

Figure 21 : Voies de signalisation associées à la toxicité du 7-cétocholestérol
Les voies de signalisations présentées regroupent des effects observés à partir de différents types cellulaires. Le 7KC s'accumule dans les radeaux lipidiques, déclenche l'externalisation de la phosphatidylsérine, module l'activité des canaux Ca^{2+}, K^+ et Na^+/K^+ tels que les récepteurs P2X7 et Kv3.1. Ceci favorise une accumulation intracellulaire de Ca^{2+} et de K^+. Le 7KC active également le stress du RE et le stress oxydant (surproduction d'ERO), ce qui contribue aux dysfonctionnements des organites (mitochondrie, peroxysome, lysosome, RE). De plus, la capacité du 7KC à inhiber la voie de signalisation PI3-K/PKB/Akt participe à la chute du potentiel transmembranaire mitochondrial (ΔΨm). Ces différents effets conduisent à une induction de l'autophagie et l'apoptose. L'activation du stress oxydant, de l'apoptose et de l'autophagie est définie comme *oxyapoptophagie* (***oxiapoptophagy*** dans les bases de données). Le 7KC est également une molécule pro-inflammatoire qui déclenche l'inflammation par l'activation du récepteur TLR4 et la sécrétion de cytokines pro-inflammatoires (IL-1β, IL-8, ICAM-1, VCAM-1, E-sélectine). Adapté de (Vejux *et al.*, 2020).

Le 7KC s'accumule dans les radeaux lipidiques et modifie la fluidité membranaire (Ragot *et al.*,

2011). Il peut ainsi perturber les signaux membranaires tels que les flux calciques et potassiques

impliqués dans la mort cellulaire (Bezine *et al.*, 2018a; Bezine *et al.*, 2018b; Mackrill, 2011; Olivier *et al.*, 2016). Le 7KC inhibe la voie PI3-K/PKB/Akt, ce qui provoque une chute du potentiel transmembranaire mitochondrial (ΔΨm) et induit l'apoptose sur des cellules monocytaires U937 (Vejux *et al.*, 2009a). D'autre part, le 7KC induit une augmentation du stress oxydant qui contribue aux dysfonctions des organites (mitochondrie, RE, lysosome, peroxysome). Une augmentation de l'inflammation via la sécrétion de cytokines peut aussi être observée via l'activation du récepteur membranaire TLR4 (Huang *et al.*, 2014). Ces différentes altérations métaboliques sont généralement accompagnées d'un processus d'autophagie et d'une mort cellulaire par apoptose (Nury *et al.*, 2014). La notion d'oxyapoptophagie n'est pas limitée au 7KC mais s'applique aussi à d'autres oxystérols cytotoxiques comme le 7β-OHC et le 24(S)-OHC (Nury *et al.*, 2015; Vejux *et al.*, 2020). Mieux connaitre l'oxyapoptophagie présente un intérêt pharmacologique et thérapeutique pour identifier des cibles afin de s'opposer à ce type de mort et aux maladies auxquelles elle serait associée.

✓ De plus, ce travail de thèse a permis de préciser les effets du 7KC sur le peroxysome et les conséquences probables sur les autres organites (mitochondrie, lysosome, RE) ainsi que sur les gouttelettes lipidiques. Les résultats obtenus ont aussi permis d'aborder les relations peroxysome, stress oxydant, apoptose et autophagie. Il a été démontré sur des oligodendrocytes murins 158N que le 7KC perturbe le métabolisme peroxysomal, qu'il soit utilisé à une concentration faiblement toxique (25 µM) ou à une concentration toxique (50 µM). Dans ces conditions, les mitochondries sont peu affectées à 25 µM alors qu'une importante chute du ΔΨm est observée à 50 µM, entrainant un phénomène d'apoptose. De plus, les modifications peroxysomales causées par le 7KC se caractérisent par une modification de leur forme en microscopie électronique à

transmission. L'expression de plusieurs protéines peroxysomales est également modifiée. Les niveaux de transporteurs membranaires peroxysomaux ABCD1 et ABCD3 sont diminués ainsi que les enzymes ACOX1 et MFP2, impliquées dans la β-oxydation des AGTLC. La première enzyme de synthèse des plasmalogènes, la DHAPAT, est également diminuée. Ces altérations d'expression de protéines peroxysomales sont accompagnées d'une accumulation d'AGTLC (C24:0, C24:1 C26:0 et C26:1) ; en revanche, le niveau de plasmalogènes total n'est pas impacté. Il est important de souligner que l'accumulation d'AGTLC induite par le 7KC pourrait contribuer à amplifier le stress oxydant, à altérer les membranes, à agir sur l'homéostasie calcique et à activer la mort cellulaire (Baarine *et al.*, 2012; Doria *et al.*, 2019; Nury *et al.*, 2017; Schonfeld *et al.*, 2016). Les effets toxiques des AGTLC et du 7KC seraient donc cumulatifs. Ces résultats suggèrent que les altérations peroxysomales induites par le 7KC joueraient ainsi un rôle important dans le processus de mort cellulaire induit par le 7KC.

- ***Impact du 7KC sur le peroxysome et conséquence sur les autres organites***

Dans son ensemble, le 7KC pertuberait la mitochondrie et le peroxysome mais aussi le RE et les lysosomes, ainsi que les relations entre ces différents organites. Ceci aurait pour conséquence une altération des fonctions et des activités cellulaires qui dans des conditions extrêmes pourraient aboutir à la mort.

- *Incidence du 7KC sur les relations peroxysome / mitochondrie :* La β-oxydation des AGTLC débute dans le peroxysome et se poursuit dans les mitochondries. Le NAD^+ nécessaire à la β-oxydation des AGTLC est produit par la mitochondrie puis transporté vers le peroxysome.

Le NADH formé ne peut alors être oxydé que dans les mitochondries (Fransen *et al.*, 2017). Le métabolisme Redox du peroxysome et de la mitochondrie sont également liés : en effet, des dysfonctions métaboliques peroxysomales (β-oxydation, activité catalase, biogénèse peroxysomale) induisent une augmentation du stress oxydant mitochondrial (Fransen *et al.*, 2017; Lismont *et al.*, 2015; Peeters *et al.*, 2015). Par ailleurs, comme la mitochondrie joue un rôle lors de la biogénèse peroxysomale (une partie des peroxysomes formés *de novo* provient de bourgeonnement mitochondriaux) (Fujiki, 2016; Sugiura *et al.*, 2017) son altération peut avoir des conséquences délétères sur la quantité et la qualité des peroxysomes par cellule. Il a été montré que le 7KC diminue le taux de NAD^+ dans les cellules 158N et perturbe le cycle de Krebs au niveau des mitochondries, induisant une diminution des acides organiques (pyruvate, citrate, fumarate, succinate) et une accumulatin de lactate (Leoni *et al.*, 2017). L'accumulation d'AGTLC observée dans les cellules traitées par le 7KC pourrait être dûe en partie à la diminution du taux de NAD^+ mitochondrial qui est nécessaire à la β-oxydation peroxysomale, soulignant ainsi l'importance des relations mitochondrie / peroxysome.

- *Incidence du 7KC sur les relations peroxysome / RE :* Le peroxysome peut aussi interagir avec le RE. Une partie des peroxysomes formés *de novo* provient de bourgeonnement de RE (Sugiura *et al.*, 2017). De plus, la synthèse de DHA, des acides biliaires et des plasmalogènes est partagée entre ces deux organites. Il a été montré qu'une accumulation d'AGTLC due à un défaut de β-oxydation entraine un stress du RE dans des fibroblastes de patients atteints d'X-ALD (van de Beek *et al.*, 2017). Dans des souris PEX2 -/-, l'expression de sterol regulatory element-binding protein-2 et 1c (SREBP-2, SREBP-1c : facteurs de transcriptions impliqués dans la régulation du métabolisme du cholestérol et des triglycérides) et insulin induced gene-2a (INSIG-2a : protéine impliquée dans la régulation du métabolisme du cholestérol) est dérégulée, ce qui entraine un

stress du RE et une perturbation de la voie de réponse aux stérols (Kovacs *et al.*, 2009). Les effets toxiques du 7KC sur le RE pourraient ainsi avoir des répercussions sur la biogenèse des peroxysomes. De plus, l'accumulation des AGTLC induite par le 7KC pourraient entrainer à son tour un stress du RE en raison de leur toxicité (van de Beek *et al.*, 2017).

- *Incidence du 7KC sur les relations peroxysome / lysosome :* Des liens existent également entre le peroxysome et le lysosome. Les membranes peroxysomales et lysosomales peuvent interagir via la synaptotagmine VII (SYT7) présente dans la membrane lysosomale et le phosphatidylinositol-4,5-biphosphate (PI(4,5)P2) de la membrane peroxysomale. Ces contacts membranaires permettent aux deux organites d'échanger du cholestérol (Chu *et al.*, 2015; Sargsyan *et al.*, 2020). Une accumulation de cholestérol est observée dans les lysosomes de souris et des fibroblastes de patients présentant des déficiences peroxysomales. Cette accumulation pourrait résulter d'un défaut d'interactions entre les peroxysomes et les lysosomes (Chen *et al.*, 2020). Cette accumulation de cholestérol associée au stress oxydant pourrait alors contribuer à faire augmenter le taux de 7KC. De plus, les perturbations lysosomales induites par le 7KC (diminution du pH, accumulation de cholestérol, diminution de l'actvité des cathepsines) pourraient altérer l'efficacité du processus d'autophagie lors de la fusion du lysosome avec les autophagosomes (Butler *et al.*, 2006; Li *et al.*, 2011).

- *Incidence du 7KC sur les relations peroxysome / goutelettes lipidiques :* Enfin, les peroxysomes peuvent interagir avec les gouttelettes lipidiques de façon à réaliser des échanges de lipides. Le contact entre les membranes des deux organites se fait par l'interaction de la spastine M1 présente dans la membrane des gouttelettes lipidiques avec le transporteur membranaire peroxysomal ABCD1 (Sargsyan *et al.*, 2020). Des acides gras peuvent ainsi entrer dans le

peroxysome pour y être dégradés. Les mutations de la spastine M1 qui perturbent les contacts entre les peroxysomes et les gouttelettes lipidiques sont la première cause de paraplégie spastique familiale (maladie neurodégénérative) (Chang *et al.*, 2019). Le 7KC diminuant l'expression d'ABCD1 dans les oligodendrocytes murins 158N, on peut supposer que cette altération pourrait entrainer des effets secondaires au niveau des contacts avec les gouttelettes lipidiques.

Ainsi, les effets toxiques du 7KC sur le peroxysome pourraient perturber les interactions avec les autres organites mais aussi avec les goutellettes lipidiques. Ceci pourrait altérer les voies métaboliques issues de ces coopérations et contribuer aux dégats cellulaires causés par le 7KC.

- ***Impact du 7KC sur le peroxysome et conséquence sur le stress oxydant***

Ce travail a montré que le 7KC perturbe le peroxysome ainsi que le stress oxydant au sein des cellules. Les niveaux d'anions superoxydes ($O_2^{\bullet -}$) et de peroxyde d'hydrogène (H_2O_2) sont augmentés. L'expression ainsi que l'activité de la catalase sont aussi induites par le 7KC. Enfin, les taux d'oxystérols formés par l'élévation du stress oxydant favorisent l'accumulation de 7β-OHC et cholestane-3β,5α,6β-triol. Plusieurs enzymes peroxysomales génèrent des ERO à un niveau basal (NOS, différentes oxydases : ACOX, urate oxydase, xanthine oxydase, D-amino acid oxidase, D-aspartate oxidase, pipecolic acid oxidase, polyamine oxidase). Le peroxysome contient également des enzymes qui dégradent les ERO de façon à maintenir l'équilibre Redox (catalase, glutathion peroxidase (GPx), SOD, epoxyde hydrolase, peroxyrédoxine) (Schrader *et al.*, 2006). Sur les cellules 158N, le niveau des transcrits de gènes peroxysomaux impliqués dans le catabolisme des ERO (SOD2 et catalase) est augmenté par le 7KC. Sur les cellules N2a traitées par le 7KC, l'expression de SOD1, SOD2, catalase et GPx1 est modifiée par le 7KC. Sur des

cellules microgliales murines BV-2, l'activité catalase est augmentée par le 7KC (Nury *et al.*, 2017). Sur les cellules 158N traitées par le 7β-OHC, les activités GPx, SOD et catalase sont augmentées (Sghaier *et al.*, 2019a). Les effets du 7KC sur les enzymes productrices d'ERO n'ont pas été étudiés à l'heure actuelle, il serait intéressant d'étudier les effets du 7KC sur ces dernières. Il est également possible que l'augmentation des activités SOD, GPx et catalase soit dûe en partie à l'augmentation générale du stress oxydant cellulaire (ERO provenant de la mitochondrie) et pas uniquement à des perturbations peroxysomales. Ainsi, le 7KC, en modifiant l'activité et / ou l'expression d'enzymes du métabolisme Redox peroxysomal pourrait contribuer par l'intermédiaire de ce dernier à l'élévation du stress oxydant.

- ***Impact du 7KC sur le peroxysome et conséquence sur l'apoptose***

Nous avons montré que le 7KC induit des dysfonctions cellulaires et peroxysomales pouvant conduire à une mort par oxyapoptophagie des cellules 158N. Une activation de l'apoptose a été mise en évidence : clivage de la caspase-3, clivage de PARP, augmentation du ratio Bad/Mcl-1 ainsi qu'une condensation / fragmentation de l'ADN. Il est bien documenté que le 7KC induit de l'apoptose par la voie mitochondriale en induisant une chute du $\Delta\psi m$, un relargage du cytochrome c, d'apoptosis inducing factor (AIF) et d'endonuclease G qui déclenche la fragmentation de l'ADN et l'activation des caspases 3, 7, 8 et 9 (Vejux *et al.*, 2008). Il est possible que les dysfonctions peroxysomales induites par le 7KC jouent un rôle dans le déclenchement de l'apoptose. En effet, les relations métaboliques entre le peroxysome et la mitochondrie sont nombreuses. Il a été montré que des anomalies de PEX entrainent des dysfonctions mitochondriales. Une délétion de PEX5 dans des hépatocytes de souris perturbe la structure de la membrane interne et externe mitochondriale, fait augmenter leur volume, réduit

l'activité des complexes de la phopsphorylation oxydative, diminue le Δψm et stimule la production d'ERO (Peeters *et al.*, 2015). La délétion de PEX3 ou de PEX5 dans des firboblastes embryonaires de souris, dans des conditions où les ERO ne sont pas augmentés, induit une fragmentation des mitochondries et un relarge de cytochrome c sans qu'il y ait activation de l'apoptose (Tanaka *et al.*, 2019). Sur ce même modèle, le traitement par un prolifératéur de peroxysome, le 4-phenylbutyrate, induit la prolifération des peroxysomes mais aussi l'élongation des mitochondries. Il est ainsi possible que la toxicité du 7KC sur le peroxysome perturbe l'expression de PEX3, PEX5, ou d'autres protéines, ce qui contribuerait à déclencher le processus d'apoptose des cellules via l'intervention de la mitochondrie.

- ***Impact du 7KC sur le peroxysome et conséquence sur l'autophagie***

Ce travail a également permis de montrer que la toxicité du 7KC est associée à des critères d'autophagie, et conduit notamment à de la pexophagie sur les cellules 158N. Des observations en microscopie électronique à transmission ont montré la présence d'autophagosomes dont certains d'entre eux contenaient des peroxysomes. Sur les oligodendrocytes 158N et les cellules microgliales murines BV-2, le ratio LC3-II / LC3-I, est augmenté par le 7KC ainsi que le taux de protéine chaperonne p62 (Debbabi *et al.*, 2016; Nury *et al.*, 2017). De nombreuses vacuoles évoquant des vésicules d'autophagie et exprimant la protéine membranaire lysosomale LAMP1 sont détectées en présence de 7KC. La pexophagie est mise en évidence par un double immunomarquage révélant p62 avec ABCD3 (Nury *et al.*, 2018). La pexophagie peut être induite dans le cas d'un stress cellulaire (privation en acides aminés, hypoxie, élévation du niveau d'ERO) et implique différentes peroxines comme PEX2, PEX3, PEX5, PEX14 et la protéine cargo NBR1 (Yao *et al.*, 2020; Zhang *et al.*, 2015). Il a été montré que PEX5 jouerait un rôle

important dans cette activation. La phosphorylation de PEX5 et son ubiquitinylation subséquente par PEX2 pourrait être augmentée par les ERO, ce qui déclencherait la pexophagie en augmentant son affinité pour p62 (Zhang *et al.*, 2015). Récemment, la kinase ataxia-telangiectasia mutated (ATM kinase), une protéine impliquée dans la réparation de l'ADN, a été identifiée comme inductrice de pexophagie lorsqu'elle est activée par les ERO. Lorsque le stress oxydant augmente, l'ATM kinase est adressée au peroxysome par PEX5. Elle peut alors activer la pexophagie de deux manières différentes : soit en réprimant le complexe mTORC1 (inhibiteur d'autophagie), soit en phosphorylant PEX5, ce qui entrainerait son ubiquitinylation puis la liaison à p62 et l'adressage du peroxysome à l'autophagosome (Eberhart *et al.*, 2018; Germain *et al.*, 2020). Les perturbations de la pexophagie sont responsable d'environ 65% des cas de maladies due à un défaut de biogénèse peroxysomale (Nazarko, 2017).

Il serait ainsi intéressant de mesurer les niveaux d'expression de PEX5, PEX2, ATM kinase et NBR1 dans les oligodendrocytes 158N pour vérifier si la pexophagie induite par le 7KC implique ces protéines et de quelle manière.

Il est par ailleurs connu que d'autres oxystérols toxiques comme le 7β-OHC ou le 24(S)-OHC induisent également de l'oxyapoptophagie mais la pexophagie reste à établir (Nury *et al.*, 2015).

A souligner que la pexophagie, et plus généralement l'autophagie induite par le 7KC sur les cellules 158N est une autophagie de survie. En effet, l'utilisation de la 3-methyladénine (inhibiteur d'autophagie) amplifie la mort cellulaire tandis que la rapamycine (activateur d'autophagie) l'inhibe. Sur des cellules vasculaires endothéliales lisses, l'autophagie induite par le 7KC est une autophagie de survie. Son inhibition augmente la mort cellulaire tandis que son activation prévient de l'apoptose (He *et al.*, 2013). Les effets toxiques du 7KC sur les organites (mitochondrie, lysosome, peroxysome, RE) via l'élévation du stress oxydant perturbe leur

métabolisme. Ainsi, le stress oxydant pourrait contribuer à déclencher l'autophagie de manière à éliminer les organites altérés et maintenir une homéostasie au sein de la cellule.

L'induction de l'autophagie induite par le 7KC sur des cellules de singe Vero et des neurones humains semble être protectrice contre l'infection au virus Zika en diminuant sa réplication (Willard *et al.*, 2018). Sur des cellules gliales de rat C6, il a été montré que le 7β-OHC pouvait induire une autophagie protectrice (Sassi *et al.*, 2019a). Il a également été montré que le 27-OHC pouvait être un inducteur d'autophagie protectrice à basse concentration sur des cellules U937. L'augmentation des ERO générée par le 27-OHC active Nrf2 par la voie PI3K/Akt. L'expression du gène de l'hème oxygénase 1 (HO-1) est alors augmentée. De plus, p62 peut interagir avec Keap1 (inhibiteur de Nrf2) ce qui déclencherait l'activité transcriptionnelle de Nrf2 et l'expression de ses gènes cibles. Nrf2 induit également l'expression de p62 (Vurusaner *et al.*, 2018). Sur les cellules 158N traitées par le 7KC, les niveaux des transcrits de gènes cibles de Nrf2 sont augmentés (SOD2, HMOX et catalase). Sur des cellules de neuroblastomes murins N2a, le 7KC modifie également l'expression de gènes cibles de Nrf2 (SOD1, SOD2 et GPx1). Sur cellules 158N, il n'est pas à exclure que le 7KC puisse activer l'autophagie en partie par le biais de Nrf2 et l'interaction avec p62.

Cependant, l'autophagie induite par les oxystérols n'est pas forcément protectrice. En effet, il a été montré que la dendrogénine A (DDA) est un inducteur d'autophagie léthale sur cellules cancéreuses via l'activation de LXR et l'accumulation de zymosténol en raison de l'inhibition de la 3β-hydroxysteroid-$\Delta^8\Delta^7$-isomérase (D8D7I) (Poirot *et al.*, 2018; Segala *et al.*, 2017).

En résumé, la toxicité induite par le 7KC sur le modèle d'oligodendrocytes murins 158N entraine une élévation du stress oxydant qui perturbe le métabolisme des organites (peroxysome, mitochondrie). L'autophagie serait ensuite activée de manière protectrice pour maintenir le bon

fonctionnement de la cellule. Lorsque les défences cellulaire sont dépassées (protections contre les ERO, autophagie), le processus d'apoptose serait déclenché. La succession de ces événements caractériserait ainsi la mort cellulaire par oxyapoptophagie (**Figure 22**).

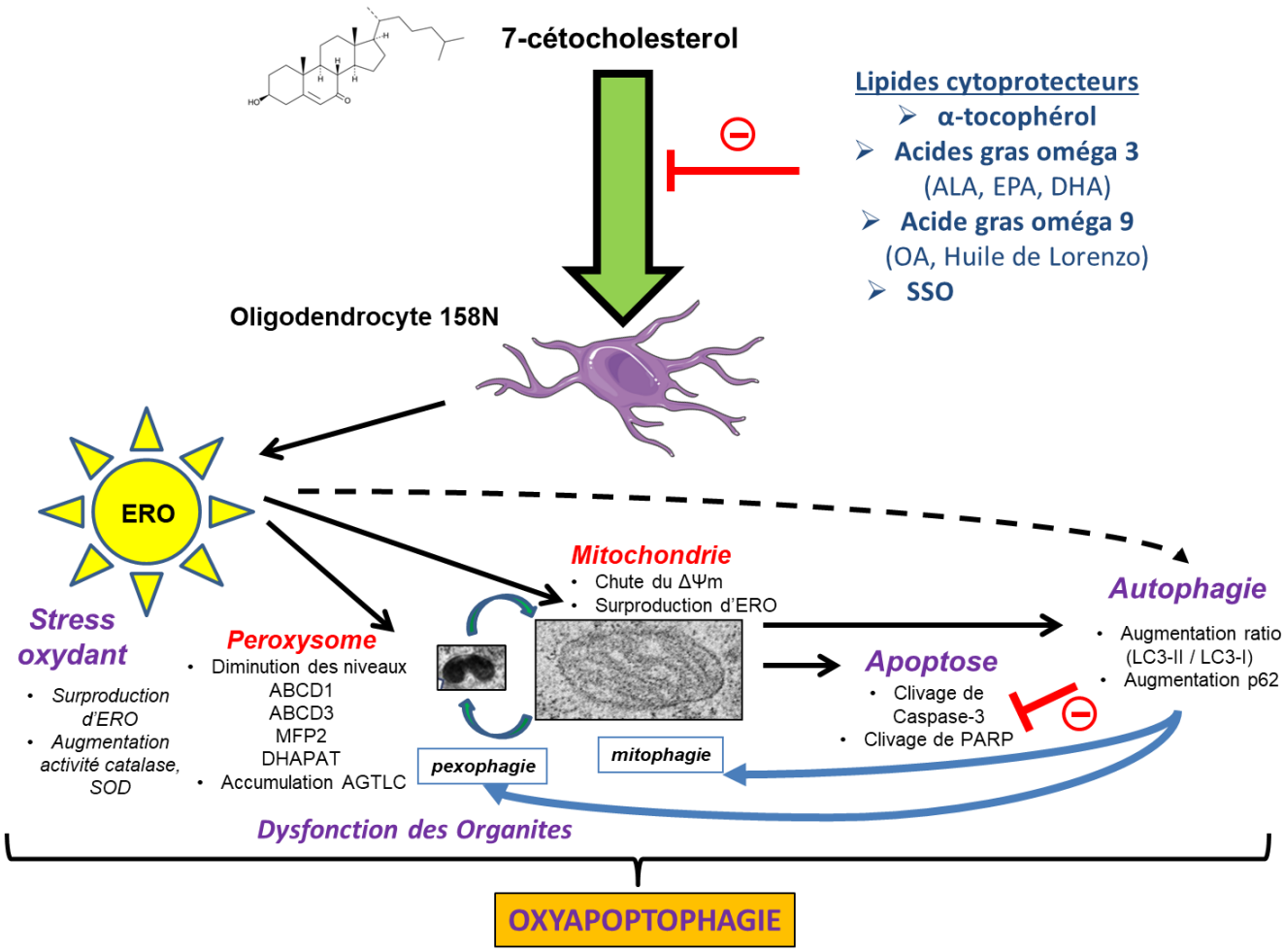

Figure 22 : Résumé de l'action du 7-cétocholestérol sur les cellules 158N menant à l'oxyapoptophagie.
Le 7KC pénètre dans les cellules et induit la surproduction d'ERO au niveau mitochondrial et peroxysomal. Des dommages peroxysomaux (diminution de niveaux d'ABCD1, ABCD3, MFP2, DHAPAT, accumulation d'AGTLC (C24:0, C24:1 et C26:0, C26:1)) et mitochondriaux (chute du Δψm) sont observés. Ces dysfonctions des organites et l'augmentation du stress oxydant induisent l'autophagie (pexophagie mais aussi très probablement mitophagie) dont le but serait de protéger la cellule en recyclant les organites dysfonctionnels. Lorsque l'autophagie est dépassée et ne parvient plus à maintenir la cellule dans un état fonctionnel, l'apoptose serait activée et la cellule meurt par oxyapoptophagie. Les molécules protectrices (α-tocophérol, ALA, EPA, DHA, OA, huile de Lorenzo et SSO) auraient un impact cytoprotecteur précoce sur cette toxicité.

✓ Au cours de ce travail de thèse, le troisième objectif a été d'identifier des lipides naturels ou synthétiques pour inhiber l'oxyapoptophagie induite par le 7KC. Certaines molécules parmi lesquelles figurent de nombreux nutriments sont déjà connues comme ayant un effet protecteur contre la toxicité du 7KC : l'α-tocophérol, le DHA, l'acide oléique, des polyphénols mais aussi des huiles végétales (huile de graines de chardon marie, huile d'olive, huile d'argan). L'ensemble des molécules testées au laboratoire ainsi que par d'autres équipes sont regroupées dans le **Tableau 2**. La seule molécule synthétique actuellement décrite pour réduire la toxicité du 7KC est le diméthylfumarate (DMF) commercialisé sous le nom de Tecfidera par la société Biogen dans le cadre d'un traitement contre la sclérose en plaques sous sa forme rémittente-récurente. Son métabolite majeur, le monométhylfumarate (MMF) est aussi cytoprotecteur vis-à-vis du 7KC (**Tableau 2**).

Tableau 2 : Molécules, mélanges de molécules ou extraits végétaux protecteurs et non protecteurs vis-à-vis du 7-cétocholestérol.

		Molécules	Concentrations	Cellules	Concentration en 7KC	Références
Molécules protectrices	**Tocophérols**	**α-tocophérol**	100 - 400 µM	Monocytes humains U937 ; Oligodendrocytes murins158N ; Cellules Musculaires lisses aortiques de rat A7R5 ; Neuroblastomes murins N2a ; Microglie murine BV-2	25 – 50 µM	Lizard *et al*., 2000; Miguet-Alfonsi *et al*., 2002; Vejux *et al*., 2009; Royer *et al*., 2009; Yammine *et al*., 2020; Debbabi *et al*., 2016; Debbabi *et al*., 2017
		γ-tocophérol	400 µM	Microglie murine BV-2	50 µM	Debbabi *et al*., 2016
	Acides gras	**Acide α-linolénique (ALA)**	50 µM	Neuroblastomes murins N2a	50 µM	Yammine *et al*., 2020a
		Acide eicosapentaénoïque (EPA)	50 µM	Neuroblastomes murins N2a	50 µM	Yammine *et al*., 2020a

		Acide docosahexaénoïque (DHA)	50 µM	Microglie murine BV-2 ; Oligodendrocytes murins158N ; Neuroblastomes murins N2a ; Neuroblastomes humains SK-N-BE	25 - 50 µM	Debbabi *et al*., 2017; Nury *et al*., 2015; Nury *et al*., 2017; Yammine *et al*., 2020a; Zarrouk *et al*., 2015)
		Acide oléique	100 - 200 µM	Oligodendrocytes murins 158N ; Microglie murine BV-2 ; Neuroblastomes murins N2a	50 µM	Badreddine *et al*., 2017; Debbabi *et al*., 2016; Debbabi *et al*., 2017; Yammine *et al*., 2020
		Acide sterculique	1 µM	Epithélium pigmentaire rétinien humain ARPE-19	12 µM	Huang *et al*., 2012; Huang *et al*., 2014
	Phospholipide	**BMP**	-	Macrophages murins RAW264.7	Prévient la formation du 7KC	Arnal-Levron *et al*., 2013 ; Arnal-Levron *et al*., 2019
	Terpénoïde	**Lycopène**	0,5 - 2 µM	Monocytes humains THP-1	10 - 25 µM	Palozza *et al*., 2010; Palozza *et al*., 2011
	Composés phénoliques	**Epicatéchine**	5 - 10 µM	Monocytes / Macrophages murins J774A,1	20 µM	Leonarduzzi *et al*., 2006
		Epigallocatéchine gallate	30 - 50 µM	Angiosarcôme humains ISO-HAS	50 µM	Yamagata *et al*., 2013
		Resvératrol	1,5 - 30 µM	Neuroblastomes murins N2a ; Monocytes humains isolés ; Epithélium pigmentaire rétinien humain ARPE-19	15 - 50 - 150 µM	Yammine *et al*., 2020b; Buttari *et al*, 2014; Dugas *et al*., 2010
		Apigénine	1,5 - 6,25 µM	Neuroblastomes murins N2a	50 µM	Yammine *et al*., 2020b
		Quercétine	1,5 - 6,25 µM	Neuroblastomes murins N2a	50 µM	Yammine *et al*., 2020b
		Hydroxytyrosol	2,5 - 10 µM	Adénocarcinome colorectal humain Caco2	187,5 µM	Atzeri *et al*., 2016; Deiana *et al*., 2010
		Tyrosol	2,5 - 10 µM	Adénocarcinome colorectal humain Caco2	187,5 µM	Atzeri *et al*., 2016; Deiana *et al*., 2010
		Alcool homovanillique	5 - 25 µM	Adénocarcinome colorectal humain Caco2	prévient l'oxydation du cholestérol	Deiana *et al*., 2010
		Taxifoline (dihydroquercétine)	15 µM	Phéochromocytome de rat PC12 ; Neuroblastomes humains SH-SY5Y	125 µM	Kim *et al*., 2017
		Acide férulique	0.5 – 1.5 mM	Epithélium pigmentaire rétinien humain ARPE-19	40 µM	(Kohno *et al.*, 2020)
	Pigment végétal	**Indicaxanthine**	1 - 5 µM	Monocytes humains THP-1 ; érythrocytes	7 - 16 µM	Tesoriere *et al*., 2014b; Tesoriere *et al*., 2013; Tesoriere *et al*., 2015
	Antioxydants	**N-acétylcystéine (NAC)**	10 - 15 mM	Monocytes humains U937 ; préostéoblastes murins MC3T3-E1	100 µM	Lizard *et al*., 1998; Lizard *et al*., 2000; Sato *et al*., 2017
		Glutathion réduit (GSH)	10 - 15 mM	Monocytes humains U937	100 µM	Lizard *et al*., 1998; Lizard *et al*., 2000

		Ergothionéine	1 mM	Cellules microvasculaires endothéliales cérébrales humaines hCMEC/D3	30 µM	Koh *et al*., 2020
	Molécules de synthèse	**Monométhylfumarate (MMF)**	25 - 50 µM	Oligodendrocytes murins 158N	25 - 50 µM	non publié
		Diméthylfumarate (DMF)	25 - 50 µM	Oligodendrocytes murins 158N	25 - 50 µM	Zarrouk *et al*., 2017
	Mélanges ou extraits végétaux	**α-tocophérol + DHA**	400 µM + 50 µM	Oligodendrocytes murins 158N	50 µM	Nury *et al*., 2015
		Extrait de levure de riz rouge	100 µg/mL	Macrophages murins RAW 264.7	70 µM	Shen *et al*., 2017
		Huile d'olive	1 / 1000	Oligodendrocytes murins 158N	50 µM	Badreddine *et al*., 2017 ; Debbabi *et al*., 2016 ; Debbabi *et al*., 2017
		Huile d'argan	2 / 1000	Oligodendrocytes murins 158N	50 µM	Badreddine *et al*., 2017
		Huile de graines de chardon-Marie	3 / 1000	Oligodendrocytes murins 158N	50 µM	Meddeb *et al*., 2018
		Extrait de vin rouge et blanc	20 - 40 mg/mL ; 1 / 10 ; 1 / 500	Adénocarcinome colorectal humain Caco2	prévient l'oxydation du cholestérol	Deckert *et al*., 2002 ; Tian *et al*., 2011
		Extrait méthanolique de *Clinacanthus nutans*	100 µg/mL	Cellules microvasculaires endothéliales cérébrales humaines hCMEC/D3	30 µM	Kuo *et al*., 2020
	Enzyme bactérienne	**Cholestérol oxydase de *Chromobacterium* DS-1**	-	Fibroblastes humains / expression lysosomale	25 - 50 µM	Mathieu *et al*., 2012

Molécules non protectrices	**Vitamines**	**Biotine**	10 - 100 nm	Oligodendrocytes murins 158N	50 µM	Non publié
		γ-tocophérol	100 µM	Muscle lisse aortique de rat A7R5	50 µM	Royer *et al*., 2009
		α-tocotriénol	25 µM	Oligodendrocytes murins 158N	25 - 50 µM	Nury *et al*., 2018
		Vitamine C	50 µM	Monocytes humains U937	100 µM	Lizard *et al*., 2000
	Acides gras	**Acide élaïdique**	100 - 200 µM	Microglie murine BV-2	50 µM	Debbabi *et al*., 2017
	Composés phénoliques	**Resvératrol**	10- 50 µM	Oligodendrocytes murins 158N	50 µM	Ragot *et al*., 2013
		Acide ellagique	10 - 50 µM	Oligodendrocytes murins 158N	50 µM	Ragot *et al*., 2013
		Acide férulique	6 – 50 µM	Oligodendrocytes murins 158N	50 µM	Non publié
	Antioxydants	**N-acétyl-glucosamine**	100 µM	Oligodendrocytes murins 158N	25 - 50 µM	Non publié
		Zinc monométhionine	20 µg/mL	Oligodendrocytes murins 158N	25 - 50 µM	Non publié
		Acide lipoïque	100 µM	Oligodendrocytes murins 158N	25 - 50 µM	Non publié
		N-acétylcystéine	5 - 15 mM	Oligodendrocytes	50 µM	Non publié

		(NAC)		murins 158N		
		Glutathion réduit (GSH)	5 - 15 mM	Oligodendrocytes murins 158N	50 µM	Non publié
	Molécules de synthèse	**Trolox**	400µM	Microglie murine BV-2	50 µM	Debbabi *et al*., 2016
		Huile de Nigelle	1/1000	Oligodendrocytes murins 158N	50 µM	Meddeb *et al*., 2018
	Mélanges ou extraits végétaux	**Extrait de gingembre**	20 µg/mL	Oligodendrocytes murins 158N	25 - 50 µM	Non publié
		Picroliv (extrait de *Picrorhiza kurroa*)	20 µg/mL	Oligodendrocytes murins 158N	25 - 50 µM	Non publié
		C3 reduct ODN (curcuminoïdes extraits de *Curcuma longa*)	20 µg/mL	Oligodendrocytes murins 158N	25 - 50 µM	Non publié
		Berbérine sulfate	100 µM	Oligodendrocytes murins 158N	25 - 50 µM	Non publié
		Berbérine hydrochloride	100 µM	Oligodendrocytes murins 158N	25 - 50 µM	Non publié
		Silymarine	50 µM	Oligodendrocytes murins 158N	25 - 50 µM	Non publié
	Autres	**Mélatonine**	1 mM	Monocytes humains U937	100 µM	Lizard *et al*., 2000
		Bézafibrate	35 µM	Oligodendrocytes murins 158N	50 µM	Non publié

Les travaux de thèse ont permis d'identifier de nouvelles molécules cytoprotectrices vis-à-vis du 7KC : ce sont les précurseurs de synthèse du DHA (ALA et EPA (deux acides gras ω3)), l'huile de Lorenzo composée de deux acides gras ω9 (acide oléique + acide érucique (en proportion 4 : 1)) et le SSO dérivant de l'acide oléique (**Figure 22**). Le traitement par ces molécules inhibe la toxicité du 7KC à plusieurs niveaux en prévenant la chute du ΔΨm, l'augmentation du stress oxydant, l'induction de l'autophagie et l'activation de l'apoptose. Dans la cascade d'évènements conduisant à l'oxyapoptophagie, ces molécules agiraient au niveau des phases précoces de la toxicité induite par le 7KC. Ces lipides pourraient réduire l'incorporation du 7KC dans la membrane plasmique (en particulier au niveau des radeaux lipidiques) et au niveau des membranes organites. Ainsi, les voies de signalisation inhibées par le 7KC, comme PI3-K / PKB / Akt mais aussi GSK3, conduisant au déclenchement de l'apoptose, ne seraient plus inhibée et la survie serait activée (Ragot *et al.*, 2011; Vejux *et al.*, 2020). L'α-tocophérol agit d'ailleurs en

inhibant l'accumulation membranaire de 7KC dans les radeaux lipidiques et en restaurant la voie PI3-K /PKB / Akt (Ragot *et al.*, 2011; Ragot *et al.*, 2013; Royer *et al.*, 2009).

Les tests réalisés avec différentes molécules et mélanges de molécules sur cellules 158N montrent une prédominance des molécules liposolubles pour prévenir la toxicité du 7KC. Seuls le DMF et le MMF, légèrement plus solubles dans des véhicules aqueux, se sont montrés cytoprotecteurs (**Tableau 2**). Il est donc envisageable d'utiliser ces molécules pour le traitement et / ou la prévention de maladies impliquant le 7KC : maladies cardiovasculaires, maladies neurodégénératives, maladies oculaires, maladies inflammatoires de l'intestin, maladies génétiques rares. Il a été montré que le DHA pouvait être protecteur vis-à-vis des AGTLC (C24:0 et C26:0) dont les taux augmentent en présence de 7KC (Nury *et al.*, 2020). Le DHA et l'EPA ont montré des activités bénéfiques dans les maladies neurodégénératives et des maladies inflammatoires : ils diminuent la sécrétion d'acide arachidonique qui est un précurseur des leucotriènes et des prostaglandines associés à l'inflammation non cytokinique, ainsi que l'activation de voies pro-inflammatoires et la sécrétion de cytokines (Troesch *et al.*, 2020). L'huile de pérille, enrichie en ALA, permet aussi de diminuer la stéatose hépatique et l'autophagie causée par le stress du RE chez des souris sous régime gras (Bae *et al.*, 2020).

Dans les maladies neurodégénératives, il est préférable que les molécules protectrices puissent traverser la BHE. Cet obstacle n'est pas rédibitoire pour des pathologies lourdes (injections intracérébrales) ou lorsque la BHE devient perméable à des stades avancés des maladies. Néanmoins, le DHA est capable de traverser la BHE mais les mécanismes de transport sont encore sujets à débat (diffusion passive, transport facilité, passage sous forme estérifiée) (Hachem *et al.*, 2020). L'ALA et l'EPA semblent également capables de traverser la BHE puisqu'une supplémentation en acides gras ω3 augmente les concentrations de ces derniers dans le liquide céphalorachidien (Freund Levi *et al.*, 2014). L'acide oléique et l'acide érucique passent

aussi la BHE (Golovko *et al.*, 2006; Murphy, 2017). De même, l'α-tocophérol traverse la BHE (Lee *et al.*, 2019). En ce qui concerne le SSO, aucune étude n'a été réalisée pour déterminer sa capacité ou non à diffuser au niveau de la BHE. Cette molécule est pour l'instant uniquement utilisée comme inhibiteur de CD36 mais il apparait qu'elle pourrait avoir d'autres activités biologiques. Il a été montré sur des mitochondries de rat isolées que le SSO inhibe la β-oxydation mitochondriale des acides gras à longue chaine ainsi que la phosphorylation oxydative au niveau des complexe I, II et III (le complexe IV et le cytochrome c ne seraient pas affectés) (Drahota *et al.*, 2010). Sur des cellules microgliales BV-2, le SSO inhibe la sécrétion d'IL-6 et de TNF-α ainsi que l'activation de COX2 et NOS2 induite par du LPS+IFNγ. De plus, lorsque des neurones primaires sont en co-culture avec les cellules BV-2 activées par LPS+IFNγ, le SSO protège les neurones de la mort cellulaire. Enfin, sur un modèle de souris ischémiques (occlusion permanente d'une artère cérébrale), le SSO diminue l'étendue de la zone de lésion (Dhungana *et al.*, 2017). Ces effets protecteurs du SSO passeraient, entre autres, par le blocage de CD36 et de la voie NFκB mais le mécanisme précis est encore inconnu.

Actuellement, les effets protecteurs de ces acides gras et dérivés (ALA, EPA, DHA, OA, huile de Lorenzo et SSO) sont essentiellement établis sur la toxicité du 7KC. Toutefois, l'α-tocophérol, le DHA, l'acide oléique, le DMF et le MMF protégent aussi de l'oxyapoptophagie induite par d'autres oxystérols (7β-OHC et 24(S)-OHC) (Nury *et al.*, 2015). La biotine (vitamine B8 / Vitamine B7 / Vitamine H) protège de l'oxyapoptophagie et des altérations peroxysomales et mitochondriales induites par le 7β-OHC sur les cellules 158N mais elle n'a aucun effet sur la toxicité du 7KC (Sghaier *et al.*, 2019b). Il serait intéressant d'identifier de nouvelles molécules protectrices contre l'oxyapoptophagie induite par le 7KC et d'autres oxystérols et d'en préciser les mécanismes pour élaborer des compléments alimentaires ou des médicaments pouvant être

administrés dans des maladies liées à l'âge et inflammatoires chroniques associées à des taux élevés d'oxystérols.

Le ciblage des organites par les composés cytoprotecteurs offre des perspectives innovantes prometteuses pour augmenter leur efficacité et pour les utiliser comme traitement. En effet, l'apport *in situ* des molécules protectrices directement aux organites pourrait permettre de conserver leurs effets tout en diminuant les doses, ce qui permettrait aussi de réduire les effets secondaires. Le ciblage des organites permettrait par exemple de réduire à la source la production d'ERO augmentée par le 7KC. Il existe différentes façons de diriger des molécules vers un organite : soit en liant le signal d'adressage directement à la molécule d'intérêt, soit en greffant la molécule sur un nanotransporteur adressé à l'organite. Pour cibler la mitochondrie, il existe plusieurs types d'adressage connus utilisant souvent des molécules cationiques lipophiles : liaison de la molécule d'intérêt avec du triphénylphosphonium (TPP) ou de la rhodamine 123 ou encore avec un signal peptidique d'adressage à la mitochondrie (Battogtokh *et al.*, 2018). Les séquences PTS1 et PTS2 nécessaires à la biogénèse du peroxysome peuvent aussi être utilisées pour cibler le peroxysome (Kim *et al.*, 2018). Le pH ainsi que des séquences peptidiques peuvent également être utilisés pour cibler les lysosomes (Sakhrani *et al.*, 2013).

Un autre projet au laboratoire dans les années à venir est de développer des nanoparticules fonctionnalisées par du resvératrol pour les cibler à la mitochondrie ou au peroxysome.

Conclusions et perspectives

Dans leur ensemble, ces travaux de thèse ont permis de mieux caractériser *in vitro* les effets du 7KC sur la mort cellulaire et de mieux décrire la mort cellulaire par oxyapoptophagie ainsi que les effets de cette mort sur le peroxysome.

Le 7KC causerait dans un premier temps une élévation du stress oxydant qui perturberait le métabolisme du peroxysome et de la mitochondrie. Afin de maintenir l'homéostasie cellulaire, l'autophagie serait activée de manière à protéger la cellule de la toxicité du 7KC. Enfin, lorsque les dommages cellulaires deviendraient trop importants, l'apoptose serait activée.

Cependant, ce type de mort cellulaire induit par certains oxystérols (7KC, 7β-OHC et 24(S)-OHC) associant stress oxydant, apoptose et autophagie, n'a pour l'instant été décrit que sur des cellules en culture murines ou humaines.

✓ Il est nécessaire d'évaluer si ce processus d'oxyapoptophagie existe également *in vivo*. Dans ce but, des coupes histologiques de plaques d'athéromes humaines ou murines pourraient être utilisées afin de réaliser des co-marquages mettant en évidence le 7KC, le stress oxydant, l'apoptose et l'autophagie au sein d'une même cellule.

✓ De plus, des effets toxiques du 7KC sur le métabolisme du peroxysome ont également été démontrés (diminution de l'expression et de l'activité de certains transporteurs (ABCD1, ABCD3) et enzymes (ACOX1, MFP2, catalase), accumulation d'AGTLC (C24:0, C24:1 et C26:0, C26:1)). L'étude des relations entre les dysfonctions peroxysomales et l'induction du stress oxydant, de l'autophagie et de l'apoptose, ainsi que les interactions avec les autres organites permettrait de mieux comprendre la place du peroxysome dans le processus de mort cellulaire par oxyapoptophagie.

✓ Il serait aussi intéressant de définir les sites d'accumulation du 7KC au sein de la cellule en particulier au niveau des membranes des organites (mitochondrie, peroxysome) en isolant ces derniers afin de mesurer les taux de 7KC. Pour cela, nous utiliserons des anticorps anti-7KC.

✓ Il est aussi nécessaire de mieux caractériser l'autophagie en déterminant quelle est la cascade d'évènements qui aboutit à l'augmentation du rapport (LC3-II / LC3-I).

✓ Enfin, des lipides cytoprotecteurs inhibant la toxicité du 7KC ont été identifiés : ALA, EPA, DHA, OA, huile de Lorenzo et SSO. Le mécanisme d'action précis de ces lipides reste à élucider de manière à pouvoir élaborer des compléments alimentaires ou des traitements préventifs et / ou curatifs pour les maladies impliquant une élévation des taux de 7KC (maladies cardiovasculaires, oculaires, neurodégénératives, inflammatoires chroniques et génétiques rares).

✓ Des tests préliminaires sur la drosophile ont par ailleurs été réalisés au laboratoire en collaboration avec l'équipe du Dr Yaël Grosjean (CSGA / CNRS, Dijon). Ce modèle a été choisi car cette mouche est auxotrophe pour le cholestérol. Il ne peut donc pas y avoir de 7KC endogène généré, sauf par l'intermédiaire de celui apporté par l'alimentation ou formé à partir du cholestérol alimentaire. Nous avons déjà nourri des mouches avec du 7KC pour préciser les cibles cellulaires et tissulaires du 7KC alimentaire. Ce modèle permettra ainsi d'étudier les conséquences d'une accumulation de 7KC alimentaire sur le développement, la longévité, la fertilité, la mobilité et le comportement. L'objectif est aussi de définir si cette accumulation de 7KC induit de l'oxyapoptophagie chez la mouche, ce qui démontrerait que ce type de mort est conservé parmi les espèces. Ce modèle permettrait également de pouvoir étudier les mécanismes de l'oxyapoptophagie *in vivo* en relation avec différents autres cofacteurs (activité, stress, environnement, alimentation, etc.). Des expériences utilisant des cellules de drosophile S2 sont envisagées *in vitro* en présence de 7KC pour aborder ses activités biologiques parallèlement aux expériences menées *in vivo*.

✓ Des tests *in vitro* sur des cultures mixtes (oligodendrocytes, neurones, microglie) pourraient être envisagés afin d'étudier les relations entre les différents types cellulaires du système nerveux central en présence de 7KC. Notre laboratoire dispose aussi de lignées de

microglie murine BV-2 (ABCD1 -/-, ABCD2 -/-, ABCD1/2 -/- et ACOX1-/- obtenues par la technique CRISPR-cas9) présentant des déficiences de la β-oxydation peroxysomales qui pourraient également être utilisées dans ce cadre.

- ✓ Un modèle de myélinisation *in vitro* (oligodendrocytes + neurones) pourrait être utilisé pour caractériser les effets de la toxicité du 7KC sur la myéline (protéines, phospholipides),
- ✓ Des coupes organotypiques de cerveaux pourraient aussi permettre d'étudier les effets du 7KC sur la quantité et la qualité de la myéline *ex vivo*,
- ✓ L'utilisation d'organoïdes et d'IPSCs combinée à des techniques microfluidiques serait une alternative à l'expérimentation animale qui mériterait d'être mise en œuvre pour aborder la toxicité du 7KC et la cytoprotection de manière multiparamétrique et dynamique.

Bibliographie

Addis PB, Emanuel HA, Bergmann SD, Zavoral JH (1989). Capillary GC quantification of cholesterol oxidation products in plasma lipoproteins of fasted humans. *Free radical biology & medicine* **7**(2)**:** 179-182.

Aksu N, Samadi A, Yalcinkaya A, Cetin T, Eser B, Lay I*, et al.* (2020). Evaluation of oxysterol levels of patients with silicosis by LC-MS/MS method. *Molecular and cellular biochemistry* **467**(1-2)**:** 117-125.

Albers JJ, Vuletic S, Cheung MC (2012). Role of plasma phospholipid transfer protein in lipid and lipoprotein metabolism. *Biochimica et biophysica acta* **1821**(3)**:** 345-357.

Anderson A, Campo A, Fulton E, Corwin A, Jerome WG, 3rd, O'Connor MS (2020). 7-Ketocholesterol in disease and aging. *Redox biology* **29:** 101380.

Antonenkov VD (1989). Dehydrogenases of the pentose phosphate pathway in rat liver peroxisomes. *European journal of biochemistry* **183**(1)**:** 75-82.

Arnal-Levron M, Chen Y, Delton-Vandenbroucke I, Luquain-Costaz C (2013). Bis(monoacylglycero)phosphate reduces oxysterol formation and apoptosis in macrophages exposed to oxidized LDL. *Biochemical pharmacology* **86**(1)**:** 115-121.

Arnal-Levron M, Chen Y, Greimel P, Calevro F, Gaget K, Riols F*, et al.* (2019). Bis(monoacylglycero)phosphate regulates oxysterol binding protein-related protein 11 dependent sterol trafficking. *Biochimica et biophysica acta. Molecular and cell biology of lipids* **1864**(9)**:** 1247-1257.

Asatryan A, Bazan NG (2017). Molecular mechanisms of signaling via the docosanoid neuroprotectin D1 for cellular homeostasis and neuroprotection. *J Biol Chem* **292**(30)**:** 12390-12397.

Atzeri A, Lucas R, Incani A, Penalver P, Zafra-Gomez A, Melis MP*, et al.* (2016). Hydroxytyrosol and tyrosol sulfate metabolites protect against the oxidized cholesterol pro-oxidant effect in Caco-2 human enterocyte-like cells. *Food & function* **7**(1)**:** 337-346.

Ayee MA, Levitan I (2016). Paradoxical impact of cholesterol on lipid packing and cell stiffness. *Front Biosci (Landmark Ed)* **21:** 1245-1259.

Baarine M, Andreoletti P, Athias A, Nury T, Zarrouk A, Ragot K*, et al.* (2012). Evidence of oxidative stress in very long chain fatty acid--treated oligodendrocytes and potentialization of ROS production using RNA interference-directed knockdown of ABCD1 and ACOX1 peroxisomal proteins. *Neuroscience* **213:** 1-18.

Baarine M, Ragot K, Genin EC, El Hajj H, Trompier D, Andreoletti P*, et al.* (2009). Peroxisomal and mitochondrial status of two murine oligodendrocytic cell lines (158N, 158JP): potential models for the

study of peroxisomal disorders associated with dysmyelination processes. *Journal of neurochemistry* **111**(1)**:** 119-131.

Babiker A, Diczfalusy U (1998). Transport of side-chain oxidized oxysterols in the human circulation. *Biochimica et biophysica acta* **1392**(2-3)**:** 333-339.

Badreddine A, Zarrouk A, Karym EM, Debbabi M, Nury T, Meddeb W*, et al.* (2017). Argan Oil-Mediated Attenuation of Organelle Dysfunction, Oxidative Stress and Cell Death Induced by 7-Ketocholesterol in Murine Oligodendrocytes 158N. *International journal of molecular sciences* **18**(10).

Bae SJ, Kim JE, Choi HJ, Choi YJ, Lee SJ, Gong JE*, et al.* (2020). alpha-Linolenic Acid-Enriched Cold-Pressed Perilla Oil Suppress High-Fat Diet-Induced Hepatic Steatosis through Amelioration of the ER Stress-Mediated Autophagy. *Molecules* **25**(11).

Barja G (2019). Towards a unified mechanistic theory of aging. *Experimental gerontology* **124:** 110627.

Battogtokh G, Cho YY, Lee JY, Lee HS, Kang HC (2018). Mitochondrial-Targeting Anticancer Agent Conjugates and Nanocarrier Systems for Cancer Treatment. *Frontiers in pharmacology* **9:** 922.

Berthier A, Lemaire-Ewing S, Prunet C, Monier S, Athias A, Bessede G*, et al.* (2004). Involvement of a calcium-dependent dephosphorylation of BAD associated with the localization of Trpc-1 within lipid rafts in 7-ketocholesterol-induced THP-1 cell apoptosis. *Cell death and differentiation* **11**(8)**:** 897-905.

Berthier A, Lemaire-Ewing S, Prunet C, Montange T, Vejux A, Pais de Barros JP*, et al.* (2005). 7-Ketocholesterol-induced apoptosis. Involvement of several pro-apoptotic but also anti-apoptotic calcium-dependent transduction pathways. *The FEBS journal* **272**(12)**:** 3093-3104.

Bezine M, Debbabi M, Nury T, Ben-Khalifa R, Samadi M, Cherkaoui-Malki M*, et al.* (2017). Evidence of K(+) homeostasis disruption in cellular dysfunction triggered by 7-ketocholesterol, 24S-hydroxycholesterol, and tetracosanoic acid (C24:0) in 158N murine oligodendrocytes. *Chemistry and physics of lipids* **207**(Pt B)**:** 135-150.

Bezine M, Maatoug S, Ben Khalifa R, Debbabi M, Zarrouk A, Wang Y*, et al.* (2018a). Modulation of Kv3.1b potassium channel level and intracellular potassium concentration in 158N murine oligodendrocytes and BV-2 murine microglial cells treated with 7-ketocholesterol, 24S-hydroxycholesterol or tetracosanoic acid (C24:0). *Biochimie* **153:** 56-69.

Bezine M, Namsi A, Sghaier R, Ben Khalifa R, Hamdouni H, Brahmi F*, et al.* (2018b). The effect of oxysterols on nerve impulses. *Biochimie* **153:** 46-51.

Bhowmik SK, An JH, Lee SH, Jung BH (2012). Alteration of bile acid metabolism in pseudo germ-free rats [corrected]. *Archives of pharmacal research* **35**(11)**:** 1969-1977.

Biasi F, Mascia C, Astegiano M, Chiarpotto E, Nano M, Vizio B*, et al.* (2009). Pro-oxidant and proapoptotic effects of cholesterol oxidation products on human colonic epithelial cells: a potential mechanism of inflammatory bowel disease progression. *Free radical biology & medicine* **47**(12)**:** 1731-1741.

Biermann J, Just WW, Wanders RJ, Van Den Bosch H (1999). Alkyl-dihydroxyacetone phosphate synthase and dihydroxyacetone phosphate acyltransferase form a protein complex in peroxisomes. *European journal of biochemistry* **261**(2)**:** 492-499.

Bjorkhem I (2006). Crossing the barrier: oxysterols as cholesterol transporters and metabolic modulators in the brain. *Journal of internal medicine* **260**(6)**:** 493-508.

Bjorkhem I, Cedazo-Minguez A, Leoni V, Meaney S (2009). Oxysterols and neurodegenerative diseases. *Molecular aspects of medicine* **30**(3)**:** 171-179.

Bjorkhem I, Diczfalusy U, Lovgren-Sandblom A, Starck L, Jonsson M, Tallman K*, et al.* (2014). On the formation of 7-ketocholesterol from 7-dehydrocholesterol in patients with CTX and SLO. *Journal of lipid research* **55**(6)**:** 1165-1172.

Bjorkhem I, Leoni V, Svenningsson P (2019). On the fluxes of side-chain oxidized oxysterols across blood-brain and blood-CSF barriers and origin of these steroids in CSF (Review). *The Journal of steroid biochemistry and molecular biology* **188:** 86-89.

Bjorkhem I, Meaney S (2004). Brain cholesterol: long secret life behind a barrier. *Arterioscler Thromb Vasc Biol* **24**(5)**:** 806-815.

Boenzi S, Deodato F, Taurisano R, Goffredo BM, Rizzo C, Dionisi-Vici C (2016). Evaluation of plasma cholestane-3beta,5alpha,6beta-triol and 7-ketocholesterol in inherited disorders related to cholesterol metabolism. *Journal of lipid research* **57**(3)**:** 361-367.

Boselli E, Velazco V, Caboni MF, Lercker G (2001). Pressurized liquid extraction of lipids for the determination of oxysterols in egg-containing food. *Journal of chromatography. A* **917**(1-2)**:** 239-244.

Bozcali E, Süzer O, Gürsoy HN, Atukeren P, Gümüstas KM (2009). Effects of erucic acid supplemented feeding on chronic doxorubucin toxicity in rats. *International journal of clinical and experimental medicine* **2**(4)**:** 337-347.

Brahmi F, Nury T, Debbabi M, Hadj-Ahmed S, Zarrouk A, Prost M*, et al.* (2018). Evaluation of Antioxidant, Anti-Inflammatory and Cytoprotective Properties of Ethanolic Mint Extracts from Algeria on 7-Ketocholesterol-Treated Murine RAW 264.7 Macrophages. *Antioxidants (Basel)* **7**(12).

Brahmi F, Vejux A, Sghaier R, Zarrouk A, Nury T, Meddeb W*, et al.* (2019). Prevention of 7-ketocholesterol-induced side effects by natural compounds. *Crit Rev Food Sci Nutr* **59**(19)**:** 3179-3198.

Braverman NE, Moser AB (2012). Functions of plasmalogen lipids in health and disease. *Biochimica et biophysica acta* **1822**(9)**:** 1442-1452.

Brites P, Waterham HR, Wanders RJ (2004). Functions and biosynthesis of plasmalogens in health and disease. *Biochimica et biophysica acta* **1636**(2-3)**:** 219-231.

Brown AJ, Dean RT, Jessup W (1996). Free and esterified oxysterol: formation during copper-oxidation of low density lipoprotein and uptake by macrophages. *Journal of lipid research* **37**(2)**:** 320-335.

Brown AJ, Jessup W (1999). Oxysterols and atherosclerosis. *Atherosclerosis* **142**(1)**:** 1-28.

Brown AJ, Jessup W (2009). Oxysterols: Sources, cellular storage and metabolism, and new insights into their roles in cholesterol homeostasis. *Molecular aspects of medicine* **30**(3)**:** 111-122.

Brown RB (2019). Phospholipid packing defects and oxysterols in atherosclerosis: Dietary prevention and the French paradox. *Biochimie* **167:** 145-151.

Brzeska M, Szymczyk K, Szterk A (2016). Current Knowledge about Oxysterols: A Review. *Journal of food science* **81**(10)**:** R2299-R2308.

Butler D, Bahr BA (2006). Oxidative stress and lysosomes: CNS-related consequences and implications for lysosomal enhancement strategies and induction of autophagy. *Antioxidants & redox signaling* **8**(1-2)**:** 185-196.

Buttari B, Profumo E, Segoni L, D'Arcangelo D, Rossi S, Facchiano F*, et al.* (2014). Resveratrol counteracts inflammation in human M1 and M2 macrophages upon challenge with 7-oxo-cholesterol: potential therapeutic implications in atherosclerosis. *Oxidative medicine and cellular longevity* **2014:** 257543.

Buttari B, Segoni L, Profumo E, D'Arcangelo D, Rossi S, Facchiano F*, et al.* (2013). 7-Oxo-cholesterol potentiates pro-inflammatory signaling in human M1 and M2 macrophages. *Biochemical pharmacology* **86**(1)**:** 130-137.

Buvelot H, Jaquet V, Krause KH (2019). Mammalian NADPH Oxidases. *Methods Mol Biol* **1982:** 17-36.

Cardenia V, Rodriguez-Estrada MT, Lorenzini A, Bandini E, Angeloni C, Hrelia S*, et al.* (2017). Effect of broccoli extract enriched diet on liver cholesterol oxidation in rats subjected to exhaustive exercise. *The Journal of steroid biochemistry and molecular biology* **169:** 137-144.

Chalubinski M, Wojdan K, Gorzelak P, Borowiec M, Broncel M (2014). The effect of oxidized cholesterol on barrier functions and IL-10 mRNA expression in human intestinal epithelium co-cultured with dendritic cells in the transwell system. *Food and chemical toxicology : an international journal published for the British Industrial Biological Research Association* **69:** 289-293.

Chan AC (1993). Partners in defense, vitamin E and vitamin C. *Canadian journal of physiology and pharmacology* **71**(9)**:** 725-731.

Chang CL, Weigel AV, Ioannou MS, Pasolli HA, Xu CS, Peale DR*, et al.* (2019). Spastin tethers lipid droplets to peroxisomes and directs fatty acid trafficking through ESCRT-III. *The Journal of cell biology* **218**(8)**:** 2583-2599.

Chemerovski-Glikman M, Mimouni M, Dagan Y, Haj E, Vainer I, Allon R*, et al.* (2018). Rosmarinic Acid Restores Complete Transparency of Sonicated Human Cataract Ex Vivo and Delays Cataract Formation In Vivo. *Scientific reports* **8**(1)**:** 9341.

Chen C, Li J, Qin X, Wang W (2020). Peroxisomal Membrane Contact Sites in Mammalian Cells. *Frontiers in cell and developmental biology* **8:** 512.

Chen L, Deng H, Cui H, Fang J, Zuo Z, Deng J*, et al.* (2018). Inflammatory responses and inflammation-associated diseases in organs. *Oncotarget* **9**(6)**:** 7204-7218.

Cheng D, Jenner AM, Shui G, Cheong WF, Mitchell TW, Nealon JR*, et al.* (2011). Lipid pathway alterations in Parkinson's disease primary visual cortex. *PloS one* **6**(2)**:** e17299.

Cho DH, Kim YS, Jo DS, Choe SK, Jo EK (2018). Pexophagy: Molecular Mechanisms and Implications for Health and Diseases. *Molecules and cells* **41**(1)**:** 55-64.

Chu BB, Liao YC, Qi W, Xie C, Du X, Wang J*, et al.* (2015). Cholesterol transport through lysosome-peroxisome membrane contacts. *Cell* **161**(2)**:** 291-306.

Cilla A, Alegria A, Attanzio A, Garcia-Llatas G, Tesoriere L, Livrea MA (2017). Dietary phytochemicals in the protection against oxysterol-induced damage. *Chemistry and physics of lipids* **207**(Pt B)**:** 192-205.

Colles SM, Irwin KC, Chisolm GM (1996). Roles of multiple oxidized LDL lipids in cellular injury: dominance of 7 beta-hydroperoxycholesterol. *Journal of lipid research* **37**(9)**:** 2018-2028.

Colles SM, Maxson JM, Carlson SG, Chisolm GM (2001). Oxidized LDL-induced injury and apoptosis in atherosclerosis. Potential roles for oxysterols. *Trends in cardiovascular medicine* **11**(3-4)**:** 131-138.

Cooper GM (2000). The Cell: A Molecular Approach. 2nd edition *Sunderland (MA): Sinauer Associates*.

Cooper RA (1978). Influence of increased membrane cholesterol on membrane fluidity and cell function in human red blood cells. *Journal of supramolecular structure* **8**(4)**:** 413-430.

Coort SL, Willems J, Coumans WA, van der Vusse GJ, Bonen A, Glatz JF*, et al.* (2002). Sulfo-N-succinimidyl esters of long chain fatty acids specifically inhibit fatty acid translocase (FAT/CD36)-mediated cellular fatty acid uptake. *Molecular and cellular biochemistry* **239**(1-2)**:** 213-219.

Cornforth JW, Robinson R (1947). Towards the synthesis of cholesterol. *Nature* **160**(4074)**:** 737-739.

Crosignani A, Zuin M, Allocca M, Del Puppo M (2011). Oxysterols in bile acid metabolism. *Clinica chimica acta; international journal of clinical chemistry* **412**(23-24)**:** 2037-2045.

De Duve C, Baudhuin P (1966). Peroxisomes (microbodies and related particles). *Physiological reviews* **46**(2)**:** 323-357.

de Medina P, Diallo K, Huc-Claustre E, Attia M, Soules R, Silvente-Poirot S*, et al.* (2020). The 5,6-epoxycholesterol metabolic pathway in breast cancer: Emergence of new pharmacological targets. *British journal of pharmacology*.

de Medina P, Paillasse MR, Segala G, Voisin M, Mhamdi L, Dalenc F*, et al.* (2013). Dendrogenin A arises from cholesterol and histamine metabolism and shows cell differentiation and anti-tumour properties. *Nature communications* **4:** 1840.

Debbabi M, Nury T, Zarrouk A, Mekahli N, Bezine M, Sghaier R*, et al.* (2016). Protective Effects of alpha-Tocopherol, gamma-Tocopherol and Oleic Acid, Three Compounds of Olive Oils, and No Effect of Trolox, on 7-Ketocholesterol-Induced Mitochondrial and Peroxisomal Dysfunction in Microglial BV-2 Cells. *International journal of molecular sciences* **17**(12).

Debbabi M, Zarrouk A, Bezine M, Meddeb W, Nury T, Badreddine A*, et al.* (2017). Comparison of the effects of major fatty acids present in the Mediterranean diet (oleic acid, docosahexaenoic acid) and in hydrogenated oils (elaidic acid) on 7-ketocholesterol-induced oxiapoptophagy in microglial BV-2 cells. *Chem Phys Lipids* **207**(Pt B)**:** 151-170.

Deckert V, Desrumaux C, Athias A, Duverneuil L, Palleau V, Gambert P*, et al.* (2002). Prevention of LDL alpha-tocopherol consumption, cholesterol oxidation, and vascular endothelium dysfunction by polyphenolic compounds from red wine. *Atherosclerosis* **165**(1)**:** 41-50.

Deiana M, Calfapietra S, Incani A, Atzeri A, Rossin D, Loi R*, et al.* (2017). Derangement of intestinal epithelial cell monolayer by dietary cholesterol oxidation products. *Free radical biology & medicine* **113:** 539-550.

Deiana M, Corona G, Incani A, Loru D, Rosa A, Atzeri A*, et al.* (2010). Protective effect of simple phenols from extravirgin olive oil against lipid peroxidation in intestinal Caco-2 cells. *Food and chemical toxicology : an international journal published for the British Industrial Biological Research Association* **48**(10)**:** 3008-3016.

Del Rio LA (2011). Peroxisomes as a cellular source of reactive nitrogen species signal molecules. *Archives of biochemistry and biophysics* **506**(1)**:** 1-11.

Dhungana H, Huuskonen MT, Jaronen M, Lemarchant S, Ali H, Keksa-Goldsteine V*, et al.* (2017). Sulfosuccinimidyl oleate sodium is neuroprotective and alleviates stroke-induced neuroinflammation. *Journal of neuroinflammation* **14**(1)**:** 237.

Di Cara F, Andreoletti P, Trompier D, Vejux A, Bulow MH, Sellin J*, et al.* (2019). Peroxisomes in Immune Response and Inflammation. *International journal of molecular sciences* **20**(16).

Diestel A, Aktas O, Hackel D, Hake I, Meier S, Raine CS*, et al.* (2003). Activation of microglial poly(ADP-ribose)-polymerase-1 by cholesterol breakdown products during neuroinflammation: a link between demyelination and neuronal damage. *The Journal of experimental medicine* **198**(11)**:** 1729-1740.

Doria M, Nury T, Delmas D, Moreau T, Lizard G, Vejux A (2019). Protective function of autophagy during VLCFA-induced cytotoxicity in a neurodegenerative cell model. *Free radical biology & medicine* **137:** 46-58.

Dragonas C, Bertsch T, Sieber CC, Brosche T (2009). Plasmalogens as a marker of elevated systemic oxidative stress in Parkinson's disease. *Clinical chemistry and laboratory medicine* **47**(7)**:** 894-897.

Drahota Z, Vrbacky M, Nuskova H, Kazdova L, Zidek V, Landa V*, et al.* (2010). Succinimidyl oleate, established inhibitor of CD36/FAT translocase inhibits complex III of mitochondrial respiratory chain. *Biochemical and biophysical research communications* **391**(3)**:** 1348-1351.

Dugas B, Charbonnier S, Baarine M, Ragot K, Delmas D, Menetrier F*, et al.* (2010). Effects of oxysterols on cell viability, inflammatory cytokines, VEGF, and reactive oxygen species production on human retinal cells: cytoprotective effects and prevention of VEGF secretion by resveratrol. *European journal of nutrition* **49**(7)**:** 435-446.

Duran MJ, Pierre SV, Lesnik P, Pieroni G, Bourdeaux M, Dignat-Georges F*, et al.* (2010). 7-ketocholesterol inhibits Na,K-ATPase activity by decreasing expression of its alpha1-subunit and membrane fluidity in human endothelial cells. *Cell Mol Biol (Noisy-le-grand)* **56 Suppl:** OL1434-1441.

Eberhart T, Kovacs WJ (2018). Pexophagy in yeast and mammals: an update on mysteries. *Histochemistry and cell biology* **150**(5)**:** 473-488.

Faust PL, Kovacs WJ (2014). Cholesterol biosynthesis and ER stress in peroxisome deficiency. *Biochimie* **98:** 75-85.

Fischer BM, Voynow JA, Ghio AJ (2015). COPD: balancing oxidants and antioxidants. *International journal of chronic obstructive pulmonary disease* **10:** 261-276.

Fraga CG, Croft KD, Kennedy DO, Tomas-Barberan FA (2019). The effects of polyphenols and other bioactives on human health. *Food & function* **10**(2)**:** 514-528.

Fransen M, Lismont C, Walton P (2017). The Peroxisome-Mitochondria Connection: How and Why? *International journal of molecular sciences* **18**(6).

Fransen M, Nordgren M, Wang B, Apanasets O (2012). Role of peroxisomes in ROS/RNS-metabolism: implications for human disease. *Biochimica et biophysica acta* **1822**(9)**:** 1363-1373.

Freeman NE, Rusinol AE, Linton M, Hachey DL, Fazio S, Sinensky MS*, et al.* (2005). Acyl-coenzyme A:cholesterol acyltransferase promotes oxidized LDL/oxysterol-induced apoptosis in macrophages. *Journal of lipid research* **46**(9)**:** 1933-1943.

Freund Levi Y, Vedin I, Cederholm T, Basun H, Faxen Irving G, Eriksdotter M*, et al.* (2014). Transfer of omega-3 fatty acids across the blood-brain barrier after dietary supplementation with a docosahexaenoic acid-rich omega-3 fatty acid preparation in patients with Alzheimer's disease: the OmegAD study. *Journal of internal medicine* **275**(4)**:** 428-436.

Fu X, Huang X, Li P, Chen W, Xia M (2014). 7-Ketocholesterol inhibits isocitrate dehydrogenase 2 expression and impairs endothelial function via microRNA-144. *Free radical biology & medicine* **71:** 1-15.

Fuda H, Javitt NB, Mitamura K, Ikegawa S, Strott CA (2007). Oxysterols are substrates for cholesterol sulfotransferase. *Journal of lipid research* **48**(6)**:** 1343-1352.

Fujiki Y (2016). Peroxisome biogenesis and human peroxisome-deficiency disorders. *Proceedings of the Japan Academy. Series B, Physical and biological sciences* **92**(10)**:** 463-477.

Fujiki Y, Abe Y, Imoto Y, Tanaka AJ, Okumoto K, Honsho M*, et al.* (2020). Recent insights into peroxisome biogenesis and associated diseases. *Journal of cell science* **133**(9).

Ganguli G, Mukherjee U, Sonawane A (2019). Peroxisomes and Oxidative Stress: Their Implications in the Modulation of Cellular Immunity During Mycobacterial Infection. *Frontiers in microbiology* **10:** 1121.

Germain K, Kim PK (2020). Pexophagy: A Model for Selective Autophagy. *International journal of molecular sciences* **21**(2).

Geuze HJ, Murk JL, Stroobants AK, Griffith JM, Kleijmeer MJ, Koster AJ*, et al.* (2003). Involvement of the endoplasmic reticulum in peroxisome formation. *Molecular biology of the cell* **14**(7)**:** 2900-2907.

Ghosh B, Hanevold CD, Dobashi K, Orak JK, Singh I (1996). Tissue differences in antioxidant enzyme gene expression in response to endotoxin. *Free radical biology & medicine* **21**(4)**:** 533-540.

Ghosh S, Khare SK (2017). Biodegradation of 7-Ketocholesterol by Rhodococcus erythropolis MTCC 3951: Process optimization and enzymatic insights. *Chemistry and physics of lipids* **207**(Pt B)**:** 253-259.

Ghosh S, Khare SK (2016). Biodegradation of cytotoxic 7-Ketocholesterol by Pseudomonas aeruginosa PseA. *Bioresource technology* **213:** 44-49.

Girao H, Mota MC, Ramalho J, Pereira P (1998). Cholesterol oxides accumulate in human cataracts. *Experimental eye research* **66**(5)**:** 645-652.

Golovko MY, Murphy EJ (2006). Uptake and metabolism of plasma-derived erucic acid by rat brain. *Journal of lipid research* **47**(6)**:** 1289-1297.

Gray E, Rice C, Hares K, Redondo J, Kemp K, Williams M*, et al.* (2014). Reductions in neuronal peroxisomes in multiple sclerosis grey matter. *Mult Scler* **20**(6)**:** 651-659.

Griffiths WJ, Wang Y (2019a). Oxysterol research: a brief review. *Biochemical Society transactions* **47**(2)**:** 517-526.

Griffiths WJ, Wang Y (2020). Oxysterols as lipid mediators: Their biosynthetic genes, enzymes and metabolites. *Prostaglandins & other lipid mediators* **147:** 106381.

Griffiths WJ, Yutuc E, Abdel-Khalik J, Crick PJ, Hearn T, Dickson A*, et al.* (2019b). Metabolism of Non-Enzymatically Derived Oxysterols: Clues from sterol metabolic disorders. *Free radical biology & medicine* **144:** 124-133.

Hachem M, Belkouch M, Lo Van A, Picq M, Bernoud-Hubac N, Lagarde M (2020). Brain targeting with docosahexaenoic acid as a prospective therapy for neurodegenerative diseases and its passage across blood brain barrier. *Biochimie* **170:** 203-211.

Hamer I, Van Beersel G, Arnould T, Jadot M (2012). Lipids and lysosomes. *Current drug metabolism* **13**(10)**:** 1371-1387.

Han JH, Kim YJ, Han ES, Lee CS (2007). Prevention of 7-ketocholesterol-induced mitochondrial damage and cell death by calmodulin inhibition. *Brain research* **1137**(1)**:** 11-19.

Harris TR, Hammock BD (2013). Soluble epoxide hydrolase: gene structure, expression and deletion. *Gene* **526**(2)**:** 61-74.

He C, Zhu H, Zhang W, Okon I, Wang Q, Li H*, et al.* (2013). 7-Ketocholesterol induces autophagy in vascular smooth muscle cells through Nox4 and Atg4B. *The American journal of pathology* **183**(2)**:** 626-637.

Helmschrodt C, Becker S, Schroter J, Hecht M, Aust G, Thiery J*, et al.* (2013). Fast LC-MS/MS analysis of free oxysterols derived from reactive oxygen species in human plasma and carotid plaque. *Clinica chimica acta; international journal of clinical chemistry* **425:** 3-8.

Heo GY, Bederman I, Mast N, Liao WL, Turko IV, Pikuleva IA (2011). Conversion of 7-ketocholesterol to oxysterol metabolites by recombinant CYP27A1 and retinal pigment epithelial cells. *Journal of lipid research* **52**(6)**:** 1117-1127.

Higgins LG, Hayes JD (2011). Mechanisms of induction of cytosolic and microsomal glutathione transferase (GST) genes by xenobiotics and pro-inflammatory agents. *Drug metabolism reviews* **43**(2)**:** 92-137.

Houten SM, Wanders RJA, Ranea-Robles P (2020). Metabolic interactions between peroxisomes and mitochondria with a special focus on acylcarnitine metabolism. *Biochimica et biophysica acta. Molecular basis of disease* **1866**(5)**:** 165720.

Hua R, Kim PK (2016). Multiple paths to peroxisomes: Mechanism of peroxisome maintenance in mammals. *Biochimica et biophysica acta* **1863**(5)**:** 881-891.

Huang JD, Amaral J, Lee JW, Larrayoz IM, Rodriguez IR (2012). Sterculic acid antagonizes 7-ketocholesterol-mediated inflammation and inhibits choroidal neovascularization. *Biochimica et biophysica acta* **1821**(4)**:** 637-646.

Huang JD, Amaral J, Lee JW, Rodriguez IR (2014). 7-Ketocholesterol-induced inflammation signals mostly through the TLR4 receptor both in vitro and in vivo. *PloS one* **9**(7)**:** e100985.

Huyghe S, Mannaerts GP, Baes M, Van Veldhoven PP (2006). Peroxisomal multifunctional protein-2: the enzyme, the patients and the knockout mouse model. *Biochimica et biophysica acta* **1761**(9)**:** 973-994.

Iborra RT, Machado-Lima A, Castilho G, Nunes VS, Abdalla DS, Nakandakare ER*, et al.* (2011). Advanced glycation in macrophages induces intracellular accumulation of 7-ketocholesterol and total sterols by decreasing the expression of ABCA-1 and ABCG-1. *Lipids in health and disease* **10:** 172.

Imanaka T (2019). Biogenesis and Function of Peroxisomes in Human Disease with a Focus on the ABC Transporter. *Biological & pharmaceutical bulletin* **42**(5)**:** 649-665.

Indaram M, Ma W, Zhao L, Fariss RN, Rodriguez IR, Wong WT (2015). 7-Ketocholesterol increases retinal microglial migration, activation, and angiogenicity: a potential pathogenic mechanism underlying age-related macular degeneration. *Scientific reports* **5:** 9144.

Iriondo A, Garcia-Sebastian M, Arrospide A, Arriba M, Aurtenetxe S, Barandiaran M*, et al.* (2020). Cerebrospinal Fluid 7-Ketocholesterol Level is Associated with Amyloid-beta42 and White Matter Microstructure in Cognitively Healthy Adults. *Journal of Alzheimer's disease : JAD*.

Iuliano L (2011). Pathways of cholesterol oxidation via non-enzymatic mechanisms. *Chemistry and physics of lipids* **164**(6)**:** 457-468.

Iuliano L, Monticolo R, Straface G, Zullo S, Galli F, Boaz M*, et al.* (2009). Association of cholesterol oxidation and abnormalities in fatty acid metabolism in cystic fibrosis. *The American journal of clinical nutrition* **90**(3)**:** 477-484.

Jang J, Park S, Jin Hur H, Cho HJ, Hwang I, Pyo Kang Y*, et al.* (2016). 25-hydroxycholesterol contributes to cerebral inflammation of X-linked adrenoleukodystrophy through activation of the NLRP3 inflammasome. *Nature communications* **7:** 13129.

Javitt NB, Javitt JC (2009). The retinal oxysterol pathway: a unifying hypothesis for the cause of age-related macular degeneration. *Current opinion in ophthalmology* **20**(3)**:** 151-157.

Jo DS, Cho DH (2019). Peroxisomal dysfunction in neurodegenerative diseases. *Archives of pharmacal research* **42**(5)**:** 393-406.

Johansson I, Monsen VT, Pettersen K, Mildenberger J, Misund K, Kaarniranta K*, et al.* (2015). The marine n-3 PUFA DHA evokes cytoprotection against oxidative stress and protein misfolding by inducing autophagy and NFE2L2 in human retinal pigment epithelial cells. *Autophagy* **11**(9)**:** 1636-1651.

Kahn E, Baarine M, Dauphin A, Ragot K, Tissot N, Seguin A*, et al.* (2011). Impact of 7-ketocholesterol and very long chain fatty acids on oligodendrocyte lipid membrane organization: evaluation via LAURDAN and FAMIS spectral image analysis. *Cytometry. Part A : the journal of the International Society for Analytical Cytology* **79**(4)**:** 293-305.

Kandutsch AA, Chen HW, Heiniger HJ (1978). Biological activity of some oxygenated sterols. *Science* **201**(4355)**:** 498-501.

Kanner J (2007). Dietary advanced lipid oxidation endproducts are risk factors to human health. *Molecular nutrition & food research* **51**(9)**:** 1094-1101.

Kanner J, Lapidot T (2001). The stomach as a bioreactor: dietary lipid peroxidation in the gastric fluid and the effects of plant-derived antioxidants. *Free radical biology & medicine* **31**(11)**:** 1388-1395.

Kawaguchi K, Morita M (2016). ABC Transporter Subfamily D: Distinct Differences in Behavior between ABCD1-3 and ABCD4 in Subcellular Localization, Function, and Human Disease. *BioMed research international* **2016:** 6786245.

Keenan SN, Watt MJ, Montgomery MK (2020). Inter-organelle Communication in the Pathogenesis of Mitochondrial Dysfunction and Insulin Resistance. *Current diabetes reports* **20**(6)**:** 20.

Kemp S, Theodoulou FL, Wanders RJ (2011). Mammalian peroxisomal ABC transporters: from endogenous substrates to pathology and clinical significance. *British journal of pharmacology* **164**(7)**:** 1753-1766.

Kim I, Bang WY, Kim S, Jin SM, Hyun JY, Han EH*, et al.* (2018). Peroxisome-targeted Supramolecular Nanoprobes Assembled with Pyrene-labelled Peptide Amphiphiles. *Chemistry, an Asian journal* **13**(22)**:** 3485-3490.

Kim P (2017). Peroxisome Biogenesis: A Union between Two Organelles. *Current biology : CB* **27**(7)**:** R271-R274.

Kim PK, Mullen RT, Schumann U, Lippincott-Schwartz J (2006). The origin and maintenance of mammalian peroxisomes involves a de novo PEX16-dependent pathway from the ER. *The Journal of cell biology* **173**(4)**:** 521-532.

Kim YJ, Lee CS (2010). Tyrosine kinase inhibitor AG126 reduces 7-ketocholesterol-induced cell death by suppressing mitochondria-mediated apoptotic process. *Neurochemical research* **35**(4)**:** 603-612.

Klionsky DJ, Abdelmohsen K, Abe A, Abedin MJ, Abeliovich H, Acevedo Arozena A*, et al.* (2016). Guidelines for the use and interpretation of assays for monitoring autophagy (3rd edition). *Autophagy* **12**(1)**:** 1-222.

Koh SS, Ooi SC, Lui NM, Qiong C, Ho LT, Cheah IK*, et al.* (2020). Effect of Ergothioneine on 7-Ketocholesterol-Induced Endothelial Injury. *Neuromolecular medicine*.

Kohno M, Musashi K, Ikeda HO, Horibe T, Matsumoto A, Kawakami K (2020). Oral administration of ferulic acid or ethyl ferulate attenuates retinal damage in sodium iodate-induced retinal degeneration mice. *Scientific reports* **10**(1)**:** 8688.

Kou J, Kovacs GG, Hoftberger R, Kulik W, Brodde A, Forss-Petter S*, et al.* (2011). Peroxisomal alterations in Alzheimer's disease. *Acta neuropathologica* **122**(3)**:** 271-283.

Kovacs WJ, Krisans S (2003). Cholesterol biosynthesis and regulation: role of peroxisomes. *Advances in experimental medicine and biology* **544:** 315-327.

Kovacs WJ, Tape KN, Shackelford JE, Wikander TM, Richards MJ, Fliesler SJ*, et al.* (2009). Peroxisome deficiency causes a complex phenotype because of hepatic SREBP/Insig dysregulation associated with endoplasmic reticulum stress. *The Journal of biological chemistry* **284**(11)**:** 7232-7245.

Kuda O, Pietka TA, Demianova Z, Kudova E, Cvacka J, Kopecky J*, et al.* (2013). Sulfo-N-succinimidyl oleate (SSO) inhibits fatty acid uptake and signaling for intracellular calcium via binding CD36 lysine 164: SSO also inhibits oxidized low density lipoprotein uptake by macrophages. *J Biol Chem* **288**(22)**:** 15547-15555.

Kuo X, Herr DR, Ong WY (2020). Anti-inflammatory and Cytoprotective Effect of Clinacanthus nutans Leaf But Not Stem Extracts on 7-Ketocholesterol Induced Brain Endothelial Cell Injury. *Neuromolecular medicine*.

Kuriakose M, Younger D, Ravula AR, Alay E, Rama Rao KV, Chandra N (2019). Synergistic Role of Oxidative Stress and Blood-Brain Barrier Permeability as Injury Mechanisms in the Acute Pathophysiology of Blast-induced Neurotrauma. *Scientific reports* **9**(1)**:** 7717.

La Marca V, Spagnuolo MS, Cigliano L, Marasco D, Abrescia P (2014). The enzyme lecithin-cholesterol acyltransferase esterifies cerebrosterol and limits the toxic effect of this oxysterol on SH-SY5Y cells. *Journal of neurochemistry* **130**(1)**:** 97-108.

Lazarow PB, Fujiki Y (1985). Biogenesis of peroxisomes. *Annual review of cell biology* **1:** 489-530.

Lee P, Ulatowski LM (2019). Vitamin E: Mechanism of transport and regulation in the CNS. *IUBMB life* **71**(4)**:** 424-429.

Lee WH, Lee CS, Kwon K, Kwon YS, Kim SW, Goo TW*, et al.* (2009). 7-ketocholesterol induces endoplasmic reticulum stress in HT-29 cells. *Zeitschrift fur Naturforschung. C, Journal of biosciences* **64**(3-4)**:** 307-310.

Leonarduzzi G, Sottero B, Poli G (2002). Oxidized products of cholesterol: dietary and metabolic origin, and proatherosclerotic effects (review). *The Journal of nutritional biochemistry* **13**(12)**:** 700-710.

Leonarduzzi G, Vizio B, Sottero B, Verde V, Gamba P, Mascia C*, et al.* (2006). Early involvement of ROS overproduction in apoptosis induced by 7-ketocholesterol. *Antioxidants & redox signaling* **8**(3-4)**:** 375-380.

Leoni V, Nury T, Vejux A, Zarrouk A, Caccia C, Debbabi M*, et al.* (2017). Mitochondrial dysfunctions in 7-ketocholesterol-treated 158N oligodendrocytes without or with alpha-tocopherol: Impacts on the cellular profil of tricarboxylic cycle-associated organic acids, long chain saturated and unsaturated fatty acids, oxysterols, cholesterol and cholesterol precursors. *J Steroid Biochem Mol Biol* **169:** 96-110.

Li W, Ghosh M, Eftekhari S, Yuan XM (2011). Lipid accumulation and lysosomal pathways contribute to dysfunction and apoptosis of human endothelial cells caused by 7-oxysterols. *Biochemical and biophysical research communications* **409**(4)**:** 711-716.

Li W, Laskar A, Sultana N, Osman E, Ghosh M, Li Q*, et al.* (2012). Cell death induced by 7-oxysterols via lysosomal and mitochondrial pathways is p53-dependent. *Free radical biology & medicine* **53**(11)**:** 2054-2061.

Lifschütz J (1913). Die Oxydation des Cholesterins durch das Blutgewebe. *Biological Chemistry* **93**(3-4).

Lin CYM, C. W (1995). Distribution of oxysterols in human serum: Characterization of 25-hydroxycholesterol association with serum albumin. *The Journal of nutritional biochemistry* **6**(11)**:** 618-625.

Linseisen J, Wolfram G (1998). Absorption of cholesterol oxidation products from ordinary foodstuff in humans. *Annals of nutrition & metabolism* **42**(4)**:** 221-230.

Lismont C, Nordgren M, Van Veldhoven PP, Fransen M (2015). Redox interplay between mitochondria and peroxisomes. *Frontiers in cell and developmental biology* **3:** 35.

Liu YM, Nepali K, Liou JP (2017). Idiopathic Pulmonary Fibrosis: Current Status, Recent Progress, and Emerging Targets. *Journal of medicinal chemistry* **60**(2)**:** 527-553.

Lizard G, Gueldry S, Sordet O, Monier S, Athias A, Miguet C*, et al.* (1998). Glutathione is implied in the control of 7-ketocholesterol-induced apoptosis, which is associated with radical oxygen species production. *FASEB journal : official publication of the Federation of American Societies for Experimental Biology* **12**(15)**:** 1651-1663.

Lizard G, Miguet C, Bessede G, Monier S, Gueldry S, Neel D*, et al.* (2000). Impairment with various antioxidants of the loss of mitochondrial transmembrane potential and of the cytosolic release of cytochrome c occuring during 7-ketocholesterol-induced apoptosis. *Free radical biology & medicine* **28**(5)**:** 743-753.

Lochhead JJ, McCaffrey G, Quigley CE, Finch J, DeMarco KM, Nametz N*, et al.* (2010). Oxidative stress increases blood-brain barrier permeability and induces alterations in occludin during hypoxia-reoxygenation. *Journal of cerebral blood flow and metabolism : official journal of the International Society of Cerebral Blood Flow and Metabolism* **30**(9)**:** 1625-1636.

Luchetti F, Canonico B, Cesarini E, Betti M, Galluzzi L, Galli L*, et al.* (2015). 7-Ketocholesterol and 5,6-secosterol induce human endothelial cell dysfunction by differential mechanisms. *Steroids* **99**(Pt B)**:** 204-211.

Luu-The V (2013). Assessment of steroidogenesis and steroidogenic enzyme functions. *The Journal of steroid biochemistry and molecular biology* **137:** 176-182.

Lyons MA, Brown AJ (2001). Metabolism of an oxysterol, 7-ketocholesterol, by sterol 27-hydroxylase in HepG2 cells. *Lipids* **36**(7)**:** 701-711.

Mackrill JJ (2011). Oxysterols and calcium signal transduction. *Chemistry and physics of lipids* **164**(6)**:** 488-495.

Malvitte L, Montange T, Joffre C, Vejux A, Maiza C, Bron A*, et al.* (2006). [Analogies between atherosclerosis and age-related maculopathy: expected roles of oxysterols]. *Journal francais d'ophtalmologie* **29**(5)**:** 570-578.

Manickam R, Wahli W (2017). Roles of Peroxisome Proliferator-Activated Receptor beta/delta in skeletal muscle physiology. *Biochimie* **136:** 42-48.

Marcello A, Civra A, Milan Bonotto R, Nascimento Alves L, Rajasekharan S, Giacobone C*, et al.* (2020). The cholesterol metabolite 27-hydroxycholesterol inhibits SARS-CoV-2 and is markedly decreased in COVID-19 patients. *Redox biology* **36:** 101682.

Massaad C, Iuliano L, Lizard G (2017). Oxysterols and phytosterols in human health. *Chemistry and physics of lipids* **207**(Pt B)**:** 49-50.

Mathieu J, Schloendorn J, Rittmann BE, Alvarez PJ (2008). Microbial degradation of 7-ketocholesterol. *Biodegradation* **19**(6)**:** 807-813.

Mathieu JM, Mohn WW, Eltis LD, LeBlanc JC, Stewart GR, Dresen C*, et al.* (2010). 7-ketocholesterol catabolism by Rhodococcus jostii RHA1. *Applied and environmental microbiology* **76**(1)**:** 352-355.

Mathieu JM, Wang F, Segatori L, Alvarez PJ (2012). Increased resistance to oxysterol cytotoxicity in fibroblasts transfected with a lysosomally targeted Chromobacterium oxidase. *Biotechnology and bioengineering* **109**(9)**:** 2409-2415.

Meaney S (2013). Epigenetic regulation of oxysterol formation. *Biochimie* **95**(3)**:** 531-537.

Meddeb W, Rezig L, Abderrabba M, Lizard G, Mejri M (2017). Tunisian Milk Thistle: An Investigation of the Chemical Composition and the Characterization of Its Cold-Pressed Seed Oils. *International journal of molecular sciences* **18**(12).

Meddeb W, Rezig L, Zarrouk A, Nury T, Vejux A, Prost M*, et al.* (2018). Cytoprotective Activities of Milk Thistle Seed Oil Used in Traditional Tunisian Medicine on 7-Ketocholesterol and 24S-Hydroxycholesterol-Induced Toxicity on 158N Murine Oligodendrocytes. *Antioxidants (Basel)* **7**(7).

Mei S, Ni HM, Manley S, Bockus A, Kassel KM, Luyendyk JP*, et al.* (2011). Differential roles of unsaturated and saturated fatty acids on autophagy and apoptosis in hepatocytes. *J Pharmacol Exp Ther* **339**(2)**:** 487-498.

Miguet-Alfonsi C, Prunet C, Monier S, Bessede G, Lemaire-Ewing S, Berthier A*, et al.* (2002). Analysis of oxidative processes and of myelin figures formation before and after the loss of mitochondrial transmembrane potential during 7beta-hydroxycholesterol and 7-ketocholesterol-induced apoptosis: comparison with various pro-apoptotic chemicals. *Biochemical pharmacology* **64**(3)**:** 527-541.

Millanvoye-Van Brussel E, Topal G, Brunet A, Do Pham T, Deckert V, Rendu F*, et al.* (2004). Lysophosphatidylcholine and 7-oxocholesterol modulate Ca2+ signals and inhibit the phosphorylation of endothelial NO synthase and cytosolic phospholipase A2. *The Biochemical journal* **380**(Pt 2)**:** 533-539.

Mitic T, Andrew R, Walker BR, Hadoke PW (2013). 11beta-Hydroxysteroid dehydrogenase type 1 contributes to the regulation of 7-oxysterol levels in the arterial wall through the inter-conversion of 7-ketocholesterol and 7beta-hydroxycholesterol. *Biochimie* **95**(3)**:** 548-555.

Monier S, Samadi M, Prunet C, Denance M, Laubriet A, Athias A*, et al.* (2003). Impairment of the cytotoxic and oxidative activities of 7 beta-hydroxycholesterol and 7-ketocholesterol by esterification with oleate. *Biochemical and biophysical research communications* **303**(3)**:** 814-824.

Moreira EF, Larrayoz IM, Lee JW, Rodriguez IR (2009). 7-Ketocholesterol is present in lipid deposits in the primate retina: potential implication in the induction of VEGF and CNV formation. *Investigative ophthalmology & visual science* **50**(2)**:** 523-532.

Moser HW, Moser AB, Hollandsworth K, Brereton NH, Raymond GV (2007). "Lorenzo's oil" therapy for X-linked adrenoleukodystrophy: rationale and current assessment of efficacy. *Journal of molecular neuroscience : MN* **33**(1)**:** 105-113.

Munn NJ, Arnio E, Liu D, Zoeller RA, Liscum L (2003). Deficiency in ethanolamine plasmalogen leads to altered cholesterol transport. *Journal of lipid research* **44**(1)**:** 182-192.

Murphy EJ (2017). The blood-brain barrier and protein-mediated fatty acid uptake: role of the blood-brain barrier as a metabolic barrier: An Editorial Comment for 'The blood-brain barrier fatty acid transport protein 1 (FATP1/SLC27A1) supplies docosahexaenoic acid to the brain, and insulin facilitates transport'. *Journal of neurochemistry* **141**(3)**:** 324-329.

Mutemberezi V, Guillemot-Legris O, Muccioli GG (2016). Oxysterols: From cholesterol metabolites to key mediators. *Progress in lipid research* **64:** 152-169.

Nakazawa T, Miyanoki Y, Urano Y, Uehara M, Saito Y, Noguchi N (2017). Effect of vitamin E on 24(S)-hydroxycholesterol-induced necroptosis-like cell death and apoptosis. *The Journal of steroid biochemistry and molecular biology* **169:** 69-76.

Namsi A, Nury T, Hamdouni H, Yammine A, Vejux A, Vervandier-Fasseur D*, et al.* (2018). Induction of Neuronal Differentiation of Murine N2a Cells by Two Polyphenols Present in the Mediterranean Diet Mimicking Neurotrophins Activities: Resveratrol and Apigenin. *Diseases* **6**(3).

Namsi A, Nury T, Khan AS, Leprince J, Vaudry D, Caccia C*, et al.* (2019). Octadecaneuropeptide (ODN) Induces N2a Cells Differentiation through a PKA/PLC/PKC/MEK/ERK-Dependent Pathway: Incidence on Peroxisome, Mitochondria, and Lipid Profiles. *Molecules* **24**(18).

Navas-Madronal M, Rodriguez C, Kassan M, Fite J, Escudero JR, Canes L*, et al.* (2019). Enhanced endoplasmic reticulum and mitochondrial stress in abdominal aortic aneurysm. *Clin Sci (Lond)* **133**(13)**:** 1421-1438.

Nazarko TY (2017). Pexophagy is responsible for 65% of cases of peroxisome biogenesis disorders. *Autophagy* **13**(5)**:** 991-994.

Nordgren M, Wang B, Apanasets O, Fransen M (2013). Peroxisome degradation in mammals: mechanisms of action, recent advances, and perspectives. *Frontiers in physiology* **4:** 145.

Nury T, Doria M, Lizard G, Vejux A (2020). Docosahexaenoic Acid Attenuates Mitochondrial Alterations and Oxidative Stress Leading to Cell Death Induced by Very Long-Chain Fatty Acids in a Mouse Oligodendrocyte Model. *International journal of molecular sciences* **21**(2).

Nury T, Samadi M, Varin A, Lopez T, Zarrouk A, Boumhras M*, et al.* (2013). Biological activities of the LXRalpha and beta agonist, 4beta-hydroxycholesterol, and of its isomer, 4alpha-hydroxycholesterol, on oligodendrocytes: effects on cell growth and viability, oxidative and inflammatory status. *Biochimie* **95**(3)**:** 518-530.

Nury T, Sghaier R, Zarrouk A, Menetrier F, Uzun T, Leoni V*, et al.* (2018). Induction of peroxisomal changes in oligodendrocytes treated with 7-ketocholesterol: Attenuation by alpha-tocopherol. *Biochimie* **153:** 181-202.

Nury T, Zarrouk A, Mackrill JJ, Samadi M, Durand P, Riedinger JM*, et al.* (2015). Induction of oxiapoptophagy on 158N murine oligodendrocytes treated by 7-ketocholesterol-, 7beta-hydroxycholesterol-, or 24(S)-hydroxycholesterol: Protective effects of alpha-tocopherol and docosahexaenoic acid (DHA; C22:6 n-3). *Steroids* **99**(Pt B)**:** 194-203.

Nury T, Zarrouk A, Ragot K, Debbabi M, Riedinger JM, Vejux A*, et al.* (2017). 7-Ketocholesterol is increased in the plasma of X-ALD patients and induces peroxisomal modifications in microglial cells: Potential roles of 7-ketocholesterol in the pathophysiology of X-ALD. *J Steroid Biochem Mol Biol* **169:** 123-136.

Nury T, Zarrouk A, Vejux A, Doria M, Riedinger JM, Delage-Mourroux R*, et al.* (2014). Induction of oxiapoptophagy, a mixed mode of cell death associated with oxidative stress, apoptosis and autophagy, on 7-ketocholesterol-treated 158N murine oligodendrocytes: impairment by alpha-tocopherol. *Biochemical and biophysical research communications* **446**(3)**:** 714-719.

Olivier E, Dutot M, Regazzetti A, Leguillier T, Dargere D, Auzeil N*, et al.* (2016). P2X7-pannexin-1 and amyloid beta-induced oxysterol input in human retinal cell: Role in age-related macular degeneration? *Biochimie* **127:** 70-78.

Olkkonen VM, Beaslas O, Nissila E (2012). Oxysterols and their cellular effectors. *Biomolecules* **2**(1)**:** 76-103.

Palozza P, Simone R, Catalano A, Boninsegna A, Bohm V, Frohlich K*, et al.* (2010). Lycopene prevents 7-ketocholesterol-induced oxidative stress, cell cycle arrest and apoptosis in human macrophages. *The Journal of nutritional biochemistry* **21**(1)**:** 34-46.

Palozza P, Simone R, Catalano A, Monego G, Barini A, Mele MC*, et al.* (2011). Lycopene prevention of oxysterol-induced proinflammatory cytokine cascade in human macrophages: inhibition of NF-kappaB

nuclear binding and increase in PPARgamma expression. *The Journal of nutritional biochemistry* **22**(3)**:** 259-268.

Pandey KB, Rizvi SI (2009). Plant polyphenols as dietary antioxidants in human health and disease. *Oxidative medicine and cellular longevity* **2**(5)**:** 270-278.

Pariente A, Pelaez R, Perez-Sala A, Larrayoz IM (2019). Inflammatory and cell death mechanisms induced by 7-ketocholesterol in the retina. Implications for age-related macular degeneration. *Experimental eye research* **187:** 107746.

Pedruzzi E, Guichard C, Ollivier V, Driss F, Fay M, Prunet C*, et al.* (2004). NAD(P)H oxidase Nox-4 mediates 7-ketocholesterol-induced endoplasmic reticulum stress and apoptosis in human aortic smooth muscle cells. *Molecular and cellular biology* **24**(24)**:** 10703-10717.

Peeters A, Shinde AB, Dirkx R, Smet J, De Bock K, Espeel M*, et al.* (2015). Mitochondria in peroxisome-deficient hepatocytes exhibit impaired respiration, depleted DNA, and PGC-1alpha independent proliferation. *Biochimica et biophysica acta* **1853**(2)**:** 285-298.

Phan HTT, Shimokawa N, Sharma N, Takagi M, Vestergaard MC (2018). Strikingly different effects of cholesterol and 7-ketocholesterol on lipid bilayer-mediated aggregation of amyloid beta (1-42). *Biochemistry and biophysics reports* **14:** 98-103.

Poirot M, Silvente-Poirot S (2018). The tumor-suppressor cholesterol metabolite, dendrogenin A, is a new class of LXR modulator activating lethal autophagy in cancers. *Biochemical pharmacology* **153:** 75-81.

Poli G, Biasi F, Leonarduzzi G (2013). Oxysterols in the pathogenesis of major chronic diseases. *Redox biology* **1:** 125-130.

Porter FD, Scherrer DE, Lanier MH, Langmade SJ, Molugu V, Gale SE*, et al.* (2010). Cholesterol oxidation products are sensitive and specific blood-based biomarkers for Niemann-Pick C1 disease. *Science translational medicine* **2**(56)**:** 56ra81.

Prieto Tenreiro A, Penacho Lazaro MA, Andres Celda R, Fernandez Fernandez M, Gonzalez Mateo C, Diez Hernandez A (2013). Dietary treatment for X-linked adrenoleukodystrophy: is "Lorenzo's oil" useful? *Endocrinologia y nutricion : organo de la Sociedad Espanola de Endocrinologia y Nutricion* **60**(1)**:** 37-39.

Prunet C, Montange T, Vejux A, Laubriet A, Rohmer JF, Riedinger JM*, et al.* (2006). Multiplexed flow cytometric analyses of pro- and anti-inflammatory cytokines in the culture media of oxysterol-treated human monocytic cells and in the sera of atherosclerotic patients. *Cytometry. Part A : the journal of the International Society for Analytical Cytology* **69**(5)**:** 359-373.

Qiu B, Simon MC (2016). BODIPY 493/503 Staining of Neutral Lipid Droplets for Microscopy and Quantification by Flow Cytometry. *Bio-protocol* **6**(17).

Ragot K, Delmas D, Athias A, Nury T, Baarine M, Lizard G (2011). alpha-Tocopherol impairs 7-ketocholesterol-induced caspase-3-dependent apoptosis involving GSK-3 activation and Mcl-1 degradation on 158N murine oligodendrocytes. *Chemistry and physics of lipids* **164**(6)**:** 469-478.

Ragot K, Mackrill JJ, Zarrouk A, Nury T, Aires V, Jacquin A*, et al.* (2013). Absence of correlation between oxysterol accumulation in lipid raft microdomains, calcium increase, and apoptosis induction on 158N murine oligodendrocytes. *Biochem Pharmacol* **86**(1)**:** 67-79.

Raleigh DR, Sever N, Choksi PK, Sigg MA, Hines KM, Thompson BM*, et al.* (2018). Cilia-Associated Oxysterols Activate Smoothened. *Molecular cell* **72**(2)**:** 316-327 e315.

Rasmiena AA, Barlow CK, Stefanovic N, Huynh K, Tan R, Sharma A*, et al.* (2015). Plasmalogen modulation attenuates atherosclerosis in ApoE- and ApoE/GPx1-deficient mice. *Atherosclerosis* **243**(2)**:** 598-608.

Ricciardi CA, Gnudi L (2020). The endoplasmic reticulum stress and the unfolded protein response in kidney disease: Implications for vascular growth factors. *Journal of cellular and molecular medicine*.

Rimbach G, Minihane AM, Majewicz J, Fischer A, Pallauf J, Virgli F*, et al.* (2002). Regulation of cell signalling by vitamin E. *The Proceedings of the Nutrition Society* **61**(4)**:** 415-425.

Rinaldo P, Matern D, Bennett MJ (2002). Fatty acid oxidation disorders. *Annual review of physiology* **64:** 477-502.

Rodriguez IR, Alam S, Lee JW (2004). Cytotoxicity of oxidized low-density lipoprotein in cultured RPE cells is dependent on the formation of 7-ketocholesterol. *Investigative ophthalmology & visual science* **45**(8)**:** 2830-2837.

Rosenblat M, Aviram M (2002). Oxysterol-induced activation of macrophage NADPH-oxidase enhances cell-mediated oxidation of LDL in the atherosclerotic apolipoprotein E deficient mouse: inhibitory role for vitamin E. *Atherosclerosis* **160**(1)**:** 69-80.

Rossin D, Barbosa-Pereira L, Iaia N, Testa G, Sottero B, Poli G*, et al.* (2019). A Dietary Mixture of Oxysterols Induces In Vitro Intestinal Inflammation through TLR2/4 Activation: The Protective Effect of Cocoa Bean Shells. *Antioxidants (Basel)* **8**(6).

Rothe G, Valet G (1990). Flow cytometric analysis of respiratory burst activity in phagocytes with hydroethidine and 2',7'-dichlorofluorescin. *Journal of leukocyte biology* **47**(5)**:** 440-448.

Royer MC, Lemaire-Ewing S, Desrumaux C, Monier S, Pais de Barros JP, Athias A*, et al.* (2009). 7-ketocholesterol incorporation into sphingolipid/cholesterol-enriched (lipid raft) domains is impaired by vitamin E: a specific role for alpha-tocopherol with consequences on cell death. *The Journal of biological chemistry* **284**(23)**:** 15826-15834.

Sabolova M, Pohorela B, Fisnar J, Kourimska L, Chrpova D, Panek J (2017). Formation of oxysterols during thermal processing and frozen storage of cooked minced meat. *Journal of the science of food and agriculture* **97**(15)**:** 5092-5099.

Sakhrani NM, Padh H (2013). Organelle targeting: third level of drug targeting. *Drug design, development and therapy* **7:** 585-599.

Sargsyan Y, Thoms S (2020). Staying in Healthy Contact: How Peroxisomes Interact with Other Cell Organelles. *Trends in molecular medicine* **26**(2)**:** 201-214.

Sasaki H, Watanabe F, Murano T, Miyashita Y, Shirai K (2007). Vascular smooth muscle cell apoptosis induced by 7-ketocholesterol was mediated via Ca2+ and inhibited by the calcium channel blocker nifedipine. *Metabolism: clinical and experimental* **56**(3)**:** 357-362.

Sassa T, Wakashima T, Ohno Y, Kihara A (2014). Lorenzo's oil inhibits ELOVL1 and lowers the level of sphingomyelin with a saturated very long-chain fatty acid. *J Lipid Res* **55**(3)**:** 524-530.

Sassi K, Nury T, Zarrouk A, Sghaier R, Khalafi-Nezhad A, Vejux A*, et al.* (2019a). Induction of a non-apoptotic mode of cell death associated with autophagic characteristics with steroidal maleic anhydrides and 7beta-hydroxycholesterol on glioma cells. *The Journal of steroid biochemistry and molecular biology* **191:** 105371.

Sassi K, Nury T, Zarrouk A, Sghaier R, Khalafi-Nezhad A, Vejux A*, et al.* (2019b). Induction of a non-apoptotic mode of cell death associated with autophagic characteristics with steroidal maleic anhydrides and 7β-hydroxycholesterol on glioma cells. *J Steroid Biochem Mol Biol* **191:** 105371.

Sato Y, Ishihara N, Nagayama D, Saiki A, Tatsuno I (2017). 7-ketocholesterol induces apoptosis of MC3T3-E1 cells associated with reactive oxygen species generation, endoplasmic reticulum stress and caspase-3/7 dependent pathway. *Molecular genetics and metabolism reports* **10:** 56-60.

Schieffer D, Naware S, Bakun W, Bamezai AK (2014). Lipid raft-based membrane order is important for antigen-specific clonal expansion of CD4(+) T lymphocytes. *BMC immunology* **15:** 58.

Schlegel RA, Stevens M, Lumley-Sapanski K, Williamson P (1993). Altered lipid packing identifies apoptotic thymocytes. *Immunology letters* **36**(3)**:** 283-288.

Schloendorn J, Webb T, Kemmish K, Hamalainen M, Jackemeyer D, Jiang L*, et al.* (2009). Medical bioremediation: a concept moving toward reality. *Rejuvenation Res* **12**(6)**:** 411-419.

Schonfeld P, Reiser G (2016). Brain Lipotoxicity of Phytanic Acid and Very Long-chain Fatty Acids. Harmful Cellular/Mitochondrial Activities in Refsum Disease and X-Linked Adrenoleukodystrophy. *Aging and disease* **7**(2)**:** 136-149.

Schrader M, Bonekamp NA, Islinger M (2012). Fission and proliferation of peroxisomes. *Biochimica et biophysica acta* **1822**(9)**:** 1343-1357.

Schrader M, Costello JL, Godinho LF, Azadi AS, Islinger M (2016). Proliferation and fission of peroxisomes - An update. *Biochimica et biophysica acta* **1863**(5)**:** 971-983.

Schrader M, Fahimi HD (2006). Peroxisomes and oxidative stress. *Biochimica et biophysica acta* **1763**(12)**:** 1755-1766.

Schwingshackl L, Morze J, Hoffmann G (2020). Mediterranean diet and health status: Active ingredients and pharmacological mechanisms. *Br J Pharmacol* **177**(6)**:** 1241-1257.

Segala G, David M, de Medina P, Poirot MC, Serhan N, Vergez F*, et al.* (2017). Dendrogenin A drives LXR to trigger lethal autophagy in cancers. *Nature communications* **8**(1)**:** 1903.

Sghaier R, Nury T, Leoni V, Caccia C, Pais De Barros JP, Cherif A*, et al.* (2019a). Dimethyl fumarate and monomethyl fumarate attenuate oxidative stress and mitochondrial alterations leading to oxiapoptophagy in 158N murine oligodendrocytes treated with 7beta-hydroxycholesterol. *The Journal of steroid biochemistry and molecular biology* **194:** 105432.

Sghaier R, Zarrouk A, Nury T, Badreddine I, O'Brien N, Mackrill JJ*, et al.* (2019b). Biotin attenuation of oxidative stress, mitochondrial dysfunction, lipid metabolism alteration and 7beta-hydroxycholesterol-induced cell death in 158N murine oligodendrocytes. *Free radical research* **53**(5)**:** 535-561.

Simons K, Toomre D (2000). Lipid rafts and signal transduction. *Nature reviews. Molecular cell biology* **1**(1)**:** 31-39.

Sottero B, Rossin D, Staurenghi E, Gamba P, Poli G, Testa G (2019). Omics analysis of oxysterols to better understand their pathophysiological role. *Free radical biology & medicine* **144:** 55-71.

Su XQ, Wang J, Sinclair AJ (2019). Plasmalogens and Alzheimer's disease: a review. *Lipids in health and disease* **18**(1)**:** 100.

Sudo R, Sato F, Azechi T, Wachi H (2015). 7-Ketocholesterol-induced lysosomal dysfunction exacerbates vascular smooth muscle cell calcification via oxidative stress. *Genes to cells : devoted to molecular & cellular mechanisms* **20**(12)**:** 982-991.

Sugiura A, Mattie S, Prudent J, McBride HM (2017). Newly born peroxisomes are a hybrid of mitochondrial and ER-derived pre-peroxisomes. *Nature* **542**(7640)**:** 251-254.

Szedlacsek SE, Wasowicz E, Hulea SA, Nishida HI, Kummerow FA, Nishida T (1995). Esterification of oxysterols by human plasma lecithin-cholesterol acyltransferase. *The Journal of biological chemistry* **270**(20)**:** 11812-11819.

Takeshi Arita TY, Shohei Moriyama, Kei Irie, Mitsuhiro Fukata, Keita Odashiro, Toru Maruyama, Seira Hazeyama,Shiro Mawatari, Takehiko Fujino, Koichi Akashi (2018). Plasma and Erythrocyte Membrane Plasmalogens in Patients with Coronary Heart Diseases Undergoing Percutaneous Intervention *Cardiology and Angiology: An International Journal* **7**(4).

Tall AR (2008). Cholesterol efflux pathways and other potential mechanisms involved in the athero-protective effect of high density lipoproteins. *Journal of internal medicine* **263**(3)**:** 256-273.

Tanaka H, Okazaki T, Aoyama S, Yokota M, Koike M, Okada Y*, et al.* (2019). Peroxisomes control mitochondrial dynamics and the mitochondrion-dependent apoptosis pathway. *Journal of cell science* **132**(11).

Targosz-Korecka M, Wnetrzak A, Chachaj-Brekiesz A, Gonet-Surowka A, Kubisiak A, Filiczkowska A*, et al.* (2020). Effect of selected B-ring-substituted oxysterols on artificial model erythrocyte membrane and isolated red blood cells. *Biochimica et biophysica acta. Biomembranes* **1862**(2)**:** 183067.

Terasaka N, Wang N, Yvan-Charvet L, Tall AR (2007). High-density lipoprotein protects macrophages from oxidized low-density lipoprotein-induced apoptosis by promoting efflux of 7-ketocholesterol via ABCG1. *Proceedings of the National Academy of Sciences of the United States of America* **104**(38)**:** 15093-15098.

Tesoriere L, Attanzio A, Allegra M, Cilla A, Gentile C, Livrea MA (2014a). Oxysterol mixture in hypercholesterolemia-relevant proportion causes oxidative stress-dependent eryptosis. *Cellular physiology and biochemistry : international journal of experimental cellular physiology, biochemistry, and pharmacology* **34**(4)**:** 1075-1089.

Tesoriere L, Attanzio A, Allegra M, Gentile C, Livrea MA (2014b). Indicaxanthin inhibits NADPH oxidase (NOX)-1 activation and NF-kappaB-dependent release of inflammatory mediators and prevents the increase of epithelial permeability in IL-1beta-exposed Caco-2 cells. *The British journal of nutrition* **111**(3)**:** 415-423.

Tesoriere L, Attanzio A, Allegra M, Gentile C, Livrea MA (2013). Phytochemical indicaxanthin suppresses 7-ketocholesterol-induced THP-1 cell apoptosis by preventing cytosolic Ca(2+) increase and oxidative stress. *The British journal of nutrition* **110**(2)**:** 230-240.

Tesoriere L, Attanzio A, Allegra M, Livrea MA (2015). Dietary indicaxanthin from cactus pear (Opuntia ficus-indica L. Mill) fruit prevents eryptosis induced by oxysterols in a hypercholesterolaemia-relevant proportion and adhesion of human erythrocytes to endothelial cell layers. *The British journal of nutrition* **114**(3)**:** 368-375.

Testa G, Rossin D, Poli G, Biasi F, Leonarduzzi G (2018). Implication of oxysterols in chronic inflammatory human diseases. *Biochimie* **153:** 220-231.

Testa G, Staurenghi E, Zerbinati C, Gargiulo S, Iuliano L, Giaccone G*, et al.* (2016). Changes in brain oxysterols at different stages of Alzheimer's disease: Their involvement in neuroinflammation. *Redox biology* **10:** 24-33.

Thakur V, Morley S, Manor D (2010). Hepatic alpha-tocopherol transfer protein: ligand-induced protection from proteasomal degradation. *Biochemistry* **49**(43)**:** 9339-9344.

Tian L, Wang H, Abdallah AM, Prinyawiwatkul W, Xu Z (2011). Red and white wines inhibit cholesterol oxidation induced by free radicals. *Journal of agricultural and food chemistry* **59**(12)**:** 6453-6458.

Tomanek L (2015). Proteomic responses to environmentally induced oxidative stress. *The Journal of experimental biology* **218**(Pt 12)**:** 1867-1879.

Troesch B, Eggersdorfer M, Laviano A, Rolland Y, Smith AD, Warnke I*, et al.* (2020). Expert Opinion on Benefits of Long-Chain Omega-3 Fatty Acids (DHA and EPA) in Aging and Clinical Nutrition. *Nutrients* **12**(9).

Trompier D, Vejux A, Zarrouk A, Gondcaille C, Geillon F, Nury T*, et al.* (2014). Brain peroxisomes. *Biochimie* **98:** 102-110.

Umetani M, Ghosh P, Ishikawa T, Umetani J, Ahmed M, Mineo C*, et al.* (2014). The cholesterol metabolite 27-hydroxycholesterol promotes atherosclerosis via proinflammatory processes mediated by estrogen receptor alpha. *Cell metabolism* **20**(1)**:** 172-182.

Vamecq J, Van Hoof F (1984). Implication of a peroxisomal enzyme in the catabolism of glutaryl-CoA. *The Biochemical journal* **221**(1)**:** 203-211.

van de Beek MC, Ofman R, Dijkstra I, Wijburg F, Engelen M, Wanders R*, et al.* (2017). Lipid-induced endoplasmic reticulum stress in X-linked adrenoleukodystrophy. *Biochimica et biophysica acta. Molecular basis of disease* **1863**(9)**:** 2255-2265.

Van Veldhoven PP, Brees C, Mannaerts GP (1991). D-aspartate oxidase, a peroxisomal enzyme in liver of rat and man. *Biochimica et biophysica acta* **1073**(1)**:** 203-208.

Vauzour D, Rodriguez-Mateos A, Corona G, Oruna-Concha MJ, Spencer JP (2010). Polyphenols and human health: prevention of disease and mechanisms of action. *Nutrients* **2**(11)**:** 1106-1131.

Vejux A, Abed-Vieillard D, Hajji K, Zarrouk A, Mackrill JJ, Ghosh S*, et al.* (2020). 7-Ketocholesterol and 7beta-hydroxycholesterol: In vitro and animal models used to characterize their activities and to identify molecules preventing their toxicity. *Biochemical pharmacology* **173:** 113648.

Vejux A, Guyot S, Montange T, Riedinger JM, Kahn E, Lizard G (2009a). Phospholipidosis and down-regulation of the PI3-K/PDK-1/Akt signalling pathway are vitamin E inhibitable events associated with 7-ketocholesterol-induced apoptosis. *The Journal of nutritional biochemistry* **20**(1)**:** 45-61.

Vejux A, Kahn E, Dumas D, Bessède G, Ménétrier F, Athias A*, et al.* (2005). 7-Ketocholesterol favors lipid accumulation and colocalizes with Nile Red positive cytoplasmic structures formed during 7-ketocholesterol-induced apoptosis: analysis by flow cytometry, FRET biphoton spectral imaging microscopy, and subcellular fractionation. *Cytometry A* **64**(2)**:** 87-100.

Vejux A, Kahn E, Menetrier F, Montange T, Lherminier J, Riedinger JM*, et al.* (2007). Cytotoxic oxysterols induce caspase-independent myelin figure formation and caspase-dependent polar lipid accumulation. *Histochemistry and cell biology* **127**(6)**:** 609-624.

Vejux A, Lizard G (2009b). Cytotoxic effects of oxysterols associated with human diseases: Induction of cell death (apoptosis and/or oncosis), oxidative and inflammatory activities, and phospholipidosis. *Molecular aspects of medicine* **30**(3)**:** 153-170.

Vejux A, Malvitte L, Lizard G (2008). Side effects of oxysterols: cytotoxicity, oxidation, inflammation, and phospholipidosis. *Brazilian journal of medical and biological research = Revista brasileira de pesquisas medicas e biologicas* **41**(7)**:** 545-556.

Vejux A, Samadi M, Lizard G (2011). Contribution of cholesterol and oxysterols in the physiopathology of cataract: implication for the development of pharmacological treatments. *Journal of ophthalmology* **2011:** 471947.

Viens L, Athias A, Lizard G, Simard G, Gueldry S, Braschi S*, et al.* (1996). Effect of lipid transfer activity and lipolysis on low density lipoprotein (LDL) oxidizability: evidence for lipolysis-generated non-esterified fatty acids as inhibitors of LDL oxidation. *Journal of lipid research* **37**(10)**:** 2179-2192.

Vine DF, Croft KD, Beilin LJ, Mamo JC (1997). Absorption of dietary cholesterol oxidation products and incorporation into rat lymph chylomicrons. *Lipids* **32**(8)**:** 887-893.

Vurusaner B, Gargiulo S, Testa G, Gamba P, Leonarduzzi G, Poli G*, et al.* (2018). The role of autophagy in survival response induced by 27-hydroxycholesterol in human promonocytic cells. *Redox biology* **17:** 400-410.

Waechter F, Bentley P, Bieri F, Staubli W, Volkl A, Fahimi HD (1983). Epoxide hydrolase activity in isolated peroxisomes of mouse liver. *FEBS letters* **158**(2)**:** 225-228.

Walther TC, Farese RV, Jr. (2012). Lipid droplets and cellular lipid metabolism. *Annual review of biochemistry* **81:** 687-714.

Wanders RJ (2004). Peroxisomes, lipid metabolism, and peroxisomal disorders. *Molecular genetics and metabolism* **83**(1-2)**:** 16-27.

Wanders RJ, Waterham HR (2006). Biochemistry of mammalian peroxisomes revisited. *Annual review of biochemistry* **75:** 295-332.

Wanders RJA, Waterham HR, Ferdinandusse S (2018). Peroxisomes and Their Central Role in Metabolic Interaction Networks in Humans. *Sub-cellular biochemistry* **89:** 345-365.

Warraich UE, Hussain F, Kayani HUR (2020). Aging - Oxidative stress, antioxidants and computational modeling. *Heliyon* **6**(5)**:** e04107.

Watanabe Y, Yamaguchi T, Ishihara N, Nakamura S, Tanaka S, Oka R*, et al.* (2018). 7-Ketocholesterol induces ROS-mediated mRNA expression of 12-lipoxygenase, cyclooxygenase-2 and pro-inflammatory cytokines in human mesangial cells: Potential role in diabetic nephropathy. *Prostaglandins & other lipid mediators* **134:** 16-23.

Waterham HR, Ferdinandusse S, Wanders RJ (2016). Human disorders of peroxisome metabolism and biogenesis. *Biochimica et biophysica acta* **1863**(5)**:** 922-933.

Willard KA, Elling CL, Stice SL, Brindley MA (2018). The Oxysterol 7-Ketocholesterol Reduces Zika Virus Titers in Vero Cells and Human Neurons. *Viruses* **11**(1).

Wu T, Yankovskaya V, McIntire WS (2003). Cloning, sequencing, and heterologous expression of the murine peroxisomal flavoprotein, N1-acetylated polyamine oxidase. *The Journal of biological chemistry* **278**(23)**:** 20514-20525.

Yalcinkaya A, Samadi A, Lay I, Unal S, Sabuncuoglu S, Oztas Y (2019). Oxysterol concentrations are associated with cholesterol concentrations and anemia in pediatric patients with sickle cell disease. *Scandinavian journal of clinical and laboratory investigation* **79**(6)**:** 381-387.

Yamagata K, Tanaka N, Suzuki K (2013). Epigallocatechin 3-gallate inhibits 7-ketocholesterol-induced monocyte-endothelial cell adhesion. *Microvascular research* **88:** 25-31.

Yamamuro D, Yamazaki H, Osuga JI, Okada K, Wakabayashi T, Takei A*, et al.* (2020). Esterification of 4beta-hydroxycholesterol and other oxysterols in human plasma occurs independently of LCAT. *Journal of lipid research*.

Yammine A, Nury T, Vejux A, Latruffe N, Vervandier-Fasseur D, Samadi M*, et al.* (2020a). Prevention of 7-Ketocholesterol-Induced Overproduction of Reactive Oxygen Species, Mitochondrial Dysfunction and Cell Death with Major Nutrients (Polyphenols, omega3 and omega9 Unsaturated Fatty Acids) of the Mediterranean Diet on N2a Neuronal Cells. *Molecules* **25**(10).

Yammine A, Nury T, Vejux A, Latruffe N, Vervandier-Fasseur D, Samadi M*, et al.* (2020b). Prevention of 7-Ketocholesterol-Induced Overproduction of Reactive Oxygen Species, Mitochondrial Dysfunction and Cell Death with Major Nutrients (Polyphenols, ω3 and ω9 Unsaturated Fatty Acids) of the Mediterranean Diet on N2a Neuronal Cells. *Molecules* **25**(10).

Yammine A, Zarrouk A, Nury T, Vejux A, Latruffe N, Vervandier-Fasseur D*, et al.* (2020c). Prevention by Dietary Polyphenols (Resveratrol, Quercetin, Apigenin) Against 7-Ketocholesterol-Induced Oxiapoptophagy in Neuronal N2a Cells: Potential Interest for the Treatment of Neurodegenerative and Age-Related Diseases. *Cells* **9**(11).

Yang C, Xie L, Gu Q, Qiu Q, Wu X, Yin L (2019). 7-Ketocholesterol disturbs RPE cells phagocytosis of the outer segment of photoreceptor and induces inflammation through ERK signaling pathway. *Experimental eye research* **189:** 107849.

Yao RQ, Ren C, Xia ZF, Yao YM (2020). Organelle-specific autophagy in inflammatory diseases: a potential therapeutic target underlying the quality control of multiple organelles. *Autophagy***:** 1-17.

Yokota S, Oda T, Fahimi HD (2001). The role of 15-lipoxygenase in disruption of the peroxisomal membrane and in programmed degradation of peroxisomes in normal rat liver. *The journal of histochemistry and cytochemistry : official journal of the Histochemistry Society* **49**(5)**:** 613-622.

Zarrouk A, Martine L, Gregoire S, Nury T, Meddeb W, Camus E*, et al.* (2019). Profile of Fatty Acids, Tocopherols, Phytosterols and Polyphenols in Mediterranean Oils (Argan Oils, Olive Oils, Milk Thistle Seed Oils and Nigella Seed Oil) and Evaluation of their Antioxidant and Cytoprotective Activities. *Current pharmaceutical design* **25**(15)**:** 1791-1805.

Zarrouk A, Nury T, Karym EM, Vejux A, Sghaier R, Gondcaille C*, et al.* (2017). Attenuation of 7-ketocholesterol-induced overproduction of reactive oxygen species, apoptosis, and autophagy by dimethyl fumarate on 158N murine oligodendrocytes. *The Journal of steroid biochemistry and molecular biology* **169:** 29-38.

Zarrouk A, Nury T, Samadi M, O'Callaghan Y, Hammami M, O'Brien NM*, et al.* (2015). Effects of cholesterol oxides on cell death induction and calcium increase in human neuronal cells (SK-N-BE) and evaluation of the protective effects of docosahexaenoic acid (DHA; C22:6 n-3). *Steroids* **99**(Pt B)**:** 238-247.

Zarrouk A, Vejux A, Mackrill J, O'Callaghan Y, Hammami M, O'Brien N*, et al.* (2014). Involvement of oxysterols in age-related diseases and ageing processes. *Ageing research reviews* **18:** 148-162.

Zerbinati C, Iuliano L (2017). Cholesterol and related sterols autoxidation. *Free radical biology & medicine* **111:** 151-155.

Zhang J, Tripathi DN, Jing J, Alexander A, Kim J, Powell RT*, et al.* (2015). ATM functions at the peroxisome to induce pexophagy in response to ROS. *Nature cell biology* **17**(10)**:** 1259-1269.

Zhou L, Shi M, Guo Z, Brisbon W, Hoover R, Yang H (2006). Different cytotoxic injuries induced by lysophosphatidylcholine and 7-ketocholesterol in mouse endothelial cells. *Endothelium : journal of endothelial cell research* **13**(3)**:** 213-226.

Zieden B, Kaminskas A, Kristenson M, Kucinskiene Z, Vessby B, Olsson AG*, et al.* (1999). Increased plasma 7 beta-hydroxycholesterol concentrations in a population with a high risk for cardiovascular disease. *Arteriosclerosis, thrombosis, and vascular biology* **19**(4)**:** 967-971.

Zmyslowski A, Szterk A (2019). Oxysterols as a biomarker in diseases. *Clinica chimica acta; international journal of clinical chemistry* **491:** 103-113.

Résumé

Le stress oxydant est souvent augmenté dans plusieurs maladies comme des maladies liées à l'âge (maladies cardiovasculaires, maladies oculaires (dégénérescence maculaire liée à l'âge (DMLA) et cataracte), des maladies neurodégénératives (Maladie d'Alzheimer, sclérose en plaques), des maladies inflammatoires chroniques (maladies inflammatoires chroniques de l'intestin (MICI)) ainsi que certaines maladies génétiques rares (maladie de Niemann Pick, adrénoleucodystrophie liée à l'X (X-ALD)). Le stress oxydant peut oxyder différentes molécules, notamment le cholestérol présent dans les membranes lipidiques, et conduire à la formation de dérivés oxydés du cholestérol : les oxystérols. Certains d'entre eux, comme le 7-cétocholestérol (7KC), sont toxiques et peuvent être à l'origine d'un type de mort cellulaire, l'oxyapoptophagie, associant une élévation du stress oxydant, une activation de l'apoptose à des critères d'autophagie. En utilisant des oligodendrocytes murins 158N, ce travail a permis de mieux caractériser l'oxyapoptophagie induite par le 7KC. La toxicité du 7KC sur les organites cellulaires comme la mitochondrie et le lysosome a été confirmée. Ce travail montre aussi que l'oxyapoptophagie est associée à des modifications topographiques, morphologiques et fonctionnelles du peroxysome. Il a été montré que le 7KC induit une diminution de l'expression et de l'activité de certains transporteurs peroxysomaux (ABCD1, ABCD3) et enzymes peroxysomales (ACOX1, MFP2, catalase) et favorise une accumulation d'acides gras à très longue chaine (C24:0, C24:1 et C26:0, C26:1) dégradés au niveau du peroxysome. Il a aussi été démontré que certains lipides (α-tocophérol, acide α-linolénique (ALA), acide éïcosapentaénoïque (EPA), acide docosahéxaénoïque (DHA), acide oléique (AO), huile de Lorenzo (acide oléique + acide érucique (4:1)) et le sulfo-N-succinimidyl oleate (SSO)) sont cytoprotecteurs et atténuent fortement l'oxyapoptophagie induite par le 7KC. Ceci permet d'envisager la prévention ou le traitement les maladies associées à des taux élevés de 7KC, en particulier certaines maladies liées à l'âge qui ne disposent pas de traitements efficaces.

Mots clés : oxystérol, 7-cétocholestérol, oxyapoptophagie, peroxysome, cytoprotection, stress oxydant.

Abstract

Oxidative stress is often increased in several diseases such as age-related diseases (cardiovascular diseases, eye diseases (age-related macular degeneration (AMD) and cataracts), neurodegenerative diseases (Alzheimer's disease, multiple sclerosis), chronic inflammatory diseases (chronic inflammatory bowel disease (IBD)) as well as certain rare genetic diseases (Niemann Pick's disease, X-linked adrenoleukodystrophy (X-ALD)). Oxidative stress can oxidize various molecules, in particular the cholesterol present in lipid membranes, and lead to the formation of oxidized cholesterol derivatives: oxysterols. Some of them, such as 7-ketocholesterol (7KC), are toxic and may be the cause of a type of cell death, oxiapoptophagy, associating an increase in oxidative stress, activation of apoptosis and autophagic criteria. Using 158N murine oligodendrocytes, this work has allowed to better characterize the oxiapoptophagy induced by 7KC. The toxicity of 7KC on cellular organelles such as mitochondria and lysosome was confirmed. This work also shows that oxyapoptophagy is associated with topographic, morphological and functional modifications of the peroxisome. It has been shown that 7KC induces a decrease in the expression and activity of certain peroxisomal transporters (ABCD1, ABCD3) and peroxisomal enzymes (ACOX1, MFP2, catalase) and promotes an accumulation of very long-chain fatty acids (C24:0, C24:1 and C26:0, C26:1) degraded in the peroxisome. It has also been shown that certain lipids (α-tocopherol, α-linolenic acid (ALA), eicosapentaenoic acid (EPA), docosahexaenoic acid (DHA), oleic acid (AO), Lorenzo's oil (oleic acid + erucic acid (4: 1)) and sulfo-N-succinimdyl oleate (SSO)) are cytoprotective and strongly attenuate 7KC-induced oxyaptophagy. This makes it possible to envisage the prevention or treatment of diseases associated with high levels of 7KC, in particular certain age-related diseases for which there are no effective treatments.

Key words: peroxisome, oxysterol, 7-ketocholesterol, oxiapoptophagy, oxidative stress, cytoprotection.